2018

Part I: Vanadium–catalyzed Asymmetric Oxidative Coupling Of Phenols And Hydroxycarbazoles And Its Mechanistic Study Part Ii: Total Synthesis Of Chaetoglobin A Part Iii: Ligand Evolution To Drive Reaction Discovery Part Iv: Oxidative Coupling Of 3-Oxindoles To Construct Quaternary Centers

Houng Kang
University of Pennsylvania, meditator19@gmail.com

Part I: Vanadium–catalyzed Asymmetric Oxidative Coupling Of Phenols And Hydroxycarbazoles And Its Mechanistic Study Part Ii: Total Synthesis Of Chaetoglobin A Part Iii: Ligand Evolution To Drive Reaction Discovery Part Iv: Oxidative Coupling Of 3-Oxindoles To Construct Quaternary Centers

Abstract

Part I: The axially chiral biaryl motif is found in many natural products as well as in ligands for catalysis such as 1,1'-binaphthol. Formation of axially chiral compounds was accomplished by means of the asymmetric oxidative coupling, which has proven to be both an efficient and environmentally benign synthetic method. Interests toward an effective asymmetric oxidative coupling of simple phenols, which are challenging substrates because of relatively high oxidation potential and regioselectivity issues, have arisen due to a lack of corresponding methods. After many efforts to design and modify the catalyst scaffold, we found that a monomeric vanadium(V) catalyst together with LiCl or HOAc as an additive accomplished C-C bond formation to afford the bisphenol moiety in good yield and good enantioselectivity. The carbazole moiety is another good candidate to apply our oxidative coupling method because of its electron-rich nature. Using various 3-substituted-2-hydroxycarbazole derivatives, oxidative coupling afforded products containing diverse functional groups, including ketone, ester, trifluoromethyl, halides, allyl, etc.

Part II: The azaphilone alkaloid, chaetoglobin A, has drawn attention due to its intriguing dimeric structure. The molecule features a 2H-isoquinoline-6,8-dione moiety containing quaternary centers and a chiral axis that connects two identical motifs. Although a variety of monomeric azaphilone alkaloids have been synthesized, a dimeric class of azaphilone has not been synthesized to date. Installing axial chirality by means of the asymmetric oxidative phenol coupling is the key step in making the natural product. Afterwards, bisformylation and oxidative dearomatization were carried out smoothly to afford highly oxygenated bicyclic cores. Thorough optimization of the selective acetyl deprotection and final amination afforded access to the synthetic chaetoglobin A in 12 linear steps.

Part III: These days, the ligand plays an important role in versatile chemical reactions. Understanding the ligand effect provided critical information to tackle challenging issues. Taking advantage of High Throughput Experimentation (HTE) allowed access to a variety of ligands in a rapid and efficient manner. Due to easy synthesis of a series of different alkynylphosphine oxides and azides, our efforts were focused on generating the diverse triazole-based phosphine ligands. The ligand was prepared by [3+2]-cycloaddition with the alkynylphosphine oxide and azide, followed by the corresponding phosphine oxide reduction. Ultimately, a one-pot protocol reinforced the efficient ligand synthesis and accomplished the synthesis of a number of ligands by HTE parallel synthesis. Currently, with the ClickPhos ligands, the ligand effect was explored under the challenging chemical reaction conditions.

Part IV: 2,2-Disubstituted indolin-3-one is not only a core structure for many natural products but also serves as a useful synthetic intermediate. To construct the C-2 quaternary center via the oxidative coupling between 3-oxindole and various aryl substrates, including indoles, pyrroles, and electron-rich aryl compounds, was achieved in the presence of a copper catalyst incorporated with a salan ligand. This milder catalytic protocol efficiently generated the quaternary center with various functional groups tolerance, such as halide, ester,

nitrile, etc. In addition, use of a chiral monomeric vanadium catalyst gave promising levels of asymmetric transformation.

Degree Type
Dissertation

Degree Name
Doctor of Philosophy (PhD)

Graduate Group
Chemistry

First Advisor
Marisa C. Kozlowski

Second Advisor
Amos B. Smith, III

Keywords
3-oxindole coupling, chaetoglobin A, Clickphos, Oxidative phenol coupling, Vanadium

Subject Categories
Organic Chemistry

PART I: VANADIUM–CATALYZED ASYMMETRIC OXIDATIVE COUPLING OF PHENOLS AND HYDROXYCARBAZOLES AND ITS MECHANISTIC STUDY
PART II: TOTAL SYNTHESIS OF CHAETOGLOBIN A
PART III: LIGAND EVOLUTION TO DRIVE REACTION DISCOVERY
PART IV: OXIDATIVE COUPLING OF 3-OXINDOLES TO CONSTRUCT QUATERNARY CENTERS

Houng Kang

A DISSERTATION

in

Chemistry

Presented to the Faculties of the University of Pennsylvania

in

Partial Fulfillment of the Requirements for the

Degree of Doctor of Philosophy

2018

Supervisor of Dissertation

_____

Marisa C. Kozlowski, Professor of Chemistry

Graduate Group Chairperson

_____

David W. Christianson, Roy and Diana Vagelos Professor in Chemistry and Chemical Biology

Dissertation Committee:

Amos B. Smith III, Rhodes-Thompson Professor of Chemistry
Gary A. Molander, Hirschmann-Makineni Professor of Chemistry
Patrick J. Walsh, Professor of Chemistry

ACKNOWLEDGMENT

ABSTRACT

PART I: VANADIUM–CATALYZED ASYMMETRIC OXIDATIVE COUPLING OF PHENOLS AND HYDROXYCARBAZOLES AND ITS MECHANISTIC STUDY

PART II: TOTAL SYNTHESIS OF CHAETOGLOBIN A

PART III: LIGAND EVOLUTION TO DRIVE REACTION DISCOVERY

PART IV: OXIDATIVE COUPLING OF 3-OXINDOLES TO CONSTRUCT QUATERNARY CENTERS

Houng Kang

Marisa C. Kozlowski

Part I: The axially chiral biaryl motif is found in many natural products as well as in ligands for catalysis such as 1,1'-binaphthol. Formation of axially chiral compounds was accomplished by means of the asymmetric oxidative coupling, which has proven to be both an efficient and environmentally benign synthetic method. Interests toward an effective asymmetric oxidative coupling of simple phenols, which are challenging substrates because of relatively high oxidation potential and regioselectivity issues, have arisen due to a lack of corresponding methods. After many efforts to design and modify the catalyst scaffold, we found that a monomeric vanadium(**V**) catalyst together with LiCl or HOAc as an additive accomplished C-C bond formation to afford the bisphenol moiety in good yield and good enantioselectivity. The carbazole moiety is another good candidate to apply our oxidative coupling method because of its electron-rich nature. Using various 3-substituted-2-hydroxycarbazole derivatives, oxidative coupling afforded products containing diverse functional groups, including ketone, ester, trifluoromethyl, halides, allyl,

etc.

Part II: The azaphilone alkaloid, chaetoglobin A, has drawn attention due to its intriguing dimeric structure. The molecule features a 2*H*-isoquinoline-6,8-dione moiety containing quaternary centers and a chiral axis that connects two identical motifs. Although a variety of monomeric azaphilone alkaloids have been synthesized, a dimeric class of azaphilone has not been synthesized to date. Installing axial chirality by means of the asymmetric oxidative phenol coupling is the key step in making the natural product. Afterwards, bisformylation and oxidative dearomatization were carried out smoothly to afford highly oxygenated bicyclic cores. Thorough optimization of the selective acetyl deprotection and final amination afforded access to the synthetic chaetoglobin A in 12 linear steps.

Part III: These days, the ligand plays an important role in versatile chemical reactions. Understanding the ligand effect provided critical information to tackle challenging issues. Taking advantage of High Throughput Experimentation (HTE) allowed access to a variety of ligands in a rapid and efficient manner. Due to easy synthesis of a series of different alkynylphosphine oxides and azides, our efforts were focused on generating the diverse triazole-based phosphine ligands. The ligand was prepared by [3+2]-cycloaddition with the alkynylphosphine oxide and azide, followed by the corresponding phosphine oxide reduction. Ultimately, a one-pot protocol reinforced the efficient ligand synthesis and accomplished the synthesis of a number of ligands by HTE parallel synthesis. Currently, with the ClickPhos ligands, the ligand effect was explored under the challenging chemical reaction conditions.

Part IV: 2,2-Disubstituted indolin-3-one is not only a core structure for many natural products but also serves as a useful synthetic intermediate. To construct the C-2 quaternary center via the oxidative coupling between 3-oxindole and various aryl

substrates, including indoles, pyrroles, and electron-rich aryl compounds, was achieved in the presence of a copper catalyst incorporated with a salan ligand. This milder catalytic protocol efficiently generated the quaternary center with various functional groups tolerance, such as halide, ester, nitrile etc. In addition, use of a chiral monomeric vanadium catalyst gave promising levels of asymmetric transformation.

TABLE OF CONTENTS

LIST OF TABLES

LIST OF FIGURES

LIST OF SCHEMES

CHAPTER 1: VANADIUM–CATALYZED ASYMMETRIC OXIDATIVE COUPLING OF PHENOLS AND HYDROXYCARBAZOLES AND ITS MECHANISTIC STUDY[1]

1.1. Background

Asymmetric oxidative catalysis offers a simple and atom-economic method to generate an enantioenriched biaryl motif, which is widely found in natural products and catalysts (**Figure 1.1**).[2,3] Naturally occurring dimeric scaffolds, connected through a chiral axis, feature intriguing structures as well as biological activities, such as agonism of neuritic streaming[2a] or inhibition of cancer cell lines.[2f] Furthermore, these axial chiral backbones have been widely utilized in asymmetric catalysts. BINOL has been proven to

[1] Adapted from Kang, H.; Lee, Y. E.; Reddy, P. V. G.; Dey, S.; Allen, S. E.; Niederer, K. A.; Sung, P.; Hewitt, K.; Torruellas, C.; Herling, M. R.; Kozlowski, M. C. Asymmetric Oxidative Coupling of Phenols and Hydroxycarbazoles. *Org. Lett.* **2017**, *19*, 5505–5508. Copyright 2017 American Chemical Society.

[2] (a) Fukuyama, Y.; Asakawa, Y. Novel Neurotrophic Isocuparane-Type Sesquiterpene Dimers, Mastigophorenes A, B, C and D, Isolated from the Liverwort Mastigophora Diclados. *J. Chem. Soc. [Perkin 1]* **1991**, *0* (11), 2737–2741. (b) Degnan, A. P.; Meyers, A. I. Total Syntheses of (−)-Herbertenediol, (−)-Mastigophorene A, and (−)-Mastigophorene B. Combined Utility of Chiral Bicyclic Lactams and Chiral Aryl Oxazolines. *J. Am. Chem. Soc.* **1999**, *121*, 2762–2769. (c) Narayan, S.; Roush, W. R. Studies Toward the Total Synthesis of Angelmicin B (Hibarimicin B): Synthesis of a Model CD−D' Arylnaphthoquinone. *Org. Lett.* **2004**, *6*, 3789–3792. (d) Kenar, J. A. Reaction Chemistry of Gossypol and Its Derivatives. *J. Am. Oil Chem. Soc.* **2006**, *83*, 269–302. (e) Buter, J.; Heijnen, D.; Vila, C.; Hornillos, V.; Otten, E.; Giannerini, M.; Minnaard, A. J.; Feringa, B. L. Palladium-Catalyzed, Tert-Butyllithium-Mediated Dimerization of Aryl Halides and Its Application in the Atropselective Total Synthesis of Mastigophorene A. *Angew. Chem. Int. Ed.* **2016**, *55*, 3620–3624. (f) Ming Ge, H.; Yun Zhang, W.; Ding, G.; Saparpakorn, P.; Chun Song, Y.; Hannongbua, S.; Xiang Tan, R. Chaetoglobins A and B, Two Unusual Alkaloids from Endophytic Chaetomium Globosum Culture. *Chem. Commun.* **2008**, 5978-5980. (g) Nutan, M. T.; Hasan, C.; Rashid, M. Bismurrayafoline E: A New Dimeric Carbazole Alkaloid from Murraya Koenigii. *Fitoterapia* **1999**, *70*, 130–133. (h) Tachibana, Y.; Kikuzaki, H.; Lajis, N. H.; Nakatani, N. Comparison of Antioxidative Properties of Carbazole Alkaloids from Murraya Koenigii Leaves. *J. Agric. Food Chem.* **2003**, *51*, 6461–6467.

[3] (a) Brunel, J. M. BINOL: A Versatile Chiral Reagent. *Chem. Rev.* **2005**, *105*, 857–898. (b) Qiu, L.; Kwong, F. Y.; Wu, J.; Lam, W. H.; Chan, S.; Yu, W.-Y.; Li, Y.-M.; Guo, R.; Zhou, Z.; Chan, A. S. C. A New Class of Versatile Chiral-Bridged Atropisomeric Diphosphine Ligands: Remarkably Efficient Ligand Syntheses and Their Applications in Highly Enantioselective Hydrogenation Reactions. *J. Am. Chem. Soc.* **2006**, *128*, 5955–5965. (c) Melhado, A. D.; Luparia, M.; Toste, F. D. Au(I)-Catalyzed Enantioselective 1,3-Dipolar Cycloadditions of Münchnones with Electron-Deficient Alkenes. *J. Am. Chem. Soc.* **2007**, *129*, 12638–12639. (d) Heiser, B.; Broger, E. A.; Crameri, Y. New Efficient Methods for the Synthesis and In-Situ Preparation of Ruthenium(II) Complexes of Atropisomeric Diphosphines and Their Application in Asymmetric Catalytic Hydrogenations. *Tetrahedron Asymmetry* **1991**, *2*, 51–62.

be effective in reduction, oxidation, and diverse asymmetric C-C bond–forming reactions, which include the ene, Diels-Alder, aldol, allylation, alkynylation, cycloaddition, and Friedel-Crafts reactions, etc.[3a] In addition, axial chiral bisphosphine ligands have been used in numerous reactions, including asymmetric hydrogenation and cycloaddition reactions.[3b-d]

a. Natural Products

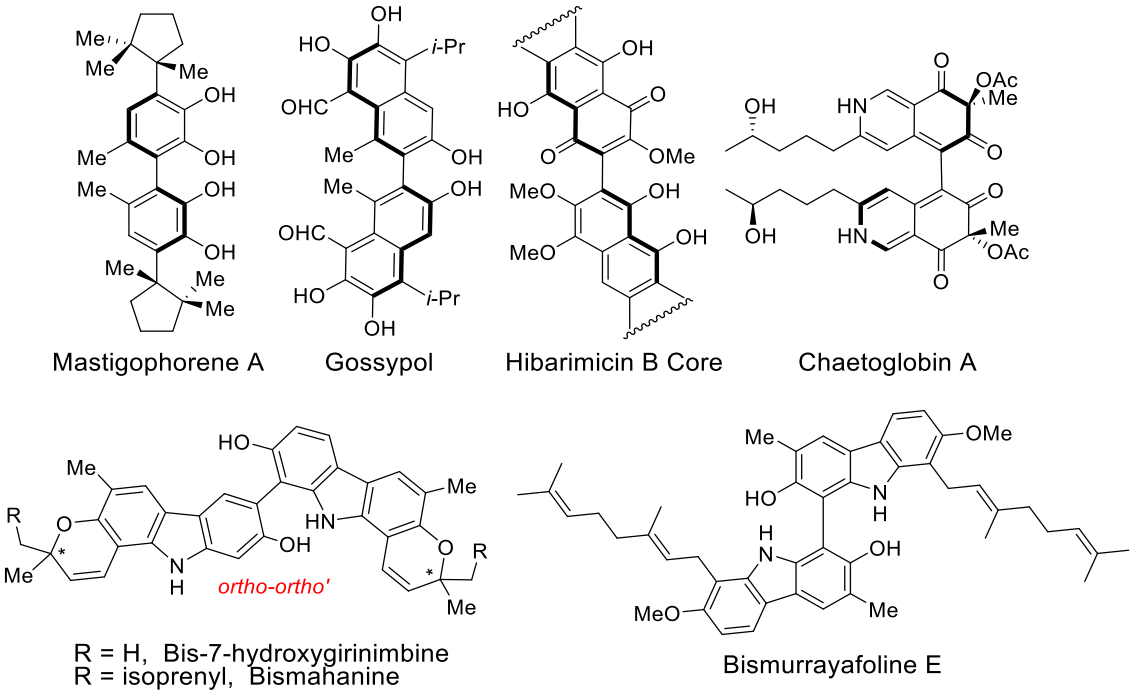

b. Ligands

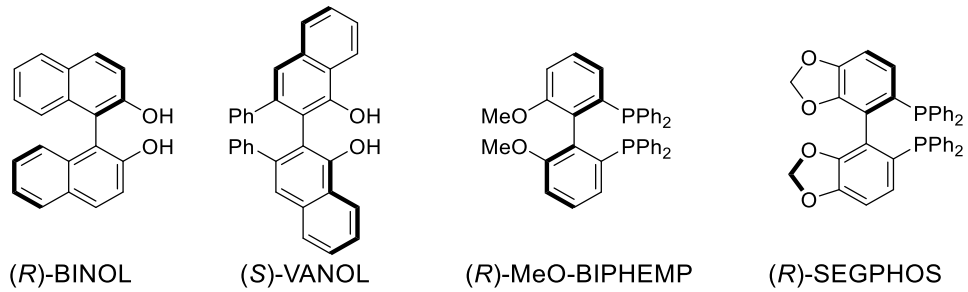

Figure 1.1. Example of a Chiral Axis in Natural Products and Catalysis[1]

In the last three decades, a variety of transition metals have been proven to effect such transformations. In 1999, Nakajima and coworkers reported that copper complexes

with proline derivatives as ligands allowed access to BINOL analogs.[4] The Kozlowski group discovered that the 1,5-diaza-*cis*-decalin ligand afforded further improvement on both reactivity and enantioselectivity.[5] The unsymmetrical H_8–BINAM ligand has been utilized to construct a chiral axis by the Ha group in 2004.[6] It was necessary, however, to have an additional coordination group next to phenol to generate the complex, which was needed to produce facial selectivity by blocking one side (**Scheme 1.1**).

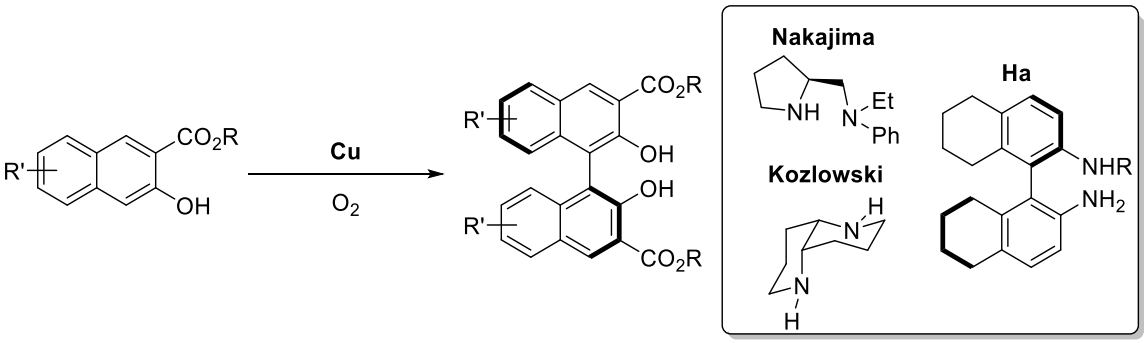

Scheme 1.1. Cu-catalyzed Asymmetric BINOL Derivative Syntheses

Vanadium also has been widely used as an asymmetric catalyst to synthesize BINOL derivatives. Monomeric vanadium complexes, by the Uang[7] and Chen groups,[8] or dimeric vanadium complexes, by the Gong[9] and Sasai groups,[10] afforded highly selective

[4] Nakajima, M.; Miyoshi, I.; Kanayama, K.; Hashimoto, S.; Noji, M.; Koga, K. Enantioselective Synthesis of Binaphthol Derivatives by Oxidative Coupling of Naphthol Derivatives Catalyzed by Chiral Diamine·Copper Complexes. *J. Org. Chem.* **1999**, *64*, 2264–2271.

[5] Li, X.; Yang, J.; Kozlowski, M. C. Enantioselective Oxidative Biaryl Coupling Reactions Catalyzed by 1,5-Diazadecalin Metal Complexes. *Org. Lett.* **2001**, *3*, 1137–1140.

[6] Kim, K. H.; Lee, D.-W.; Lee, Y.-S.; Ko, D.-H.; Ha, D.-C. Enantioselective Oxidative Coupling of Methyl 3-Hydroxy-2-Naphthoate Using Mono-N-Alkylated Octahydrobinaphthyl-2,2′-Diamine Ligand. *Tetrahedron* **2004**, *60*, 9037–9042.

[7] Chu, C.-Y.; Uang, B.-J. Catalytic Enantioselective Coupling of 2-Naphthols by New Chiral Oxovanadium Complexes Bearing a Self Accelerating Functional Group. *Tetrahedron Asymmetry* **2003**, *14*, 53–55.

[8] Barhate, N. B.; Chen, C.-T. Catalytic Asymmetric Oxidative Couplings of 2-Naphthols by Tridentate N-Ketopinidene-Based Vanadyl Dicarboxylates. *Org. Lett.* **2002**, *4*, 2529–2532.

[9] Guo, Q.-X.; Wu, Z.-J.; Luo, Z.-B.; Liu, Q.-Z.; Ye, J.-L.; Luo, S.-W.; Cun, L.-F.; Gong, L.-Z. Highly Enantioselective Oxidative Couplings of 2-Naphthols Catalyzed by Chiral Bimetallic Oxovanadium Complexes with Either Oxygen or Air as Oxidant. *J. Am. Chem. Soc.* **2007**, *129*, 13927–13938.

[10] Takizawa, S.; Katayama, T.; Somei, H.; Asano, Y.; Yoshida, T.; Kameyama, C.; Rajesh, D.; Onitsuka, K.; Suzuki, T.; Mikami, M.; Yamataka, H.; Jayaprakash, D.; Sasai, H. Dual Activation in

BINOL analogs (**Scheme 1.2**).

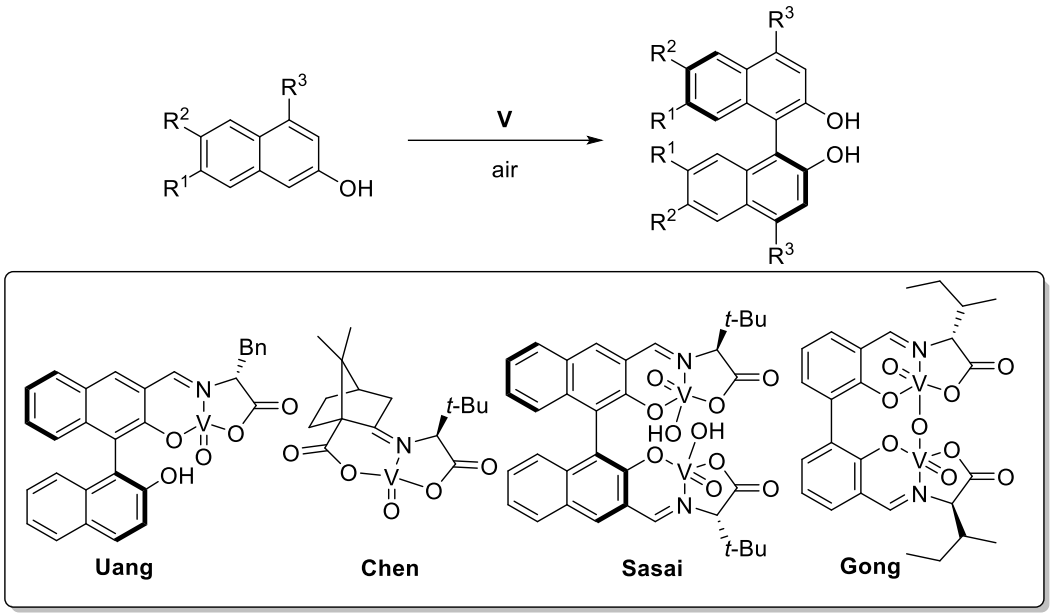

Scheme 1.2. V-catalyzed Asymmetric BINOL Derivative Syntheses

Later, Katsuki and coworkers disclosed that a Schiff base-iron complex was able to construct bisnaphthols efficiently, which are connected through a chiral axis.[11] Using an asymmetric phosphoric acid coordinated to iron, Toste and Pappo introduced the axial chiral bond in BINOL analogs in 2016 (**Scheme 1.3**).[12]

Oxidative Coupling of 2-Naphthols Catalyzed by Chiral Dinuclear Vanadium Complexes. *Tetrahedron* **2008**, *64*, 3361–3371.

[11] Egami, H.; Katsuki, T. Iron-Catalyzed Asymmetric Aerobic Oxidation: Oxidative Coupling of 2-Naphthols. *J. Am. Chem. Soc.* **2009**, *131*, 6082–6083.

[12] Narute, S.; Parnes, R.; Toste, F. D.; Pappo, D. Enantioselective Oxidative Homocoupling and Cross-Coupling of 2-Naphthols Catalyzed by Chiral Iron Phosphate Complexes. *J. Am. Chem. Soc.* **2016**, *138*, 16553–16560.

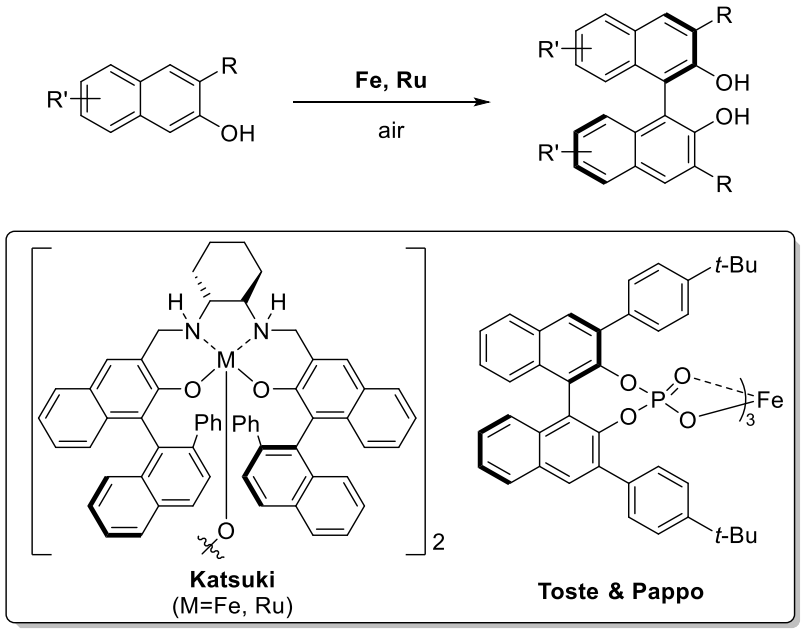

Scheme 1.3. Ru or Fe-catalyzed Asymmetric BINOL Derivative Syntheses

Compared to 2-naphthols, phenol couplings have been limited and less explored (**Scheme 1.4**). Furthermore, no highly selective oxidative phenol homocoupling is known to date. In 1999, Uang and coworkers (**Scheme 1.4.A**) reported oxidative phenol dimerization by means of a vanadium catalyst.[13] Recently, Kozlowski and Pappo highlighted that Cr[14] or Fe-catalyzed[15] oxidative phenol coupling allowed access to cross-coupled bisphenols (**Scheme 1.4.C**). Notably, the Liu and Kurti groups have reported highly enantioselective phenol couplings by utilizing preoxidized compounds, which

[13] Hwang, D.-R.; Chen, C.-P.; Uang, B.-J. Aerobic Catalytic Oxidative Coupling of 2-Naphthols and Phenols by $VO(Acac)_2$. *Chem. Commun.* **1999**, 1207–1208.
[14] Lee, Y. E.; Cao, T.; Torruellas, C.; Kozlowski, M. C. Selective Oxidative Homo- and Cross-Coupling of Phenols with Aerobic Catalysts. *J. Am. Chem. Soc.* **2014**, *136*, 6782–6785.
[15] Libman, A.; Shalit, H.; Vainer, Y.; Narute, S.; Kozuch, S.; Pappo, D. Synthetic and Predictive Approach to Unsymmetrical Biphenols by Iron-Catalyzed Chelated Radical–Anion Oxidative Coupling. *J. Am. Chem. Soc.* **2015**, *137*, 11453–11460.

impose constraints on the product types that can be formed (**Scheme 1.4.D**).[16,17]

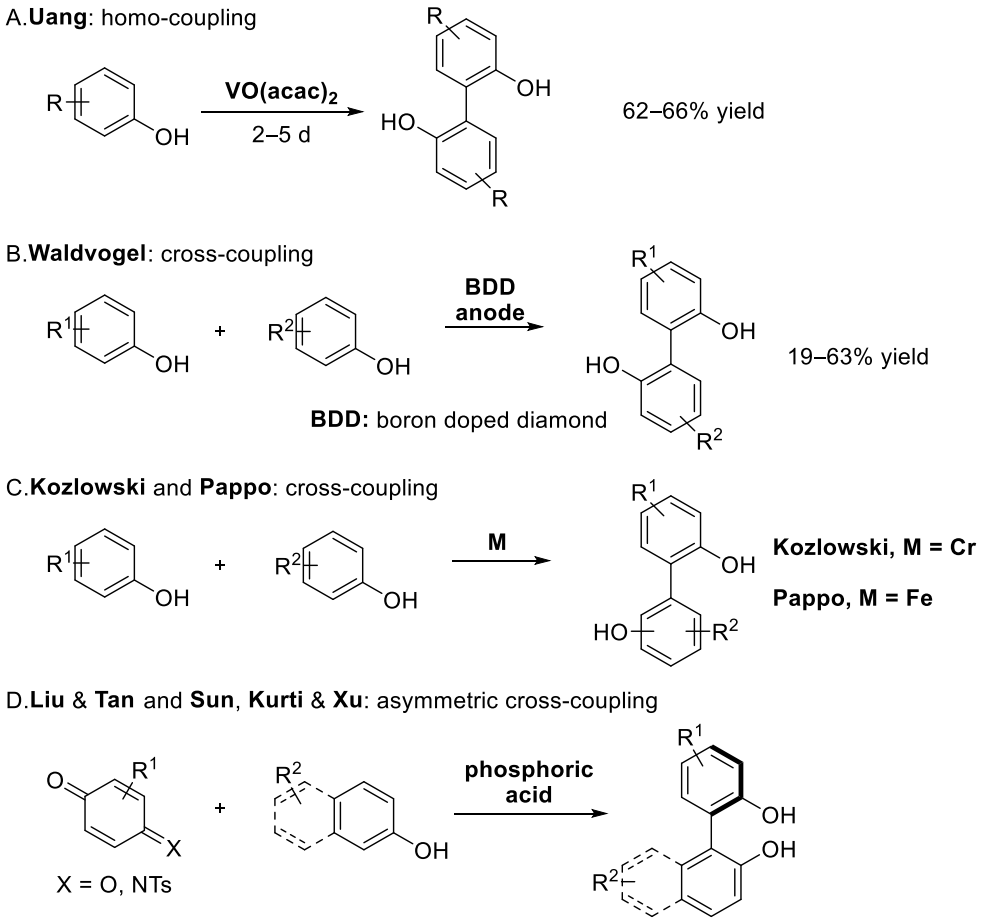

Scheme 1.4. Previous Oxidative Phenol Couplings

Hydroxycarbazoles have been found to be effective in oxidative coupling due to their electron-rich nature (**Scheme 1.5**). A variety of different oxidants have enabled the formation of the central bond. Benzoyl peroxide was utilized by Moody and coworkers to

[16] Chen, Y.-H.; Cheng, D.-J.; Zhang, J.; Wang, Y.; Liu, X.-Y.; Tan, B. Atroposelective Synthesis of Axially Chiral Biaryldiols via Organocatalytic Arylation of 2-Naphthols. *J. Am. Chem. Soc.* **2015**, *137*, 15062–15065.
[17] Wang, J.-Z.; Zhou, J.; Xu, C.; Sun, H.; Kürti, L.; Xu, Q.-L. Symmetry in Cascade Chirality-Transfer Processes: A Catalytic Atroposelective Direct Arylation Approach to BINOL Derivatives. *J. Am. Chem. Soc.* **2016**, *138*, 5202–5205.

make biscarbazole in 1989.[18] Bringmann and other groups used *tert*-butyl peroxide to introduce the C-C bond oxidatively from 1-hydroxycarbazoles.[19] Later, Knölker reported that tetrachloro-*para*-benzoquinone produced an axial bond *ortho* to the hydroxyl group.[20] In 2015, the Kozlowski group revealed that the vanadium-catalyzed oxidative coupling with *N*-protected 2-hydroxycarbazole generated the *ortho*-*ortho'* adduct as the major product.[21]

[18] Moody, C. J.; Shah, P. Diels-Alder Reactivity of Pyrano[3,4-b]Indol-3-Ones. Part 4. Synthesis of the Carbazole Alkaloids Carbazomycin A and B and Hyellazole. *J. Chem. Soc. [Perkin 1]* **1989**, 2463–2471.

[19] (a) Bringmann, G.; Ledermann, A.; Stahl, M.; Gulden, K. Bismurrayaquinone A: Synthesis, Chromatographic Enantiomer Resolution, and Stereoanalysis by Computational and Experimental CD Investigations. *Tetrahedron* **1995**, *51*, 9353–9360. (b) Lin, G.; Zhang, A. Synthesis of Optically Pure Clausenamine-A and Its Demethoxylated Analogs. *Tetrahedron* **2000**, *56*, 7163–7171. (c) Fillion, H.; Bouaziz, Z.; Nebois, P.; Poumaroux, A. Carbazole-1,4-Diones: Syntheses and Properties. *HETEROCYCLES* **2000**, *52*, 977–1000.

[20] Knölker, H.-J.; Goesmann, H.; Hofmann, C. Transition Metal Complexes in Organic Synthesis, Part 31.1 A Novel Molybdenum-Mediated Synthesis of Carbazole Derivatives: Application to the Total Synthesis of Mukonal and 1,1'-Bis(2-Hydroxy-3-Methylcarbazole). *Synlett* **1996**, *1996*, 737–740.

[21] Liu, L.; Carroll, P. J.; Kozlowski, M. C. Vanadium-Catalyzed Regioselective Oxidative Coupling of 2-Hydroxycarbazoles. *Org. Lett.* **2015**, *17*, 508–511.

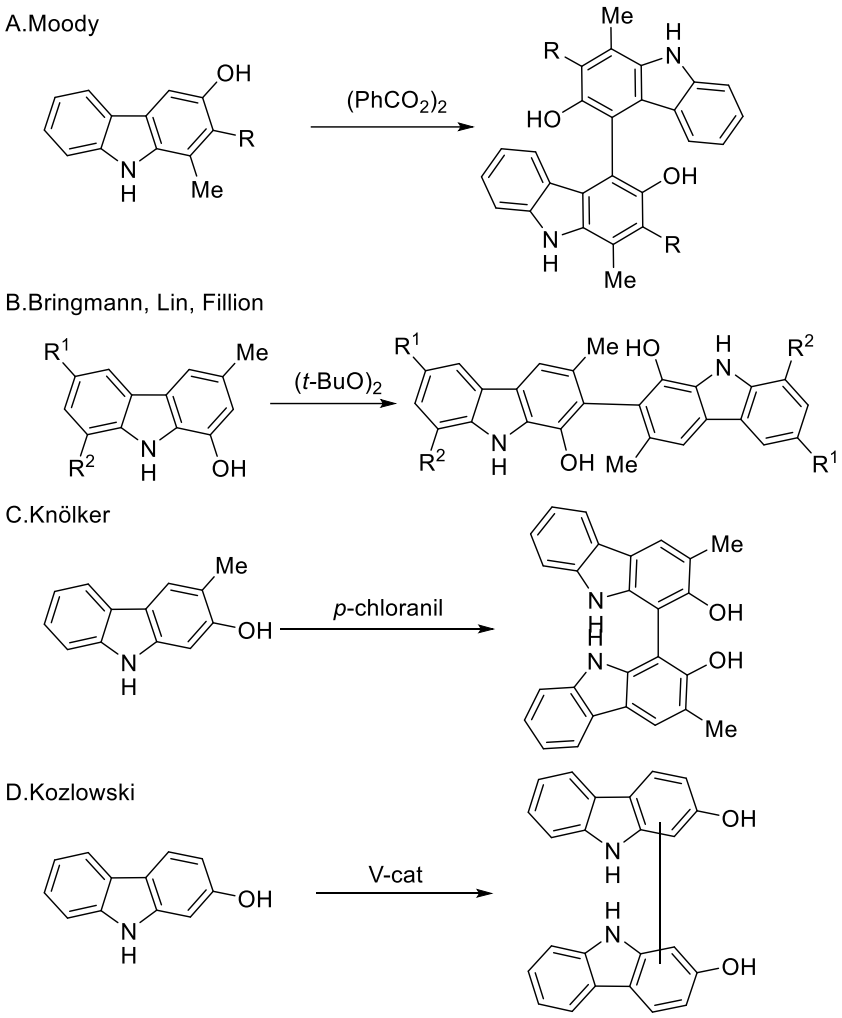

Scheme 1.5. Oxidative Hydroxycarbazole Couplings with Various Oxidants

1.2. Catalyst Optimization

Inspired by an effective oxidative coupling with $VO(acac)_2$,[13] 2,3,5-trimethylphenol (**1.1a**) was examined as the substrate in initial studies (**Scheme 1.6**). Its success in asymmetric BINOL derivative syntheses indicates that vanadium catalysts are highly efficient at introducing a chiral axis. Encouragingly, our initial attempts coupling **1.1a** with dimeric vanadium catalyst **V0** provided only *ortho-ortho* **1.2a** and *para-para* **1.3a** products among the many potential outcomes.

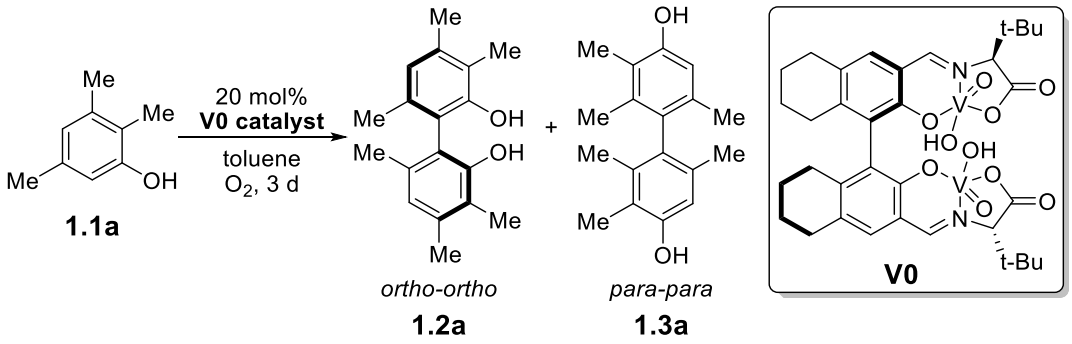

Scheme 1.6. Preliminary Oxidative Phenol Coupling with **V0** Catalyst[1]

However, the outcome from trial to trial was found to vary considerably. Part of the irreproducibility was attributed to the exact preparation of the catalyst, for which several protocols have been reported using different vanadium sources including $VO(SO_4)$[9,22a-d] and $VO(Cl)_3$.[22e-h] A base is sometimes used for ligand deprotonation prior to complexation, and removal of inorganic salts is effected with an aqueous wash. For the phenol couplings, we discovered that the hydration state of the catalyst had a great influence on reactivity. For example, an inactive catalyst was produced when the complex was placed under high vacuum. We attributed this reduced reactivity to formation of a less potent, oxo-bridged species. Fortunately, using $VO(OEt)_3$ as previously described for asymmetric

[22] (a) Chu, C.-Y.; Hwang, D.-R.; Wang, S.-K.; Uang, B.-J. Chiral Oxovanadium Complex Catalyzed Enantioselective Oxidative Coupling of 2-Naphthols. *Chem. Commun.* **2001**, *0* (11), 980–981. (b) Hon, S.-W.; Li, C.-H.; Kuo, J.-H.; Barhate, N. B.; Liu, Y.-H.; Wang, Y.; Chen, C.-T. Catalytic Asymmetric Coupling of 2-Naphthols by Chiral Tridentate Oxovanadium(IV) Complexes. *Org. Lett.* **2001**, *3*, 869–872. (c) Luo, Z.; Liu, Q.; Gong, L.; Cui, X.; Mi, A.; Jiang, Y. The Rational Design of Novel Chiral Oxovanadium(IV) Complexes for Highly Enantioselective Oxidative Coupling of 2-Naphthols. *Chem. Commun.* **2002**, *0* (8), 914–915. (d) Somei, H.; Asano, Y.; Yoshida, T.; Takizawa, S.; Yamataka, H.; Sasai, H. Dual Activation in a Homolytic Coupling Reaction Promoted by an Enantioselective Dinuclear Vanadium(IV) Catalyst. *Tetrahedron Lett.* **2004**, *45*, 1841–1844. (e) Takizawa, S.; Katayama, T.; Kameyama, C.; Onitsuka, K.; Suzuki, T.; Yanagida, T.; Kawai, T.; Sasai, H. Chiral Dinuclear Vanadium(V) Catalysts for Oxidative Coupling of 2-Naphthols. *Chem. Commun.* **2008**, *0* (15), 1810–1812. (f) Takizawa, S.; Katayama, T.; Sasai, H. Dinuclear Chiral Vanadium Catalysts for Oxidative Coupling of 2-Naphtholsvia a Dual Activation Mechanism. *Chem. Commun.* **2008**, *0* (35), 4113–4122. (g) Takizawa, S.; Kodera, J.; Yoshida, Y.; Sako, M.; Breukers, S.; Enders, D.; Sasai, H. Enantioselective Oxidative-Coupling of Polycyclic Phenols. *Tetrahedron* **2014**, *70*, 1786–1793. (h) Sako, M.; Takeuchi, Y.; Tsujihara, T.; Kodera, J.; Kawano, T.; Takizawa, S.; Sasai, H. Efficient Enantioselective Synthesis of Oxahelicenes Using Redox/Acid Cooperative Catalysts. *J. Am. Chem. Soc.* **2016**, *138*, 11481–11484.

homoallylic oxidation,[23] some catalysts provided reproducible results. The dimeric **V1** catalyst afforded a 37% *ee* for **1.2a**, although low conversion (49%) and the mixture of products were observed (28:21 **1.2a:1.3a**, **Figure 1.2**).

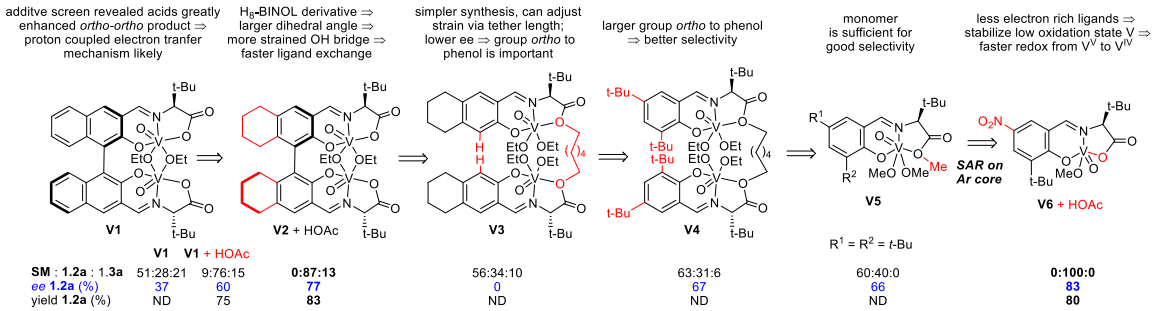

Figure 1.2. Catalyst Evolution in the Asymmetric Phenol Coupling[1,24]

To improve conversion and regioselectivity, it was necessary to modify the reaction conditions. We speculated that the phenoxide substrate accelerates the reaction rate. Using Et_3N as an additive, however, led to no product formation. Conversely, a protic acid additive, which was capable of catalyst activation by means of protonation, afforded both enhanced reactivity (91% conv, 75% isolated yield) and selectivity (60% *ee*) to produce *ortho-ortho* (**1.2a**) product (**Figure 1.2**).

Additional improvement was achieved by manipulating the catalyst backbone. The use of a scaffold with a greater dihedral angle between the upper and lower portions (**V2**, **Figure 1.2**) improved yields to 83% and enantioselectivity to 77%. No further readily optimized parameters were available within this scaffold, so an alternate linker was explored. The free acid positions were not found to be crucial since similar results were obtained with the methyl ester derived ligands. However, linking via the carboxylic acids

[23] Hartung, J.; Drees, S.; Greb, M.; Schmidt, P.; Svoboda, I.; Fuess, H.; Murso, A.; Stalke, D. (Schiff-Base)Vanadium(V) Complex-Catalyzed Oxidations of Substituted Bis(Homoallylic) Alcohols − Stereoselective Synthesis of Functionalized Tetrahydrofurans. *Eur. J. Org. Chem.* **2003**, *2003* (13), 2388–2408.

[24] These catalysts engineering work had done by Dr. Scott E. Allen, Dr. Young Eun Lee and Gina Kim.

was not effective with the original tetrahydronaphthol backbone using a variety of tether lengths (**V3**, 34% **1.2a**, 0% *ee*). We hypothesized that a large group is needed where the chiral axis had seen to offer selective coupling. Thus, a *tert*-butyl–substituted phenol was employed. With a linker length of six carbons being optimal (**V4**), a larger improvement in selectivity was seen (67% *ee*). To interrogate whether a dimeric catalyst was really necessary, a trial with monomer **V5** was undertaken, which revealed results similar to those of the dimer.

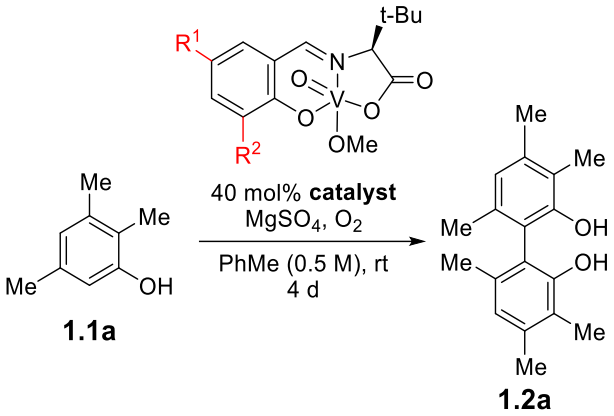

1.1a **1.2a**

Entry	R^1	R^2	Conversion (%)[a]	*ee* (%)[b]
1	*t*-Bu	*t*-Bu	40	66
2	*t*-Bu	2-tolyl	78	49
3	*t*-Bu	2,6-xylyl	92	50
4	*t*-Bu	1-naphthyl	85	38
5	*t*-Bu	2-methoxy-1-naphthyl	81	57
6	*t*-Bu	$SiMe_3$	70	73
7	*t*-Bu	$SiEt_3$	58	75
8	*t*-Bu	Si^iPr_3	35	76
9	*t*-Bu	$SiPh_2{}^tBu$	13	60
10	*t*-Bu	adamantyl	24	66
11	*t*-Bu	CPh_3	15	56
12	*t*-Bu	CMe_2Ph	37	76
13	OMe	*t*-Bu	47	65
14	OAc	*t*-Bu	43	62
15	NO_2	*t*-Bu	86	75

16	NO_2	$SiEt_3$	100	75

[a]Determined from 1H NMR; isolated yield in parentheses. [b]Determined using CSP HPLC.

Table 1.1. SAR of Monomeric Vanadium Catalyst[31]

In line with the previous results, bulky groups, such as *tert*-butyl (**Table 1.1**, entry 1), SiR_3 (entry 6–8), or adamantyl (entry 10), at the R^2 position tend to provide better selectivity. A sterically more congested substituent, 1,1-dimethylbenzyl, gave higher selectivity (entry 12, 76% *ee*). However, the reactivity declined as R^2 became larger than TMS (entry 6–8). To tackle the low conversion issue, we modulated the electronics by substituting at R^1. Our objective was to achieve a more powerful oxidizing catalyst by destabilizing the higher oxidation state of the vanadium catalyst. An electron-withdrawing substituent ($R^1 = NO_2$, entry 15) facilitated the reaction in accordance with our hypothesis (entry 13 vs 15). With the modified monomeric catalyst (**V6**), in the presence of HOAc, the *ortho-ortho* coupled product (**1.2a**) was obtained in 80% isolated yield as the only product with 83% *ee*.

1.3. Phenol Scope

A variety of phenols were examined with the optimized conditions (**Table 1.4**). The substituent *ortho* to the phenol possessed an important role in obtaining enantioselectivity, with methyl being optimal. Smaller groups, such as a hydrogen, showed drastically decreased selectivity (entries 2, 5). The larger *tert*-butyl group gave no selectivity (entry 3). 2,3,5-Trisubstituted phenols generally provided better results.

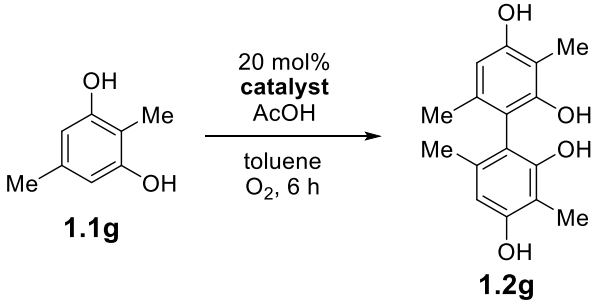

Entry	Temperature (°C)	Conversion (%)[a]	*ee* (%)
1	23	72	50
2	0	53	63
3	–20	30	75
4	–40	15	85

Table 1.2. Oxdative Coupling of Dihydroxyarene **1.1g** at Various Temperatures

Dioxygenated substrates such as **1.1g** were examined next, with the expectation that the more electron-rich systems would undergo oxidative coupling more readily. In line with this hypothesis, reaction of **1.1g** occurred quickly at room temperature (**Table 1.2**, entry 1), and the selectivity could be increased by lowering the temperature (entries 2-4). However, below 0 °C reaction rates were compromised.

As a result, additional additive screening was undertaken with this class of substrates (**Table 1.3**). Most additives resulted in lesser reactivity although cationic lithium species resulted in significantly higher reactivity (entries 10, 12, 17). LiCl (entry 5) afforded the highest enantioselectivity (entry 5, 85% *ee*), which did not appear to devolve solely from the chloride (c.f., entries 6-8). Using the LiCl additive with substrate **1.1f** gave a similar boost in selectivity (**Table 1.4**, entry 6, 82% *ee*). Unfortunately, LiCl did not provide equal levels of improvement for all of these substrates.

Entry	Additives	Conversion (%)[b]	*ee* (%)
1	-	70	52
2	$Sn(OTf)_2$	33	43
3	$Sc(OTf)_3$	43	67
4	$Yb(OTf)_3$	48	69
5	LiCl	46	**85**
6	NaCl	52	47
7	KCl	59	45
8	$MgCl_2$	28	78
9	LiF	46	46
10	LiBr	**100**	63
11	LiI	12	57
12	$LiClO_4$	**94**	73

13	LiOAc	43	18
14	Li_2CO_3	53	27
15	4Å MS	-	68
16	$MgSO_4$	50	70
17	LiCl + 12-crown-4	**100**	60

[a]Reaction conditions: 20 mol % **V6**, 40 mol % additive, $PhCH_3$, O_2, 0 °C, 6 h. [b]Conversion was determined by ^1H NMR.

Table 1.3. Additive Screening with Dihydroxyarene **1.1g**[31]

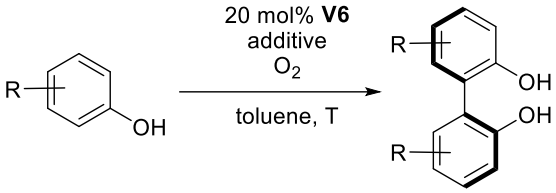

1.1 **1.2**

Entry	Substrate	Additive[b]	Temp	Yield (%)[c]	ee (%)[d]
1	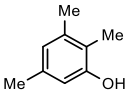 **1.1a**	HOAc	rt	89(72)[e]	85(95)[e]
2	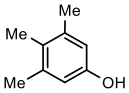 **1.1b**	HOAc	rt	100[f]	10
3	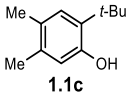 **1.1c**	HOAc	rt	100[f]	0
4	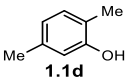 **1.1d**	HOAc	rt	ND	60
5	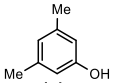 **1.1e**	HOAc	rt	38[f]	38
6	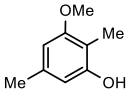 **1.1f**	HOAc	rt	100[f]	50
		LiCl	0 °C	80(76)[e]	82(95)[e]
7	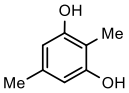 **1.1g**	HOAc	rt	89	63
		LiCl	0 °C	81	86
8	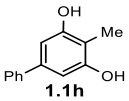 **1.1h**	HOAc	0 °C	65	50

Entry	Substrate	Additive[b]	Temp	Yield (%)[c]	ee (%)[d]
9	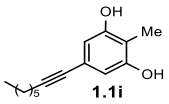 **1.1i**	LiCl	0 °C	66	89
10	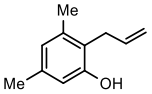 **1.1j**	HOAc	rt	56(99)[g]	77
11	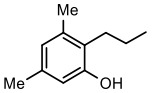 **1.1k**	HOAc	rt	80(98)[g]	72
12	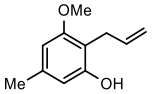 **1.1l**	HOAc	rt	44[f]	34
13	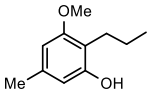 **1.1m**	HOAc	rt	100[f]	10
14	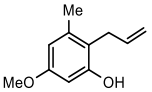 **1.1n**	HOAc	0 °C	78	40
15	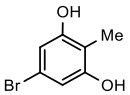 **1.1o**	HOAc	rt	24[f]	20
16	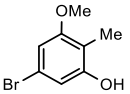 **1.1p**	HOAc	rt	12[f]	47

[a]Reaction conditions: 20 mol% catalyst, x equiv additives, O_2, 0.5 M $PhCH_3$. [b]6.25 equiv HOAc, 0.4 equiv LiCl. [c]Isolated yield. [d] ee determined by chiral HPLC. [e]After trituration in parentheses. [f]Conversion. [g]Isolated yield based on recovered substrate

Table 1.4. Scope of Phenol Coupling[a,1]

Other substituents, such as allyl or propyl, *ortho* to the phenol, resulted in

comparable selectivity (**Table 1.4**, entry 10, 11). However, the allyl or propyl groups were no longer tolerated with either 3-methoxy or 5-methoxy substrates (entry 12–14) in contrast to 3-methoxy with 2-methyl substituent (entry 6). To examine the effects of substituents at the 5-position, experiments were conducted with a phenyl (entry 8), alkynyl chain (entry 9), and electron-withdrawing groups (entries 15, 16). Notably, oxidative coupling of the phenol bearing an alkynyl chain afforded good selectivity (entry 9, 89% *ee*) in the presence of LiCl. As we expected, 5-bromo analogs caused slower oxidation with only 24% (**1.1o**) and 12% (**1.1p**) conversion after 48 h. Racemic biaryl products have much poorer solubility than enantiopure biaryls in hexane. Exploiting this difference, one trituration was found to increase the enantiomeric excess of the filtrate. For example, substrates **1.1a** and **1.1f** were enhanced to 95% *ee* following trituration.

1.4. Hydroxycarbazole Scope

The electron rich nature of hydroxycarbazoles allows access to dimeric compounds via oxidative coupling (**Scheme 1.5**). Accordingly, hydroxycarbazole **1.4** was examined in our asymmetric oxidative coupling.[20] Our previous report demonstrated that the *N*-protecing group was essential for selective oxidation *ortho* to the hydroxyl group by excluding reaction with the amine.[21]

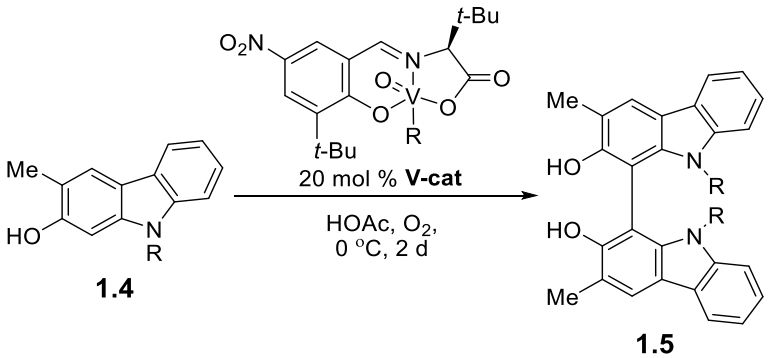

1.4 **1.5**

Entry	R	Catalyst	Solvent	Yield (%)	*ee* (%)
1	Bn (**1.4b**)	**V6** (R = OMe)	PhMe	78	70

2	Bn (**1.4b**)	**V7** (R = F)	PhMe	40	70
3	Bn (**1.4b**)	**V8** (R = O*i*-Pr)	PhMe	71	78
4	Bn (**1.4b**)	**V9** (R = O*t*-Bu)	PhMe	44	74
5	Bn (**1.4b**)	**V8** (R = O*i*-Pr)	PhCl	91	87
6	Me (**1.4c**)	**V8** (R = O*i*-Pr)	PhCl	82	71
7	allyl (**1.4d**)	**V8** (R = O*i*-Pr)	PhCl	71	76
8	*i*-Pr (**1.4e**)	**V8** (R = O*i*-Pr)	PhCl	58	42
9	2,4,6-Me_3Bn (**1.4f**)	**V8** (R = O*i*-Pr)	PhCl	27	37

[a]Reaction Conditions: 20 mol% catalyst, 6.5 equiv AcOH, O_2, 0.5 M solvent, 0 °C, 48 h.

Table 1.5. Oxidative Coupling of 2-Hydroxycarbazole Optimization[31]

With the nitrogen position protected with a benzyl substituent, promising levels of selectivity (70% *ee*) were observed (**Table 1.5**, entry 1). Examining related vanadium catalysts **V7** (R = F, entry 2) and **V8** (R = O*i*-Pr, entry 3) revealed that a larger ligand on the vanadium center gave rise to higher selectivity (78% *ee*). However, even larger substituents on vanadium (R = O*t*-Bu, entry 4) did not afford further improvement. Finally, optimization of solvent (CH_2Cl_2, DCE, $CHCl_3$, toluene, dichlorobenzene) revealed that chlorobenzene (entry 5) provided the best result (91% yield, 87% *ee*). With the optimal catalyst (**V8**), examination of the nitrogen substituent showed that either smaller (Me, entry 6, 71% *ee*) or larger groups (*i*-Pr; 2,4,6-trimethylbenzyl, entries 8-9) were detrimental. Moderate–sized groups such as allyl (entry 7, 76% *ee*) and benzyl (entry 5, 87% *ee*) were superior.

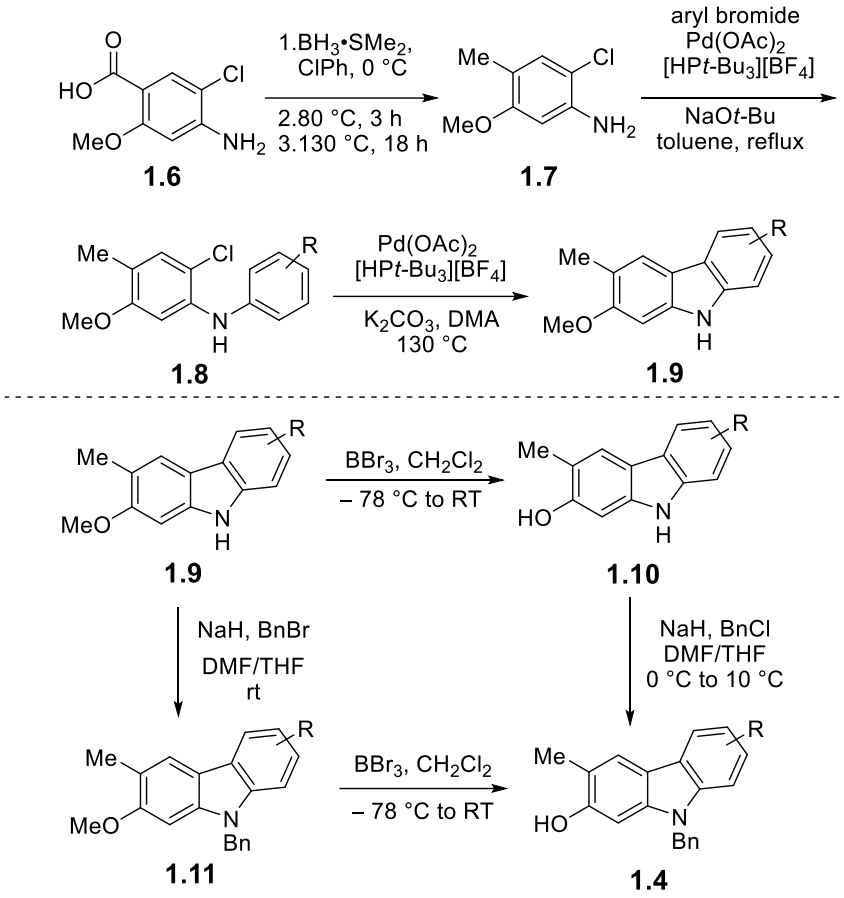

Scheme 1.7. 2-Hydroxy-3-methylcarbazole Analog Synthesis[1]

Various 2-hydroxycarbazole analog syntheses are outlined in **Scheme 1.7–10**. Most of the substituted carbazoles were prepared from commercially available aniline **1.6** (**Scheme 1.7**). Carboxylic acid was reduced to methyl with BH_3•SMe_2, followed by a Buchwald–Hartwig amination using a wide range of aryl bromides, which allowed access to a variety of substituted precursors (**1.7**).[25] Cyclization was achieved in the presence of $Pd(OAc)_2$ and monodentate trialkyl phosphine ligand to generate carbazole **1.9**.[25] To obtain nitrogen protected hydroxycarbazoles, BBr_3 demethylation,[21] followed by selective

[25] Bedford, R. B.; Betham, M. N-H Carbazole Synthesis from 2-Chloroanilines via Consecutive Amination and C−H Activation. *J. Org. Chem.* **2006**, *71*, 9403–9410.

benzylation afforded 2-hydroxy-3-methylcarbazoles (**1.4**) or vice versa.[26]

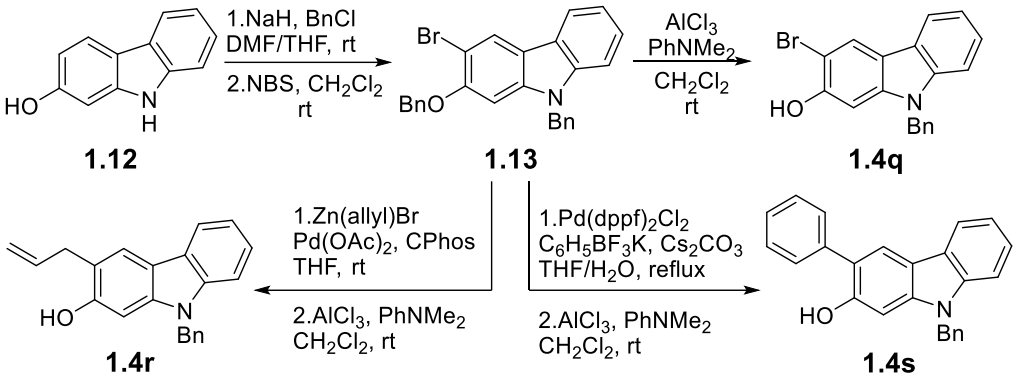

Scheme 1.8. 3-Substituted-2-hydroxycarbazole Syntheses[1]

Substrates that contained a different moiety *ortho* to the phenol were prepared form the commercially available hydroxycarbazole **1.12** by Kyle Niederer, 3rd year graduate student in our laboratory (**Scheme 1.8**). A one-pot benzylation of the oxygen and nitrogen was followed by a bromination, using NBS, to obtain **1.13**. Suzuki and Negishi[27] couplings, respectively, introduced a phenyl and allyl group to the C-3 position. Thereafter, deprotection of the phenol was achieved in the presence of $AlCl_3$ to afford **1.4q**, **1.4r**, and **1.4s**.[28]

[26] Albanese, D.; Landini, D.; Penso, M.; Spanò, G.; Trebicka, A. Chemoselective *N*-Alkylation of 2-Hydroxycarbazole as a Model for the Synthesis of N-Substituted Pyrrole Derivatives Containing Acidic Functions. *Tetrahedron* **1995**, *51*, 5681–5688.
[27] Duggan, K. A. Preparation of biphenyl propanamide compounds for the treatment of hypertension and/or fibrosis. *PCT Int. Appl.* WO 2015039172 A1, Mar. 26, 2015.
[28] Akiyama, T.; Hirofuji, H.; Ozaki, S. $AlCl_3$-*N,N*-Dimethylaniline: A New Benzyl and Allyl Ether Cleavage Reagent. *Tetrahedron Lett.* **1991**, *32*, 1321–1324.

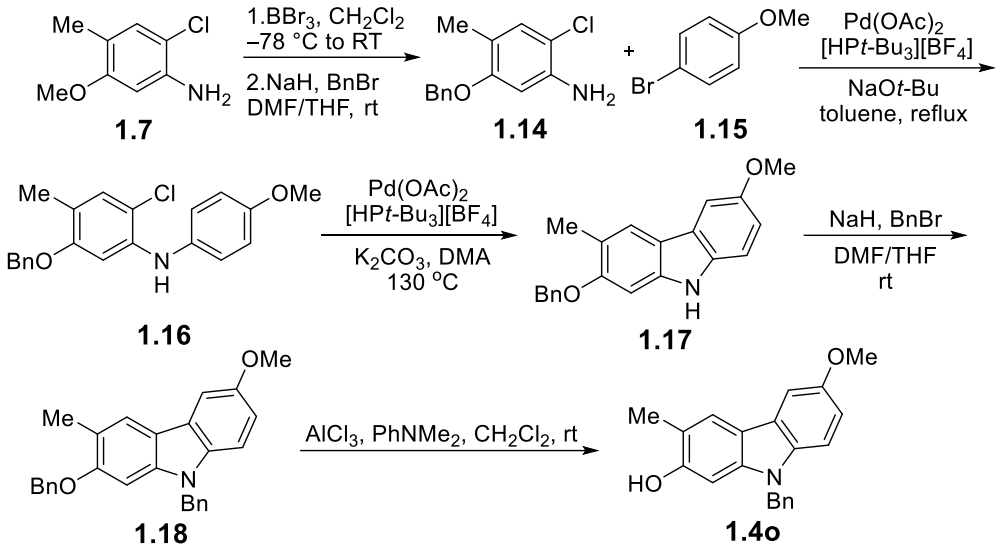

Scheme 1.9. 6-Methoxy-2-hydroxycarbazole (**1.4o**) Synthesis[1]

To investigate how introducing an electron donating group to the carbazole affected enantioselectivity, a substrate with a methoxy group at the C-6 position was also synthesized by Kyle Niederer (**Scheme 1.9**). For substrates containing two methoxy substituents, selective deprotection of the oxygen at the C-2 position proved untenable. To synthesize the desired substrate, the carboxylic acid **1.6** was reduced to methyl with borane to provide **1.7**. A demethylation with BBr_3 was followed by a selective benzylation of the phenol to yield the aniline **1.14**. Thereafter, a Buchwald Hartwig amination with aryl bromide **1.15** was followed by cyclization in the presence of $Pd(OAc)_2$ and a monodentate trialkyl phosphine ligand to generate carbazole **1.17**. Finally, N-benzylation followed by selective O-debenzylation with $AlCl_3$ afforded **1.4o**.

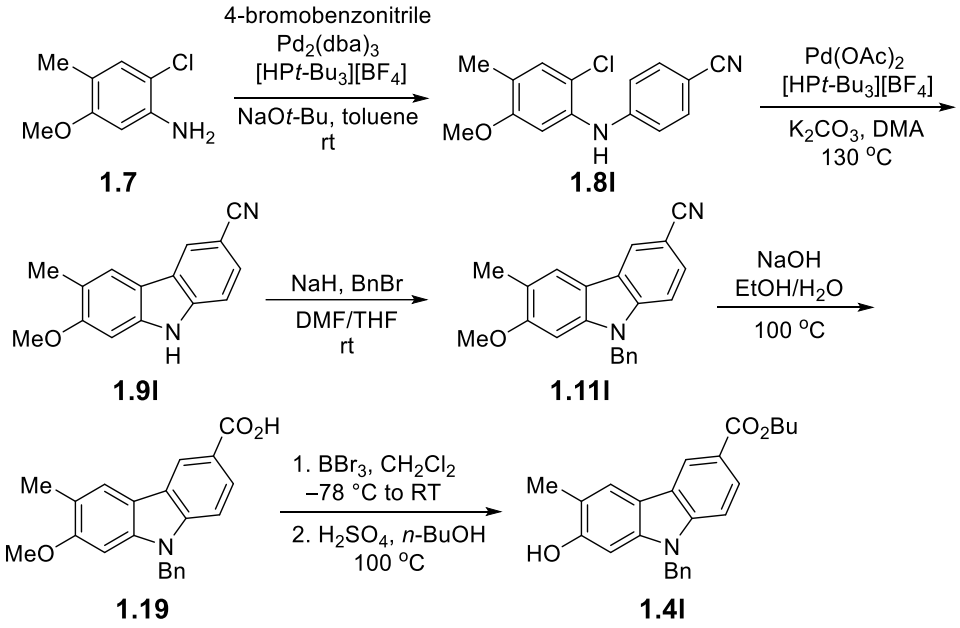

Scheme 1.10. Synthesis of 6-Carboalkoxy-2-hydroxycarbazole **1.4l**[1]

To prepare the ester-functionalized hydroxycarbazole, we conducted the C-N coupling with 4-bromobenzonitrile, followed by intramolecular cyclization reaction to obtain carbazole **1.9l** (**Scheme 1.10**). After benzyl protection, the nitrile was converted to the benzoic acid (**1.19**) by treatment with sodium hydroxide in EtOH and water.[29] Subsequent demethylation with boron tribromide followed by esterification afforded **1.4l**.

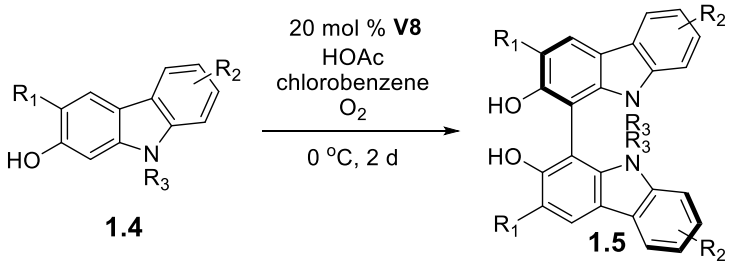

Entry	Substrate	Yield (%)[b]	*ee* (%)[c]	Entry	Substrate	Yield (%)[b]	*ee* (%)[c]
1	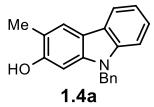 **1.4a**	91	87	9	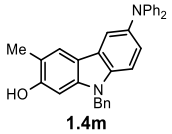 **1.4m**	62	37

[29] Baba, K.; Tobisu, M.; Chatani, N. Palladium-Catalyzed Synthesis of Six-Membered Benzofuzed Phosphacycles via Carbon–Phosphorus Bond Cleavage. *Org. Lett.* **2015**, *17*, 70–73.

2	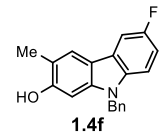 **1.4f**	87	92	10	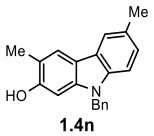 **1.4n**	90(45)[f]	60(76)[f]
3	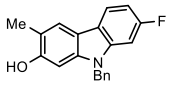 **1.4g**	73	92	11[g]	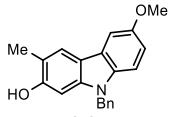 **1.4o**	82	74
4	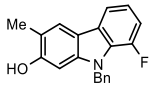 **1.4h**	80	91	12	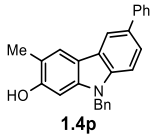 **1.4p**	70	82
5	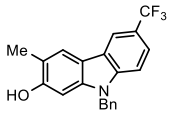 **1.4i**	70	93	13	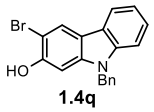 **1.4q**	17(30)[e]	72
6	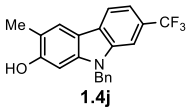 **1.4j**	60	94	14	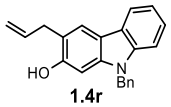 **1.4r**	75	83
7[d]	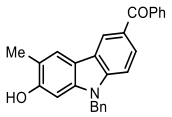 **1.4k**	53(76)[e]	85	15	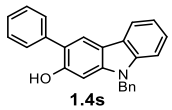 **1.4s**	26(43)[e]	60
8	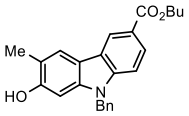 **1.4l**	46(67)[e]	96				

[a]Reaction Conditions: 20 mol% **V8** catalyst, 6.5 equiv HOAc, O_2, 0.5 M chlorobenzene, 48 h. [b]Isolated yield. [c]ee determined by chiral HPLC. [d]HFIP/PhCl as a solvent. [e]Isolatted yield based on recovered substrate. [f]Reaction was conducted at −15 °C. [g]Reaction time was 26 h.

Table 1.6. Scope of 2-Hydroxycarbazole Coupling[a,1]

Thereafter, we investigated the scope of a variety of 2-hydroxycarbazoles (Table 6). Electron-withdrawing substituents gave good to excellent selectivity (85–96% *ee*) along with moderate to good conversions (46–87% yield). Highly enantioenriched bishydroxycarbazoles were obtained with the fluoride substituent regardless of their position (entries 2–4, 91–92% *ee*). More electron-deficient hydroxycarbazoles, 6-CF_3 (entry 5) and 7-CF_3 (entry 6), offered excellent selectivities (93% and 94% *ee*) with good

yields. Incorporating another electron–withdrawing substituent, a carbonyl group (entry 7), gave rise to solubility issues. A mixed solvent system, which included hexafluoroisopropanol as a co-solvent, was needed. Accordingly, compromised conversion was observed along with slightly lower selectivity (85% *ee*). The ester–substituted compound provided the most selective coupling result (entry 8, 96% *ee*). The diphenylamino group was an outlier, with drastically lower selectivity (entry 9, 37% *ee*). Faster oxidative coupling reactions were observed with electron-donating substituents. For example, the 6-methoxyhydroxycarbazole coupling reaction was completed in 26 hours with moderate selectivity (entry 11, 74% *ee*). With a methyl or allyl group adjacent to the phenol, good enantioselectivites were observed (entry 1, 13). On the other hand, an electron-withdrawing bromide (entry 14) or an aryl group (entry 15) at this site compromised reactivity while retaining moderate levels of selectivity.

1.5. Mechanistic Study

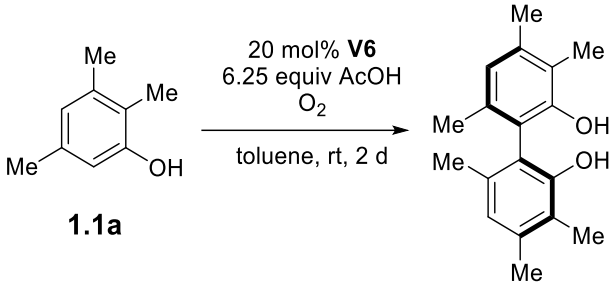

1.1a **1.2a**

entry	catalyst	condition[a]	conversion
1	20 mol% **V6**	control	100%
2	20 mol% **V6**	0.2 equiv TEMPO	35%
3	20 mol% **V6**	N_2 atmosphere	9% (3 days)
4	50 mol% **V6**	N_2 atmosphere	26% (3 days)

[a]Reaction Conditions: 6.25 equiv HOAc, toluene, O_2, rt, 2 d.

Table 1.7. Control Experiments[1]

With 20 mol% of **V6**, the oxidative coupling of 2,3,5-trimethylphenol was completed within 2 days at ambient temperature under oxygen (**Table 1.7**, entry 1). However, the

addition of an equimolar amount of the radical inhibitor TEMPO relative to catalyst led to low conversion (35%, entry 2), which suggested a radical process. Under an inert atmosphere, 9% and 26% conversions were detected in the presence of 20 and 50 mol% of **V6** catalyst (entry 3–4). Accordingly, vanadium(V) species were implicated as the active oxidants. Further, the stoichiometry is consistent with each vanadium(V) abstracting one electron.

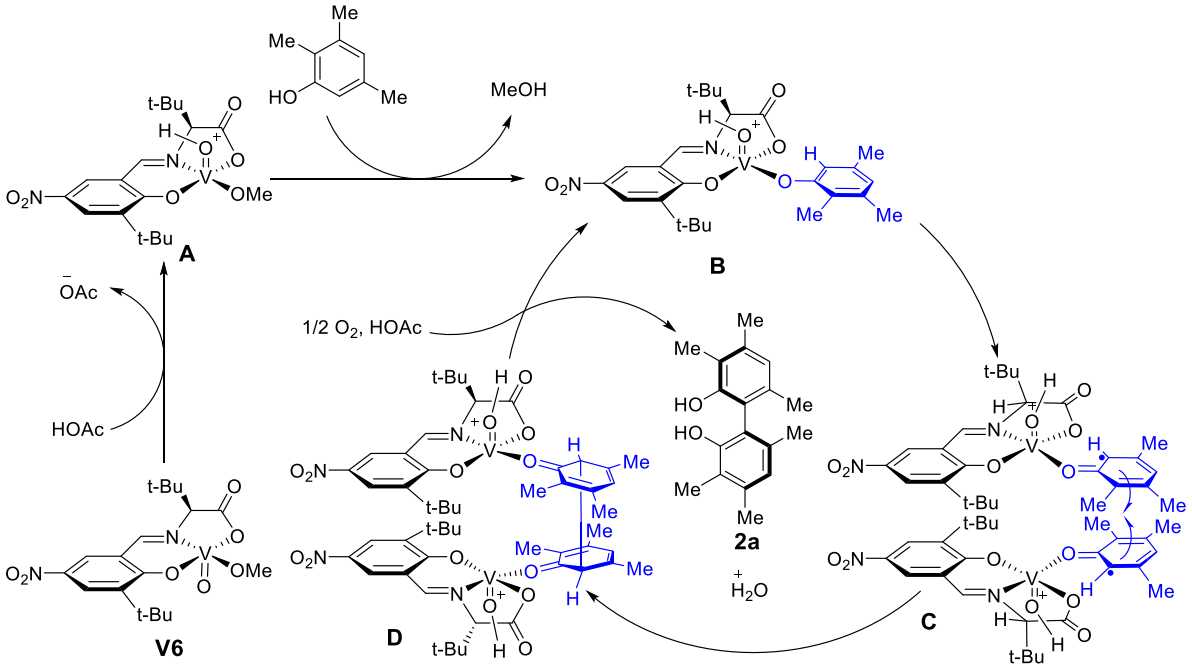

Figure 1.3. Proposed Mechanism[1]

Based on the control experiments, our proposed mechanism is described in **Figure 1.3**. Initially, we speculated that catalyst activation would be achieved through protonation by excess acetic acid to produce **A**. We excluded the possibility of H• abstraction due to the absence of an isotope effect between HOAc and acetic acid-D_4 (**Figure 1.4.b**).[30] Ligand exchange with phenol **1.1a** would generate intermediate **B**, which was observed by LCMS analysis. Subsequent single electron transfer to oxidize the phenol, would be

[30] Wiberg, K. B. The Deuterium Isotope Effect. *Chem. Rev.* **1955**, *55*, 713–743.

followed by coupling (**C**). The control experiment in **Table 1.7** (entry 2) supports such a radical coupling. To test this theory further, we performed the cross-coupling experiment with **1.1a** and **1.1g** (Scheme 1.11). The major product was **1.2g**, which is derived from more readily oxidizable phenol **1.1g**. The overall product distribution is consistent with a radical-radical mechanism where oxidizability dictates the rate of radical formation and a statistical distribution is observed.[9] Bond formation via dimeric cluster **D** was supported by positive non-linear effect (**Figure 1.4.a**), which was determined by Kirsten Hewitt. Oxygen as the terminal oxidant enabled regeneration of vanadium (V) and product **1.2a** was produced after tautomerization.

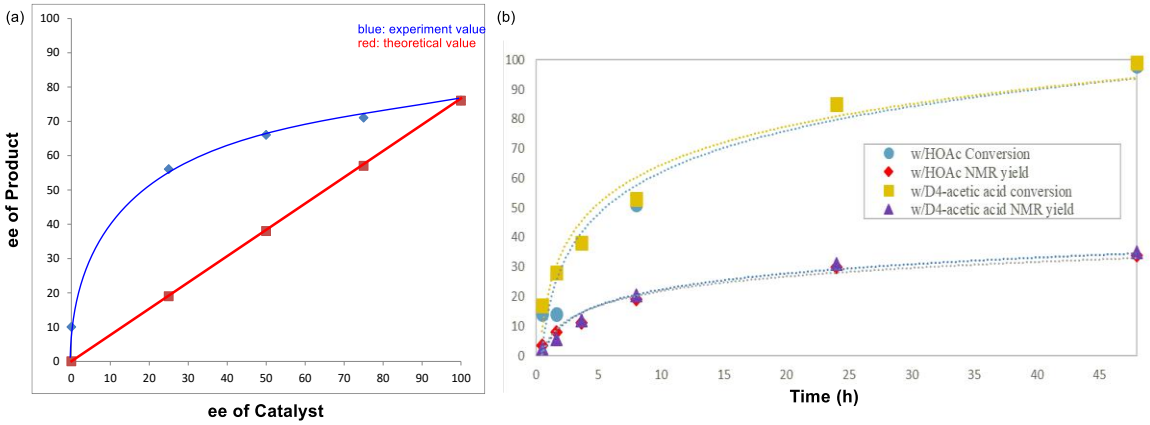

Figure 1.4. (a) Theoretical vs Measured Nonlinear Effect (b) CH_3COOH vs CD_3COOD[1]

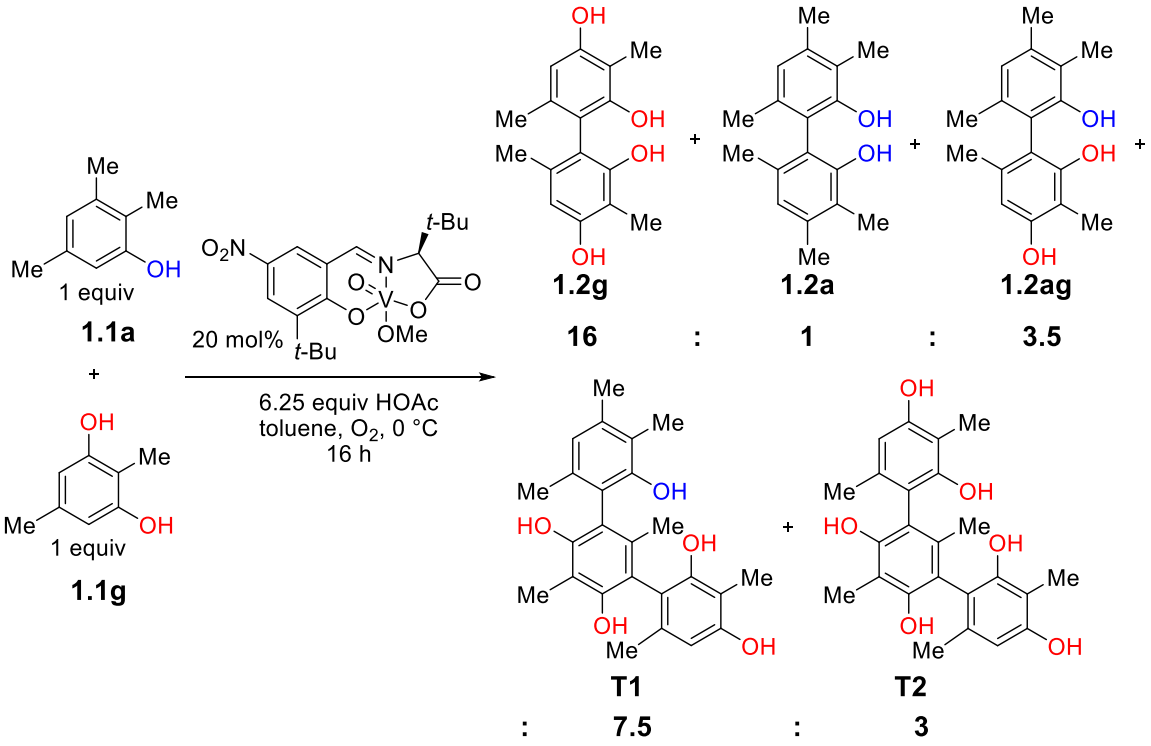

Scheme 1.11. Cross-coupling Experiment with **1.1a** and **1.1g**

1.6. DFT Calculations

To understand the origin of regio- and enantioselectivity further, we initiated a DFT study of the catalytic cycle using a simplified catalyst structure. Calculations by Madison Herling, a 2nd year graduate student, suggest a stepwise radical coupling (**Figure 1.5**). Formation of the acetate-bridged aggregate ***Int B1*** was predicted to be exergonic by 7.5 kcal/mol. Singlet-triplet transition of the aggregate was speculated to lead to stable diradical intermediate ***Int B2***. Coupling was shown to be rate-limiting with $\Delta G^{\ddagger}$ of 16.6 kcal/mol and proceed through transition state ***TS A*** to form intermediate ***Int C***. Additional calculations demonstrated both that the μ^2-acetate bridge was essential for a reasonable activation energy and that the singlet-triplet transition was not rate-determining. Finally, our computations suggest that dissociation of product **1.2a** from the aggregate and oxidation to regenerate the catalyst may occur sequentially rather than in tandem. The

transition state leading to *ortho–para* coupled product was predicted to be disfavored by 5.5 kcal/mol, which explains why the *ortho–para* product is not observed and suggests that the coupling step is regiodetermining. To model the enantioselectivity, we computed two diastereomeric transition structures incorporating the complete Schiff base ligand, which lead to formation of the *S* and *R* product enantiomers, respectively. Our model predicts an enantiomeric excess of 84% in favor of the *S*-enantiomer, which agrees with the experimentally obtained value of 86% ee and supports the notion that the coupling step is enantiodetermining.

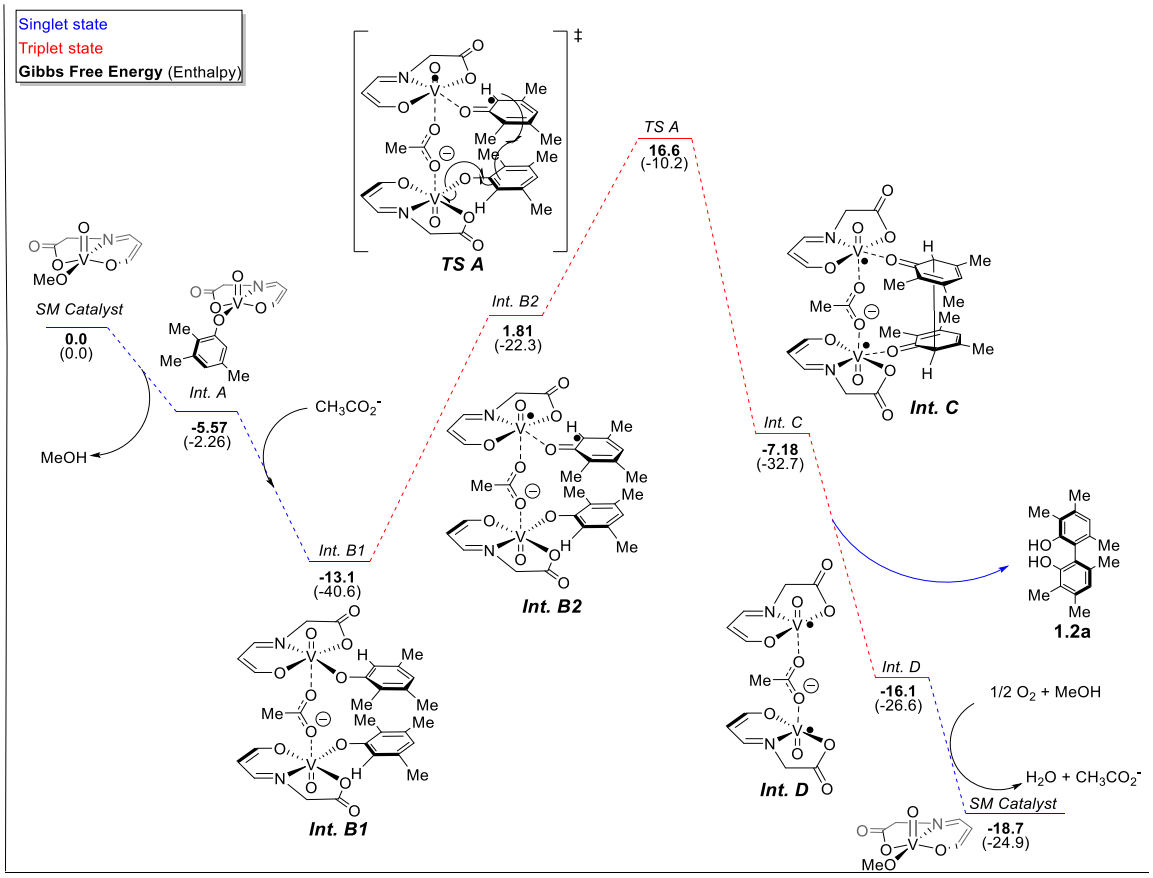

Figure 1.5. Reaction Energy Diagram Representing Alternative Calculated Pathway

1.7. Absolute Stereochemistry Determination

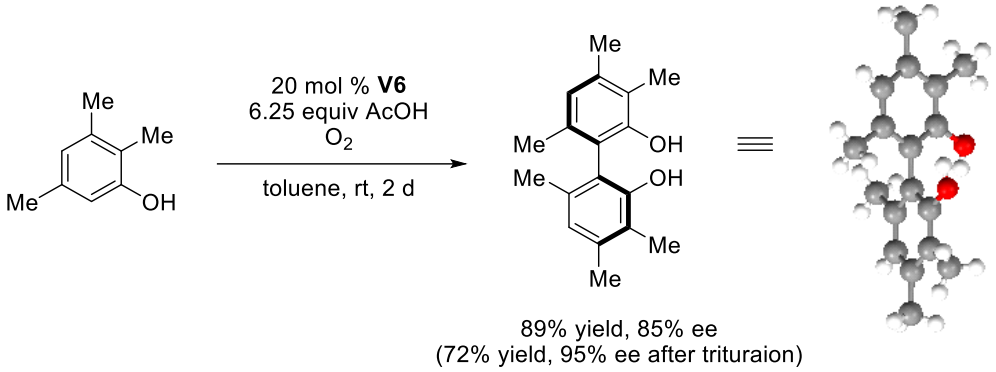

Figure 1.6. X-ray Crystallographic Analysis of **1.2a**[31]

X-Ray crystallographic analysis of **1.2a** indicated the (*S*) absolute axial configuration was present (**Figure 1.6**). On this basis, a preliminary stereochemical model can be proposed as illustrated in intermediate **C** of **Figure 1.6**. The phenol coordinates to minimize steric interactions; namely, the less hindered lone pair of the phenol coordinates to the vanadium and the less substituted *ortho*-position orients closest to the catalyst, placing the larger *ortho*-substituent into unoccupied space. Approach of the second phenol from the face opposite the *tert*-butyl group then gives rise to the observed stereochemistry.

1.8. Conclusions

In summary, the first enantioselective oxidative coupling of phenols and 2-hydroxycarbazoles has been accomplished and gives rise to adducts not available with alternate approaches. A much more active vanadium oxidative catalyst was developed capable of acting on these less reactive substrates to form the axial chiral dimers efficiently. Less electron-rich ligands were employed, which stabilize the low valent vanadium(IV) and destabilize the high valent vanadium(V), giving rise to a more potent

[31] Reprinted with permission from Kang, H.; Lee, Y. E.; Reddy, P. V. G.; Dey, S.; Allen, S. E.; Niederer, K. A.; Sung, P.; Hewitt, K.; Torruellas, C.; Herling, M. R.; Kozlowski, M. C. Asymmetric Oxidative Coupling of Phenols and Hydroxycarbazoles. *Org. Lett.* **2017**, *19*, 5505–5508. Copyright 2017 American Chemical Society.

oxidizing species. Counterintuitively, the addition of a Brønsted or Lewis acid was found to accelerate the process, indicating that ligand exchange of the substrate is not driven by deprotonation of the phenol. Rather, the Brønsted acid likely activates the vanadium catalyst, enhancing both its oxidizing properties and its ability to coordinate a neutral phenol. Together, these features should prove useful in the design of other asymmetric oxidants.

1.9. Experimental Section

General Considerations

Unless otherwise noted, all non-aqueous reactions were carried out under an atmosphere of dry N_2 in dried glassware. When necessary, solvents and reagents were dried prior to use. THF was distilled from sodium benzophenone ketyl. CH_2Cl_2, $ClCH_2CH_2Cl$, and toluene were distilled from CaH_2. High throughput experiments were performed at the Penn/Merck High Throughput Experimentation Laboratory at the University of Pennsylvania. The screens were analyzed by HPLC by addition of an internal standard.

Analytical thin layer chromatography (TLC) was performed on EM Reagents 0.25 mm silica-gel 254-F plates. Visualization was accomplished with UV light. Chromatography was performed using a forced flow of the indicated solvent system on EM Reagents Silica Gel 60 (230-400 mesh). When necessary, the column was pre-washed with 1% Et_3N in the eluent system. ^1H NMR spectra were recorded on a 500 MHz spectrometer. Chemical shifts are reported in ppm from tetramethylsilane (0 ppm) or from the solvent resonance ($CDCl_3$ 7.26 ppm, DMSO-d_6 3.58 ppm, acetone-d_6 2.05 ppm, DMF-d_7 2.50 ppm, CD_3CN 1.94 ppm, CD_2Cl_2 5.32 ppm). Data are reported as follows: chemical shift, multiplicity (s = singlet, d = doublet, t = triplet, q = quartet, br = broad, m = multiplet), coupling constants, and number of protons. Decoupled ^{13}C NMR spectra were recorded at 125 MHz. IR

spectra were taken on an FT-IR spectrometer using a thin film on NaCl plate. Accurate mass measurement analyses were conducted via time-of-flight mass analyzer GCMS with electron ionization (EI) or via time-of-flight mass analyzer LCMS with electrospray ionization (ESI). The signals were measured against an internal reference of perfluorotributylamine for EI-GCMS and leucine enkephalin for ESI-LCMS. The instrument was calibrated and measurements were made using neutral atomic masses; the mass of the electron removed or added to create the charged species is not taken into account. Low resolution LCMS data were obtained by use of a UPLC system with a SQD mass analyzer equipped with electrospray ionization. Circular dichroism and UV-vis spectroscopy measurements carried out at ambient temperature (23 C). Solution spectra in methanol recorded in 10-mm quartz cuvettes and corrected by subtracting the spectrum of the pure solvent at the same temperature. A scan rate of 100 nm/min with a response time of 1 s and a bandwidth of 1 nm was used to measure the CD spectra, which were recorded in low sensitivity mode with 4 accumulations. Melting points are corrected. Enantiomeric excesses were determined using analytical HPLC with UV detection at 254 nm. Analytical Chiralpak columns (4.6 mm x 250 mm, 5 µm) from Daicel were used. Optical rotations were measured on a polarimeter with a sodium lamp.

Table 1.S1. CD Spectrum of Compound 1.2a in MeOH

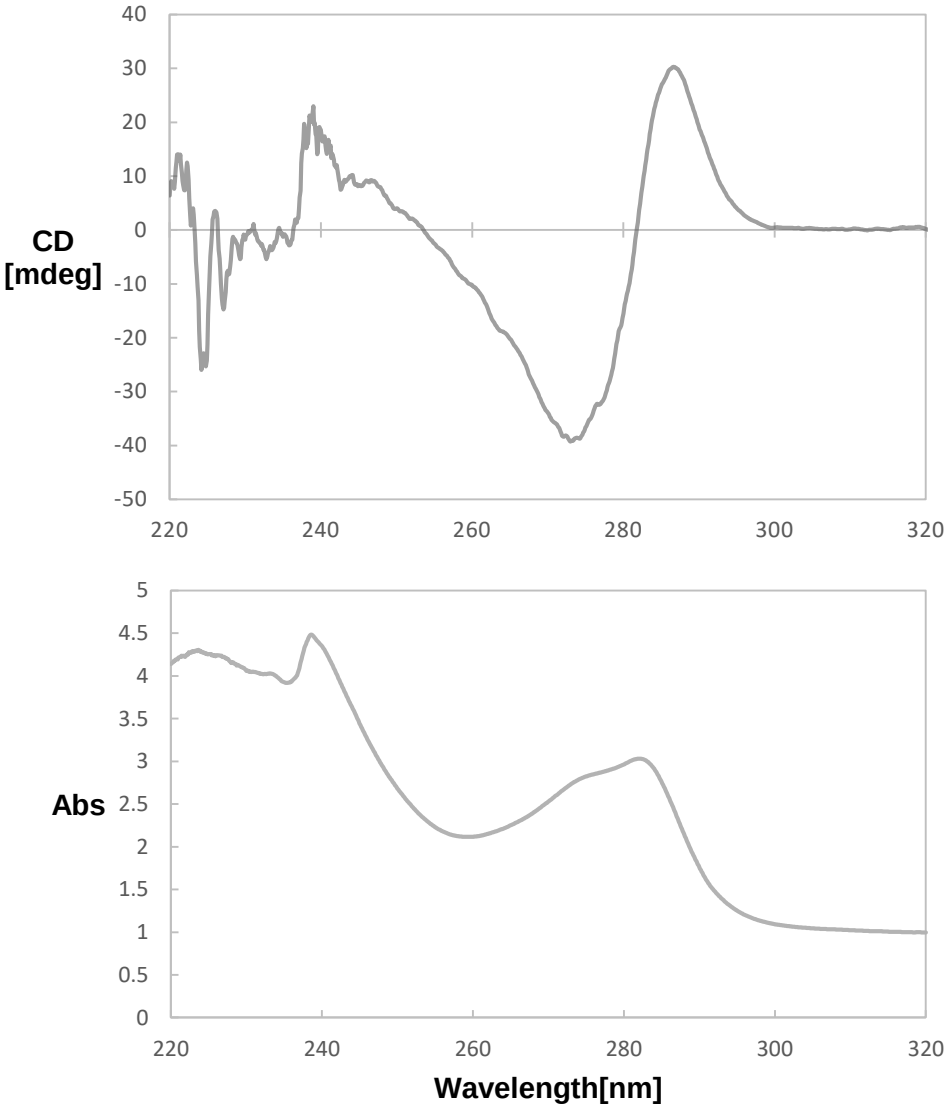

Table 1.S2. CD Spectrum of Compound 1.4l in MeOH

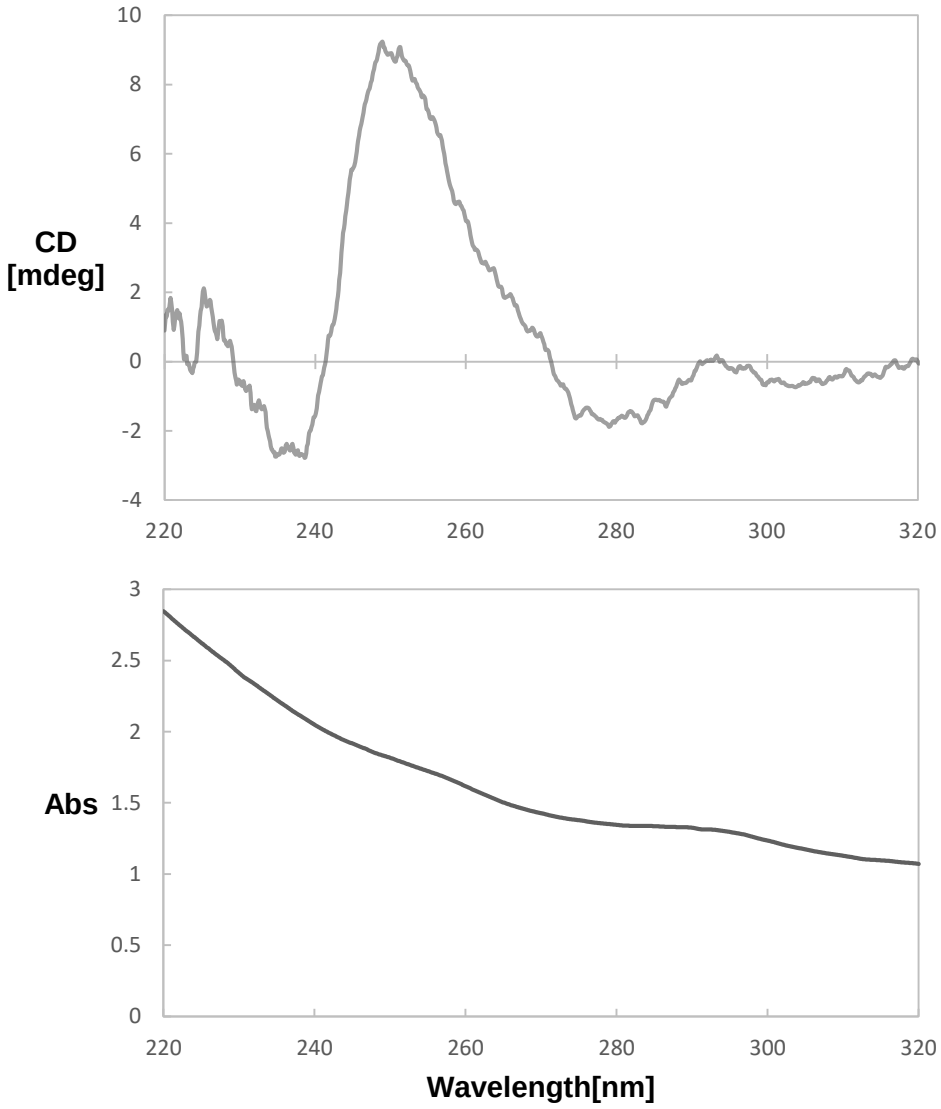

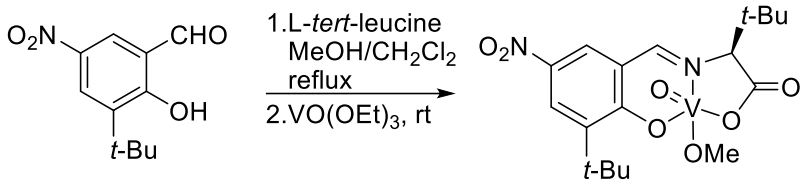

(*S*)-Vanadium Catalyst V6. All glassware was flame dried. A mixture of L-*tert*-leucine (45 mg, 0.34 mmol) and 3-*tert*-butyl-5-nitro-2-hydroxybenzaldehyde (76 mg, 0.34 mmol) in MeOH:CH_2Cl_2 (2 mL, 1:1) was heated at reflux and monitored by TLC. The reaction mixture was cooled to room temperature and $VO(OEt)_3$ (69 mg, 0.34 mmol) was added followed by stirring for 3 h under Ar. Removal of solvent afforded the catalyst (147 mg, 99%) as a deep blue solid: HRMS (ESI-TOF) *m/z* = 433.1180 calcd for $C_{18}H_{26}N_2O_7V$ $[M+H]^+$, found 433.1179.

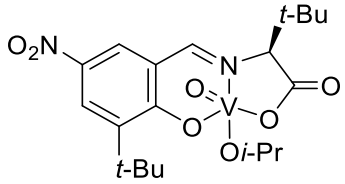

(*S*)-Vanadium Catalyst V8. 3-*tert*-Butyl-5-nitro-2-hydroxybenzaldehyde (300 mg, 1.34 mmol) and L-*tert*-leucine (176 mg, 1.34 mmol) in MeOH:CH_2Cl_2 (7.6 mL, 1:1) were added to an oven-dried round-bottom flask. The resultant mixture was heated at reflux for 3 h. After evaporation of organic solvents, the residual solid was redissolved in CH_2Cl_2 (6.7 mL). $VO(O\textit{i}\text{-Pr})_3$ (0.32 mL, 1.34 mmol) was introduced to the mixture followed by stirring for 3 h under Ar. Removal of solvent afforded the catalyst (590 mg, 99%) as a deep blue solid: HRMS (ESI-TOF) *m/z* = 461.1493 calcd for $C_{20}H_{30}N_2O_7V$ $[M+H]^+$, found 461.1476.

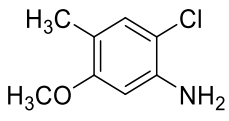

2-Chloro-5-methoxy-4-methylaniline (1.7) 4-Amino-5-chloro-2-methoxybenzoic acid (5.00 g, 24.8 mmol) was suspended in chlorobenzene (50 mL) and cooled to 0 °C. Neat

BH_3•SMe_2 (7.1 mL, 74.4 mmol) was added with vigorous stirring. When effervescence ceased, the mixture was heated for 3 h at 80 °C and then for 18 h at 130 °C. The reaction was quenched by addition of aqueous Na_2CO_3 (aq) (1 M, 82 mL). The mixture was extracted with CH_2Cl_2 (50 mL X 3), dried ($MgSO_4$), filtered, and the solvent was removed under reduced pressure to give a yellow solid. Chromatography (9:1 = hexane/EtOAc) afforded the product as a white powder (2.76 g 65%): **^{1}H NMR** (360 MHz, $CDCl_3$) δ 6.90 (s, 1H), 6.40 (s, 1H), 5.05 (s, 2H), 3.68 (s, 3H), 1.96 (s, 3H). Spectra are in accord with those previously reported.[25]

General procedure A: Buchwald-Hartwig *C-N* coupling. A mixture of NaO*t*-Bu (2.8 g, 29.1 mmol), $Pd(OAc)_2$ (52 mg, 0.23 mmol), and [HP(*t*-Bu)$_3$][BF_4] (85 mg, 0.29 mmol) was suspended in toluene (0.17 M). 2-Chloro-5-methoxy-4-methylaniline (1.0 g, 5.83 mmol) and an aryl bromide (5.94 mmol) were added. The reaction mixture was heated at reflux for 18 h. After the resultant mixture was cooled to ambient temperature, the mixture was quenched by addition of 2 M HCl (aq) (35 mL). The mixture was extracted with CH_2Cl_2 (30 mL X 3), dried over Na_2SO_4, filtered, and the solvent was removed under reduced pressure. Chromatography afforded the product.

General procedure B: palladium catalyzed cyclization. Chlorobiphenylaniline (1.89 mmol), K_2CO_3 (783 mg, 5.67 mmol), $Pd(OAc)_2$ (21 mg, 0.09 mmol), and [HP(*t*-Bu)$_3$][BF_4] (55 mg, 0.19 mmol) were combined with DMA (7.6 mL) under an Ar atmosphere. After stirring at 130 ^{o}C for 18 h, the mixture was cooled and then quenched by addition of 2 M HCl (aq) (7 mL). The mixture was poured into excess amount of water and extracted with EtOAc (30 mL X 3). The combined organic layers were washed thoroughly with H_2O (2 mL X 5) and brine followed by drying over Na_2SO_4. After filtration and removal of solvent, the compounds was chromatographed.

General procedure C: demethylation. The 2-methoxycarbazole (1.62 mmol) was

dissolved in CH_2Cl_2 (23 mL). After cooling to –78 ºC, a solution of BBr_3 (1 M in dichloromethane, 3.24 mmol) was added dropwise. The resultant mixture was allowed to warm to room temperature and stirred until completion as judged by TLC (30 min – 18 h). The mixture was subsequently quenched with water (15 mL) under ice bath. The solution was then extracted with EtOAc (30 mL X 3), washed with brine and the combined organic layers were dried over Na_2SO_4. Removal of solvent was followed by chromatography.

General procedure D: protection of carbazole nitrogen. To a stirring solution of DMF (1.4 mL) and NaH (85 mg, 3.55 mmol) was added a solution of 2-hydroxycarbazole (1.42 mmol) in THF (14 mL) at 0 °C. After stirring for 30 minutes at room temperature, BnCl (1.6 mL, 1.56 mmol, 1.0 M in THF) was added to the solution. After stirring for 18 h at 10 ºC, the solution was quenched with ice-water (15 mL), extracted with EtOAc (30 mL X 3). After washing the combined organic layers with water (2 mL X 5) and brine, the organic phase was dried with Na_2SO_4. Removal of solvent was followed by chromatography.

General procedure E: asymmetric oxidative 2-hydroxycarbazole coupling. To a microwave vial was added *N*-protected 2-hydroxycarbazole (0.42 mmol), catalyst **V8** (38 mg, 0.08 mmol) and AcOH (0.16 mL, 2.71 mmol). The vial was sealed with a septum and the chlorobenzene (0.84 mL) was added. After degassing and purging with O_2 three times, the vial was sealed with a microwave vial cap and was stirred at 0 ºC for 48 h. Upon completion, the reaction mixture was then directly chromatographed using silica gel.

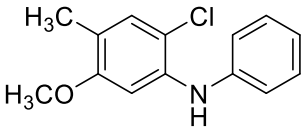

2-Chloro-5-methoxy-4-methyl-*N*-phenylaniline (1.8a). Following **General Procedure A** for 23 h, the product was obtained as brown oil (1.26 g) in 87% yield. $\mathbf{R_f}$ = 0.6 (EtOAc/Hexanes = 1/4): **^{1}H NMR** (500 MHz, acetone-d_6) δ 7.30 (t, J = 6.3 Hz, 2H), 7.13-

7.10 (m, 3H), 6.99 (s, 1H), 6.8 (s, 1H), 5.94 (s, 1H), 3.71 (s, 3H), 2.13 (s, 3H); **^{13}C NMR** (125 MHz, acetone-d_6) δ 157.1, 143.3, 138.8, 130.7, 129.2, 120.9, 120.0, 118.2, 113.8, 101.3, 55.0, 14.5; **IR** (neat) 3400, 2925, 2850, 1512, 1200, 605 cm^{-1}; **HRMS** (ESI-TOF) calcd for $C_{14}H_{15}ClNO$ $[M+H]^+$ 248.0842, found 248.0842.

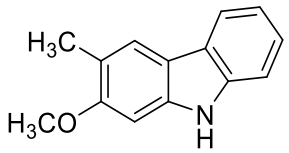

2-Methoxy-3-methyl-9*H*-carbazole (1.9a). Following **General Procedure B** for 20 h, the product was obtained as a white solid (342 mg) in 86% yield. Spectral data were in agreement with those reported.[32]

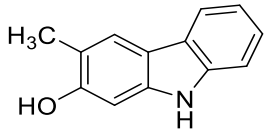

3-Methyl-9*H*-carbazol-2-ol (1.10a). Following **General Procedure C** for 23 h, the product was obtained as a white solid (342 mg) in 86% yield. Spectral data were in agreement with those reported.[32]

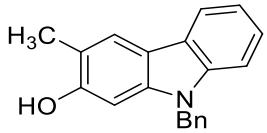

9-Benzyl-3-methyl-9*H*-carbazol-2-ol (1.4a). Following **General Procedure D** for 24 h, the product was obtained as an off-white powder (72 mg) in 52% yield. Spectral data were in agreement with those reported.[32]

[32] Dai, J.; Ma, D.; Fu, C.; Ma, S. Gram Scale Total Synthesis of 2-Hydroxy-3-Methylcarbazole, Pyrano[3,2-a]Carbazole and Prenylcarbazole Alkaloids. *Eur. J. Org. Chem.* **2015**, *2015* (25), 5655–5662.

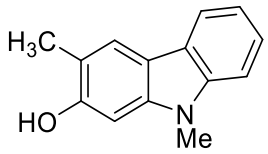

3,9-Dimethyl-9*H*-carbazol-2-ol (1.4b). Following **General Procedure D** using a 1.0 M solution of MeI in THF (0.067 mL) for 2 h, the product was obtained as a brown solid (10 mg) in 23% yield. $\mathbf{R_f}$ = 0.4 (EtOAc:Hexanes = 1:4): **^{1}H NMR** (500 MHz, acetone-d_6) δ 8.29 (s, 1H), 7.94 (d, J = 7.5 Hz, 1H), 7.80 (s, 1H) 7.39 (d, J = 8.0 Hz, 1H), 7.30 (dt, J = 7.5, 1.0 Hz, 1H), 7.10 (dt, J = 8.0, 0.5 Hz, 1H), 6.89 (s, 1H), 3.76 (s, 3H), 2.35 (s, 3H); **^{13}C NMR** (125 MHz, acetone-d_6) δ 155.9, 142.1, 141.8, 124.6, 124.0, 122.4, 119.7, 119.3, 117.6, 116.4, 109.1, 95.2, 29.2, 16.6; **IR** (neat) 3391, 2922, 2853, 1634, 1604, 815, 740, 719, 621 cm^{-1}; **HRMS** (ESI-TOF) calcd for $C_{14}H_{12}NO$ $[M-H]^-$ 212.1075, Found 212.1083.

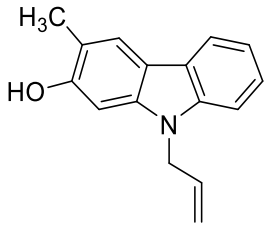

9-Allyl-3-methyl-9*H*-carbazol-2-ol (1.4c). Following **General Procedure D**, the product was obtained as a colorless solid (71 mg) in 43% yield. $\mathbf{R_f}$ = 0.47 (EtOAc:Hexanes = 1:4): **^{1}H NMR** (500 MHz, $CDCl_3$) δ 7.98 (d, J = 7.7 Hz, 1H), 7.82 (s, 1H), 7.37 (td, J = 8.2, 1.1 Hz, 1H), 7.31 (d, J = 8.1 Hz, 1H), 7.20 (td, J = 7.8, 0.9 Hz, 1H), 6.79 (s, 1H), 6.00-5.93 (m, 1H), 5.16 (dd, J = 10.3, 1.3 Hz, 1H), 5.04 (dd, J = 17.1, 1.2 Hz, 1H), 4.85 (s, 1H), 4.81-4.80 (m, 2H), 2.42 (s, 3H); **^{13}C NMR** (125 MHz, $CDCl_3$) δ 153.3, 140.6, 132.4, 124.4, 123.2, 122.0, 119.5, 119.1, 117.0, 116.9, 115.9, 108.6, 95.1, 45.5, 16.2; **IR** (neat) 3350, 2918, 1633, 1604, 1495, 1461, 1326, 1251, 1183, 1141, 1120, 1022, 923, 808, 744, 721 cm^{-1}; **HRMS** (EI-TOF) calcd for $C_{16}H_{15}NO$ $[M]^+$ m/z = 237.1154; found 237.1152.

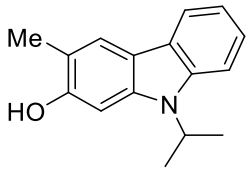

9-Isopropyl-3-methyl-9*H*-carbazol-2-ol (1.4d). Following **General Procedure D**, the product was obtained as a white solid (65 mg) in 39% yield. $\mathbf{R_f}$ = 0.43 (EtOAc:Hexanes = 1:4): **^{1}H NMR** (500 MHz, $CDCl_3$) δ 7.97 (d, *J* = 7.7 Hz, 1H), 7.81 (s, 1H), 7.45 (d, *J* = 8.3 Hz, 1H), 7.35 (td, *J* = 8.2, 1.2 Hz, 1H), 7.17 (td, *J* = 7.8, 0.8 Hz, 1H), 6.95 (s, 1H), 4.91-4.84 (m, 1H), 4.82 (s, 1H), 2.42 (s, 3H), 1.67 (d, *J* = 7.0 Hz, 6H); **^{13}C NMR** (125 MHz, $CDCl_3$) δ 152.8, 139.7, 139.4, 124.0, 123.5, 121.9, 119.5, 118.6, 117.5, 115.4, 109.7, 96.4, 46.8, 20.8, 16.1; **IR** (neat) 3383, 2972, 2917, 2849, 1635, 1602, 1459, 1350, 1223, 1101, 996, 1879, 721 cm^{-1}; **HRMS** (EI-TOF) calcd for $C_{16}H_{17}NO$ $[M]^+$ *m/z* = 239.1310; found 239.1321.

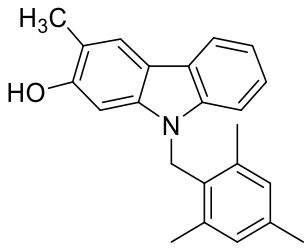

3-Methyl-9-(2,4,6-trimethylbenzyl)-9*H*-carbazol-2-ol (1.4e). Following **General Procedure D** using 2,4,6-trimethylbenzylchloride (0.117 g, 0.70 mmol), the product was obtained as a white solid (92 mg) in 40% yield. $\mathbf{R_f}$ = 0.4 (EtOAc:Hexanes = 1:4): **^{1}H NMR** (500 MHz, $CDCl_3$) δ 7.95 (d, *J* = 7.7 Hz, 1H), 7.79 (s, 1H), 7.25 (td, *J* = 8.3, 1.2 Hz, 1H), 7.15 (td, *J* = 7.9, 0.8 Hz, 1H), 7.09 (d, *J* = 8.2 Hz, 1H), 6.89 (s, 2H), 6.50 (s, 1H), 5.34 (s, 2H), 4.69 (s, 1H), 2.38 (s, 3H), 2.30 (s, 3H), 2.18 (s, 6H); **^{13}C NMR** (125 MHz, $CDCl_3$) δ 153.0, 140.9, 140.8, 137.7, 137.6, 129.9, 129.6, 124.3, 123.3, 121.8, 119.3, 118.9, 117.1, 115.8, 109.2, 95.7, 43.3, 21.1, 20.5, 16.2; **IR** (neat) 3241, 2954, 1604, 1460, 1300, 1188,

742 cm^{-1}; **HRMS** (EI-TOF) calcd for $C_{23}H_{23}NO$ $[M]^+$ *m/z* = 329.1780; found 329.1798.

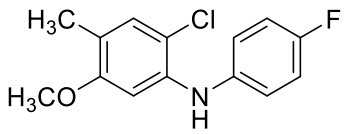

2-Chloro-*N*-(4-fluorophenyl)-5-methoxy-4-methylaniline (1.8f). Following **General Procedure A**, the product was obtained as brown oil (1.55 g) in 99% yield. $\mathbf{R_f}$ = 0.65 (EtOAc:Hexanes = 1:4): **^{1}H NMR** (500 MHz, acetone-d_6) δ 7.20-7.17 (m, 2H), 7.12 (s, 1H), 7.07-7.04 (m, 2H), 6.83 (s, 1H), 6.78 (s, 1H), 3.72 (s, 3H), 2.09 (s, 3H); **^{13}C NMR** (125 MHz, acetone-d_6) δ 158.0 (d, *J* = 238 Hz), 157.2, 139.54 (d, *J* = 2.1 Hz), 139.5, 130.9 (d, *J* = 1.8 Hz), 121.0 (d, *J* = 8.2 Hz), 119.6, 115.7 (d, *J* = 22.0 Hz), 113.2, 100.5 (d *J* = 3.9 Hz), 55.1, 14.6; **IR** (neat) 3420, 2925, 1609, 1200, 602, cm^{-1}; **HRMS** (ESI-TOF) calcd for $C_{14}H_{14}ClFNO$ $[M+H]^+$ 266.0748, found 266.0743.

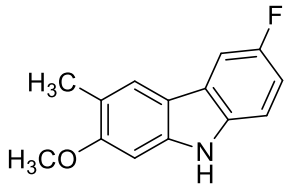

6-Fluoro-2-methoxy-3-methyl-9*H*-carbazole (1.9f). Following **General Procedure B**, the product was obtained as a yellow solid (104 mg) in 72% yield. $\mathbf{R_f}$ = 0.20 (EtOAc:Hexanes = 1:4): **^{1}H NMR** (500 MHz, acetone-d_6) δ 10.08 (s, 1H), 7.81 (s, 1H), 7.69 (dd, *J* = 9.3, 2.5 Hz, 1H), 7.40 (dd, *J* = 8.8, 4.4 Hz, 1H), 7.04 (td, *J* = 9.4, 2.4 Hz, 1H), 7.01 (s, 1H), 3.89 (s, 3H), 2.30 (3H); **^{13}C NMR** (125 MHz, acetone-d_6) δ 157.9, 157.3 (d, *J* = 233 Hz), 141.2, 136.3, 123.9 (d, *J* = 10.1 Hz), 121.4, 118.5, 115.7 (d, *J* = 3.8 Hz), 111.1, 111.0 (d, *J* = 15.1 Hz), 104.4 (d, *J* = 23.9 Hz), 92.6, 54.9, 16.0; **IR** (neat) 3395, 2910, 1486, 847, 822, 803, 783, cm^{-1}; **HRMS** (ESI-TOF) calcd for $C_{14}H_{13}FNO$ $[M+H]^+$ 230.0981, Found 230.0986.

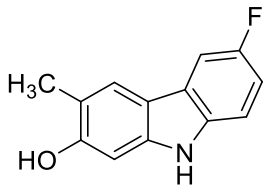

6-Fluoro-3-methyl-9*H*-carbazol-2-ol (1.10f). Following **General Procedure C**, the product was obtained as a brown solid (166 mg) in 90% yield. $\mathbf{R_f}$ = 0.20 (EtOAc:Hexanes = 1:2): **^{1}H NMR** (500 MHz, acetone-d_6) δ 9.94 (s, 1H), 8.34 (s, 1H), 7.78 (s, 1H), 7.66 (dd, *J* = 9.5, 2.6 Hz, 1H), 7.35 (dd, *J* = 8.8, 4.5 Hz, 1H), 7.01 (td, *J* = 9.0, 2.5 Hz, 1H), 6.97 (s, 1H), 2.35 (s, 3H); **^{13}C NMR** (125 MHz, acetone-d_6) δ 157.0 (d, *J* = 233 Hz), 155.3, 141.3, 136.3, 124.2 (d, *J* = 10.1 Hz), 121.6, 117.2, 115.8 (d, *J* = 3.8 Hz), 110.9, 110.7 (d, *J* = 14.8 Hz), 104.4 (d, *J* = 23.9 Hz), 96.2, 15.8; **IR** (neat) 3406, 2919, 1485, 1406, 1257, 1146, 1013, 600 cm^{-1}; **HRMS** (ESI-TOF) calcd for $C_{13}H_9NOF$ $[M-H]^+$ 214.0668, Found 214.0672.

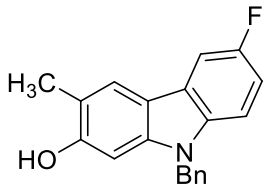

9-Benzyl-6-fluoro-3-methyl-9*H*-carbazol-2-ol (1.4f). Following **General Procedure D**, the product was obtained as a yellow solid (193 mg) in 81% yield. $\mathbf{R_f}$ = 0.35 (EtOAc:Hexanes = 1:4): **^{1}H NMR** (500 MHz, acetone-d_6) δ 8.40 (s, 1H), 7.85 (s, 1H), 7.73 (dd, *J* = 9.0, 5.0 Hz, 1H), 7.41 (dd, *J* = 10.0, 5.0 Hz, 1H), 7.28-7.19 (m, 3H), 7.15-7.13 (m, 2H), 7.05 (td, *J* = 10.0, 1.0 Hz, 1H), 6.89 (s, 1H), 5.50 (s, 2H), 2.34 (s, 3H); **^{13}C NMR** (125 MHz, acetone-d_6) δ 157.4 (d, *J* = 233 Hz), 155.6, 141.7, 137.9, 137.0, 128.6, 127.2, 126.5, 123.9, (d, *J* = 10.6 Hz), 122.0, 117.5, 115.3, 110.9 (d, *J* = 25.6 Hz), 109.3 (d, *J* = 9.3 Hz), 104.6 (d, *J* = 24.3 Hz), 94.9, 46.1, 15.7; **IR** (neat) 3301, 2922, 2851, 1633, 862, 828, 791, 729, 696, 626 cm^{-1}; **HRMS** (ESI-TOF) calcd for $C_{20}H_{17}FNO$ $[M+H]^+$ 306.1494 Found: 306.1497

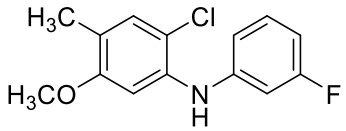

2-Chloro-*N*-(3-fluorophenyl)-5-methoxy-4-methylaniline (1.8g). Following **General Procedure A**, the product was obtained as brown oil (826 mg) in 65% yield. $\mathbf{R_f}$ = 0.78 (EtOAc:Hexanes = 1:4): **^{1}H NMR** (500 MHz, acetone-d_6) δ 7.24 (dd, J = 15.0, 8.0 Hz, 1H), 7.18 (s, 1H), 7.11 (br s, 1H), 6.95 (s, 1H), 6.90 (dd, J = 8.0, 2.0 Hz, 1H), 6.80 (dt, J = 11.5, 2.5 Hz, 1H), 6.58 (td, J = 8.0, 2.5 Hz, 1H), 3.79 (s, 3H), 2.13 (s, 3H); **^{13}C NMR** (125 MHz, acetone-d_6) δ 163.8 (d, J = 243 Hz), 156.9, 144.6 (d, J = 10.0 Hz), 137.1, 131.0, 130.6 (d, J = 10.0 Hz), 121.3, 114.2, 113.6 (d, J = 2.5 Hz), 108.0 (d, J = 21.3 Hz), 104.7 (d, J = 25.0 Hz), 101.3, 55.7, 15.4; **IR** (neat) 3405, 2920, 2851, 1604, 1582, 1518, 834, 815, 776, 767, 678, 615 cm^{-1}; **HRMS** (ESI-TOF) calcd for $C_{14}H_{14}FClNO$ $[M+H]^+$ 266.0748, found 266.0740.

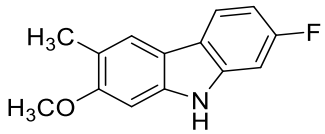

7-Fluoro-2-methoxy-3-methyl-9*H*-carbazole (1.9g). Following **General Procedure B**, the product was obtained as a yellow solid (60 mg) in 5% yield. $\mathbf{R_f}$ = 0.10 (EtOAc:Hexanes = 1:4): **^{1}H NMR** (500 MHz, acetone-d_6) δ 10.18 (s, 1H), 7.92 (dd, J = 8.6, 5.5 Hz, 1H), 7.78 (s, 1H), 7.15 (dd, J = 10.0, 2.4 Hz, 1H), 7.03 (s, 1H), 6.90-6.86 (m, 1H), 3.89 (s, 3H), 2.30 (s, 3H); **^{13}C NMR** (125 MHz, acetone-d_6) δ 158.7 (d, J = 245 Hz), 158.5, 143.2 (d, J = 11.0 Hz), 140.6, 125.4 (d, J = 8.2 Hz), 124.0 (d, J = 2.9 Hz), 120.0, 114.0, 112.3, 107.6 (d, J = 3.5 Hz), 105.0 (d, J = 19.1 Hz), 93.5, 55.8, 16.8; **IR** (neat) 3396, 2921, 1611, 841, 808, 742 cm^{-1}; **HRMS** (ESI-TOF) calcd for $C_{14}H_{11}FNO$ $[M-H]^-$ 228.0825, Found 228.0822.

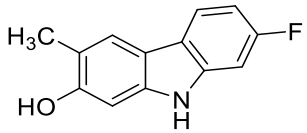

7-Fluoro-3-methyl-9*H*-carbazol-2-ol (1.10g). Following **General Procedure C**, the product was obtained as a brown solid (69 mg) in 99% yield. $\mathbf{R_f}$ = 0.20 (EtOAc:Hexanes = 1:2): **^{1}H NMR** (500 MHz, acetone-d_6) δ 10.06 (s, 1H), 8.26, (s, 1H), 7.89 (dd, J = 8.5, 5.5 Hz, 1H), 7.74 (s, 1H), 7.11 (dd, J = 10.5, 2.5 Hz, 1H), 6.96 (s, 1H), 6.88-6.84 (m, 1H) 2.33 (s, 3H); **^{13}C NMR** (125 MHz, acetone-d_6) δ 161.0 (d, J = 235 Hz), 154.6, 140.6 (d, J = 14.8 Hz), 140.6, 121.2, 120.3, 119.7 (d, J = 10.5 Hz), 117.4, 115.7, 106.2 (d, J = 24.1 Hz), 97.0 (d, J = 26.3 Hz), 96.5, 15.9; **IR** (neat) 3406, 2920, 1486, 1293, 834, 820, 810, 781, 600, cm^{-1}; **HRMS** (ESI-TOF) calcd for $C_{13}H_9FNO$ $[M-H]^-$ 214.0668, Found: 214.0669.

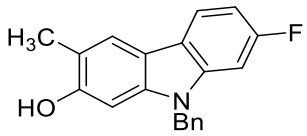

9-Benzyl-7-fluoro-3-methyl-9*H*-carbazol-2-ol (1.4g). Following **General Procedure D**, the product was obtained as a yellow solid (57 mg) in 83% yield. $\mathbf{R_f}$ = 0.17 (EtOAc:Hexanes = 1:4): **^{1}H NMR** (500 MHz, acetone-d_6) δ 8.38 (s, 1H), 7.84 (s, 1H), 7.28-7.19 (m, 5H), 7.14 (d, J = 7.0 Hz, 2H), 6.91 (s, 1H), 6.84 (ddd, J = 8.5, 7.0, 1.5 Hz, 1H), 5.50 (s, 2H), 2.33 (s, 3H); **^{13}C NMR** (125 MHz, acetone-d_6) δ 157.6 (d, J = 245 Hz), 155.0, 143.0, 140.3, 137.5, 128.5, 127.2, 126.4, 124.5 (d, J = 8.3 Hz), 123.7 (d, J = 3.0 Hz), 117.9, 112.8, 111.0, (d, J = 21.0 Hz), 104.9, 104.4 (d, J = 19.3 Hz), 94.3, 46.2, 15.5; **IR** (neat) 3456, 3370, 2918, 1470, 883, 776, 741, 715, 702, 693 cm^{-1}; **HRMS** (ESI-TOF) calcd for $C_{20}H_{15}FNO$ $[M-H]^-$ 304.0876 Found: 304.0875

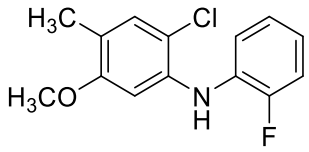

2-Chloro-*N*-(2-fluorophenyl)-5-methoxy-4-methylaniline (1.8h). Following **General Procedure A** for 20 h, the product was obtained as brown oil (398 mg) in 64% yield. Spectral data were in agreement with those reported.[33]

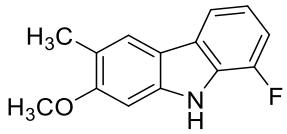

1-Fluoro-7-methoxy-6-methyl-9*H*-carbazole (1.9h). Following **General Procedure B** for 20 h, the product was obtained as a light brown solid (313 mg) in 91% yield. Spectral data were in agreement with those reported.[33]

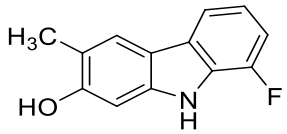

8-Fluoro-3-methyl-9*H*-carbazol-2-ol (1.10h). Following **General Procedure C**, the product was obtained as a brown solid (200 mg) in 69% yield. $\mathbf{R_f}$ = 0.38 (EtOAc:Hexanes = 1:2): **^{1}H NMR** (500 MHz, acetone-d_6) δ 10.28 (br s, 1H), 8.43 (s, 1H), 7.80 (s, 1H), 7.75-7.74 (m, 1H), 7.06-7.03 (m, 3H), 2.37 (s, 3H); **^{13}C NMR** (125 MHz, acetone-d_6) δ 156.3, 149.8 (d, J = 240.5 Hz), 141.2, 128.3 (d, J = 6.0 Hz), 128.1, 122.4 (d, J = 4.0 Hz), 119.6 (d, J = 5.9 Hz), 118.6, 116.8 (d, J = 2.6 Hz), 115.6, 109.6 (d, J = 16.6 Hz), 97.4, 16.7; **IR** (neat) 3540, 3404, 2911, 1623, 1576, 1475, 1450, 1429, 1299, 1290, 1262, 1237, 1219, 1200, 1174, 1157, 1137, 1057, 1050, 833 cm^{-1}; **HRMS** (EI-TOF) calcd for $C_{13}H_{10}FNO$ $[M]^+$ m/z = 215.0746, found 215.0758.

[33] Bedford, R. B.; Betham, M.; Charmant, J. P. H.; Weeks, A. L. Intramolecular Direct Arylation in the Synthesis of Fluorinated Carbazoles. *Tetrahedron* **2008**, *64*, 6038–6050.

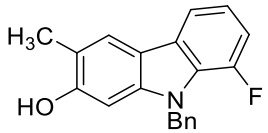

9-Benzyl-8-fluoro-3-methyl-9*H*-carbazol-2-ol (1.4h). Following **General Procedure D**, the product was obtained as a yellow solid (55 mg) in 28% yield. $\mathbf{R_f}$ = 0.65 (EtOAc:Hexanes = 1:2): **^{1}H NMR** (500 MHz, acetone-d_6) δ 8.49 (br s, 1H), 7.86 (s, 1H), 7.81 (d, J = 7.5 Hz, 1H), 7.27 (t, J = 7.0 Hz, 2H), 7.22 (t, J = 7.2 Hz, 1H), 7.15 (d, J = 7.2 Hz, 2H), 7.11-7.02 (m, 2H), 6.93 (s, 1H), 5.65 (s, 2H), 2.34 (s, 3H); **^{13}C NMR** (125 MHz, acetone-d_6) δ 156.5, 150.2 (d, J = 241.5 Hz), 142.1, 139.4, 129.5, 129.4, 128.3 (d, J = 5.0 Hz), 128.0, 127.1, 122.6, 120.1 (d, J = 6.3 Hz), 119.0, 116.6, 115.9 (d, J = 3.8 Hz), 110.8 (d, J = 18.9 Hz), 95.9, 49.0, 16.6; **IR** (neat) 3310, 2918, 1577, 1472, 1454, 1423, 1347, 1296, 1235, 1219, 1186, 1137, 1105, 1058, 1000, 819 cm^{-1}; **HRMS** (ESI-TOF) calcd for $C_{20}H_{17}FNO$ $[M+H]^+$ m/z = 306.1294, found 306.1314.

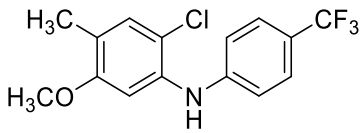

2-Chloro-5-methoxy-4-methyl-*N*-(4-(trifluoromethyl)phenyl)aniline (1.8i). Following **General Procedure A** using $Pd_2(dba)_3$ as the catalyst at room temperature for 10 min, the product was obtained as a white solid (252 mg) in 45% yield. $\mathbf{R_f}$ = 0.57 (EtOAc:Hexanes = 1:4): **^{1}H NMR** (500 MHz, $CDCl_3$) δ 7.54 (d, J = 8.5 Hz, 2H), 7.18 (s, 1H), 7.10 (d, J = 8.5 Hz, 2H), 6.89 (s, 1H), 6.08 (br s, 1H), 3.78 (s, 3H), 2.21 (s, 3H); **^{13}C NMR** (125 MHz, $CDCl_3$) δ 157.0, 146.3, 136.4, 131.2, 126.9, 124.6 (q, J = 271 Hz), 122.6 (q, J = 32.7 Hz), 122.5, 116.4, 115.5, 102.6, 55.7, 15.5; **IR** (neat) 3400, 2925, 1604, 1525, 1509, 1481, 1450, 1395, 1323, 1289, 1244, 1201, 1186, 1159, 1103, 1066, 990, 946, 873 cm^{-1}; **HRMS** (ESI-TOF) calcd for $C_{15}H_{14}ClF_3NO$ $[M+H]^+$ m/z = 316.0716, found 316.0742.

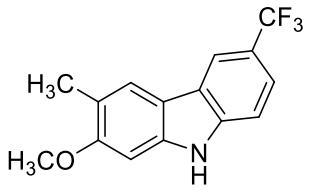

2-methoxy-3-methyl-6-(trifluoromethyl)-9*H*-carbazole (1.9i) Following **General Procedure B** for 48 h, the product was obtained as a light brown solid (94 mg) in 84% yield. $\mathbf{R_f}$ = 0.44 (EtOAc:Hexanes = 1:2): **^{1}H NMR** (500 MHz, $CDCl_3$) δ 8.21 (s, 1H), 7.87 (br s, 1H), 7.81 (s, 1H), 7.55 (d, *J* = 8.5 Hz, 1H), 7.30 (d, *J* = 8.5 Hz, 1H), 6.72 (s, 1H), 3.87 (s, 3H), 2.39 (s, 3H); **^{13}C NMR** (125 MHz, $CDCl_3$) δ 158.2, 140.7, 139.8, 125.5 (q, *J* = 271 Hz), 123.2, 121.8, 121.7 (q, *J* = 31.8 Hz), 121.0, 120.5, 116.8, 115.6, 110.3, 92.5, 55.6, 16.8; **IR** (neat) 3360, 2915, 1614, 1458, 1334, 1297, 1261, 1230, 1197, 1164, 1145, 1112, 1095, 1051, 1039, 1015, 978, 880, 819 cm^{-1}; **HRMS** (EI-TOF) calcd for $C_{15}H_{13}F_3NO$ $[M+H]^+$ *m/z* = 279.0871, found 279.0877.

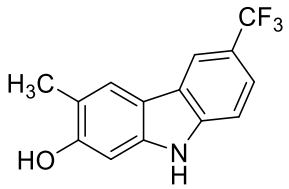

3-Methyl-6-(trifluoromethyl)-9*H*-carbazol-2-ol (1.10i). Following **General Procedure C**, the product was obtained as a light tan solid (98 mg) in 71% yield. $\mathbf{R_f}$ = 0.29 (EtOAc:Hexanes = 1:1): **^{1}H NMR** (500 MHz, acetone-d_6) δ 10.36 (br s, 1H), 8.44 (s, 1H), 8.31 (s, 1H), 7.95 (s, 1H), 7.57-7.53 (m, 2H), 7.04 (s, 1H), 2.37 (s, 3H); **^{13}C NMR** (125 MHz, acetone-d_6) δ 156.5, 142.5, 141.7, 126.7 (q, *J* = 270 Hz), 124.2, 122.7, 121.1 (q, *J* = 3.8 Hz), 121.0 (q, *J* = 31.4 Hz), 119.0, 117.1 (q, *J* = 3.8 Hz), 116.3, 111.4, 97.3, 16.7; **IR** (neat) 3412, 3270, 2925, 1641, 1616, 1414, 1330, 1298, 1255, 1225, 1210, 1194, 1169, 1156, 1137, 1108, 1052, 1015, 883 cm^{-1}; **HRMS** (EI-TOF) calcd for $C_{14}H_{10}F_3NO$ $[M]^+$ m/z = 265.0714, found 265.0714.

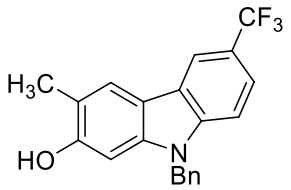

9-Benzyl-3-methyl-6-(trifluoromethyl)-9*H*-carbazol-2-ol (1.4i). Following **General Procedure D**, the product was obtained as a white powder (24 mg) in 29% yield. $\mathbf{R_f}$ = 0.50 (EtOAc:Hexanes = 1:2): **^{1}H NMR** (500 MHz, acetone-d_6) δ 8.52 (s, 1H), 8.37 (s, 1H), 8.01 (s, 1H), 7.64-7.58 (m, 2H), 7.30-7.24 (m, 3H), 7.17 (d, *J* = 7.0 Hz, 2H), 6.97 (s, 1H), 5.58 (s, 2H), 2.37 (s, 3H); **^{13}C NMR** (125 MHz, acetone-d_6) δ 156.7, 143.0, 142.4, 138.3, 129.5, 128.2, 127.4, 126.6 (q, *J* = 270 Hz), 124.0, 123.0, 121.4 (q, *J* = 3.6 Hz), 121.3 (q, *J* = 31.7 Hz), 119.4, 117.2 (q, *J* = 4.3 Hz), 116.0, 109.8, 96.1, 47.0, 16.6; **IR** (neat) 3350, 2923, 1613, 1453, 1371, 1330, 1301, 1260, 1213, 1175, 1158, 1141, 1103, 1068, 1044, 1013, 963, 882 cm^{-1}; **HRMS** (EI-TOF) calcd for $C_{21}H_{16}F_3NO$ $[M]^+$ *m/z* = 355.1184, found 355.1175.

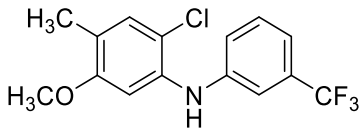

2-Chloro-5-methoxy-4-methyl-*N*-(3-(trifluoromethyl)phenyl)aniline (1.8j). Following **General Procedure A** using $Pd_2(dba)_3$ as the catalyst at room temperature for 10 min, the product was obtained as a yellow oil (677 mg) in 92% yield. $\mathbf{R_f}$ = 0.69 (EtOAc:Hexanes = 1:5): **^{1}H NMR** (500 MHz, $CDCl_3$) δ 7.40-7.36 (m, 2H), 7.23-7.19 (m, 2 H), 7.15 (s, 1H), 6.81 (s, 1H), 6.03 (s, 1H), 3.74 (s, 3H), 2.16 (s, 3H); **IR** (neat) 3405, 2940, 1607, 1598, 1518, 1496, 1466, 1447, 1434, 1398, 1332, 1320, 1236, 1200, 1162, 1120, 1098, 1069, 1000, 875, 789, 697 cm^{-1}; **HRMS** (ESI-TOF) *m/z* = 315.0638 calcd for $C_{15}H_{13}ClF_3NO$ $[M]^+$, found 315.0627.

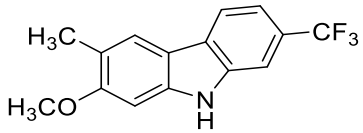

2-Methoxy-3-methyl-7-(trifluoromethyl)-9*H*-carbazole (1.9j). Following **General Procedure B** for 24 h, the product was obtained as a light tan solid (295 mg) in 67% yield. $\mathbf{R_f}$ = 0.10 (EtOAc:Hexanes = 1:6): **^{1}H NMR** (500 MHz, acetone-d_6) δ 10.43 (br s, 1H), 8.13 (d, J = 8.2 Hz, 1H), 7.91 (s, 1H), 7.77 (s, 1H), 7.41 (d, J = 8.1 Hz, 1H), 7.10 (s, 1H), 3.93 (s, 3H), 2.33 (s, 3H); **^{13}C NMR** (125 MHz, acetone-d_6) δ 159.6, 142.3, 139.9, 127.2, 126.5 (q, J = 269 Hz), 125.8 (q, J = 31.0 Hz), 122.7, 120.5, 120.4, 116.1 (q, J = 4.0 Hz), 116.0, 108.6, (q, J = 4.0 Hz), 93.7, 56.0, 17.0; **IR** (neat) 3395, 2935, 1630, 1478, 1448, 1332, 1323, 1293, 1217, 1197, 1163, 1146, 1114, 1070, 1057, 1035, 1002, 920, 874, 821, 791, 666 cm^{-1}; **HRMS** (ESI-TOF) m/z = 279.0871 calcd for $C_{15}H_{12}F_3NO$ $[M]^+$, found 279.0866.

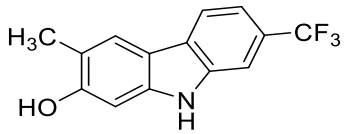

3-Methyl-7-(trifluoromethyl)-9*H*-carbazol-2-ol (1.10j). Following **General Procedure C**, the product was obtained as a tan solid (144 mg) in 68% yield. $\mathbf{R_f}$ = 0.15 (EtOAc:Hexanes = 1:5): **^{1}H NMR** (500 MHz, acetone-d_6) δ 10.31 (br s, 1H), 8.52 (s, 1H), 8.11 (d, J = 8.1 Hz), 7.89 (s, 1H), 7.73 (s, 1H), 7.40 (d, J = 8.0 Hz, 1H), 7.03, (s, 1H), 2.36 (s, 3H); **IR** (neat) 3505, 3380, 2920, 1635, 1620, 1473, 1451, 1433, 1351, 1322, 1302, 1285, 1217, 1161, 1115, 1056, 1010 917, 873, 843, 822, 727, 669 cm^{-1}; **HRMS** (ESI-TOF) m/z = 265.0714 calcd for $C_{14}H_{10}F_3NO$ $[M]^+$, found 265.0726.

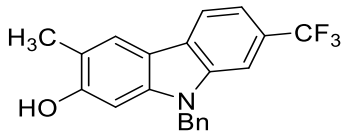

9-Benzyl-3-methyl-7-(trifluoromethyl)-9*H*-carbazol-2-ol (1.4j). Following **General**

Procedure D, the product was obtained as a white solid (77 mg) in 58% yield. $\mathbf{R_f}$ = 0.28 (EtOAc:Hexanes = 1:4): **^{1}H NMR** (500 MHz, acetone-d_6) δ 8.60 (s, 1H), 8.18 (d, *J* = 8.2 Hz, 1H), 7.96 (s, 1H), 7.83 (s, 1H), 7.45 (d, *J* = 8.1 Hz, 1H), 7.30-7.24 (m, 3H), 7.16 (d, *J* = 7.1 Hz, 2H), 6.96 (s, 1H), 5.63 (s, 2H), 2.36 (s, 3H); **^{13}C NMR** (125 MHz, acetone-d_6) δ 156.3, 142.0, 139.8, 137.5, 128.7, 127.3, 126.5, 126.2, 125.5 (q, *J* = 269 Hz), 125.1 (q, *J* = 31.0 Hz), 122.4, 119.4, 118.5, 115.3 (q, *J* = 4.0 Hz), 114.7, 105.8 (q, *J* = 4.0 Hz), 95.1, 46.1, 15.7; **IR** (neat) 3345(w), 2915, 1640, 1453, 1370, 1317, 1296, 1262, 1248, 1214, 1168, 1142, 1132, 1116, 1063, 1042, 1011, 887, 858, 821, 702, 665, 653 cm^{-1}; **HRMS** (ESI-TOF) *m/z* = 356.1262 calcd for $C_{21}H_{16}F_3NO$ $[M]^+$, found 356.1247.

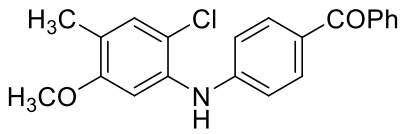

(4-((2-Chloro-5-methoxy-4-methylphenyl)amino)phenyl)(phenyl)methanone (1.8k). Following **General Procedure A** using $Pd_2(dba)_3$ (4 mol %) as a catalyst at room temperature for 20 min, the product was obtained as a brown solid (497 mg) in 81% yield. $\mathbf{R_f}$ = 0.44 (EtOAc:Hexanes = 1:4): **^{1}H NMR** (500 MHz, $CDCl_3$) δ 7.81 (d, *J* = 8.5 Hz, 2H), 7.77 (d, *J* = 7.0 Hz, 2H), 7.55 (t, *J* = 7.5 Hz, 1H), 7.46 (t, *J* = 8.0 Hz, 2H), 7.16 (s, 1H), 7.05 (d, *J* = 6.5 Hz, 2H), 6.92 (s, 1H), 6.31 (s, 1H), 3.76 (s, 3H), 2.18 (s, 3H); **^{13}C NMR** (125 MHz, $CDCl_3$) δ 195.2, 156.8, 147.5, 138.5, 135.7, 132.6, 131.7, 131.1, 129.6, 129.3, 128.2, 122.9, 116.0, 115.1, 103.3, 55.7, 15.6; **IR** (neat) 3360, 3000, 2949, 1584, 1574, 1516, 1500, 1480, 1465, 1443, 1394, 1309, 1282, 1249, 1201, 1174, 1165, 1143, 837 cm^{-1}; **HRMS** (ESI-TOF) calcd for $C_{21}H_{19}ClNO_2$ $[M+H]^+$ *m/z* = 352.1104, found 352.1100.

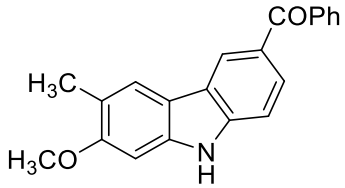

(7-Methoxy-6-methyl-9*H*-carbazol-3-yl)(phenyl)methanone (1.9k). Following **General Procedure B** for 23 h, the product was obtained as a brown solid (288 mg) in 65% yield. $\mathbf{R_f}$ = 0.19 (EtOAc:Hexanes = 1:2): **^{1}H NMR** (500 MHz, DMF-d_7) δ 11.55 (br s, 1H), 8.53 (s, 1H), 7.99 (s, 1H), 7.84 (d, *J* = 8.4 Hz, 3H), 7.70 (t, *J* = 7.4 Hz, 1H), 7.63-7.60 (m, 3H), 7.15 (s, 1H), 3.96 (s, 3H), 2.33 (s, 3H); **^{13}C NMR** (125 MHz, DMF-d_7) δ 196.0, 158.2, 143.1, 141.2, 139.6, 131.9, 129.8, 128.6, 128.5, 126.6, 123.1, 122.7, 121.9, 119.4, 116.1, 110.6, 93.4, 55.5, 16.3; **IR** (neat) 3300, 2910, 1629, 1599, 1565, 1473, 1332, 1312, 1282, 1247, 1195, 1147, 1131, 1036, 1001, 876, 825 cm^{-1}; **HRMS** (ESI-TOF) calcd for $C_{21}H_{18}NO_2$ $[M+H]^+$ *m/z* = 316.1338, found 316.1347.

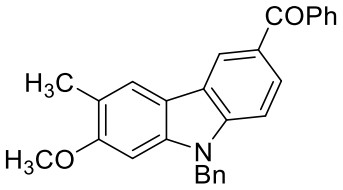

(9-Benzyl-7-methoxy-6-methyl-9*H*-carbazol-3-yl)(phenyl)methanone (1.11k). Following **General Procedure D** at room temperature for 22 h, the product was obtained as a pale yellow solid (206 mg) in 80% yield. $\mathbf{R_f}$ = 0.80 (EtOAc:Hexanes = 1:1): **^{1}H NMR** (500 MHz, acetone-d_6) δ 8.51 (s, 1H), 7.97 (s, 1H), 7.84 (dd, *J* = 8.6, 1.6 Hz, 1H), 7.81 (dd, *J* = 8.1, 1.5 Hz, 2H), 7.64-7.54 (m, 4H), 7.31-7.24 (m, 6H), 5.72 (s, 2H), 3.91 (s, 3H), 2.32 (s, 3H); **^{13}C NMR** (125 MHz, acetone-d_6) δ 196.2, 159.1, 143.7, 142.4, 140.1, 138.4, 132.3, 130.4, 129.6, 129.5, 129.0, 128.2, 127.6, 127.3, 123.6, 123.1, 122.6, 120.6, 116.5, 109.6, 92.6, 56.0, 47.0, 16.8; **IR** (neat) 2925, 1649, 1630, 1600, 1452, 1356, 1310, 1283, 1254, 1194, 1174, 1161, 1140, 877 cm^{-1}; **HRMS** (ESI-TOF) calcd for $C_{28}H_{24}NO_2$ $[M+H]^+$ m/z = 406.1807, found 406.1792.

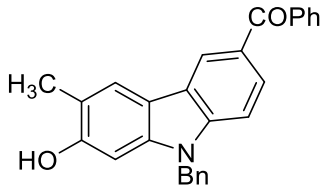

(9-Benzyl-7-hydroxy-6-methyl-9*H*-carbazol-3-yl)(phenyl)methanone (1.4k). Following **General Procedure C** at room temperature for 45 min, the product was obtained as an off-white powder (97 mg) in quantitative yield. $\mathbf{R_f}$ = 0.34 (EtOAc:Hexanes = 1:2): **^{1}H NMR** (500 MHz, acetone-d_6) δ 8.48 (d, J = 3.9 Hz, 2H), 7.94 (s, 1H), 7.84 (dd, J = 8.5, 1.6 Hz, 1H), 7.81 (d, J = 7.0 Hz, 2H), 7.65 (t, J = 7.5 Hz, 1H), 7.61-7.55 (m, 3H), 7.32-7.25 (m, 3H), 7.21 (d, J = 7.0 Hz, 2 H), 6.98 (s, 1H), 5.61 (s, 2H), 2.35 (s, 3H); **^{13}C NMR** (125 MHz, acetone-d_6) δ 196.2, 156.5, 144.0, 142.3, 140.2, 138.3, 132.3, 130.4, 129.6, 129.5, 129.1, 128.3, 127.5, 127.4, 123.8, 122.98, 122.97, 119.3, 116.6, 109.2, 96.3, 47.1, 16.6; **IR** (neat) 3381, 2924, 2854, 1649, 1597, 1449, 1414, 1318, 1281, 1251, 1183, 1136, 1072, 1028, 1002, 948 cm^{-1}; **HRMS** (ESI-TOF) calcd for $C_{27}H_{22}NO_2$ $[M+H]^+$ m/z = 392.1651, found 392.1664.

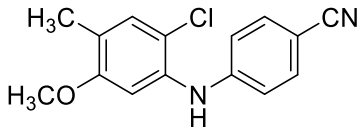

4-((2-Chloro-5-methoxy-4-methylphenyl)amino)benzonitrile (1.8l). Following **General Procedure A** using $Pd_2(dba)_3$ as a catalyst at room temperature for 10 min, the product was obtained as a yellow powder (412 mg) in 86% yield. $\mathbf{R_f}$ = 0.41 (EtOAc:Hexanes = 1:4): **^{1}H NMR** (500 MHz, $CDCl_3$) δ 7.51 (d, J = 8.5 Hz, 2H), 7.17 (s, 1H), 6.99 (d, J = 8.5 Hz, 2H), 6.83 (s, 1H), 6.11 (br s, 1H), 3.77 (s, 3H), 2.17 (s, 3H); **^{13}C NMR** (125 MHz, $CDCl_3$) δ 157.0, 147.5, 135.1, 133.9, 131.3, 124.0, 119.7, 116.9, 115.8, 104.1, 102.6, 55.8, 15.7; **IR** (neat) 3402, 2925, 2217, 1599, 1506, 1469, 1455, 1441, 1396, 1372, 1333, 1299, 1283, 1251, 1202, 1169, 985, 868, 815 cm^{-1}; **HRMS** (ESI-TOF) calcd for $C_{15}H_{13}ClN_2O$ $[M]^+$

m/z = 272.0716, found 272.0706.

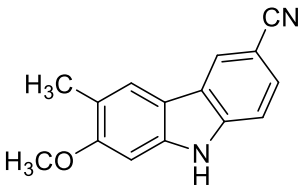

7-Methoxy-6-methyl-9*H*-carbazole-3-carbonitrile (1.9l). Following **General Procedure B** for 48 h, the product was obtained as a light brown powder (249 mg) in 78% yield. $\mathbf{R_f}$ = 0.33 (EtOAc:Hexanes = 1:2): **^{1}H NMR** (500 MHz, acetone-d_6) δ 10.62 (br s, 1H), 8.38 (s, 1H), 7.93 (s, 1H), 7.57 (s, 2H), 7.09 (s, 1H), 3.92 (s, 3H), 2.32 (s, 3H); **^{13}C NMR** (125 MHz, acetone-d_6) δ 159.3, 142.5, 141.4, 127.8, 124.6, 124.4, 122.4, 121.2, 120.8, 115.7, 112.2, 102.2, 93.7, 55.8, 16.8; **IR** (neat) 3311, 2910, 2217, 1609, 1466, 1444, 1323, 1297, 1272, 1234, 1200, 1160, 1136, 1118, 1039, 1003, 862, 806 cm^{-1}; **HRMS** (EI-TOF) calcd for $C_{15}H_{12}N_2O$ $[M]^+$ *m/z* = 236.0950, found 236.0964.

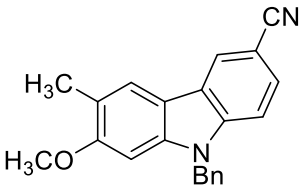

9-Benzyl-7-methoxy-6-methyl-9*H*-carbazole-3-carbonitrile (1.11l). Following **General Procedure D** at room temperature for 22 h, the product was obtained as a yellow solid (249 mg) in 90% yield. $\mathbf{R_f}$ = 0.63 (EtOAc:Hexanes = 1:2): **^{1}H NMR** (500 MHz, acetone-d_6) δ 8.46 (s, 1H), 8.02 (s, 1H), 7.64-7.60 (m, 2H), 7.30-7.20 (m, 6H), 5.72 (s, 2H), 3.92 (s, 3H), 2.34 (s, 3H); **^{13}C NMR** (125 MHz, acetone-d_6) δ 159.6, 142.9, 142.4, 138.1, 129.6, 128.3, 128.0, 127.6, 124.7, 124.3, 122.8, 121.1, 121.0, 115.5, 110.8, 102.5, 92.7, 56.1, 47.0, 16.8; **IR** (neat) 2923, 2852, 2211, 1632, 1602, 1487, 1469, 1455, 1352, 1326, 1255, 1198, 1171, 1141, 1051, 1039, 873 cm^{-1}; **HRMS** (EI-TOF) calcd for $C_{22}H_{18}N_2O$ $[M]^+$ m/z = 326.1419, found 326.1436.

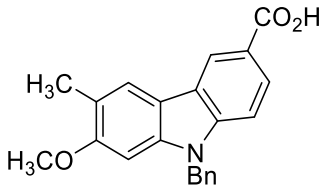

9-Benzyl-7-methoxy-6-methyl-9H-carbazole-3-carboxylic acid (1.19). To a solution of **S-5t** (90 mg, 0.28 mmol) in EtOH (1.0 mL) and H_2O (0.5 mL) was added NaOH (276 mg, 6.89 mmol). The reaction mixture was refluxed overnight and then cooled to room temperature. EtOH was removed under reduced pressure, and the resultant aqueous mixture was acidified at 0 ^oC with 2 M HCl (3.5 mL). The resultant insoluble solid was filtered, washed with water (20 mL X 2), and dried to give the product as a white solid (95 mg) in quantitative yield. $\mathbf{R_f}$ = 0.20 (EtOAc:Hexanes = 1:2): **^{1}H NMR** (500 MHz, DMSO-d_6) δ 12.50 (br s, 1H), 8.64 (d, J = 1.0 Hz, 1H), 8.01 (s, 1H), 7.92 (dd, J = 8.5, 1.5 Hz, 1H), 7.56 (d, J = 9.0 Hz, 1H), 7.29-7.18 (m, 6H), 5.69 (s, 2H), 3.87 (s, 3H), 2.30 (s, 3H); **^{13}C NMR** (125 MHz, DMSO-d_6) δ 168.0, 157.5, 142.3, 140.9, 137.4, 128.5, 127.2, 126.7, 125.4, 122.2, 121.6, 121.3, 121.2, 118.9, 114.8, 108.8, 92.1, 55.6, 45.7, 16.4; **IR** (neat) 3350, 2924, 1605, 1556, 1495, 1446, 1391, 1351, 1324, 1254, 1192, 1161, 1133, 1054, 1037, 884 cm^{-1}; **HRMS** (ESI-TOF) calcd for $C_{22}H_{20}NO_3$ $[M+H]^+$ m/z = 346.1443, found 346.1460.

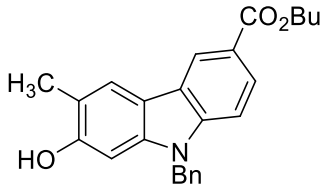

Butyl 9-benzyl-7-hydroxy-6-methyl-9*H*-carbazole-3-carboxylate (1.4l). To a solution of **S-5t** (267 mg, 0.77 mmol) in CH_2Cl_2 (11 mL) at –78 ^oC, a solution of BBr_3 (1 M in CH_2Cl_2, 1.5 mL, 1.54 mmol) was added dropwise. The resultant mixture was allowed to warm to room temperature and stirred for 40 min. The mixture was subsequently quenched with

water (15 mL) with cooling in an ice bath. The solution was extracted with EtOAc (30 mL X 3), washed with brine, and the combined organic layers were dried over Na_2SO_4. Removal of solvent yielded the product (234 mg). No further purification was necessary.

A microwave vial was charged with above product (103 mg, 0.31 mmol), *n*-BuOH (3.9 mL), and two drops of concentrated H_2SO_4. After stirring at at 100 ^oC for 22 h, the solvent was removed and the resultant residue was basified with satd $NaHCO_3$ (aq) to a pH of 8. The mixture was extracted with EtOAc (10 mL X 3) and the combined organic layers were washed with brine, dried over Na_2SO_4, filtered, and concentrated. Chromatography (hexane:ethyl acetate = 10:1) afforded the product as a tan amorphous solid (59 mg) in 49% yield. $\mathbf{R_f}$ = 0.47 (EtOAc:Hexanes = 1:2): **^{1}H NMR** (500 MHz, acetone-d_6) δ 8.70 (d, J = 1.4 Hz, 1H), 8.44 (s, 1H), 8.01 (dd, J = 8.6, 1.7 Hz, 1H), 7.96 (s, 1H), 7.52 (d, J = 8.5 Hz, 1H), 7.29-7.23 (m, 3H), 7.17 (d, J = 7.1 Hz, 2H), 6.95 (s, 1H), 5.56 (s, 2H), 4.34 (t, J = 6.5 Hz, 2H), 2.38 (s, 3H), 1.81-1.76 (m, 2H), 1.56-1.48 (m, 2H), 1.00 (t, J = 7.4 Hz, 3H); **^{13}C NMR** (125 MHz, acetone-d_6) δ 167.5, 156.4, 144.1, 142.2, 138.3, 129.5, 128.2, 127.4, 126.3, 124.0, 122.8, 122.1, 121.8, 119.2, 116.5, 109.1, 96.2, 64.7, 47.0, 31.8, 20.0, 16.6, 14.1; **IR** (neat) 3351, 2955, 2930, 1674, 1633, 1602, 1450, 1388, 1353, 1297, 1281, 1241, 1178, 1134, 1100, 1020, 997, 972, 768 cm^{-1}; **HRMS** (ESI-TOF) calcd for $C_{25}H_{26}NO_3$ $[M+H]^+$ m/z = 388.1913, found 388.1911.

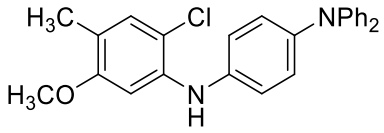

***N*^{1}-(2-Chloro-5-methoxy-4-methylphenyl)-*N*^{4},*N*^{4}-diphenylbenzene-1,4-diamine (1.8m).** Following **General Procedure A** for 18 h, the product was obtained as a pale brown solid (720 mg) in 87% yield. $\mathbf{R_f}$ = 0.40 (EtOAc:Hexanes = 1:9): **^{1}H NMR** (500 MHz, acetone-d_6) δ 7.26 (t, J = 7.4 Hz, 4H), 7.16 (d, J = 8.7 Hz, 2H), 7.13 (s, 1H), 7.03 (d, J =

7.7 Hz, 6H), 6.98 (t, *J* = 7.4 Hz, 2H), 6.90 (s, 1H), 6.83 (br s, 1H), 3.75 (s, 3H), 2.10 (s, 3H); **^{13}C NMR** (125 MHz, acetone-d_6) δ 157.9, 149.0, 142.1, 140.1, 139.8, 131.6, 130.0, 127.4, 126.7, 124.1, 123.9, 123.3, 123.2, 123.0, 120.52, 120.49, 114.2, 101.8, 55.9, 15.4; **IR** (neat) 3401, 3036, 2926, 1586, 1506, 1463, 1395, 1313, 1246, 1200, 1186, 995, 876, 819 cm^{-1}; **HRMS** (EI-TOF) calcd for $C_{26}H_{23}ClN_2O$ $[M]^+$ *m/z* = 414.1499; found 414.1508.

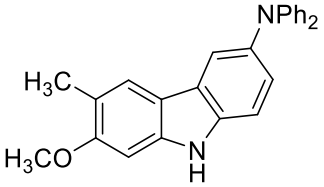

7-Methoxy-6-methyl-*N*, *N*´-diphenyl-9*H*-carbazol-3-amine (1.9m). Following **General Procedure B** for 24 h, the product was obtained as a colorless solid (529 mg) in 70% yield. **R_f** = 0.25 (EtOAc:Hexanes = 3:7): **^{1}H NMR** (500 MHz, acetone-d_6) δ 10.11 (br s, 1H), 7.75 (d, *J* = 1.9 Hz, 1H), 7.73 (s,1H), 7.43 (d, *J* = 8.5 Hz, 1H), 7.23 (t, *J* = 8.0 Hz, 4H), 7.07 (dd, *J* = 8.5, 2.0 Hz, 1H), 7.04 (d, *J* = 8.7 Hz, 5H), 6.93 (t, *J* = 7.3 Hz, 2H), 3.90 (s, 3H), 2.27 (s, 3H); **^{13}C NMR** (125 MHz, acetone-d_6) δ 158.5, 149.8, 141.6, 141.4, 140.1, 138.3, 138.1, 129.9, 125.4, 125.3, 124.7, 123.2, 122.2, 119.3, 118.7, 116.7, 112.4, 112.3, 93.50, 93.45, 55.8, 16.8; **IR** (neat) 3403, 3042, 2908, 1584, 1484, 1433, 1310, 1275, 1228, 1200, 1037 cm^{-1}; **HRMS** (EI-TOF) calcd for $C_{26}H_{22}N_2O$ $[M]^+$ *m/z* = 378.1732; found 378.1732.

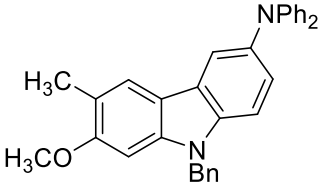

9-Benzyl-7-methoxy-6-methyl-*N*,*N*´-diphenyl-9*H*-carbazol-3-amine (1.11m). Following **General Procedure D** at room temperature for 2 h, the product was obtained as a colorless solid (222 mg) in 95% yield. **R_f** = 0.46 (EtOAc:Hexanes = 1:4): **^{1}H NMR** (500 MHz, acetone-d_6) δ 7.79 (dd, *J* = 7.8, 2.1 Hz, 2H), 7.44 (d, *J* = 8.6 Hz, 1H), 7.31-7.20 (m,

9H), 7.15 (s, 1H), 7.10 (dd, *J* = 8.6, 2.1 Hz, 1H), 7.03 (dd, *J* = 8.7, 1.0 Hz, 4H), 6.93 (t, *J* = 7.4 Hz, 2H), 5.62 (s, 2H), 3.89 (s, 3H), 2.28 (s, 3H); **^{13}C NMR** (125 MHz, acetone-d_6) δ 158.8, 149.7, 142.3, 140.5, 138.9, 138.7, 129.9, 129.5, 128.2, 127.7, 125.1, 124.6, 123.3, 122.5, 122.3, 119.5, 118.7, 116.2, 110.8, 92.2, 56.0, 47.0, 16.7; **IR** (neat) 3021, 2912, 1632, 1585, 1490, 1470, 1423, 1354, 1317, 1254, 1193, 1037, 805, 736 cm^{-1}; **HRMS** (EI-TOF) calcd for $C_{33}H_{28}N_2O$ $[M]^+$ *m/z* = 468.2202; found 468.2215.

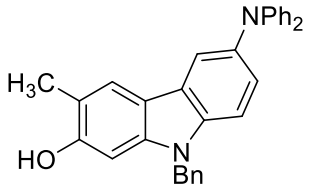

9-Benzyl-6-(diphenylamino)-3-methyl-9*H*-carbazol-2-ol (1.4m). Following **General Procedure C** at room temperature for 1.5 h, the product was obtained as a white solid (105 mg) in 93% yield. **R_f** = 0.30 (EtOAc:Hexanes = 1:4): **^{1}H NMR** (500 MHz, $CDCl_3$) δ 7.77 (br s, 1H), 7.67 (s, 1H), 7.29-7.07 (m, 15H), 6.92 (s, 2H), 6.71 (s, 1H), 5.36 (s, 2H), 4.76 (s, 1H), 2.34 (s, 3H); **^{13}C NMR** (125 MHz, acetone-d_6) δ 155.2, 148.8, 141.2, 139.4, 137.93, 137.90, 128.9, 128.5, 127.1, 126.6, 124.3, 123.6, 122.3, 121.8, 121.3, 117.6, 117.3, 115.4, 109.5, 94.8, 46.1, 15.6; **IR** (neat) 3421, 2923, 1632, 1585, 1490, 1393, 1367, 1355, 1310, 648 cm^{-1}; **HRMS** (EI-TOF) calcd for $C_{32}H_{26}N_2O$ $[M]^+$ *m/z* 454.2045; found 454.2072.

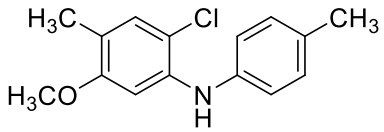

2-Chloro-5-methoxy-4-methyl-*N*-(*p*-tolyl)aniline (1.8n). Following **General Procedure A** for 20 h, the product was obtained as yellow oil (443 mg) in 73% yield. **R_f** = 0.75 (EtOAc:Hexanes = 1:4): **^{1}H NMR** (500 MHz, acetone-d_6) δ 7.12 (d, *J* = 8.0, 2H), 7.08 (s, 1H), 7.04 (d, *J* = 8.5, 2H), 6.72 (s, 1H), 6.72 (s, 1H), 5.88 (br s, 1H), 3.96 (s, 3H), 2.32 (s,

3H), 2.12 (s, 3H); **^{13}C NMR** (125 MHz, acetone-d_6) δ 2 rotamers; **IR** (neat) 3420, 2921, 1589, 606 cm^{-1}; **HRMS** (ESI-TOF) calcd for $C_{15}H_{17}ClNO$ $[M+H]^+$ 262.0999, found 262.1003.

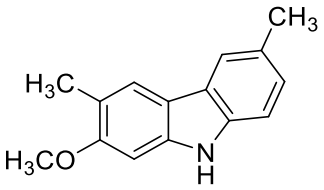

2-Methoxy-3,6-dimethyl-9*H*-carbazole (1.9n). Following **General Procedure B**, the product was obtained as a brown solid (1.39 g) in 83% yield. **R_f** = 0.30 (EtOAc:Hexanes = 1:4): **^{1}H NMR** (500 MHz, acetone-d_6) δ 7.79 (s, 1H), 7.74 (s, 2H), 7.25 (d, *J* = 8.0 Hz, 1H), 7.12 (d, *J* = 7.0 Hz, 1H), 6.84 (s, 1H), 3.91 (s, 3H), 2.56 (s, 3H), 2.35 (s, 3H); **^{13}C NMR** (125 MHz, acetone-d_6) δ 157.3, 140.3, 138.2, 127.5, 125.0, 123.5, 121.0, 118.9, 117.9, 115.8, 110.1, 92.6, 54.8, 20.6, 15.0; **IR** (neat) 3390, 2920, 1634, 1615, 818, 746 cm^{-1}; **HRMS** (ESI-TOF) calcd for $C_{15}H_{16}NO$ $[M+H]^+$ 226.1232, found 226.1229.

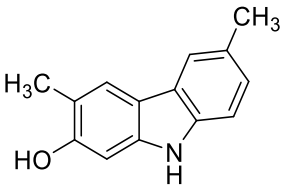

3,6-Dimethyl-9*H*-carbazol-2-ol (1.10n). Following **General Procedure C**, the product was obtained as a brown solid (510 mg) in 94% yield. **R_f** = 0.24 (EtOAc:Hexanes = 1:2): **^{1}H NMR** (500 MHz, acetone-d_6) δ 9.75 (s, 1H), 8.15 (s, 1H), 7.74 (s, 1H), 7.72 (d, *J* = 0.6 Hz, 1H), 7.26 (d, *J* = 8.2 Hz, 1H), 7.06 (dd, *J* = 8.2, 1.3 Hz, 1H), 6.93 (s, 1H), 2.44 (s, 3H), 2.34 (s, 3H); **^{13}C NMR** (125 MHz, acetone-d_6) δ 155.5, 141.3, 139.1, 128.2, 125.8, 124.6, 122.1, 119.7, 117.4, 116.9, 110.9, 97.1, 21.5, 16.8; **IR** (neat) 3398, 2921, 1603, 826, 744, 719, 640 cm^{-1}; **HRMS** (ESI-TOF) calcd for $C_{14}H_{14}NO$ $[M+H]^+$ 212.1075, Found 212.1080.

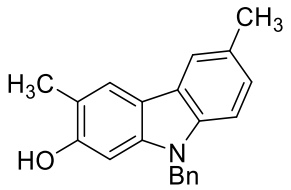

9-Benzyl-3,6-dimethyl-9*H*-carbazol-2-ol (1.4n). Following **General Procedure D**, the product was obtained as a yellow solid (81 mg) in 53% yield. $\mathbf{R_f}$ = 0.40 (EtOAc:Hexanes = 1:4): **^{1}H NMR** (500 MHz, acetone-d_6) δ 8.22 (s, 1H), 7.80 (s, 1H), 7.79 (s, 1H), 7.30 (d, *J* = 8.3 Hz, 1H), 7.27-7.21 (m, 3H), 7.14 (d, *J* = 7.0 Hz, 2H), 7.10 (dd, *J* = 8.3, 1.1 Hz, 1H), 6.86 (s, 1H), 5.46 (s, 2H), 2.46 (s, 3H), 2.35 (s, 3H); **^{13}C NMR** (125 MHz, acetone-d_6) δ 154.8, 140.9, 138.9, 138.2, 128.5, 127.8, 127.1, 126.5, 125.1, 123.5, 121.5, 119.0, 116.8, 115.6, 108.3, 94.8, 45.9, 20.5, 15.7. **IR** (neat) 3421, 2919, 2852, 1494, 863, 796, 735, 697 cm^{-1}; **HRMS** (ESI-TOF) calcd for $C_{21}H_{20}NO$ $[M+H]^+$ 302.1545, Found: 302.1545.

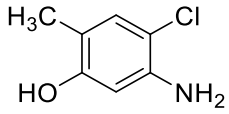

5-Amino-4-chloro-2-methylphenol. Following **General Procedure C**, the product was obtained as a light tan solid (244 mg) in 49% yield. $\mathbf{R_f}$ = 0.22 (EtOAc:Hexanes = 1:5): **^{1}H NMR** (500 MHz, CD_3CN) δ 6.97 (s, 1H), 6.25 (s, 1H), 4.50 (s, 1H), 3.82 (br s, 2H), 2.12 (s, 3H); **^{13}C NMR** (125 MHz, CD_3CN) δ 155.4, 143.5, 131.4, 115.8, 110.0, 103.3, 15.2; **IR** (neat) 3405, 3416, 3195 (w), 2923, 1618, 1515, 1413, 1378, 1311, 1274, 1197, 1164, 988, 847, 723, 630, 460 cm^{-1}; **HRMS** (ESI-TOF) *m/z* = 158.0373 calcd for C_7H_9ClNO $[M+H]^+$, found 158.0380.

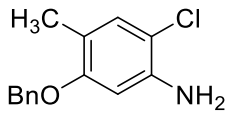

5-(Benzyloxy)-2-chloro-4-methylaniline (1.14). Following **General Procedure D** using 1 equiv NaH, 1 equiv BnBr, 2.4 mL DMF and 24 mL THF on a 2.41 mmol scale, the product

was obtained as a light tan solid (372 mg) in 62% yield. $\mathbf{R_f}$ = 0.40 (EtOAc:Hexanes = 1:5): **^{1}H NMR** (500 MHz, $CDCl_3$) δ 7.43-7.31 (m, 5H), 7.01 (s, 1H), 6.34 (s, 1H), 5.01 (s, 2H), 3.88 (s, 2H), 2.15 (s, 3H); **^{13}C NMR** (125 MHz, $CDCl_3$) δ 156.3, 141.2, 137.2, 130.6, 128.5, 127.8, 127.0, 118.3, 110.4, 100.4, 70.1, 15.3; **IR** (neat) 3465, 3390, 2945, 1619, 1506, 1454, 1413, 1380, 1282, 1265, 1215, 1201, 1169. 1079, 1045, 1028, 988, 875, 819, 801, 734, 695, 651 cm^{-1}; **HRMS** (ESI-TOF) *m/z* = 248.0842 calcd for $C_{14}H_{15}ClNO$ $[M+H]^+$, found 248.0839.

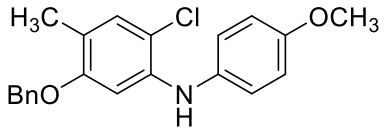

5-(Benzyloxy)-2-chloro-*N*-(4-methoxyphenyl)-4-methylaniline (1.16). Following **General Procedure A**, the product was obtained as red oil (316 mg) in 68% yield. $\mathbf{R_f}$ = 0.80 (EtOAc:Hexanes = 1:5): **^{1}H NMR** (500 MHz, $CDCl_3$) δ 7.38-7.31 (m, 5H), 7.09 (s, 1H), 6.97 (dd, *J* = 6.7, 2.2 Hz, 2H), 6.84 (dd, *J* = 5.7, 3.5 Hz, 2H), 6.55 (s, 1H), 5.79 (s, 1H), 4.92 (s, 2H), 3.82 (s, 3H), 2.18 (s, 3H); **^{13}C NMR** (125 MHz, acetone-d_6) δ 157.3, 157.0, 141.8, 138.8, 136.5, 132.1, 129.8, 129.0, 128.5, 124.0, 119.6, 115.9, 112.9, 101.4, 71.0, 56.3, 16.1; **IR** (neat) 3400, 2940, 1611, 1578, 1508, 1489, 1454, 1416, 1399, 1375, 1287, 1242, 1164, 1032, 1002, 841, 820, 775, 735, 696, 655, 600 cm^{-1}; **HRMS** (ESI-TOF) *m/z* = 354.1261 calcd for $C_{21}H_{21}ClNO_2$ $[M+H]^+$, found 354.1268.

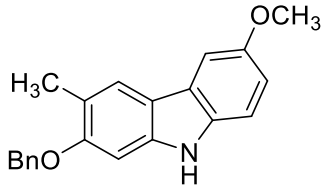

2-(Benzyloxy)-6-methoxy-3-methyl-9*H*-carbazole (1.17). Following **General Procedure B**, the product was obtained as a light tan solid (161 mg) in 80% yield. $\mathbf{R_f}$ = 0.23 (EtOAc:Hexanes = 1:4): **^{1}H NMR** (500 MHz, acetone-d_6) δ 9.86 (br s, 1H), 7.83 (s,

1H), 7.55-7.53 (m, 3H), 7.41 (td, *J* = 5.8, 1.6 Hz, 2H), 7.34-7.31 (m, 2H), 7.07 (s, 1H), 6.91 (dd, *J* = 8.7, 2.5 Hz, 1H), 5.19 (s, 2H), 3.86 (s, 3H), 2.38 (s, 3H); **^{13}C NMR** (125 MHz, acetone-d_6) δ 157.3, 154.7, 141.5, 138.8, 135.7, 129.3, 128.5, 128.1, 124.7, 122.1, 119.0, 117.3, 113.8, 111.9, 103.2, 95.0, 70.6, 56.1, 17.1; **IR** (neat) 3385, 2910, 1648, 1486, 1472, 1450, 1429, 1298, 1276, 1217, 1203, 1179, 1170, 1135, 1113, 1026, 839, 837, 813, 743, 699, 468 cm^{-1}; **HRMS** (ESI-TOF) *m/z* = 317.1416 calcd for $C_{21}H_{19}NO_2$ $[M]^+$, found 317.1430.

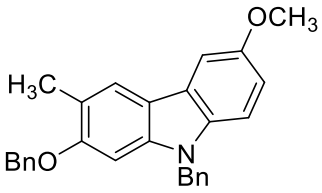

9-Benzyl-2-(benzyloxy)-6-methoxy-3-methyl-9*H*-carbazole (1.18). Following **General Procedure D** using 1.1 equiv NaH, 1.1 equiv BnBr, 0.51 mL DMF and 5.1 mL THF on a 0.51 mmol scale, the product was obtained as a light tan solid (129 mg) in 62% yield. **R_f** = 0.65 (EtOAc:Hexanes = 1:5): **^{1}H NMR** (500 MHz, acetone-d_6) δ 7.88 (s, 1H), 7.60 (d, *J* = 2.5 Hz, 1H), 7.52 (d, *J* = 7.5 Hz, 2H), 7.39 (t, *J* = 7.2 Hz, 2H), 7.33-7.31 (m, 2H), 7.24-7.20 (m, 4H), 7.16 (dd, *J* = 8.2 Hz, 1.5 Hz, 2H), 6.93 (dd, *J* = 8.8, 2.5 Hz, 1H), 5.86 (s, 2H), 5.21 (s, 2H), 3.86 (s, 3H), 2.39 (s, 3H); **^{13}C NMR** (125 MHz, acetone-d_6) δ 157.5, 155.0, 142.0, 139.1, 138.7, 136.3, 129.4, 129.3, 128.5, 128.3, 128.0, 127.6, 124.5, 122.4, 119.2, 116.8, 113.7, 110.5, 103.5, 93.7, 70.7, 56.1, 46.9, 17.0; **IR** (neat) 2910, 1645, 1494, 1474, 1464, 1454, 1441, 1431, 1305, 1252, 1234, 1226, 1202, 1181, 1141, 1053, 1027, 807, 793, 778, 732, 698 cm^{-1}; **HRMS** (ESI-TOF) *m/z* = 408.1964 calcd for $C_{28}H_{26}NO_2$ $[M+H]^+$, found 408.1960.

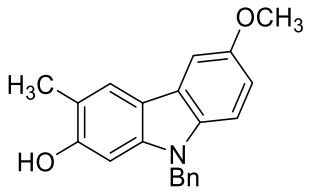

2-(Benzyloxy)-6-methoxy-3,9-dimethyl-9*H*-carbazole (1.4o). Mono debenzylation of **S-5j** following the procedure for **4h** afforded a tan solid (39 mg) in 58% yield. $\mathbf{R_f}$ = 0.17 (EtOAc:Hexanes = 1:5): **^{1}H NMR** (500 MHz, acetone-d_6) δ 8.29 (s, 1H), 7.83 (s, 1H), 7.59 (dd, *J* = 2.4 Hz, 1H), 7.31 (d, *J* = 8.8 Hz, 1H), 7.25-7.20 (m, 3H), 7.13 (d, *J* = 7.1 Hz, 2H), 6.92 (dd, *J* = 8.8, 2.5 Hz, 1H), 6.86 (s, 1H), 5.44 (s, 2H), 3.86 (s, 3H), 2.35 (s, 3H); **^{13}C NMR** (125 MHz, acetone-d_6) δ 156.0, 155.0, 142.3, 139.2, 136.5, 129.5, 128.1, 127.5, 124.8, 122.7, 117.7, 116.8, 113.4, 110.2, 103.6, 95.8, 56.2, 47.0, 16.7; **IR** (neat) 3375, 2910, 1633, 1474, 1453, 1433, 1298, 1275, 1253, 1233, 1219, 1202, 1182, 1170, 1140, 1046, 1014, 823, 803, 732, 700, 632 cm^{-1}; **HRMS** (ESI-TOF) *m/z* = 318.1494 calcd for $C_{21}H_{20}NO_2$ $[M+H]^+$, found 318.1492.

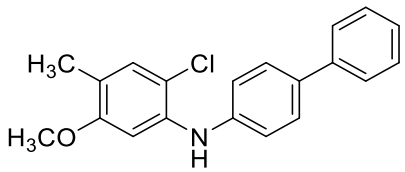

***N*-(2-Chloro-5-methoxy-4-methylphenyl)-[1,1'-biphenyl]-4-amine (1.8p).** Following **General Procedure A**, the product was obtained as a white solid (412 mg) in 73% yield. $\mathbf{R_f}$ = 0.75 (EtOAc:Hexanes = 1:4): **^{1}H NMR** (500 MHz, $CDCl_3$) δ 7.60 (d, *J* = 8.0 Hz, 2H), 7.57 (d, *J* = 9.0 Hz, 2H), 7.45 (t, *J* = 7.5 Hz, 2H), 7.33 (t, *J* = 7.5 Hz, 1H), 7.21 (d, *J* = 8.5 Hz, 2H), 7.15 (s, 1H), 6.89 (s, 1H), 6.03(br s, 1H), 3.76 (s, 3H), 2.17 (s, 3H); **^{13}C NMR** (125 MHz, $CDCl_3$) δ 157.0, 141.9, 140.8, 138.1, 134.8, 131.0, 128.9, 128.2, 126.9, 126.2, 120.2, 119.1, 113.4, 100.4, 55.7, 15.4; **IR** (neat) 3400, 2921, 1589, 1523, 1486, 1450, 1412, 1374, 1248, 1232, 992, 822 cm^{-1}; **HRMS** (ESI-TOF) calcd for $C_{20}H_{19}ClNO$ $[M+H]^+$ *m/z* =

324.1155, found 324.1176.

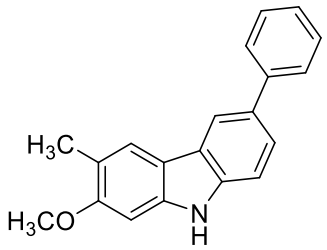

2-Methoxy-3-methyl-6-phenyl-9*H*-carbazole (1.9p). Following **General Procedure B**, the product was obtained as a brown solid (143 mg) in 83% yield. $\mathbf{R_f}$ = 0.25 (EtOAc:Hexanes = 1:4): **^{1}H NMR** (500 MHz, $CDCl_3$) δ 8.20 (s, 1H), 7.86 (s, 1H), 7.74 (d, *J* = 7.0 Hz, 2H), 7.64 (br s, 1H), 7.58 (d, *J* = 8.0 Hz, 1H), 7.50 (t, *J* = 7.5 Hz, 2H), 7.37 (t, *J* = 7.5 Hz, 1H), 7.29 (d, *J* = 8.0 Hz, 1H), 6.68 (s, 1H), 3.84 (s, 3H), 2.42 (s, 3H); **^{13}C NMR** (125 MHz, $CDCl_3$) δ 157.7, 142.4, 139.9, 138.9, 132.9, 128.8, 127.4, 126.5, 124.1, 123.8, 121.6, 119.5, 117.9, 116.3, 110.6, 92.7, 55.5, 16.8; **IR** (neat) 3390, 2925, 1621, 1481, 1323, 1284, 1226, 1195, 1171, 1034, 881, 752 cm^{-1}; **HRMS** (ESI-TOF) calcd for $C_{20}H_{18}NO$ $[M+H]^+$ *m/z* = 288.1388, found 288.1387.

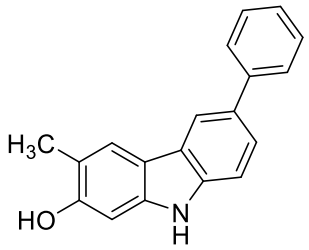

3-Methyl-6-phenyl-9*H*-carbazol-2-ol (1.10p), Following **General Procedure C**, the product was obtained as a dark brown solid (103 mg) in 76% yield. $\mathbf{R_f}$ = 0.21 (EtOAc:Hexanes = 1:2): **^{1}H NMR** (500 MHz, CD_3CN) δ 8.74 (br s, 1H), 7.88 (d, *J* = 1.5 Hz, 1H), 7.52 (s, 1H), 7.39 (dd, *J* = 8.0, 1.0 Hz, 2H), 7.23 (dd, *J* = 8.0, 1.5 Hz, 1H), 7.15-7.12 (m, 3H), 6.99 (td, *J* = 8.0, 1.0 Hz, 1H), 6.67 (br s, 1H), 6.59 (s, 1H), 2.00 (s, 3H); **^{13}C NMR** (125 MHz, CD_3CN) δ 155.5, 143.1, 141.2, 140.3, 132.9, 129.8, 127.9, 127.3, 124.9, 124.2,

122.6, 118.4, 118.1, 117.2, 111.7, 97.3, 16.7; **IR** (neat) 3409, 2923, 1635, 1480, 1398, 1264, 1175, 1122, 1009, 879, 764 cm^{-1}; **HRMS** (ESI-TOF) calcd for $C_{19}H_{16}NO$ $[M+H]^+$ m/z = 274.1232, found 274.1245.

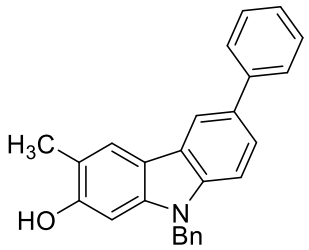

9-Benzyl-3-methyl-6-phenyl-9*H*-carbazol-2-ol (1.4p). Following **General Procedure D**, the product was obtained as a white powder (71 mg) in 52% yield. $\mathbf{R_f}$ = 0.45 (EtOAc:Hexanes = 1:2): **^{1}H NMR** (500 MHz, $CDCl_3$) δ 8.22 (d, *J* = 1.5 Hz, 1H), 7.89 (s, 1H), 7.70 (dd, *J* = 8.5, 1.5 Hz, 2H), 7.59 (dd, *J* = 8.5, 1.5 Hz, 1H), 7.47 (t, *J* = 8.0 Hz, 2H), 7.36-7.32 (m, 2H), 7.30-7.24 (m, 3H), 7.16 (d, *J* = 8.0 Hz, 2H), 6.76 (s, 1H), 5.43 (s, 2H), 4.81 (s, 1H), 2.43 (s, 3H); **^{13}C NMR** (125 MHz, $CDCl_3$) δ 153.5, 142.3, 141.2, 140.3, 137.2, 132.8, 128.9, 128.8, 127.6, 127.4, 126.5, 126.4, 124.0, 123.8, 122.1, 118.1, 117.1, 116.4, 108.8, 95.3, 46.8, 16.2; **IR** (neat) 3305, 2920, 1634, 1607, 1482, 1466, 1454, 1368, 1348, 1300, 1249, 1219, 1174, 1139, 998, 871 cm^{-1}; **HRMS** (ESI-TOF) calcd for $C_{26}H_{22}NO$ $[M+H]^+$ *m/z* = 364.1701, found 364.1692.

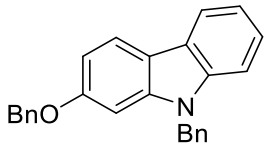

9-Benzyl-2-(benzyloxy)-9*H*-carbazole. To a stirring solution of DMF (20 mL) and NaH concentrated to a volume of 25 mL and EtOAc was added. The resultant precipitate was filtered and (784 mg, 32.7 mmol) was added a solution of 2-hydroxycarbazole (2.00 g, 10.9 mmol) in THF (75 mL). After stirring 30 min at room temperature, BnBr (4.50 mL, 38.5 mmol) was added to the solution. After stirring 3 h, the solution was quenched with

H_2O (100 mL), extracted with CH_2Cl_2 (3 X 100 mL), washed with brine (100 mL), and dried with $MgSO_4$. After filtration, the solution was washed with cold EtOAc to afford a white powder (3.85 g) in 97% yield. $\mathbf{R_f}$ = 0.5 (EtOAc:Hexanes = 1:4): **^{1}H NMR** (500 MHz, CD_2Cl_2) δ 8.02 (d, *J* = 7.6 Hz, 1H), 7.99 (d, *J* = 8.5 Hz, 1H), 7.45 (d, *J* = 7.1 Hz, 2H), 7.38 (td, *J* = 8.6, 1.0 Hz, 2H), 7.36-7.31 (m, 3H), 7.24 (m, 4H), 7.13 (d, *J* = 6.7 Hz, 2H), 6.95-6.92 (m, 2H), 5.45 (s, 2H) 5.12 (s, 2H); **^{13}C NMR** (125 MHz, CD_2Cl_2) δ 159.0 142.6, 141.4, 137.87, 137.85, 129.3, 129.0, 128.5, 128.2, 128.0, 127.1, 125.2, 123.7, 121.6, 120.0, 119.9, 117.6, 109.3, 108.9, 95.2, 71.0, 47.1; **IR** (neat) 3020, 1626, 1598, 1495, 1460, 1451, 1437, 1359, 1328, 1246, 1179, 1120, 1009, 993, 944, 820, 804, 735, 726, 719, 695 cm^{-1}; **HRMS** (ESI-TOF) *m/z* = 363.1623 calcd for $C_{26}H_{21}NO$ $[M]^+$, found 363.1612.

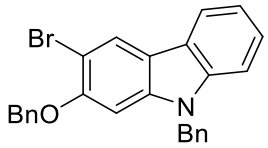

9-Benzyl-2-(benzyloxy)-3-bromo-9*H*-carbazole (1.13). To a stirring solution of 9-benzyl-2-(benzyloxy)-9*H*-carbazole (1.45 g, 3.99 mmol) and CH_2Cl_2 (40 mL) was added *N*-bromosuccinimide (729 mg, 4.11 mmol). After stirring 30 min at room temperature, the mixture was quenched with ice-cold water, extracted with EtOAc, washed (3 X 20 mL) with brine (30 mL), and dried with $MgSO_4$. After filtration and concentration, trituration with acetone (3 X 10 mL) afforded a white solid (1.46 g) in 83% yield. $\mathbf{R_f}$ = 0.43 (EtOAc:Hexanes = 1:4): **^{1}H NMR** (500 MHz, $CDCl_3$) δ 8.26 (s, 1H), 7.98 (d, *J* = 7.7 Hz, 1H), 7.47 (d, *J* = 7.5 Hz, 2H), 7.35 (m, 5H), 7.24 (m, 4H), 7.08 (dd, *J* = 5.2, 1.7 Hz, 2H), 6.87 (s, 1H), 5.42 (s, 2H), 5.16 (s, 2H); **^{13}C NMR** (125 MHz, CD_2Cl_2) δ 154.2, 141.31, 141.29, 137.4, 137.2, 129.4, 129.1, 128.5, 128.1, 127.9, 127.0, 125.8, 125.1, 122.7, 120.3, 120.2, 118.4, 109.5, 104.4, 95.2, 71.8, 47.1; **IR** (neat) 3015, 1597, 1469, 1445, 1433, 1356, 1307, 1273, 1249, 1182, 1151, 1121, 1024, 996, 748, 736, 724, 715, 695, 673, 616

cm^{-1}; **HRMS** (ESI-TOF) *m/z* = 363.1623 calcd for $C_{26}H_{20}BrNO$ $[M]^+$, found 363.1612.

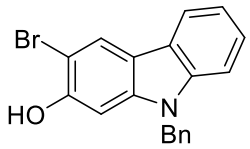

9-Benzyl-3-bromo-9*H*-carbazol-2-ol (1.4q). To a stirring solution of 9-benzyl-2-(benzyloxy)-3-bromo-9*H*-carbazole (1.20 g, 2.72 mmol) in CH_2Cl_2 (30.0 mL) was added *N,N*-dimethylaniline (3.40 mL, 27.2 mmol) followed by the slow addition of $AlCl_3$ (2.18 g, 16.32 mmol). After stirring 10 min at room temperature, the solution was cooled to 0 ^{0}C and quenched with H_2O (30 mL). The solution was extracted with EtOAc (3 X 30 mL), washed with brine (30 mL), and dried with $MgSO_4$. Removal of solvent and chromatography (5:1 Hex/EtOAc) afforded a white solid (382 mg) in 40% yield. $\mathbf{R_f}$ = 0.27 (EtOAc:Hexanes = 1:4): **^{1}H NMR** (500 MHz, acetone-d_6) δ 8.72 (br s, 1H), 8.29 (s, 1H), 8.08 (d, *J* = 8.5 Hz, 1H), 7.47 (d, *J* = 8.2 Hz, 1H), 7.36 (td, *J* = 8.3, 1.1 Hz, 1H), 7.28-7.18 (m, 4H), 7.16(d, *J* = 7.1 Hz, 2H), 7.10 (s, 1H), 5.52 (s, 2H); **^{13}C NMR** (125 MHz, acetone-d_6) δ 153.4, 142.2, 142.0, 138.5, 129.6, 128.3, 127.5, 126.0, 125.1, 123.3, 120.53, 120.45, 118.5, 110.0, 102.9, 97.3, 47.0; **IR** (neat) 3410 (w), 2925, 1601, 1475, 1451, 1380, 1360, 1337, 1318, 1262, 1216, 1157, 1120, 1079, 1059, 1020, 946, 883, 824, 738, 717, 696 cm^{-1}; **HRMS** (ESI-TOF) *m/z* = 351.0259 calcd for $C_{19}H_{14}BrNO$ $[M]^+$, found 351.0283.

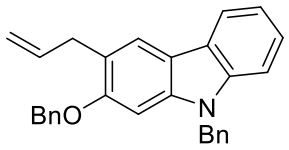

3-Allyl-9-benzyl-2-(benzyloxy)-9*H*-carbazole. To a flask charged with 9-benzyl-2-(benzyloxy)-3-bromo-9*H*-carbazole (300 mg, 0.680 mmol), $Pd(OAc)_2$ (7.60 mg, 0.034 mmol), and CPhos(24 mg, 0.068 mmol), was added THF (0.7 mL) followed by allyl zinc bromide[27] (1.85 mL, 1.02 mmol). After stirring 18 h under Ar atmosphere, the solution was

quenched with H_2O (10 mL), extracted with EtOAc (3 X 20 mL), washed with brine (20 mL), and dried with $MgSO_4$. Removal of solvent and chromatography (10:1 Hex/EtOAc) afforded a white solid (183 mg) in 67% yield. $\mathbf{R_f}$ = 0.6 (EtOAc:Hexanes = 1:5): **^{1}H NMR** (500 MHz, acetone-d_6) δ 8.04 (dt, J = 7.9, 1.0 Hz, 1H), 7.92 (d, J = 7.7 Hz, 1H), 7.52 (dt, J = 7.5, 0.5 Hz, 2H), 7.46 (d, J = 8.5 Hz, 1H), 7.39 (td, J = 7.5, 1.5 Hz, 2H), 7.32-7.25 (m, 6H), 7.19 (dd, J = 8.3, 1.5 Hz, 2H), 7.14 (td, J = 7.0, 0.5 Hz, 1H), 6.14-6.09 (m, 1H), 5.62 (s, 2H), 5.23 (s, 2H), 5.10 (dd, J = 17.1, 3.8 Hz, 1H), 5.01 (dd, J = 11.3, 2.4 Hz, 1H), 3.57 (d, J = 6.6 Hz, 2H); **^{13}C NMR** (125 MHz, acetone-d_6) δ 157.1, 141.7, 141.5, 139.0, 138.9, 138.6, 129.5, 129.4, 128.6, 128.4, 128.2, 127.7, 125.1, 124.1, 122.1, 121.9, 120.2, 120.0, 117.03, 115.4, 110.0, 94.1, 71.0, 46.9, 35.7; **IR** (neat) 3010, 1602, 1495, 1480, 1462, 1448, 1355, 1328, 1254, 1175, 1156, 1145, 1122, 1056, 1028, 910, 807, 740, 731, 719, 694 cm^{-1}; **HRMS** (ESI-TOF) m/z = 403.1936 calcd for $C_{29}H_{25}NO$ $[M]^+$, found 403.1939.

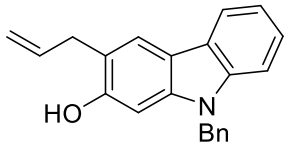

3-Allyl-9-benzyl-9*H*-carbazol-2-ol (1.4r). Mono debenzylation of **S-9** following the procedure for **1.4q** afforded a white solid (22 mg) in 63% yield. $\mathbf{R_f}$ = 0.23 (EtOAc:Hexanes = 1:5): **^{1}H NMR** (500 MHz, acetone-d_6) δ 8.35 (s, 1H), 8.01 (dd, J = 7.6, 0.7 Hz, 1H), 7.85 (s, 1H), 7.45 (d, J = 8.2 Hz, 1H), 7.31-7.21 (m, 4H), 7.18-7.12 (m, 3H), 6.91 (s, 1H), 6.15-6.07 (m, 1H), 5.51 (s, 2H), 5.11 (dd, J = 19.1, 2.1 Hz, 1H), 5.01 (dd, J = 10.1, 1.3 Hz, 1H), 3.53 (d, J = 6.6 Hz, 2H); **^{13}C NMR** (125 MHz, acetone-d_6) δ 155.4, 141.8, 141.6, 138.98, 138.97, 129.5, 128.2, 127.5, 125.0, 124.3, 122.0, 120.6, 120.0, 119.9, 116.9, 115.2, 109.6, 96.0, 46.9, 35.4; **IR** (neat) 3300 (w), 2995, 1636, 1604, 1495, 1467, 1450, 1441, 1348, 1319, 1247, 1178, 1139, 1122, 959, 914, 823, 741, 729, 709, 697, 603 cm^{-1}; **HRMS** (ESI-TOF) m/z = 313.1467 calcd for $C_{22}H_{19}NO$ $[M]^+$, found 313.1466.

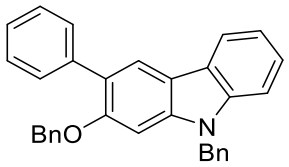

9-Benzyl-2-(benzyloxy)-3-phenyl-9*H*-carbazole. 9-Benzyl-2-(benzyloxy)-3-bromo-9*H*-carbazole (300 mg, 0.680 mmol), potassium phenyl trifluoroborate (188 mg, 1.02 mmol), $Pd(dppf)Cl_2$ (28 mg, 0.0340 mmol), and cesium carbonate (775 mg, 2.38 mmol) were treated with a 2:1 mixture of THF and H_2O (30 mL). After stirring 18 h at 70 ^{0}C, the solution was cooled to room temperature and diluted with H_2O (20 mL). The solution was then extracted with EtOAc (3 X 30 mL), washed with brine (30 mL), and dried with $MgSO_4$. Removal of solvent and chromatography (5:1 = Hex/EtOAc) afforded a white solid (257 mg) in 88% yield. $\mathbf{R_f}$ = 0.52 (EtOAc:Hexanes = 1:5): **^{1}H NMR** (500 MHz, CD_2Cl_2) δ 8.12 (s, 1H), 8.10 (d, *J* = 7.5 Hz, 1H), 7.73 (d, *J* = 7.5 Hz, 2H), 7.50 (t, *J* = 7.5 Hz, 2H), 7.41-7.28 (m, 12H), 7.19 (d, *J* = 6.0 Hz, 2H), 7.04 (s, 1H), 5.49 (s, 2H), 5.15 (s, 2H); **^{13}C NMR** (125 MHz, CD_2Cl_2) δ 155.8, 141.7, 141.3, 140.1, 137.8, 137.7, 130.6, 129.3, 129.0, 128.5, 128.3, 128.1, 127.7, 127.1, 127.0, 125.3, 124.8, 123.8, 123.0, 120.1, 120.0, 117.3, 109.4, 94.2, 71.3, 47.1; **IR** (neat) 2940, 1601, 1456, 1448, 1430, 1351, 1314, 1262, 1225, 1210, 1179, 1125, 1028, 1021, 809, 764, 737, 732, 701, 692, 662 cm^{-1}; **HRMS** (ESI-TOF) *m/z* = 440.2014 calcd for $C_{32}H_{26}NO$ $[M+H]^+$, found 440.2003.

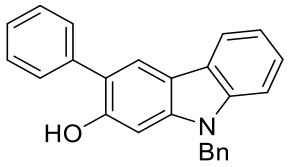

9-Benzyl-3-phenyl-9*H*-carbazol-2-ol (1.4s). Mono debenzylation of **S-10** following the procedure for **1.4q** afforded a white solid (25 mg) in 71% yield. $\mathbf{R_f}$ = 0.24 (EtOAc:Hexanes = 1:5): **^{1}H NMR** (500 MHz, acetone-d_6) δ 8.39 (br s, 1H), 8.10 (d, *J* = 7.7 Hz, 1H), 8.06 (s,

1H), 7.66 (dd, *J* = 8.3, 1.3 Hz, 2H), 7.51 (d, *J* = 8.2 Hz, 1H), 7.42 (t, *J* = 5.8 Hz, 2H), 7.36-7.30 (m, 4H), 7.29 (dd, *J* = 6.0, 1.7 Hz, 1H), 7.22 (dd, *J* = 8.5, 1.4 Hz, 2H), 7.18 (td, *J* = 7.8, 0.8 Hz, 1H), 7.03 (s, 1H), 5.58, (s, 2H); **^{13}C NMR** (125 MHz, $CDCl_3$) δ 152.0, 142.0, 141.2, 138.0, 137.2, 129.8, 129.6, 129.0, 127.8, 127.7, 126.7, 125.0, 123.5, 121.9, 121.6, 119.74, 119.65, 117.4, 109.0, 95.6, 46.9 cm^{-1}; **IR** (neat) 3495 (w), 2910, 1633, 1603, 1490, 1477, 1453, 1431, 1353, 1324, 1291, 1263, 1218, 1167, 1122, 950, 822, 744, 723, 700, 660, 608 cm^{-1}; **HRMS** (ESI-TOF) *m/z* = 350.1545 calcd for $C_{25}H_{20}NO$ $[M+H]^+$, found 350.1556.

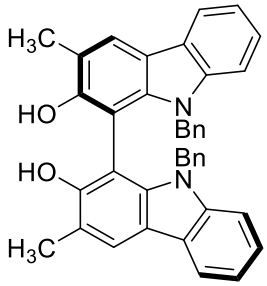

9,9'-Dibenzyl-3,3'-dimethyl-9H,9'H-[1,1'-bicarbazole]-2,2'-diol (1.5a). Following **General Procedure E**, the product was obtained as a yellow solid (109 mg) in 91% yield. R_f = 0.65 (EtOAc:Hexanes = 1:4): ^{1}H NMR (500 MHz, acetone-d_6) δ 8.06 (d, *J* = 8.0 Hz, 2H), 7.94 (s, 2H), 7.23 (td, *J* = 8.2, 1.2 Hz, 2H), 7.17 (t, *J* = 7.2 Hz, 2H), 7.08 (d, *J* = 8.1 Hz, 2H), 6.85-6.82 (m, 8H), 6.46-6.44 (m, 4H), 4.83 (d, *J* = 17.3 Hz, 2H), 4.61 (d, *J* = 17.3 Hz, 2H), 2.21 (s, 6H); ^{13}C NMR (125 MHz, acetone-d_6) δ 153.6, 141.7, 139.0, 138.0, 127.5, 126.0, 125.4, 123.9, 123.1, 122.0, 119.0, 118.6, 117.5, 116.8, 109.0, 101.0, 46.5, 16.2; IR (neat) 3513, 2923, 1603, 736, 706 cm^{-1}; HRMS (ESI-TOF) calcd for $C_{40}H_{33}N_2O_2$ $[M-H]$ $C_{40}H_{32}N_2O_2$ 571.2386, found 571.2380; $[\alpha]_D^{22}$ +164 (*c* 0.35, 87% ee, CH_2Cl_2); Chiral HPLC: Chiralpak IA column (10% *i*-PrOH/hexanes, 1 mL/min) t_R(*1*) = 8.12 min, t_R(*2*) = 11.8 min.

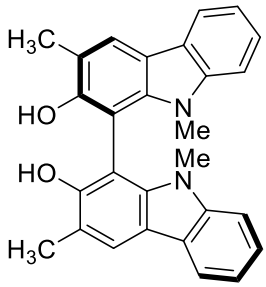

3,3',9,9'-Tetramethyl-9*H*,9'*H*-[1,1'-bicarbazole]-2,2'-diol (1.5b). Following **General Procedure E**, the product was obtained as a yellow solid (9.0 mg) in 82% yield. R_f = 0.63 (EtOAc:Hexanes = 1:4): ^{1}H NMR (500 MHz, acetone-d_6) δ 8.03 (dd, *J* = 7.8, 0.8 Hz, 2H), 8.00 (d, *J* = 1.0 Hz, 2H), 7.31-7.30 (m, 4H), 7.25 (s, 2H), 7.16 (ddd, *J* = 2.9, 5.2, 7.9 Hz, 2H), 3.45 (s, 6H), 2.45 (s, 6H); ^{13}C NMR (125 MHz, acetone-d_6) δ 153.9, 141.7, 139.8, 123.9, 122.9, 122.1, 118.8, 118.6, 117.0, 116.3, 108.4, 101.7, 29.3, 16.3; IR (neat) 3509, 2924, 2854, 1626, 1603, 882, 768, 737 cm^{-1}; HRMS (ESI-TOF) calcd for $C_{28}H_{25}N_2O_2$ $[M+H]^+$ 421.1916, found: 421.1928. $[\alpha]_D^{22}$ +180 (*c* 0.43, 60% ee, CH_2Cl_2); CSP HPLC (Chiralpak AD, 1.0 mL/min, 90:10 hexanes:i-PrOH): t_R(*1*) = 16.6 min, t_R(*2*) = 20.9 min.

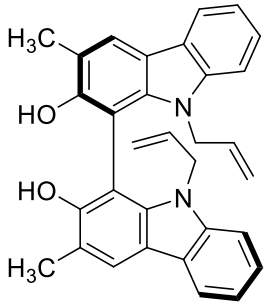

9,9'-Diallyl-3,3'-dimethyl-9*H*,9'*H*-[1,1'-bicarbazole]-2,2'-diol (1.5c). Following **General Procedure E**, the product was obtained as pale yellow oil (5.7 mg) in 71% yield. R_f = 0.48 (EtOAc:Hexanes = 1:9): ^{1}H NMR (500 MHz, $CDCl_3$) δ 8.05 (d, *J* = 7.7 Hz, 2H), 8.03 (s, 2H), 7.36 (td, *J* = 8.2, 1.0 Hz, 2H), 7.25 (t, *J* = 7.6 Hz, 2H), 7.20 (d, *J* = 8.2 Hz, 2H), 5.40-5.33 (m, 2H), 5.17 (br s, 2H), 4.74 (dd, *J* = 10.4, 1.2 Hz, 2H), 4.41 (dd, *J* = 17.2, 1.2 Hz, 2H), 4.25-4.15 (m, 4H), 2.46 (s, 6H); ^{13}C NMR (125 MHz, $CDCl_3$) δ 152.4, 141.2, 138.2,

132.5, 124.8, 123.6, 122.9, 119.7, 119.2, 117.6, 117.4, 115.8, 109.3, 98.3, 46.0, 16.8; IR (neat) 3510, 2919, 1603, 1477, 1459, 1355, 1235, 1184, 1072, 737cm^{-1}; HRMS (ESI-TOF) calcd for $C_{32}H_{29}N_2O_2$ $[M+H]^+$ *m/z* = 473.2229; found 473.2236; $[\alpha]_D^{22}$ +177 (*c* 0.28, 76% ee, CH_2Cl_2); Chiral HPLC: Chiralpak IA column (10% *i*-PrOH/hexanes, 1 mL/min) t_R(*1*) = 11.5 min, t_R(*2*) = 21.1 min.

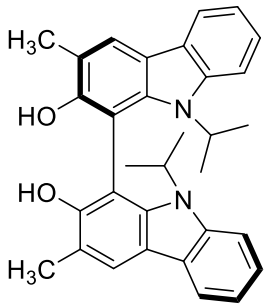

9,9'-Diisopropyl-3,3'-dimethyl-9*H*,9'*H*-[1,1'-bicarbazole]-2,2'-diol (1.5d). Following **General Procedure E**, the product was obtained as pale yellow oil (3.5 mg) in 58% yield. R_f = 0.60 (EtOAc:Hexanes = 1:9): ^{1}H NMR (500 MHz, $CDCl_3$) δ 8.07 (d, *J* = 7.7 Hz, 2H), 8.00 (s, 2H), 7.52 (d, *J* = 8.2 Hz, 2H), 7.33 (td, *J* = 8.3, 1.2 Hz, 2H), 7.23 (t, *J* = 7.7 Hz, 2H), 5.16 (s, 2H), 4.62-4.54 (m, 2H), 2.45 (s, 6H), 1.38 (d, *J* = 7.0 Hz, 6H), 1.18 (d, *J* = 7.0 Hz, 6H); ^{13}C NMR (125 MHz, $CDCl_3$) δ 152.0, 139.1, 137.5, 124.2, 124.1, 123.2, 119.4, 119.2, 117.5, 117.2, 112.6, 99.2, 46.8, 20.9, 20.7, 16.7; IR (neat) 3510, 2918, 2832, 1601, 1459, 1395, 1183, 1133, 1066, 738 cm^{-1}; HRMS (ESI-TOF) calcd for $C_{32}H_{33}N_2O_2$ $[M+H]^+$ *m/z* = 477.2542; found 477.2522; $[\alpha]_D^{22}$ +18 (*c* 0.15, 42% ee, CH_2Cl_2); Chiral HPLC: Chiralpak IA column (10% *i*-PrOH/hexanes, 1 mL/min) t_R(*1*) = 7.46 min, t_R(*2*) = 11.0 min.

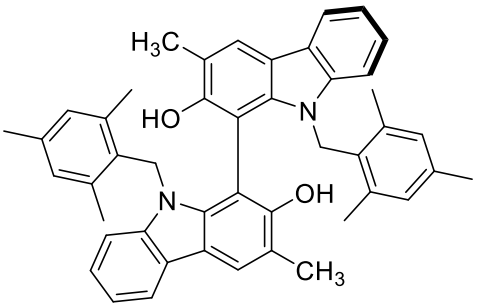

3,3'-Dimethyl-9,9'-bis(2,4,6-trimethylbenzyl)-9*H*,9'*H*-[1,1'-bicarbazole]-2,2'-diol (1.5e). Following **General Procedure E**, the product was obtained as yellow oil (4.0 mg) in 37% yield. R_f = 0.50 (EtOAc:Hexanes = 1:9): ^{1}H NMR (500 MHz, $CDCl_3$) δ 7.96 (d, *J* = 7.7 Hz, 2H), 7.94 (s, 2H), 7.12 (t, *J* = 7.8 Hz, 2H), 7.03 (td, *J* = 8.4, 1.2 Hz, 2H), 6.70 (s, 2H), 6.64 (s, 2H), 6.48 (d, *J* = 8.5 Hz, 2H), 5.30 (br s, 2H), 4.91 (d, *J* = 15.3 Hz, 2H), 4.75 (d, *J* = 15.3 Hz, 2H), 2.37 (s, 6H), 2.19 (s, 6H), 1.82 (s, 6H), 1.64 (s, 6H); ^{13}C NMR (125 MHz, $CDCl_3$) δ 152.3, 141.4, 139.4, 137.2, 136.7, 130.0, 129.8, 129.22, 129. 124.6, 123.6, 123.4, 119.4, 119.0, 117.9, 117.5, 110.6, 100.2, 44.7, 20.9, 20.1, 19.6, 16.7; IR (neat) 3509, 2920, 1603, 1456, 1180, 1135, 1076, 1041, 851, 743m^{-1}; HRMS (EI-TOF) calcd for $C_{46}H_{43}N_2O_2$ $[M-H]^-$ *m/z* = 655.3325; found 655.3322; $[\alpha]_D^{22}$ +182 (*c* 0.18, 37% ee, CH_2Cl_2); Chiral HPLC: Chiralpak IA column (5% *i*-PrOH/hexanes, 1 mL/min) t_R(*1*) = 5.09 min, t_R(*2*) = 14.9 min.

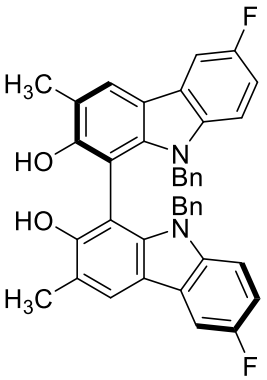

9,9'-Dibenzyl-6,6'-difluoro-3,3'-dimethyl-9*H*,9'*H*-[1,1'-bicarbazole]-2,2'-diol (1.5f).

Following **General Procedure E**, the product was obtained as a yellow solid (26 mg) in 87% yield. R_f = 0.58 (EtOAc:Hexanes = 1:4): ^{1}H NMR (500 MHz, acetone-d_6) δ 7.94 (s, 2H), 7.78 (dd, *J* = 9.0, 2.5 Hz, 2H), 7.06 -6.98 (m, 6H), 6.86-6.84 (m, 6H), 6.47-6.45 (m, 4H), 4.82 (d, *J* = 17.3 Hz, 2H), 4.60 (d, *J* = 17.3 Hz, 2H), 2.21 (s, 6H); ^{13}C NMR (125 MHz, acetone-d_6) δ 158.5 (d, *J* = 233 Hz), 155.3, 140.9, 139.0, 138.8, 128.5, 127.1, 126.2, 124.6 (d, *J* = 8.8 Hz), 123.4, 118.7, 117.4 (d, *J* = 3.8 Hz), 112.1 (d, *J* = 26.4 Hz), 110.7 (d, *J* = 10.1 Hz), 105.2 (d, *J* = 23.9 Hz), 101.9, 47.7, 17.1; IR (neat) 3515, 2923, 1627, 856, 796, 781, 703 cm^{-1}; HRMS (ESI-TOF) calcd for $C_{40}H_{31}F_2N_2O_2$ $[M+H]^+$ 609.2354, found 609.2368; $[\alpha]_D^{22}$ +183 (*c* 0.40, 92% ee, CH_2Cl_2); Chiral HPLC: Chiralpak IA column (10% *i*-PrOH/hexanes, 1 mL/min) t_R(*1*) = 9.52 min, t_R(*2*) = 10.4 min.

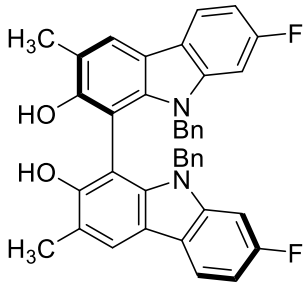

9,9'-Dibenzyl-7,7'-difluoro-3,3'-dimethyl-9*H*,9'*H*-[1,1'-bicarbazole]-2,2'-diol (1.5g). Following **General Procedure E**, the product was obtained as a yellow solid (17.8 mg) in 93% yield. R_f = 0.60 (EtOAc:Hexanes = 1:4): ^{1}H NMR (500 MHz, acetone-d_6) δ 7.95 (s, 2H), 7.21 (td, *J* = 8.1, 5.5 Hz, 2H), 7.06 (s, 2H), 6.91 (d, *J* = 8.1 Hz, 2H), 6.89 (d, *J* = 8.1 Hz, 2H), 6.84-6.82 (m, 6H), 6.45-6.43 (m, 4H), 4.85 (d, *J* = 17.9 Hz, 2H), 4.60 (d, *J* = 17.4 Hz, 2H), 2.21 (s, 6H); ^{13}C NMR (125 MHz, acetone-d_6) δ 157.7 (d, *J* = 243 Hz), 153.9, 144.1 (d, *J* = 10.6 Hz), 138.7, 137.5, 127.5, 126.1, 125.2, 124.6 (d, *J* = 20.1 Hz), 124.4 (d, *J* = 20.1 Hz), 118.4, 114.1, 110.8, 105.3, 104.7 (d, *J* = 18.7 Hz), 101.0, 47.0, 16.2; IR (neat) 3519, 2925, 1601, 965, 709 cm^{-1}; HRMS (ESI-TOF) calcd for $C_{40}H_{29}F_2N_2O_2$ $[M-H]^-$ 607.2197, found 607.2191, $[\alpha]_D^{22}$ +157 (*c* 0.35, 92% ee, CH_2Cl_2); Chiral HPLC: Chiralpak

IA column (5% *i*-PrOH/hexanes, 1 mL/min) t_R(*1*) = 6.80 min, t_R(*2*) = 7.61 min.

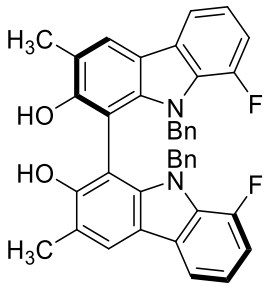

9,9'-Dibenzyl-8,8'-difluoro-3,3'-dimethyl-9*H*,9'*H*-[1,1'-bicarbazole]-2,2'-diol (1.5h). Following **General Procedure E**, the product was obtained as yellow oil (12 mg) in 80% yield. R_f = 0.65 (EtOAc:Hexanes = 1:4): ^{1}H NMR (500 MHz, acetone-d_6) δ 7.97 (s, 2H), 7.90 (d, *J* = 5.0 Hz, 2H), 7.16-7.12 (m, 2H), 7.00-6.96 (m, 4H), 6.87-6.83 (m, 6H), 6.38 (d, *J* = 5.0 Hz, 4H), 4.95 (d, *J* = 15.0 Hz, 2H), 4.81 (d, *J* = 15.0 Hz, 2H), 2.19 (s, 6H); ^{13}C NMR (125 MHz, acetone-d_6) δ 155.2, 150.2 (d, *J* = 243 Hz), 140.2, 139.9, 129.5 (d, *J* = 7.5 Hz), 128.3, 128.1 (d, *J* = 5.0 Hz), 126.8, 125.6, 123.1, 120.4 (d, *J* = 6.3 Hz), 119.5, 117.8, 115.6 (d, *J* = 2.5 Hz), 111.1 (d, *J* = 18.9 Hz), 102.0, 49.5, 17.1; IR (neat) 3516, 2920, 1630, 1613, 1579, 1497, 1450, 1414, 1380, 1348, 1239, 1216, 1192, 1178, 1160, 1141, 1124, 1062, 987 cm^{-1}; HRMS (ESI-TOF) calcd for $C_{40}H_{31}F_2N_2O_2$ $[M+H]^+$ *m/z* = 609.2354, found 609.2370; $[\alpha]_D^{22}$ +211 (*c* 0.25, 91% ee, CH_2Cl_2); Chiral HPLC: Chiralpak IA column (10% *i*-PrOH/hexanes, 1 mL/min) t_R(*1*) = 8.29 min, t_R(*2*) = 9.39 min.

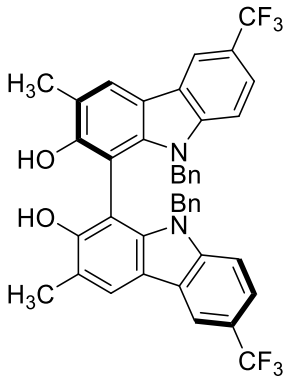

9,9'-Dibenzyl-3,3'-dimethyl-6,6'-bis(trifluoromethyl)-9*H*,9'*H*-[1,1'-bicarbazole]-2,2'-

diol (1.5i). Following **General Procedure E**, the product was obtained as light yellow oil (12 mg) in 70% yield. R_f = 0.53 (EtOAc:Hexanes = 1:4): ^{1}H NMR (500 MHz, acetone-d_6) δ 8.43 (s, 2H), 8.12 (s, 2H), 7.54 (d, J = 8.5 Hz, 2H), 7.25 (d, J = 8.5 Hz, 2H), 7.23 (s, 2H), 6.86-6.83 (m, 6H), 6.45-6.43 (m, 4H), 4.89 (d, J = 17.4 Hz, 2H), 4.68 (d, J = 17.4 Hz, 2H), 2.23 (s, 6H); ^{13}C NMR (125 MHz, acetone-d_6) δ 155.6, 144.0, 140.7, 138.2, 128.5, 127.1, 126.6 (q, J = 270 Hz), 126.0, 123.8, 123.5, 121.6 (q, J = 31.4 Hz), 121.5 (q, J = 2.5 Hz), 119.0, 117.2, 117.0 (q, J = 3.8 Hz), 110.3, 102.2, 47.7, 17.1; IR (neat) 3525, 2925, 1609, 1451, 1411, 1365, 1346, 1325, 1300, 1262, 1186, 1163, 1148, 1113, 1080, 1069, 1051, 1034, 1005 cm^{-1}; HRMS (ESI-TOF) calcd for $C_{42}H_{31}F_6N_2O_2$ $[M+H]^+$ m/z = 709.2292, found 709.2290; $[\alpha]_D^{22}$ +175 (c 0.6, 93% ee, CH_2Cl_2); Chiralpak IA column (10% i-PrOH/hexanes, 1 mL/min) t_R(1) = 8.61 min, t_R(2) = 9.89 min.

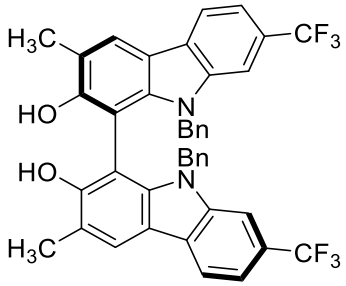

9,9'-Dibenzyl-3,3'-dimethyl-7,7'-bis(trifluoromethyl)-9*H*,9'*H*-[1,1'-bicarbazole]-2,2'-diol (1.5j). Following **General Procedure E**, the product was obtained as yellow oil (15 mg) in 60% yield. R_f = 0.55 (EtOAc:Hexanes = 1:4): ^{1}H NMR (500 MHz, acetone-d_6) δ 8.25 (d, J = 8.2 Hz, 2H), 8.07 (s, 2H), 7.48 (d, J = 8.3 Hz, 2H), 7.42 (s, 2H), 7.29 (s, 2H), 6.86-6.79 (m, 6H), 6.44 (d, J = 7.0 Hz, 4H), 4.93 (d, J = 17.5 Hz, 2H), 4.73 (d, J = 17.5 Hz, 2H), 2.24 (s, 6H); ^{13}C NMR (125 MHz, acetone-d_6) δ 156.0, 141.6, 141.2, 138.3, 128.5, 127.1, 126.9, 126.3 (q, J = 271.1 Hz), 126.1 (q, J = 31.2 Hz), 126.0, 123.7, 120.0, 119.8, 116.8, 116.5 (q, J = 3.6 Hz), 107.0 (q, J = 4.1 Hz), 102.0, 47.7, 17.1; IR (neat) 3519, 2925, 1629, 1574, 1451, 1351, 1321, 1294, 1280, 1264, 1232, 1164, 1135, 1118, 1061, 1005,

910 cm^{-1}; HRMS (ESI-TOF) calcd for $C_{42}H_{31}F_6N_2O_2$ $[M+H]^+$ *m/z* = 709.2290, found 709.2270; $[\alpha]_D^{22}$ +254 (*c* 0.42, 94% ee, CH_2Cl_2); Chiral HPLC: Chiralpak IA column (5% *i*-PrOH/hexanes, 1 mL/min) t_R(*1*) = 6.42 min, t_R(*2*) = 21.8 min.

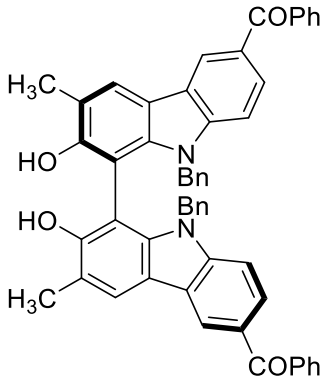

(9,9'-Dibenzyl-2,2'-dihydroxy-3,3'-dimethyl-9*H*,9'*H*-[1,1'-bicarbazole]-6,6'-diyl)bis(phenylmethanone) (1.5k). Following **General Procedure E** with chlorobenzene/HFIP(1:1, 0.5 M) as a solvent, the product was obtained as an off-white solid (9.1 mg) in 76% yield based on recovered starting material. R_f = 0.50 (EtOAc:Hexanes = 1:2): ^{1}H NMR (500 MHz, acetone-d_6) δ 8.56 (d, *J* = 1.0 Hz, 2H), 8.03 (s, 2H), 7.85 (d, *J* = 8.0 Hz, 4H), 7.79 (dd, *J* = 8.5, 1.5 Hz, 2H), 7.67 (d, *J* = 7.5 Hz, 2H), 7.60 (t, *J* = 7.5 Hz, 4H), 7.25 (br s, 2H), 7.22 (d, *J* = 8.5 Hz, 2H), 6.89-6.86 (m, 6H), 6.50-6.48 (m, 4H), 4.94 (d, *J* = 15.0 Hz, 2H), 4.70 (d, *J* = 15.0 Hz, 2H), 2.23 (s, 6H); ^{13}C NMR (125 MHz, acetone-d_6) δ 196.2, 155.4, 145.0, 140.7, 140.1, 138.2, 132.4, 130.4, 129.8, 129.1, 128.5, 127.4, 127.2, 126.1, 123.6, 123.4, 122.6, 119.7, 117.8, 109.6, 102.4, 47.8, 17.1; IR (neat) 3500, 2923, 2853, 1645, 1596, 1569, 1494, 1449, 1412, 1365, 1346, 1318, 1286, 1250, 1184, 1134, 1072, 1003, 948 cm^{-1}; HRMS (ESI-TOF) calcd for $C_{54}H_{41}N_2O_4$ $[M+H]^+$ *m/z* = 781.3066, found 781.3054; $[\alpha]_D^{22}$ +55 (*c* 0.15, 85% ee, CH_2Cl_2); Chiral HPLC: Chiralpak IA column (20% *i*-PrOH/hexanes, 1 mL/min) t_R(*1*) = 29.8 min, t_R(*2*) = 39.8 min.

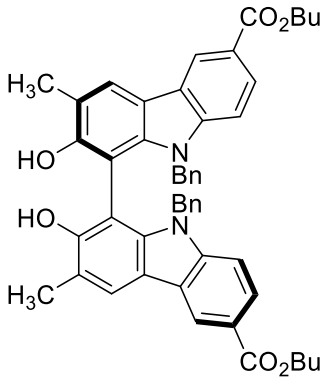

Dibutyl 9,9'-dibenzyl-2,2'-dihydroxy-3,3'-dimethyl-9*H*,9'*H*-[1,1'-bicarbazole]-6,6'-dicarboxylate (1.5l). Following **General Procedure E**, the product was obtained as light yellow oil (16 mg) in 67% yield based on recovered starting material. R_f = 0.41 (EtOAc:Hexanes = 1:4): ^{1}H NMR (500 MHz, acetone-d_6) δ 8.75 (d, J = 1.5 Hz, 2H), 8.08 (s, 2H), 7.95 (dd, J = 8.6, 1.7 Hz, 2H), 7.15 (d, J = 8.9 Hz, 2H), 7.14 (s, 2H), 6.84-6.82 (m, 6H), 6.43-6.41 (m, 4H), 4.87 (d, J = 17.3 Hz, 2H), 4.65 (d, J = 17.3 Hz, 2H), 4.39-4.34 (m, 4H), 2.23 (s, 6H), 1.84-1.78 (m, 4H), 1.59-1.51 (m, 4H), 1.02 (t, J = 7.4 Hz, 6H); ^{13}C NMR (125 MHz, acetone-d_6) δ 167.6, 155.3, 145.2, 140.6, 138.2, 128.5, 127.1, 126.4, 126.1, 123.8, 123.3, 122.4, 121.5, 119.7, 117.7, 109.6, 102.4, 64.8, 47.8, 31.8, 20.0, 17.1, 14.1; IR (neat) 3395, 2958, 2926, 1697, 1603, 1577, 1495, 1451, 1412, 1382, 1364, 1348, 1287, 1240, 1182, 1132, 1102, 1071, 1004, 972 cm^{-1}; HRMS (ESI-TOF) calcd for $C_{50}H_{49}N_2O_6$ $[M+H]^+$ m/z = 773.3591, found 773.3585; $[\alpha]_D^{22}$ +100 (c 0.30, 96% ee, CH_2Cl_2); Chiral HPLC: Chiralpak IA column (20% i-PrOH/hexanes, 1 mL/min) t_R(*1*) = 9.80 min, t_R(*2*) = 19.9 min.

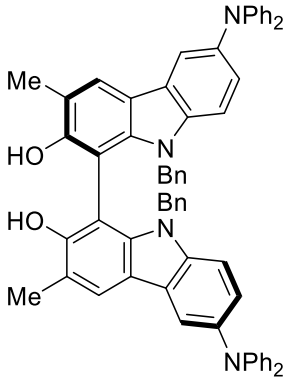

9,9'-Dibenzyl-6,6'-bis(diphenylamino)-3,3'-dimethyl-9*H*,9'*H*-[1,1'-bicarbazole]-2,2'-diol (1.5m). Following **General Procedure E**, the product was obtained as a colorless solid (8.0 mg) in 62% yield. R_f = 0.58 (EtOAc:Hexanes = 1:9): ^{1}H NMR (500 MHz, acetone-d_6) δ 7.85 (s, 2H), 7.83 (d, J = 2.0 Hz, 2H), 7.27 (t, J = 8.6 Hz, 8H), 7.09-7.03 (m, 12H), 7.00 (s, 2H), 6.96 (t, J = 7.4 Hz, 4H), 6.91-6.88 (m, 6H), 6.54 d, (J = 6.6 Hz, 4H), 4.87 (d, J = 17.2 Hz, 2H), 4.61 (d, J = 17.2 Hz, 2H), 2.19 (s, 6H); ^{13}C NMR (125 MHz, acetone-d_6) δ 154.9, 149.7, 140.6, 140.5, 140.0, 138.9, 129.9, 128.5, 127.1, 126.3, 125.1, 124.7, 123.2, 122.3, 121.8, 118.6, 118.2, 117.5, 110.9, 101.8, 47.8, 17.1; IR (neat) 3526, 3032, 2919, 1635, 1585, 1490, 1454, 1326, 1285, 1257, 1217, 1164, 1132, 1028, 998, 804, 752 cm^{-1}; HRMS (EI-TOF) calcd for $C_{64}H_{50}N_4O_2Na$ $[M+Na]^+$ *m/z* 929.3831; found 929.3810; $[\alpha]_D^{22}$ +31 (*c* 0.35, 37% ee, CH_2Cl_2); Chiral HPLC: Chiralpak IA column (5% *i*-PrOH/hexanes, 1 mL/min) t_R(*1*) = 6.95 min, t_R(*2*) = 8.19 min.

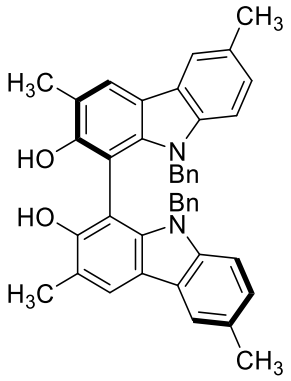

9,9'-Dibenzyl-3,3',6,6'-tetramethyl-9*H*,9'*H*-[1,1'-bicarbazole]-2,2'-diol (1.5n). Following **General Procedure E**, the product was obtained as a yellow solid (13 mg) in 93% yield. R_f = 0.74 (EtOAc:Hexanes = 1:4): ^{1}H NMR (500 MHz, acetone-d_6) δ 7.89 (s, 2H), 7.84 (s, 2H), 7.06 (dd, J = 1.8, 7.5, 2H), 6.97 (d, J = 8.0, 2H), 6.86-6.82 (m, 6H), 6.71 (s, 2H), 6.45 (s, 2H), 6.46-6.42 (m, 2H), 4.77 (d, J = 17.1, 2H), 4.58 (d, J = 17.1, 2H), 2.49 (s, 6H), 2.19 (s, 6H); ^{13}C NMR (125 MHz, acetone-d_6) δ 140.0, 139.2, 138.3, 128.1, 127.3, 126.1, 125.4, 125.2, 123.3, 121.9, 118.6, 117.2, 116.7, 108.9, 108.8, 100.9, 46.6, 20.5, 16.2; IR (neat) 3503, 2920, 1608, 793, 733, 701 cm^{-1}; HRMS(ESI-TOF) calcd for $C_{42}H_{37}N_2O_2$ $[M+H]^+$ 601.2855, found 601.2849 $[\alpha]_D^{22}$ +180 (*c* 0.43, 60% ee, CH_2Cl_2); Chiral HPLC: Chiralpak IA column (10% *i*-PrOH/hexanes, 1 mL/min): t_R(*1*) = 8.97 min, t_R(*2*) = 13.3 min.

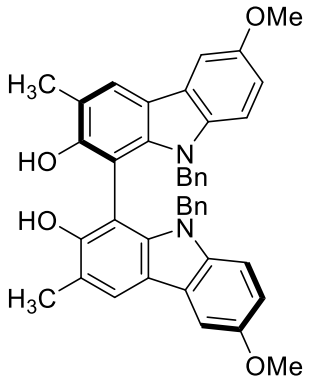

9,9'-Dibenzyl-6,6'-dimethoxy-3,3'-dimethyl-9H,9'H-[1,1'-bicarbazole]-2,2'-diol (1.5o). Following **General Procedure E** for 26 h, the product was obtained as a light brown powder (10.6 mg) in 82% yield. R_f = 0.33 (EtOAc:Hexanes = 1:4): ^{1}H NMR (500 MHz, acetone-d_6) δ 7.91 (s, 2H), 7.63 (d, *J* = 2.5 Hz, 2H), 6.98 (d, *J* = 8.8 Hz, 2H), 6.88-6.83 (m, 8H), 6.81 (s, 2H), 6.46 (d, *J* = 7.8 Hz, 4H), 4.78 (d, *J* = 17.2 Hz, 2H), 4.56 (d, *J* = 17.2 Hz, 2H), 3.90 (s, 6H), 2.20 (s, 6H); ^{13}C NMR (125 MHz, acetone-d_6) δ 155.1, 154.5, 140.4, 139.2, 137.4, 128.4, 126.9, 126.3, 124.4, 123.0, 117.9, 117.6, 113.5, 110.6, 102.9, 101,7, 56.1, 47.5, 17.1; IR (neat) 3500, 2925, 1627, 1482, 1450, 1433, 1409, 1349, 1298, 1229,

1191, 1181, 1159, 1145, 1073, 1055, 1027, 1004 cm^{-1}; HRMS (ESI-TOF) calcd for $C_{42}H_{37}N_2O_4$ $[M+H]^+$ *m/z* = 633.2753, found 633.2766. $[\alpha]_D^{22}$ +142 (*c* 0.45, 74% ee, CH_2Cl_2); Chiral HPLC: Chiralpak IA column (15% *i*-PrOH/hexanes, 1 mL/min) t_R(*1*) = 12.6 min, t_R(*2*) = 14.1 min.

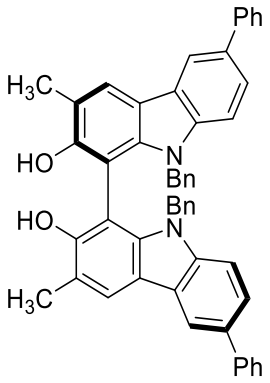

9,9'-Dibenzyl-3,3'-dimethyl-6,6'-diphenyl-9*H*,9'*H*-[1,1'-bicarbazole]-2,2'-diol (1.5p). Following **General Procedure E**, the product was obtained as a yellow solid (23 mg) in 70% yield. R_f = 0.64 (EtOAc:Hexanes = 1:4): ^{1}H NMR (500 MHz, $CDCl_3$) δ 8.32 (d, *J* = 1.5 Hz, 2H), 8.04 (s, 2H), 7.77 (d, *J* = 7.0 Hz, 4H), 7.61 (dd, *J* = 8.5, 2.0 Hz, 2H), 7.52 (t, *J* = 7.5 Hz, 4H), 7.34 (t, *J* = 7.0 Hz, 2H), 7.18 (d, *J* = 8.5 Hz, 2H), 6.94 (t, *J* = 7.0 Hz, 2H), 6.89 (t, *J* = 7.0 Hz, 4H), 6.31 (d, *J* = 7.0 Hz, 4H), 4.78 (s, 2H), 4.74 (d, *J* = 17.0 Hz, 2H), 4.69 (d, *J* = 17.0 Hz, 2H), 2.22 (s, 6H); ^{13}C NMR (125 MHz, $CDCl_3$) δ 152.7, 142.2, 141.4, 138.7, 137.3, 133.3, 128.9, 128.0, 127.4, 126.8, 126.6, 125.1, 124.4, 123.4, 123.3, 118.0, 117.8, 117.7, 109.3, 99.2, 47.0, 16.6; IR (neat) 3502, 2921, 1603, 1468, 1450, 1406, 1361, 1347, 1290, 1251, 1178, 1135, 1076, 1003, 964, 878 cm^{-1}; HRMS (ESI-TOF) calcd for $C_{52}H_{41}N_2O_2$ $[M+H]^+$ *m/z* = 725.3168, found 725.3168. $[\alpha]_D^{22}$ +82 (*c* 0.25, 82% ee, CH_2Cl_2); Chiral HPLC: Chiralpak IA column (10% *i*-PrOH/hexanes, 1 mL/min) t_R(*1*) = 14.6 min, t_R(*2*) = 27.1 min.

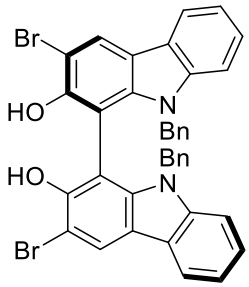

9,9'-Dibenzyl-3,3'-dibromo-9*H*,9'*H*-[1,1'-bicarbazole]-2,2'-diol (1.5q). Following **General Procedure E**, the product was obtained as yellow oil (12.0 mg) in 30% yield based on recovered starting material. R_f = 0.63 (EtOAc:Hexanes = 1:4): ^{1}H NMR (500 MHz, acetone-d_6) δ 8.37 (s, 2H), 8.14 (d, J = 7.4 Hz, 2H), 7.56 (s, 2H), 7.31 (td, J = 8.3, 1.2 Hz, 2H), 7.23 (td, J = 7.8, 0.8 Hz, 2H), 7.13 (d, J = 8.2 Hz, 2H), 6.87-6.82 (m, 6H), 6.48 (dd, J = 8.1, 1.9 Hz, 4H), 4.90 (d, J = 17.3 Hz, 2H), 4.63 (d, J = 17.4 Hz, 2H); ^{13}C NMR (125 MHz, acetone-d_6) δ 152.1, 143.0, 140.6, 138.4, 128.6, 127.3, 126.2, 126.1, 125.1, 123.1, 120.7, 120.1, 119.5, 110.3, 104.7, 103.6, 47.8; IR (neat) 3503, 2924, 2853, 1591, 1473, 1446, 1412, 1340, 1319, 1259, 1205, 1184, 1123, 1027, 960, 777, 746, 730 cm^{-1}; HRMS (ESI-TOF) calcd for $C_{38}H_{27}Br_2N_2O_2$ $[M+H]^+$ m/z = 701.0439, found 701.0462; $[\alpha]_D^{22}$ +58 (c 0.25, 72% ee, CH_2Cl_2); Chiral HPLC: Chiralpak IA column (20% i-PrOH/hexanes, 1 mL/min) t_R(*1*) = 12.0 min, t_R(*2*) = 19.6 min.

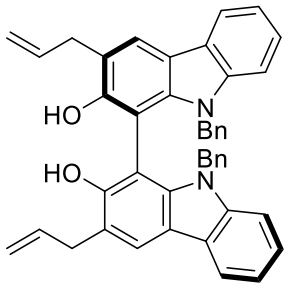

3,3'-Diallyl-9,9'-dibenzyl-9*H*,9'*H*-[1,1'-bicarbazole]-2,2'-diol (1.5r). Following **General Procedure E**, the product was obtained as a yellow powder (9.0 mg) in 75% yield. R_f = 0.72 (EtOAc:Hexanes = 1:4): ^{1}H NMR (500 MHz, acetone-d_6) δ 8.07 (d, J = 7.5 Hz, 2H),

7.94 (s, 2H), 7.23 (dt, *J* = 8.3, 1.3 Hz, 2H), 7.18 (dt, *J* = 7.8, 1.0 Hz, 2H), 7.06 (d, *J* = 8.0 Hz, 2H), 7.00 (br s, 2H), 6.83-6.81 (m, 6H), 6.48-6.46 (m, 4H), 6.00-5.93 (m, 2H), 5.11 (dq, *J* = 17.1, 1.6 Hz, 2H), 4.98 (dq, *J* = 10.0, 1.2 Hz, 2H), 4.88 (d, *J* = 17.2 Hz, 2H), 4.58 (d, *J* = 17.2 Hz, 2H), 3.42-3.33 (m, 4H); ^{13}C NMR (125 MHz, acetone-d_6) δ 154.1, 142.5, 140.0, 138.8, 138.6, 128.4, 126.9, 126.2, 125.0, 124.1, 122.3, 120.8, 120.0, 119.5, 118.0, 115.3, 110.1, 101.9, 47.4, 35.7; IR (neat) 3513, 2923, 1603, 1477, 1449, 1417, 1348, 1244, 1180, 1124, 919 cm^{-1}; HRMS (ESI-TOF) calcd for $C_{44}H_{36}N_2O_2Na$ $[M+Na]^+$ *m/z* = 647.2674, found 647.2659; $[\alpha]_D^{22}$ +268 (*c* 0.10, 83% ee, CH_2Cl_2); Chiral HPLC: Chiralpak IA column (10% *i*-PrOH/hexanes, 1 mL/min) t_R(*1*) = 9.72 min, t_R(*2*) = 11.0 min.

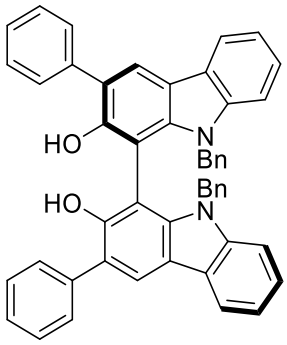

9,9'-Dibenzyl-3,3'-diphenyl-9*H*,9'*H*-[1,1'-bicarbazole]-2,2'-diol (1.5s). Following **General Procedure E**, the product was obtained as orange oil (12 mg) in 43% based on recovery of starting material yield. R_f = 0.62 (EtOAc:Hexanes = 1:4): ^{1}H NMR (500 MHz, acetone-d_6) δ 8.16 (d, *J* = 10.0 Hz, 2H), 8.14 (s, 2H), 7.40 (d, *J* = 10.0 Hz, 4H), 7.35 (d, *J* = 10.0 Hz, 4H), 7.29-7.20 (m, 8H), 7.09 (d, *J* = 5.0 Hz, 2H), 6.88-6.86 (m, 6H), 6.63-6.61 (m, 4H), 5.10 (d, *J* = 20.0 Hz, 2H), 4.74 (d, *J* = 20.0 Hz, 2H); ^{13}C NMR (125 MHz, acetone-d_6) δ 153.3, 142.7, 140.7, 140.3, 138.8, 130.6, 128.69, 128.65, 127.1, 127.0, 126.3, 125.3, 124.3, 123.4, 123.3, 120.3, 119.8, 118.5, 110.3, 102.8, 47.5; IR (neat) 3506, 2923, 1625, 1603, 1495, 1474, 1448, 1434, 1411, 1347, 1320, 1264, 1228, 1203, 1182, 1152, 1125, 958 cm^{-1}; HRMS (ESI-TOF) calcd for $C_{50}H_{37}N_2O_2$ $[M+H]^+$ *m/z* = 697.2855, found 697.2839.

$[\alpha]_D^{22}$ +39 (*c* 0.25, 60% ee, CH_2Cl_2); Chiral HPLC: Chiralpak IA column (10% *i*-PrOH/hexanes, 1 mL/min) t_R(*1*) = 10.4 min, t_R(*2*) = 15.7 min.

CHAPTER 2: Total Synthesis of Chaetoglobin A[1]

2.1. Introduction

Chaetoglobin A is one of the azaphilone dimers, which contains two identical oxygenated bicyclic cores incorporating quaternary stereocenters that are connected through an axial chiral bond (**Figure 2.1**). It is isolated from the endophytic fungus *chaetomium globosum*, which lives in the stem of *Imperata cylindrical*. In 2008, Tan et al. reported its inhibitory ability on the propagation of human breast cancer and colon cancer cell lines.[2] Previous studies on the biosynthesis of azaphilone alkaloids indicate that its core backbone is polyketide in origin.[3] However, the nature of the dimerization and generation of attendant axial chiral stereochemistry has not been delineated. Specifically, it is unclear whether the stereochemistry of the chiral axis forms first and directs formation of the quaternary centers (via **2.3**), if the quaternary centers form first and then direct formation of the chiral axis (via **2.4**), or if these stereoelements are formed independently.

[1] Adapted from Kang, H.; Pagan, C. T.; Liu, J.; Kozlowski, M. C. *Org*. *Lett*. **2018** *submitted*. Copyright 2018 American Chemical Society.

[2] Ming Ge, H.; Yun Zhang, W.; Ding, G.; Saparpakorn, P.; Chun Song, Y.; Hannongbua, S.; Xiang Tan, R. Chaetoglobins A and B, Two Unusual Alkaloids from Endophytic Chaetomium Globosum Culture. *Chem. Commun.* **2008**, 5978-5980.

[3] (a) Colombo, L.; Gennari, C.; Ricca, G. S.; Scolastico, C.; Aragozzini, F. Detection of One Symmetrical Precursor during the Biosynthesis of the Fungal Metabolite Austdiol Using [1,2-13C2]Acetate and [Me-13C]Methionine. *J. Chem. Soc. Chem. Commun.* **1981**, 575-576. (b) Takahashi, M.; Koyama, K.; Natori, S. Four New Azaphilones from Chaetomium Globosum Var. Flavo-Viridae. *Chem. Pharm. Bull. (Tokyo)* **1990**, *38*, 625–628. (c) Seto, H.; Tanabe, M. Utilization of 13C-13C Coupling in Structural and Biosynthetic Studies. III. Ochrephilone - a New Fungal Metabolite. *Tetrahedron Lett.* **1974**, *15*, 651–654. (d) Duncan, S. J.; Williams, D. H.; Ainsworth, M.; Martin, S.; Ford, R.; Wrigley, S. K. On the Biosynthesis of an Inhibitor of the P53/MDM2 Interaction. *Tetrahedron Lett.* **2002**, *43*, 1075–1078. (e) Nakazawa, T.; Ishiuchi, K.; Sato, M.; Tsunematsu, Y.; Sugimoto, S.; Gotanda, Y.; Noguchi, H.; Hotta, K.; Watanabe, K. Targeted Disruption of Transcriptional Regulators in Chaetomium Globosum Activates Biosynthetic Pathways and Reveals Transcriptional Regulator-Like Behavior of Aureonitol. *J. Am. Chem. Soc.* **2013**, *135*, 13446–13455.

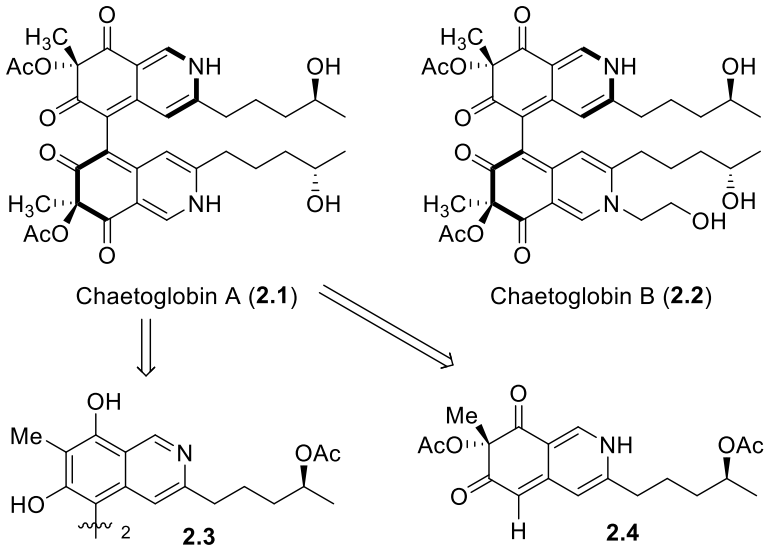

Figure 2.1. Structure of Chaetoglobin A (**2.1**) and B (**2.2**)[1]

Due to their intriguing structures and biological activities, numerous attempts to synthesize the azaphilone alkaloids have been reported since the early 1970s.[4] Approaches to introducing the bicyclic core proceed from either a keto-formyl precursor or alkynyl-formyl precursor that generate benzopyrylium salts or pyronoquinones as key intermediates. Often, acid-catalyzed cycloisomerization, followed by oxidation, was used to construct the 2*H*-isoquinoline-2,6-dione backbone. However, no synthetic efforts have been reported toward azaphilone dimers to date. Recently, we reported an efficient

[4] (a) Galbraith, M. N.; Whalley, W. B. The Chemistry of Fungi. Part LIX. The Synthesis of (±)-Ascochitine. *J Chem Soc C* **1971**, 3557–3559. (b) Chong, R.; Gray, R. W.; King, R. R.; Whalley, W. B. The Chemistry of Fungi. Part LXII. The Synthesis of (+/-)-Mitorubrin, a Metabolite of Penicillium Rubrum. *J Chem Soc C* **1971**, 3571–3575. (c) Zhu, J.; Grigoriadis, N. P.; Lee, J. P.; Porco, J. A. Synthesis of the Azaphilones Using Copper-Mediated Enantioselective Oxidative Dearomatization. *J. Am. Chem. Soc.* **2005**, *127*, 9342–9343. (d) Marsini, M. A.; Gowin, K. M.; Pettus, T. R. R. Total Synthesis of (±)-Mitorubrinic Acid. *Org. Lett.* **2006**, *8*, 3481–3483. (e) Clark, R. C.; Yeul Lee, S.; Boger, D. L. Total Synthesis of Chlorofusin, Its Seven Chromophore Diastereomers, and Key Partial Structures. *J. Am. Chem. Soc.* **2008**, *130*, 12355–12369. (f) Germain, A. R.; Bruggemeyer, D. M.; Zhu, J.; Genet, C.; O'Brien, P.; Porco, J. A. Synthesis of the Azaphilones (+)-Sclerotiorin and (+)-8-O-Methylsclerotiorinamine Utilizing (+)-Sparteine Surrogates in Copper-Mediated Oxidative Dearomatization. *J. Org. Chem.* **2011**, *76*, 2577–2584. (g) Somoza, A. D.; Lee, K.-H.; Chiang, Y.-M.; Oakley, B. R.; Wang, C. C. C. Reengineering an Azaphilone Biosynthesis Pathway in Aspergillus Nidulans to Create Lipoxygenase Inhibitors. *Org. Lett.* **2012**, *14*, 972–975. (h) Gao, J.-M.; Yang, S.-X.; Qin, J.-C. Azaphilones: Chemistry and Biology. *Chem. Rev.* **2013**, *113*, 4755–4811.

method to construct a chiral biaryl axis by means of vanadium-catalyzed enantioselective oxidative phenol coupling.[5] The oxidative coupling permits the formation of chiral axes effectively. Here, we describe the total synthesis of chaetoglobin A utilizing this asymmetric oxidative phenol coupling to generate an axial chiral bisphenol dimer **2.7** as a key intermediate.

2.2. Retrosynthetic Analysis

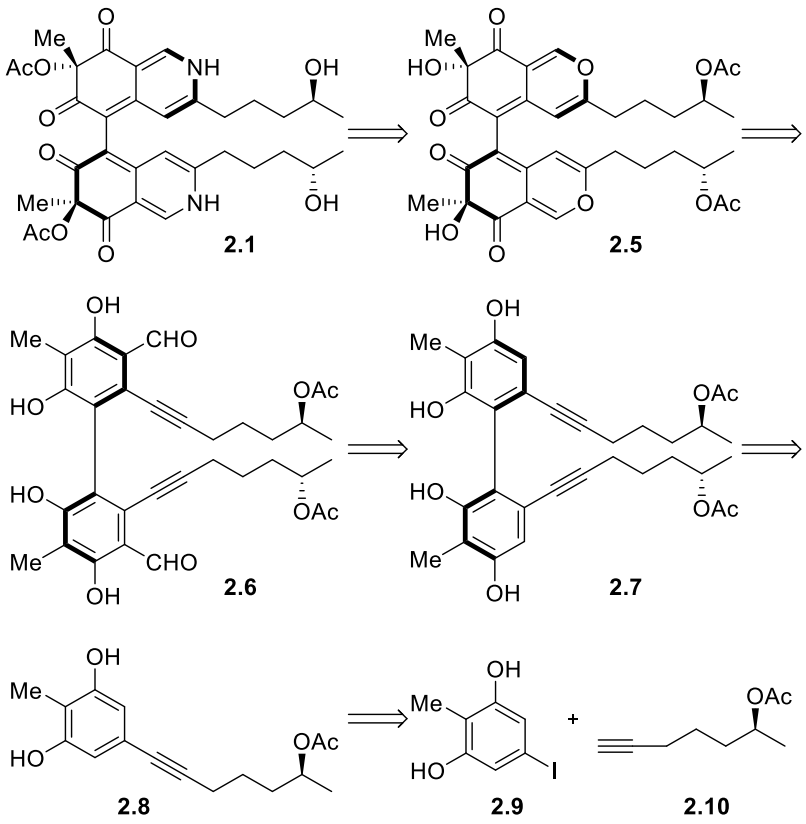

Scheme 2.1. Retrosynthetic Analysis of Chaetoglobin A (**2.1**)[1]

In our retrosynthetic analysis, the final isoquinoline moiety could be prepared by amination of **2.5** (**Scheme 2.1**). Lewis acid-catalyzed dearomatization followed by oxidation would allow the construction of the corresponding bicyclic core from formylated

[5] Kang, H.; Lee, Y. E.; Reddy, P. V. G.; Dey, S.; Allen, S. E.; Niederer, K. A.; Sung, P.; Hewitt, K.; Torruellas, C.; Herling, M. R.; Kozlowski, M. C. Asymmetric Oxidative Coupling of Phenols and Hydroxycarbazoles. *Org. Lett.* **2017**, *19*, 5505–5508.

dimer **2.6**. We hypothesized that the axial chirality of **2.6** could direct formation of the quaternary centers of **2.5**. In doing so, we could determine the feasibility one of the possible biosynthetic pathways (i.e., via **2.3**, **Figure 2.1**). Vilsmeier-Haack formylation could install the necessary formyl groups on tetraphenol **2.7**. We envisioned the asymmetric oxidative phenol coupling of **2.8** to afford pure atropoisomer **2.7**. It was anticipated that the acetoxy stereocenters of **2.8** would have little effect on stereochemical course of the phenol coupling with the chiral catalyst exerting control. Internal alkynyl monomer **2.8** would be prepared from the Sonogashira cross-coupling of bisphenol **2.9** and alkyne **2.10**.

2.3. Preparation of Sonogashira Coupling Pair

Synthetic efforts commenced with preparation of phenol **2.9** and alkyne **2.10** as shown in **Scheme 2.2**. Iridium-catalyzed borylation of commercially available **2.11**, followed by halogenation, allowed the formation of bromide **2.13**.[6] Due to need for a more reactive electrophile for Sonogashira cross-coupling, halogen exchange was undertaken to generate iodophenol **2.9** after demethylation. Surprisingly, stepwise iodination via halogen exchange[7] from bromide **2.13** proved to be more efficient than direct iodination[8] from boronic ester **2.12**.

[6] Murphy, J. M.; Liao, X.; Hartwig, J. F. Meta Halogenation of 1,3-Disubstituted Arenes via Iridium-Catalyzed Arene Borylation. *J. Am. Chem. Soc.* **2007**, *129*, 15434–15435.
[7] Klapars, A.; Buchwald, S. L. Copper-Catalyzed Halogen Exchange in Aryl Halides: An Aromatic Finkelstein Reaction. *J. Am. Chem. Soc.* **2002**, *124*, 14844–14845.
[8] Partridge, B. M.; Hartwig, J. F. Sterically Controlled Iodination of Arenes via Iridium-Catalyzed C–H Borylation. *Org. Lett.* **2013**, *15*, 140–143.

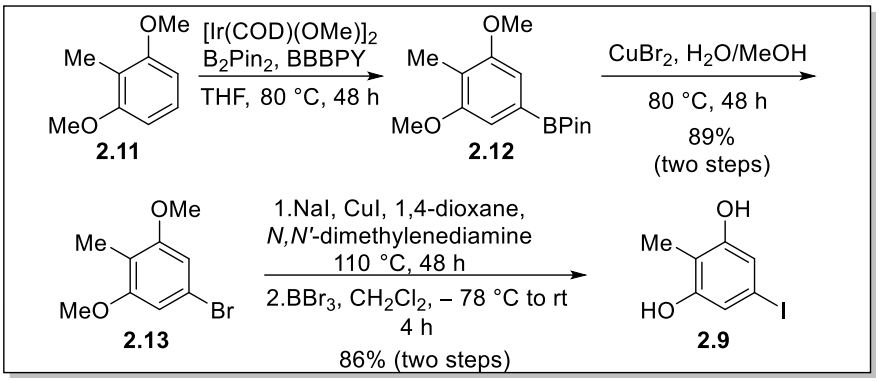

Scheme 2.2. Synthesis of 2,6-Dihydroxy-4-iodotoluene (**2.9**)[1]

Following a literature report[9] to prepare enantiomerically pure hydroxyalkyne **2.17**, a nucleophilic ring opening with commercially available propylene oxide **2.14** and butyne **2.15** gave internal alkyne **2.16**. Sequential alkyne isomerization was effected with a Li/KO*t*-Bu in 1,3-diaminopropane. Acetate protection of the free hydroxyl group provided the desired alkyne **2.10** in 74% yield over three steps (**Scheme 2.3**).

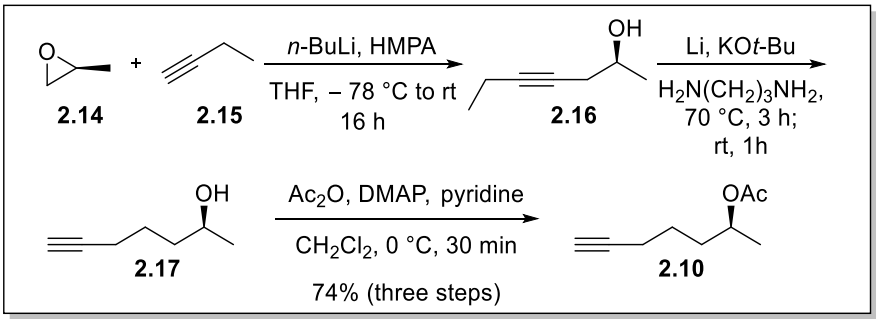

Scheme 2.3. Synthesis of Terminal Alkyne (**2.10**)[1]

2.4. Diastereoselective Oxidative Phenol Coupling to Generate Chiral Axis

[9] Wu, Y.; Gao, J. Total Synthesis of (+)-Brefeldin A. *Org. Lett.* **2008**, *10*, 1533–1536.

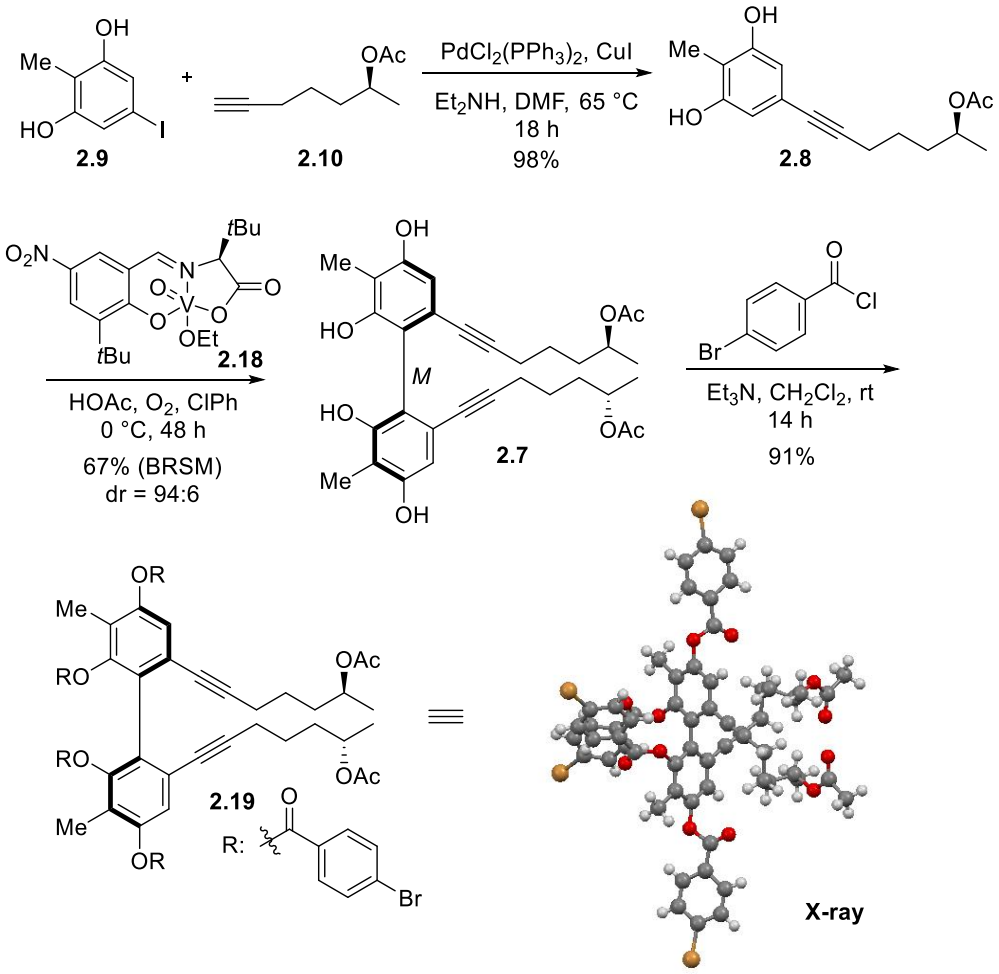

Scheme 2.4. Asymmetric Oxidative Phenol Coupling and Determination of its Absolute Stereochemistry[1]

Optimization of Sonogashira coupling between iodide **2.9** and alkyne **2.10** led to the formation of oxidative phenol coupling precursor **2.8** in 98% yield (**Scheme 2.4**). Using our recently reported atroposelective oxidative coupling of phenols,[5] vanadium catalyst **2.18** was applied to this transformation. Notably, complete catalyst control over the diastereoselectivity was observed with the opposite enantiomer of the catalyst providing the diastereomeric product with comparable dr**.** The additives, LiCl and HOAc, which are theorized to activate the vanadium catalyst, result in significant improvements (**Table 2.1**). Treatment of **2.8** with LiCl as an additive gave high diastereoselectivity (**Table 2.1**, entry

2). Increased catalyst loading showed neither a significant improvement in yield nor selectivity (entry 3). Among alternative solvents, chlorobenzene seemed a promising candidate in terms of improving yield (entry 2 vs 4 and entry 5 vs 6). Improved yield and comparable selectivity of dimer was realized with HOAc as the additive and chlorobenzene as solvent (entry 6). Finally, further improved yield and diastereoselectivity was achieved under more concentrated reaction conditions (entry 7). Use of asymmetric vanadyl catalyst **2.18** under the optimized conditions allowed access to the axially chiral dimer **2.7** in 67% yield with >15:1 dr. The absolute stereochemistry of product **2.7** was confirmed by X-ray crystallographic analysis of the *para*-bromobenzoyl substituted derivative **2.19**.[10]

entry	v-cat **2.18**	additive[a]	solvent[b]	yield (%)[c]	dr
1	20 mol%	–	Chlorobenzene[d]	34 (44)	79:21
2	20 mol%	LiCl	Toluene	52 (59)	92:8
3	40 mol%	LiCl	Toluene	49 (52)	93:7
4	20 mol%	LiCl	Chlorobenzene	54 (60)	90:10
5	20 mol%	HOAc	Toluene	49 (55)	87:13
6	20 mol%	HOAc	Chlorobenzene	49 (64)	90:10
7	20 mol%	HOAc	Chlorobenzene[d]	58 (67)	94:6

[a]20 mol% [b]0.3 M [c]Isolated yield based on recovery of substrate in parentheses [d]0.5 M

Table 2.1. Diastereoselective Oxidative Coupling of **2.8**[1]

2.5. Formylation

[10] Opposite chiral axis compound (*P*)-**19** crystallographic data included in Experimental Section.

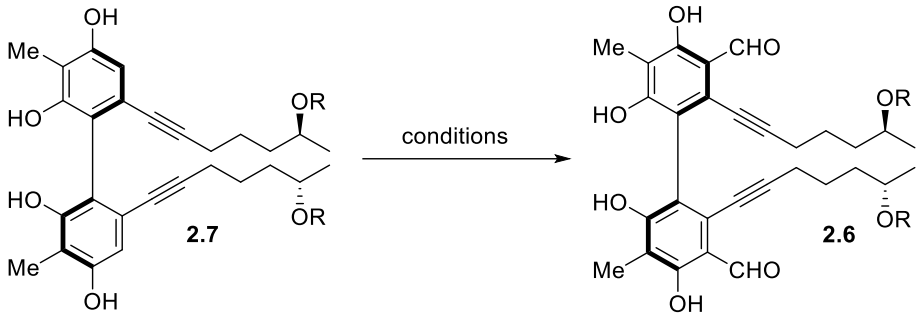

Entry	R	condition	T (°C)	Time	Yield (%)
1	TBDPS	$POCl_3$, DMF, CH_2Cl_2	25	20 min	16
2	TBDPS	$POCl_3$, DMF, CH_2Cl_2	0	20 min	27
3	TBDPS	Cl_2CHOMe, AgOTf, CH_2Cl_2	–78	3 h	<10
4	TBDPS	$MgCl_2$, $(CH_2O)_n$, Et_3N, THF	70	3 h	–[a]
5[b]	TBDPS	$ClCHN(CH_3)_2Cl$, CH_2Cl_2	25	20 min	36
6[b]	TBDPS	$ClCHN(CH_3)_2Cl$, CH_2Cl_2	0	20 min	42
7	Ac	$ClCHN(CH_3)_2Cl$, CH_2Cl_2	25	3 h	23[c]
8	Ac	$ClCHN(CH_3)_2Cl$, CH_2Cl_2	0	20 min	43
9	Ac	$ClCHN(CH_3)_2Cl$, CH_2Cl_2	–35	12 h	75 (86)[d]

[a]Substrates decomposition occured.[b]TBDPS deprotection detected in ^{1}H NMR.[c]No deprotection was observed. [d]Based on recovery of starting material yield in parentheses. TBDPS=*tert*-butyldiphenyl silyl, Ac=acetyl

Table 2.2. Formylation Optimization

With the coupled atropoisomer in hand, our attention turned to generating the formyl functional group adjacent to the alkyne chain. Attempts at formylation with various methods[11] are shown in **Table 2.2**. Owing to inherent acidic conditions of the formylation

[11] (a) Ramadas, S.; Krupadanam, G. L. D. Enantioselective Acylation of 2-Hydroxymethyl-2,3-Dihydrobenzofurans Catalysed by Lipase from Pseudomonas Cepacia (Amano PS) and Total Stereoselective Synthesis of (−)-(R)-MEM-Protected Arthrographol. *Tetrahedron Asymmetry* **2000**, *11*, 3375–3393. (b) Phan, D. H. T.; Kim, B.; Dong, V. M. Phthalides by Rhodium-Catalyzed Ketone Hydroacylation. *J. Am. Chem. Soc.* **2009**, *131*, 15608–15609. (c) Ohsawa, K.; Yoshida, M.; Doi, T. A Direct and Mild Formylation Method for Substituted Benzenes Utilizing Dichloromethyl Methyl Ether–Silver Trifluoromethanesulfonate. *J. Org. Chem.* **2013**, *78*, 3438–3444.

reaction, the *tert*–butyldiphenylsilyl (TBDPS) was used as an initial hydroxyl protecting group. The Vilsmeier–Haack formylation gave promising results (entry 1–2), compared to Lewis acid assisted conditions (entry 3–4). Interestingly, use of the preformed Vilsmeier reagent improved the reaction yield to 42% (entry 6). However, TBDPS deprotection was faster than the formylation under these conditions. Surprisingly, an acetyl group was tolerated under Vilsmeier–Haack conditions without the ester deprotection (entry 7). Finally, it was revealed that the Vilsmeier-Haack formylation with preformed (chloromethylene)dimethyliminium chloride at –35 ºC provided bisformylated product **2.6** in 86% yield without acyl deprotection (entry 9).

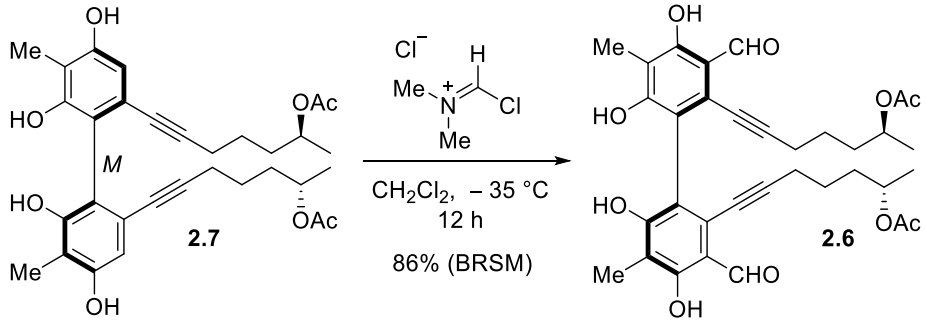

Scheme 2.5. Vilsmeier–Haack Formylation[1]

2.6. Oxidative Dearomatization

Subsequently, an oxidative dearomatization reaction, which was developed by Porco and coworkers, was used to generate the bicyclic core featuring a quaternary stereocenter.[12] Initially, we tested this transformation using monomeric formylated phenol **2.20**, which was easily prepared from monomer **2.8** in 85% yield (**Scheme 2.6**). Based on the literature, $Au(OAc)_3$ was the optimal Lewis acid for this transformation. These

[12] Zhu, J.; Germain, A. R.; Porco, J. A. Synthesis of Azaphilones and Related Molecules by Employing Cycloisomerization of O-Alkynylbenzaldehydes. *Angew. Chem. Int. Ed.* **2004**, *43*, 1239–1243.

conditions efficiently provided the desired oxygenated core **2.21** upon IBX oxidation as gaining access to a monomer **2.22** after acetylation (72% yield over three steps).

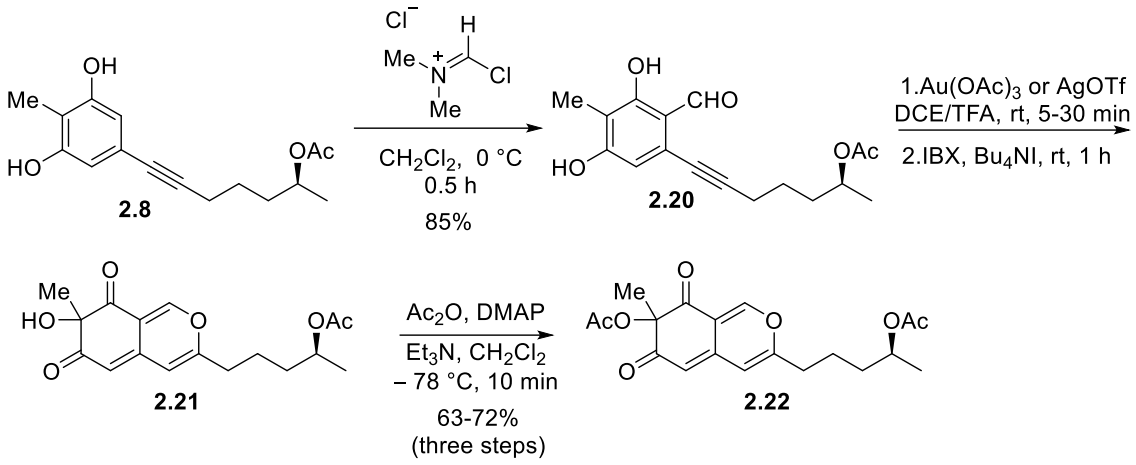

Scheme 2.6. Oxidative Dearomatization with Monomer **2.20**[1]

With dimer **2.6**, however, $Au(OAc)_3$-catalyzed dearomatization did not generate desired product **2.5**. The use of Au catalyst to activate bisformyl **2.6** causing decomposition. After screening several Lewis acids, we found that AgOTf[13] gave a similar result (63% overall yield from **2.20**) as in the model system (**Scheme 2.6**). Cycloisomerization of **2.6** occured in the presence of AgOTf, and subsequent oxidation with hypervalent iodine, IBX, allowed access to bicyclic dimer **2.5** (**Scheme 2.7**). We had theorized that the chiral axis would influence the stereochemistry during formation of this quaternary center, with the bulk of the 2*H*-isoquinoline-2,6-dione backbone blocking one stereoface. That the reaction gave a 1:1:1 mixture of the three possible isomers (7*S*,7'*S*, 7*S*,7'*R*, and 7*R*,7'*R*) indicates that such a stereocontrol scenario is most likely not active in the biosynthesis. Fortunately, sufficient amounts of each isomer were obtained to proceed with the synthesis. The following section describes the results obtained with the

[13] Feng, X.; Wang, H.; Yang, B.; Fan, R. One-Pot Synthesis of Highly Substituted 4-Acetonylindoles via Sequential Dearomatization and Silver-Catalyzed Domino Reaction. *Org. Lett.* **2014**, *16*, 3600–3603.

faster eluting symmetric diastereomer, which could not be definitively assigned as 7*S*,7'*S* or 7*R*,7'*R* at this stage.

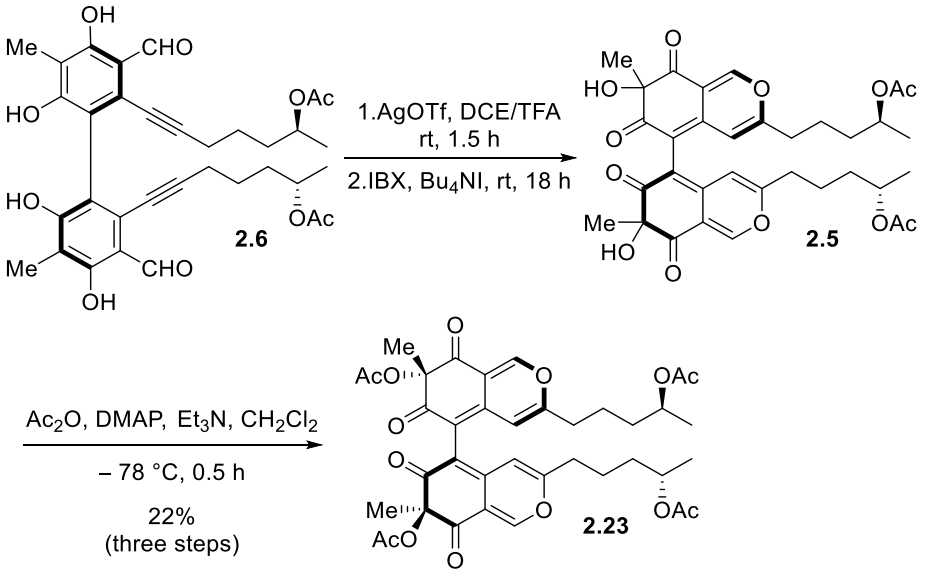

Scheme 2.7. Oxidative Dearomatization with Dimer **2.6**[1]

At this juncture, selective acylation of the tertiary alcohol centers was needed, which was achieved either by deacylation of the secondary alcohols followed by selective acylation of the tertiary alcohols or by global acetylation followed by selection deacylation of the less hindered secondary alcohols. The former possibility takes advantage of the greater reactivity of the alcohols adjacent to the ketone.[14] Upon removal of the acetyl groups from **2.5**, the resultant product was found to be prone to decomposition. As such, the latter alternative became a focus. Acetylation of **2.5** afforded product **2.23** in 22% over three steps from **2.6**, which represent six sets of chemical transformations due to the dimeric nature of the material (**Scheme 2.7**).

[14] Holton, R. A.; Zhang, Z.; Clarke, P. A.; Nadizadeh, H.; Procter, D. J. Selective Protection of the C(7) and C(10) Hydroxyl Groups in 10-Deacetyl Baccatin III. *Tetrahedron Lett.* **1998**, *39*, 2883–2886.

2.7. Selective Acetyl Deprotection

Unexpectedly, selective deprotection of the secondary acetoxy group in the presence of the sterically congested quaternary acetoxy group was challenging. Attempted hydrolysis of **2.23** with acidic or basic conditions led to decomposition that was faster than deprotection. We explored a wide range of hydrolysis conditions,[15] including enzymatic methods (see Experimental Section),[16] and finally established that 10 equiv of

[15] (a) Plattner, J. J.; Gless, R. D.; Rapoport, H. Synthesis of Some DE and CDE Ring Analogs of Camptothecin. *J. Am. Chem. Soc.* **1972**, *94*, 8613–8615. (b) Mori, K.; Tominaga, M.; Takigawa, T.; Matsui, M. A Mild Transesterification Method. *Synthesis* **1973**, 790–791. (c) Askin, D.; Angst, C.; Danishefsky, S. An Approach to the Synthesis of Bactobolin and the Total Synthesis of N-Acetylactinobolamine: Some Remarkably Stable Hemiacetals. *J. Org. Chem.* **1987**, *52*, 622–635. (d) Nudelman, A.; Herzig, J.; Gottlieb, H. E.; Keinan, E.; Sterling, J. Selective Deacetylation of Anomeric Sugar Acetates with Tin Alkoxides. *Carbohydr. Res.* **1987**, *162*, 145–152. (e) Baptistella, L. H. B.; Santos, J. F. D.; Ballabio, K. C.; Marsaioli, A. J. 1,8-Diazabicyclo[5.4.0]Undec-7-Ene as a Mild Deprotective Agent for Acetyl Groups. *Synthesis* **1989**, *21*, 436–439. (f) Roush, W. R.; Lin, X.-F. Studies on the Synthesis of Aureolic Acid Antibiotics: Highly Stereoselective Synthesis of Aryl 2-Deoxy-.Beta.-Glycosides via the Mitsunobu Reaction and Synthesis of the Olivomycin A-B Disaccharide. *J. Am. Chem. Soc.* **1995**, *117*, 2236–2250. (g) Yamamoto, N.; Nishikawa, T.; Isobe, M. Synthesis of Bicyclic Hydroxy Lactone Intermediates toward (-)-Tetrodotoxin. *Synlett* **1995**, 505–506. (h) Yanada, R.; Negoro, N.; Bessho, K.; Yanada, K. Metallic Samarium and Iodine in Alcohol. Deacylation and Dealkyloxycarbonylation of Protected Alcohols and Lactams. *Synlett* **1995**, 1261–1263. (i) Xu, Y.-C.; Bizuneh, A.; Walker, C. A Reagent for Selective Deprotection of Alkyl Acetates. *J. Org. Chem.* **1996**, *61*, 9086–9089. (j) Kajiro, H.; Mitamura, S.; Mori, A.; Hiyama, T. Scandium Trifluoromethanesulfonate-Catalyzed Mild, Efficient, and Selective Cleavage of Acetates Bearing a Coordinative Group. *Tetrahedron Lett.* **1999**, *40*, 1689–1692. (k) Sharma, G. V. M.; Ilangovan, A. Ytterbium Triflate Mediated Selective Deprotection of Acetates. *Synlett* **1999**, 1963–1965. (l) Yoshimoto, K.; Kawabata, H.; Nakamichi, N.; Hayashi, M. Tris(2,4,6-Trimethoxyphenyl)Phosphine (TTMPP): A Novel Catalyst for Selective Deacetylation. *Chem. Lett.* **2001**, *30*, 934–935. (m) Ravindranathan Kartha, K. P.; Mukhopadhyay, B.; Field, R. A. Practical De-O-Acylation Reactions Promoted by Molecular Sieves. *Carbohydr. Res.* **2004**, *339*, 729–732. (n) Wang, S.-M.; Ge, W.-Z.; Liu, H.-M.; Zou, D.-P.; Yan, X.-B. Syntheses of Acetylated Steroid Glycosides and Selective Cleavage of O-Acetyl Groups in Sugar Moiety. *Steroids* **2004**, *69*, 599–604. (o) Ren, B.; Cai, L.; Zhang, L.-R.; Yang, Z.-J.; Zhang, L.-H. Selective Deacetylation Using Iodine–methanol Reagent in Fully Acetylated Nucleosides. *Tetrahedron Lett.* **2005**, *46*, 8083–8086. (p) Yeom, C.-E.; Lee, S. Y.; Kim, Y. J.; Kim, B. M. Mild and Chemoselective Deacetylation Method Using a Catalytic Amount of Acetyl Chloride in Methanol. *Synlett* **2005**, 1527–1530. (q) B. C. Ranu, S. K. Guchhait, M. Saha, *J. Indian Chem. Soc.* **1999**, *76*, 547.

[16] (a) Sakaki, J.; Sakoda, H.; Sugita, Y.; Sato, M.; Kaneko, C. Lipase-Catalyzed Asymmetric Synthesis of 6-(3-Chloro-2-Hydroxypropyl)-1,3-Dioxin-4-Ones and Their Conversion to Chiral 5,6-Epoxyhexanoates. *Tetrahedron Asymmetry* **1991**, *2*, 343–346. (b) Lopez, R.; Montero, E.; Sanchez, F.; Canada, J.; Fernandez-Mayoralas, A. Regioselective Acetylations of Alkyl .Beta.-D-Xylopyranosides by Use of Lipase PS in Organic Solvents and Application to the Chemoenzymic Synthesis of Oligosaccharides. *J. Org. Chem.* **1994**, *59*, 7027–7032. (c) Houille, O.; Schmittberger, T.; Uguen, D. A Remarkably Simple Process for Monoprotecting Diols. *Tetrahedron Lett.* **1996**, *37*, 625–628.

Ti(O*i*-Pr)$_4$ in CH_2Cl_2 at elevated temperature afforded free hydroxylated **2.24** in 52% yield (**Scheme 2.8**).[15p] Exposure of oxygenated bicycle **2.24** to excess NH_4OAc furnished synthetic chaetoglobin A (**2.1**) in nearly quantitative yield.

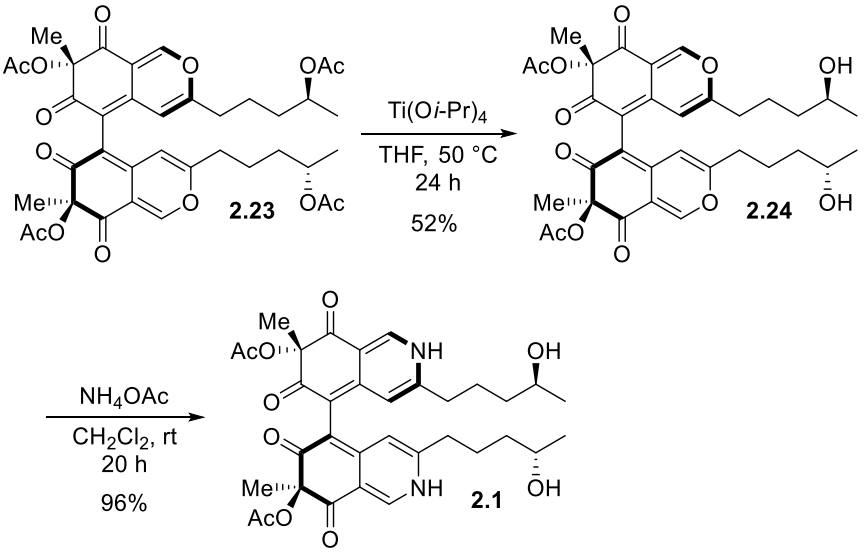

Scheme 2.8. Selective Acetyl Deprotection and Amination to make Chaetoglobin A (**2.1**)[1]

2.8. Confirmation of Synthetic Product 2.1

The spectroscopic data from synthetic **2.1** was in accord with those reported in the literature for chaetoglobin A (**Table 2.3**).[2] In particular, the ^{13}C NMR gave rise to 17 differentiable carbons supporting the symmetric structure, and the chemical shifts of those signals closely matched those from the natural product, securing evidence that the correct diastereomeric relationship between the quaternary carbons and the stereoaxis had been generated (**Table 2.3**). Importantly, circular dichroism data obtained from the synthetic material proved identical to that from the natural product (**Figure 2.2**), which indicates that both the correct absolute and relative stereochemistries are established.

Natural Product			**Synthetic Product**		
^1H (ppm)	IR (cm^{-1})	^{13}C (ppm)	^1H (ppm)	IR (cm^{-1})	^{13}C (ppm)

1.16 (d)	3384	20.4	1.12 (d)	3383	20.6
1.45 (m)	2931	23.3	1.39–1.45 (m)	2928	23.4
1.64 (s)	1732	23.4	1.60 (s)	1732	23.6
1.72 (m)	1692	25.3	1.63–1.72 (m)	1692	25.5
2.19 (s)	1644	33.9	2.15 (s)	1643	34.1
2.49 (t)	1549	39.0	2.45 (t)	1547	39.2
3.73 (m)	1471	67.8	3.67–3.73 (m)	1465	68.1
6.42 (s)	1372	85.7	6.37 (s)	1373	86.0
8.05 (s)	1247	103.7	8.00 (s)	1248	104.0
	1204	116.0		1206	116.1
	1128	116.7		1130	116.9
	1080	139.6		1081	139.7
		151.2			151.3
		153.2			153.2
		171.8			172.0
		189.6			189.9
		197.8			198.0

[a]20 mol% [b]0.3 M [c]Isolated yield based on recovery of substrate in parentheses [d]0.5 M

Table 2.3. Comparing Spectral Data between Natural Product vs Synthetic Product (**2.1**)

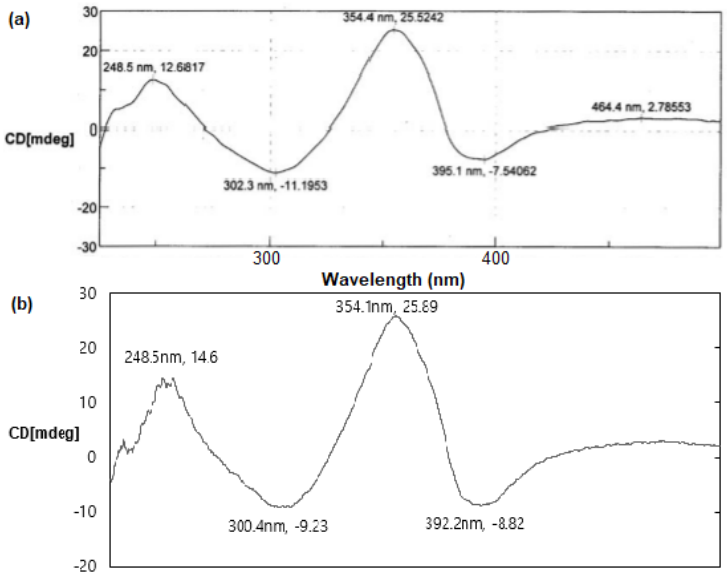

Figure 2.2. Comparing Circular Dichroism of Chaetoglobin A (**2.1**) (a) CD Spectrum of Natural Product Isolate. Adapted from reference 2 with permission of The Royal Society of Chemistry; (b) Synthetic **2.1** CD Spectrum.[1]

2.9. Conclusions

In conclusion, we have accomplished the first total synthesis of chaetoglobin A in 4.3% overall yield, with 12 steps in the longest linear sequence. A vanadium-catalyzed asymmetric oxidative phenol coupling serves as a key step in the formation of stereoaxis of chiral azaphilone dimer **1**. The stereochemical results from oxidative cyclization after formation of the stereoaxis raise interesting questions about the operating biosynthetic pathways; oxidative cyclization after dimerization appears unlikely.

2.10. Experimental Section

General Information

Unless otherwise noted, all non-aqueous reactions were carried out under an atmosphere of dry N_2 in dried glassware. When necessary, solvents and reagents were dried prior to use. THF was distilled from sodium benzophenone ketyl. CH_2Cl_2, and toluene were distilled from CaH_2. High throughput experiments were performed at the Penn/Merck

High Throughput Experimentation Laboratory at the University of Pennsylvania. The screens were analyzed by HPLC using an internal standard.

Analytical thin layer chromatography (TLC) was performed on EM Reagents 0.25 mm silica-gel 254-F plates. Visualization was accomplished with UV light. Chromatography was performed using a forced flow of the indicated solvent system on EM Reagents Silica Gel 60 (230-400 mesh). When necessary, the column was pre-washed with 1% Et_3N in the eluent system. ^1H NMR spectra were recorded on a 500 MHz spectrometer. Chemical shifts are reported in ppm from tetramethylsilane (0 ppm) or from the solvent resonance ($CDCl_3$ 7.26 ppm, acetone-d_6 2.05 ppm, DMF-d_7 2.50 ppm, CD_3CN 1.94 ppm, CD_2Cl_2 5.32 ppm). Data are reported as follows: chemical shift, multiplicity (s = singlet, d = doublet, t = triplet, q = quartet, br = broad, m = multiplet), coupling constants, and number of protons. Decoupled ^{13}C NMR spectra were recorded at 125 MHz. IR spectra were taken on an FT-IR spectrometer using a neat film. Accurate mass measurement analyses were conducted via time-of-flight mass analyzer GCMS with electron ionization (EI) or via time-of-flight mass analyzer LCMS with electrospray ionization (ESI). The signals were measured against an internal reference of perfluorotributylamine for EI-GCMS and leucine enkephalin for ESI-LCMS. The instrument was calibrated and measurements were made using neutral atomic masses; the mass of the electron removed or added to create the charged species is not taken into account. Low resolution LCMS data were obtained by use of a UPLC system with a SQD mass analyzer equipped with electrospray ionization. Melting points are corrected. Enantiomeric excesses were determined using analytical HPLC with UV detection at 254 nm. Analytical Chiralpak columns (4.6 mm x 250 mm, 5 µm) from Daicel were used. Optical rotations were measured on a polarimeter with a sodium lamp.

Experimental Procedures and Characterization Data

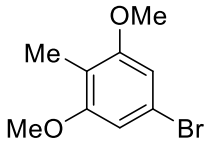

5-Bromo-1,3-dimethoxy-2-methylbenzene (2.13). In a glove box, $[Ir(COD)(OMe)]_2$ (54 mg, 0.08 mmol), 4,4'-di-*tert*-butyl-2,2'-dipyridyl (44 mg, 0.16 mmol), B_2Pin_2 (7.09 g, 27.9 mmol), and 2,6-dimethoxytoluene (5.00 g, 32.9 mmol) were added to a Schlenk flask, which was then sealed with septum. The reactants were dissolved in distilled THF (41 mL) under an argon atmosphere and the resultant mixture was heated at 80 °C for 44 h. The mixture was cooled to ambient temperature and concentrated. After standing under vacuum for 3 h, the ester was subjected to MeOH (230 mL) and $CuBr_2$ (22.0 g, 98.6 mmol) in distilled H_2O (230 mL). The resultant mixture was heated at 80 °C for 48 h and then, cooled to ambient temperature. The mixture was extracted with EtOAc (150 mL X 3) and the combined organic layer were washed with brine, dried over Na_2SO_4, filtered, and concentrated. Column chromatography (Hex:EtOAc = 99:1) afforded a white powder (6.78 g) in 89% overall yield[17]: $\mathbf{R_f}$ = 0.56 (Hexane:EtOAc = 40:1); **^{1}H NMR** (500 MHz, $CDCl_3$) δ 6.67 (s, 2H), 3.80 (s, 6H), 2.02 (s, 3H); **^{13}C NMR** (125 MHz, $CDCl_3$) δ 158.9, 119.3, 113.7, 107.4, 56.0, 8.2; **IR** (neat) 2938, 2834, 1586, 1464, 1402, 1310, 1283, 1253, 1227, 1181, 1139, 1126, 1041, 843 cm^{-1}; **HRMS** (EI-TOF) *m/z* calcd for $C_9H_{11}BrO_2$ $[M]^+$ 229.9942, found 229.9927

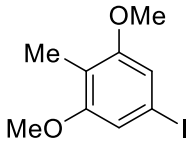

5-Iodo-1,3-dimethoxy-2-methylbenzene (2.S1). A Schlenk flask was charged with CuI

[17] Murphy, J. M.; Liao, X.; Hartwig, J. F. Meta Halogenation of 1,3-Disubstituted Arenes via Iridium-Catalyzed Arene Borylation. *J. Am. Chem. Soc.* **2007**, *129*, 15434–15435.

(279 mg, 1.47 mmol), NaI (8.80 g, 58.7 mmol), and **2.13** (6.78 g, 29.3 mmol). The reactants were dissolved in 1,4-dioxane (29 mL) and *N,N'*-dimethylethylenediamine (0.32 mL, 2.93 mmol) under an argon atmosphere. The resultant mixture was stirred at 110 °C for 48 h. The resulting suspension was allowed to cool to ambient temperature, diluted with satd NH_4Cl, poured into water and extracted with CH_2Cl_2 (15 mL X 3). The combined organic phases were dried over Na_2SO_4 and filtered. Removal of solvent and chromatography (Hex:EtOAc = 99:1) afforded a white powder (7.75 g) in 95% yield. ^{1}H NMR spectrum is in accord with that previously reported[18]: $\mathbf{R_f}$ = 0.61 (Hexane:EtOAc = 40:1); **^{1}H NMR** (500 MHz, $CDCl_3$) δ 6.85 (s, 2H), 3.80 (s, 6H), 2.03 (s, 3H); **^{13}C NMR** (125 MHz, $CDCl_3$) δ 158.9, 114.8, 113.4, 89.7, 56.1, 8.2; **IR** (neat) 2996, 2911, 2852, 1575, 1485, 1448, 1435, 1396, 1304, 1279, 1234, 1180, 1132, 841 cm^{-1}; **HRMS** (EI-TOF) *m/z* calcd for $C_9H_{11}IO_2$ $[M]^+$ 277.9804, found 277.9804

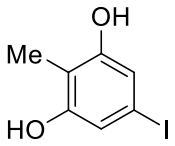

5-Iodo-2-methylbenzene-1,3-diol (2.9). 2.S1 (6.94 g, 25.0 mmol) was dissolved in CH_2Cl_2 (50 mL). After cooling to –78 ºC, a solution of BBr_3 (1 M in dichloromethane, 62 mL) was added dropwise. The resultant mixture was allowed to warm to ambient temperature and stirred until completion as judged by TLC (24 h). The mixture was subsequently quenched with water (15 mL) in an ice bath. The solution was extracted with CH_2Cl_2 (20 mL X 3). The combined organic phases were washed with brine and dried over Na_2SO_4. Removal of solvent followed by chromatography (100 % CH_2Cl_2) afforded a white powder (5.62 g) in 90% yield: $\mathbf{R_f}$ = 0.22 (100 % CH_2Cl_2); **^{1}H NMR** (500 MHz, $(CD_3)_2CO$) δ

[18] Duggan, K. A. Compositions for the Treatment of Hypertension and/or Fibrosis. WO2015039172 (A1), March 26, **2015**.

8.37 (br s, 2H), 6.78 (s, 2H), 2.02 (s, 3H); **^{13}C NMR** (125 MHz, CD_3CN) δ 157.6, 116.8, 112.1, 89.6, 8.4; **IR** (neat) 3367, 2918, 2496, 1580, 1494, 1442, 1396, 1324, 1274, 1229, 1055, 952, 845 cm^{-1}; **HRMS** (EI-TOF) *m/z* calcd for $C_7H_7IO_2$ $[M]^+$ 249.9491, found 249.9475

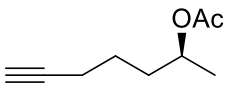

(*S*)-Hept-6-yn-2-yl acetate (2.10). To a stirred solution of **2.17** (35.7 mmol), which was prepared over two steps without chromatography,[9] in CH_2Cl_2 (71 mL) was added pyridine (5.8 mL, 71.4 mmol), at 0 ºC followed by the addition of 4-(dimethylamino)pyridine (1.09 g, 8.93 mmol) and Ac_2O (3.7 mL, 39.3 mmol). The resultant mixture was stirred for 30 min and then was quenched with 1*N* HCl (95 mL) in an ice bath. The resulting mixture was extracted with CH_2Cl_2 (20 mL X 3) and the combined organic phases were sequentially washed with H_2O (50 mL) and satd $NaHCO_3$ (50 mL). The organic layer was dried over Na_2SO_4 and filtered. Removal of the solvent followed by chromatography (Hex:EtOAc = 10:1) gave the desired product as clear liquid (4.09 g) in 74% over three steps: $\mathbf{R_f}$ = 0.75 (Hexane:EtOAc = 4:1); $\mathbf{[\alpha]_D^{22}}$ = +4.1 (c 1.4, CH_3OH); **^{1}H NMR** (500 MHz, $CDCl_3$) δ 4.88-4.94 (m, 1H), 2.20 (td, *J* = 7.0, 2.5 Hz, 2H), 2.02 (s, 3H), 1.95 (t, *J* = 2.5 Hz, 1H), 1.49-1.71 (m, 4H), 1.22 (d, *J* = 6.5 Hz, 3H); **^{13}C NMR** (125 MHz, $CDCl_3$) δ 170.9, 84.1, 70.6, 68.8, 35.1, 24.5, 21.5, 20.1, 18.4; **IR** (neat) 3295, 2978, 2937, 2870, 1731, 1436, 1371, 1241, 1133, 1073, 1049, 1018, 976 cm^{-1}; **HRMS** (EI-TOF) *m/z* calcd for $C_9H_{14}O_2$ $[M]^+$ 154.0994, found 154.0982

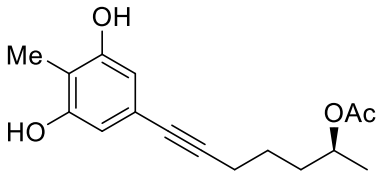

(*S*)-7-(3,5-Dihydroxy-4-methylphenyl)hept-6-yn-2-yl acetate (2-8). To an oven-dried

Schlenk flask was added **2.9** (2.67 g, 10.7 mmol), $Pd(PPh_3)_2Cl_2$ (750 mg, 1.07 mmol), CuI (203 mg, 1.07 mmol) and **2.10** (1.81 g, 11.7 mmol). The flask was sealed with a septum and purged with argon. The resultant mixture was dissolved in DMF (36 mL) and Et_2NH (3.9 mL, 37.4 mmol). The mixture was stirred at 65 ºC for 18 h. After cooling to ambient temperature, the reaction mixture was treated with satd NH_4Cl (15 mL). The resultant mixture was poured into water and extracted with Et_2O (40 mL X 3). The combined organic layers were washed thoroughly with satd LiCl (3 mL X 3) and brine. The organic layer was dried over Na_2SO_4 and filtered. Removal of the solvent followed by chromatography (Hex:EtOAc = 4:1) afforded a brown oil (2.88 g) in 98% yield: $\mathbf{R_f}$ = 0.36 (Hexane:EtOAc = 2:1); $\mathbf{[\alpha]_D^{22}}$ = –4.5 (c 0.24, CH_3OH); **^{1}H NMR** (500 MHz, $CDCl_3$) δ 6.46 (s, 2H), 5.99 (br s, 2H), 4.96-5.02 (m, 1H), 2.38 (t, *J* = 7.0 Hz, 2H), 2.11 (s, 3H), 2.06 (s, 3H), 1.53-1.77 (m, 4H), 1.24 (d, *J* = 6.5 Hz, 3H); **^{13}C NMR** (125 MHz, $CDCl_3$) δ 172.1, 154.8, 121.5, 111.6, 110.9, 88.7, 80.9, 71.4, 35.0, 24.5, 21.5, 19.9, 19.2, 8.2; **IR** (neat) 3386, 2935, 1699, 1616, 1583, 1413, 1375, 1341, 1323, 1265, 1165, 1133, 1078, 1023, 950 cm^{-1}; **HRMS** (ESI-TOF) *m/z* calcd for $C_{16}H_{20}O_4Na$ $[M+Na]^+$ 299.1259, found 299.1273

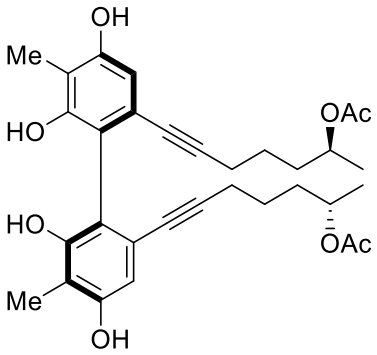

(2*S*,2'*S*)-((*R*)-4,4',6,6'-Tetrahydroxy-5,5'-dimethyl-[1,1'-biphenyl]-2,2'-diyl)bis(hept-6-yne-7,2-diyl) diacetate (2.7). To a microwave vial was added phenol **2.8** (320 mg, 1.15 mmol), vanadium catalyst **2.18** (103 mg, 0.23 mmol), and HOAc (13 mL, 0.23 mmol). The vial was sealed and chlorobenzene (2.3 mL) was added. Oxygen was added via an active

purge. The deep blue solution was stirred for 42 h at 0 °C. The reaction mixture was directly chromatographed (Hex:EtOAc = 4:1) to afford the mixture of coupled products (214 mg) in 67% yield with 94:6 dr (the diastereoselectivity varies depending on batch of the catalyst from 4:1 to >15:1). The combined mixture of products (1.497 g) was dissolved in methanol (10 mL). This solution was used as feeding solution (150 mg/mL) for Supercritical Fluid Chromatographic separation (SFC). The separation of the two isomers was performed using a Lux Celluiose-4 column (21 x 250 mm) with 30% MeOH / 70% CO_2 at 35 °C (flow rate 60 mL/min, BP 100 bar, detector 210 nm). Five hundred μL of feeding solution was injected at a time and two fractions (2.2-2.5 min, and 3.1-3.7 min) were collected for each run. Concentration of the two fractions afforded 180 mg of the (*P*)**-7** as light yellow powder and 1.05 g of **2.7** as light yellow powder: $\mathbf{R_f}$ = 0.23 (Hexane:EtOAc = 2:1); $\mathbf{[\alpha]_D^{22}}$ = –33.5 (c 0.30, CH_3OH); **^{1}H NMR** (500 MHz, $CDCl_3$) δ 6.53 (s, 2H), 5.76 (br s, 2H), 5.03 (br s, 2H), 4.76-4.83 (m, 2H), 2.16-2.19 (m, 4H), 2.17 (s, 6H), 2.06 (s, 6H), 1.20-1.43 (m, 8H), 1.15 (d, *J* = 6.5 Hz, 6H); **^{13}C NMR** (125 MHz, $CDCl_3$) δ 171.7, 155.1, 153.6, 123.1, 115.3, 112.0, 111.3, 92.1, 79.2, 71.1, 34.7, 24.6, 21.6, 20.0, 19.3, 8.8; **IR** (neat) 3540, 3375, 2950, 1708, 1683, 1604, 1585, 1431, 1404, 1377, 1345, 1323, 1288, 1277, 1239, 1163, 1136, 1076, 1047, 1020, 839 cm^{-1}; **HRMS** (ESI-TOF) *m/z* calcd for $C_{32}H_{39}O_8$ $[M+H]^+$ 551.2645, found 551.2650; **HPLC** (Chiralpak IA column) 20% *i*-PrOH/Hexane (1 mL/min), t(**7**) = 10.5 min, t((*P*)-**7**) = 28.7 min

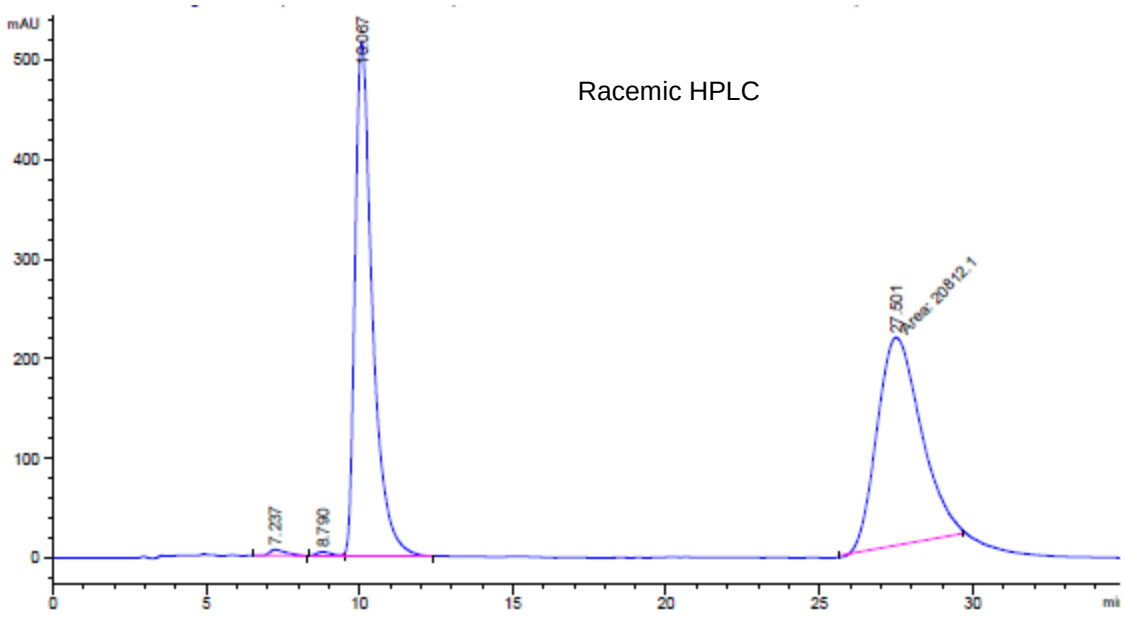

Peak #	RetTime [min]	Type	Width [min]	Area [mAU*s]	Height [mAU]	Area %
1	7.237	BB	0.5406	228.06839	5.94642	0.5487
2	8.790	BV E	0.4962	130.41409	3.96127	0.3138
3	10.067	VB R	0.5965	2.03943e4	515.99664	49.0662
4	27.501	MM	1.6603	2.08121e4	208.91748	50.0713

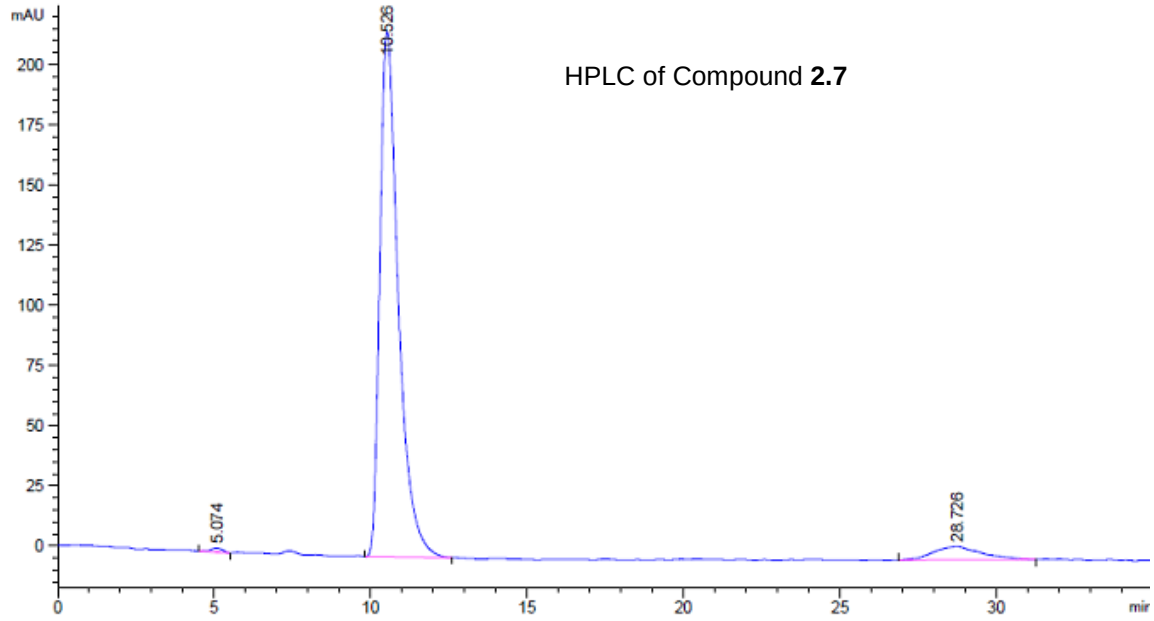

HPLC of Compound **2.7**

Peak #	RetTime [min]	Type	Width [min]	Area [mAU*s]	Height [mAU]	Area %
1	5.074	BB	0.3663	44.76253	1.70340	0.4657
2	10.526	BB	0.6224	8974.86426	218.29311	93.3712
3	28.726	BB	1.3393	592.39465	5.55268	6.1631

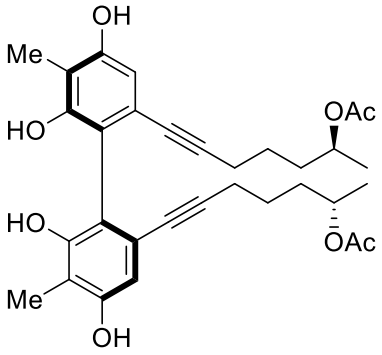

(2*S*,2'*S*)-((*S*)-4,4',6,6'-Tetrahydroxy-5,5'-dimethyl-[1,1'-biphenyl]-2,2'-diyl)bis(hept-6-yne-7,2-diyl) diacetate [(*P*)-2.7]: **R_f** = 0.23 (Hexane:EtOAc = 2:1); **$[\alpha]_D^{22}$** = +8.4 (c 0.39, CH_3OH); **^{1}H NMR** (500 MHz, $CDCl_3$) δ 6.76 (br s, 2H), 6.59 (s, 2H), 5.23 (br s, 2H), 4.75-4.80 (m, 2H), 2.12-2.22 (m, 4H), 2.13 (s, 6H), 2.02 (s, 6H), 1.31-1.43 (m, 6H), 1.17 (d, *J* = 6.5 Hz, 6H), 1.05-1.18 (m, 2H); **^{13}C NMR** (125 MHz, $CDCl_3$) δ 171.9, 155.3, 153.7, 122.9, 115.4, 112.1, 111.0, 92.0, 79.5, 71.6, 34.6, 24.5, 21.5, 20.0, 19.2, 8.8; **IR** (neat) 3406,

2944, 1709, 1604, 1582, 1398, 1374, 1348, 1322, 1267, 1164, 1132, 1077, 1032, 991, 952 cm^{-1}; **HRMS** (ESI-TOF) *m/z* calcd for $C_{32}H_{38}O_8Na$ $[M+Na]^+$ 573.2464, found 573.2479

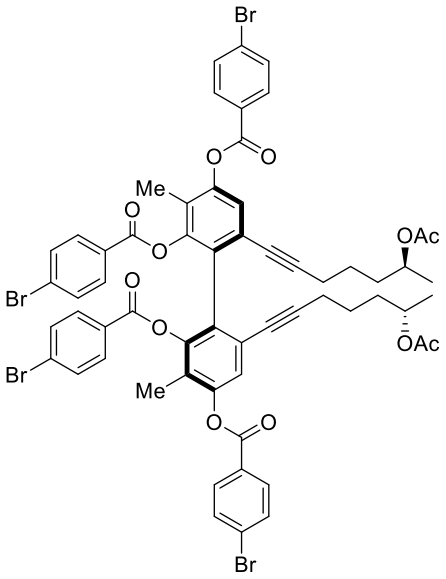

6,6'-Bis((*S*)-6-acetoxyhept-1-yn-1-yl)-3,3'-dimethyl-[1,1'-biphenyl]-2,2',4,4'-tetrayl tetrakis(4-bromobenzoate) (2.19). To a stirred solution of **2.7** (50 mg, 0.09 mmol) in CH_2Cl_2 (0.91 mL) was added 4-bromobenzoyl chloride (90 mg, 0.41 mmol) and Et_3N (40 μL, 0.27 mmol) at room temperature. The mixture was stirred for 14 h and the resultant solution was washed with 1 *N* HCl (2 mL X 2) and brine. The organic layer was dried over Na_2SO_4 and filtered. Removal of the solvent and chromatography (Hex:EtOAc = 10:1) afforded light yellow powder (105 mg) in 91% yield. Crystallization from EtOAc and pentane via the vapor diffusion method gave white crystals. The absolute axial configuration was determined as *M* from the X-Ray crystal structure: $\mathbf{R_f}$ = 0.44 (Hexane:EtOAc = 4:1); $\mathbf{[\alpha]_D^{22}}$ = –13.1 (c 2.30, CH_2Cl_2); **^{1}H NMR** (500 MHz, $CDCl_3$) δ 8.07 (d, *J* = 8.5 Hz, 4H), 7.75 (d, *J* = 8.5 Hz, 4H), 7.67 (d, *J* = 8.5 Hz, 4H), 7.58 (d, *J* = 8.5 Hz, 4H), 7.20 (s, 2H), 4.81-4.88 (m, 2H), 2.25 (t, *J* = 6.0 Hz, 4H), 1.98 (s, 12H), 1.33-1.53 (m, 8H), 1.17 (d, *J* = 6.5 Hz, 6H); **^{13}C NMR** (125 MHz, $CDCl_3$) δ 170.8, 163.6, 162.9, 149.4,

148.4, 132.3, 132.1, 131.8, 131.7, 130.1, 129.2, 128.8, 128.2, 128.1, 124.9, 123.8, 123.1, 94.6, 78.2, 70.8, 34.8, 24.3, 21.5, 20.0, 19.4, 11.2; **IR** (neat) 2940, 1737, 1588, 1484, 1398, 1371, 1246, 1173, 1154, 1132, 1110, 1084, 1068, 1009, 954 cm^{-1}; **HRMS** (ESI-TOF) *m/z* calcd for $C_{60}H_{51}Br_4O_{12}$ $[M+H]^+$ 1279.0114, found 1279.0121

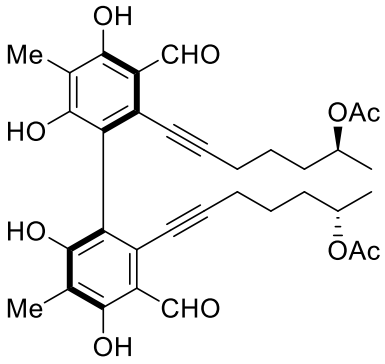

(2*S*,2'*S*)-(3,3'-Diformyl-4,4',6,6'-tetrahydroxy-5,5'-dimethyl-[1,1'-biphenyl]-2,2'-diyl)bis(hept-6-yne-7,2-diyl) diacetate (2.6). The bisphenol **2.7** (457 mg, 0.83 mmol) was dissolved in CH_2Cl_2 (41 mL). After cooling to –35 ºC, five portions of commercial (chloromethylene)dimethyliminium chloride (424 mg, 3.31 mmol) was added every 20 min. The reaction mixture was stirred for 12 h and the mixture was subsequently quenched with satd $NaHCO_3$ (20 mL) in an ice bath. The solution was extracted with EtOAc (40 mL X 3), washed thoroughly with satd LiOH solution (2 mLX 5), and brine. The combined organic layers were dried over Na_2SO_4. Removal of the solvent followed by chromatography (Hex:EtOAc = 4:1) provided a yellow oil (433 mg) in 86 % yield: $\mathbf{R_f}$ = 0.32 (Hexane:EtOAc = 2:1); $\mathbf{[\alpha]_D^{22}}$ = –138.1 (c 0.43, CH_3OH); **^{1}H NMR** (500 MHz, $CDCl_3$) δ 12.32 (s, 2H), 10.21 (s, 2H), 5.92 (s, 2H), 4.76-4.82 (m, 2H), 2.27 (t, *J* = 6.5 Hz, 4H), 2.17 (s, 6H), 2.01 (s, 6H), 1.28-1.44 (m, 8H), 1.12 (d, *J* = 6.5 Hz, 6H); **^{13}C NMR** (125 MHz, $CDCl_3$) δ 195.5, 170.9, 163.5, 159.8, 128.4, 115.5, 114.8, 112.9, 101.4, 74.2, 70.2, 34.7, 24.2, 21.5, 20.0, 19.4, 7.9; **IR** (neat) 3350, 2936, 1734, 1622, 1417, 1368, 1324, 1292, 1248, 1177, 1142, 1104, 1021, 952 cm^{-1}; **HRMS** (ESI-TOF) *m/z* calcd for $C_{34}H_{39}O_{10}$

$[M+H]^+$ 607.2543, found 607.2546

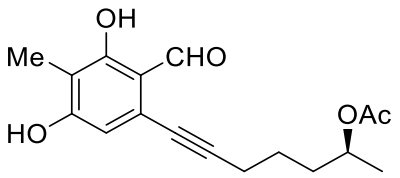

(*S*)-7-(2-Formyl-3,5-dihydroxy-4-methylphenyl)hept-6-yn-2-yl acetate (2.20). Following the same procedure as **2.6** for 30 min using **2.8**, the product was obtained as yellow oil (601 mg) in 85% yield after chromatography (CH_2Cl_2:EtOAc = 20:1): $\mathbf{R_f}$ = 0.68 (CH_2Cl_2:EtOAc = 10:1); $\mathbf{[\alpha]_D^{22}}$ = +9.3 (c 1.85, $CHCl_3$); **^{1}H NMR** (500 MHz, $CDCl_3$) δ 12.25 (s, 1H), 10.15 (s, 1H), 6.50 (s, 1H), 5.83 (s, 1H), 4.95-4.98 (m, 1H), 2.45 (t, *J* = 7.0 Hz, 2H), 2.09 (s, 3H), 2.06 (s, 3H), 1.57-1.78 (m, 4H), 1.24 (d, *J* = 6.0 Hz, 3H); **^{13}C NMR** (125 MHz, $CDCl_3$) δ 195.1, 171.9, 163.1, 161.5, 127.0, 114.2, 112.5, 112.1, 96.2, 76.5, 71.0, 35.1, 24.4, 21.5, 19.9, 19.4, 7.3; **IR** (neat) 3250, 2933, 1732, 1703, 1614, 1487, 1432, 1368, 1305, 1248, 1174, 1139, 1107, 1080, 1046, 1023, 848 cm^{-1}; **HRMS** (ESI-TOF) *m/z* calcd for $C_{17}H_{20}O_5Na$ $[M+Na]^+$ 327.1208, found 327.1202

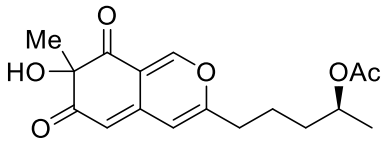

(2*S*)-5-(7-Hydroxy-7-methyl-6,8-dioxo-7,8-dihydro-6H-isochromen-3-yl)pentan-2-yl acetate (2.21). An oven-dried round bottom flask was charged with **2.20** (445 mg, 1.46 mmol) and $Au(OAc)_3$ (27 mg, 0.07 mmol) or AgOTf (38 mg, 0.15 mmol). The mixture was dissolved in 1,2-dichloroethane (7.3 mL), followed by trifluoroacetic acid (0.73 mL). The resulting mixture was stirred for 15 min at rt and then, 2-iodoxybenzoic acid (1.23 g, 4.39 mmol) and tetrabutylammonium iodide (27 mg, 0.07 mmol) were added. The mixture was stirred for 1.5 h and quenched with satd NaS_2O_3 (10 mL). The resultant mixture was extracted with EtOAc (10 mL X 3) and the combined organic layers were washed with

brine. The solution was dried over Na_2SO_4 and filtered. Removal of the solvent was followed by chromatography (Hex:EtOAc = 1:2) afforded red brown oil (379 mg) in 81 % yield: $\mathbf{R_f}$ = 0.44 (100 % EtOAc); **^{1}H NMR** (500 MHz, $CDCl_3$) δ 7.85 (s, 1H), 6.10 (s, 1H), 5.49 (s, 1H), 4.89-4.92 (m, 1H), 3.93 (br s, 1H), 2.39-2.43 (m, 2H), 2.01 (s, 3H), 1.54-1.68 (m, 4H), 1.52 (s, 3H), 1.21 (d, *J* = 6.5 Hz, 3H); **^{13}C NMR** (125 MHz, $CDCl_3$) δ 196.3, 195.8, 170.7, 162.2, 152.9, 143.9, 115.9, 108.6, 105.3, 83.5, 70.1, 35.1, 32.9, 28.5, 22.5, 21.3, 20.0; **IR** (neat) 3441, 2977, 2934, 1718, 1665, 1621, 1548, 1443, 1371, 1346, 1242, 1214, 1169, 1133, 1077, 1047, 1020, 963, 907 cm^{-1}; **HRMS** (ESI-TOF) *m/z* calcd for $C_{17}H_{21}O_6$ $[M+H]^+$ 321.1338, found 321.1333

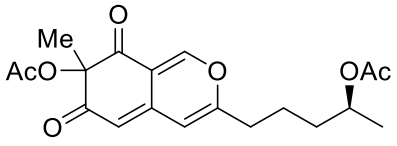

(2*S*)-5-(7-Acetoxy-7-methyl-6,8-dioxo-7,8-dihydro-6H-isochromen-3-yl)pentan-2-yl acetate (2.22). Alcohol **2.21** was subject to the same procedure used for **2.10** for –78 ºC for 10 min with Et_3N as the base. The product was obtained as a red brown oil (379 mg) in 89% yield after chromatography (Hex:EtOAc = 1:1): $\mathbf{R_f}$ = 0.43 (Hexane:EtOAc = 1:2); **^{1}H NMR** (500 MHz, $CDCl_3$) δ 7.82 (d, *J* = 1.0 Hz, 1H), 6.06 (s, 1H), 5.46 (d, *J* = 1.0 Hz, 1H), 4.86-4.89 (m, 1H), 2.36-2.39 (m, 2H), 2.10 (s, 3H), 1.99 (s, 3H), 1.49-1.63 (m, 4H), 1.47 (s, 3H), 1.18 (d, *J* = 6.5 Hz, 3H); **^{13}C NMR** (125 MHz, $CDCl_3$) δ 193.2, 192.6, 170.6, 169.9, 161.6, 153.8, 142.5, 115.2, 108.9, 106.9, 84.4, 70.0, 35.0, 32.7, 22.4, 22.2, 21.3, 20.1, 19.9; **IR** (neat) 2940, 1716, 1669, 1634, 1592, 1553, 1446, 1370, 1343, 1308, 1243, 1181, 1132, 1088, 1045, 1019, 975, 939 cm^{-1}; **HRMS** (ESI-TOF) *m/z* calcd for $C_{19}H_{23}O_7$ $[M+H]^+$ 363.1444, found 363.1463

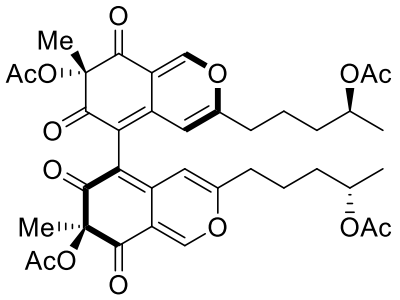

(7*S*,7'*S*)-3,3'-Bis((*S*)-4-acetoxypentyl)-7,7'-dimethyl-6,6',8,8'-tetraoxo-7,7',8,8'-tetrahydro-6H,6'H-[5,5'-biisochromene]-7,7'-diyl diacetate (2.23). To **2.6** (244 mg, 0.40 mmol) and AgOTf (10 mg, 0.04 mmol) was added 1,2-dichloroethane (4 mL) and trifluoroacetic acid (0.2 mL) addition. The resulting mixture was stirred for 1.5 h at rt and then, 2-iodoxybenzoic acid (676 mg, 2.41 mmol) and tetrabutylammonium iodide (7.4 mg, 0.02 mmol) were added. The mixture was stirred for additional 18 h, followed by quenching with satd $Na_2S_2O_3$ (8 mL). The resultant mixture was extracted with EtOAc (10 mL X 3) and the combined organic layers were washed with brine. The solution was dried over Na_2SO_4 and filtered. Removal of the solvent followed by chromatography (Hex:EtOAc = 1:2 to 1:5) afforded one separable isomer and mixture of two isomers (1:1). Both fractions were contaminated with IBX waste.

Without further purification, the pure isomer (0.13 mmol) was dissolved in CH_2Cl_2 (7 mL) and the mixture was cooled to –78 ºC. To the solution was added Ac_2O (76 μL, 0.80 mmol), 4-(dimethylamino)pyridine (33 mg, 0.27 mmol), and Et_3N (75 μL, 0.54 mmol). After stirring 15 min, the solution was quenched with 1*N* HCl (2 mL) in an ice bath. The resulting mixture was extracted with CH_2Cl_2 (10 mL X 3) and the combined organic phases were washed with brine. The organic layer was dried over Na_2SO_4 and filtered. Removal of the solvent followed by chromatography (Hex:EtOAc = 1:1) gave the product as orange oil (64 mg) in 22% yield over three steps: $\mathbf{R_f}$ = 0.52 (Hexane:EtOAc = 1:2); $\mathbf{[\alpha]_D^{22}}$ = –11.5 (c 0.24, CH_2Cl_2); **^{1}H NMR** (500 MHz, $CDCl_3$) δ 7.92 (s, 2H), 5.95 (s, 2H), 4.84-4.90 (m,

2H), 2.35 (t, *J* = 7.0 Hz, 4H), 2.16 (s, 6H), 2.01 (s, 6H), 1.48-1.66 (m, 14H), 1.20 (d, *J* = 6.5 Hz, 6H); **^{13}C NMR** (125 MHz, $CDCl_3$) δ 193.5, 190.7, 170.8, 170.5, 162.4, 153.7, 141.9, 115.6, 110.6, 107.8, 84.9, 70.4, 35.2, 33.2, 22.4, 22.3, 21.5, 20.4, 20.0; **IR** (neat) 2936, 1730, 1715, 1631, 1582, 1528, 1431, 1371, 1335, 1244, 1131, 1087, 1022, 985, 936 cm^{-1}; **HRMS** (ESI-TOF) *m/z* calcd for $C_{38}H_{43}O_{14}$ $[M+H]^+$ 723.2653, found 723.2661

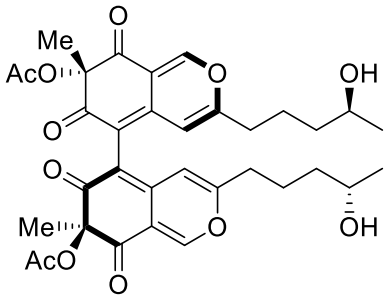

(7*S*,7'*S*)-3,3'-bis((*S*)-4-hydroxypentyl)-7,7'-dimethyl-6,6',8,8'-tetraoxo-7,7',8,8'-tetrahydro-6H,6'H-[5,5'-biisochromene]-7,7'-diyl diacetate (2.24). Compound **2.23** (24 mg, 0.03 mmol) was dissolved in THF (0.66 mL) In a microwave vial under an argon atmosphere. Freshly distilled Ti(O*i*-Pr)$_4$ (0.10 mL, 0.33 mmol) added to the mixture and the vial was sealed. The resultant mixture was stirred at 50 ºC for 24 h. After cooling to ambient temperature, the reaction mixture was diluted with EtOAc (50 mL) and washed with satd Na_2SO_4 until the organic phase became clear. The combined aqueous layers were back-extracted with EtOAc (5 mL) and the organic layer was washed with brine. The solution was dried over $MgSO_4$ and filtered. Removal of the solvent followed by chromatography (Hex:EtOAc = 1:5 to 100 % EtOAc) afforded yellow oil (11 mg) in 52% yield: **R_f** = 0.13 (Hexane:EtOAc = 1:2); **$[\alpha]_D^{22}$** = +14.3 (c 0.22, CH_3OH); **^{1}H NMR** (500 MHz, $CDCl_3$) δ 7.93 (s, 2H), 5.97 (s, 2H), 3.75-3.81 (m, 2H), 2.39 (t, *J* = 7.5 Hz, 4H), 2.17 (s, 6H), 1.68-1.77 (m, 2H), 1.54-1.62 (m, 10H), 1.42-1.47 (m, 4H), 1.17 (d, *J* = 6.2 Hz, 6H); **^{13}C NMR** (125 MHz, $CDCl_3$) δ 193.4, 190.6, 170.9, 162.9, 153.9, 142.1, 115.6, 110.4, 107.7, 85.2, 67.6, 38.2, 33.0, 23.5, 22.49, 22.47, 20.5; **IR** (neat) 3463, 2924, 1713, 1663,

1629, 1582, 1525, 1432, 1372, 1247, 1183, 1132, 1086, 986, 937, 875 cm^{-1}; **HRMS** (ESI-TOF) *m/z* calcd for $C_{34}H_{39}O_{12}$ $[M+H]^+$ 639.2442, found 639.2450

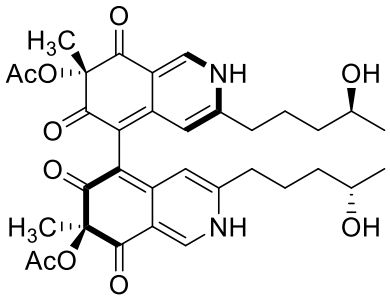

Chaetoglobin A (2.1). Compound **2.24** (9.0 mg, 0.01 mmol) in CH_2Cl_2 (0.28 mL) was treated with NH_4OAc (22 mg, 0.28 mmol) and stirred for 20 h at room temperature. Removal of the solvent followed by chromatography (CH_2Cl_2:MeOH = 9:1) afforded an orange red gum (8.6 mg) in 96% yield: $\mathbf{R_f}$ = 0.10 (CH_2Cl_2:CH_3OH = 10:1); $\mathbf{[\alpha]_D^{22}}$ = +478.4 (c 0.10, CH_3OH); **^{1}H NMR** (500 MHz, CD_3OD) δ 8.00 (s, 2H), 6.37 (s, 2H), 3.67-3.73 (m, 2H), 2.45 (t, *J* = 7.5 Hz, 4H), 2.15 (s, 6H), 1.63-1.72 (m, 4H), 1.60 (s, 6H), 1.39-1.45 (m, 4H), 1.12 (d, *J* = 6.2 Hz, 6H); **^{13}C NMR** (125 MHz, CD_3OD) δ 198.0, 189.9, 172.0, 153.2, 151.3, 139.7, 116.9, 116.1, 104.0, 86.0, 68.1, 39.2, 34.1, 25.5, 23.6, 23.4, 20.6; **IR** (neat) 3383, 2928, 1732, 1692, 1643, 1547, 1465, 1373, 1248, 1206, 1130, 1081, 994 cm^{-1}; **HRMS** (ESI-TOF) *m/z* calcd for $C_{34}H_{41}N_2O_{10}$ $[M+H]^+$ 637.2761, found 637.2775

X-ray Crystallographic Data for compound 2.19

Table 1. Summary of Structure Determination of Compound 2.19

Empirical formula	$C_{60}H_{50}Br_4O_{12}$
Formula weight	1282.64
Temperature/K	100
Crystal system	orthorhombic

Space group	$P2_12_12$
a	25.002(2)Å
b	7.8642(7)Å
c	16.1018(14)Å
Volume	3165.9(5)Å^3
Z	2
d_{calc}	1.346 g/cm^3
μ	2.597 mm^{-1}
F(000)	1292.0
Crystal size, mm	0.15 × 0.08 × 0.02
2θ range for data collection	2.53 - 55.14°
Index ranges	-18 ≤ h ≤ 32, -10 ≤ k ≤ 10, -20 ≤ l ≤ 20
Reflections collected	47673
Independent reflections	7260[R(int) = 0.0853]
Data/restraints/parameters	7260/0/346
Goodness-of-fit on F^2	1.028
Final R indexes [I>=2σ (I)]	R_1 = 0.0835, wR_2 = 0.2093
Final R indexes [all data]	R_1 = 0.1317, wR_2 = 0.2316
Largest diff. peak/hole	1.84/-0.62 eÅ^{-3}
Flack parameter	0.028(7)

Table 2 . Refined Positional Parameters for Compound 2.19

Atom	*x*	*y*	*z*	U(eq)
Br1	0.81867(5)	1.58691(16)	0.30710(9)	0.0682(5)
Br2	0.57919(10)	-0.16032(17)	-0.11975(9)	0.1081(8)
O1	0.3861(3)	0.3655(8)	0.6913(5)	0.0442(17)
O2	0.4023(4)	0.6339(10)	0.7322(5)	0.058(2)
O3	0.6287(3)	0.9713(7)	0.2937(4)	0.0348(15)
O4	0.6625(3)	0.9073(12)	0.4189(5)	0.062(2)
O5	0.5706(3)	0.4322(7)	0.1879(4)	0.0405(15)
O6	0.5555(4)	0.6027(8)	0.0787(4)	0.057(2)
C1	0.5190(4)	0.5739(10)	0.2920(5)	0.031(2)
C2	0.5130(4)	0.7071(9)	0.3486(5)	0.0232(18)
C3	0.5500(4)	0.8382(11)	0.3503(5)	0.030(2)
C4	0.5927(4)	0.8329(10)	0.2981(6)	0.032(2)
C5	0.6027(4)	0.7018(11)	0.2414(6)	0.033(2)
C6	0.5631(4)	0.5749(10)	0.2413(5)	0.037(2)
C7	0.4702(4)	0.7072(10)	0.4072(6)	0.0276(19)
C8	0.4355(4)	0.7054(10)	0.4587(6)	0.033(2)
C9	0.3936(4)	0.6984(13)	0.5244(6)	0.041(2)
C10	0.3661(5)	0.5168(14)	0.5266(6)	0.045(3)
C11	0.4043(4)	0.3754(11)	0.5446(6)	0.042(3)

C12	0.4293(4)	0.3709(11)	0.6279(7)	0.041(2)
C13	0.4634(6)	0.2167(16)	0.6427(9)	0.067(4)
C14	0.3772(5)	0.5022(16)	0.7372(7)	0.050(3)
C15	0.3297(5)	0.4807(18)	0.7916(7)	0.061(3)
C16	0.6627(4)	0.9970(11)	0.3604(6)	0.034(2)
C17	0.6967(4)	1.1442(11)	0.3461(6)	0.034(2)
C18	0.6988(5)	1.2367(13)	0.2741(7)	0.048(3)
C19	0.7348(5)	1.3659(16)	0.2626(8)	0.058(3)
C20	0.7689(5)	1.4088(15)	0.3253(8)	0.056(3)
C21	0.7677(4)	1.3176(15)	0.3992(6)	0.046(3)
C22	0.7337(4)	1.1902(14)	0.4102(6)	0.041(2)
C23	0.6512(5)	0.7016(15)	0.1865(8)	0.060(3)
C24	0.5636(5)	0.4653(10)	0.1066(6)	0.041(2)
C25	0.5686(5)	0.3080(11)	0.0551(6)	0.045(3)
C26	0.5706(6)	0.3281(13)	-0.0313(7)	0.061(4)
C27	0.5759(6)	0.1930(15)	-0.0812(7)	0.070(4)
C28	0.5745(7)	0.0300(15)	-0.0465(7)	0.070(4)
C29	0.5712(6)	0.0079(13)	0.0360(7)	0.057(3)
C30	0.5691(6)	0.1438(13)	0.0875(6)	0.057(3)

Table 3 . Positional Parameters for Hydrogens in Compound 2.19

Atom	*x*	*y*	*z*	U(eq)
H3	0.545484	0.930904	0.387447	0.036
H9a	0.366152	0.786339	0.513315	0.049
H9b	0.409893	0.722789	0.579112	0.049
H10a	0.337757	0.517092	0.56947	0.054
H10b	0.348829	0.495295	0.472245	0.054
H11a	0.385195	0.266543	0.53619	0.051
H11b	0.433377	0.380336	0.502877	0.051
H12	0.451255	0.475749	0.636085	0.049
H13a	0.481798	0.227962	0.696168	0.101
H13b	0.489972	0.206778	0.598138	0.101
H13c	0.440845	0.114924	0.64338	0.101
H15a	0.297994	0.526779	0.763677	0.091
H15b	0.335448	0.541577	0.843949	0.091
H15c	0.324196	0.359561	0.803082	0.091
H18	0.674553	1.210241	0.230599	0.058
H19	0.735914	1.425392	0.211309	0.07
H21	0.791679	1.347056	0.442637	0.055
H22	0.733787	1.129	0.461108	0.049
H23a	0.654621	0.590391	0.159599	0.09
H23b	0.683081	0.724149	0.220077	0.09

H23c	0.647431	0.790084	0.14407	0.09
H26	0.568263	0.438737	-0.054676	0.073
H27	0.58045	0.20766	-0.139347	0.085
H29	0.570353	-0.103838	0.058458	0.069
H30	0.567885	0.127161	0.145867	0.069

Table 4 . Refined Thermal Parameters (U's) for Compound 2.19

Atom	**U_{11}**	**U_{22}**	**U_{33}**	**U_{23}**	**U_{13}**	**U_{12}**
Br1	0.0683(8)	0.0432(6)	0.0932(10)	-0.0002(7)	-0.0194(7)	-0.0234(6)
Br2	0.226(2)	0.0378(7)	0.0607(9)	-0.0248(6)	0.0131(12)	0.0185(10)
O1	0.058(4)	0.026(3)	0.049(4)	-0.005(3)	0.012(4)	0.003(3)
O2	0.074(6)	0.039(5)	0.061(5)	-0.013(4)	0.011(4)	-0.003(4)
O3	0.050(4)	0.020(3)	0.034(4)	-0.001(3)	-0.006(3)	-0.012(3)
O4	0.060(5)	0.070(5)	0.057(5)	0.026(5)	-0.020(4)	-0.017(4)
O5	0.078(5)	0.011(3)	0.032(3)	-0.003(2)	0.006(3)	-0.003(3)
O6	0.114(7)	0.017(3)	0.041(4)	0.005(3)	0.007(4)	0.006(4)
C1	0.055(6)	0.006(3)	0.032(5)	0.000(3)	0.003(4)	-0.003(4)
C2	0.039(5)	0.009(3)	0.021(4)	0.008(3)	-0.007(4)	0.002(3)
C3	0.045(6)	0.016(4)	0.029(5)	0.000(3)	-0.006(4)	-0.003(4)
C4	0.049(6)	0.015(4)	0.033(5)	0.005(4)	-0.005(5)	-0.011(4)
C5	0.050(6)	0.019(4)	0.031(5)	0.001(3)	0.014(4)	-0.002(4)

C6	0.074(7)	0.007(4)	0.029(5)	-0.004(3)	0.003(5)	-0.001(4)
C7	0.038(5)	0.015(4)	0.030(5)	0.001(3)	-0.004(4)	-0.004(4)
C8	0.056(6)	0.015(4)	0.029(5)	0.001(3)	0.008(5)	-0.005(4)
C9	0.041(6)	0.036(6)	0.045(6)	0.005(4)	0.002(5)	-0.002(4)
C10	0.050(7)	0.054(7)	0.032(5)	0.003(5)	0.007(5)	-0.014(5)
C11	0.061(7)	0.016(4)	0.050(6)	-0.004(4)	0.015(5)	-0.016(4)
C12	0.043(6)	0.022(5)	0.057(6)	-0.001(4)	0.014(5)	-0.002(4)
C13	0.079(9)	0.043(7)	0.079(9)	-0.001(6)	0.016(7)	0.008(6)
C14	0.054(7)	0.061(8)	0.035(6)	0.010(5)	-0.007(5)	0.019(6)
C15	0.063(8)	0.072(8)	0.047(7)	0.006(6)	0.026(6)	0.007(6)
C16	0.048(6)	0.026(5)	0.029(5)	0.004(4)	0.000(4)	0.002(4)
C17	0.032(5)	0.022(4)	0.049(6)	-0.004(4)	0.001(4)	0.007(4)
C18	0.068(8)	0.031(5)	0.046(6)	0.009(4)	-0.018(5)	-0.016(5)
C19	0.071(8)	0.052(7)	0.051(7)	0.009(5)	-0.019(6)	-0.021(6)
C20	0.051(7)	0.038(6)	0.078(9)	-0.010(6)	0.001(6)	0.002(5)
C21	0.048(7)	0.060(7)	0.029(5)	-0.004(5)	-0.009(5)	-0.004(5)
C22	0.033(6)	0.051(7)	0.038(5)	-0.005(5)	0.002(5)	0.006(5)
C23	0.079(9)	0.040(6)	0.060(7)	-0.004(6)	0.030(7)	-0.005(6)
C24	0.069(7)	0.012(4)	0.041(6)	0.004(4)	0.002(5)	-0.006(4)
C25	0.073(8)	0.014(4)	0.047(6)	-0.007(4)	0.012(5)	0.008(5)
C26	0.110(11)	0.032(6)	0.042(6)	0.013(5)	0.019(7)	0.020(6)
C27	0.130(12)	0.042(7)	0.040(6)	0.005(5)	0.020(7)	-0.007(7)

C28	0.130(13)	0.038(6)	0.043(6)	-0.019(5)	0.017(7)	0.025(7)
C29	0.102(10)	0.019(5)	0.051(7)	0.002(4)	0.016(7)	0.005(6)
C30	0.109(10)	0.037(6)	0.025(5)	0.004(4)	0.026(6)	-0.007(6)

Table 5 . Bond Distances in Compound 2.19, Å

Br1-C20	1.896(12)	Br2-C28	1.909(10)	O1-C12	1.487(12)
O1-C14	1.324(13)	O2-C14	1.213(14)	O3-C4	1.414(10)
O3-C16	1.384(11)	O4-C16	1.177(11)	O5-C6	1.426(10)
O5-C24	1.345(11)	O6-C24	1.188(11)	C1-C1	1.502(16)
C1-C2	1.397(11)	C1-C6	1.371(13)	C2-C3	1.385(12)
C2-C7	1.428(13)	C3-C4	1.360(13)	C4-C5	1.399(12)
C5-C6	1.405(13)	C5-C23	1.500(15)	C7-C8	1.199(13)
C8-C9	1.490(14)	C9-C10	1.585(14)	C10-C11	1.495(15)
C11-C12	1.479(16)	C12-C13	1.502(15)	C14-C15	1.487(16)
C16-C17	1.454(13)	C17-C18	1.369(14)	C17-C22	1.433(14)
C18-C19	1.369(15)	C19-C20	1.364(17)	C20-C21	1.390(16)
C21-C22	1.326(15)	C24-C25	1.495(12)	C25-C26	1.400(15)
C25-C30	1.393(14)	C26-C27	1.338(16)	C27-C28	1.400(17)
C28-C29	1.342(16)	C29-C30	1.353(14)		

Table 6 . Bond Angles in Compound 2.19, °

C14-O1-C12	118.8(8)	C16-O3-C4	117.6(7)	C24-O5-C6	114.7(7)
C2-C1-C1	120.8(8)	C6-C1-C1	120.9(8)	C6-C1-C2	118.1(8)
C1-C2-C7	120.9(7)	C3-C2-C1	119.9(8)	C3-C2-C7	119.2(8)
C4-C3-C2	119.4(8)	C3-C4-O3	120.5(8)	C3-C4-C5	124.4(8)
C5-C4-O3	114.9(8)	C4-C5-C6	113.6(8)	C4-C5-C23	121.9(9)
C6-C5-C23	124.5(9)	C1-C6-O5	117.4(8)	C1-C6-C5	124.7(8)
C5-C6-O5	117.9(8)	C8-C7-C2	177.5(10)	C7-C8-C9	177.9(10)
C8-C9-C10	110.7(8)	C11-C10-C9	113.4(9)	C12-C11-C10	117.6(8)
O1-C12-C13	106.3(8)	C11-C12-O1	108.5(9)	C11-C12-C13	113.8(9)
O1-C14-C15	111.7(11)	O2-C14-O1	124.8(10)	O2-C14-C15	123.3(12)
O3-C16-C17	110.6(8)	O4-C16-O3	122.0(9)	O4-C16-C17	127.4(9)
C18-C17-C16	125.5(9)	C18-C17-C22	116.8(9)	C22-C17-C16	117.6(9)
C19-C18-C17	122.3(10)	C20-C19-C18	119.6(11)	C19-C20-Br1	118.6(10)
C19-C20-C21	119.5(11)	C21-C20-Br1	121.9(9)	C22-C21-C20	121.2(10)
C21-C22-C17	120.5(10)	O5-C24-C25	111.7(7)	O6-C24-O5	124.5(8)
O6-C24-C25	123.8(9)	C26-C25-C24	117.5(8)	C30-C25-C24	124.0(9)
C30-C25-C26	118.4(9)	C27-C26-C25	120.7(10)	C26-C27-C28	119.0(10)
C27-C28-Br2	118.0(9)	C29-C28-Br2	120.9(9)	C29-C28-C27	121.0(10)
C28-C29-C30	120.4(10)	C29-C30-C25	120.2(9)		

X-ray Crystallographic Data for compound (*P*)**-2.19**

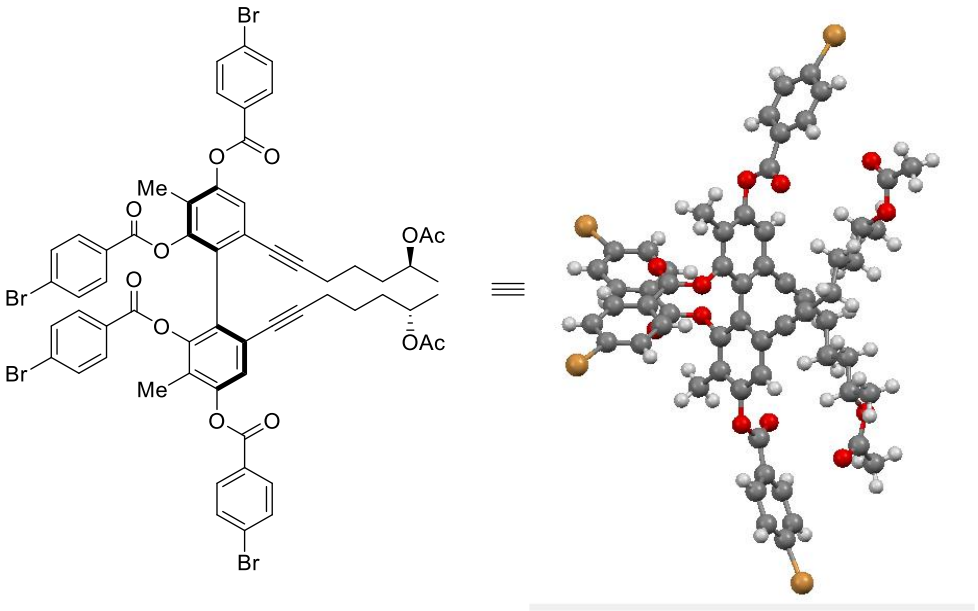

Table 1. Summary of Structure Determination of Compound (*P*)-**2.19**

Empirical formula	$C_{60}H_{50}O_{12}Br_4$
Formula weight	1282.64
Temperature/K	100
Crystal system	orthorhombic
Space group	$P2_12_12_1$
a	7.9305(4)Å
b	24.3507(11)Å
c	28.5067(13)Å
Volume	5505.0(4)Å^3
Z	4

d_{calc}	1.548 g/cm^3
μ	2.987 mm^{-1}
F(000)	2584.0
Crystal size, mm	0.49 × 0.13 × 0.13
2θ range for data collection	2.2 - 55.132°
Index ranges	-10 ≤ h ≤ 10, -31 ≤ k ≤ 31, -37 ≤ l ≤ 37
Reflections collected	136749
Independent reflections	12717[R(int) = 0.0454]
Data/restraints/parameters	12717/0/691
Goodness-of-fit on F^2	1.112
Final R indexes [I>=2σ (I)]	R_1 = 0.0464, wR_2 = 0.1120
Final R indexes [all data]	R_1 = 0.0511, wR_2 = 0.1140
Largest diff. peak/hole	1.56/-0.96 eÅ^{-3}
Flack parameter	0.012(3)

Table 2 . Refined Positional Parameters for Compound (*P*)-**2.19**

Atom	***x***	***y***	***z***	**U(eq)**
Br1	1.23685(8)	0.44568(3)	0.05928(2)	0.02343(14)
Br2	-0.52858(8)	0.21531(3)	0.38159(2)	0.02642(15)
Br3	-0.19236(10)	0.61127(3)	0.06765(3)	0.03514(19)
Br4	1.49398(8)	0.83407(3)	0.40537(2)	0.02286(14)

O1	0.7559(6)	0.6684(2)	0.47351(15)	0.0236(9)
O2	1.0083(6)	0.69479(19)	0.44614(17)	0.0275(10)
O3	0.6209(5)	0.44265(18)	0.22661(15)	0.0186(9)
O4	0.4624(6)	0.4637(2)	0.16369(16)	0.0233(10)
O5	0.0827(6)	0.3682(2)	0.27720(18)	0.0256(10)
O6	0.2430(7)	0.3146(2)	0.3227(2)	0.0468(16)
O7	0.2761(6)	0.34866(19)	0.47353(16)	0.0252(10)
O8	0.0348(8)	0.3127(2)	0.4469(2)	0.0467(15)
O9	0.4156(7)	0.5887(2)	0.23501(18)	0.0319(12)
O10	0.5757(7)	0.5769(2)	0.1715(2)	0.0360(13)
O11	0.9358(6)	0.66063(19)	0.30152(16)	0.0222(10)
O12	0.7542(6)	0.7132(2)	0.3418(2)	0.0324(12)
C1	0.4553(8)	0.4895(3)	0.2839(2)	0.0169(12)
C2	0.4733(7)	0.4450(3)	0.2537(2)	0.0174(11)
C3	0.3556(8)	0.4022(3)	0.2505(2)	0.0229(14)
C4	0.2138(8)	0.4077(3)	0.2787(2)	0.0241(14)
C5	0.1892(8)	0.4508(3)	0.3096(2)	0.0238(14)
C6	0.3129(8)	0.4917(3)	0.3131(2)	0.0193(12)
C7	0.2945(8)	0.5350(3)	0.3463(2)	0.0205(13)
C8	0.2898(8)	0.5699(3)	0.3756(2)	0.0205(13)
C9	0.2977(8)	0.6151(3)	0.4097(2)	0.0218(13)
C10	0.4781(8)	0.6371(3)	0.4145(2)	0.0214(13)

C11	0.5912(8)	0.5969(3)	0.4412(2)	0.0225(13)
C12	0.7689(8)	0.6171(3)	0.4476(2)	0.0220(13)
C13	0.8804(9)	0.5774(3)	0.4734(3)	0.0337(17)
C14	0.8835(8)	0.7049(3)	0.4681(2)	0.0205(13)
C15	0.8453(9)	0.7583(3)	0.4922(3)	0.0284(15)
C16	0.5984(8)	0.4551(2)	0.1804(2)	0.0192(13)
C17	0.7592(8)	0.4549(2)	0.1532(2)	0.0172(12)
C18	0.7500(8)	0.4657(3)	0.1061(2)	0.0193(12)
C19	0.8918(8)	0.4648(3)	0.0783(2)	0.0199(13)
C20	1.0451(7)	0.4518(2)	0.0991(2)	0.0168(11)
C21	1.0615(8)	0.4424(3)	0.1464(2)	0.0214(13)
C22	0.9162(8)	0.4440(3)	0.1739(2)	0.0203(13)
C23	0.384(1)	0.3530(3)	0.2194(3)	0.0285(16)
C24	0.1104(9)	0.3261(3)	0.3063(3)	0.0300(16)
C25	-0.0518(9)	0.2953(3)	0.3173(3)	0.0297(16)
C26	-0.0376(9)	0.2551(3)	0.3501(3)	0.0312(16)
C27	-0.1800(9)	0.2301(3)	0.3683(3)	0.0290(15)
C28	-0.3351(8)	0.2464(3)	0.3526(2)	0.0207(13)
C29	-0.3529(9)	0.2860(3)	0.3186(3)	0.0304(16)
C30	-0.2073(10)	0.3108(3)	0.3012(3)	0.0330(17)
C31	0.5844(8)	0.5335(3)	0.2868(2)	0.0173(12)
C32	0.5645(9)	0.5831(3)	0.2621(2)	0.0239(14)

C33	0.6759(9)	0.6267(3)	0.2661(2)	0.0243(14)
C34	0.8112(8)	0.6194(3)	0.2963(2)	0.0190(12)
C35	0.8382(8)	0.5718(3)	0.3216(2)	0.0182(12)
C36	0.7215(7)	0.5289(2)	0.3176(2)	0.0164(12)
C37	0.7384(8)	0.4810(2)	0.3469(2)	0.0192(12)
C38	0.7415(8)	0.4425(3)	0.3725(2)	0.0250(13)
C39	0.7325(10)	0.3945(3)	0.4047(3)	0.0340(16)
C40	0.5511(10)	0.3744(3)	0.4111(3)	0.0320(16)
C41	0.4366(9)	0.4168(3)	0.4342(3)	0.0302(15)
C42	0.2621(9)	0.3960(3)	0.4420(2)	0.0265(14)
C43	0.1462(10)	0.4383(3)	0.4629(3)	0.0344(17)
C44	0.1594(9)	0.3094(3)	0.4703(2)	0.0267(15)
C45	0.204(1)	0.2602(3)	0.5006(3)	0.0350(17)
C46	0.4387(9)	0.5836(3)	0.1894(3)	0.0311(16)
C47	0.2771(8)	0.5875(3)	0.1606(3)	0.0297(16)
C48	0.2919(9)	0.5867(3)	0.1133(3)	0.0290(15)
C49	0.1511(9)	0.5927(3)	0.0868(3)	0.0309(16)
C50	-0.0045(8)	0.5998(3)	0.1081(2)	0.0206(12)
C51	-0.0257(9)	0.5998(3)	0.1554(2)	0.0291(15)
C52	0.1214(11)	0.5930(3)	0.1832(3)	0.0342(17)
C53	0.6477(12)	0.6799(3)	0.2397(3)	0.041(2)
C54	0.8936(8)	0.7046(3)	0.3286(2)	0.0223(14)

C55	1.0431(8)	0.7387(2)	0.3408(2)	0.0183(12)
C56	1.0144(8)	0.7848(3)	0.3682(2)	0.0229(13)
C57	1.1492(8)	0.8140(3)	0.3869(2)	0.0216(13)
C58	1.3116(7)	0.7965(2)	0.3765(2)	0.0175(12)
C59	1.3440(8)	0.7528(3)	0.3478(2)	0.0205(13)
C60	1.2074(8)	0.7230(3)	0.3293(2)	0.0210(13)

Table 3 . Positional Parameters for Hydrogens in Compound (*P*)-**2.19**

Atom	***x***	***y***	***z***	**U(eq)**
H5	0.092	0.4525	0.3278	0.032
H9a	0.2585	0.6022	0.44	0.029
H9b	0.2238	0.6446	0.3996	0.029
H10a	0.5248	0.6435	0.3835	0.028
H10b	0.4757	0.6719	0.431	0.028
H11a	0.5422	0.59	0.4718	0.03
H11b	0.594	0.5623	0.4243	0.03
H12	0.8182	0.6246	0.4167	0.029
H13a	0.8849	0.5433	0.4565	0.051
H13b	0.8356	0.5711	0.5042	0.051
H13c	0.9919	0.5925	0.4759	0.051
H15a	0.9488	0.7773	0.4986	0.043

H15b	0.7873	0.7512	0.5211	0.043
H15c	0.7755	0.7805	0.4722	0.043
H18	0.6461	0.4738	0.0926	0.026
H19	0.8852	0.4726	0.0464	0.026
H21	1.1663	0.4352	0.1596	0.028
H22	0.9233	0.4378	0.206	0.027
H23a	0.3345	0.3597	0.1892	0.043
H23b	0.3326	0.3213	0.2333	0.043
H23c	0.5029	0.3468	0.2158	0.043
H26	0.0686	0.2442	0.3604	0.041
H27	-0.1704	0.2027	0.3909	0.039
H29	-0.4589	0.2959	0.3075	0.04
H30	-0.2159	0.3381	0.2785	0.044
H35	0.9322	0.5683	0.3408	0.024
H39a	0.7788	0.4046	0.4349	0.045
H39b	0.8006	0.3648	0.3921	0.045
H40a	0.505	0.3648	0.3807	0.043
H40b	0.5521	0.3414	0.4301	0.043
H41a	0.4849	0.4274	0.4641	0.04
H41b	0.4317	0.4492	0.4145	0.04
H42	0.2154	0.3837	0.412	0.035
H43a	0.1287	0.4674	0.4406	0.052

H43b	0.1961	0.4531	0.4908	0.052
H43c	0.04	0.4216	0.4704	0.052
H45a	0.1781	0.227	0.4839	0.052
H45b	0.1399	0.2614	0.5291	0.052
H45c	0.3222	0.261	0.5078	0.052
H48	0.3968	0.5822	0.0993	0.039
H49	0.1589	0.592	0.0543	0.041
H51	-0.1315	0.604	0.169	0.039
H52	0.1145	0.5921	0.2158	0.045
H53a	0.7364	0.685	0.2172	0.062
H53b	0.6477	0.71	0.2615	0.062
H53c	0.5412	0.6785	0.2238	0.062
H56	0.9045	0.7962	0.374	0.03
H57	1.1311	0.8445	0.4058	0.029
H59	1.4544	0.7431	0.3406	0.027
H60	1.2263	0.6931	0.3097	0.028

Table 4 . Refined Thermal Parameters (U's) for Compound (*P*)-**2.19**

Atom	**U_{11}**	**U_{22}**	**U_{33}**	**U_{23}**	**U_{13}**	**U_{12}**
Br1	0.0168(3)	0.0284(3)	0.0251(3)	0.0014(3)	0.0061(2)	0.0030(2)
Br2	0.0226(3)	0.0298(3)	0.0269(3)	-0.0007(3)	0.0052(3)	-0.0114(3)

Br3	0.0371(4)	0.0336(4)	0.0347(4)	-0.0031(3)	-0.0171(3)	0.0107(3)
Br4	0.0183(3)	0.0248(3)	0.0255(3)	-0.0002(2)	-0.0047(3)	-0.0078(3)
O1	0.018(2)	0.031(2)	0.022(2)	-0.0094(19)	0.0004(18)	0.000(2)
O2	0.020(2)	0.031(2)	0.032(2)	-0.006(2)	0.006(2)	0.001(2)
O3	0.014(2)	0.021(2)	0.021(2)	-0.0017(18)	0.0015(17)	-0.0018(17)
O4	0.014(2)	0.034(3)	0.021(2)	-0.0053(19)	-0.0039(18)	0.0028(19)
O5	0.017(2)	0.027(2)	0.032(3)	0.000(2)	-0.0011(19)	-0.0073(19)
O6	0.019(3)	0.041(3)	0.080(4)	0.018(3)	-0.005(3)	-0.005(2)
O7	0.027(3)	0.026(2)	0.024(2)	0.0030(18)	-0.004(2)	-0.002(2)
O8	0.037(3)	0.043(3)	0.060(4)	0.015(3)	-0.019(3)	-0.015(3)
O9	0.035(3)	0.032(3)	0.028(3)	0.007(2)	-0.010(2)	-0.012(2)
O10	0.026(3)	0.044(3)	0.038(3)	-0.005(3)	-0.001(2)	0.001(2)
O11	0.019(2)	0.022(2)	0.026(2)	-0.0016(19)	0.0010(18)	-0.0117(18)
O12	0.014(2)	0.023(2)	0.060(3)	-0.009(2)	-0.002(2)	-0.007(2)
C1	0.013(3)	0.021(3)	0.016(3)	0.002(2)	0.000(2)	-0.001(2)
C2	0.011(2)	0.024(3)	0.018(3)	0.001(2)	0.003(2)	-0.005(2)
C3	0.023(3)	0.017(3)	0.028(3)	-0.007(3)	0.004(3)	-0.009(3)
C4	0.018(3)	0.026(3)	0.029(3)	-0.002(3)	-0.001(3)	-0.012(3)
C5	0.015(3)	0.036(4)	0.020(3)	-0.007(3)	0.004(2)	-0.005(3)
C6	0.015(3)	0.023(3)	0.020(3)	-0.003(2)	0.003(2)	-0.005(2)
C7	0.014(3)	0.023(3)	0.025(3)	0.001(3)	0.002(2)	-0.004(2)
C8	0.014(3)	0.026(3)	0.022(3)	-0.001(3)	0.004(2)	0.002(2)

C9	0.018(3)	0.024(3)	0.024(3)	-0.011(3)	0.002(2)	0.003(2)
C10	0.021(3)	0.022(3)	0.022(3)	-0.009(2)	-0.002(3)	0.000(3)
C11	0.021(3)	0.026(3)	0.020(3)	-0.002(3)	0.001(3)	-0.004(3)
C12	0.022(3)	0.024(3)	0.020(3)	-0.001(2)	0.002(2)	0.002(3)
C13	0.025(4)	0.037(4)	0.039(4)	0.008(3)	0.004(3)	0.005(3)
C14	0.015(3)	0.029(3)	0.018(3)	-0.003(3)	-0.005(2)	0.003(2)
C15	0.023(3)	0.032(4)	0.031(4)	-0.013(3)	-0.002(3)	0.004(3)
C16	0.017(3)	0.013(3)	0.028(3)	-0.005(2)	-0.002(2)	-0.003(2)
C17	0.014(3)	0.016(3)	0.022(3)	-0.007(2)	0.003(2)	-0.002(2)
C18	0.011(3)	0.023(3)	0.024(3)	-0.003(2)	-0.003(2)	0.000(2)
C19	0.018(3)	0.020(3)	0.021(3)	0.003(2)	-0.004(2)	-0.003(2)
C20	0.013(3)	0.016(3)	0.022(3)	0.000(2)	0.002(2)	-0.001(2)
C21	0.016(3)	0.023(3)	0.024(3)	0.000(3)	-0.004(2)	0.001(2)
C22	0.014(3)	0.031(3)	0.016(3)	0.001(3)	-0.001(2)	-0.004(3)
C23	0.032(4)	0.021(3)	0.033(4)	-0.012(3)	0.011(3)	-0.012(3)
C24	0.027(4)	0.027(4)	0.036(4)	-0.008(3)	-0.006(3)	0.009(3)
C25	0.025(4)	0.018(3)	0.046(4)	-0.008(3)	0.009(3)	-0.008(3)
C26	0.016(3)	0.027(4)	0.051(5)	-0.006(3)	0.002(3)	-0.001(3)
C27	0.026(3)	0.024(3)	0.037(4)	0.002(3)	0.005(3)	-0.002(3)
C28	0.013(3)	0.018(3)	0.031(3)	-0.002(3)	0.005(2)	-0.009(2)
C29	0.016(3)	0.039(4)	0.037(4)	0.013(3)	-0.002(3)	-0.004(3)
C30	0.026(4)	0.034(4)	0.039(4)	0.012(3)	0.007(3)	-0.005(3)

C31	0.017(3)	0.017(3)	0.018(3)	-0.005(2)	0.001(2)	-0.006(2)
C32	0.025(3)	0.025(3)	0.022(3)	0.003(3)	-0.007(3)	-0.008(3)
C33	0.030(4)	0.023(3)	0.020(3)	0.005(2)	-0.010(3)	-0.007(3)
C34	0.015(3)	0.019(3)	0.023(3)	-0.003(2)	0.002(2)	-0.008(2)
C35	0.013(3)	0.017(3)	0.024(3)	-0.002(2)	0.000(2)	0.001(2)
C36	0.011(3)	0.018(3)	0.021(3)	-0.003(2)	-0.002(2)	0.000(2)
C37	0.011(3)	0.015(3)	0.031(3)	0.000(2)	0.001(3)	-0.005(2)
C38	0.012(3)	0.025(3)	0.038(4)	0.002(3)	-0.006(3)	0.002(3)
C39	0.030(4)	0.024(3)	0.048(4)	0.013(3)	-0.008(3)	0.005(3)
C40	0.032(4)	0.019(3)	0.044(4)	0.011(3)	0.002(3)	0.000(3)
C41	0.035(4)	0.025(3)	0.031(4)	0.007(3)	-0.005(3)	-0.002(3)
C42	0.027(3)	0.022(3)	0.031(3)	-0.004(3)	-0.008(3)	0.001(3)
C43	0.032(4)	0.035(4)	0.037(4)	-0.007(3)	-0.007(3)	0.006(3)
C44	0.027(4)	0.027(4)	0.026(3)	0.001(3)	0.006(3)	0.003(3)
C45	0.034(4)	0.027(4)	0.044(4)	0.006(3)	0.003(4)	-0.002(3)
C46	0.026(4)	0.023(3)	0.044(4)	-0.004(3)	0.005(3)	0.000(3)
C47	0.016(3)	0.019(3)	0.054(5)	0.005(3)	-0.005(3)	-0.001(3)
C48	0.021(3)	0.026(3)	0.040(4)	-0.003(3)	0.002(3)	-0.002(3)
C49	0.027(4)	0.024(3)	0.042(4)	-0.006(3)	0.003(3)	-0.002(3)
C50	0.012(3)	0.024(3)	0.026(3)	0.004(2)	-0.009(2)	0.002(2)
C51	0.020(3)	0.041(4)	0.026(3)	0.001(3)	-0.002(3)	-0.009(3)
C52	0.046(5)	0.033(4)	0.023(4)	0.006(3)	-0.003(3)	-0.005(3)

C53	0.050(5)	0.031(4)	0.043(5)	0.016(3)	-0.025(4)	-0.020(4)
C54	0.018(3)	0.018(3)	0.030(4)	0.003(3)	-0.004(3)	-0.006(2)
C55	0.016(3)	0.015(3)	0.024(3)	0.005(2)	-0.005(2)	-0.003(2)
C56	0.015(3)	0.019(3)	0.035(3)	-0.002(3)	-0.002(3)	-0.001(3)
C57	0.019(3)	0.012(3)	0.033(4)	-0.003(3)	0.002(3)	0.000(2)
C58	0.013(3)	0.019(3)	0.021(3)	0.003(2)	-0.002(2)	-0.007(2)
C59	0.011(3)	0.023(3)	0.028(3)	0.003(3)	0.002(2)	-0.006(2)
C60	0.021(3)	0.019(3)	0.023(3)	-0.001(2)	-0.001(2)	-0.006(3)

Table 5 . Bond Distances in Compound (*P*)-**2.19, Å**

Br1-C20	1.904(6)	Br2-C28	1.900(6)	Br3-C50	1.904(6)
Br4-C58	1.900(6)	O1-C12	1.456(8)	O1-C14	1.354(8)
O2-C14	1.196(8)	O3-C2	1.404(7)	O3-C16	1.363(8)
O4-C16	1.198(8)	O5-C4	1.418(7)	O5-C24	1.337(9)
O6-C24	1.184(9)	O7-C42	1.465(8)	O7-C44	1.334(9)
O8-C44	1.195(9)	O9-C32	1.417(8)	O9-C46	1.318(10)
O10-C46	1.212(9)	O11-C34	1.417(7)	O11-C54	1.360(8)
O12-C54	1.187(9)	C1-C2	1.389(9)	C1-C6	1.405(8)
C1-C31	1.484(8)	C2-C3	1.403(8)	C3-C4	1.390(9)
C3-C23	1.506(9)	C4-C5	1.382(9)	C5-C6	1.402(9)
C6-C7	1.426(9)	C7-C8	1.190(9)	C8-C9	1.471(8)

C9-C10	1.533(9)	C10-C11	1.530(9)	C11-C12	1.504(9)
C12-C13	1.501(9)	C14-C15	1.502(9)	C16-C17	1.492(8)
C17-C18	1.371(9)	C17-C22	1.403(8)	C18-C19	1.375(9)
C19-C20	1.389(8)	C20-C21	1.373(9)	C21-C22	1.395(9)
C24-C25	1.522(10)	C25-C26	1.358(11)	C25-C30	1.369(11)
C26-C27	1.383(10)	C27-C28	1.367(10)	C28-C29	1.373(10)
C29-C30	1.395(10)	C31-C32	1.408(9)	C31-C36	1.402(9)
C32-C33	1.386(9)	C33-C34	1.389(9)	C33-C53	1.513(10)
C34-C35	1.380(9)	C35-C36	1.401(8)	C36-C37	1.440(9)
C37-C38	1.188(9)	C38-C39	1.488(9)	C39-C40	1.530(10)
C40-C41	1.524(10)	C41-C42	1.491(10)	C42-C43	1.504(10)
C44-C45	1.518(10)	C46-C47	1.525(10)	C47-C48	1.353(11)
C47-C52	1.399(11)	C48-C49	1.357(10)	C49-C50	1.386(10)
C50-C51	1.360(9)	C51-C52	1.420(11)	C54-C55	1.490(8)
C55-C56	1.384(9)	C55-C60	1.398(9)	C56-C57	1.391(9)
C57-C58	1.388(9)	C58-C59	1.365(9)	C59-C60	1.408(9)

Table 6 . Bond Angles in Compound (*P*)-**2.19, °**

C14-O1-C12	116.8(5)	C16-O3-C2	114.4(5)	C24-O5-C4	112.5(5)
C44-O7-C42	118.0(5)	C46-O9-C32	114.3(6)	C54-O11-C34	116.4(5)
C2-C1-C6	118.6(6)	C2-C1-C31	121.8(5)	C6-C1-C31	119.6(6)

C1-C2-O3	117.3(5)	C1-C2-C3	123.5(6)	C3-C2-O3	119.1(5)
C2-C3-C23	122.1(6)	C4-C3-C2	115.3(6)	C4-C3-C23	122.6(6)
C3-C4-O5	120.7(6)	C5-C4-O5	115.5(6)	C5-C4-C3	123.8(6)
C4-C5-C6	119.1(6)	C1-C6-C7	120.3(6)	C5-C6-C1	119.6(6)
C5-C6-C7	120.1(6)	C8-C7-C6	175.2(7)	C7-C8-C9	174.7(7)
C8-C9-C10	111.1(5)	C11-C10-C9	111.6(5)	C12-C11-C10	113.7(5)
O1-C12-C11	106.0(5)	O1-C12-C13	110.2(6)	C13-C12-C11	113.7(6)
O1-C14-C15	111.4(5)	O2-C14-O1	122.9(6)	O2-C14-C15	125.7(6)
O3-C16-C17	112.9(5)	O4-C16-O3	122.8(6)	O4-C16-C17	124.3(6)
C18-C17-C16	117.6(6)	C18-C17-C22	119.7(6)	C22-C17-C16	122.7(5)
C17-C18-C19	121.2(6)	C18-C19-C20	118.2(6)	C19-C20-Br1	117.5(5)
C21-C20-Br1	119.8(5)	C21-C20-C19	122.7(6)	C20-C21-C22	118.0(6)
C21-C22-C17	120.1(6)	O5-C24-C25	111.6(6)	O6-C24-O5	124.8(7)
O6-C24-C25	123.6(7)	C26-C25-C24	115.3(7)	C26-C25-C30	120.3(7)
C30-C25-C24	123.8(7)	C25-C26-C27	120.5(7)	C28-C27-C26	119.0(7)
C27-C28-Br2	117.9(5)	C27-C28-C29	121.8(6)	C29-C28-Br2	120.2(5)
C28-C29-C30	118.0(6)	C25-C30-C29	120.4(7)	C32-C31-C1	120.9(6)
C36-C31-C1	120.8(6)	C36-C31-C32	118.0(6)	C31-C32-O9	116.6(6)
C33-C32-O9	120.2(6)	C33-C32-C31	123.0(6)	C32-C33-C34	116.4(6)
C32-C33-C53	121.4(6)	C34-C33-C53	122.1(6)	C33-C34-O11	120.8(6)
C35-C34-O11	115.6(6)	C35-C34-C33	123.5(6)	C34-C35-C36	118.9(6)
C31-C36-C37	120.0(5)	C35-C36-C31	120.1(6)	C35-C36-C37	119.8(5)

C38-C37-C36	175.2(7)	C37-C38-C39	176.1(7)	C38-C39-C40	111.7(6)
C41-C40-C39	113.3(6)	C42-C41-C40	112.8(6)	O7-C42-C41	106.8(5)
O7-C42-C43	110.1(6)	C41-C42-C43	113.1(6)	O7-C44-C45	111.4(6)
O8-C44-O7	124.3(7)	O8-C44-C45	124.3(7)	O9-C46-C47	114.1(6)
O10-C46-O9	123.6(7)	O10-C46-C47	122.3(7)	C48-C47-C46	117.6(7)
C48-C47-C52	122.5(7)	C52-C47-C46	120.0(7)	C47-C48-C49	118.8(7)
C48-C49-C50	120.1(7)	C49-C50-Br3	116.7(5)	C51-C50-Br3	120.3(5)
C51-C50-C49	123.0(6)	C50-C51-C52	116.9(7)	C47-C52-C51	118.6(7)
O11-C54-C55	112.1(5)	O12-C54-O11	123.2(6)	O12-C54-C55	124.6(6)
C56-C55-C54	117.0(6)	C56-C55-C60	120.5(6)	C60-C55-C54	122.2(6)
C55-C56-C57	120.3(6)	C58-C57-C56	118.3(6)	C57-C58-Br4	117.8(5)
C59-C58-Br4	119.4(5)	C59-C58-C57	122.8(6)	C58-C59-C60	118.8(6)
C55-C60-C59	119.2(6)				

Table 2.S1. Selective Acetyl Deprotection

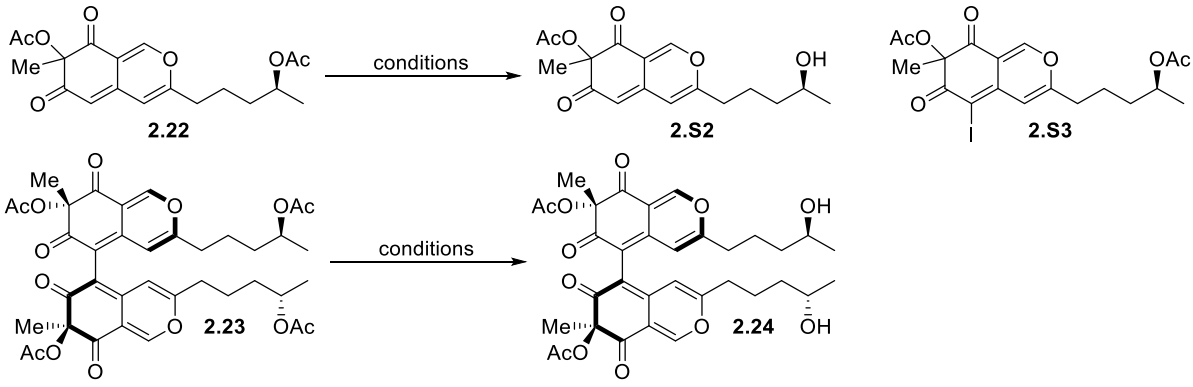

entry	substrate	condition	yield (%)

1	**2.22**	KCN, EtOH, rt, 1.5 h	decomposition
2	**2.22**	I_2, MeOH, 20 min	**2.S3**
3	**2.22**	BF_3•Et_2O, CH_3CN, 50 ºC, 2 d	decomposition
4	**2.22**	$Sc(OTf)_3$, MeOH/H_2O, 50 ºC, 2 d	decomposition
5	**2.22**	AcCl, MeOH, rt, 1 h	17
6	**2.22**	K_2CO_3, MeOH, rt, 19 h	29
7	**2.22**	Lipase PS, toluene, *n*-BuOH, 80 ºC, 5 d	34
8	**2.22**	Bu_4NOH, MeOH, rt, 10 h	54
9	**2.22**	Ti(O*i*-Pr)$_4$, THF, 50 ºC, 1 d	44
10	**2.23**	AcCl, MeOH, rt, 2 d	18
11	**2.23**	K_2CO_3, MeOH, rt, 12 h	8~44[a]
12	**2.23**	Sm, I_2, MeOH, rt, 3.5 h	19
13	**2.23**	Lipase PS, toluene, *n*-BuOH, 100 ºC, 5 d	N/R[b]
14	**2.23**	Bu_4NOH, MeOH, rt, 2.5 h	30
15	**2.23**	Ti(O*i*-Pr)$_4$, THF, 50 ºC, 1 d	**52**

[a]Reproducibility issue [b]Substrate decomposition occurred.

CHAPTER 3: LIGAND EVOLUTION TO DRIVE REACTION DISCOVERY

3.1. Introduction

Addressing unsolved challenges in organometallic chemistry, such as selective Heck coupling of complex substrates,[1] selective cross coupling of dihalides,[2] and hindered C–N bond formation,[3] is an important aspect of academic research and industrial development. Promoting these types of reactivity requires the design and rapid synthesis of ligand scaffolds possessing diverse physical properties. The goal of this research is to develop a platform for the synthesis, characterization, and purification of novel phosphine ligands in *parallel*, thus creating large ligand libraries to expand the current ligand landscape. Microscale parallel ligand synthesis, paired with High–Throughput Experimentation, will be valuable in expediting reaction discovery or resolving challenging issues via exploring new chemical reactivity.

[1] Beletskaya, I. P.; Cheprakov, A. V. The Heck Reaction as a Sharpening Stone of Palladium Catalysis. *Chem. Rev.* **2000**, *100* (8), 3009–3066.

[2] (a) Strotman, N. A.; Chobanian, H. R.; He, J.; Guo, Y.; Dormer, P. G.; Jones, C. M.; Steves, J. E. Catalyst-Controlled Regioselective Suzuki Couplings at Both Positions of Dihaloimidazoles, Dihalooxazoles, and Dihalothiazoles. J. Org. Chem. 2010, 75 (5), 1733–1739. (b) Rossi, R.; Bellina, F.; Lessi, M. Highly Selective Palladium-Catalyzed Suzuki–Miyaura Monocoupling Reactions of Ethene and Arene Derivatives Bearing Two or More Electrophilic Sites. *Tetrahedron* **2011**, *67* (37), 6969–7025. (c) Dai, X.; Chen, Y.; Garrell, S.; Liu, H.; Zhang, L.-K.; Palani, A.; Hughes, G.; Nargund, R. Ligand-Dependent Site-Selective Suzuki Cross-Coupling of 3,5-Dichloropyridazines. *J. Org. Chem.* **2013**, *78* (15), 7758–7763. (d) Manabe, K.; Yamaguchi, M. ChemInform Abstract: Catalyst-Controlled Site-Selectivity Switching in Pd-Catalyzed Cross-Coupling of Dihaloarenes. *Catalysts* **2014**, *4*, 307–320.

[3] Qiao, J. X.; Lam, P. Y. S. Copper-Promoted Carbon-Heteroatom Bond Cross-Coupling with Boronic Acids and Derivatives. *Synthesis* **2011**, *2011* (6), 829–856.

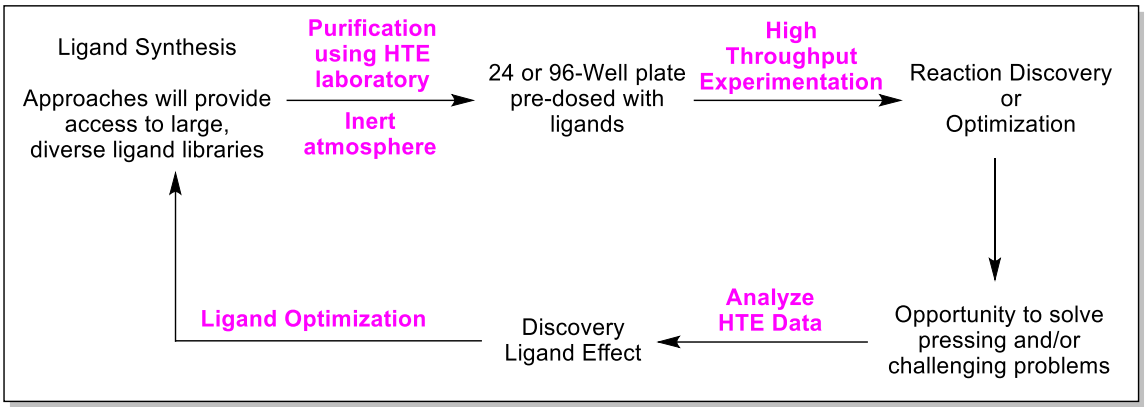

Figure 3.1. Ligand Evolution to Drive Reaction Discovery

3.2. Significance of Triazole-based Monophosphine Ligand

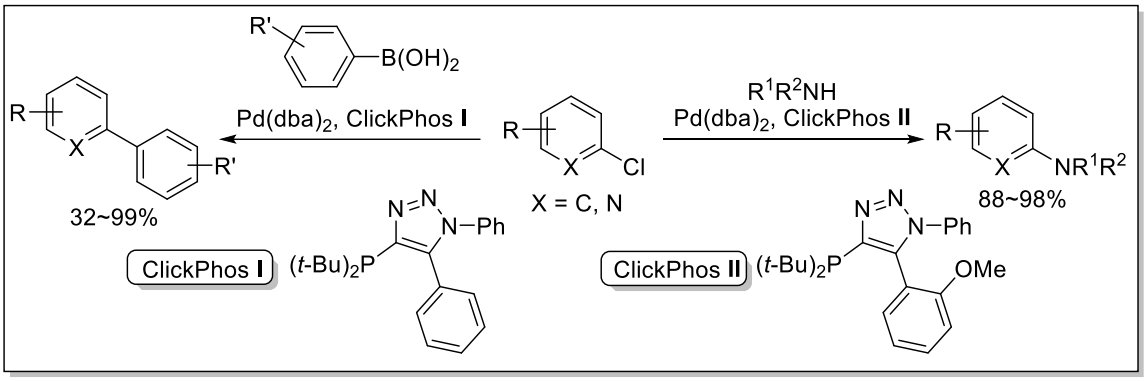

Scheme 3.1. Utility of ClickPhos Ligands in Suzuki-Miyaura Coupling and Amination Reaction

One of the most widely-employed methods for C-C bond formation is the Suzuki-Miyaura coupling reaction.[4] Utilizing aryl chlorides in this reaction is especially advantageous due to the reduced cost and greater diversity of available compounds.[5] Fu[6] and Buchwald[7] reported that electron–rich and sterically hindered phosphine ligands, such

[4] Miyaura, N.; Suzuki, A. Palladium-Catalyzed Cross-Coupling Reactions of Organoboron Compounds. *Chem. Rev.* **1995**, *95*, 2457–2483.
[5] Littke, A. F.; Fu, G. C. Palladium-Catalyzed Coupling Reactions of Aryl Chlorides. *Angew. Chem. Int. Ed.* **2002**, *41*, 4176–4211.
[6] Littke, A. F.; Dai, C.; Fu, G. C. Versatile Catalysts for the Suzuki Cross-Coupling of Arylboronic Acids with Aryl and Vinyl Halides and Triflates under Mild Conditions. *J. Am. Chem. Soc.* **2000**, *122*, 4020–4028.
[7] Yin, J.; Rainka, M. P.; Zhang, X.-X.; Buchwald, S. L. A Highly Active Suzuki Catalyst for the Synthesis of Sterically Hindered Biaryls: Novel Ligand Coordination. *J. Am. Chem. Soc.* **2002**, *124*, 1162–1163.

as *t*-Bu_3P and dialkylbisphenylphosphine, are effective for this type of transformation. Recently, Zhang demonstrated that triazole-based monophosphines are promising candidates for palladium-catalyzed $C(sp^2)$–$C(sp^2)$ bond formation and the amination with aryl chlorides (**Scheme 3.1**).[8] The triazole moiety not only supports the production of numerous analogs but also features diverse physical properties (**Figure 3.2**). For example, triazole contains an acidic site (pK_a of triazole ~9.2)[9] and supports a diverse array of steric, electronic, and hemilabile environments. Inspired by the untapped structural diversity possible with the triazole scaffolds, we decided to develop a triazole-based monophosphine ligand library through [3+2]-cycloaddition between alkynylphosphine oxides and azides. Subsequent reduction of the resultant phosphine oxides in the same reaction flask provides a protocol that can be implemented in a parallel manner.

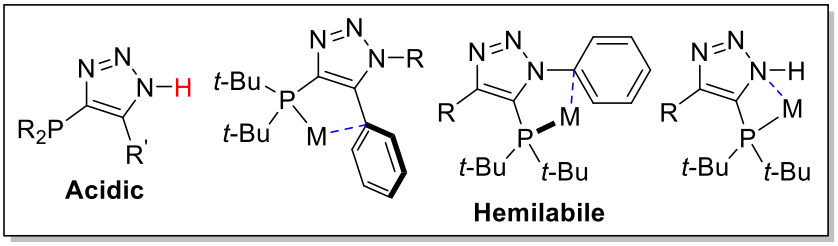

Figure 3.2. Diversity of ClickPhos Ligand Physical Properties

3.3. Previous Approaches to Prepare Triazole Moiety and ClickPhos Ligand

[8] (a) Liu, D.; Gao, W.; Dai, Q.; Zhang, X. Triazole-Based Monophosphines for Suzuki−Miyaura Coupling and Amination Reactions of Aryl Chlorides. *Org. Lett.* **2005**, *7*, 4907–4910. (b) Dai, Q.; Gao, W.; Liu, D.; Kapes, L. M.; Zhang, X. Triazole-Based Monophosphine Ligands for Palladium-Catalyzed Cross-Coupling Reactions of Aryl Chlorides. *J. Org. Chem.* **2006**, *71*, 3928–3934. (c) Spinella, S.; Guan, Z.-H.; Chen, J.; Zhang, X. Suzuki Coupling of Heteroaromatic Chlorides Using Highly Electron-Donating ClickPhos Ligands. *Synthesis* **2009**, *2009* (18), 3094–3098.

[9] Tanaka, Y.; Velen, S. R.; Miller, S. I. Syntheses and Properties of H-1,2,3-Triazoles. *Tetrahedron* **1973**, *29*, 3271–3283.

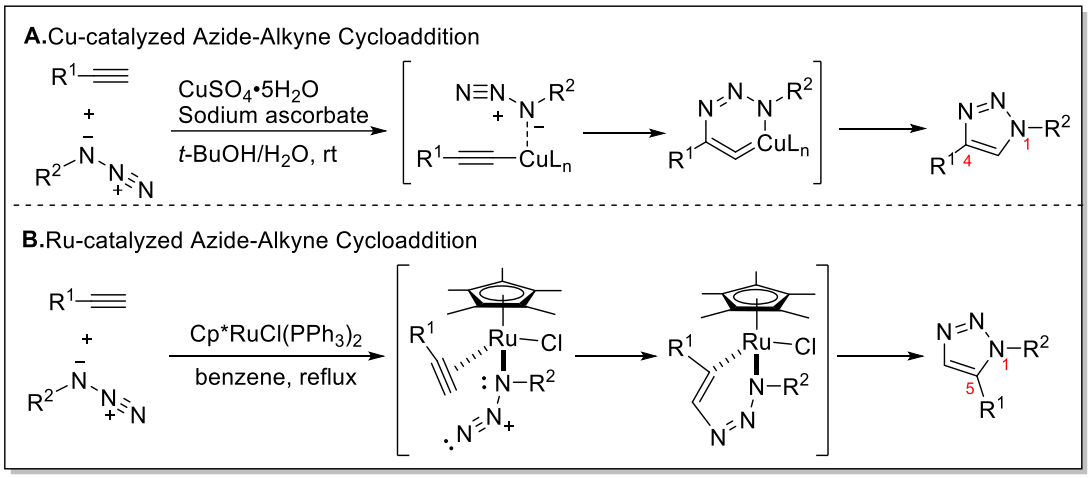

Scheme 3.2. Regioselective [3+2]-Cycloaddition

Over the last two decades, the 1,3-dipolar cycloaddition reaction between organic azides and alkynes, known as Huisgen's dipolar cycloaddition,[10] has been explored extensively with and without metal catalysts.[11] Thermal Huisgen cycloaddition reactions afford a mixture of 1,4- and 1,5-disubstituted 1,2,3-triazole products (1:1). In 2002, Sharpless and coworkers reported that a Cu-catalyzed azide-alkyne cycloaddition (CuAAC) with terminal alkynes permits access to 1,4-disubstituted-1,2,3-triazole selectively (**Scheme 3.2.A**).[12] Alternatively, the Sharpless group also utilized Mg-acetylide to form 1,4,5-trisubstituted-1,2,3-triazoles preferentially by quenching with a variety of electrophiles (**Scheme 3.3.A**).[13] On the other hand, Fokin and Jia achieved inverted

[10] Huisgen, R. 1.3-Dipolare Cycloadditionen Rückschau und Ausblick. *Angew. Chem.* **1963**, *75*, 604–637.
[11] (a) Spiteri, C.; Moses, J. E. Copper-Catalyzed Azide–Alkyne Cycloaddition: Regioselective Synthesis of 1,4,5-Trisubstituted 1,2,3-Triazoles. *Angew. Chem. Int. Ed.* **2010**, *49*, 31–33. (b) Schulze, B.; Schubert, U. S. Beyond Click Chemistry – Supramolecular Interactions of 1,2,3-Triazoles. *Chem. Soc. Rev.* **2014**, *43*, 2522. (c) Johansson, J. R.; Beke-Somfai, T.; Said Stålsmeden, A.; Kann, N. Ruthenium-Catalyzed Azide Alkyne Cycloaddition Reaction: Scope, Mechanism, and Applications. *Chem. Rev.* **2016**, *116*, 14726–14768.
[12] Rostovtsev, V. V.; Green, L. G.; Fokin, V. V.; Sharpless, K. B. A Stepwise Huisgen Cycloaddition Process: Copper(I)-Catalyzed Regioselective "Ligation" of Azides and Terminal Alkynes. *Angew. Chem. Int. Ed.* **2002**, *41*, 2596–2599.
[13] Krasiński, A.; Fokin, V. V.; Sharpless, K. B. Direct Synthesis of 1,5-Disubstituted-4-Magnesio-1,2,3-Triazoles, Revisited. *Org. Lett.* **2004**, *6*, 1237–1240.

regioselectivity compared to CuAAC with terminal alkynes by means of a Ru-catalyzed azide-alkyne cycloaddition (RuAAC) to produce another regioisomer, 1,5-disubstituted-1,2,3-triazole (**Scheme 3.2.B**).[14] Furthermore, RuAAC afforded the cycloaddition product not only with terminal alkynes, but also with internal alkynes to generate the 1,4,5-trisubstituted-1,2,3-triazole moiety (**Scheme 3.3.B**).[14,15]

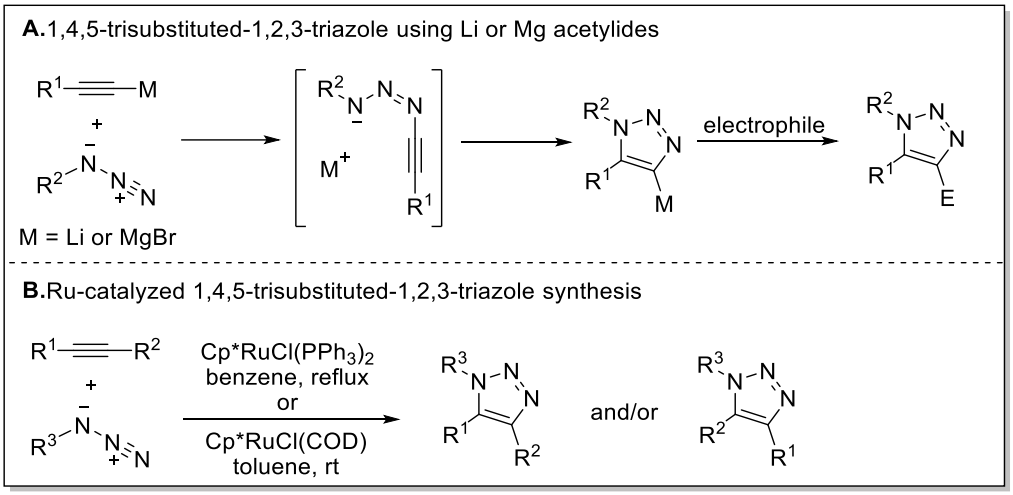

Scheme 3.3. Syntheses of 1,4,5-Trisubstituted-1,2,3-triazole

Owing to their ease of purification,[16] Zhang's ClickPhos ligands were synthesized in a two-step sequence; (1) [3+2]-cycloaddition between azide and Mg-acetylide to yield 1,5-disubstituted triazole after quenching with NH_4Cl, then (2) treatment with LDA followed by addition of chlorophosphine to generate the triazole-based monophosphine ligand (**Scheme 3.4**).[8]

---

[14] Zhang, L.; Chen, X.; Xue, P.; Sun, H. H. Y.; Williams, I. D.; Sharpless, K. B.; Fokin, V. V.; Jia, G. Ruthenium-Catalyzed Cycloaddition of Alkynes and Organic Azides. *J. Am. Chem. Soc.* **2005**, *127*, 15998–15999.

[15] (a) Majireck, M. M.; Weinreb, S. M. A Study of the Scope and Regioselectivity of the Ruthenium-Catalyzed [3 + 2]-Cycloaddition of Azides with Internal Alkynes. *J. Org. Chem.* **2006**, *71* (22), 8680–8683. (b) Boren, B. C.; Narayan, S.; Rasmussen, L. K.; Zhang, L.; Zhao, H.; Lin, Z.; Jia, G.; Fokin, V. V. Ruthenium-Catalyzed Azide−Alkyne Cycloaddition: Scope and Mechanism. *J. Am. Chem. Soc.* **2008**, *130* (28), 8923–8930.

[16] One pot synthesis was capable by means of directly quenching with chlorophosphine.

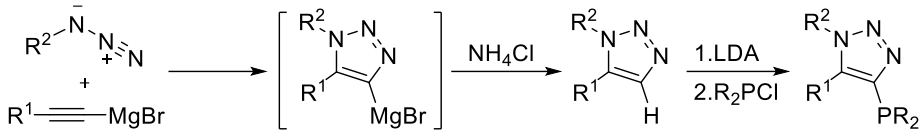

Scheme 3.4. Zhang's Approach to the Synthesis of ClickPhos

3.4. Preparation of Alkynylphosphine Oxides and Azides

To build the 1,2,3-triazole monophosphine scaffold, we designed a route that utilizes alkynylphosphine oxides and azides. The advantages of this route include the ability to generate both isomeric adducts and to synthesize many triazole phosphines easily by simply combining different substrates. Both substrates are simple to prepare from commericial sources– the alkynylphosphine oxides were synthesized in a linear sequence of 3–5 steps from commercially available aldehydes or alkynes (**Scheme 3.5.A**) and azides were prepared in ≤2 steps from either corresponding bromides or anilines (**Scheme 3.5.B**).

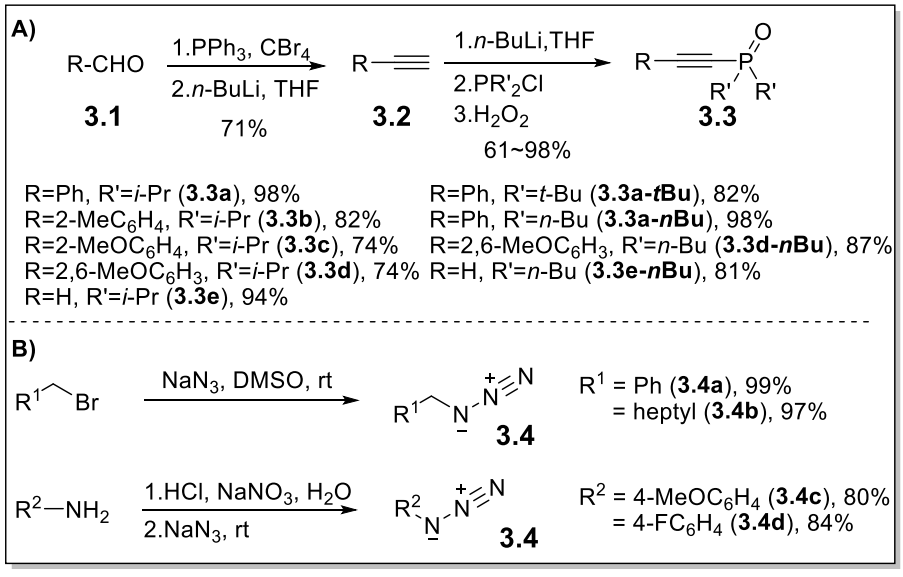

Scheme 3.5. Preparation of Alkynylphosphine Oxides and Azides

The Corey-Fuchs alkyne synthesis has been utilized to generate terminal alkynes from aldehydes. In the presence of PPh_3 and CBr_4, a one-carbon homolyzed dibromide

alkene intermediate was generated. Subsequent treatment of the dibromide with two equivalents of *n*-butyllithium afforded the corresoponding terminal alkyne. To prepare the phosphine oxide, a substitution reaction was conducted by alkyne deprotonation with *n*-butyllihium, followed by treatment with chloro dialkyl phosphines to make alkynylphosphine oxides in one-pot after quenching with H_2O_2 (**Scheme 3.5.A**).

Various organic azides were synthesized within 2 steps. Benzyl (**3.4a**)[17] and octyl azides (**3.4b**)[18] were prepared directly from their corresponding bromides by means of an S_N2 reaction. Aromatic azides (**3.4c–d**) were prepared via diazotization and sequential nucleophilic aromatic substitution reaction in one pot (**Scheme 3.5.B**).[19]

[17] Daskalaki, E.; Le Droumaguet, B.; Gérard, D.; Velonia, K. Multifunctional Giant Amphiphiles via Simultaneous Copper(I)-Catalyzed Azide–Alkynecycloaddition and Living Radical Polymerization. *Chem Commun* **2012**, *48* (10), 1586–1588.
[18] Ngai, M. H.; Yang, P.-Y.; Liu, K.; Shen, Y.; Wenk, M. R.; Yao, S. Q.; Lear, M. J. Click-Based Synthesis and Proteomic Profiling of Lipstatin Analogues. *Chem. Commun.* **2010**, *46* (44), 8335.
[19] Hu, M.; Li, J.; Q. Yao, S. In Situ “Click” Assembly of Small Molecule Matrix Metalloprotease Inhibitors Containing Zinc-Chelating Groups. *Org. Lett.* **2008**, *10* (24), 5529–5531.

3.5. [3+2]-Cycloaddition Reaction

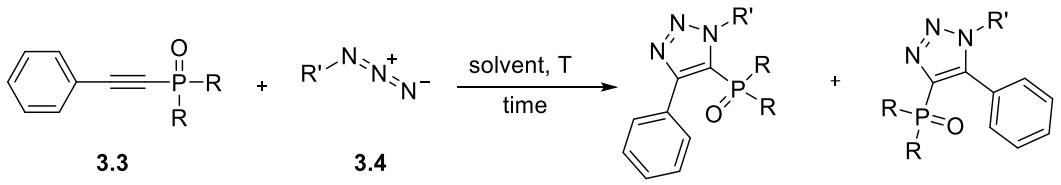

3.3 + 3.4 → 3.5 + 3.6

Entry	R	R'	Solvent	T (°C)	Time	Conversion[a]
1	*i*-Pr (**3.3a**)	Bn (**3.4a**)	toluene	110	3 d	94%
2	*i*-Pr (**3.3a**)	Bn (**3.4a**)	toluene	150	3 d	100%
3[b]	*i*-Pr (**3.3a**)	4-OMeC$_6$H$_4$ (**3.4c**)	toluene	110	5 d	50%
4[b]	*i*-Pr (**3.3a**)	4-FC$_6$H$_4$ (**3.4d**)	toluene	110	5 d	75%
5[c]	*i*-Pr (**3.3a**)	4-OMeC$_6$H$_4$ (**3.4c**)	toluene	110	10 min	N/R
6[b,c]	*i*-Pr (**3.3a**)	4-OMeC$_6$H$_4$ (**3.4c**)	toluene	150	30 min	trace
7[b,c]	*i*-Pr (**3.3a**)	4-OMeC$_6$H$_4$ (**3.4c**)	DMF	110	30 min	N/R
8[b,c]	*i*-Pr (**3.3a**)	4-OMeC$_6$H$_4$ (**3.4c**)	NMP	110	30 min	N/R
9[d]	*i*-Pr (**3.3a**)	4-OMeC$_6$H$_4$ (**3.4c**)	toluene	110	3 d	95%

[a]Determined by ^{1}H NMR.[b]Azide decomposition was observed.[c]Reaction was carried out in microwave reactor.[d]Additional 2 equiv of azide added after 1 d.

Table 3.1. [3+2]-Cycloaddition Optimization

To obtain as many triazole phosphine ligands as possible, the cycloaddition reaction was conducted under thermal conditions, which yields both isomeric cycloadducts. Attempts to optimize the thermal [3+2]-cycloaddition are shown in **Table 3.1**. Increased temperature was necessary to achieve full conversion with benzyl azide **3.4a** (entry 1 vs 2). Thermal cycloaddition with aryl azides, however, gave lower conversion even after the prolonged reaction time (entry 3,4). In addition, thermal decomposition of both azides was detected during the course of the reaction. Use of a

microwave reactor neither improved the reactivity nor resolved the observed decomposition (entry 5–8). Addition of a second portion of azide after one day eventually enabled access to triazole phosphine oxides in good conversion and yield (entry 9).

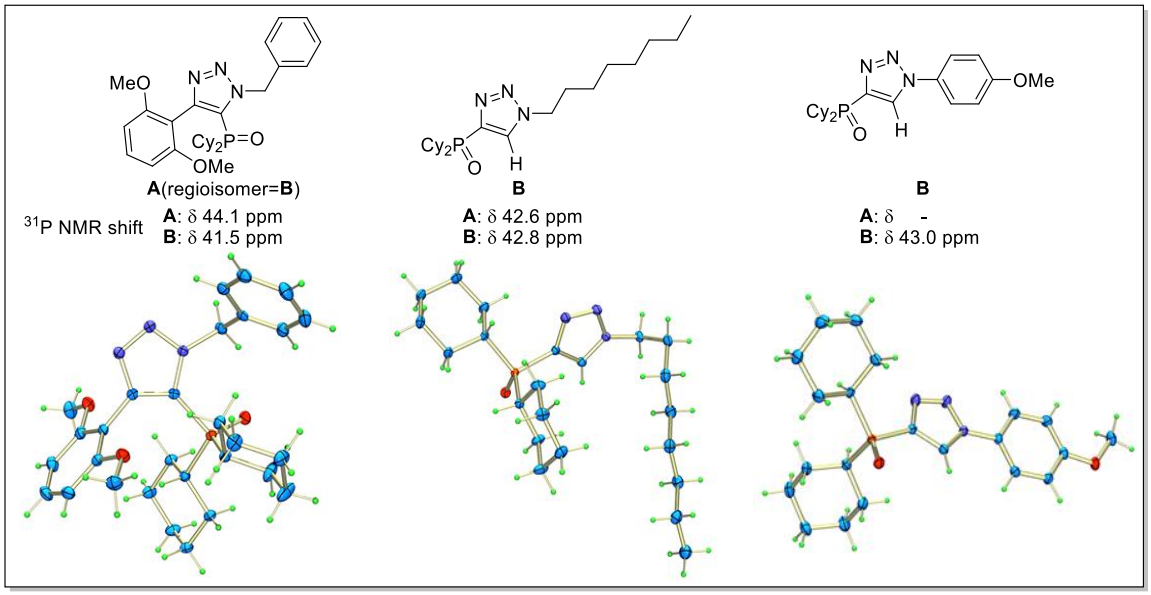

Figure 3.3. Regioisomer Characterization by X-ray Crystal Structures[20]

To verify the structure of both regioisomers, Dr. Rosaura Padilla–Salinas performed crystallographic analysis on several triazole phosphine oxides (**Figure 3.3**). Based on this analysis, the less polar compound (on TLC) was found to be the phosphine oxide at the C-5 position (**Figure 3.3.A**). In terms of the phosphine NMR shifts, the relationship between the regioisomers varies, depending on the azide source. With a C-1 benzyl substituent, the shift in the ^{31}P NMR of isomer **A** is more downfield than that of the other isomer **B**. With an octyl substituent at C-1, however, the opposite relationship is observed in the phosphine NMR shifts (**Figure 3.3**).

3.6. Scope of Triazole Phosphine Oxides

With optimized conditions in hand for the synthesis of triazole phosphine oxides,

[20] Dr. Rosaura Padilla–Salinas conducted X-ray crystallographic structure determinations.

the substrate scope of the cycloaddition was investigated first with alkyl azides (**Table 3.2**). Use of phenylalkynylphosphine oxide (**3.3a**) with benzyl azide (**3.4a**) produced triazole-based phosphine oxides in good yield (**Table 3.2**, 87%). *ortho*-Substituted arylalkynylphosphine oxides (**3.3b–c**) were also used to produce the cyclized products in good yield. In addition, 2,6-dimethoxyphenylalkynylphosphine oxide (**3.3d**) generated the corresponding electron-rich heterocycles in excellent yield (91%). The expected product ratio between regioisomers was observed in most cases (~1:1). Interestingly, 2,6-dimethoxyphenyl–substituted alkynylphosphine oxide (**3.3d**) resulted in some preferential formation of phosphine oxide substituted at the C-4 position (**3.6i**). Compared to benzyl azide (**3.4a**), the reaction with octyl azide (**3.4b**) required prolonged reaction times (5 days).

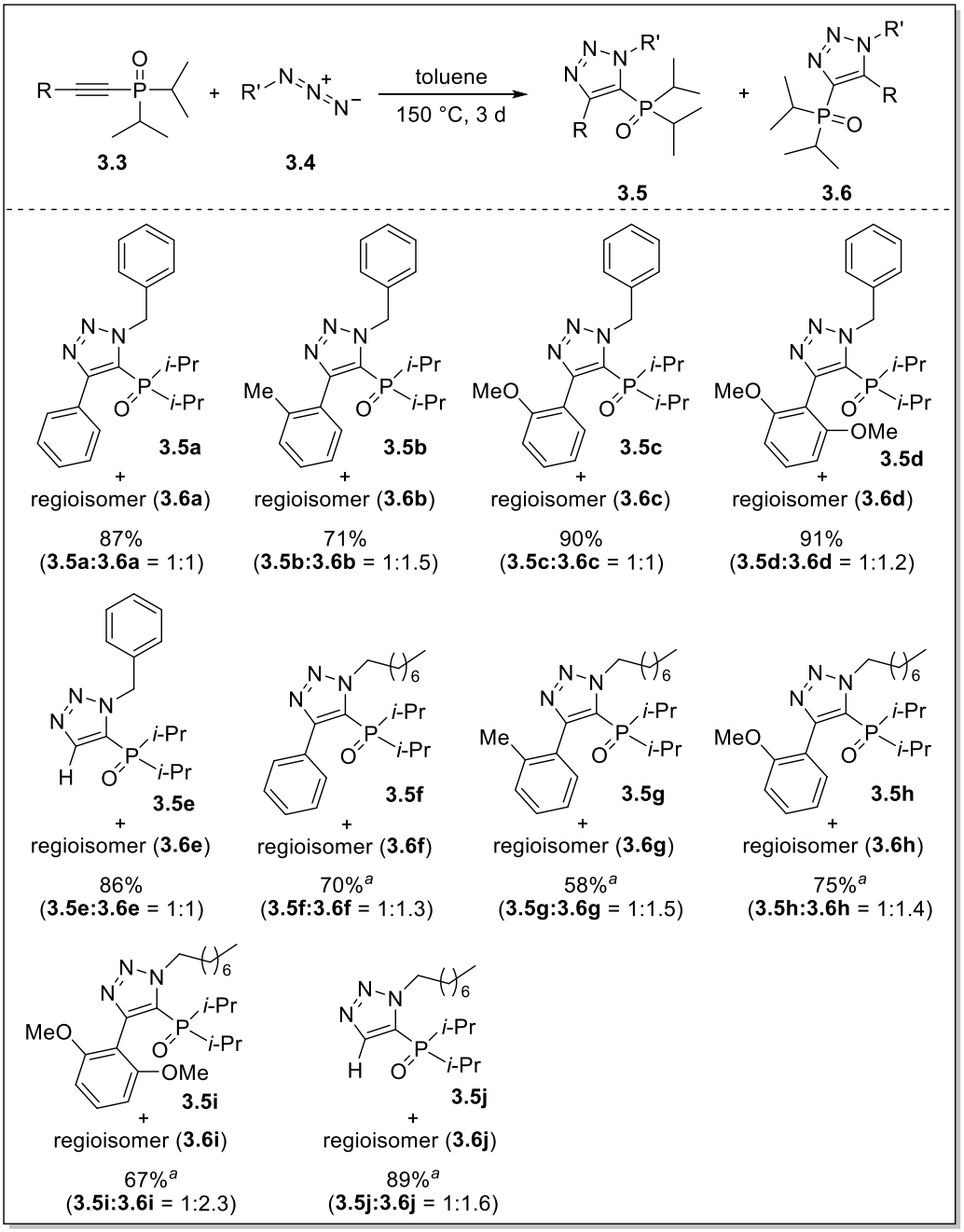

[a]Reaction conducted for 5 d.

Table 3.2. Scope of [3+2]-Cycloaddition with Alkyl Azides

Given success in the cycloaddition with alkyl azides, triazole synthesis using aryl azides was explored (**Table 3.3**). 4-Methoxyphenyl azide (**3.4c**) afforded 1,4,5-trisubstituted triazoles in good yield (58–84%). Notably, significant regioselectivity was

detected when an electron-donating aryl azide (**3.4c**) was employed, implicating that the azide electronics play a key role to induce the regioselectivity (**3.5k–o:3.6k–o** = ~1:10). Electron-withdrawing aryl azides (**3.4d**) were also treated with a variety of alkynylphosphine oxides to yield the corresponding triazole phosphine oxides in yields of 42–77% (**Table 3.3**). Slightly lower regioselectivity was observed across the series of electron-deficient aryl azide substrates (**3.5p–t:3.6p–t** = ~1:6).

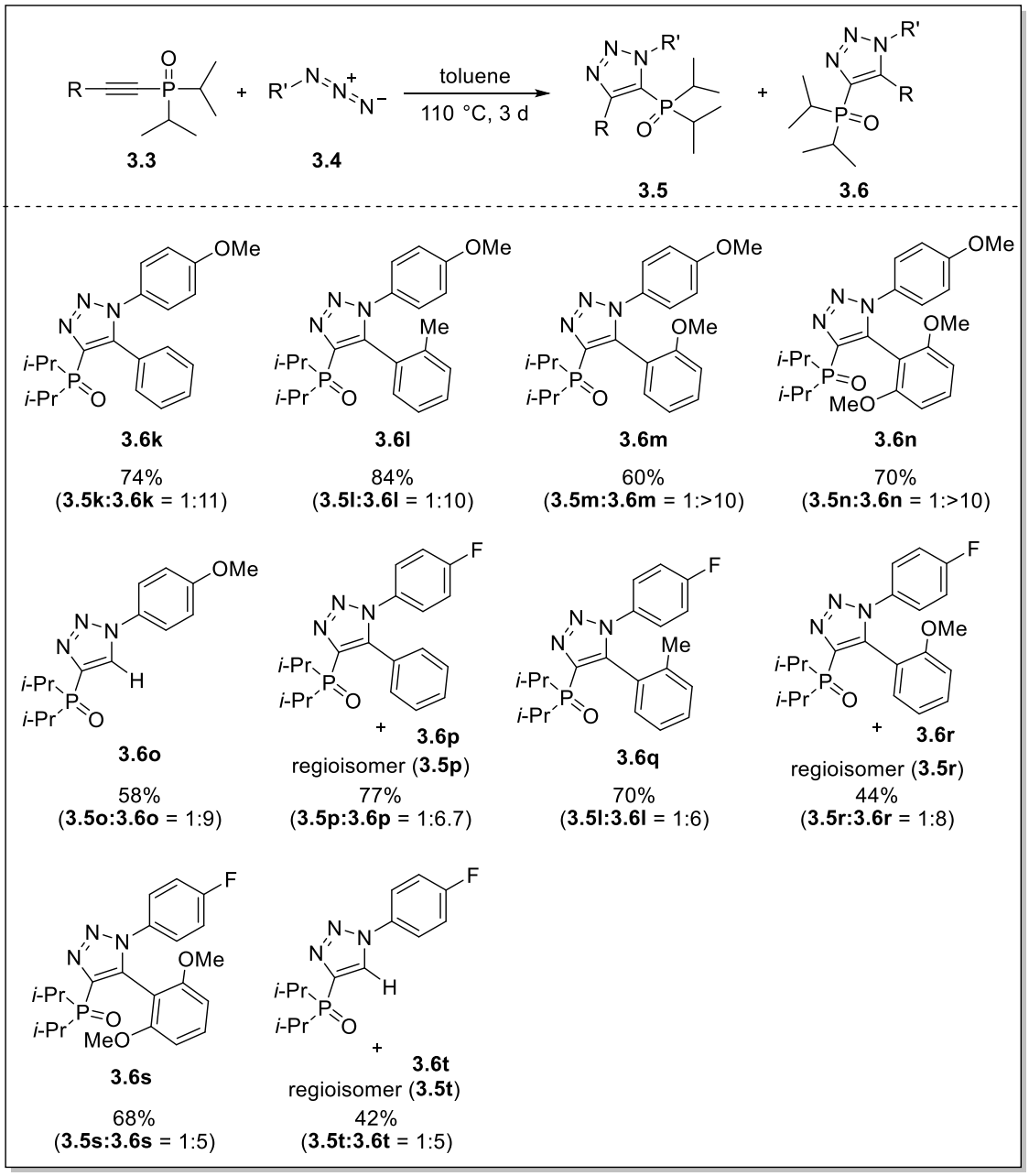

Table 3.3. Scope of [3+2]-Cycloaddition with Aryl Azides

To produce more active phosphine ligands, other electron-rich phosphine sources (*n*-Bu, *t*-Bu) were used to make triazole phosphine oxides (**Table 3.4**). The click reaction afforded the corresponding triazole phosphine oxides, incorporating electron-rich substituents, in good to excellent yields and similar regioselectivity.

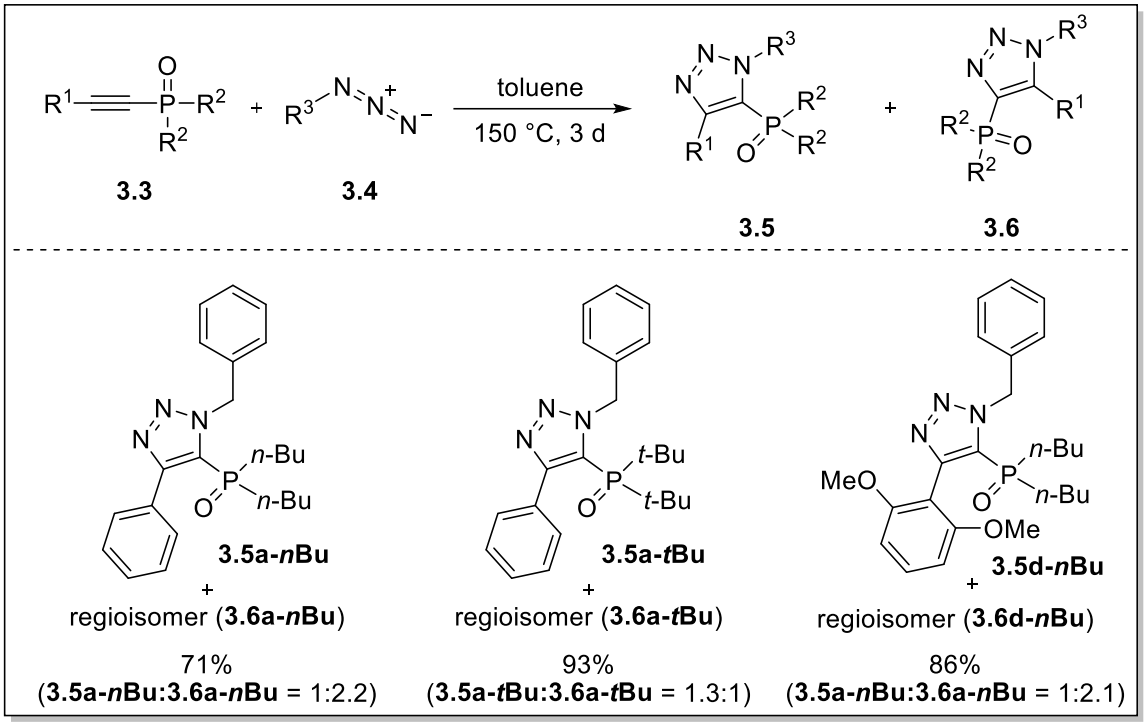

Table 3.4. Scope of [3+2]-Cycloaddition with Other Phosphine Sources

3.7. Reduction of Triazole Phosphine Oxides

Upon successful transformation to triazole phosphine oxides, the reduction of phosphine oxide was performed to generate heterocyclic phosphines. In 2012, the Beller group reported that the acid-catalyzed reduction of phosphine oxides in the presence of silane enables efficient transformation to phosphines.[21] Initial attempts at reduction were carried out with the more sterically hindered isomer of triazole phosphine oxide (**3.5a**) with the reported phosphoric acid and silane (**Table 3.5**). However, Beller's representative conditions did not convert the phosphine oxide (**3.5a**) into the corresponding phosphine, even after 2 days (entry 1). Increasing the amount of phosphoric acid catalyst and silane gave a promising result (entry 2). Unfortunately, no further improvement was achieved, even with elevated temperature (entry 3). A Cu-catalyzed tertiary phosphine oxide

[21] Li, Y.; Lu, L.-Q.; Das, S.; Pisiewicz, S.; Junge, K.; Beller, M. Highly Chemoselective Metal-Free Reduction of Phosphine Oxides to Phosphines. *J. Am. Chem. Soc.* **2012**, *134* (44), 18325–18329.

reduction method was also developed by Beller and coworkers.[22] However, the Cu-catalyzed condition failed to produce triazole phosphine ligand (**3.7a**), even after 3 days (entry 4). Next, Ti(O*i*-Pr)$_4$-assisted phosphine oxide reduction, reported by the Nishibayashi group in 2005,[23] was examined with various silane sources (entry 5–9). This mild method allowed access to the reduced phosphine product (**3.7a**). Use of Ti(O*i*-Pr)$_4$ and triethoxysilane in benzene was found to be one of the most effective conditions (entry 9). At a later time, use of trichlorosilane was found to convert phosphine oxide to its corresponding ClickPhos ligand in excellent yield, without additional additives (entry 10).[24]

[22] Li, Y.; Das, S.; Zhou, S.; Junge, K.; Beller, M. General and Selective Copper-Catalyzed Reduction of Tertiary and Secondary Phosphine Oxides: Convenient Synthesis of Phosphines. *J. Am. Chem. Soc.* **2012**, *134* (23), 9727–9732.
[23] Onodera, G.; Matsumoto, H.; Milton, M. D.; Nishibayashi, Y.; Uemura, S. Ruthenium-Catalyzed Formation of Aryl(Diphenyl)Phosphine Oxides by Reactions of Propargylic Alcohols with Diphenylphosphine Oxide. *Org. Lett.* **2005**, *7* (18), 4029–4032.
[24] Gray, M.; Chapell, B. J.; Felding, J.; Taylor, N. J.; Snieckus, V. The Di- *t* -Butylphosphinyl Directed *Ortho* Metalation Group. Synthesis of Hindered Dialkylarylphosphines. *Synlett* **1998**, *1998* (4), 422–424.

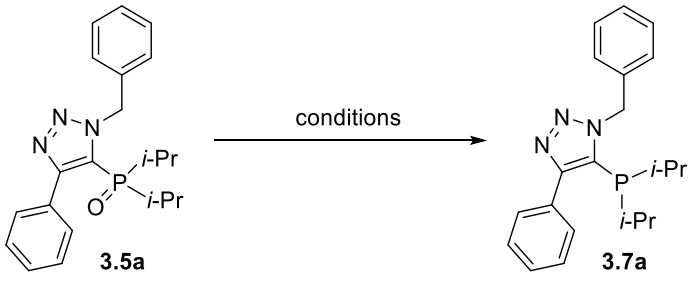

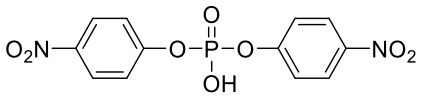

acid catalyst

Entry	conditions	solvent	Time	Conversion[a]
1	cat (7.5 mol%), $(EtO)_2MeSiH$ (4 equiv), 110 °C	toluene	2 d	N/R
2	cat (30 mol%), $(EtO)_2MeSiH$ (8 equiv), 110 °C	toluene	3 d	33%
3	cat (30 mol%), $(EtO)_2MeSiH$ (8 equiv), 150 °C	mesitylene	2 d	22%
4	$Cu(OTf)_2$ (10 mol%), TMDS (3 equiv), 100 °C	toluene	3 d	N/R
5	$Ti(O\textit{i}\text{-}Pr)_4$ (30 mol%), $(EtO)_2MeSiH$ (3 equiv), 80 °C	benzene	16 h	66%
6	$Ti(O\textit{i}\text{-}Pr)_4$ (30 mol%), $(MeO)_3SiH$ (3 equiv), 80 °C	benzene	16 h	68%
7	$Ti(O\textit{i}\text{-}Pr)_4$ (30 mol%), Ph_2SiH_2 (3 equiv), 80 °C	benzene	16 h	49%
8	$Ti(O\textit{i}\text{-}Pr)_4$ (30 mol%), TMDS (3 equiv), 80 °C	benzene	16 h	70%
9	$Ti(O\textit{i}\text{-}Pr)_4$ (30 mol%), $(EtO)_3SiH$ (3 equiv), 80 °C	benzene	16 h	92%
10	Cl_3SiH, 80 °C	toluene	20 h	95%[b]

[a]Determined by ^1H NMR.[b]Isolated yield.

Table 3.5. Phosphine Oxide Reduction Optimization

To explore the validity of this synthetic approach in rapidly generating a large ligand library, High Throughput Experimentation (HTE) was employed. Using the optimized reduction protocol, a one-pot synthesis was tested using phenylalkynylphosphine oxide (**3.3a**) and benzyl azide (**3.4a**). The click reaction and subsequent reduction in benzene gave the corresponding triazole phosphines in good

yield (**Scheme 3.6**). In addition, mass-directed liquid chromatography (MDLC) allowed efficient separation of the regioisomeric mixture of phosphine ligands.

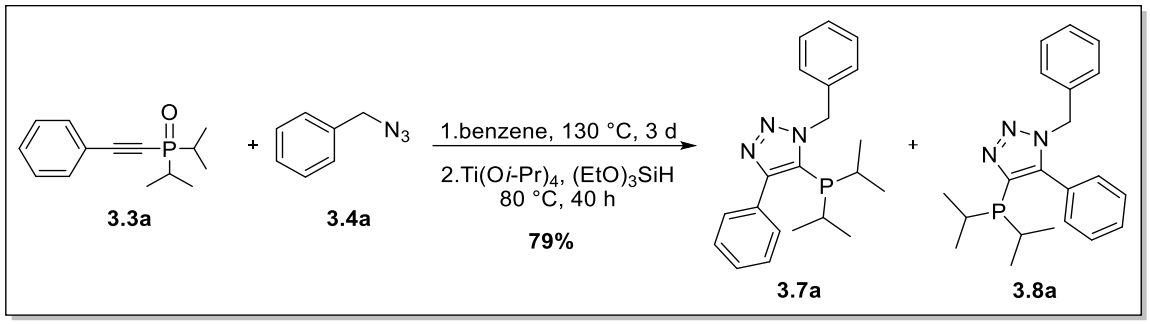

Scheme 3.6. One-pot Synthesis of ClickPhos Ligand

3.8. Preliminary Studies toward Suzuki Coupling of 3,5-Dichloropyridazine

With a small array of ClickPhos ligands, we began to investigate ligand effects in selective Suzuki-Miyaura cross-coupling. Based on the literature by Dai and coworkers,[2c] variable chemoselectivity was achieved by utilizing different ligands. An electron-deficient bidentate ligand, DPPF, gave **3.11** as a major and an electron-rich monodentate ligand, Q-Phos, showed inverted selectivity. Inspired by this site-selective cross-coupling precedent,[2c] Suzuki coupling of 3,5-dichloropyridazine with 13 pairs of ClickPhos ligands[25] was screened under the reported condition (**Scheme 3.7**).

As shown in **Figure 3.4**, screening results support the reported hypothesis of Dai and coworkers. Due to the electron-rich nature of the triazole-based phosphine ligands, we anticipated formation of the challenging C-5 substituted pyridazine (**3.12**) as the major product. Across the plate, most of the ClickPhos ligands generated the 5-substituted product (**3.12**) preferentially over the 3-substituted (**3.11**) or 3,5-disubstituted products (**3.13**). Notably, the most electron-rich ClickPhos ligand (**3.7d-Cy**) produced the highest C-5:C-3 ratio of 4.9:1. Interestingly, the least electron-rich triazole phosphine (**3.8e**) gave

[25] Sobia Jabeen, visiting student, assisted to synthesize ClickPhos ligands.

C-3 substituted pyridazine (**3.11**) as the major product.

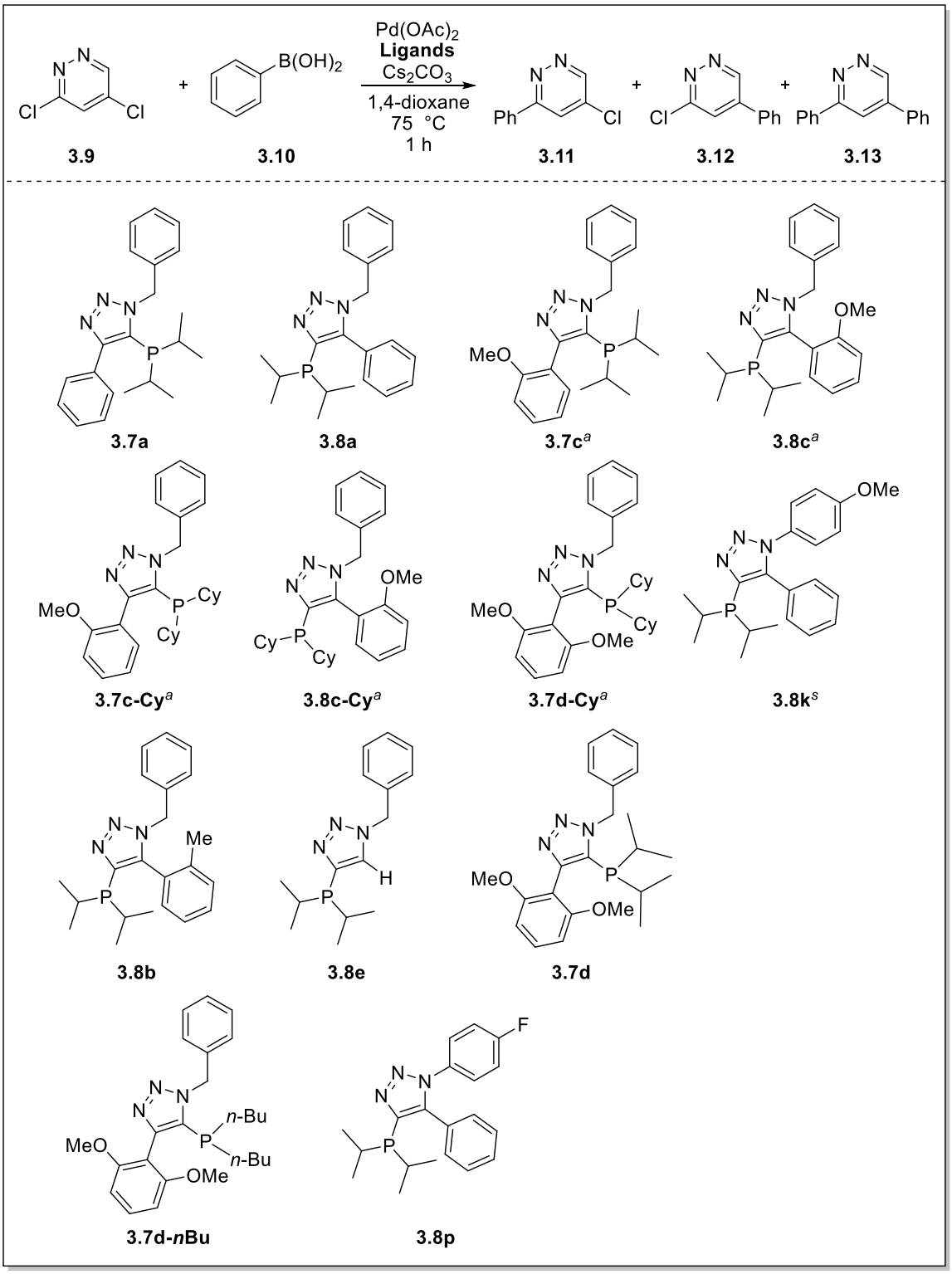

Reaction condition:1.0 equiv **3.9**, 1.1 equiv **3.10**, 10 mol% $Pd(OAc)_2$, 10 or 20 mol% ligands, 3.0 equiv Cs_2CO_3, 0.1 M 1,4-dioxane. [a]Ligands were synthesized by Sobia Jabeen.

Scheme 3.7. Preliminary Screening of Suzuki-Miyaura Coupling with Diverse ClickPhos Ligands

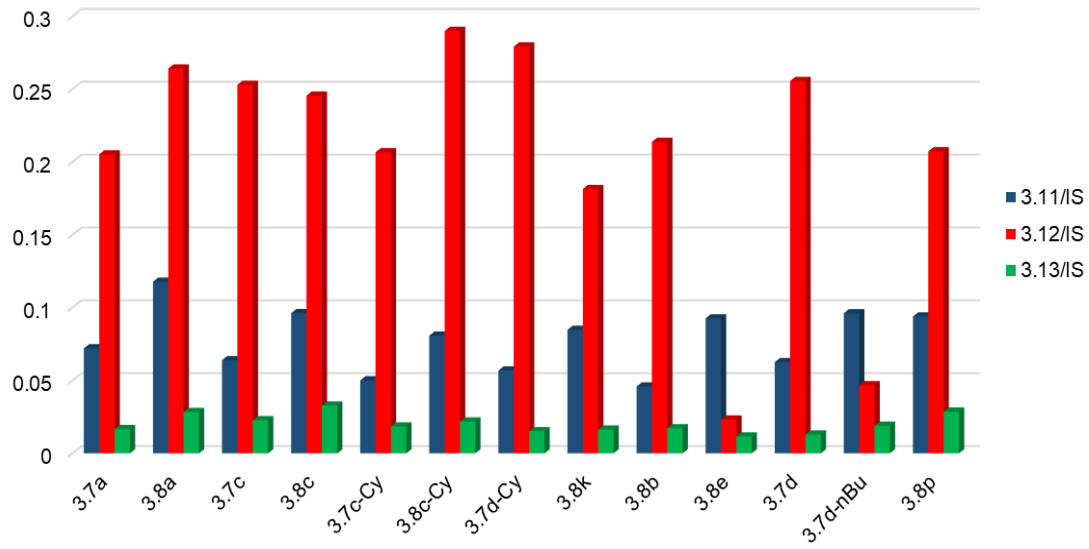

Figure 3.4. Screening Results of 13 ClickPhos Ligands

3.9. Conclusion

In conclusion, a variety of triazole-based phosphine ligands have been synthesized via thermal [3+2]-cycloaddition, followed by phosphine oxide reduction. A one-pot protocol has also been developed, which will allow rapid expansion of the ligand library through the use of High–Throughput Experimentation. Although a small array of phosphine ligands was tested, the preliminary reaction screen gave promising results that seem to indicate selective substitution of chemically challenging substrates. To expand the ligand library, it is necessary to develop a more efficient phosphine oxide reduction method. The current conditions cannot reduce sterically hindered phosphine oxides, such as the di-*tert*-butyl phosphine oxides (**3.5a-*t*Bu**), which will be more active ligands based on the preliminary data. Furthermore, additional data, obtained from a larger collection of ligands, need to be collected to disclose novel ligand effects.

3.10. Experimental Section

General Considerations

Unless otherwise noted, all non-aqueous reactions were carried out under an atmosphere of dry N_2 in dried glassware. When necessary, solvents and reagents were dried prior to use. THF was distilled from sodium benzophenone ketyl. CH_2Cl_2, $ClCH_2CH_2Cl$, and toluene were distilled from CaH_2. High throughput experiments were performed at the Penn/Merck High Throughput Experimentation Laboratory at the University of Pennsylvania. The screens were analyzed by HPLC by addition of an internal standard.

Analytical thin layer chromatography (TLC) was performed on EM Reagents 0.25 mm silica-gel 254-F plates. Visualization was accomplished with UV light. Chromatography was performed using a forced flow of the indicated solvent system on EM Reagents Silica Gel 60 (230-400 mesh). When necessary, the column was pre-washed with 1% Et_3N in the eluent system. ^1H NMR spectra were recorded on a 500 MHz spectrometer. Chemical shifts are reported in ppm from tetramethylsilane (0 ppm) or from the solvent resonance ($CDCl_3$ 7.26 ppm, DMSO-d_6 3.58 ppm, acetone-d_6 2.05 ppm, DMF-d_7 2.50 ppm, CD_3CN 1.94 ppm, CD_2Cl_2 5.32 ppm). Data are reported as follows: chemical shift, multiplicity (s = singlet, d = doublet, t = triplet, q = quartet, br = broad, m = multiplet), coupling constants, and number of protons. Decoupled ^{13}C NMR spectra were recorded at 125 MHz. IR spectra were taken on an FT-IR spectrometer. Accurate mass measurement analyses were conducted via time-of-flight mass analyzer GCMS with electron ionization (EI) or via time-of-flight mass analyzer LCMS with electrospray ionization (ESI). The signals were measured against an internal reference of perfluorotributylamine for EI-GCMS and leucine enkephalin for ESI-LCMS. The instrument was calibrated and measurements were made using neutral atomic masses; the mass of

the electron removed or added to create the charged species is not taken into account. Low resolution LCMS data were obtained by use of a UPLC system with a SQD mass analyzer equipped with electrospray ionization. Circular dichroism and UV-vis spectroscopy measurements carried out at ambient temperature (23 C). Enantiomeric excesses were determined using analytical HPLC with UV detection at 254 nm. Analytical Chiralpak columns (4.6 mm x 250 mm, 5 µm) from Daicel were used.

General procedure A: preparation of alkynylphosphine oxide. A solution of *n*-BuLi (1.6 M in hexane) (9.4 mL, 15.0 mmol) was added dropwise to the solution of the acetylene (13.7 mmol) in THF (45 mL) at –78 °C. The reaction was allowed to warm to 0 °C, stirred for 20 min, and then again cooled to –78 °C. Chlorodiisopropylphosphine (2.2 mL, 13.7 mmol), or di-*tert*-butylchlorophosphine (2.6 mL, 13.7 mmol), or chlorodibutylphosphine (2.6 mL, 13.7 mmol) was added dropwise. The solution was allowed to warm to room temperature and was stirred for a further 2.5 h. The reaction was then cooled to 0 °C and hydrogen peroxide (30% aq solution, 2.0 mL, 6.7 M) was added dropwise. The solution was warmed to room temperature. After stirring 30 min at room temperature, the reaction mixture was dried over Na_2SO_4, filtered, and concentrated. Chromatography afforded the desired product.

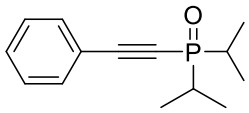

Diisopropyl(phenylethynyl)phosphine oxide (3.3a). Following **General procedure A**, the product was obtained as a colorless oil (3.16 g) in 98% yield. $\mathbf{R_f}$ = 0.21 (100% EtOAc): **^{1}H NMR** (500 MHz, $CDCl_3$) δ 7.54 (d, *J* = 7.0 Hz, 2H), 7.43 (t, *J* = 7.5 Hz, 1H), 7.37 (t, *J* = 7.5 Hz, 2H), 2.18–2.10 (m, 2H), 1.35–1.24 (m, 12H); **^{13}C NMR** (125 MHz, $CDCl_3$) δ 132.3, 130.2, 128.4, 120.2, 103.1 (d, *J* = 21.9 Hz), 80.6 (d, *J* = 135.9 Hz), 27.1 (d, *J* = 78.5 Hz),

16.1 (d, *J* = 1.8 Hz), 14.9 (d, *J* = 1.8 Hz); **^{31}P NMR** δ 40.8; **IR** (neat) 2964, 2933, 2873, 2173, 1489, 1463, 1443, 1263, 1223, 1188, 1156, 1025 cm^{-1}; **HRMS** (ESI-TOF) calcd for $C_{14}H_{19}OPNa$ $[M+Na]^+$ 257.1071, found 257.1075.

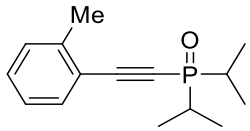

Diisopropyl(*o*-tolylethynyl)phosphine oxide (3.3b). Following **General procedure A**, the product was obtained as a white solid (0.90 g) in 82% yield. **R_f** = 0.17 (100% EtOAc): **^{1}H NMR** (500 MHz, $CDCl_3$) δ 7.45 (d, *J* = 7.5 Hz, 1H), 7.26 (t, *J* = 7.5 Hz, 1H), 7.17 (d, *J* = 7.5 Hz, 1H), 7.12 (t, *J* = 7.5 Hz, 1H), 2.41 (s, 3H), 2.13–2.03 (m, 2H), 1.30–1.24 (m, 12H); **^{13}C NMR** (125 MHz, $CDCl_3$) δ 141.3, 132.9, 130.2, 129.7, 125.8, 120.2 (d, *J* = 3.3 Hz), 102.1 (d, *J* = 21.8 Hz), 84.5 (d, *J* = 136.3 Hz), 27.2 (d, *J* = 78.4 Hz), 20.7, 16.2 (d, *J* = 2.5 Hz), 15.0 (d, *J* = 3.3 Hz); **^{31}P NMR** δ 41.7; **IR** (neat) 2968, 2171, 1457, 1177, 1144, 1114, 1032, 884 cm^{-1}; **HRMS** (ESI-TOF) calcd for $C_{15}H_{22}OP$ $[M+H]^+$ 249.1408, found 249.1423.

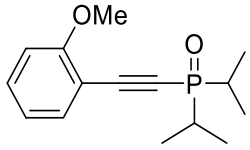

Diisopropyl((2-methoxyphenyl)ethynyl)phosphine oxide (3.3c). Following **General Procedure A**, the product was obtained as a off-white oil (1.01 g) in 74% yield. **R_f** = 0.20 (100% EtOAc): **^{1}H NMR** (500 MHz, $CDCl_3$) δ 7.42 (dd, *J* = 7.5, 1.5 Hz, 1H), 7.33 (td, *J* = 7.5, 1.5 Hz, 1H), 6.88 (t, *J* = 7.5 Hz, 1H), 6.84 (d, *J* = 8.0 Hz, 1H), 3.81 (s, 3H), 2.14–2.03 (m, 2H), 1.28 (dd, *J* = 16.5, 7.0 Hz, 6H), 1.27 (dd, *J* = 17.0, 7.0 Hz, 6H); **^{13}C NMR** (125 MHz, $CDCl_3$) δ 161.4, 134.1, 131.8, 120.5, 110.8, 109.8 (d, *J* = 3.4 Hz), 100.0 (d, *J* = 22.6 Hz), 84.6 (d, *J* = 139.2 Hz), 55.8, 27.2 (d, *J* = 78.6 Hz), 16.2 (d, *J* = 2.4 Hz), 15.0 (d, *J* = 3.1 Hz); **^{31}P NMR** δ 42.0; **IR** (neat) 2964, 2172, 1595, 1490, 1462, 1435, 1290, 1258, 1185,

1157, 1114, 1045, 1022 cm^{-1}; **HRMS** (ESI-TOF) calcd for $C_{15}H_{22}O_2P$ $[M+H]^+$ 265.1357, found 265.1345.

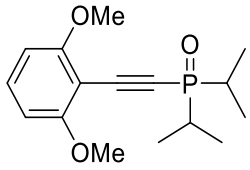

((2,6-Dimethoxyphenyl)ethynyl)diisopropylphosphine oxide (3.3d). Following **General procedure A**, the product was obtained as a white solid (1.08 g) in 74% yield. $\mathbf{R_f}$ = 0.13 (100% EtOAc): **^{1}H NMR** (500 MHz, $CDCl_3$) δ 7.24 (t, *J* = 8.5 Hz, 1H), 6.45 (d, *J* = 8.5 Hz, 2H), 3.79 (s, 6H), 2.10–2.05 (m, 2H), 1.27 (dd, *J* = 17.0, 7.0 Hz, 12H); **^{13}C NMR** (125 MHz, $CDCl_3$) δ 162.7, 131.9, 103.4, 99.2 (d, *J* = 3.6 Hz), 96.7 (d, *J* = 24.4 Hz), 88.6 (d, *J* = 143.0 Hz), 56.0, 27.2 (d, *J* = 78.8 Hz), 16.1 (d, *J* = 2.5 Hz), 15.0 (d, *J* = 3.4 Hz); **^{31}P NMR** δ 41.0; **IR** (neat) 2955, 2872, 2174, 1593, 1579, 1474, 1447, 1438, 1258, 1176, 1149, 1108, 1025, 884 cm^{-1}; **HRMS** (ESI-TOF) calcd for $C_{16}H_{24}O_3P$ $[M+H]^+$ 295.1463, found 295.1443.

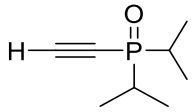

Ethynyldiisopropylphosphine oxide (3.3e). Following **General Procedure A**, the product was obtained as a white solid (1.59 g) in 94% yield. $\mathbf{R_f}$ = 0.21 (100% EtOAc): **^{1}H NMR** (500 MHz, $CDCl_3$) δ 3.00 (d, *J* = 8.5 Hz, 1H), 2.05–1.97 (m, 2H), 1.24–1.17 (m, 12H); **^{13}C NMR** (125 MHz, $CDCl_3$) δ 91.9 (d, *J* = 19.4 Hz), 76.6 (d, *J* = 127.5 Hz), 26.9 (d, *J* = 77.9 Hz), 16.0 (d, *J* = 2.6 Hz), 14.8 (d, *J* = 3.0 Hz); **^{31}P NMR** δ 42.2; **IR** (neat) 3129, 2966, 2934, 2907, 2874, 2044, 1464, 1448, 1387, 1251, 1176, 1154, 1025 cm^{-1}; **HRMS** (ESI-TOF) calcd for $C_8H_{15}OP$ $[M]^+$ 158.0861, found 158.0864.

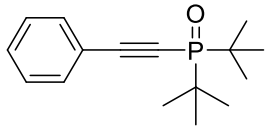

Di-*tert*-butyl(phenylethynyl)phosphine oxide (3.3a-*t*Bu). Following **General Procedure A**, the product was obtained as a white solid (1.38 g) in 82% yield. $\mathbf{R_f}$ = 0.15 (100% EtOAc): **^{1}H NMR** (500 MHz, $CDCl_3$) δ 7.46 (d, *J* = 7.0 Hz, 2H), 7.35 (td, *J* = 7.0, 1.0 Hz, 1H), 7.29 (t, *J* = 7.0 Hz, 2H), 1.32 (d, *J* = 15.0 Hz, 18H); **^{13}C NMR** (125 MHz, $CDCl_3$) δ 132.2 (d, *J* = 1.3 Hz), 130.1, 128.5, 120.5 (d, *J* = 3.4 Hz), 102.9 (d, *J* = 18.8 Hz), 81.7 (d, *J* = 127.4 Hz), 36.1 (d, *J* = 72.4 Hz), 26.4; **^{31}P NMR** δ 48.3. Spectral data were in agreement with those reported.[26]

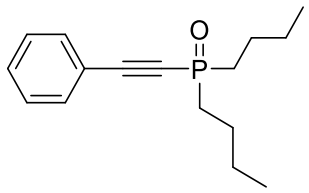

Dibutyl(phenylethynyl)phosphine oxide (3.3a-*n*Bu). Following **General Procedure A**, the product was obtained as a white solid (0.94 g) in 98% yield. $\mathbf{R_f}$ = 0.23 (100% EtOAc): **^{1}H NMR** (500 MHz, $CDCl_3$) δ 7.53 (d, *J* = 7.5 Hz, 2H), 7.43 (t, *J* = 7.0 Hz, 1H), 7.36 (t, *J* = 7.5 Hz, 2H), 1.96–1.89 (m, 4H), 1.79–1.66 (m, 4H), 1.52–1.44 (m, 4H), 0.96 (t, *J* = 7.5 Hz, 6H); **^{13}C NMR** (125 MHz, $CDCl_3$) δ 132.3, 130.3, 128.5, 120.2, 102.4 (d, *J* = 25.4 Hz), 82.9 (d, *J* = 144.5 Hz), 31.1 (d, *J* = 79.9 Hz), 24.0 (d, *J* = 4.0 Hz), 23.9 (d, *J* = 16.1 Hz), 13.6; **^{31}P NMR** δ 26.2. Spectral data were in agreement with those reported.[27]

[26] Kondoh, A.; Yorimitsu, H.; Oshima, K. Synthesis of 2-Indolylphosphines by Palladium-Catalyzed Annulation of 1-Alkynylphosphine Sulfides with 2-Iodoanilines. *Org. Lett.* **2010**, *12* (7), 1476–1479.
[27] Yang, J.; Chen, T.; Zhou, Y.; Yin, S.; Han, L.-B. Palladium-Catalyzed Dehydrogenative Coupling of Terminal Alkynes with Secondary Phosphine Oxides. *Chem. Commun.* **2015**, *51* (17), 3549–3551.

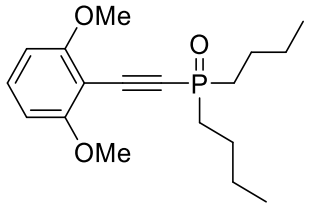

Dibutyl((2,6-dimethoxyphenyl)ethynyl)phosphine oxide (3.3d-*n*Bu). Following **General Procedure A**, the product was obtained as an off-white solid (1.04 g) in 87% yield. $\mathbf{R_f}$ = 0.26 (100% EtOAc): **^{1}H NMR** (500 MHz, $CDCl_3$) δ 7.29 (t, *J* = 8.5 Hz, 1H), 6.50 (d, *J* = 8.5 Hz, 2H), 3.84 (s, 6H), 1.96–1.87 (m, 4H), 1.81–1.71 (m, 4H), 1.48 (sext, *J* = 7.5 Hz, 4H), 0.96 (t, *J* = 7.5 Hz, 6H); **^{13}C NMR** (125 MHz, $CDCl_3$) δ 162.8, 132.0, 103.5, 99.5, 96.3 (d, *J* = 27.4 Hz), 91.2 (d, *J* = 150.0 Hz), 56.1, 31.4 (d, *J* = 80.1 Hz), 24.2 (d, *J* = 4.3 Hz), 24.1 (d, *J* = 15.8 Hz), 13.8; **^{31}P NMR** δ 26.0; **IR** (neat) 2957, 2934, 2871, 2169, 1593, 1581, 1475, 1433, 1403, 1298, 1258, 1223, 1173, 1109, 1029 cm^{-1}; **HRMS** (EI-TOF) calcd for $C_{18}H_{27}O_3P$ $[M]^+$ 322.1698, found 322.1701.

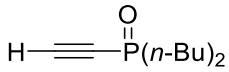

Dibutyl(ethynyl)phosphine oxide (3.3e-*n*Bu). Following **General procedure A**, the product was obtained as a white solid (0.25 g) in 81% yield. $\mathbf{R_f}$ = 0.30 (100% EtOAc): **^{1}H NMR** (500 MHz, $CDCl_3$) δ 3.00 (d, *J* = 9.0 Hz, 1H), 1.89–1.78 (m, 4H), 1.71–1.60 (m, 4H), 1.45 (sext, *J* = 7.5 Hz, 4H), 0.94 (t, *J* = 7.5 Hz, 6H); **^{13}C NMR** (125 MHz, $CDCl_3$) δ 91.0 (d, *J* = 23.0 Hz), 79.0 (d, *J* = 135.6 Hz), 31.0 (d, *J* = 79.5 Hz), 24.0 (d, *J* = 13.9 Hz), 23.9 (d, *J* = 2.8 Hz), 13.7; **^{31}P NMR** δ 27.1; **IR** (neat) 3109, 2959, 2929, 2873, 2043, 1465, 1379, 1222, 1202, 1163, 1088, 1053, 967 cm^{-1}; **HRMS** (ESI-TOF) calcd for $C_{10}H_{20}OP$ $[M+H]^+$ 187.1252, found 187.1256.

General procedure B: [3+2]-cycloaddition with alkyl azides. Azide (0.70 mmol) was added in the solution of the corresponding alkynylphosphine oxide (0.63 mmol) in toluene

(1.3 mL) under argon and sealed with a cap. The reaction mixture was stirred for 3–5 d at 150 °C. The resultant mixture was cooled to room temperature and removal of solvent was followed by chromatography.

General procedure C: [3+2]-cycloaddition with aryl azides. Azide (0.88 mmol) was added in the solution of the corresponding alkynylphosphine oxide (0.44 mmol) in toluene (0.88 mL) under argon and sealed with a cap. The reaction mixture was stirred for 1 d at 110 °C. Subsequent addition of the second portion of azide (0.88 mmol) added into the reaction mixture and stirred for 2 d. The resultant mixture was cooled to room temperature and removal of solvent was followed by chromatography.

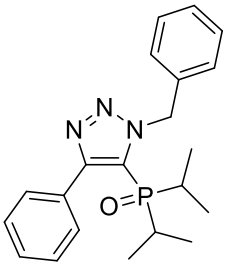

(1-Benzyl-4-phenyl-1*H*-1,2,3-triazol-5-yl)diisopropylphosphine oxide (3.5a). Following **General procedure B**, the product was obtained as an off-white solid (0.32 g) in 41% yield. $\mathbf{R_f}$ = 0.58 (100% EtOAc): **^{1}H NMR** (500 MHz, $CDCl_3$) δ 7.55 (d, *J* = 7.0 Hz, 2H), 7.45–7.43 (m, 3H), 7.35 (dd, *J* = 8.0, 1.5 Hz, 2H), 7.33–7.29 (m, 3H), 6.14 (s, 2H), 1.81–1.75 (m, 2H), 1.11 (dd, *J* = 16.0, 7.0 Hz, 6H), 0.78 (dd, *J* = 17.0, 7.5 Hz, 6H); **^{13}C NMR** (125 MHz, $CDCl_3$) δ 150.4 (d, *J* = 14.3 Hz), 136.3, 131.6, 129.5, 129.4, 129.0, 128.6, 128.5, 128.2, 124.2 (d, *J* = 83.9 Hz), 54.0, 29.1 (d, *J* = 69.9 Hz), 16.5 (d, *J* = 3.8 Hz), 15.4 (d, *J* = 2.8 Hz); **^{31}P NMR** δ 49.7; **IR** (neat) 2967, 2932, 1496, 1464, 1445, 1190, 1151, 1073, 1029 cm^{-1}; **HRMS** (ESI-TOF) calcd for $C_{21}H_{27}N_3OP$ $[M+H]^+$ 368.1892, found 368.1886.

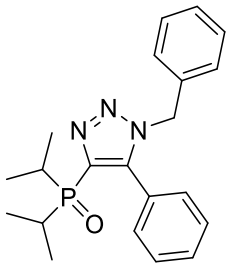

(1-Benzyl-5-phenyl-1*H*-1,2,3-triazol-4-yl)diisopropylphosphine oxide (3.6a). Following **General procedure B**, the product was obtained as an off-white solid (0.37 g) in 47% yield. $\mathbf{R_f}$ = 0.21 (100% EtOAc): **^{1}H NMR** (500 MHz, $CDCl_3$) δ 7.44 (t, *J* = 7.5 Hz, 1H), 7.39 (t, *J* = 7.5 Hz, 2H), 7.31–7.26 (m, 5H), 7.01–6.99 (m, 2H), 5.44 (s, 2H), 2.46–2.38 (m, 2H), 1.14 (dd, *J* = 16.5, 7.0 Hz, 6H), 1.10 (dd, *J* = 15.5, 7.0 Hz, 6H); **^{13}C NMR** (125 MHz, $CDCl_3$) δ 145.6 (d, *J* = 18.2 Hz), 136.2 (d, *J* = 110.3 Hz), 135.1, 130.5, 130.0, 128.9, 128.4, 128.3, 127.4, 125.9, 51.9, 26.4 (d, *J* = 70.6 Hz), 16.0 (d, *J* = 2.5 Hz), 14.9 (d, *J* = 2.9 Hz); **^{31}P NMR** δ 46.4; **IR** (neat) 2963, 2932, 2872, 1454, 1407, 1278, 1243, 1202, 1181, 1154, 1027 cm^{-1}; **HRMS** (ESI-TOF) calcd for $C_{21}H_{27}N_3OP$ $[M+H]^+$ 368.1892, found 368.1864.

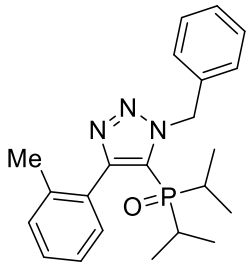

(1-Benzyl-4-(*o*-tolyl)-1*H*-1,2,3-triazol-5-yl)diisopropylphosphine oxide (3.5b). Following **General procedure B**, the product was obtained as a white solid (40 mg) in 26% yield. $\mathbf{R_f}$ = 0.60 (100% EtOAc): **^{1}H NMR** (500 MHz, $CDCl_3$) δ 7.53 (d, *J* = 7.0 Hz, 2H), 7.35–7.27 (m, 5H), 7.20 (t, *J* = 7.5 Hz, 1H), 7.07 (d, *J* = 7.5 Hz, 1H), 6.14 (s, 2H), 2.16 (s, 3H), 1.75–1.67 (m, 2H), 1.06 (dd, *J* = 16.5, 7.0 Hz, 6H), 0.79 (dd, *J* = 16.5, 7.0 Hz, 6H);

^{13}C NMR (125 MHz, $CDCl_3$) δ 149.4 (d, *J* = 14.4 Hz), 138.7, 136.4, 130.9, 130.6, 129.7, 129.6, 128.9, 128.5, 128.2, 125.6, 124.9 (d, *J* = 83.7 Hz), 54.0, 29.2 (d, *J* = 69.9 Hz), 20.2, 16.5 (d, *J* = 3.8 Hz), 15.4 (d, *J* = 2.8 Hz); **^{31}P NMR** δ 50.5; **IR** (neat) 2964, 2929, 1456, 1191, 1151, 1019, 880, 769 cm^{-1}; **HRMS** (ESI-TOF) calcd for $C_{22}H_{29}N_3OP$ $[M+H]^+$ 382.2048, found 382.2063.

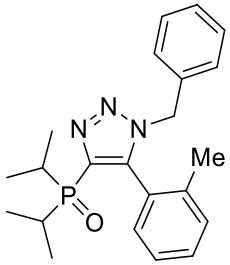

(1-Benzyl-5-(*o*-tolyl)-1*H*-1,2,3-triazol-4-yl)diisopropylphosphine oxide (3.6b). Following **General procedure B**, the product was obtained a white solid (71 mg) in 46% yield. **R_f** = 0.23 (100% EtOAc): **^{1}H NMR** (500 MHz, $CDCl_3$) δ 7.32 (t, *J* = 7.5 Hz, 1H), 7.23–7.15 (m, 5H), 6.94 (d, *J* = 7.0 Hz, 1H), 6.89 (d, *J* = 7.0 Hz, 2H), 5.27 (d, *J* = 14.5 Hz, 1H), 5.22 (d, *J* = 14.5 Hz, 1H), 2.53–2.46 (m, 1H), 2.24–2.16 (m, 1H), 1.80 (s, 3H), 1.19–1.13 (m, 6H), 1.10–1.01 (m, 6H); **^{13}C NMR** (125 MHz, $CDCl_3$) δ 144.6 (d, *J* = 18.2 Hz), 138.6, 136.9 (d, *J* = 110.9 Hz), 134.3, 130.3, 130.2, 130.1, 128.7, 128.4, 128.2, 125.8, 125.5, 52.0, 26.9 (d, *J* = 70.3 Hz), 26.0 (d, *J* = 70.5 Hz), 19.8, 16.0 (d, *J* = 3.1 Hz), 15.9 (d, *J* = 1.4 Hz), 15.2 (d, *J* = 3.1 Hz), 14.6 (d, *J* = 1.5 Hz); **^{31}P NMR** δ 46.9; **IR** (neat) 2962, 2933, 1456, 1406, 1364, 1197, 1178, 1154, 1025, 880 cm^{-1}; **HRMS** (ESI-TOF) calcd for $C_{22}H_{29}N_3OP$ $[M+H]^+$ 382.2048, found 382.2056.

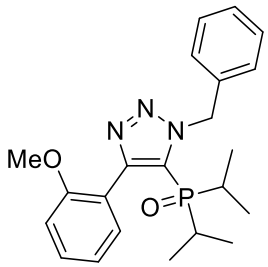

(1-Benzyl-4-(2-methoxyphenyl)-1*H*-1,2,3-triazol-5-yl)diisopropylphosphine oxide (3.5c). Following **General procedure B**, the product was obtained as a light yellow solid (67 mg) in 43% yield. $\mathbf{R_f}$ = 0.64 (100% EtOAc): **^{1}H NMR** (500 MHz, $CDCl_3$) δ 7.56 (d, *J* = 7.0 Hz, 2H), 7.43 (td, *J* = 8.5, 1.5 Hz, 1H), 7.33 (t, *J* = 7.5 Hz, 2H), 7.29 (d, *J* = 7.0 Hz, 1H), 7.16 (dd, *J* = 7.5, 1.5 Hz, 1H), 6.99 (td, *J* = 7.5, 1.0 Hz, 1H), 6.95 (d, *J* = 8.5 Hz, 1H), 6.13 (s, 2H), 3.70 (s, 3H), 1.73–1.66 (m, 2H), 1.09 (dd, *J* = 16.0, 7.0 Hz, 6H), 0.81 (dd, *J* = 17.0, 7.5 Hz, 6H); **^{13}C NMR** (125 MHz, $CDCl_3$) δ 158.0, 146.7 (d, *J* = 14.0 Hz), 136.3, 131.6, 131.3, 129.0, 128.4, 128.1, 125.5 (d, *J* = 84.8 Hz), 120.4, 120.3, 111.1, 55.2, 53.8, 28.7 (d, *J* = 70.1 Hz), 16.4 (d, *J* = 3.6 Hz), 15.3 (d, *J* = 2.8 Hz); **^{31}P NMR** δ 50.1; **IR** (neat) 2965, 2934, 1496, 1471, 1435, 1281, 1245, 1188, 1151, 1112, 1049, 1023 cm^{-1}; **HRMS** (ESI-TOF) calcd for $C_{22}H_{29}N_3O_2P$ $[M+H]^+$ 398.1997, found 398.1994.

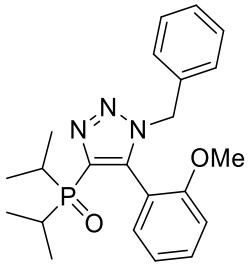

(1-Benzyl-5-(2-methoxyphenyl)-1*H*-1,2,3-triazol-4-yl)diisopropylphosphine oxide (3.6c). Following **General procedure B**, the product was obtained as a light yellow solid (74 mg) in 47% yield. $\mathbf{R_f}$ = 0.23 (100% EtOAc): **^{1}H NMR** (500 MHz, $CDCl_3$) δ 7.39 (td, *J* = 8.5, 1.5 Hz, 1H), 7.20–7.17 (m, 3H), 7.14 (dd, *J* = 7.5, 1.5 Hz, 1H), 6.95–6.92 (m, 3H), 6.89 (d, *J* = 8.0 Hz, 1H), 5.42 (d, *J* = 15.0 Hz, 1H), 5.20 (d, *J* = 15.0 Hz, 1H), 3.61 (s, 3H),

2.56–2.45 (m, 1H), 2.25–2.17 (m, 1H), 1.24–1.18 (m, 6H), 1.05–0.94 (m, 6H); **^{13}C NMR** (125 MHz, $CDCl_3$) δ 156.8, 142.5 (d, *J* = 18.1 Hz), 136.6 (d, *J* = 111.9 Hz), 134.9, 133.0, 131.8, 128.6, 128.1, 127.9, 120.6, 114.9, 110.6, 55.2, 52.2, 26.9 (d, *J* = 70.8 Hz), 25.8 (d, *J* = 71.0 Hz), 16.0 (d, *J* = 2.3 Hz), 15.8 (d, *J* = 2.0 Hz), 14.8 (d, *J* = 3.1 Hz), 14.5 (d, *J* = 4.0 Hz); **^{31}P NMR** δ 46.7; **IR** (neat) 2963, 2933, 1477, 1456, 1411, 1293, 1274, 1245, 1199, 1182, 1155, 1115, 1024 cm^{-1}; **HRMS** (EI-TOF) calcd for $C_{22}H_{29}N_3O_2P$ $[M+H]^+$ 398.1997, found 398.2017.

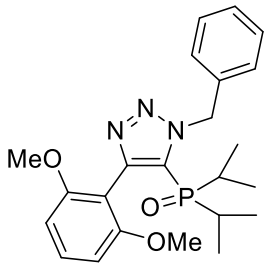

(1-Benzyl-4-(2,6-dimethoxyphenyl)-1*H*-1,2,3-triazol-5-yl)diisopropylphosphine oxide (3.5d). Following **General procedure B**, the product was obtained as an off-white solid (65 mg) in 39% yield. **R_f** = 0.47 (100% EtOAc): **^{1}H NMR** (500 MHz, $CDCl_3$) δ 7.53 (d, *J* = 7.5 Hz, 2H), 7.33 (t, *J* = 8.5 Hz, 1H), 7.30–7.22 (m, 3H), 6.55 (d, *J* = 8.5 Hz, 2H), 6.09 (s, 2H), 3.61 (s, 6H), 1.68–1.61 (m, 2H), 1.04 (dd, *J* = 16.5, 7.0 Hz, 6H), 0.78 (dd, *J* = 16.5, 7.0 Hz, 6H); **^{13}C NMR** (125 MHz, $CDCl_3$) δ 159.3, 143.2 (d, *J* = 13.8 Hz), 136.5, 131.6, 128.9, 128.3, 127.9, 126.5 (d, *J* = 85.5 Hz), 108.4, 103.6, 55.3, 53.7, 28.8 (d, *J* = 70.4 Hz), 16.3 (d, *J* = 3.8 Hz), 15.4 (d, *J* = 2.6 Hz); **^{31}P NMR** δ 50.5; **IR** (neat) 2960, 2942, 1603, 1587, 1473, 1458, 1433, 1289, 1252, 1183, 1149, 1109, 1031, 994 cm^{-1}; **HRMS** (ESI-TOF) calcd for $C_{23}H_{31}N_3O_3P$ $[M+H]^+$ 428.2103, found 428.2110.

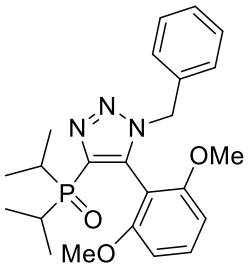

(1-Benzyl-5-(2,6-dimethoxyphenyl)-1*H*-1,2,3-triazol-4-yl)diisopropylphosphine oxide (3.6d). Following **General procedure B**, the product was obtained as an off-white solid (88 mg) in 53% yield. $\mathbf{R_f}$ = 0.08 (100% EtOAc): **^{1}H NMR** (500 MHz, $CDCl_3$) δ 7.33 (t, *J* = 8.5 Hz, 1H), 7.20–7.19 (m, 3H), 6.99–6.98 (m, 2H), 6.49 (d, *J* = 8.5 Hz, 2H), 5.25 (s, 2H), 3.52 (s, 6H), 2.33–2.28 (m, 2H), 1.12 (dd, *J* = 16.0, 7.0 Hz, 12H); **^{13}C NMR** (125 MHz, $CDCl_3$) δ 158.6, 139.4 (d, *J* = 18.9 Hz), 137.3 (d, *J* = 114.4 Hz), 134.9, 132.1, 128.3, 128.1, 127.9, 103.8, 103.5, 55.4, 52.1, 26.8 (d, *J* = 70.4 Hz), 15.8 (d, *J* = 1.3 Hz), 14.7 (d, *J* = 2.5 Hz); **^{31}P NMR** δ 47.5; **IR** (neat) 2964, 2936, 2874, 1607, 1589, 1476, 1434, 1292, 1254, 1201, 1176, 1151, 1111, 1028, 779 cm^{-1}; **HRMS** (ESI-TOF) calcd for $C_{23}H_{31}N_3O_3P$ $[M+H]^+$ 428.2103, found 428.2103.

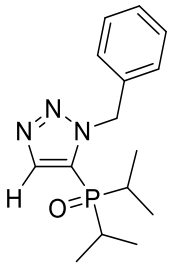

(1-Benzyl-1*H*-1,2,3-triazol-5-yl)diisopropylphosphine oxide (3.5e). Following **General procedure B**, the product was obtained as a white solid (78 mg) in 42% yield. $\mathbf{R_f}$ = 0.37 (100% EtOAc): **^{1}H NMR** (500 MHz, $CDCl_3$) δ 7.67 (s, 1H), 7.47 (d, *J* = 8.0 Hz, 2H), 7.30–7.23 (m, 3H), 6.01 (s, 2H), 2.14–2.08 (m, 2H), 1.05 (dd, *J* = 16.5, 7.0 Hz, 6H), 1.02 (dd, *J* = 17.0, 7.0 Hz, 6H); **^{13}C NMR** (125 MHz, $CDCl_3$) δ 137.7 (d, *J* = 14.3 Hz), 136.0, 128.9,

128.7, 128.5, 125.5 (d, *J* = 85.3 Hz), 53.6, 27.7 (d, *J* = 70.9 Hz), 15.8 (d, *J* = 2.6 Hz), 14.7 (d, *J* = 3.1 Hz); **^{31}P NMR** δ 47.1; **IR** (neat) 2966, 2933, 2874, 1496, 1457, 1388, 1367, 1271, 1182, 1150, 1028 cm^{-1}; **HRMS** (ESI-TOF) calcd for $C_{15}H_{23}N_3OP$ $[M+H]^+$ 292.1579, found 292.1572.

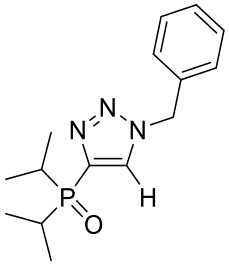

(1-Benzyl-1*H*-1,2,3-triazol-4-yl)diisopropylphosphine oxide (3.6e). Following **General procedure B**, the product was obtained as a white solid (81 mg) in 44% yield. $\mathbf{R_f}$ = 0.11 (100% EtOAc): **^{1}H NMR** (500 MHz, $CDCl_3$) δ 7.98 (s, 1H), 7.34–7.32 (m, 3H), 7.23–7.22 (m, 2H), 5.53 (s, 2H), 2.40–2.30 (m, 2H), 1.15 (dd, *J* = 16.0, 7.5 Hz, 6H), 1.07 (dd, *J* = 16.5, 7.5 Hz, 6H); **^{13}C NMR** (125 MHz, $CDCl_3$) δ 139.7 (d, *J* = 112.0 Hz), 133.9, 131.6 (d, *J* = 18.5 Hz), 129.3, 129.1, 128.3, 54.3, 25.8 (d, *J* = 70.1 Hz), 15.6 (d, *J* = 2.4 Hz), 14.7 (d, *J* = 3.3 Hz); **^{31}P NMR** δ 48.2; **IR** (neat) 2963, 2933, 2874, 1498, 1457, 1367, 1267, 1212, 1176, 1148, 1104, 1048, 1024 cm^{-1}; **HRMS** (ESI-TOF) calcd for $C_{15}H_{23}N_3OP$ $[M+H]^+$ 292.1579, found 292.1572.

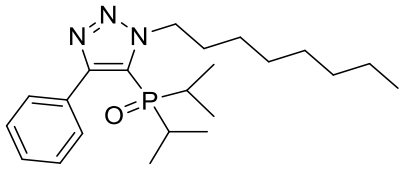

Diisopropyl(1-octyl-4-phenyl-1*H*-1,2,3-triazol-5-yl)phosphine oxide (3.5f). Following **General procedure B**, the product was obtained as a white solid (56 mg) in 30% yield. $\mathbf{R_f}$ = 0.67 (100% EtOAc): **^{1}H NMR** (500 MHz, $CDCl_3$) δ 7.45–7.40 (m, 3H), 7.35 (dd, *J* = 7.5, 1.5 Hz, 2H), 4.86 (t, *J* = 7.5 Hz, 2H), 2.02 (quint, *J* = 7.5 Hz, 2H), 1.89–1.82 (m, 2H), 1.42–

1.24 (m, 10H), 1.18 (dd, *J* = 16.0, 7.0 Hz, 6H), 0.97 (dd, *J* = 17.0, 7.5 Hz, 6H), 0.86 (t, *J* = 7.0 Hz, 3H); **^{13}C NMR** (125 MHz, $CDCl_3$) δ 150.1 (d, *J* = 14.5 Hz), 131.9, 129.7, 129.5, 128.6, 124.2 (d, *J* = 84.3 Hz), 51.6, 31.9, 31.8, 29.3, 29.0 (d, *J* = 70.6 Hz), 26.8, 22.79 (2), 16.8 (d, *J* = 3.8 Hz), 15.4 (d, *J* = 2.9 Hz), 14.2; **^{31}P NMR** δ 49.2; **IR** (neat) 2925, 2855, 1525, 1464, 1405, 1330, 1265, 1188, 1149, 1073, 1016, 919 cm^{-1}; **HRMS** (ESI-TOF) calcd for $C_{22}H_{37}N_3OP$ $[M+H]^+$ 390.2674, found 390.2654.

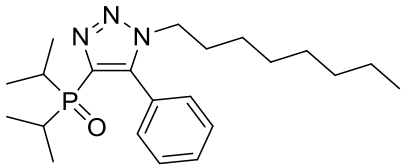

Diisopropyl(1-octyl-5-phenyl-1*H*-1,2,3-triazol-4-yl)phosphine oxide (3.6f). Following **General procedure B**, the product was obtained as a colorless oil (74 mg) in 40% yield. **R_f** = 0.25 (100% EtOAc): **^{1}H NMR** (500 MHz, $CDCl_3$) δ 7.44–7.39 (m, 5H), 4.21 (t, *J* = 7.5 Hz, 2H), 2.42–2.34 (m, 2H), 1.74 (quint, *J* = 7.0 Hz, 2H), 1.22–1.05 (m, 22H), 0.81 (t, *J* = 7.5 Hz, 3H); **^{13}C NMR** (125 MHz, $CDCl_3$) δ 145.2 (d, *J* = 18.2 Hz), 135.8 (d, *J* = 110.9 Hz), 130.3, 129.8, 128.4, 126.3, 48.4, 31.7, 29.9, 29.0, 28.8, 26.34 (d, *J* = 70.4 Hz), 26.31, 22.6, 16.0 (d, *J* = 2.5 Hz), 14.9 (d, *J* = 3.8 Hz), 14.1; **^{31}P NMR** δ 47.2; **IR** (neat) 2959, 2927, 2872, 2856, 1461, 1409, 1385, 1264, 1204, 1180, 1153, 1025, 1006, 883 cm^{-1}; **HRMS** (ESI-TOF) calcd for $C_{22}H_{37}N_3OP$ $[M+H]^+$ 390.2674, found 390.2658.

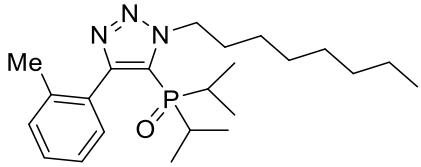

Diisopropyl(1-octyl-4-(*o*-tolyl)-1*H*-1,2,3-triazol-5-yl)phosphine oxide (3.5g). Following **General procedure B**, the product was obtained as a brown oil (61 mg) in 23% yield. **R_f** = 0.64 (100% EtOAc): **^{1}H NMR** (500 MHz, $CDCl_3$) δ 7.31 (td, *J* = 7.5, 1.0 Hz, 1H), 7.26 (d,

J = 7.5 Hz, 1H), 7.18 (t, *J* = 7.5 Hz, 1H), 7.07 (d, *J* = 7.5 Hz, 1H), 4.85 (t, *J* = 7.5 Hz, 2H), 2.14 (s, 3H), 2.00 (quint, *J* = 7.5 Hz, 2H), 1.80–1.73 (m, 2H), 1.39–1.20 (m, 10H), 1.13 (dd, *J* = 16.0, 7.0 Hz, 6H), 0.96 (dd, *J* = 17.0, 7.5 Hz, 6H), 0.83 (t, *J* = 7.0 Hz, 3H); **^{13}C NMR** (125 MHz, $CDCl_3$) δ 149.0 (d, *J* = 14.3 Hz), 138.6, 130.9, 130.7, 129.64, 129.63, 125.5, 124.8 (d, *J* = 84.4 Hz), 51.5, 31.8, 31.7, 29.24, 29.23, 29.1 (d, *J* = 70.0 Hz), 26.7, 22.7, 20.2, 16.7 (d, *J* = 3.8 Hz), 15.4 (d, *J* = 2.9 Hz), 14.2; **^{31}P NMR** δ 48.5; **IR** (neat) 2957, 2925, 2856, 1463, 1382, 1187, 1151, 1037, 1016, 996, 878 cm^{-1}; **HRMS** (ESI-TOF) calcd for $C_{23}H_{39}N_3OP$ $[M+H]^+$ 404.2831, found 404.2829.

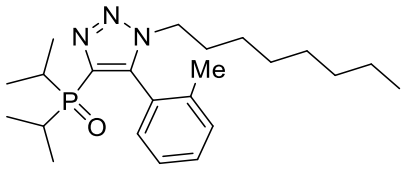

Diisopropyl(1-octyl-5-(*o*-tolyl)-1*H*-1,2,3-triazol-4-yl)phosphine oxide (3.6g). Following **General procedure B**, the product was obtained as a yellow oil (92 mg) in 35% yield. **R_f** = 0.31 (100% EtOAc): **^{1}H NMR** (500 MHz, $CDCl_3$) δ 7.32 (t, *J* = 7.5 Hz, 1H), 7.24 (d, *J* = 7.5 Hz, 1H), 7.20 (t, *J* = 7.5 Hz, 1H), 7.08 (d, *J* = 7.5 Hz, 1H), 4.11–4.05 (m, 1H), 3.93–3.87 (m, 1H), 2.47–2.39 (m, 1H), 2.27–2.19 (m, 1H), 2.07 (s, 3H), 1.72–1.64 (m, 2H), 1.19–1.02 (m, 22H), 0.79 (t, *J* = 7.5 Hz, 3H); **^{13}C NMR** (125 MHz, $CDCl_3$) δ 144.5 (d, *J* = 18.3 Hz), 137.8, 136.0 (d, *J* = 112.0 Hz), 130.5, 130.3, 130.0, 126.0, 125.6, 48.0, 31.6, 29.6, 28.9, 28.7, 26.7 (d, *J* = 81.5 Hz), 26.3, 26.1 (d, *J* = 81.7 Hz), 22.5, 20.0, 15.9 (d, *J* = 3.5 Hz), 15.8 (d, *J* = 2.0 Hz), 15.1 (d, *J* = 2.9 Hz), 14.5 (d, *J* = 2.6 Hz), 14.0; **^{31}P NMR** δ 45.9; **IR** (neat) 2958, 2926, 2872, 2856, 1461, 1410, 1384, 1264, 1183, 1154, 1024, 1003, 883 cm^{-1}; **HRMS** (ESI-TOF) calcd for $C_{23}H_{39}N_3OP$ $[M+H]^+$ 404.2831, found 404.2829.

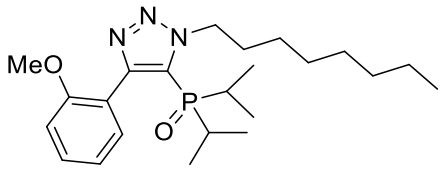

Diisopropyl(4-(2-methoxyphenyl)-1-octyl-1*H*-1,2,3-triazol-5-yl)phosphine oxide (3.5h). Following **General procedure B**, the product was obtained as an off-white solid (58 mg) in 31% yield. $\mathbf{R_f}$ = 0.64 (100% EtOAc): **^{1}H NMR** (500 MHz, $CDCl_3$) δ 7.38 (t, *J* = 7.5 Hz, 1H), 7.14 (dd, *J* = 7.5, 1.5 Hz, 1H), 6.95 (t, *J* = 7.5 Hz, 1H), 6.90 (d, *J* = 8.5 Hz, 1H), 4.81 (t, *J* = 7.5 Hz, 2H), 3.66 (s, 3H), 1.99 (quint, *J* = 7.5 Hz, 2H), 1.76–1.69 (m, 2H), 1.39–1.22 (m, 10H), 1.12 (dd, *J* = 16.0, 7.0 Hz, 6H), 0.95 (dd, *J* = 16.5, 7.0 Hz, 6H), 0.82 (t, *J* = 7.5 Hz, 3H); **^{13}C NMR** (125 MHz, $CDCl_3$) δ 157.9, 146.3 (d, *J* = 15.1 Hz), 131.5, 131.2, 125.3 (d, *J* = 85.5 Hz), 120.42, 120.35, 111.0, 55.2, 51.3, 31.8, 31.67 (2), 29.2, 28.6 (d, *J* = 70.4 Hz), 26.7, 22.7, 16.5 (d, *J* = 3.5 Hz), 15.4 (d, *J* = 2.8 Hz), 14.1; **^{31}P NMR** δ 50.0; **IR** (neat) 2957, 2928, 1473, 1435, 1282, 1242, 1183, 1163, 1147, 1029, 879 cm^{-1}; **HRMS** (ESI-TOF) calcd for $C_{23}H_{39}N_3O_2P$ $[M+H]^+$ 420.2780, found 420.2791.

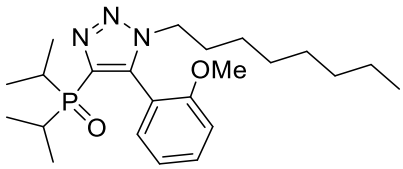

Diisopropyl(5-(2-methoxyphenyl)-1-octyl-1*H*-1,2,3-triazol-4-yl)phosphine oxide (3.6h). Following **General procedure B**, the product was obtained as a yellow solid (83 mg) in 44% yield. $\mathbf{R_f}$ = 0.19 (100% EtOAc): **^{1}H NMR** (500 MHz, $CDCl_3$) δ 7.39 (td, *J* = 8.5, 1.5 Hz, 1H), 7.31 (dd, *J* = 7.5, 1.5 Hz, 1H), 7.00 (t, *J* = 7.5 Hz, 1H), 6.91 (d, *J* = 8.5 Hz, 1H), 4.18–4.13 (m, 1H), 3.99–3.91 (m, 1H), 3.70 (s, 3H), 2.54–2.44 (m, 1H), 2.20–2.12 (m, 1H), 1.76–1.66 (m, 2H), 1.21–1.08 (m, 16H), 0.96 (dd, *J* = 16.5, 7.0 Hz, 3H), 0.90 (dd, *J* = 15.5, 7.0 Hz, 3H), 0.79 (t, *J* = 7.0 Hz, 3H); **^{13}C NMR** (125 MHz, $CDCl_3$) δ 156.8, 142.2

(d, *J* = 18.2 Hz), 135.9 (d, *J* = 112.6 Hz), 133.0, 131.7, 120.5, 115.0, 110.6, 55.3, 48.3, 31.6, 29.5, 28.9, 28.8, 26.8 (d, *J* = 70.6 Hz), 26.3, 25.6 (d, *J* = 70.6 Hz), 22.6, 15.9 (d, *J* = 2.9 Hz), 15.7 (d, *J* = 1.5 Hz), 14.7 (d, *J* = 2.4 Hz), 14.4 (d, *J* = 3.0 Hz), 14.0; **^{31}P NMR** δ 45.8; **IR** (neat) 2958, 2927, 2872, 2856, 1464, 1415, 1293, 1243, 1179, 1152, 1122, 1047, 1023, 1001, 883 cm^{-1}; **HRMS** (ESI-TOF) calcd for $C_{23}H_{39}N_3O_2P$ [M+H]$^+$ 420.2780, found 420.2786.

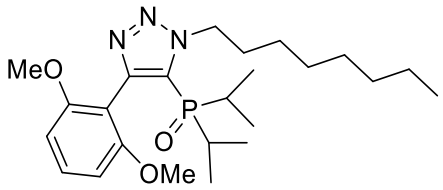

(4-(2,6-Dimethoxyphenyl)-1-octyl-1*H*-1,2,3-triazol-5-yl)diisopropylphosphine oxide (3.5i). Following **General procedure B**, the product was obtained as a light yellow solid (25 mg) in 18% yield. **R$_f$** = 0.69 (100% EtOAc): **^{1}H NMR** (500 MHz, $CDCl_3$) δ 7.33 (t, *J* = 8.5 Hz, 1H), 6.55 (d, *J* = 8.5 Hz, 2H), 4.83 (t, *J* = 7.5 Hz, 2H), 3.64 (s, 6H), 2.00 (quint, *J* = 7.5 Hz, 2H), 1.74–1.68 (m, 2H), 1.40–1.23 (m, 10H), 1.13 (dd, *J* = 16.0, 7.0 Hz, 6H), 0.97 (dd, *J* = 16.5, 7.0 Hz, 6H), 0.84 (t, *J* = 7.0 Hz, 3H); **^{13}C NMR** (125 MHz, $CDCl_3$) δ 159.3, 142.8 (d, *J* = 14.2 Hz), 131.5, 126.5 (d, *J* = 87.1 Hz), 108.8, 103.7, 55.4, 51.3, 31.8, 31.7, 29.3, 29.2, 28.8 (d, *J* = 70.5 Hz), 26.7, 22.7, 16.6 (d, *J* = 3.8 Hz), 15.5 (d, *J* = 2.6 Hz), 14.1; **^{31}P NMR** δ 50.3; **IR** (neat) 2923, 1605, 1588, 1472, 1433, 1253, 1185, 1146, 1107, 992, 880 cm^{-1}; **HRMS** (ESI-TOF) calcd for $C_{24}H_{41}N_3O_3P$ [M+H]$^+$ 450.2886, found 450.2886.

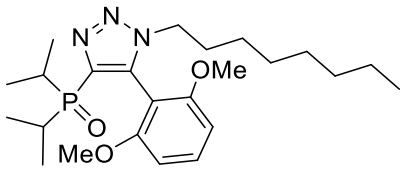

(5-(2,6-dimethoxyphenyl)-1-octyl-1*H*-1,2,3-triazol-4-yl)diisopropylphosphine oxide

(3.6i). Following **General procedure B**, the product was obtained as an off-white solid (69 mg) in 50% yield. $\mathbf{R_f}$ = 0.08 (100% EtOAc): **^{1}H NMR** (500 MHz, $CDCl_3$) δ 7.35 (t, *J* = 8.5 Hz, 1H), 6.57 (d, *J* = 8.5 Hz, 2H), 4.03 (t, *J* = 7.0 Hz, 2H), 3.68 (s, 6H), 2.32–2.28 (m, 2H), 1.73 (quint, *J* = 7.0 Hz, 2H), 1.24–1.16 (m, 10H), 1.11 (dd, *J* = 16.0, 7.0 Hz, 6H), 1.10 (dd, *J* = 15.5, 7.0 Hz, 6H), 0.83 (t, *J* = 7.5 Hz, 3H); **^{13}C NMR** (125 MHz, $CDCl_3$) δ 158.8, 139.0 (d, *J* = 18.9 Hz), 136.5 (d, *J* = 113.2 Hz), 132.0, 104.1, 103.7, 55.6, 48.2, 31.8, 29.5, 29.1, 29.0, 26.7 (d, *J* = 71.7 Hz), 26.4, 22.7, 15.8 (d, *J* = 2.5 Hz), 14.6 (d, *J* = 2.5 Hz), 14.1; **^{31}P NMR** δ 47.3; **IR** (neat) 2958, 2925, 1607, 1590, 1475, 1463, 1434, 1254, 1173, 1146, 1108, 1025, 883 cm^{-1}; **HRMS** (ESI-TOF) calcd for $C_{24}H_{41}N_3O_3P$ $[M+H]^+$ 450.2886, found 450.2893.

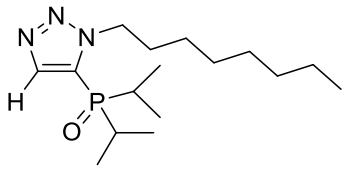

Diisopropyl(1-octyl-1*H*-1,2,3-triazol-5-yl)phosphine oxide (3.5j). Following **General procedure B**, the product was obtained as a white solid (68 mg) in 34% yield. $\mathbf{R_f}$ = 0.37 (100% EtOAc): **^{1}H NMR** (500 MHz, $CDCl_3$) δ 7.63 (s, 1H), 4.75 (t, *J* = 7.5 Hz, 2H), 2.23–2.16 (m, 2H), 1.96 (quint, *J* = 7.5 Hz, 2H), 1.34–1.20 (m, 10H), 1.19 (dd, *J* = 16.5, 7.5 Hz, 6H), 1.07 (dd, *J* = 17.0, 7.5 Hz, 6H), 0.83 (t, *J* = 7.0 Hz, 3H); **^{13}C NMR** (125 MHz, $CDCl_3$) δ 137.3 (d, *J* = 14.2 Hz), 125.3 (d, *J* = 86.1 Hz), 50.8, 31.8, 31.3, 29.2, 29.1, 27.5 (d, *J* = 71.5 Hz), 26.6, 22.7, 15.7 (d, *J* = 2.5 Hz), 14.7 (d, *J* = 3.3 Hz), 14.1; **^{31}P NMR** δ 48.1; **IR** (neat) 3093, 2959, 2923, 2872, 2855, 1487, 1459, 1369, 1278, 1255, 1179, 1154, 1129, 1031, 976 cm^{-1}; **HRMS** (ESI-TOF) calcd for $C_{16}H_{33}N_3OP$ $[M+H]^+$ 314.2361, found 314.2369.

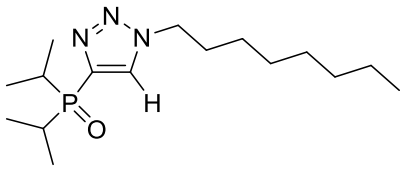

Diisopropyl(1-octyl-1*H*-1,2,3-triazol-4-yl)phosphine oxide (3.6j). Following **General procedure B**, the product was obtained as a white solid (109 mg) in 55% yield. $\mathbf{R_f}$ = 0.12 (100% EtOAc): **^{1}H NMR** (500 MHz, $CDCl_3$) δ 8.09 (s, 1H), 4.35 (t, *J* = 7.5 Hz, 2H), 2.36–2.31 (m, 2H), 1.86 (quint, *J* = 7.0 Hz, 2H), 1.23–1.12 (m, 16H), 1.05 (dd, *J* = 16.5, 7.0 Hz, 6H), 0.78 (t, *J* = 7.0 Hz, 3H); **^{13}C NMR** (125 MHz, $CDCl_3$) δ 138.8 (d, *J* = 113.2 Hz), 131.6 (d, *J* = 17.6 Hz), 50.5, 31.6, 30.1, 29.0, 28.8, 26.3, 25.7 (d, *J* = 70.2 Hz), 22.6, 15.5 (d, *J* = 1.9 Hz), 14.6 (d, *J* = 2.9 Hz), 14.0; **^{31}P NMR** δ 48.3; **IR** (neat) 3102, 2959, 2927, 2872, 2857, 1498, 1464, 1213, 1176, 1148, 1124, 1098, 1045, 1025, 998, 883 cm^{-1}; **HRMS** (ESI-TOF) calcd for $C_{16}H_{33}N_3OP$ $[M+H]^+$ 314.2361, found 314.2365.

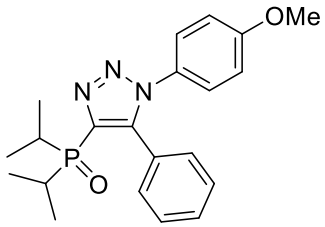

Diisopropyl(1-(4-methoxyphenyl)-5-phenyl-1*H*-1,2,3-triazol-4-yl)phosphine oxide (3.6k). Following **General procedure C**, the product was obtained as a dark brown solid (128 mg) in 74% yield. $\mathbf{R_f}$ = 0.22 (100% EtOAc): **^{1}H NMR** (500 MHz, $CDCl_3$) δ 7.42 (dd, *J* = 7.5, 1.0 Hz, 2H) 7.38–7.30 (m, 3H), 7.21 (d, *J* = 9.0 Hz, 2H), 6.87 (d, *J* = 9.0 Hz, 2H), 3.82 (s, 3H), 2.54–2.46 (m, 2H), 1.19 (dd, *J* = 16.5, 7.0 Hz, 6H), 1.13 (dd, *J* = 15.5, 7.0 Hz, 6H); **^{13}C NMR** (125 MHz, $CDCl_3$) δ 160.2, 145.2 (d, *J* = 18.1 Hz), 136.4 (d, *J* = 108.9 Hz), 131.0, 129.8, 129.3, 128.3, 126.8, 126.1, 114.6, 55.7, 26.6 (d, *J* = 70.6 Hz), 16.2 (d, *J* = 2.5 Hz), 15.1 (d, *J* = 2.8 Hz); **^{31}P NMR** δ 48.0; **IR** (neat) 2966, 1513, 1464, 1303 1251,

1181, 1155, 1110, 1028 cm^{-1}; **HRMS** (EI-TOF) calcd for $C_{21}H_{26}N_3O_2P$ $[M]^+$ 383.1763, found 383.1748.

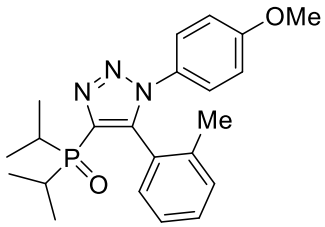

Diisopropyl(1-(4-methoxyphenyl)-5-(*o*-tolyl)-1*H*-1,2,3-triazol-4-yl)phosphine oxide (3.6l). Following **General procedure C**, the product was obtained as a dark brown oil (147 mg) in 84% yield. $\mathbf{R_f}$ = 0.20 (100% EtOAc): **^{1}H NMR** (500 MHz, $CDCl_3$) δ 7.28 (t, *J* = 7.5 Hz, 2H) 7.22–7.16 (m, 3H), 7.11 (d, *J* = 7.5 Hz, 1H), 6.80 (d, *J* = 9.0 Hz, 2H), 3.76 (s, 3H), 2.47–2.38 (m, 2H), 1.92 (s, 3H), 1.25–1.09 (m, 12H); **^{13}C NMR** (125 MHz, $CDCl_3$) δ 159.9, 144.6 (d, *J* = 18.0 Hz), 137.5, 136.9 (d, *J* = 110.0 Hz), 131.5, 130.2, 130.1, 129.3, 126.0, 125.6, 125.5, 114.4, 55.5, 26.62 (d, *J* = 70.6 Hz), 26.56 (d, *J* = 70.3 Hz), 20.1, 16.10 (d, *J* = 2.0 Hz), 16.06 (d, *J* = 2.6 Hz), 15.2 (d, *J* = 2.9 Hz), 14.7 (d, *J* = 2.8 Hz); **^{31}P NMR** δ 47.5; **IR** (neat) 2965, 1608, 1514, 1463, 1303, 1252, 1181, 1029, 883 cm^{-1}; **HRMS** (ESI-TOF) calcd for $C_{22}H_{29}N_3O_2P$ $[M+H]^+$ 398.1997, found 398.2016.

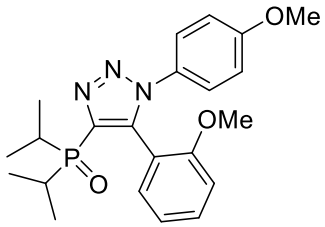

Diisopropyl(5-(2-methoxyphenyl)-1-(4-methoxyphenyl)-1*H*-1,2,3-triazol-4-yl)phosphine oxide (3.6m). Following **General procedure C**, the product was obtained as a dark brown oil (100 mg) in 60% yield. $\mathbf{R_f}$ = 0.11 (100% EtOAc): **^{1}H NMR** (500 MHz, $CDCl_3$) δ 7.47 (d, *J* = 7.5 Hz, 1H) 7.31 (t, *J* = 7.5 Hz, 1H), 7.17 (d, *J* = 8.5 Hz, 2H), 6.97 (t, *J* = 7.5 Hz, 1H), 6.78 (d, *J* = 8.5 Hz, 2H), 6.70 (d, *J* = 8.0 Hz, 1H), 3.73 (s, 3H), 3.37 (s,

3H), 2.62–2.56 (m, 1H), 2.26–2.21 (m, 1H), 1.30–1.22 (m, 6H), 1.03 (dd, *J* = 16.0, 7.0 Hz, 3H), 0.94 (dd, *J* = 15.0, 6.5 Hz, 3H); **^{13}C NMR** (125 MHz, $CDCl_3$) δ 159.7, 156.6, 142.4 (d, *J* = 17.7 Hz), 136.4 (d, *J* = 110.5 Hz), 132.9, 131.6, 129.9, 125.4, 120.4, 115.2, 113.9, 110.7, 55.5, 55.0, 27.0 (d, *J* = 69.3 Hz), 25.6 (d, *J* = 71.2 Hz), 16.0 ,15.8, 14.7, 14.5; **^{31}P NMR** δ 47.7; **IR** (neat) 2964, 1608, 1513, 1463, 1301, 1281, 1247, 1177, 1152, 1118, 1048, 1024, 993, 882 cm^{-1}; **HRMS** (ESI-TOF) calcd for $C_{22}H_{29}N_3O_3P$ $[M+H]^+$ 414.1947, found 414.1935.

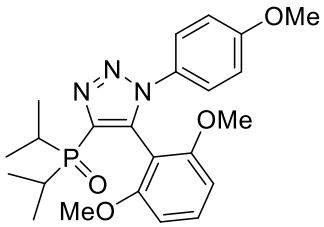

(5-(2,6-Dimethoxyphenyl)-1-(4-methoxyphenyl)-1*H*-1,2,3-triazol-4-yl)diisopropylphosphine oxide (3.6n). Following **General procedure C**, the product was obtained as a dark brown solid (106 mg) in 70% yield. **R_f** = 0.09 (100% EtOAc): **^{1}H NMR** (500 MHz, $CDCl_3$) δ 7.31–7.27 (m, 3H), 6.82 (d, *J* = 8.5 Hz, 2H), 6.48 (d, *J* = 8.0 Hz, 2H), 3.77 (s, 3H), 3.63 (s, 6H), 2.41–2.34 (m, 2H), 1.26–1.15 (m, 12H); **^{13}C NMR** (125 MHz, $CDCl_3$) δ 159.9, 158.7, 139.5 (d, *J* = 17.9 Hz), 137.2 (d, *J* = 113.0 Hz), 131.9, 129.7, 125.7, 113.9, 104.6, 103.7, 55.6, 55.5, 26.8 (d, *J* = 70.7 Hz), 15.8 (d, *J* = 2.5 Hz), 14.7 (d, *J* = 2.8 Hz); **^{31}P NMR** δ 46.5; **IR** (neat) 2959, 1609, 1588, 1516, 1474, 1306, 1253, 1201, 1182, 1146, 1107, 1019, 991, 833 cm^{-1}; **HRMS** (ESI-TOF) calcd for $C_{23}H_{31}N_3O_4P$ $[M+H]^+$ 444.2052, found 444.2057.

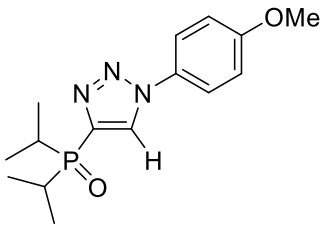

Diisopropyl(1-(4-methoxyphenyl)-1*H*-1,2,3-triazol-4-yl)phosphine oxide (3.6o). Following **General procedure C**, the product was obtained as a dark brown solid (125 mg) in 58% yield. $\mathbf{R_f}$ = 0.07 (100% EtOAc): **^{1}H NMR** (500 MHz, $CDCl_3$) δ 8.47 (s, 1H), 7.66 (d, *J* = 9.0 Hz, 2H), 7.03 (d, *J* = 9.0 Hz, 2H), 3.86 (s, 3H), 2.49–2.42 (m, 2H), 1.25 (dd, *J* = 16.0, 7.0 Hz, 6H), 1.17 (dd, *J* = 16.5, 7.0 Hz, 6H); **^{13}C NMR** (125 MHz, $CDCl_3$) δ 160.2, 140.1 (d, *J* = 110.7 Hz), 130.0, 129.8 (d, *J* = 18.9 Hz), 122.2, 115.1, 55.8, 26.0 (d, *J* = 70.4 Hz), 15.8 (d, *J* = 2.5 Hz), 14.8 (d, *J* = 3.8 Hz); **^{31}P NMR** δ 46.5; **IR** (neat) 3052, 2964, 1519, 1469, 1253, 1228, 1203, 1181, 1149, 1042, 1026, 982, 884 cm^{-1}; **HRMS** (ESI-TOF) calcd for $C_{15}H_{23}N_3O_2P$ $[M+H]^+$ 308.1528, found 308.1533.

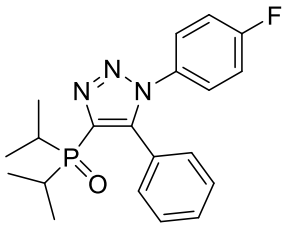

(1-(4-Fluorophenyl)-5-phenyl-1*H*-1,2,3-triazol-4-yl)diisopropylphosphine oxide (3.6p). Following **General procedure C**, the product was obtained as an off-white solid (108 mg) in 67% yield. $\mathbf{R_f}$ = 0.20 (100% EtOAc): **^{1}H NMR** (500 MHz, $CDCl_3$) δ 7.38 (d, *J* = 8.5 Hz, 2H) 7.35–7.30 (m, 3H), 7.28–7.25 (m, 2H), 7.05 (t, *J* = 8.5 Hz, 2H), 2.52–2.44 (m, 2H), 1.17 (dd, *J* = 16.0, 7.0 Hz, 6H), 1.11 (dd, *J* = 15.5, 7.0 Hz, 6H); **^{13}C NMR** (125 MHz, $CDCl_3$) δ 162.7 (d, *J* = 250.5 Hz), 145.2 (d, *J* = 17.9 Hz), 136.6 (d, *J* = 108.9 Hz), 132.3, 130.9, 129.9, 128.3, 127.2 (d, *J* = 8.9 Hz), 125.6, 116.4 (d, *J* = 23.3 Hz), 26.5 (d, *J* = 70.3 Hz), 16.1 (d, *J* = 2.5 Hz), 14.9 (d, *J* = 3.1 Hz); **^{31}P NMR** δ 48.1; **IR** (neat) 3050, 2955, 1510, 1469, 1219, 1202, 1177, 1166, 1157, 1140, 1105, 881 cm^{-1}; **HRMS** (ESI-TOF) calcd for $C_{20}H_{24}FN_3OP$ $[M+H]^+$ 372.1641, found 372.1638.

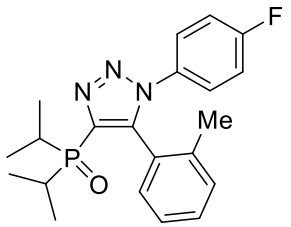

(1-(4-Fluorophenyl)-5-(*o*-tolyl)-1*H*-1,2,3-triazol-4-yl)diisopropylphosphine oxide (3.6q). Following **General procedure C**, the product was obtained as a brown solid (115 mg) in 70% yield. $\mathbf{R_f}$ = 0.19 (100% EtOAc): **^{1}H NMR** (500 MHz, $CDCl_3$) δ 7.30–7.24 (m, 4H), 7.21 (t, *J* = 7.0 Hz, 1H), 7.12 (d, *J* = 7.5 Hz, 1H), 7.00 (t, *J* = 8.0 Hz, 2H), 2.45–2.40 (m, 2H), 1.92 (s, 3H), 1.25–1.08 (m, 12H); **^{13}C NMR** (125 MHz, $CDCl_3$) δ 162.6 (d, *J* = 249.9 Hz), 144.8 (d, *J* = 18.2 Hz), 137.4, 137.3 (d, *J* = 108.3 Hz), 132.4, 131.4, 130.4 (d, *J* = 8.2 Hz), 126.04, 125.97, 125.8, 125.7, 116.4 (d, *J* = 23.3 Hz), 26.64 (d, *J* = 70.2 Hz), 26.57 (d, *J* =70.7 Hz), 20.0, 16.1 (d, *J* = 2.9 Hz), 16.0 (d, *J* = 3.6 Hz), 15.1 (d, *J* = 2.8 Hz), 14.7 (d, *J* = 2.8 Hz); **^{31}P NMR** δ 47.0; **IR** (neat) 3048, 2953, 1510, 1475, 1221, 1199, 1180, 1159, 1141, 1114, 1025, 875 cm^{-1}; **HRMS** (ESI-TOF) calcd for $C_{21}H_{26}FN_3OP$ $[M+H]^+$ 386.1798, found 386.1802.

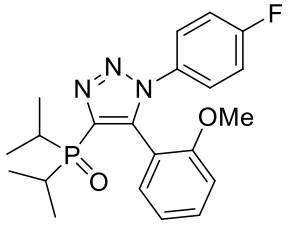

(1-(4-Fluorophenyl)-5-(2-methoxyphenyl)-1*H*-1,2,3-triazol-4-yl)diisopropylphosphine oxide (3.6r). Following **General procedure C**, the product was obtained as a brown solid (64 mg) in 39% yield. $\mathbf{R_f}$ = 0.15 (100% EtOAc): **^{1}H NMR** (500 MHz, $CDCl_3$) δ 7.53 (dd, *J* = 7.5, 1.0 Hz, 1H), 7.35 (t, *J* = 7.5 Hz, 1H), 7.28–7.25 (m, 2H), 7.02–6.99 (m, 3H), 6.71 (d, *J* = 8.0 Hz, 1H), 3.37 (s, 3H), 2.64–2.59 (m, 1H), 2.27–2.21 (m, 1H), 1.31–1.22 (m, 6H), 1.03 (dd, *J* = 16.5, 6.5 Hz, 3H), 0.94 (dd, *J* = 15.0, 6.5 Hz,

3H); **^{13}C NMR** (125 MHz, $CDCl_3$) δ 162.5 (d, *J* = 249.0 Hz), 156.5, 142.5 (d, *J* = 17.6 Hz), 136.9 (d, *J* = 110.7 Hz), 133.1, 132.0, 126.0, 125.9, 120.7, 115.9 (d, *J* = 22.6 Hz), 114.9, 110.7, 55.0, 27.1 (d, *J* = 70.4 Hz), 25.6 (d, *J* =70.4 Hz), 16.1 (d, *J* = 1.8 Hz), 15.9 (d, *J* = 3.5 Hz), 14.8 (d, *J* = 1.8 Hz), 14.6 (d, *J* = 2.9 Hz); **^{31}P NMR** δ 46.1; **IR** (neat) 2958, 2928, 1505, 1475, 1241, 1223, 1196, 1178, 1151, 1122, 1098, 1027, 996, 844 cm^{-1}; **HRMS** (ESI-TOF) calcd for $C_{21}H_{26}FN_3O_2P$ $[M+H]^+$ 402.1747, found 402.1725.

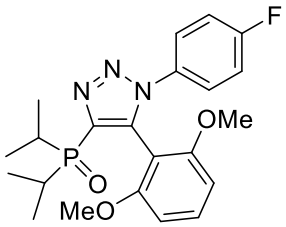

(5-(2,6-Dimethoxyphenyl)-1-(4-fluorophenyl)-1*H*-1,2,3-triazol-4-yl)diisopropylphosphine oxide (3.6s). Following **General procedure C**, the product was obtained as a brown solid (104 mg) in 68% yield. **R_f** = 0.05 (100% EtOAc): **^{1}H NMR** (500 MHz, $CDCl_3$) δ 7.34–7.31 (m, 2H), 7.26 (t, *J* = 8.5 Hz, 1H), 6.99 (t, *J* = 8.5 Hz, 2H), 6.46 (d, *J* = 8.5 Hz, 2H), 3.60 (s, 6H), 2.37–2.32 (m, 2H), 1.23–1.12 (m, 12H); **^{13}C NMR** (125 MHz, $CDCl_3$) δ 162.6 (d, *J* = 249.1 Hz), 158.6, 139.6 (d, *J* = 17.7 Hz), 137.5 (d, *J* = 112.2 Hz), 132.7 (d, *J* = 2.9 Hz), 132.1, 115.8 (d, *J* = 23.2 Hz), 104.1, 103.7, 55.6, 26.8 (d, *J* = 70.3 Hz), 15.8 (d, *J* = 2.5 Hz), 14.7 (d, *J* = 2.6 Hz); **^{31}P NMR** δ 46.6; **IR** (neat) 2926, 1590, 1509, 1476, 1435, 1256, 1227, 1199, 1181, 1143, 1106, 1081, 1026, 853 cm^{-1}; **HRMS** (ESI-TOF) calcd for $C_{22}H_{28}FN_3O_3P$ $[M+H]^+$ 432.1852, found 432.1855.

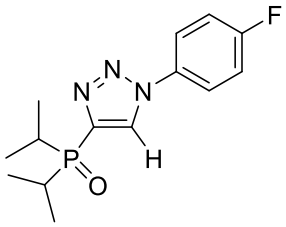

(1-(4-Fluorophenyl)-1*H*-1,2,3-triazol-4-yl)diisopropylphosphine oxide (3.6t).

Following **General procedure C**, the product was obtained as a brown solid (65 mg) in 35% yield. $\mathbf{R_f}$ = 0.08 (100% EtOAc): **^{1}H NMR** (500 MHz, $CDCl_3$) δ 8.59 (s, 1H), 7.78–7.76 (m, 2H), 7.22 (t, *J* = 8.5 Hz, 2H), 2.46–2.42 (m, 2H), 1.24 (dd, *J* = 16.0, 7.0 Hz, 6H), 1.15 (dd, *J* = 16.5, 7.0 Hz, 6H); **^{13}C NMR** (125 MHz, $CDCl_3$) δ 162.7 (d, *J* = 249.7 Hz), 140.6 (d, *J* = 109.6 Hz), 132.9 (d, *J* = 2.4 Hz), 130.0 (d, *J* = 18.7 Hz), 122.6 (d, *J* = 8.4 Hz), 117.0 (d, *J* = 23.4 Hz), 25.9 (d, *J* = 70.2 Hz), 15.7 (d, *J* = 2.5 Hz), 14.8 (d, *J* = 2.9 Hz); **^{31}P NMR** δ 48.3; **IR** (neat) 3071, 2965, 1519, 1466, 1229, 1202, 1179, 1150, 1041, 1032, 1022, 981, 883 cm^{-1}; **HRMS** (ESI-TOF) calcd for $C_{14}H_{20}FN_3OP$ $[M+H]^+$ 296.1328, found 296.1325.

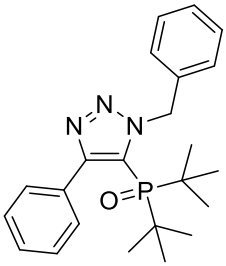

(1-Benzyl-4-phenyl-1*H*-1,2,3-triazol-5-yl)di-*tert*-butylphosphine oxide (3.5a-*t*Bu). Following **General procedure B**, the product was obtained as a light yellow powder (0.11 g) in 59% yield. $\mathbf{R_f}$ = 0.65 (100% EtOAc): **^{1}H NMR** (500 MHz, $CDCl_3$) δ 7.46 (d, *J* = 7.0 Hz, 2H), 7.41–7.36 (m, 5H), 7.28 (t, *J* = 7.5 Hz, 2H), 7.23 (t, *J* = 7.0 Hz, 1H), 6.28 (s, 2H), 1.03 (d, *J* = 15.5 Hz, 18H); **^{13}C NMR** (125 MHz, $CDCl_3$) δ 150.0 (d, *J* = 12.4 Hz), 137.0, 132.9, 131.5, 129.4, 128.7, 128.4, 128.0, 127.9, 124.2 (d, *J* = 69.9 Hz), 54.9, 37.5 (d, *J* = 62.3 Hz), 26.5; **^{31}P NMR** δ 59.5; **IR** (neat) 2951, 2870, 1475, 1457, 1428, 1199, 1165, 1149, 992, 811 cm^{-1}; **HRMS** (ESI-TOF) calcd for $C_{23}H_{31}N_3OP$ $[M+H]^+$ 396.2205, found 396.2229.

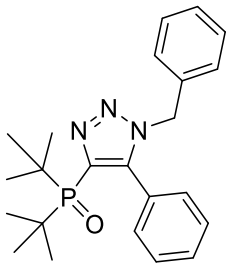

(1-Benzyl-5-phenyl-1*H*-1,2,3-triazol-4-yl)di-*tert*-butylphosphine oxide (3.6a-*t*Bu). Following **General procedure B**, the product was obtained as a yellow solid (63 mg) in 35% yield. $\mathbf{R_f}$ = 0.35 (100% EtOAc): **^{1}H NMR** (500 MHz, $CDCl_3$) δ 7.32 (t, *J* = 7.0 Hz, 1H), 7.26 (t, *J* = 7.5 Hz, 2H), 7.18–7.17 (m, 3H), 7.11 (d, *J* = 7.0 Hz, 2H), 6.91–6.90 (m, 2H), 5.30 (s, 2H), 1.20 (d, *J* = 14.5 Hz, 18H); **^{13}C NMR** (125 MHz, $CDCl_3$) δ 145.6 (d, *J* = 16.6 Hz), 137.0 (d, *J* = 103.2 Hz), 135.0, 130.1, 129.5, 128.6, 128.1, 127.8, 127.3, 126.2, 51.6, 36.1 (d, *J* = 63.5 Hz), 26.3; **^{31}P NMR** δ 48.4; **IR** (neat) 2950, 1474, 1455, 1398, 1390, 1368, 1198, 1153, 814 cm^{-1}; **HRMS** (ESI-TOF) calcd for $C_{23}H_{31}N_3OP$ $[M+H]^+$ 396.2205, found 396.2209.

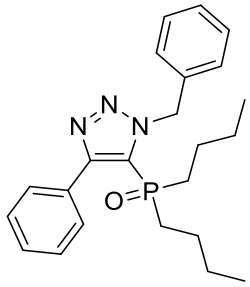

(1-Benzyl-4-phenyl-1*H*-1,2,3-triazol-5-yl)dibutylphosphine oxide (3.5a-*n*Bu). Following **General procedure B**, the product was obtained as an off-white solid (33 mg) in 22% yield. $\mathbf{R_f}$ = 0.70 (100% EtOAc): **^{1}H NMR** (500 MHz, $CDCl_3$) δ 7.46–7.40 (m, 5H), 7.35–7.30 (m, 5H), 6.11 (s, 2H), 1.60–1.52 (m, 2H), 1.40–1.28 (m, 4H), 1.14–1.03 (m, 6H), 0.69 (t, *J* = 7.0 Hz, 6H); **^{13}C NMR** (125 MHz, $CDCl_3$) δ 151.2 (d, *J* = 16.3 Hz), 136.2, 131.3, 129.62, 129.56, 128.71, 128.69, 128.67, 128.4, 124.9 (d, *J* = 90.5 Hz), 54.1, 30.9 (d, *J* =

72.9 Hz), 23.8 (d, *J* = 15.1 Hz), 23.1 (d, *J* = 5.0 Hz), 13.5; **^{31}P NMR** δ 35.8; **IR** (neat) 2957, 2928, 1466, 1455, 1448, 1403, 1178, 1160, 1132, 1073, 905 cm^{-1}; **HRMS** (ESI-TOF) calcd for $C_{23}H_{31}N_3OP$ $[M+H]^+$ 396.2205, found 396.2175.

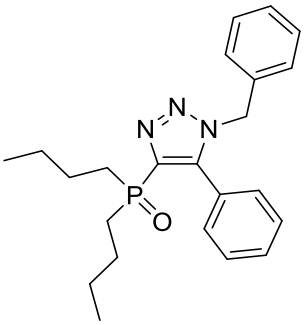

(1-Benzyl-5-phenyl-1*H*-1,2,3-triazol-4-yl)dibutylphosphine oxide (3.6a-*n*Bu). Following **General procedure B**, the product was obtained as a white solid (74 mg) in 49% yield. **R_f** = 0.33 (100% EtOAc): **^{1}H NMR** (500 MHz, $CDCl_3$) δ 7.47–7.39 (m, 3H), 7.32–7.30 (m, 2H), 7.26–7.23 (m, 3H), 7.00–6.98 (m, 2H), 5.43 (s, 2H), 2.05–1.96 (m, 2H), 1.92–1.84 (m, 2H), 1.50–1.42 (m, 4H), 1.34–1.27 (m, 4H), 0.82 (t, *J* = 7.5 Hz, 6H); **^{13}C NMR** (125 MHz, $CDCl_3$) δ 143.5 (d, *J* = 21.4 Hz), 139.1 (d, *J* = 119.5 Hz), 134.8, 130.3, 130.2, 128.9, 128.8, 128.4, 127.6, 125.7, 52.0, 29.0 (d, *J* = 72.9 Hz), 24.1 (d, *J* = 16.3 Hz), 23.6 (d, *J* = 3.8 Hz), 13.6; **^{31}P NMR** δ 35.4; **IR** (neat) 2956, 2931, 2870, 1454, 1407, 1279, 1221, 1207, 1166, 1118, 1092, 1075, 1049, 1008, 902 cm^{-1}; **HRMS** (ESI-TOF) calcd for $C_{23}H_{31}N_3OP$ $[M+H]^+$ 396.2205, found 396.2212.

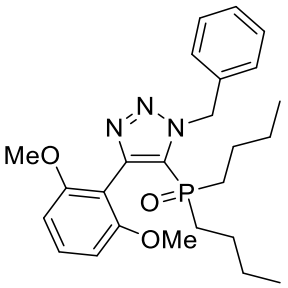

(1-Benzyl-4-(2,6-dimethoxyphenyl)-1*H*-1,2,3-triazol-5-yl)dibutylphosphine oxide

(3.5d-*n*Bu). Following **General procedure B**, the product was obtained as a white solid (47 mg) in 28% yield. $\mathbf{R_f}$ = 0.57 (100% EtOAc): **^{1}H NMR** (500 MHz, $CDCl_3$) δ 7.47 (d, *J* = 7.0 Hz, 2H), 7.37 (t, *J* = 8.5 Hz, 1H), 7.35–7.27 (m, 3H), 6.60 (d, *J* =8.5 Hz, 2H), 6.10 (s, 2H), 3.67 (s, 6H), 1.53–1.45 (m, 2H), 1.39–1.31 (m, 2H), 1.24–1.08 (m, 8H), 0.72 (t, *J* = 7.5 Hz, 6H); **^{13}C NMR** (125 MHz, $CDCl_3$) δ 159.2, 143.9 (d, *J* = 14.6 Hz), 136.5, 131.7, 128.7, 128.6, 128.2, 127.0 (d, *J* = 94.2 Hz), 108.6, 103.9, 55.7, 53.9, 30.1 (d, *J* = 73.0 Hz), 24.2 (d, *J* = 16.3 Hz), 23.0 (d, *J* = 4.6 Hz), 13.7; **^{31}P NMR** δ 37.0; **IR** (neat) 2960, 2931, 1605, 1589, 1474, 1433, 1289, 1253, 1218, 1175, 1159, 1113, 1035, 996 cm^{-1}; **HRMS** (ESI-TOF) calcd for $C_{25}H_{35}N_3O_3P$ $[M+H]^+$ 456.2416, found 456.2410.

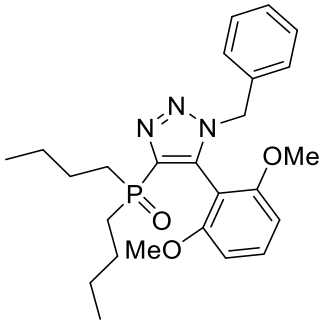

(1-Benzyl-5-(2,6-dimethoxyphenyl)-1*H*-1,2,3-triazol-4-yl)dibutylphosphine oxide (3.6d-*n*Bu). Following **General procedure B**, the product was obtained as a light yellow solid (99 mg) in 59% yield. $\mathbf{R_f}$ = 0.12 (100% EtOAc): **^{1}H NMR** (500 MHz, $CDCl_3$) δ 7.32 (t, *J* = 8.5 Hz, 1H), 7.17–7.12 (m, 3H), 6.92–6.90 (m, 2H), 6.47 (d, *J* = 8.5 Hz, 2H), 5.22 (s, 2H), 3.49 (s, 6H), 1.89–1.84 (m, 4H), 1.53–1.39 (m, 4H), 1.26 (sext, *J* = 7.5 Hz, 4H), 0.81 (t, *J* = 7.5 Hz, 6H); **^{13}C NMR** (125 MHz, $CDCl_3$) δ 158.3, 139.7 (d, *J* = 123.2 Hz), 136.6 (d, *J* = 21.4 Hz), 134.6, 132.4, 128.2, 127.9, 127.8, 103.6, 103.3, 55.4, 52.1, 29.2 (d, *J* = 71.7 Hz), 24.1 (d, *J* = 15.1 Hz), 23.3 (d, *J* = 2.5 Hz), 13.6; **^{31}P NMR** δ 35.7; **IR** (neat) 2956, 2932, 2871, 1605, 1587, 1475, 1456, 1434, 1413, 1292, 1254, 1220, 1205, 1169, 1109, 1030, 1002 cm^{-1}; **HRMS** (ESI-TOF) calcd for $C_{25}H_{35}N_3O_3P$ $[M+H]^+$ 456.2416, found

456.2391.

General procedure D: reduction of triazole phosphine oxide. To the stirring solution of the triazole phosphine oxide (0.20 mmol,) in toluene (0.20 M), was added trichlorosilane (4.00 mmol) under argon. After stirring for 20 h at 80 °C, the reaction mixture was diluted with CH_2Cl_2 (10 mL) and cooled in an ice bath. Aqueous NaOH (20%) was added dropwise at 0°C with continuous stirring until gas evolution ceased. The resulting organic and aqueous phases were separated. The organic layer was dried by Na_2SO_4, filtered, and removal of solvent was followed by chromatography.

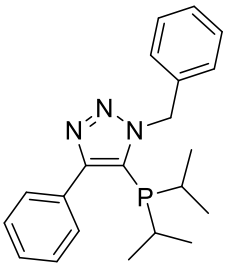

1-Benzyl-5-(diisopropylphosphaneyl)-4-phenyl-1*H*-1,2,3-triazole (3.7a). Following **General procedure D**, the product was obtained as a white solid (67 mg) in 95% yield. $\mathbf{R_f}$ = 0.68 (EtOAc:Hexane=1:2): **^{1}H NMR** (500 MHz, $CDCl_3$) δ 7.50 (dd, *J* = 7.5, 2.0 Hz, 2H), 7.42–7.40 (m, 3H), 7.37 (d, *J* = 8.0 Hz, 2H), 7.34–7.29 (m, 3H), 5.84 (s, 2H), 2.08–2.01 (m, 2H), 1.04 (dd, *J* = 14.0, 7.0 Hz, 6H), 0.54 (dd, *J* = 14.0, 7.0 Hz, 6H); **^{13}C NMR** (125 MHz, $CDCl_3$) δ 152.5 (d, *J* = 4.5 Hz), 136.2, 132.9, 130.5 (d, *J* = 29.6 Hz), 129.5, 128.8, 128.7, 128.45, 128.42, 128.3, 53.1 (d, *J* = 12.7 Hz), 25.0 (d, *J* = 8.0 Hz), 21.7 (d, *J* = 26.3 Hz), 20.9 (d, *J* = 10.4 Hz); **^{31}P NMR** δ –17.8; **IR** (neat) 2953, 2924, 2865, 1464, 1384, 1260, 1223, 1153, 1132, 1073, 1028 cm^{-1}; **HRMS** (ESI-TOF) calcd for $C_{21}H_{27}N_3P$ $[M+H]^+$ 352.1943, found 352.1940.

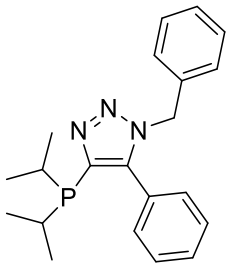

1-Benzyl-4-(diisopropylphosphaneyl)-5-phenyl-1*H*-1,2,3-triazole (3.8a). Following **General procedure D**, the product was obtained as an off-white solid (65 mg) in 92% yield. $\mathbf{R_f}$ = 0.69 (EtOAc:Hexane=1:2): **^{1}H NMR** (500 MHz, $CDCl_3$) δ 7.44–7.37 (m, 3H), 7.25 (d, *J* = 6.5 Hz, 2H), 7.14 (dd, *J* = 8.0, 1.5 Hz, 2H), 7.00–6.98 (m, 3H), 5.44 (s, 2H), 2.42–2.37 (m, 2H), 1.04–1.00 (m, 12H); **^{13}C NMR** (125 MHz, $CDCl_3$) δ 135.8, 130.5 (d, *J* = 42.7 Hz), 129.6, 129.0, 128.9, 128.8, 128.5, 128.4, 128.3, 127.4, 52.1, 23.7 (d, *J* = 6.4 Hz), 20.3 (d, *J* = 17.6 Hz), 19.7 (d, *J* = 8.2 Hz); **^{31}P NMR** δ –18.7; **IR** (neat) 2955, 2865, 1496, 1455, 1410, 1382, 1363, 1240, 1183, 1155, 1114, 1028, 1007 cm^{-1}; **HRMS** (ESI-TOF) calcd for $C_{21}H_{27}N_3P$ $[M+H]^+$ 352.1943, found 352.1951.

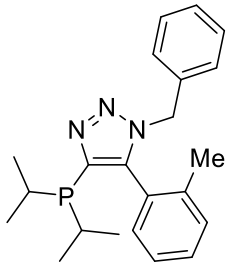

1-Benzyl-4-(diisopropylphosphaneyl)-5-(*o*-tolyl)-1*H*-1,2,3-triazole (3.8b). Following **General procedure D**, the product was obtained as a white solid (28 mg) in 99% yield. $\mathbf{R_f}$ = 0.49 (EtOAc:Hex=1:4): **^{1}H NMR** (500 MHz, $CDCl_3$) δ 7.34 (td, *J* = 7.5, 1.0 Hz, 1H), 7.24–7.17 (m, 5H), 6.91–6.89 (m, 3H), 5.31 (d, *J* = 15.0 Hz, 1H), 5.25 (d, *J* = 15.0 Hz, 1H), 2.67–2.60 (m, 1H), 2.11–2.05 (m, 1H), 1.75 (s, 3H), 1.08 (dd, *J* = 15.5, 7.0 Hz, 3H), 1.05–0.99 (m, 6H), 0.91 (dd, *J* = 16.0, 7.0 Hz, 3H); **^{13}C NMR** (125 MHz, $CDCl_3$) δ 144.2 (d, *J* = 39.0

Hz), 140.9 (d, *J* = 21.4 Hz), 137.9, 135.0, 130.9, 130.5, 130.0, 128.7, 128.3, 128.1, 127.0, 125.8, 52.2, 24.2 (d, *J* = 8.8 Hz), 22.5 (d, *J* = 5.0 Hz), 20.42 (d, *J* = 30.2 Hz), 20.40, 19.9 (d, *J* = 18.9 Hz), 19.7 (d, *J* = 3.8 Hz), 18.9 (d, *J* = 3.8 Hz); **^{31}P NMR** δ 46.9; **IR** (neat) 2950, 2923, 2864, 1637, 1455, 1410, 1381, 1363, 1236, 1181 cm^{-1}; **HRMS** (ESI-TOF) calcd for $C_{22}H_{29}N_3P$ $[M+H]^+$ 366.2099, found 366.2085.

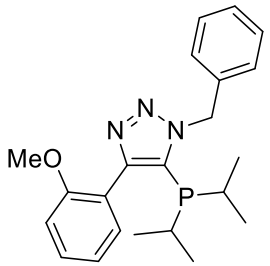

1-Benzyl-5-(diisopropylphosphaneyl)-4-(2-methoxyphenyl)-1*H*-1,2,3-triazole (3.7c). Following **General procedure D**, the product was obtained as an off-white solid (73 mg) in 96% yield. **R_f** = 0.48 (EtOAc:Hex=1:2): **^{1}H NMR** (500 MHz, $CDCl_3$) δ 7.41–7.37 (m, 3H), 7.33 (t, *J* = 7.0 Hz, 2H), 7.29 (d, *J* = 7.5 Hz, 1H), 7.18 (dd, *J* = 7.5, 1.5 Hz, 1H), 6.96 (t, *J* = 8.0 Hz, 1H), 6.93 (d, *J* = 8.0 Hz, 1H), 5.82 (s, 2H), 3.71 (s, 3H), 1.93–1.86 (m, 2H), 0.96 (dd, *J* = 17.0, 7.0 Hz, 6H), 0.60 (dd, *J*= 14.0, 7.0 Hz, 6H); **^{13}C NMR** (125 MHz, $CDCl_3$) δ 158.2, 136.1, 131.74, 131.67 (d, *J* = 26.5 Hz), 130.4, 128.7 (d, *J* = 65.3 Hz), 128.6, 128.3, 128.1, 121.7, 120.0, 110.8, 55.2, 52.8 (d, *J* = 12.4 Hz), 24.5 (d, *J* = 7.2 Hz), 21.3 (d, *J* = 23.7 Hz), 20.8 (d, *J* = 11.6 Hz); **^{31}P NMR** δ –15.4; **IR** (neat) 2925, 2865, 1607, 1526, 1496, 1470, 1434, 1384, 1331, 1281, 1248, 1182, 1160, 1113, 1049, 1026 cm^{-1}; **HRMS** (ESI-TOF) calcd for $C_{22}H_{29}N_3OP$ $[M+H]^+$ 382.2048, found 382.2034.

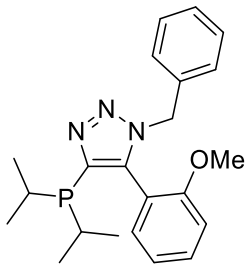

1-Benzyl-4-(diisopropylphosphaneyl)-5-(2-methoxyphenyl)-1*H*-1,2,3-triazole (3.8c). Following **General procedure D**, the product was obtained as a light yellow solid (72 mg) in 94% yield. $\mathbf{R_f}$ = 0.65 (EtOAc:Hex=1:2): **^{1}H NMR** (500 MHz, $CDCl_3$) δ 7.42–7.38 (m, 1H), 7.22–7.18 (m, 3H), 6.97–6.90 (m, 5H), 5.43 (d, *J* = 14.5 Hz, 1H), 5.24 (d, *J* = 14.5 Hz, 1H), 3.59 (s, 3H), 2.53–2.44 (m, 1H), 2.25–2.13 (m, 1H), 1.08–0.88 (m, 12H); **^{13}C NMR** (125 MHz, $CDCl_3$) δ 157.2, 142.0 (d, *J* = 41.0 Hz), 141.1 (d, *J* = 19.5 Hz), 135.6, 132.5, 131.4, 128.5, 127.8, 127.7, 120.7, 116.5, 110.9, 55.2, 52.2, 23.7 (d, *J* = 7.8 Hz), 23.0 (d, *J* = 7.0 Hz), 20.1 (d, *J* = 19.1 Hz), 19.9 (d, *J* = 8.2 Hz), 19.8 (d, *J* = 18.6 Hz), 19.1 (d, *J* = 5.6 Hz); **^{31}P NMR** δ –20.7; **IR** (neat) 2951, 2925, 2864, 1607, 1476, 1455, 1414, 1289, 1266, 1244, 1181, 1162, 1114, 1046, 1025, 1001 cm^{-1}; **HRMS** (ESI-TOF) calcd for $C_{22}H_{29}N_3OP$ $[M+H]^+$ 382.2048, found 382.2055.

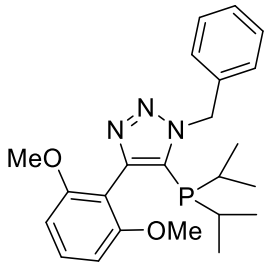

1-Benzyl-5-(diisopropylphosphaneyl)-4-(2,6-dimethoxyphenyl)-1*H*-1,2,3-triazole (3.7d). Following **General procedure D**, the product was obtained as a white solid (22 mg) in 41% yield. $\mathbf{R_f}$ = 0.14 (EtOAc:Hex=1:4): **^{1}H NMR** (500 MHz, $CDCl_3$) δ 7.36 (t, *J* = 8.0 Hz, 2H), 7.33–7.25 (m, 4H), 6.56 (d, *J* = 8.5 Hz, 2H), 5.83 (s, 2H), 3.64 (s, 6H), 1.93–1.85 (m, 2H), 0.94 (dd, *J* = 16.0, 6.5 Hz, 6H), 0.61 (dd, *J* = 15.0, 7.0 Hz, 6H); **^{13}C NMR** (125 MHz, $CDCl_3$) δ 159.5, 144.9 (d, *J* = 5.5 Hz), 136.3, 132.8 (d, *J* = 25.7 Hz), 130.8, 128.5, 128.3, 128.0, 110.0, 103.4, 55.3, 52.9 (d, *J* = 12.4 Hz), 24.3 (d, *J* = 7.0 Hz), 21.2 (d, *J* = 22.1 Hz), 21.0 (d, *J* = 13.6 Hz); **^{31}P NMR** δ –15.1; **IR** (neat) 2947, 2865, 1603, 1587, 1472, 1456, 1432, 1328, 1287, 1251, 1215, 1109, 1031, 992 cm^{-1}; **HRMS** (ESI-TOF) calcd

for $C_{23}H_{31}N_3O_2P$ $[M+H]^+$ 412.2154, found 412.2151.

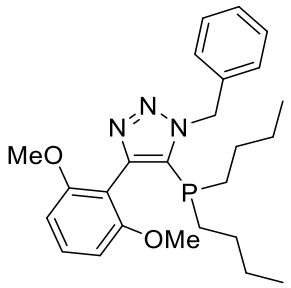

1-Benzyl-5-(dibutylphosphaneyl)-4-(2,6-dimethoxyphenyl)-1*H*-1,2,3-triazole (3.7d-*n*Bu). Following **General procedure D**, the product was obtained as an off-white solid (82 mg) in 93% yield. $\mathbf{R_f}$ = 0.45 (EtOAc:Hex=1:2): **^{1}H NMR** (500 MHz, $CDCl_3$) δ 7.32 (t, *J* = 8.5 Hz, 1H), 7.19–7.14 (m, 3H), 6.94 (dd, *J* = 6.5, 2.0 Hz, 2H), 6.49 (d, *J* = 8.5 Hz, 2H), 5.24 (s, 2H), 3.51 (s, 6H), 1.96–1.87 (m, 2H), 1.64–1.59 (m, 2H), 1.31–1.25 (m, 8H), 0.81 (t, *J* = 7.0 Hz, 6H); **^{13}C NMR** (125 MHz, $CDCl_3$) δ 158.6, 144.5 (d, *J* = 14.8 Hz), 136.7 (d, *J* = 35.2 Hz), 135.6, 131.9, 128.2, 128.0, 127.7, 104.9, 103.7, 55.4, 52.3, 28.5 (d, *J* = 13.8 Hz), 26.8 (d, *J* = 6.5 Hz), 24.5 (d, *J* = 4.7 Hz), 14.0; **^{31}P NMR** δ –-49.8; **IR** (neat) 2956, 2929, 2871, 1605, 1589 1497, 1475, 1456, 1434, 1292, 1253, 1185, 1111, 1031. 1001 cm^{-1}; **HRMS** (ESI-TOF) calcd for $C_{25}H_{35}N_3O_2P$ $[M+H]^+$ 440.2467, found 440.2458.

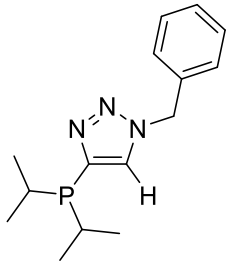

1-Benzyl-4-(diisopropylphosphaneyl)-1*H*-1,2,3-triazole (3.8e). Following **General procedure D**, the product was obtained as an off-white solid (52 mg) in 94% yield. $\mathbf{R_f}$ = 0.80 (EtOAc:Hex=1:2): **^{1}H NMR** (500 MHz, $CDCl_3$) δ 7.71 (s, 1H) 7.29–7.23 (m, 5H), 5.71 (s, 2H), 2.03–1.94 (m, 2H), 0.92 (dd, *J* = 16.0, 7.0 Hz, 6H), 0.84 (dd, *J* = 12.5, 7.0 Hz, 6H);

^{13}C NMR (125 MHz, $CDCl_3$) δ 138.8 (d, *J* = 5.5 Hz), 136.0, 132.8 (d, *J* = 26.4 Hz), 128.7, 128.3, 128.1, 52.6 (d, *J* = 9.8 Hz), 24.0 (d, *J* = 8.4 Hz), 19.7 (d, *J* = 17.6 Hz), 19.0 (d, *J* = 8.3 Hz); **^{31}P NMR** δ –23.4; **IR** (neat) 2954, 2928, 2867, 1456, 1433, 1384, 1270, 1211, 1187, 1153, 1121, 1028 cm^{-1}; **HRMS** (ESI-TOF) calcd for $C_{15}H_{23}N_3P$ $[M+H]^+$ 276.1630, found 276.1639.

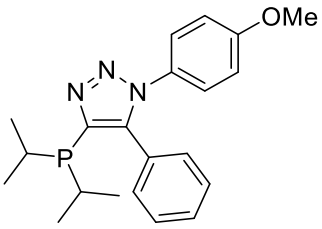

4-(Diisopropylphosphaneyl)-1-(4-methoxyphenyl)-5-phenyl-1*H*-1,2,3-triazole (3.8k). Following **General procedure D**, the product was obtained as a white solid (65 mg) in 89% yield. **R_f** = 0.70 (EtOAc:Hex=1:2): **^{1}H NMR** (500 MHz, $CDCl_3$) δ 7.36–7.33 (m, 3H), 7.25 (dd, *J* = 7.5, 2.0 Hz, 2H), 7.21 (dd, *J* = 7.0, 2.0 Hz, 2H), 6.86 (dd, *J* = 7.0, 2.0 Hz, 2H), 3.81 (s, 3H), 2.53–2.47 (m, 2H), 1.11–1.05 (m, 12H); **^{13}C NMR** (125 MHz, $CDCl_3$) δ 159.8, 144.2 (d, *J* = 33.7 Hz), 140.6 (d, *J* = 23.6 Hz), 130.5 (d, *J* = 3.1 Hz), 129.9, 129.1, 128.6, 127.7, 126.4, 114.3, 55.6, 23.6 (d, *J* = 7.8 Hz), 20.1 (d, *J* = 18.1 Hz), 19.7 (d, *J* = 8.5 Hz); **^{31}P NMR** δ –18.8; **IR** (neat) 2951, 2924, 2864, 1609, 1513, 1463, 1301, 1251, 1181, 1171, 1108, 1067, 1030 cm^{-1}; **HRMS** (ESI-TOF) calcd for $C_{21}H_{27}N_3OP$ $[M+H]^+$ 368.1892, found 368.1879.

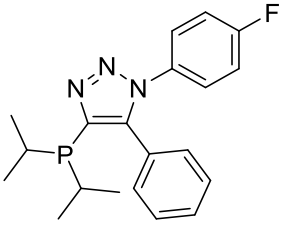

4-(Diisopropylphosphaneyl)-1-(4-fluorophenyl)-5-phenyl-1*H*-1,2,3-triazole (3.8p). Following **General procedure D**, the product was obtained as an off-white solid (10 mg)

in 83% yield. $\mathbf{R_f}$ = 0.68 (EtOAc:Hex=1:4): **^{1}H NMR** (500 MHz, $CDCl_3$) δ 7.38–7.34 (m, 3H) 7.31–7.28 (m, 2H), 7.23 (dd, *J* = 7.5, 2.0 Hz, 2H), 7.06 (t, *J* = 8.5 Hz, 2H), 2.48–2.39 (m, 2H), 1.09–1.03 (m, 12H); **^{13}C NMR** (125 MHz, $CDCl_3$) δ 162.5 (d, *J* = 249.0 Hz), 144.3 (d, *J* = 33.5 Hz), 141.1 (d, *J* = 24.5 Hz), 130.9, 130.5 (d, *J* = 2.8 Hz), 129.4, 128.8, 127.4, 126.9 (d, *J* = 8.6 Hz), 116.3 (d, *J* = 23.1 Hz), 23.6 (d, *J* = 7.7 Hz), 20.2 (d, *J* = 18.0 Hz), 19.7 (d, *J* = 8.6 Hz); **^{31}P NMR** δ –19.6; **IR** (neat) 2956, 2924, 2865, 1509, 1466, 1449, 1265, 1234, 1221, 1180, 1157, 1140, 1067, 839 cm^{-1}; **HRMS** (ESI-TOF) calcd for $C_{20}H_{24}FN_3P$ $[M+H]^+$ 356.1692, found 356.1685.

Parallel Microscale Experimentation Data

The solutions of clickphos ligands (0.1 M), $Pd(OAc)_2$ (0.05 M), and Cs_2CO_3 (0.086 M) in THF were prepared. First, each ligand (20 μL, 2 μmol) was dosed into the 24-well plate vials and removed the solvent by Genevac. The $Pd(OAc)_2$ (20 μL, 1 μmol) was introduced across the plate and stripped off the solvent by Genevac. Next, the base (350 μL, 30 μmol) was added as a slurry, followed by removal of solvent by Genevac. Finally, 0.2 M concentration of both a solution of 3,5-dichloropyridazine (50 μL, 10 μmol) and phenylboronic acid (50 μL, 10 μmol) in 1,4-dioxane were dosed into each vial. After purging with the micro stirbar to each vial, the reaction plate was sealed and stirred for 1 h at 75 °C. Upon cooling to room temperature, the reaction mixture vials were diluted with 500 μL of the 4,4'-di-*tert*-butylbiphenyl in MeCN solution (10 μmol). The plate was stirred vigorously for 2 min after sealing the plate. To a 96-well plate LC block were added 700 μL of MeCN, followed by 25 μL of the mixture from the reaction well-plate addition. The diluted mixture was then analyzed using Agilent Technologies UPLC with a 96-well plate auto-sampler.

HTE Results of Suzuki-Miyaura Coupling with 3,5-Dichloropyridazine (Scheme 3.7)

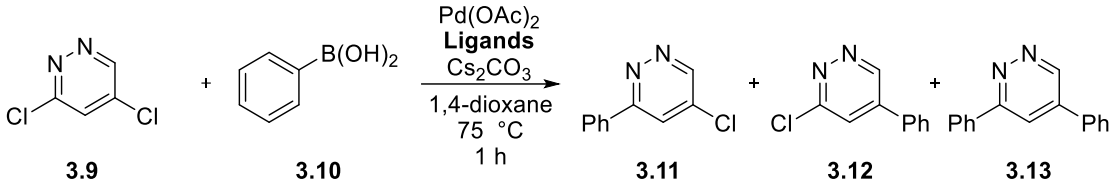

3.9 **3.10** **3.11** **3.12** **3.13**

Ligand	**3.11**/IS	**3.12**/IS	**3.13**/IS	**3.12/3.11**
3.7a	0.072	0.205	0.017	2.847
3.8a	0.118	0.264	0.028	2.242
3.7c	0.064	0.253	0.023	3.959
3.8c	0.096	0.246	0.033	2.553
3.7c-Cy	0.050	0.207	0.018	4.123
3.8c-Cy	0.081	0.290	0.022	3.589
3.7d-*n*Bu	0.057	0.279	0.015	4.912
3.8k	0.085	0.181	0.016	2.140
3.8b	0.046	0.214	0.017	4.661
3.8e	0.093	0.023	0.012	0.250
3.7d	0.063	0.256	0.013	4.08
3.7d-*n*Bu	0.096	0.047	0.019	0.486
3.8p	0.094	0.207	0.029	2.207

CHAPTER 4: OXIDATIVE COUPLING OF 3-OXINDOLE TO CONSTRUCT QUATERNARY CENTERS

4.1. Introduction

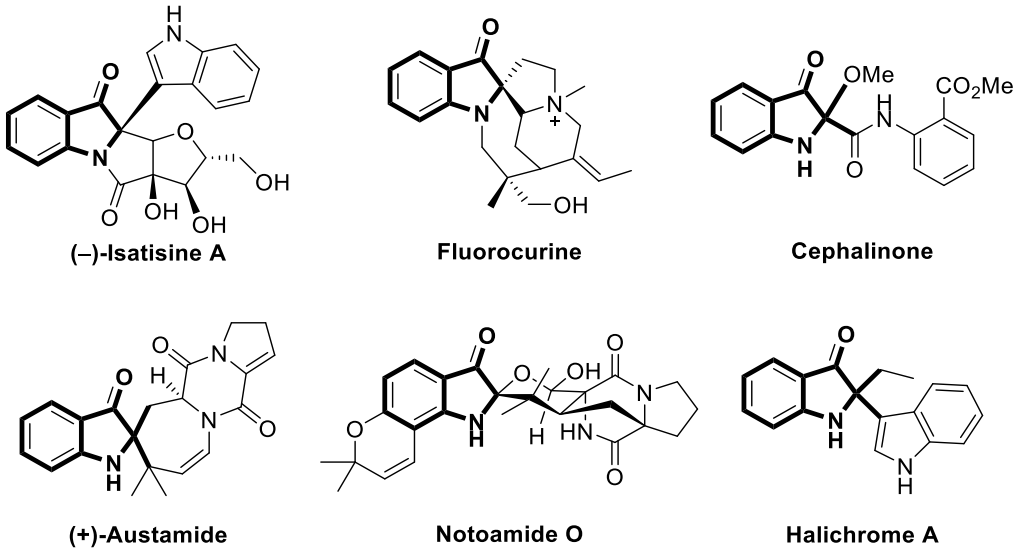

Figure 4.1. Representative Natural Prodcuts Containing 2,2-Disubstituted Indolin-3-one

Many natural products featuring the 2,2-disubstituted-3-oxindole backbone are found in indole alkaloids such as isatisine A, cephalinone, austimide, and halichrome A etc (**Figure 4.1**).[1] Moreover, C-2 quaternary indolin-3-one scaffolds have been utilized as useful synthetic intermediates in numerous natural product syntheses (**Scheme 4.1**).[2] In

[1] (a) Wu, P.-L.; Hsu, Y.-L.; Jao, C.-W. Indole Alkaloids from *Cephalanceropsis Gracilis*. *J. Nat. Prod.* **2006**, *69* (10), 1467–1470. (b) Liu, J.-F.; Jiang, Z.-Y.; Wang, R.-R.; Zheng, Y.-T.; Chen, J.-J.; Zhang, X.-M.; Ma, Y.-B. Isatisine A, a Novel Alkaloid with an Unprecedented Skeleton from Leaves of *Isatis Indigotica*. *Org. Lett.* **2007**, *9* (21), 4127–4129. (c) Tsukamoto, S.; Umaoka, H.; Yoshikawa, K.; Ikeda, T.; Hirota, H. Notoamide O, a Structurally Unprecedented Prenylated Indole Alkaloid, and Notoamides P−R from a Marine-Derived Fungus, *Aspergillus* Sp. *J. Nat. Prod.* **2010**, *73* (8), 1438–1440. (d) Liu, R.-R.; Ye, S.-C.; Lu, C.-J.; Zhuang, G.-L.; Gao, J.-R.; Jia, Y.-X. Dual Catalysis for the Redox Annulation of Nitroalkynes with Indoles: Enantioselective Construction of Indolin-3-Ones Bearing Quaternary Stereocenters. *Angew. Chem. Int. Ed.* **2015**, *54* (38), 11205–11208. (e) Baran, P. S.; Corey, E. J. A Short Synthetic Route to (+)-Austamide, (+)-Deoxyisoaustamide, and (+)-Hydratoaustamide from a Common Precursor by a Novel Palladium-Mediated Indole → Dihydroindoloazocine Cyclization. *J. Am. Chem. Soc.* **2002**, *124* (27), 7904–7905.

[2] (a) Pearson, W. H.; Mi, Y.; Lee, I. Y.; Stoy, P. Total Synthesis of the *Kopsia Lapidilecta* Alkaloid (±)-Lapidilectine B. *J. Am. Chem. Soc.* **2001**, *123* (27), 6724–6725. (b) Wang, C.; Wang, Z.; Xie, X.; Yao, X.; Li, G.; Zu, L. Total Synthesis of (±)-Grandilodine B. *Org. Lett.* **2017**, *19* (7), 1828–1830.

2001, the Pearson group demonstrated that the treatment of *ortho*-azidoaryl ketones with KOH, referred to as the Smalley cyclization,[3] was able to construct key 1,2-dihydro-3*H*-indol-3-one successfully during the synthesis of lapidilectine B.[2a] The 2-spirocyclic indolin-3-one backbone was employed via a Diels-Alder reaction in grandilodine B synthesis by Zhu and coworkers.[2b] The Kawasaki group disclosed that the Mannich-type nucleophilic addition reaction enabled generating a key intermediate, the C-2 quaternary indolin-3-one, from 2-hydroxyindolin-3-one in the presence of acid to accomplish the first total synthesis of hinckdentine A.[2c] Stepwise 2,2-disubstituted-3-oxindole moiety was obtained from 2-hydroxyindolin-3-one via a Grignard reaction followed by a pinacol-like rearrangement under acidic conditions.[2d] In 2011, the Tamber and Movassaghi groups individually reported that the efficient strategy of oxindole preparation could be achieved by means of oxidation and Wagner–Meerwein [1,2]-rearrangement in the synthesis of (–)-trigonoliimine C.[2e,f] Recently, simple Michael addition afforded 2,2-dialkylated indolin-3-one as a synthetic building block for lundurine A by Nishida and coworkers.[2g]

(c) Higuchi, K.; Sato, Y.; Tsuchimochi, M.; Sugiura, K.; Hatori, M.; Kawasaki, T. First Total Synthesis of Hinckdentine A. *Org. Lett.* **2009**, *11* (1), 197–199. (d) Liu, Y.; McWhorter, W. W. Synthesis of 8-Desbromohinckdentine A[1]. *J. Am. Chem. Soc.* **2003**, *125* (14), 4240–4252. (e) Han, S.; Movassaghi, M. Concise Total Synthesis and Stereochemical Revision of All (−)-Trigonoliimines. *J. Am. Chem. Soc.* **2011**, *133* (28), 10768–10771. (f) Qi, X.; Bao, H.; Tambar, U. K. Total Synthesis of (±)-Trigonoliimine C via Oxidative Rearrangement of an Unsymmetrical Bis-Tryptamine. *J. Am. Chem. Soc.* **2011**, *133* (26), 10050–10053. (g) Arai, S.; Nakajima, M.; Nishida, A. A Concise and Versatile Synthesis of Alkaloids from Kopsia Tenuis: Total Synthesis of (±)-Lundurine A and B. *Angew. Chem. Int. Ed.* **2014**, *53* (22), 5569–5572.

[3] Ardakani, M. A.; Smalley, R. K. Base-Induced Intramolecular Cyclisation of *o*-Azidophenyl *sec*-Alkyl Ketones. A New Synthesis of 2,2-Dialkylindoxyls. *Tetrahedron Lett.* **1979**, *20* (49), 4769–4772.

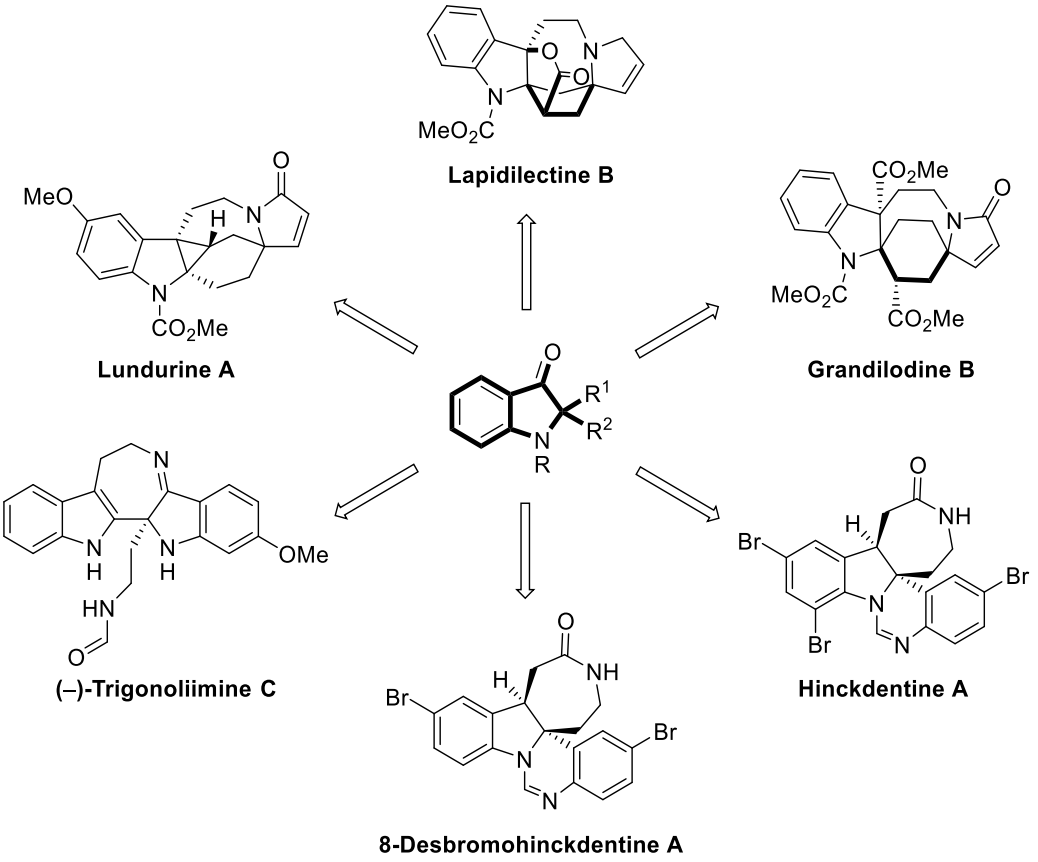

Scheme 4.1. Examples of 2,2-Disubstituted Indolin-3-ones as Efficient Intermediates for Natural Product Syntheses

4.2. Approaches to Construct 2,2-Disubstituted Indolin-3-one

Due to the versatile use of 3-oxindoles bearing C-2 quaternary centers in bioactive molecule syntheses,[2] diverse synthetic methods have been developed for several decades.[4] In the early 1950s, acid-catalyzed rearrangement with

[4] (a) Witkop, B. The Structure of the So-Called 11-Hydroxytetrahydrocarbazolenine. *J. Am. Chem. Soc.* **1950**, *72* (1), 614–620. (b) Witkop, B.; Patrick, J. B. The Course and Kinetics of the Acid-Base-Catalyzed Rearrangements of 11-Hydroxytetrahydrocarbazolenine [1]. *J. Am. Chem. Soc.* **1951**, *73* (5), 2188–2195. (c) Liu, Y.; McWhorter, W. W. Study of the Addition of Grignard Reagents to 2-Aryl-3 *H* -Indol-3-Ones [1]. *J. Org. Chem.* **2003**, *68* (7), 2618–2622. (d) Altinis Kiraz, C. I.; Emge, T. J.; Jimenez, L. S. Oxidation of Indole Substrates by Oxodiperoxomolybdenum·Trialkyl(Aryl)-Phosphine Oxide Complexes. *J. Org. Chem.* **2004**, *69* (6), 2200–2202. (e) S. Baran, P.; Jessing, M. Oxidative Coupling of Indoles with 3-Oxindoles. *HETEROCYCLES* **2010**, *82* (2), 1739. (f) Wetzel, A.; Gagosz, F. Gold-Catalyzed Transformation of 2-Alkynyl Arylazides: Efficient Access to the Valuable Pseudoindoxyl and Indolyl Frameworks. *Angew. Chem. Int. Ed.* **2011**, *50* (32), 7354–7358. (g) Goriya, Y.; Ramana, C. V. Synthesis of Pseudo-Indoxyl Derivatives via Sequential Cu-

hydroxytetrahydrocarbazole afforded a simple 2-spirocycloindolin-3-one (**Scheme 4.2**).[4a,b] This Wagner–Meerwein rearrangement strategy is still utilized in natural product synthesis as mentioned above (**Scheme 4.1**).[2e,f]

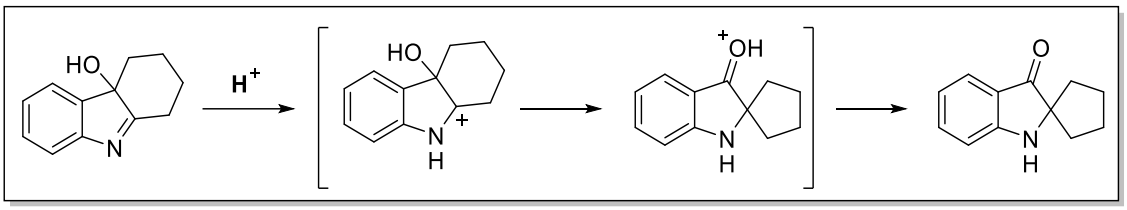

Scheme 4.2. Wagner–Meerwein Rearrangement to Construct 2,2-Disubstituted Indolin-3-one

Base-induced intramolecular cyclization enabled easy access to 2,2-dialkylated indolin-3-one from *ortho*-azidoaryl ketones by Smalley in 1979.[3] Later, the Ramana group modified the process via Cu-catalyzed S_NAr and Smalley reaction in one pot.[4g] Instead of conventional multi-step synthesis of *ortho*-azidoaryl ketones, the modified procedure generated the corresponding cyclized C-2 quaternary indolin-3-one in the presence of catalytic Cu(I) salt, sodium ascorbate, NaN_3 and K_2CO_3 from *ortho*-bromoaryl ketone (**Scheme 4.3**).

Catalyzed SNAr and Smalley Cyclization. *Chem. Commun.* **2013**, *49* (57), 6376. (h) Dhara, K.; Mandal, T.; Das, J.; Dash, J. Synthesis of Carbazole Alkaloids by Ring-Closing Metathesis and Ring Rearrangement–Aromatization. *Angew. Chem. Int. Ed.* **2015**, *54* (52), 15831–15835. (i) Guchhait, S. K.; Chaudhary, V.; Rana, V. A.; Priyadarshani, G.; Kandekar, S.; Kashyap, M. Oxidative Dearomatization of Indoles via Pd-Catalyzed C–H Oxygenation: An Entry to C2-Quaternary Indolin-3-Ones. *Org. Lett.* **2016**, *18* (7), 1534–1537. (j) Zhang, C.; Li, S.; Bureš, F.; Lee, R.; Ye, X.; Jiang, Z. Visible Light Photocatalytic Aerobic Oxygenation of Indoles and pH as a Chemoselective Switch. *ACS Catal.* **2016**, *6* (10), 6853–6860. (k) Li, Y.-J.; Yan, N.; Liu, C.-H.; Yu, Y.; Zhao, Y.-L. Gold/Copper-Co-Catalyzed Tandem Reactions of 2-Alkynylanilines: A Synthetic Strategy for the C2-Quaternary Indolin-3-Ones. *Org. Lett.* **2017**, *19* (5), 1160–1163. (l) Xia, Z.; Hu, J.; Gao, Y.-Q.; Yao, Q.; Xie, W. Facile Access to 2,2-Disubstituted Indolin-3-Ones via a Cascade Fischer Indolization/Claisen Rearrangement Reaction. *Chem. Commun.* **2017**, *53* (54), 7485–7488. (m) Fu, W.; Song, Q. Copper-Catalyzed Radical Difluoroalkylation and Redox Annulation of Nitroalkynes for the Construction of C2-Tetrasubstituted Indolin-3-Ones. *Org. Lett.* **2018**, *20* (2), 393–396. (n) Zhou, X.-Y.; Chen, X.; Wang, L.-G.; Yang, D.; Li, J.-H. Ruthenium-Catalyzed Oxidative Dearomatization of Indoles for the Construction of C2-Quaternary Indolin-3-Ones. *Synlett* **2018**, *29* (06), 835–839.

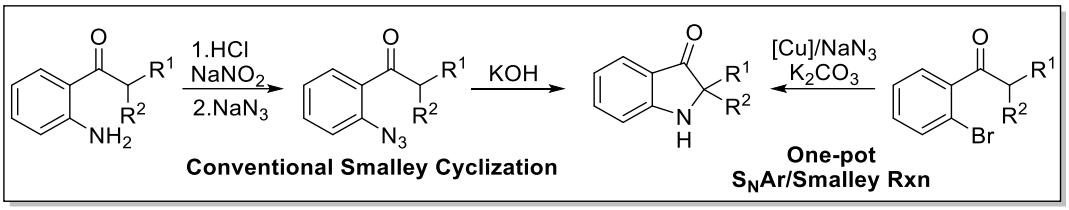

Scheme 4.3. Approaches to C-2 Quaternary Indolin-3-one via Smalley Cyclization

In 2003, McWhorter and Liu reported that Grignard addition to 2-aryl-3*H*-indol-3-one followed by acid-induced rearrangement provided 2,2-disubstituted-3-oxindole (**Scheme 4.4**).[4c] This protocol was used as one of the key steps to synthesize the indoxyl natural product analog, 8-desbromohinckdentine A.[2d]

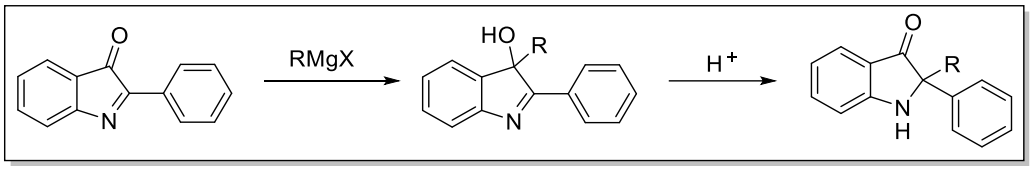

Scheme 4.4. Grignard Addition and Pinacol-type Rearrangement to Access 2,2-Disubstituted-3-oxindole

The Gagosz group developed a Au-catalyzed cylcoisomerization with 2-alkynyl aryl azides followed by Claisen rearrangement to generate various C-2 allyl–functionalized quaternary indolin-3-ones (**Scheme 4.5.a**).[4f] In 2017, Xie and coworkers demonstrated that readily accessible hydrazines and allyloxy ketones enabled access to similar 3-allyloxy indole intermediates by means of a Fischer-Indole reaction (**Scheme 4.5.b**).[4l] After Claisen rearrangement, this protocol gave rise to 2,2-disubstituted-3-oxindoles, especially C-2 allyl–substituted indolin-3-ones, in good yield.

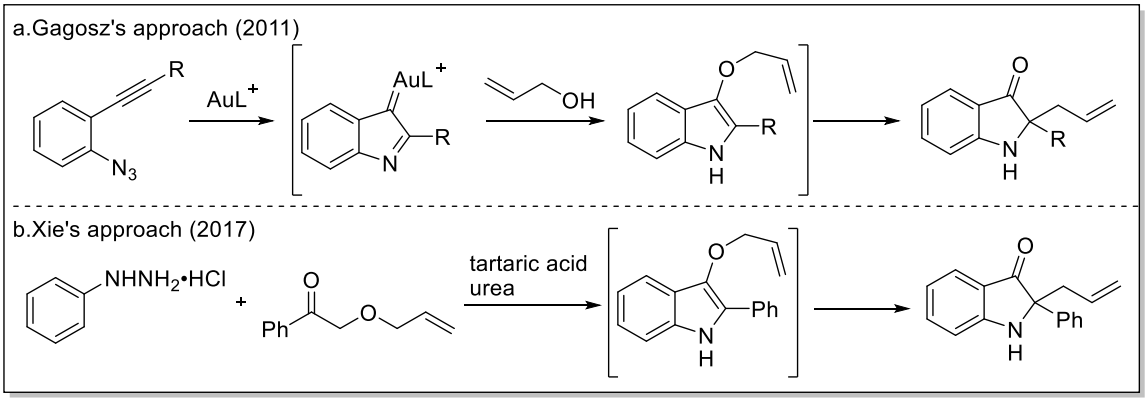

Scheme 4.5. Access to 2,2-Disubstituted Indolin-3-one via Au-catalyzed Cycloisomerization or Fischer Indolization and Claisen Rearrangement

Recently, owing to the efficiency of oxidation chemistry, a number of different types of oxidative routes have been employed to construct 2,2-disubstituted-3-oxindole. Oxidative coupling between 3-oxindoles, which can be prepared in two steps from commercial methyl anthranilate, and amino heterocycles was achieved by treatment with excess oxidant, CAN, in the presence of $NaHCO_3$ (**Scheme 4.6.a**).[4e] The oxidative dearomatization of indole under Pd-catalyzed C-H oxygenation conditions achieved the construction of 2-tetrasubstituted indolin-3-one (**Scheme 4.6.b**).[4i] Moreover, Zhou and coworkers revealed that $RuCl_3$ and $NaIO_4$ were able to generate C-2 quaternary-3-oxindole via oxidative indole dearomatization in 2018 (**Scheme 4.6.c**).[4n]

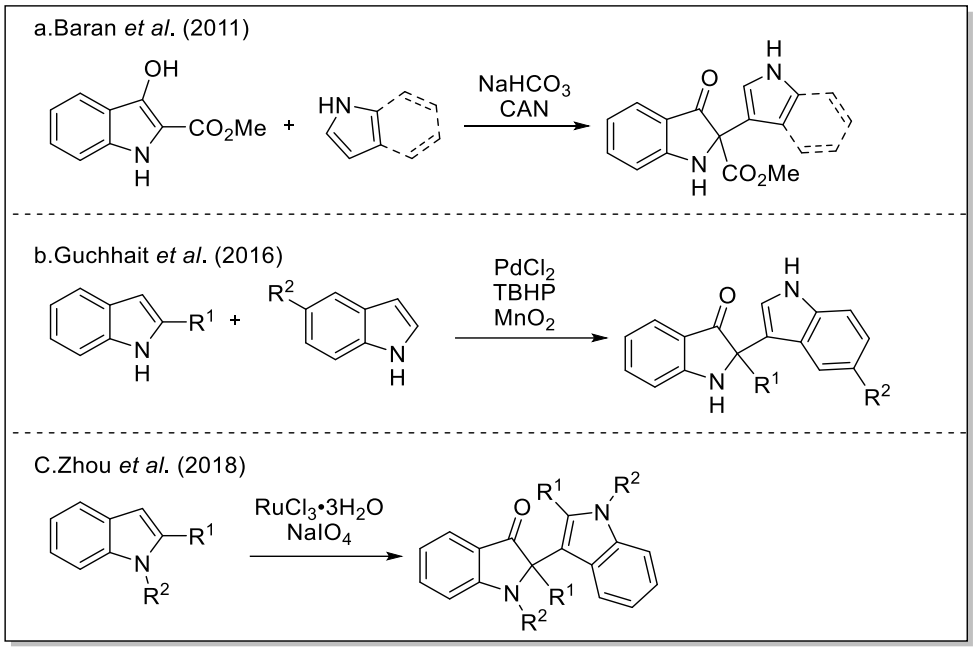

Scheme 4.6. Oxidative Approaches to Build C-2 Quaternary Indolin-3-one

Along with a variety of synthetic methods shown above, asymmetric approaches have also been developed over the past 10 years.[5] In 2007, the Kawasaki group demonstrated that *N*-benzylated cinchonidine salt, a phase transfer catalyst, induced asymmetric prenylation at the C-2 position with moderate selectivity (**Scheme 4.7.a**).[5a] An asymmetric Friedel-Crafts reaction was accomplished to generate 2,2-disubstituted

[5] (a) Kawasaki, T.; Higuchi, K.; Masuda, K.; Koseki, T.; Hatori, M.; Sakamoto, M. Asymmetric Alkylation of 2-Monosubstituted Indolin-3-Ones. *HETEROCYCLES* **2007**, *73* (1), 641. (b) Rueping, M.; Raja, S.; Núñez, A. Asymmetric Brønsted Acid-Catalyzed Friedel-Crafts Reactions of Indoles with Cyclic Imines - Efficient Generation of Nitrogen-Substituted Quaternary Carbon Centers. *Adv. Synth. Catal.* **2011**, *353* (4), 563–568. (c) Jin, C.-Y.; Wang, Y.; Liu, Y.-Z.; Shen, C.; Xu, P.-F. Organocatalytic Asymmetric Michael Addition of Oxindoles to Nitroolefins for the Synthesis of 2,2-Disubstituted Oxindoles Bearing Adjacent Quaternary and Tertiary Stereocenters. *J. Org. Chem.* **2012**, *77* (24), 11307–11312. (d) Parra, A.; Alfaro, R.; Marzo, L.; Moreno-Carrasco, A.; García Ruano, J. L.; Alemán, J. Enantioselective Aza-Henry Reactions of Cyclic α-Carbonyl Ketimines under Bifunctional Catalysis. *Chem. Commun.* **2012**, *48* (78), 9759. (e) Guo, C.; Schedler, M.; Daniliuc, C. G.; Glorius, F. N- Heterocyclic Carbene Catalyzed Formal [3+2] Annulation Reaction of Enals: An Efficient Enantioselective Access to Spiro- Heterocycles. *Angew. Chem. Int. Ed.* **2014**, *53* (38), 10232–10236. (f) Zhao, Y.-L.; Wang, Y.; Cao, J.; Liang, Y.-M.; Xu, P.-F. Organocatalytic Asymmetric Michael–Michael Cascade for the Construction of Highly Functionalized N-Fused Piperidinoindoline Derivatives. *Org. Lett.* **2014**, *16* (9), 2438–2441.

indolin-3-one in high selectivity by using chiral phosphoric acid (**Scheme 4.7.b**).[5b]

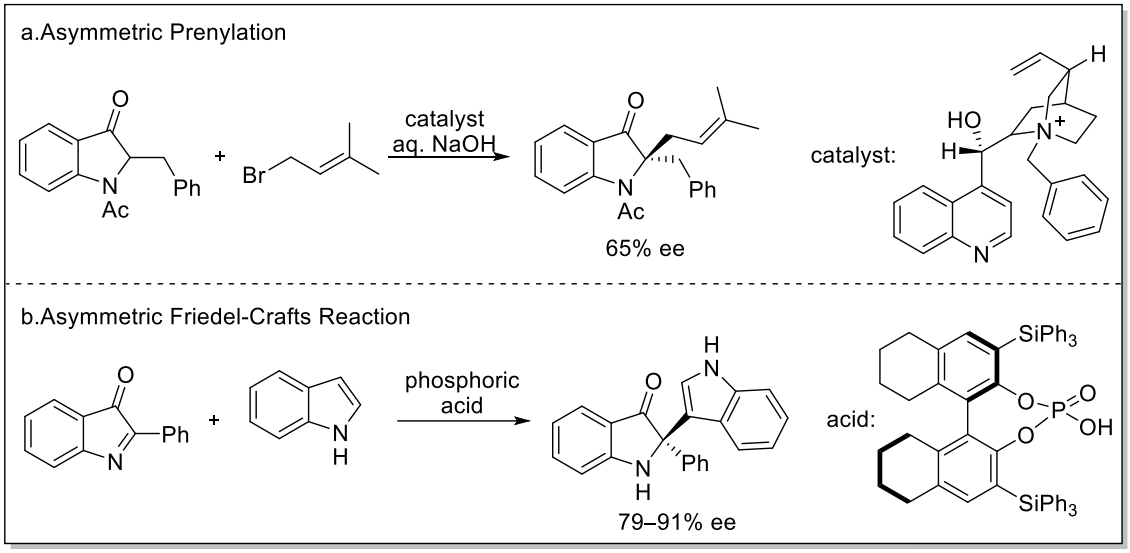

Scheme 4.7. Asymmetric Organocatalyzed Installation of Optically Active C-2 Quaternary Indolin-3-one

Notably, bifunctionalized thioureas have been known for efficient asymmetric transformation of 2-tetrasubstituted indolin-3-one derivatives via either Michael addition (**Scheme 4.8.a**)[5c,f] or aza-Henry reaction (**Scheme 4.8.b**).[5d] According to the proposed transition state model, facial selectivity could be explained by means of hydrogen bonding between the thiourea and both substrates (**Scheme 4.8**).

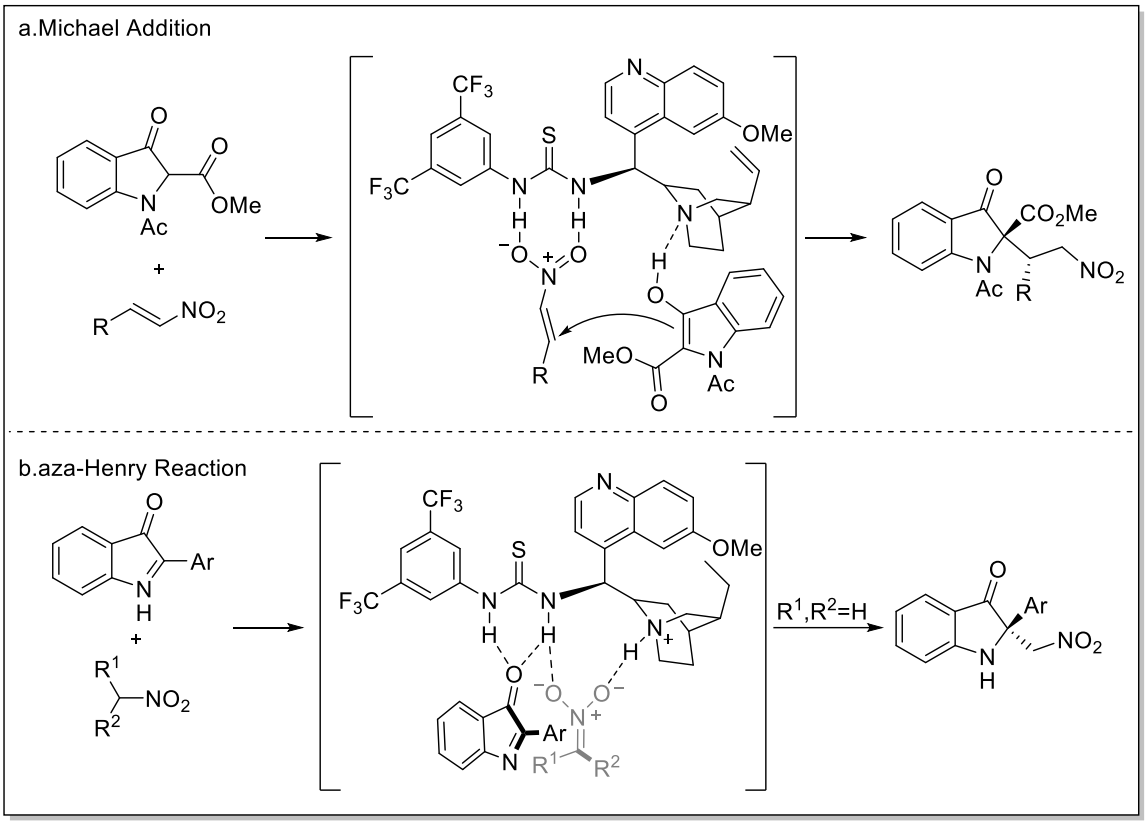

Scheme 4.8. Chiral Thiourea-catalyzed Asymmetric Formation of 2,2-Disubstituted-3-oxindole

4.3. Initial Screening to Optimize Oxidative Coupling of 3-Oxindole

Because of the structural importance of 3-oxindoles bearing a C-2 quaternary center in many natural products (**Figure 4.1**), the Kozlowski group began to develop an efficient strategy for constructing the corresponding 2,2-disubstituted indolin-3-one via transition metal-catalyzed aerobic oxidative coupling pathway. Due to the easy access of 2-substituted-3-oxindoles (**Scheme 4.9**),[4e] as well as its favorable oxidation potential and possible transformations of the 2-ester group into versatile synthetic moieties,[2c,6] 2-carboxymethyl-3-oxindole (**4.1**) was adopted as our initial substrate.

[6] Karadeolian, A.; Kerr, M. A. Total Synthesis of (+)-Isatisine A. *Angew. Chem. Int. Ed.* **2010**, *49* (6), 1133–1135.

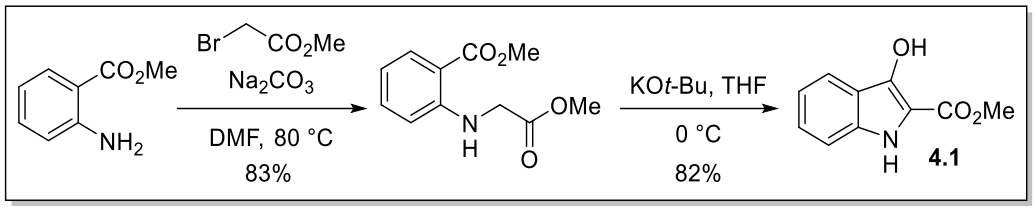

Scheme 4.9. Preparation of 2-Carboxymethyl-3-oxindole (**4.1**)

Additional transition metals with salan/salen ligand complexes have proven to be effective for aerobic oxidative coupling of phenols.[7] To find the optimal catalyst, a previous student, Erin Nigro, conducted HTE screening with 24 different combinations of 7 metals (Co,Cu, Cr, Ru, Mn, Fe, V) and 5 Schiff base ligands (**Figure 4.2**). Copper was found to be the most effective transition metal for the transformation, with the diphenyl salan (**Figure 4.2, D**) being the most efficient complex.

[7] Lee, Y. E.; Cao, T.; Torruellas, C.; Kozlowski, M. C. Selective Oxidative Homo- and Cross-Coupling of Phenols with Aerobic Catalysts. *J. Am. Chem. Soc.* **2014**, *136* (19), 6782–6785.

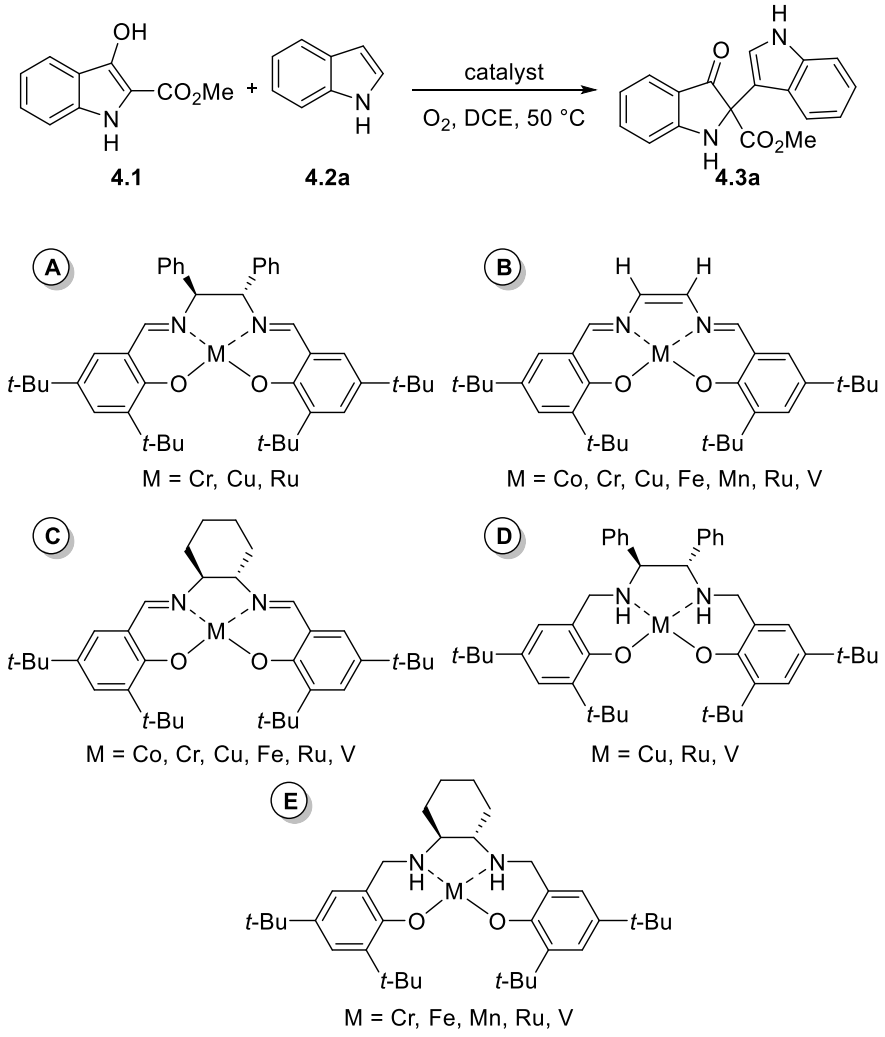

Figure 4.2. HTE Screening with Metal-Schiff Base Complexes

With the optimal conditions, Erin Nigro tested the reaction with selected indoles and pyrroles from a previous report[4e] to prove the concept of the oxidative cross-coupling of 3-oxindole (**Table 4.1**). The 3-oxindole oxidative cross-coupling reaction was catalyzed by Cu-Salan-Ph (**Table 4.1**) with molecular oxygen as an oxidant. Across the table, coupling efficiency was shown to be similar to that of Baran or even better. For example, coupling with **4.2n** yielded 65% coupled product instead of 18% yield according to the Baran's protocol.[4e]

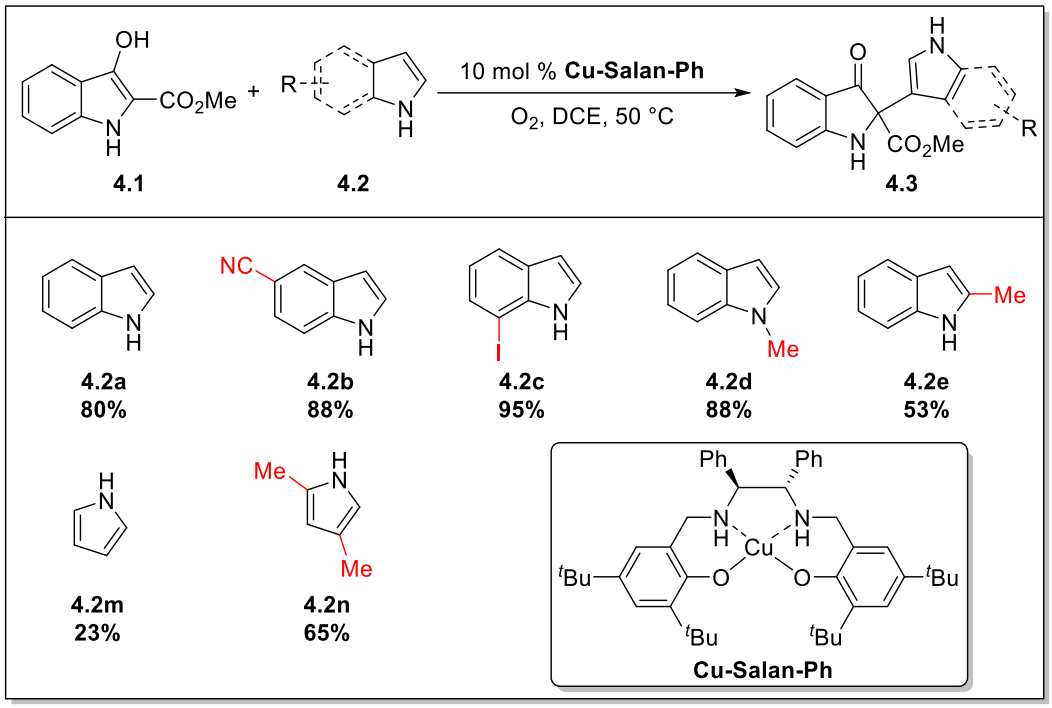

Table 4.1. Scope of 3-Oxindole Oxidative Cross-coupling by Erin Nigro

4.4. Scope of 3-Oxindole Oxidative Cross-coupling

Success with Erin's preliminary results enabled expansion of the substrate scope with a diverse array of substituted indoles and other heterocycles, including electron-rich arenes and is shown in **Table 4.2–3**. The Cu-catalyzed oxidative coupling condition tolerated both electron-rich and electron-deficient indoles (**Table 4.2**). Indoles with aromatic groups at the C-2 position afforded facile quaternary formation of 3-oxindoles in good to excellent yield (**4.2f–h**). Notably, our method shows much higher efficiency with electron-rich substrate (**4.2k**, 84%) compared to the previously reported protocol (17%).[4e] Furthermore, other improved results were able to be obtained such as **4.2i** (62% vs 48%[4e]) and **4.2j** (94% vs 66%[4e]).

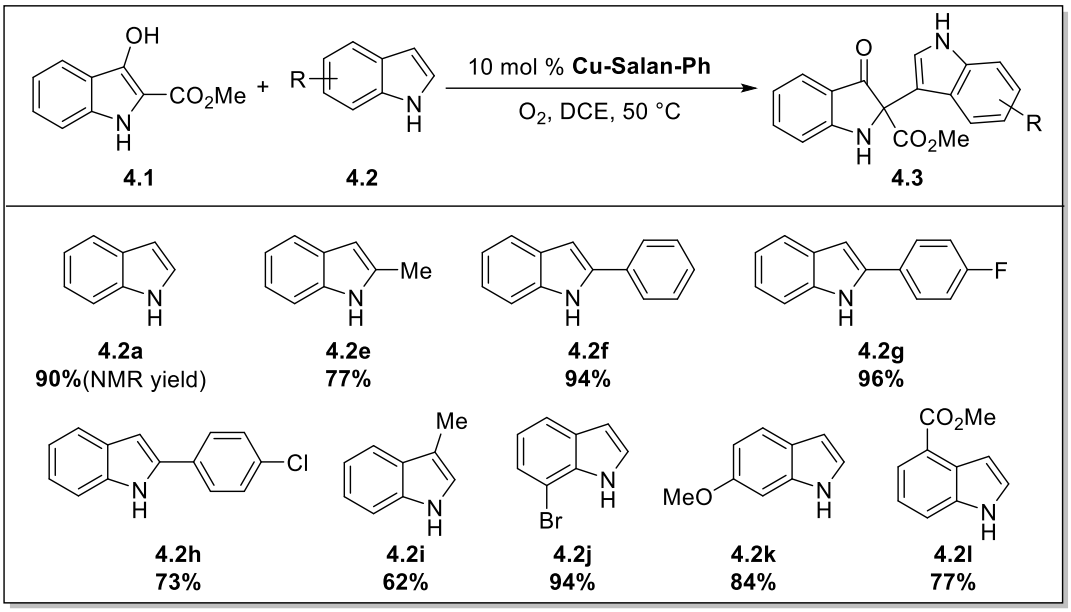

Table 4.2. Expanded Substrate Scope of Indoles

Beyond the indoles, our attention moved onto other heterocycles to construct C-2 quaternary 3-oxindoles (**Table 4.3**). Pyrrole smoothly converted to form a C-2 quaternary center. However, electronics plays a key role in pyrroles and furans that affect the transformation. In the case of pyrroles, a dramatic decrease in reactivity was observed in electron-poor substrate **4.2o**. Interestingly, *N*-substituted pyrroles (**4.2p, 4.2q**) were able to couple with 3-oxindole in moderate yields (37–60%). The electron-donor substituted furan (**4.2r**) also produced 2,2-disubstituted indolin-3-one in 68% yield. Based on the observations in **Table 4.3**, we hypothesized that the oxidative coupling with 3-oxindole could be applied to the electron-rich aryl substrates, such as aniline or anisole. Representative electron-rich substrates, *N,N*-dialkylated aniline (**4.2s, 4.2t**) and 1,3,5-trimethoxybenzene (**4.2u**), allowed extension of the reaction scope into simple arene moieties in good yields (52–66%).

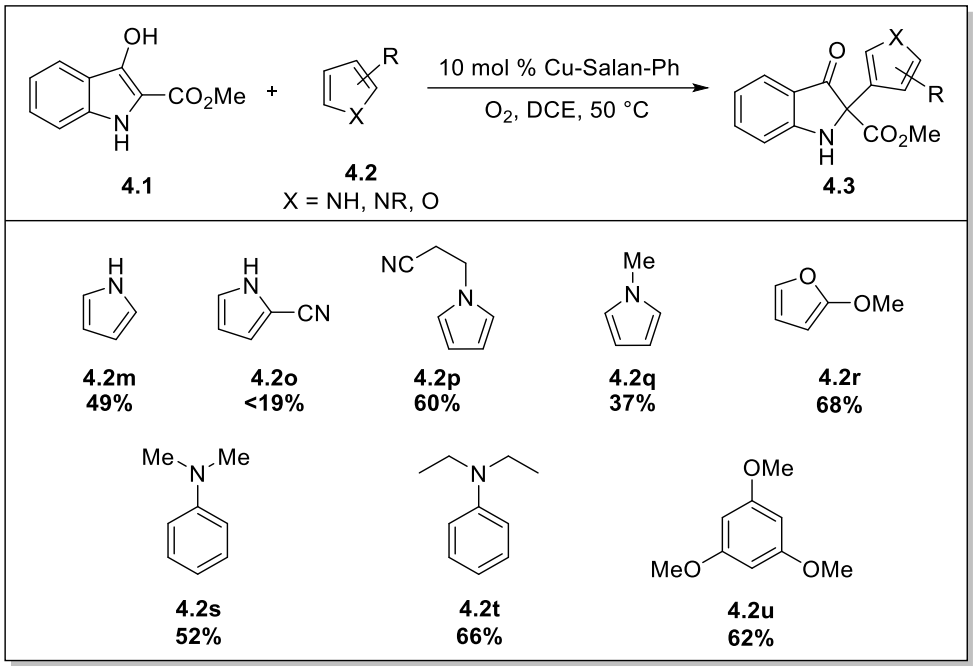

Table 4.3. Other Heterocycles and Electron-rich Aryl Scope of 3-Oxindole Coupling

4.5. Attempts to Develop Asymmetric Oxidative Coupling

After thorough studies on substrate scope, our attention turned to formation of the quaternary carbon in asymmetric fashion. Due to easy access to the asymmetric salan ligand, initial attempts examined the optimized catalyst, which was copper metal incorporated with an enantiomerically pure salan-Ph ligand (**Table 4.4**). Unfortunately, no asymmetric induction occurred with the chiral Cu-salan complex (entry 1). In addition, the bis(oxazoline) scaffold produced racemic C-2 quaternary indolin-3-one, and slowing the reaction did not improve the outcome (entries 2–3). Using a vanadium catalyst, which had been shown to be effective in asymmetric oxidative phenol coupling,[8] however, gave a promising result (entry 5, 26% ee).

[8] Kang, H.; Lee, Y. E.; Reddy, P. V. G.; Dey, S.; Allen, S. E.; Niederer, K. A.; Sung, P.; Hewitt, K.; Torruellas, C.; Herling, M. R.; et al. Asymmetric Oxidative Coupling of Phenols and Hydroxycarbazoles. *Org. Lett.* **2017**, *19* (20), 5505–5508.

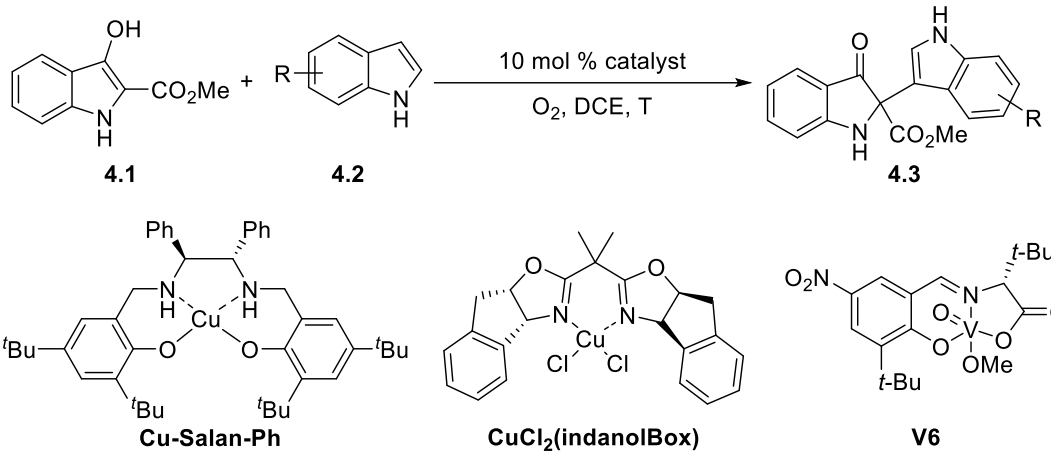

Entry	Indole	Catalyst	Temperature (°C)	ee (%)
1	**4.2f**	Cu-salan-Ph	50	0
2	**4.2f**	$CuCl_2$(indanolBox)	50	0
3	**4.2f**	$CuCl_2$(indanolBox)	25	0
4	**4.2d**	$CuCl_2$(indanolBox)	25	0
5	**4.2f**	**V6**	0	26

Table 4.4. Initial Attempts at Asymmetric Oxidative Coupling of 3-Oxindole

To improve the selectivity, further investigation was conducted concerning the steric environment around the reaction center by changing to larger ester groups at the C-2 position of the 3-oxindole. 2-*tert*-Butylcarboxyl-3-oxindole (**4.4**) was synthesized by means of Cossy's Ir-catalyzed hydrogen transfer protocol (**Scheme 4.10**).[9]

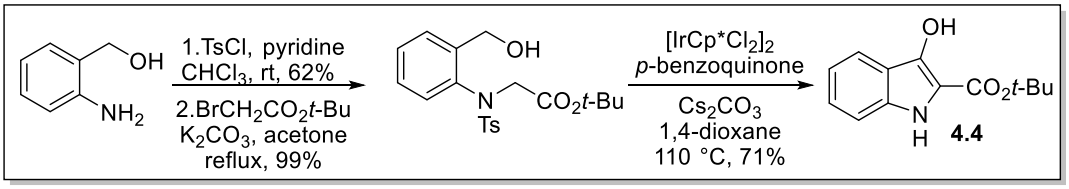

Scheme 4.10. Preparation of 2-*tert*-Butylcarboxylated-3-oxindole (**4.4**)

[9] Anxionnat, B.; Gomez Pardo, D.; Ricci, G.; Rossen, K.; Cossy, J. Iridium-Catalyzed Hydrogen Transfer: Synthesis of Substituted Benzofurans, Benzothiophenes, and Indoles from Benzyl Alcohols. *Org. Lett.* **2013**, *15* (15), 3876–3879.

With 2-*tert*-buylcarboxylated 3-oxindole (**4.4**) and 2-phenylindole (**4.2f**), the same levels of selectivity were produced in the presence of **V6** at room temperature (**Table 4.5**, entry 1). Improved enantiomeric excess was observed at lower temperatures (entry 2). Next, we utilized other amino acids and vanadium sources to study the effect of catalyst scaffold. Introducing smaller groups than *tert*-butyl at the amino acid branch resulted in slightly decreased selectivity (entry 5,6). Notably, varying enantioselectivity was detected depending on the vanadium source. A larger alkoxy–substituted vanadium catalyst engendered slightly higher selectivity (entry 3). Vanadium fluoride turned out to be the optimal group, and use of LiCl as an additive futher increased the selectivity (entry 4). Based on the improved results, we speculated that the sterics around the reaction center would be the key to induce a highly enantioselctive transformation.

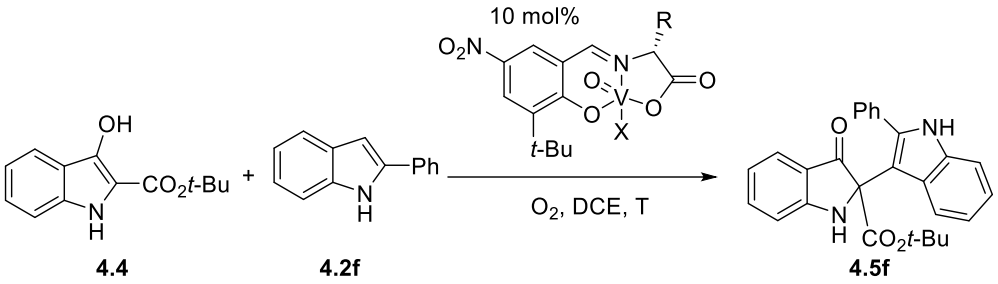

4.4 **4.2f** **4.5f**

Entry	R	X	Temperature (°C)	ee (%)
1	*t*-Bu	OMe (**V6**)	25	26
2	*t*-Bu	OMe (**V6**)	0	40
3	*t*-Bu	O*i*-Pr (**V7**)	25	44
4	*t*-Bu	F (**V8**)	25	48(52)[a]
5	Bn	OMe (**V6**)	25	30
6	CH_2(2-naphthyl)	F (**V8**)	25	20

[a]0.5 equiv LiCl added as an additive

Table 4.5. Optimization with 2-*tert*-Butylcarboxylated Indolin-3-one

An adamantyl ester at C-2 was next chosen (**4.6**) according this hypothesis. In accordance with our hypothesis, it promoted the enantioselectivity in 68% ee (**Table 4.6**, entry 1). Additional modification was undertaken with a number of solvents, revealing that halogenated solvents are more effective with respect to both reactivity and selectivity (entry 2–5). The highest selectivity was obtained in chloroform (entry 5, 74% ee).

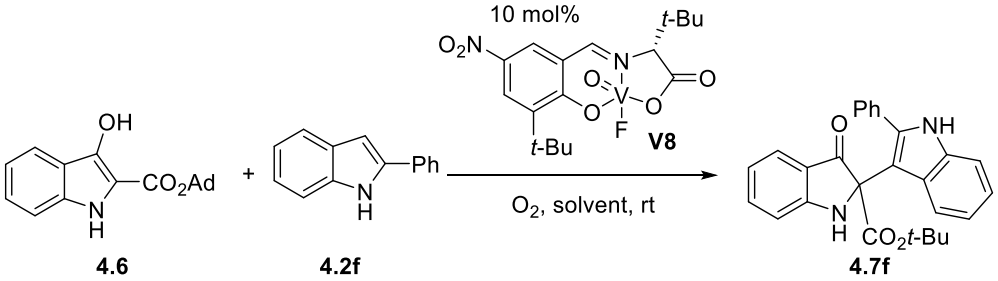

4.6 **4.2f** **4.7f**

Entry	Solvent	Yield (%)	ee (%)
1	1,2-dichloroethane	77	68
2	toluene	47	46
3	CH_2Cl_2	75	60
4	1,2-dichlorobenzene	72	54
5	$CHCl_3$	66	74

Table 4.6. Optimization with 2-Adamantylcarboxylated Indolin-3-one

4.6. Conclusions and Future Directions

In summary, Cu-catalyzed oxidative cross-coupling of 3-oxindole has been accomplished under aerobic conditions, and the protocol allowed access to a larger scope of 2,2-disubstituted indolin-3-ones bearing synthetically useful heterocycles such as indoles, pyrroles and furan. In addition, promising levels of the asymmetric transformation also has been developed with an asymmetric vanadium catalyst.

Future work is required to tackle further selectivity improvement on the asymmetric

transformation and to perform the mechanistic investigation of this oxidative cross-coupling reaction. We plan to explore additives to enhance enantioselectivity. Inspired by previous asymmetric methods to synthesize C-2 quaternary indolin-3-ones,[5] an array of bifunctionalized thioureas bearing enantio-enriched cinchonidine moieties would be the initial additive candidates.

4.4 Experimental Section

General Considerations

Unless otherwise noted, all non-aqueous reactions were carried out under an atmosphere of dry N_2 in dried glassware. When necessary, solvents and reagents were dried prior to use. THF was distilled from sodium benzophenone ketyl. CH_2Cl_2, $ClCH_2CH_2Cl$, and toluene were distilled from CaH_2. High throughput experiments were performed at the Penn/Merck High Throughput Experimentation Laboratory at the University of Pennsylvania. The screens were analyzed by HPLC by addition of an internal standard.

Analytical thin layer chromatography (TLC) was performed on EM Reagents 0.25 mm silica-gel 254-F plates. Visualization was accomplished with UV light. Chromatography was performed using a forced flow of the indicated solvent system on EM Reagents Silica Gel 60 (230-400 mesh). When necessary, the column was pre-washed with 1% Et_3N in the eluent system. ^1H NMR spectra were recorded on a 500 MHz spectrometer. Chemical shifts are reported in ppm from tetramethylsilane (0 ppm) or from the solvent resonance ($CDCl_3$ 7.26 ppm, DMSO-d_6 3.58 ppm, acetone-d_6 2.05 ppm, DMF-d_7 2.50 ppm, CD_3CN 1.94 ppm, CD_2Cl_2 5.32 ppm). Data are reported as follows: chemical shift, multiplicity (s = singlet, d = doublet, t = triplet, q = quartet, br = broad, m = multiplet), coupling constants, and number of protons. Decoupled ^{13}C NMR spectra were recorded at 125 MHz. IR spectra were taken on an FT-IR spectrometer. Accurate mass measurement analyses

were conducted via time-of-flight mass analyzer GCMS with electron ionization (EI) or via time-of-flight mass analyzer LCMS with electrospray ionization (ESI). The signals were measured against an internal reference of perfluorotributylamine for EI-GCMS and leucine enkephalin for ESI-LCMS. The instrument was calibrated and measurements were made using neutral atomic masses; the mass of the electron removed or added to create the charged species is not taken into account. Low resolution LCMS data were obtained by use of a UPLC system with a SQD mass analyzer equipped with electrospray ionization. Circular dichroism and UV-vis spectroscopy measurements carried out at ambient temperature (23 C). Enantiomeric excesses were determined using analytical HPLC with UV detection at 254 nm. Analytical Chiralpak columns (4.6 mm x 250 mm, 5 μm) from Daicel were used. Optical rotations were measured on a polarimeter with a sodium lamp.

General procedure: oxidative 3-oxindole coupling. To a microwave vial was added 3-oxindole (0.13 mmol), indole (0.13 mmol) and Cu-salan-Ph catalyst (9.3 mg, 0.01 mmol). The vial was sealed with a septum and the 1,2-dichloroethane (1.3 mL) was added. After degassing and purging with O_2 three times, the vial was sealed with a microwave vial cap and was stirred at 50 ^{o}C for 20 h. Upon completion, the reaction mixture was then directly chromatographed using silica gel.

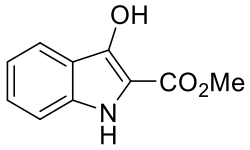

Methyl 3-hydroxy-1*H*-indole-2-carboxylate (4.1). Following the literature protocol, the product was obtained as a yellow solid (1.74 g). Spectral data were in agreement with those reported.[4e]

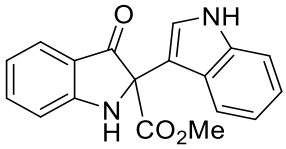

Methyl 2-(1*H*-indol-3-yl)-3-oxoindoline-2-carboxylate (4.2a). Following the **General Procedure** for 22 h, the product was obtained as a yellow solid in 90% NMR yield (50 mg, 82% isolated yield). Spectral data were in agreement with those reported.[4e]

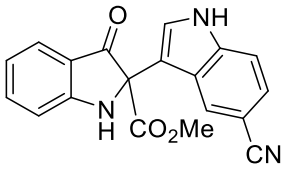

Methyl 2-(5-cyano-1*H*-indol-3-yl)-3-oxoindoline-2-carboxylate (4.2b). Following the **General Procedure** for 16 h, the product was obtained as a yellow solid (39 mg) in 88% yield. Spectral data were in agreement with those reported.[4e]

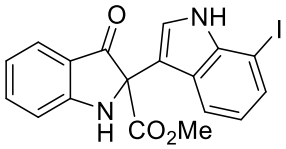

Methyl 2-(7-iodo-1*H*-indol-3-yl)-3-oxoindoline-2-carboxylate (4.2c). Following the **General Procedure** for 16 h, the product was obtained as a yellow solid (58 mg) in 95% yield. $\mathbf{R_f}$ = 0.27 (EtOAc:Hexanes = 1:2): **^{1}H NMR** (500 MHz, $CDCl_3$) δ 8.35 (br s, 1H), 7.68 (d, *J* = 8.0 Hz, 1H), 7.62 (d, *J* = 8.0 Hz, 1H), 7.55–7.50 (m, 2H), 7.48 (d, *J* = 2.0 Hz, 1H), 7.00 (d, *J* = 8.5 Hz, 1H), 6.93 (t, *J* = 7.5 Hz, 1H), 6.86 (t, *J* = 8.0 Hz, 1H), 5.76 (br s, 1H), 3.80 (s, 3H); **^{13}C NMR** (125 MHz, $CDCl_3$) δ 194.4, 168.8, 161.1, 138.3, 138.0, 131.4, 125.6, 124.0, 122.0, 120.6, 120.0, 119.8, 113.6, 113.2, 77.0, 72.6, 53.9, 29.8; **IR** (neat) 3348, 2920, 2850, 1731, 1693, 1611, 1485, 1466, 1428, 1323, 1291, 1230, 1150, 1101, 1083, 1050, 971 cm^{-1}; **HRMS** (ESI-TOF) calcd for $C_{18}H_{14}IN_2O_3$ $[M+H]^+$ 433.0049, found 433.0045.

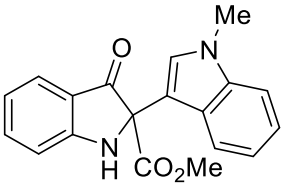

Methyl 2-(1-methyl-1*H*-indol-3-yl)-3-oxoindoline-2-carboxylate (4.2d). Following the **General Procedure** for 19 h, the product was obtained as a yellow solid (45 mg) in 88% yield. Spectral data were in agreement with those reported.[4e]

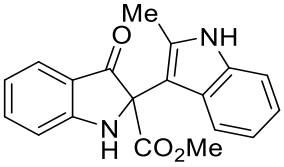

Methyl 2-(2-methyl-1*H*-indol-3-yl)-3-oxoindoline-2-carboxylate (4.2e). Following the **General Procedure** for 19 h, the product was obtained as a yellow solid (58 mg) in 77% yield. Spectral data were in agreement with those reported.[4e]

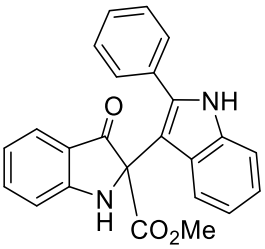

Methyl 3-oxo-2-(2-phenyl-1*H*-indol-3-yl)indoline-2-carboxylate (4.2f). Following the **General Procedure** for 19 h, the product was obtained as a yellow solid (47 mg) in 94% yield. $\mathbf{R_f}$ = 0.27 (EtOAc:Hexanes = 1:2): **^{1}H NMR** (500 MHz, $CDCl_3$) δ 8.31 (br s, 1H), 7.62 (d, *J* = 7.5 Hz, 1H), 7.54 (t, *J* = 7.5 Hz, 1H), 7.42 (d, *J* = 7.5 Hz, 2H), 7.37–7.34 (m, 3H), 7.30 (d, *J* = 8.0 Hz, 1H), 7.19–7.14 (m, 2H), 7.01 (t, *J* = 7.5 Hz, 1H), 6.96 (d, *J* = 8.5 Hz, 1H), 6.93 (t, *J* = 7.5 Hz, 1H), 5.61 (br s, 1H), 3.18 (s, 3H); **^{13}C NMR** (125 MHz, $CDCl_3$) δ 195.2, 168.8, 160.9, 138.1, 138.0, 135.5, 132.5, 129.6, 128.8, 128.4, 126.8, 125.3, 122.7, 120.6, 120.4, 120.2, 119.7, 113.4, 111.2, 108.2, 73.3, 53.2; **IR** (neat) 3345, 3052, 2950,

2920, 1697, 1613, 1485, 1457, 1431, 1323, 1292, 1233, 1196, 1150, 1099, 1072, 1013, 972, 896 cm^{-1}; **HRMS** (ESI-TOF) calcd for $C_{24}H_{19}N_2O_3$ $[M+H]^+$ *m/z* = 383.1396; found 383.1414.

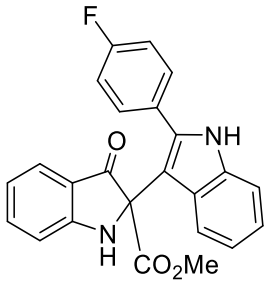

Methyl 2-(2-(4-fluorophenyl)-1*H*-indol-3-yl)-3-oxoindoline-2-carboxylate (4.2g). Following the **General Procedure** for 21 h, the product was obtained as a yellow solid (50 mg) in 96% yield. $\mathbf{R_f}$ = 0.4 (EtOAc:Hexanes = 1:2): **^{1}H NMR** (500 MHz, $CDCl_3$) δ 8.35 (br s, 1H), 7.57 (d, *J* = 8.0 Hz, 1H), 7.54 (td, *J* = 8.0, 1.0 Hz, 1H), 7.38-7.35 (m, 2H), 7.29 (d, *J* = 8.0 Hz, 1H), 7.21 (d, *J* = 8.0 Hz, 1H), 7.16 (td, *J* = 8.0, 1.0 Hz, 1H), 7.03 (td, *J* = 8.0, 1.0 Hz, 1H), 6.99–6.95 (m, 3H), 6.93 (t, *J* = 7.5 Hz, 1H), 5.62 (br s, 1H), 3.30 (s, 3H); **^{13}C NMR** (125 MHz, $CDCl_3$) δ 195.2, 168.9, 163.0 (d, *J* = 249 Hz), 160.7, 138.1, 136.8, 135.5, 131.6 (d, *J* = 8.3 Hz), 128.7, 126.9, 125.3, 122.8, 120.7, 120.5, 120.3, 119.5, 115.4 (d *J* = 21.5 Hz), 113.4, 111.4, 108.5, 73.1, 53.4; **IR** (neat) 3354, 2951, 1704, 1613, 1498, 1457, 1434, 1325, 1294, 1225, 1197, 1157, 1094, 1015, 974, 894 cm^{-1}; **HRMS** (ESI-TOF) calcd for $C_{24}H_{18}FN_2O_3$ $[M+H]^+$ 401.1301, found 401.1306.

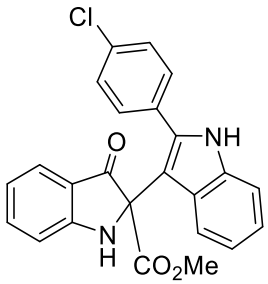

Methyl 2-(2-(4-chlorophenyl)-1*H*-indol-3-yl)-3-oxoindoline-2-carboxylate (4.2h).

Following the **General Procedure** for 22 h, the product was obtained as a yellow solid (40 mg) in 73% yield. $\mathbf{R_f}$ = 0.40 (EtOAc:Hexanes = 1:2): **^{1}H NMR** (500 MHz, $CDCl_3$) δ 8.27 (br s, 1H), 7.59 (d, *J* = 8.0 Hz, 1H), 7.55 (td, *J* = 8.5, 1.5 Hz, 1H), 7.35 (d, *J* = 8.5 Hz, 2H), 7.32 (d, *J* = 8.0 Hz, 1H), 7.28 (d, *J* =8.0 Hz, 2H), 7.22 (d, *J* = 8.5 Hz, 1H), 7.18 (td, *J* = 8.0, 1.0 Hz, 1H), 7.03 (td, *J* = 8.0, 1.0 Hz, 1H), 6.98 (d, *J* = 8.0 Hz, 1H), 6.95 (t, *J* = 7.5 Hz, 1H), 5.59 (br s, 1H), 3.32 (s, 3H); **^{13}C NMR** (125 MHz, $CDCl_3$) δ 195.0, 168.9, 160.6, 138.1, 136.6, 135.6, 135.0, 131.1, 130.9, 128.6, 126.9, 125.3, 123.0, 120.8, 120.6, 120.3, 119.6, 113.4, 111.3, 108.8, 73.1, 53.4; **IR** (neat) 3341, 3052, 2950, 1698, 1610, 1483, 1467, 1456, 1432, 1324, 1293, 1234, 1196, 1150, 1089, 1014, 973, 893, cm^{-1}; **HRMS** (ESI-TOF) calcd for $C_{24}H_{18}ClN_2O_3$ $[M+H]^+$ 417.1006, Found 417.1012.

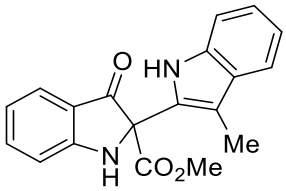

Methyl 2-(3-methyl-1*H*-indol-2-yl)-3-oxoindoline-2-carboxylate (4.2i). Following the **General Procedure** for 19 h, the product was obtained as a yellow solid (26 mg) in 62% yield. Spectral data were in agreement with those reported.[4e]

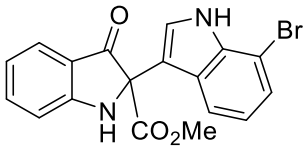

Methyl 2-(7-bromo-1*H*-indol-3-yl)-3-oxoindoline-2-carboxylate (4.2j). Following the **General Procedure** for 22 h, the product was obtained as a brown solid (47 mg) in 94% yield. Spectral data were in agreement with those reported.[4e]

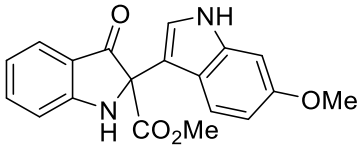

Methyl 2-(6-methoxy-1*H*-indol-3-yl)-3-oxoindoline-2-carboxylate (4.2k). Following the **General Procedure** for 21 h, the product was obtained as a yellow solid (37 mg) in 84% yield. Spectral data were in agreement with those reported.[4e]

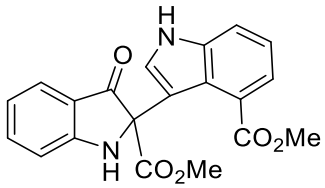

Methyl 3-(2-(methoxycarbonyl)-3-oxoindolin-2-yl)-1*H*-indole-4-carboxylate (4.2l). Following the **General Procedure** for 22 h at 80 °C, the product was obtained as a yellow solid (37 mg) in 77% yield. Spectral data were in agreement with those reported.[4e]

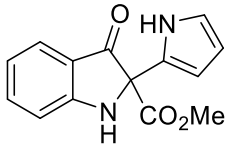

Methyl 3-oxo-2-(1*H*-pyrrol-2-yl)indoline-2-carboxylate (4.2m). Following the **General Procedure** for 15 h, the product was obtained as a brown oil (16 mg) in 49% yield. $\mathbf{R_f}$ = 0.50 (EtOAc:Hexanes = 1:2): **^{1}H NMR** (500 MHz, $CDCl_3$) δ 9.38 (br s, 1H), 7.59 (d, J = 7.5 Hz, 1H), 7.52 (td, J = 8.5, 1.0 Hz, 1H), 7.05 (d, J = 8.5 Hz, 1H), 6.91 (t, J = 7.5 Hz, 1H), 6.83–6.82 (m, 1H), 6.30–6.28 (m, 1H), 6.15–6.14 (m, 1H), 5.61 (br s, 1H), 3.81 (s, 3H); **^{13}C NMR** (125 MHz, $CDCl_3$) δ 193.2, 167.7, 161.7, 138.1, 125.8, 124.9, 120.8, 119.3, 118.9, 113.6, 108.3, 106.3, 71.9, 54.0; **IR** (neat) 3364, 2951, 1733, 1693, 1613, 1486, 1467, 1433, 1324, 1233, 1197, 1153, 1139, 1101, 1028, 1008, 950 cm^{-1}; **HRMS** (ESI-TOF) calcd for $C_{14}H_{12}N_2O_3Na$ $[M+Na]^+$ m/z = 279.0746; found 279.0756.

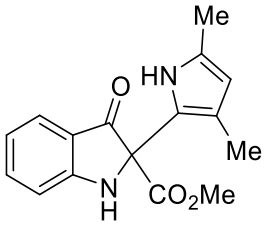

Methyl 2-(3,5-dimethyl-1*H*-pyrrol-2-yl)-3-oxoindoline-2-carboxylate (4.2n). Following the **General Procedure** for 16 h, the product was obtained as a yellow solid (25 mg) in 65% yield. Spectral data were in agreement with those reported.[4e]

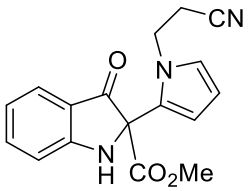

Methyl 2-(1-(2-cyanoethyl)-1*H*-pyrrol-2-yl)-3-oxoindoline-2-carboxylate (4.2p). Following the **General Procedure** for 24 h at 80 °C , the product was obtained as a brown oil (24 mg) in 60% yield. $\mathbf{R_f}$ = 0.25 (EtOAc:Hexanes = 1:2): **^{1}H NMR** (500 MHz, $CDCl_3$) δ 7.67 (dd, *J* = 8.0, 1.0 Hz, 1H), 7.57 (td, *J* = 8.0, 1.0 Hz, 1H), 7.04 (d, *J* = 8.0 Hz, 1H), 7.00 (t, *J* = 7.5 Hz, 1H), 6.80 (t, *J* = 2.0 Hz, 1H), 6.16 (d, *J* = 2.0 Hz, 2H), 5.55 (s, 1H), 3.98–3.89 (m, 2H), 3.88 (s, 3H), 2.73 (t, *J* = 7.0 Hz, 2H); **^{13}C NMR** (125 MHz, $CDCl_3$) δ 193.8, 168.1, 160.4, 138.4, 125.7, 125.6, 124.0, 121.5, 119.6, 117.4, 113.8, 111.7, 109.0, 73.1, 54.3, 43.3, 20.0; **IR** (neat) 3347, 2952, 2250, 1737, 1704, 1613, 1483, 1468, 1434, 1323, 1292, 1234, 1198, 1151, 1085, 1045, 979, 894 cm^{-1}; **HRMS** (ESI-TOF) calcd for $C_{17}H_{16}N_3O_3$ $[M+H]^+$ *m/z* = 310.1192; found 310.1180.

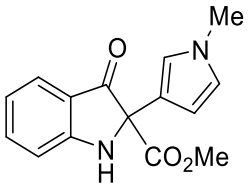

Methyl 2-(1-methyl-1*H*-pyrrol-3-yl)-3-oxoindoline-2-carboxylate (4.2q). Following the

General Procedure for 18 h, the product was obtained as a yellow solid (13 mg) in 37% yield. $\mathbf{R_f}$ = 0.5 (EtOAc:Hexanes = 1:2): **^{1}H NMR** (500 MHz, $CDCl_3$) δ 7.67 (d, *J* = 7.5 Hz, 1H), 7.53 (td, *J* = 7.5, 1.2 Hz, 1H), 7.00 (d, *J* = 8.0 Hz, 1H), 6.95 (t, *J* = 7.5 Hz, 1H), 6.61–6.60 (m, 1H), 6.13–6.12 (m, 1H), 6.07–6.06 (m, 1H), 5.50 (br s, 1H), 3.87 (s, 3H), 3.42 (s, 3H); **^{13}C NMR** (125 MHz, $CDCl_3$) δ 193.8, 168.4, 160.6, 138.1, 126.2, 125.5, 125.4, 120.9, 119.9, 113.8, 110.8, 107.2, 73.1, 54.2, 35.0; **IR** (neat) 3352, 2950, 1737, 1703, 1613, 1484, 1467, 1434, 1322, 1306, 1291, 1246, 1230, 1196, 1150, 1092, 1027 cm^{-1}; **HRMS** (ESI-TOF) calcd for $C_{15}H_{15}N_2O_3$ $[M+H]^+$ 271.1083, found 271.1095.

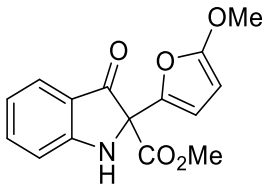

Methyl 2-(5-methoxyfuran-2-yl)-3-oxoindoline-2-carboxylate (4.2r). Following the **General Procedure** for 21 h, the product was obtained as a brown oil (26 mg) in 68% yield. $\mathbf{R_f}$ = 0.33 (EtOAc:Hexanes = 1:2): **^{1}H NMR** (500 MHz, $CDCl_3$) δ 7.64 (d, *J* = 8.0 Hz, 1H), 7.51 (td, *J* = 8.0, 1.0 Hz, 1H), 6.97 (d, *J* = 8.0 Hz, 1H), 6.91 (t, *J* = 8.0 Hz, 1H), 6.37 (d, *J* = 3.5 Hz, 1H), 5.56 (br s, 1H), 5.12 (d, *J* = 3.5 Hz, 1H), 3.81 (s, 6H); **^{13}C NMR** (125 MHz, $CDCl_3$) δ 191.8, 167.1, 162.0, 161.2, 138.4, 138.2, 125.7, 120.7, 119.4, 113.7, 110.7, 80.5, 71.6, 58.0, 54.2; **IR** (neat) 3358, 2920, 1744, 1705, 1613, 1576, 1486, 1467, 1435, 1367, 1324, 1295, 1258, 1199, 1152, 1099, 1027, 962 cm^{-1}; **HRMS** (ESI-TOF) calcd for $C_{15}H_{14}NO_5$ $[M+H]^+$ 288.0872, found 288.0860.

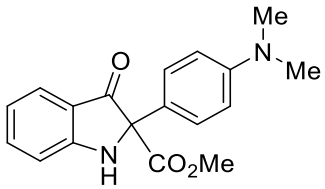

Methyl 2-(4-(dimethylamino)phenyl)-3-oxoindoline-2-carboxylate (4.2s). Following

the **General Procedure** for 19 h at 80 °C, the product was obtained as a yellow solid (21 mg) in 52% yield. $\mathbf{R_f}$ = 0.4 (EtOAc:Hexanes = 1:2): **^{1}H NMR** (500 MHz, $CDCl_3$) δ 7.60 (d, *J* = 8.0 Hz, 1H), 7.57 (d, *J* = 9.0 Hz, 2H), 7.49 (td, *J* = 7.0, 1.0 Hz, 1H), 7.01 (d, *J* = 8.0 Hz, 1H), 6.88 (t, *J* = 7.5 Hz, 1H), 6.70 (d, *J* = 9.0 Hz, 2H), 5.61 (br s, 1H), 3.80 (s, 3H), 2.93 (s, 6H); **^{13}C NMR** (125 MHz, $CDCl_3$) δ 194.5, 169.0, 160.8, 150.8, 137.6, 127.2, 125.6, 123.4, 120.3, 120.0, 113.3, 112.5, 74.8, 53.8, 40.6; **IR** (neat) 3352, 2950, 2922, 1740, 1698, 1608, 1519, 1485, 1468, 1434, 1355, 1322, 1291, 1233, 1195, 1166, 1152, 1096, 1061, 984 cm^{-1}; **HRMS** (ESI-TOF) calcd for $C_{18}H_{19}N_2O_3$ $[M+H]^+$ 311.1396, Found 311.1408.

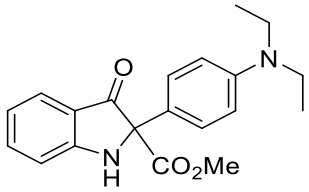

Methyl 2-(4-(diethylamino)phenyl)-3-oxoindoline-2-carboxylate (4.2t). Following the **General Procedure** for 18 h at 80 °C, the product was obtained as a yellow solid (29 mg) in 66% yield. $\mathbf{R_f}$ = 0.50 (EtOAc:Hexanes = 1:2): **^{1}H NMR** (500 MHz, $CDCl_3$) δ 7.60 (d, *J* = 7.5 Hz, 1H), 7.51 (d, *J* = 9.0 Hz, 2H), 7.48 (td, *J* = 7.5, 1.0 Hz, 1H), 7.00 (d, *J* = 8.0 Hz, 1H), 6.87 (t, *J* = 7.5 Hz, 1H), 6.63 (d, *J* = 9.0 Hz, 2H), 5.60 (br s, 1H), 3.80 (s, 3H), 3.33 (q, *J* = 7.0 Hz, 4H), 1.13 (t, *J* = 7.0 Hz, 6H); **^{13}C NMR** (125 MHz, $CDCl_3$) δ 194.7, 169.1, 160.8, 148.0, 137.6, 127.4, 125.6, 124.3, 120.2, 120.0, 113.3, 111.6, 74.9, 53.7, 44.5, 12.7; **IR** (neat) 3355, 2970, 1738, 1697, 1607, 1589, 1517, 1486, 1468, 1452, 1434, 1355, 1321, 1291, 1264, 1231, 1194, 1153, 1089 cm^{-1}; **HRMS** (ESI-TOF) calcd for $C_{20}H_{23}N_2O_3$ $[M+H]^+$ 339.1709, Found 339.1719.

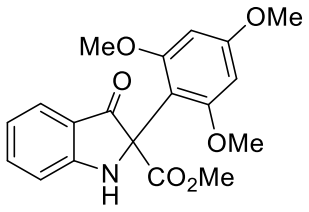

Methyl 3-oxo-2-(2,4,6-trimethoxyphenyl)indoline-2-carboxylate (4.2u). Following the **General Procedure** for 24 h at 80 °C, the product was obtained as a yellow solid (29 mg) in 62% yield. $\mathbf{R_f}$ = 0.13 (EtOAc:Hexanes = 1:2): **^{1}H NMR** (500 MHz, $CDCl_3$) δ 7.66 (d, *J* = 8.0 Hz, 1H), 7.45 (t, *J* = 8.0 Hz, 1H), 6.95 (d, *J* = 8.0 Hz, 1H), 6.89 (t, *J* = 7.5 Hz, 1H), 6.13 (s, 2H), 5.47 (br s, 1H), 3.77 (s, 6H), 3.65 (s, 6H); **^{13}C NMR** (125 MHz, $CDCl_3$) δ 195.1, 169.8, 161.7, 160.2, 159.4, 136.7, 124.7, 120.9, 120.0, 113.5, 108.5, 92.5, 72.3, 56.0, 55.6, 53.6; **IR** (neat) 3353, 2948, 1716, 1605, 1587, 1484, 1468, 1435, 1417, 1322, 1226, 1204, 1152, 1126, 1093, 1057, 1029, 993 cm^{-1}; **HRMS** (ESI-TOF) calcd for $C_{19}H_{20}NO_6$ $[M+H]^+$ 358.1291 Found: 358.1281.

Asymmetric oxidative 3-oxindole coupling

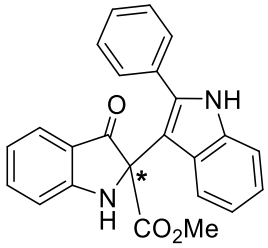

Methyl 3-oxo-2-(2-phenyl-1*H*-indol-3-yl)indoline-2-carboxylate (4.2f). Following the **General Procedure** using **V6** (5.8 mg, 0.01 mmol) as a catalyst for 18 h at 0 °C, the product was obtained as a yellow solid in 26% ee. $\mathbf{[\alpha]_D^{22}}$ = –14.3 (c 0.15, 26% ee, CH_2Cl_2); **Chiral HPLC**: Chiralpak IA column (20% *i*-PrOH/hexanes, 1 mL/min) t_R(*1*) = 29.3 min, t_R(*2*) = 34.5 min.

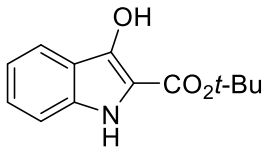

Methyl 3-hydroxy-1*H*-indole-2-carboxylate (4.4). Following a literature protocol, the product was obtained as a light yellow oil (335 mg). Spectral data were in agreement with those reported.[9]

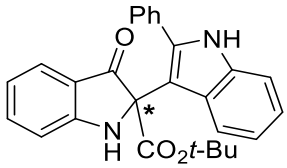

***tert*-Butyl 3-oxo-2-(2-phenyl-1*H*-indol-3-yl)indoline-2-carboxylate (4.5f).** Following the **General Procedure** using **V8** (4.7 mg, 0.01 mmol, 0.1 equiv) as a catalyst for 20 h at room temperature, the product was obtained as a yellow solid (41 mg) in 87% yield (48% ee). $\mathbf{R_f}$ = 0.21 (EtOAc:Hexanes = 1:4): **^{1}H NMR** (500 MHz, $CDCl_3$) δ 8.13 (br s, 1H), 7.62 (d, *J* = 7.5 Hz, 1H), 7.51 (td, *J* = 8.5, 1.5 Hz, 1H), 7.47–7.45 (m, 2H), 7.40–7.36 (m, 4H), 7.33 (d, *J* = 8.0 Hz, 1H), 7.16 (td, *J* = 8.0, 1.0 Hz, 1H), 7.03 (td, *J* = 8.0, 1.0 Hz, 1H), 6.92 (td, *J* = 8.0, 0.5 Hz, 1H), 6.89 (d, *J* = 8.0 Hz, 1H), 5.40 (br s, 1H), 1.10 (s, 9H); **^{13}C NMR** (125 MHz, $CDCl_3$) δ 195.6, 167.2, 160.7, 137.63, 137.57, 135.8, 133.6, 129.5, 128.8, 128.7, 127.2, 125.3, 122.7, 120.7, 120.5, 120.4, 120.2, 113.2, 111.1, 108.2, 83.6, 74.2, 27.4; **IR** (neat) 3350, 2925, 1703, 1614, 1485, 1458, 1393, 1368, 1322, 1251, 1149, 1099, 1073, 1013, 893 cm^{-1}; **HRMS** (ESI-TOF) calcd for $C_{27}H_{25}N_2O_3$ $[M+H]^+$ 425.1865, found 425.1855.; $\mathbf{[\alpha]_D^{22}}$ = +23.7 (c 0.35, 48% ee, CH_2Cl_2); **Chiral HPLC**: Chiralpak IA column (25% *i*-PrOH/hexanes, 1 mL/min) t_R(*1*) = 10.7 min, t_R(*2*) = 11.7 min.

Synthesis of 2-Adamantyl carboxylated 3-oxindole (4.6)

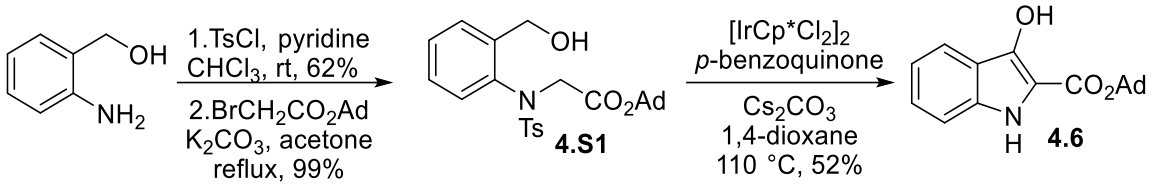

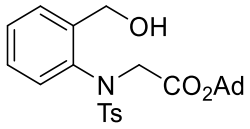

Adamantan-1-yl *N*-(2-(hydroxymethyl)phenyl)-*N*-tosylglycinate (4.S1). Following literature procedure using $BrCH_2CO_2Ad$ (2.96 g, 10.8 mmol, 1.5 equiv)[10] for 23 h,[9] the product was obtained as a pale yellow oil (3.35 g) in 99% yield. $\mathbf{R_f}$ = 0.22 (EtOAc:Hexanes = 1:4): **^{1}H NMR** (500 MHz, $CDCl_3$) δ 7.52 (dd, *J* = 7.5, 1.5 Hz, 1H), 7.46 (d, *J* = 8.5 Hz, 2H), 7.29 (td, *J* = 7.5, 1.0 Hz, 1H), 7.24 (d, *J* = 8.5 Hz, 2H), 7.08 (td, *J* = 7.5, 1.5 Hz, 1H), 6.49 (d, *J* = 7.5 Hz, 1H), 4.97 (d, *J* = 10.0 Hz, 1H), 4.73 (d, *J* = 10.0 Hz, 1H), 4.35 (d, *J* = 17.0 Hz, 1H), 3.91 (d, *J* =16.5 Hz, 1H), 3.69 (br s, 1H), 2.40 (s, 3H), 2.09 (br s, 3H), 1.98 (br s, 6H), 1.58 (br s, 6H); **^{13}C NMR** (125 MHz, $CDCl_3$) δ 167.5, 144.3, 142.7, 138.3, 134.2, 131.4, 129.6, 129.3, 128.4, 128.3, 127.5, 83.0, 61.7, 54.2, 41.1, 36.0, 30.9, 21.6; **IR** (neat) 3450, 2911, 1728, 1454, 1351, 1275, 1205, 1186, 1159, 1125, 1090, 1049, 1015, 865 cm^{-1}; **HRMS** (ESI-TOF) calcd for $C_{26}H_{32}NO_5S$ $[M+H]^+$ 470.2001 Found: 470.2009.

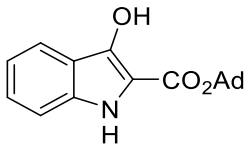

Adamantan-1-yl 3-hydroxy-1*H*-indole-2-carboxylate (4.6). Following the literature procedure for 18 h,[9] the product was obtained as a light yellow powder (397 mg) in 52% yield. $\mathbf{R_f}$ = 0.75 (EtOAc:Hexanes = 1:4): **^{1}H NMR** (500 MHz, $(CD_3)_2CO$) δ 9.89 (br s, 1H),

[10] Dang, H.-S.; Elsegood, M. R. J.; Kim, K.-M.; Roberts, B. P. Radical-Chain Reductive Alkylation of Electron-Rich Alkenes Mediated by Silanes in the Presence of Thiols as Polarity-Reversal Catalysts. *J. Chem. Soc. [Perkin 1]* **1999**, No. 15, 2061–2068.

8.18 (br s, 1H), 7.64 (d, *J* = 8.0 Hz, 1H), 7.35 (d, *J* = 8.5 Hz, 1H), 7.28 (td, *J* = 8.0, 1.0 Hz, 1H), 7.03 (td, *J* = 7.5, 1.0 Hz, 1H), 2.29 (br s, 6H), 2.21 (br s, 3H), 1.73 (br s, 6H); **^{13}C NMR** (125 MHz, $(CD_3)_2CO$) δ 163.8, 146.8, 136.1, 127.2, 120.2, 119.8, 118.4, 113.2, 110.2, 82.4, 42.4 (3), 36.8 (3), 31.9 (3); **IR** (neat) 3475, 3320, 2906, 2850, 1682, 1581, 1547, 1508, 1493, 1337, 1250, 1230, 1196, 1183, 1125, 1096, 1040, 922 cm^{-1}; **HRMS** (ESI-TOF) calcd for $C_{19}H_{22}NO_3$ $[M+H]^+$ 312.1600 Found: 312.1591.

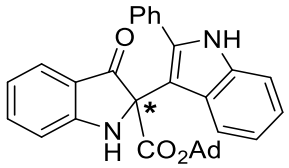

Adamantan-1-yl 3-oxo-2-(2-phenyl-1*H*-indol-3-yl)indoline-2-carboxylate (4.7f). Following the **General Procedure** using **V8** (2.7 mg, 6.4 μmol, 0.1 equiv) as a catalyst in $CHCl_3$ (0.64 mL) for 21 h at room temperature, the product was obtained as a yellow solid (21 mg) in 66% yield (74% ee). **R_f** = 0.20 (EtOAc:Hexanes = 1:4): **^{1}H NMR** (500 MHz, $CDCl_3$) δ 8.24 (br s, 1H), 7.59 (d, *J* = 7.5 Hz, 1H), 7.49 (td, *J* = 7.5, 1.0 Hz, 1H), 7.42–7.40 (m, 3H), 7.36–7.28 (m, 4H), 7.14 (td, *J* = 7.5, 1.0 Hz, 1H), 7.04 (td, *J* = 7.5, 1.0 Hz, 1H), 6.90 (t, *J* = 7.5 Hz, 1H), 6.86 (d, *J* = 8.5 Hz, 1H), 5.42 (br s, 1H), 1.99 (br s, 3H), 1.76 (d, *J* = 11.5 Hz, 3H), 1.69 (d, *J* = 11.0 Hz, 3H), 1.53–1.46 (m, 6H) ; **^{13}C NMR** (125 MHz, $CDCl_3$) δ 195.7, 166.9, 160.6, 137.6, 137.5, 135.7, 133.5, 129.5, 128.7, 128.6, 127.2, 125.2, 122.5, 120.6, 120.4, 120.3, 120.1, 113.2, 111.2, 108.1, 83.6, 74.2, 40.5, 36.0, 30.9; **IR** (neat) 3348, 2910, 1703, 1614, 1484, 1457, 1320, 1291, 1233, 1196, 1150, 1101, 1046, 1013, 963 cm^{-1}; **HRMS** (ESI-TOF) calcd for $C_{33}H_{31}N_2O_3$ $[M+H]^+$ 503.2335 Found: 503.2344; **$[\alpha]_D^{22}$** = +33.7 (c 0.18, 74% ee, CH_2Cl_2); **Chiral HPLC**: Chiralpak IA column (20% *i*-PrOH/hexanes, 1 mL/min) t_R(*1*) = 17.9 min, t_R(*2*) = 25.4 min.

APPENDIX A: SPECTROSCOPIC DATA

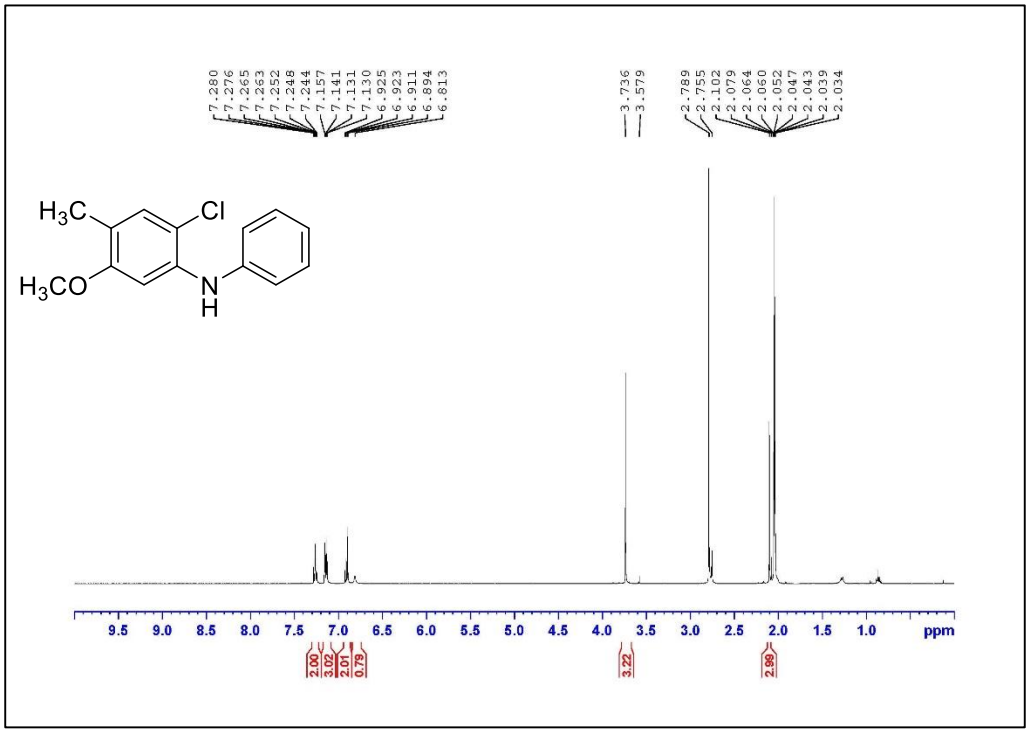

Figure A.1. ^{1}H NMR Spectrum of Compound **1.8a** (500 MHz, acetone-d_6)

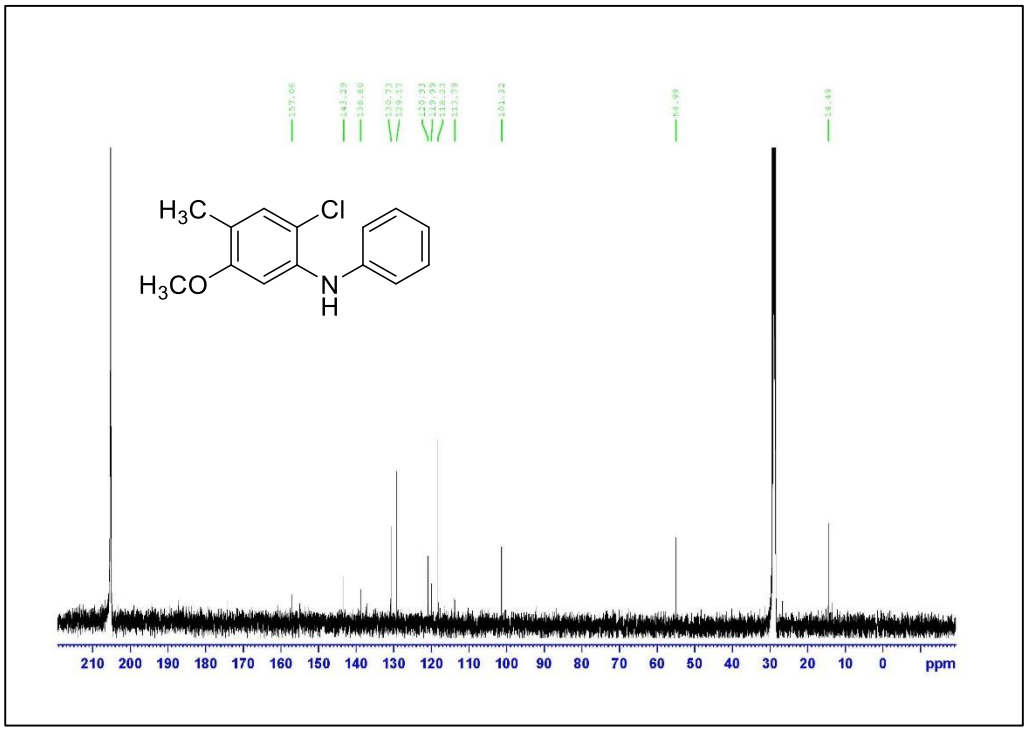

Figure A.2. ^{13}C NMR Spectrum of Compound **1.8a** (125 MHz, acetone-d_6)

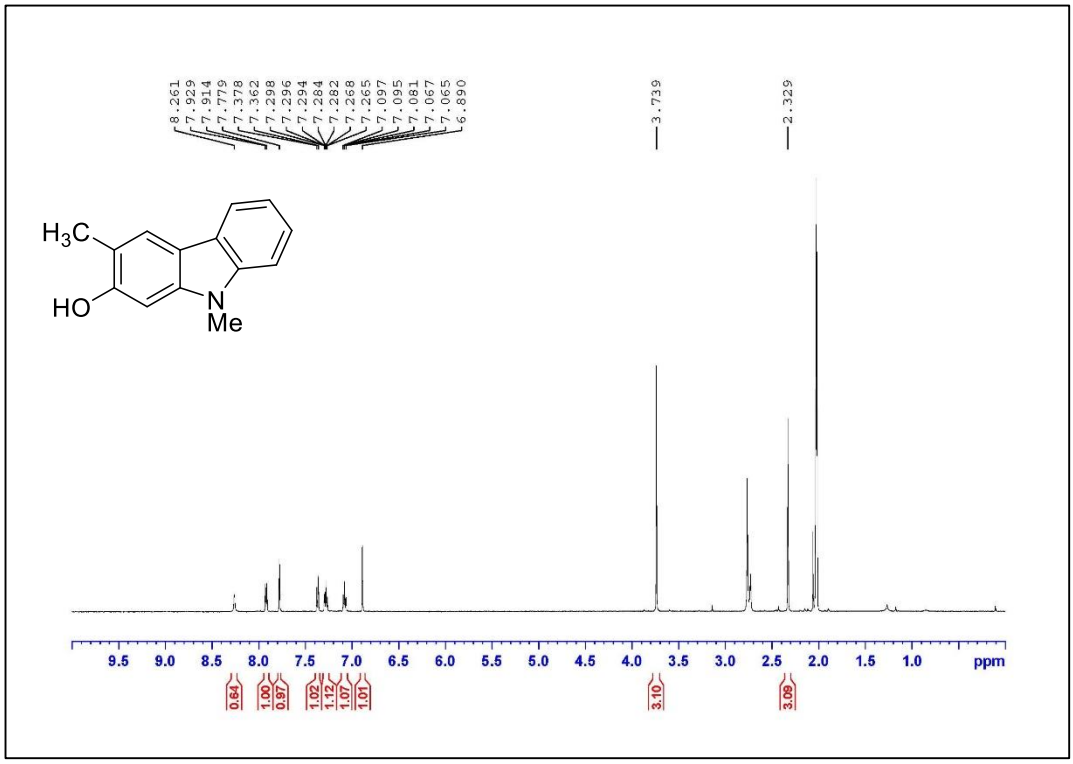

Figure A.3. ^{1}H NMR Spectrum of Compound **1.4b** (500 MHz, acetone-d_6)

오류! 책갈피가 정의되어 있지 않습니다.

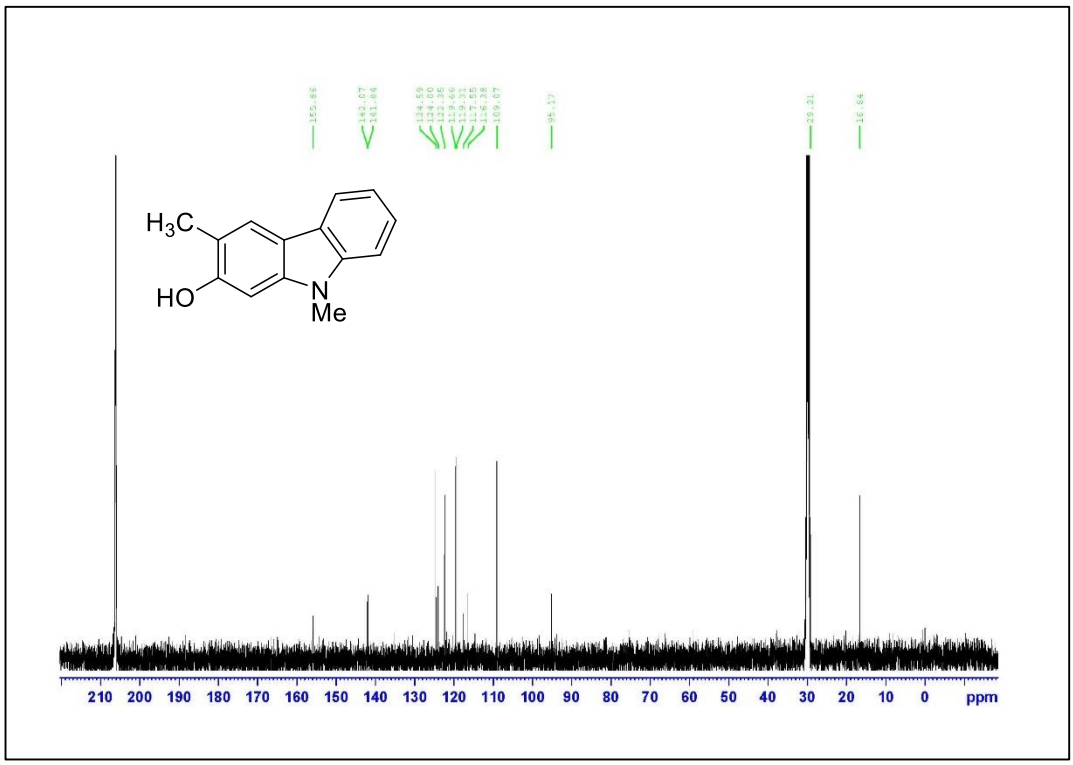

Figure A.4. ^{13}C NMR Spectrum of Compound **1.4b** (125 MHz, acetone-d_6)

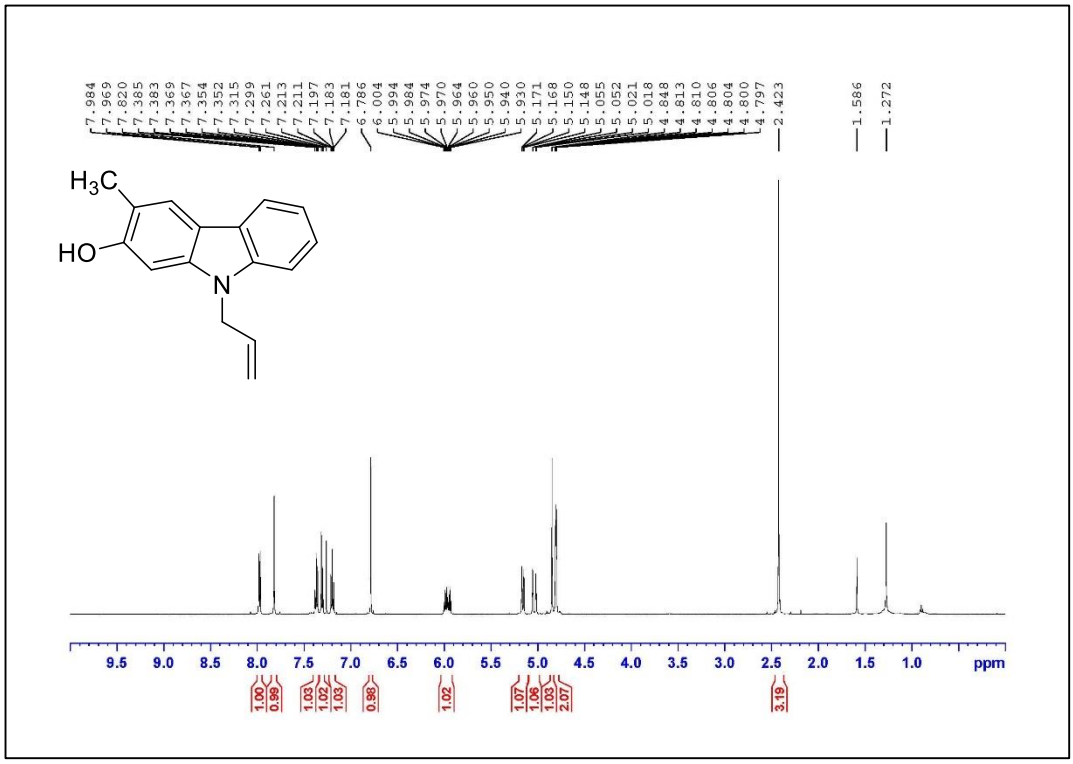

Figure A.5. ^{1}H NMR Spectrum of Compound **1.4c** (500 MHz, $CDCl_3$)

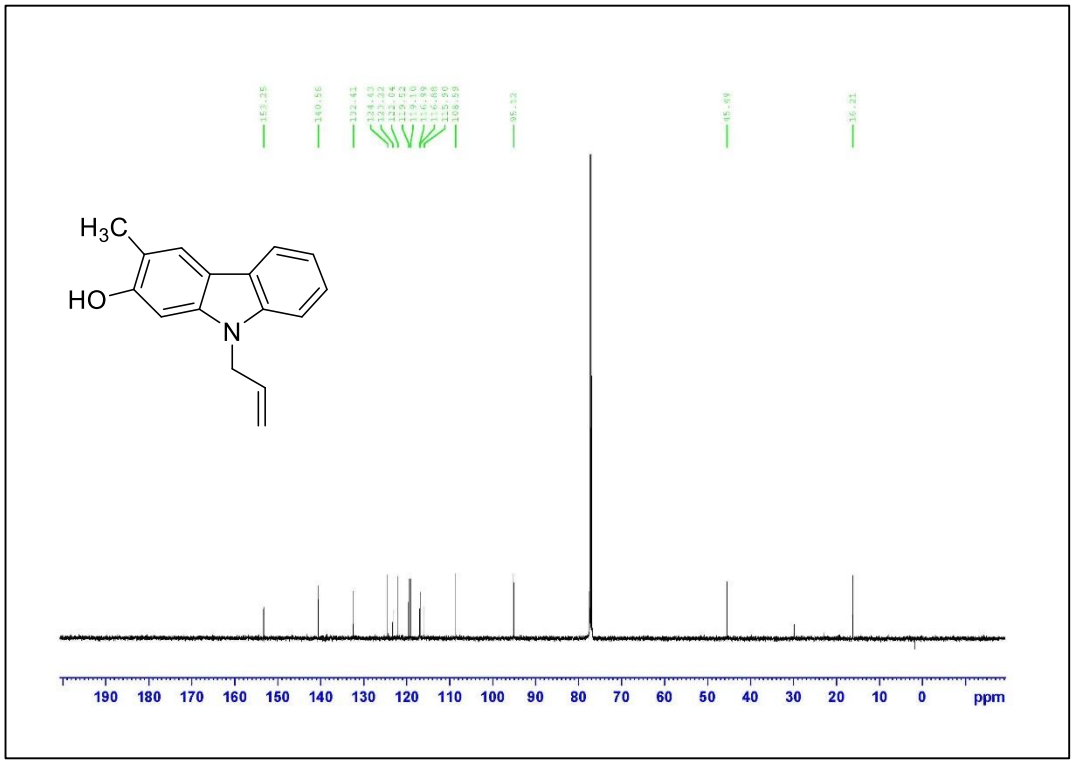

Figure A.6. ^{13}C NMR Spectrum of Compound **1.4c** (125 MHz, $CDCl_3$)

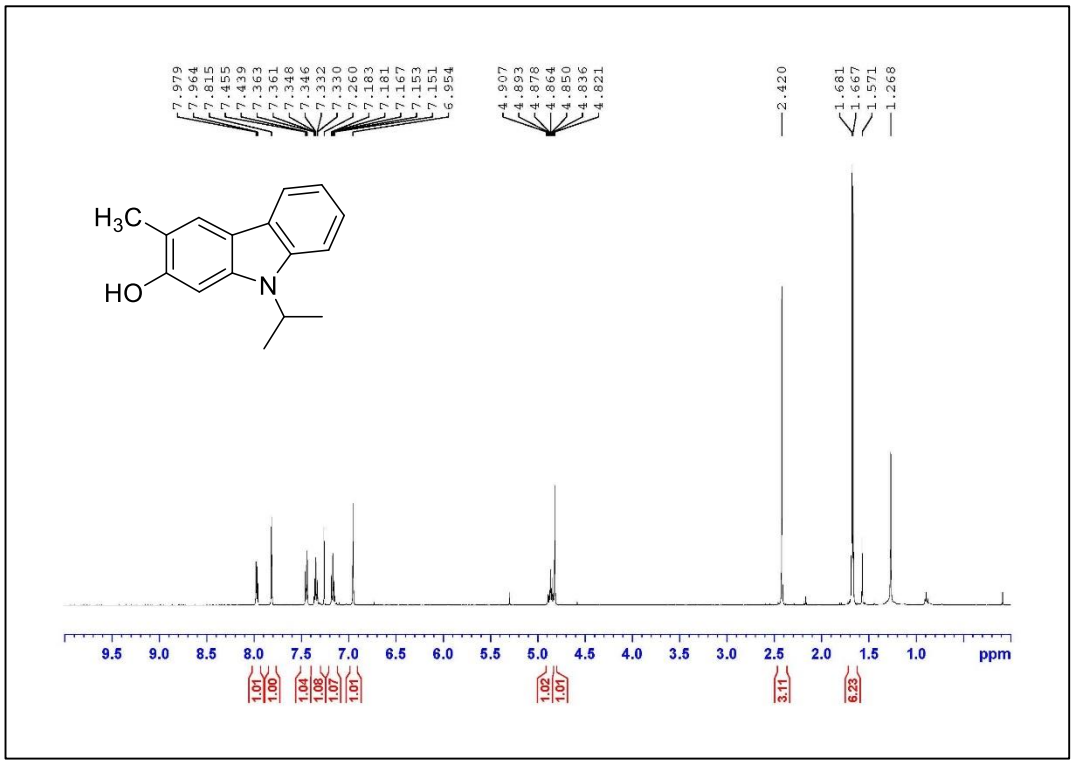

Figure A.7. ^{1}H NMR Spectrum of Compound **1.4d** (500 MHz, $CDCl_3$)

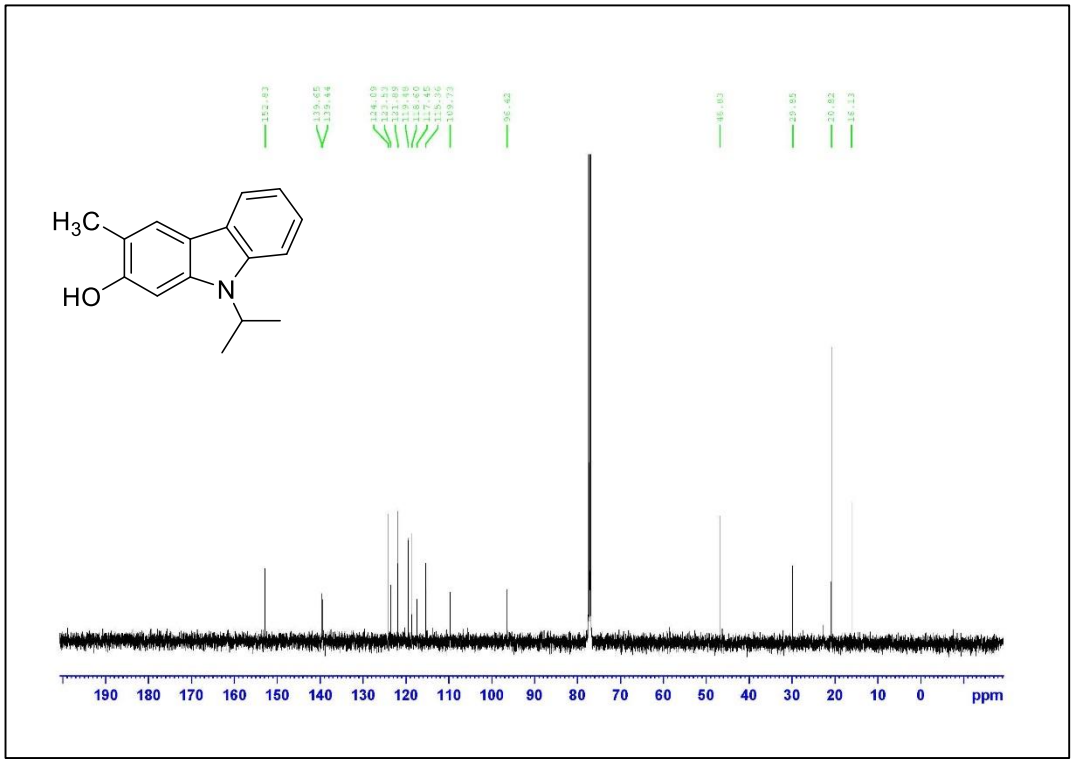

Figure A.8. ^{13}C NMR Spectrum of Compound **1.4d** (125 MHz, $CDCl_3$)

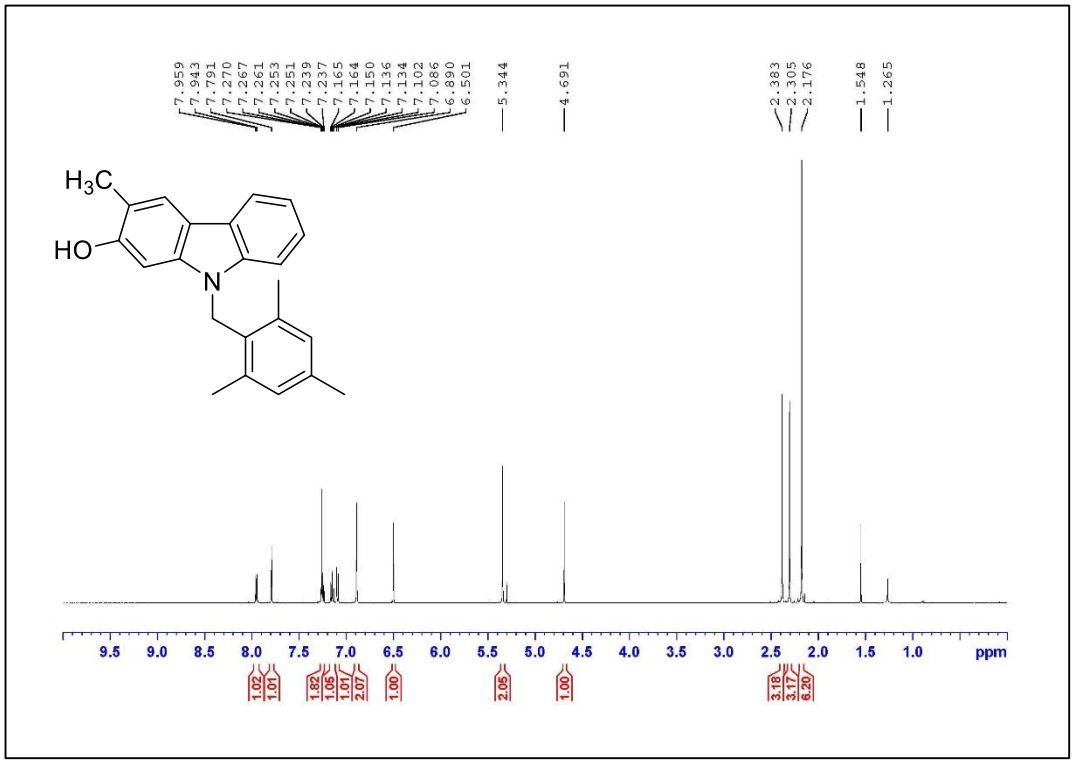

Figure A.9. ^{1}H NMR Spectrum of Compound **1.4e** (500 MHz, $CDCl_3$)

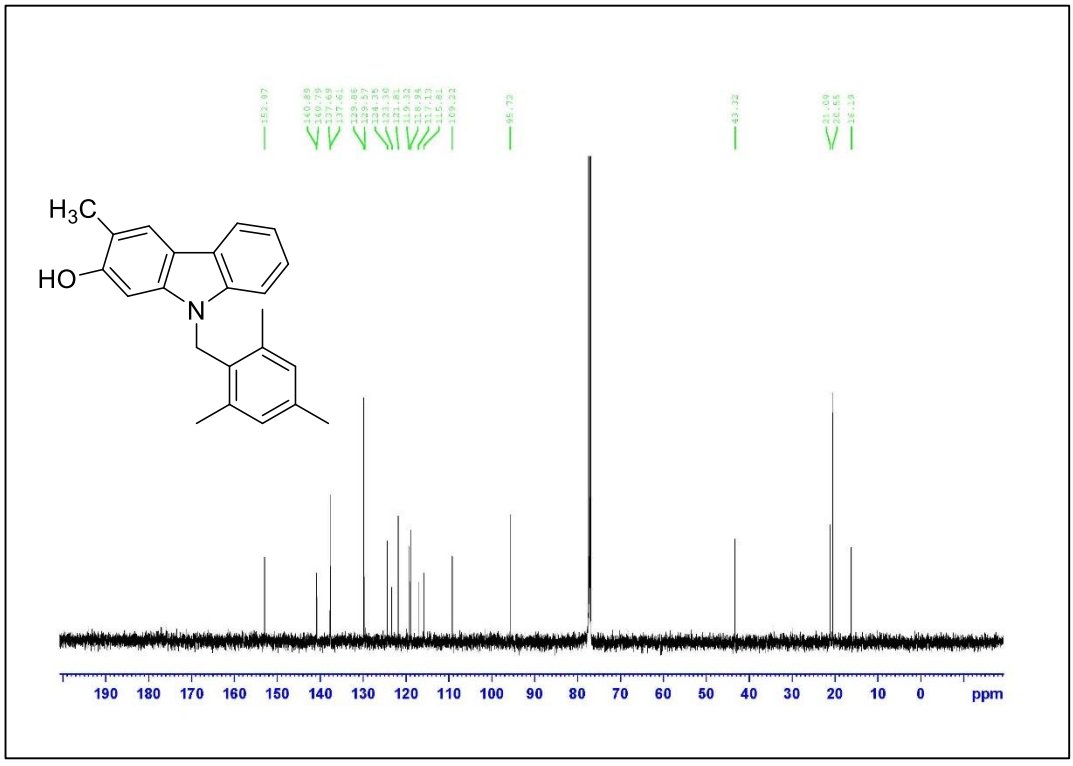

Figure A.10. ^{13}C NMR Spectrum of Compound **1.4e** (125 MHz, $CDCl_3$)

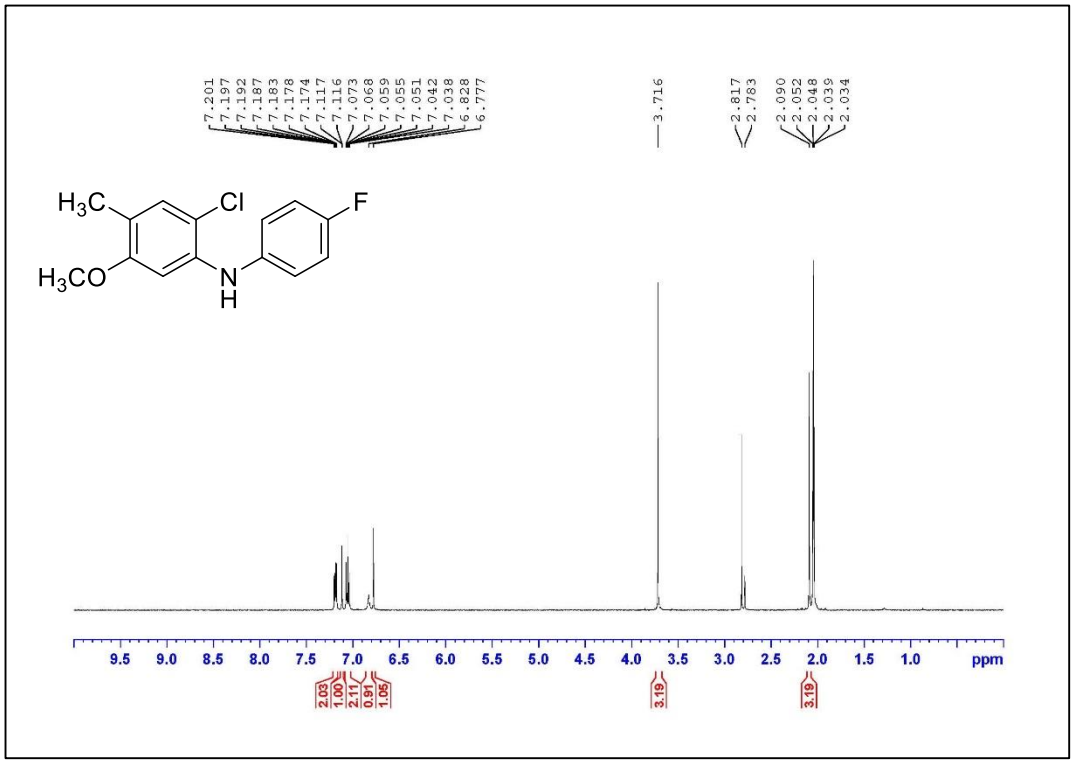

Figure A.11. ^{1}H NMR Spectrum of Compound **1.8f** (500 MHz, acetone-d_6)

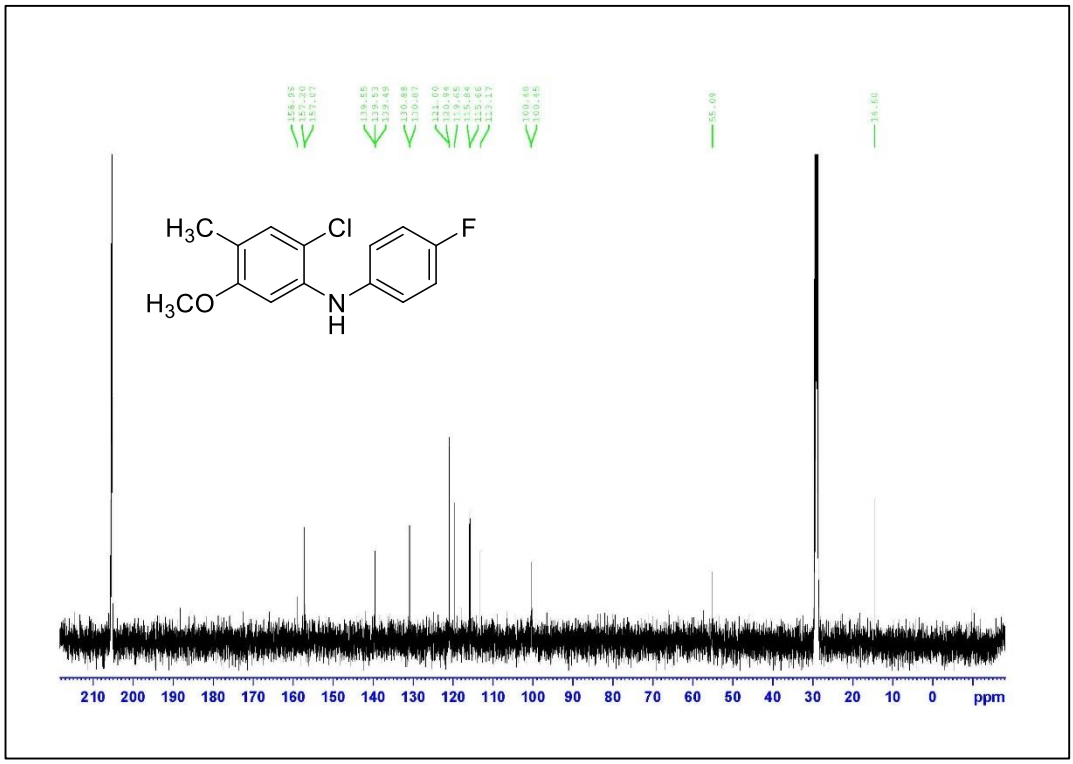

Figure A.12. ^{13}C NMR Spectrum of Compound **1.8f** (125 MHz, acetone-d_6)

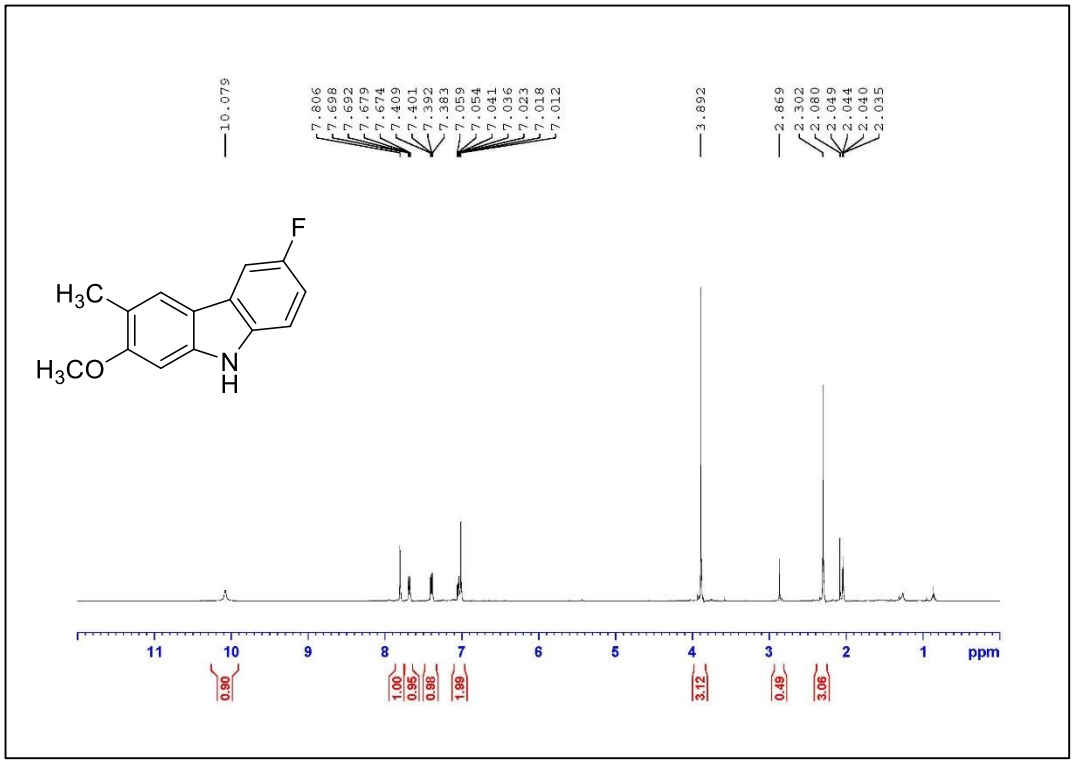

Figure A.13. ^{1}H NMR Spectrum of Compound **1.9f** (500 MHz, acetone-d_6)

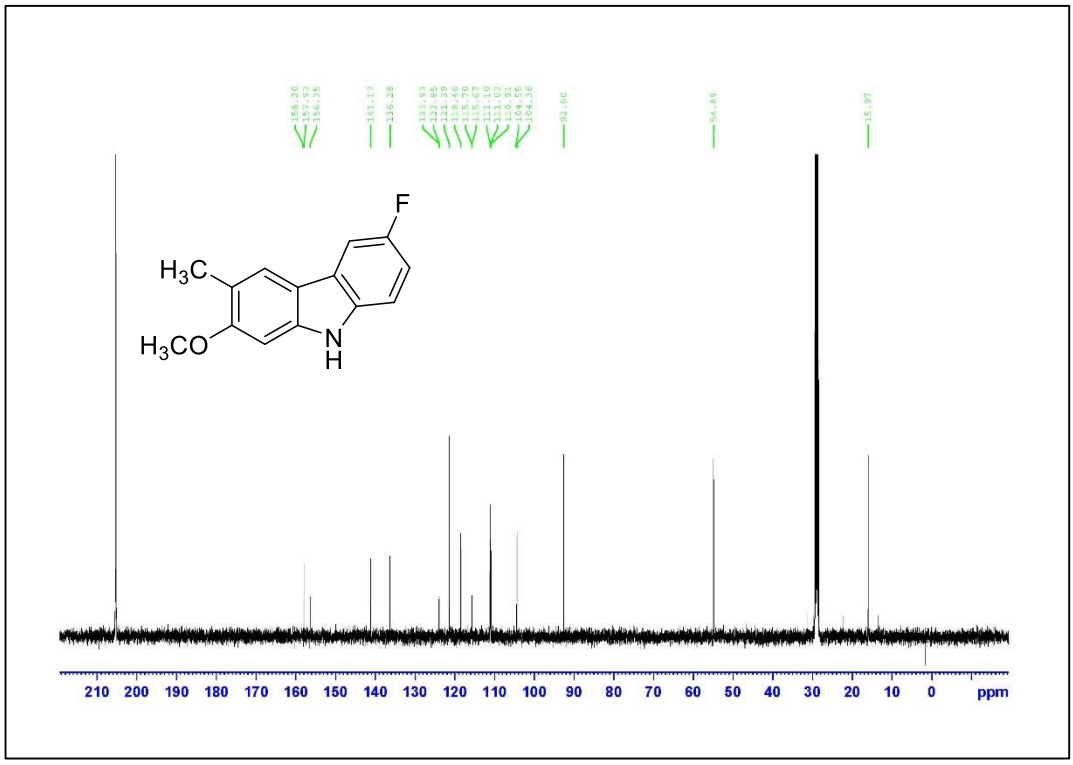

Figure A.14. ^{13}C NMR Spectrum of Compound **1.9f** (125 MHz, acetone-d_6)

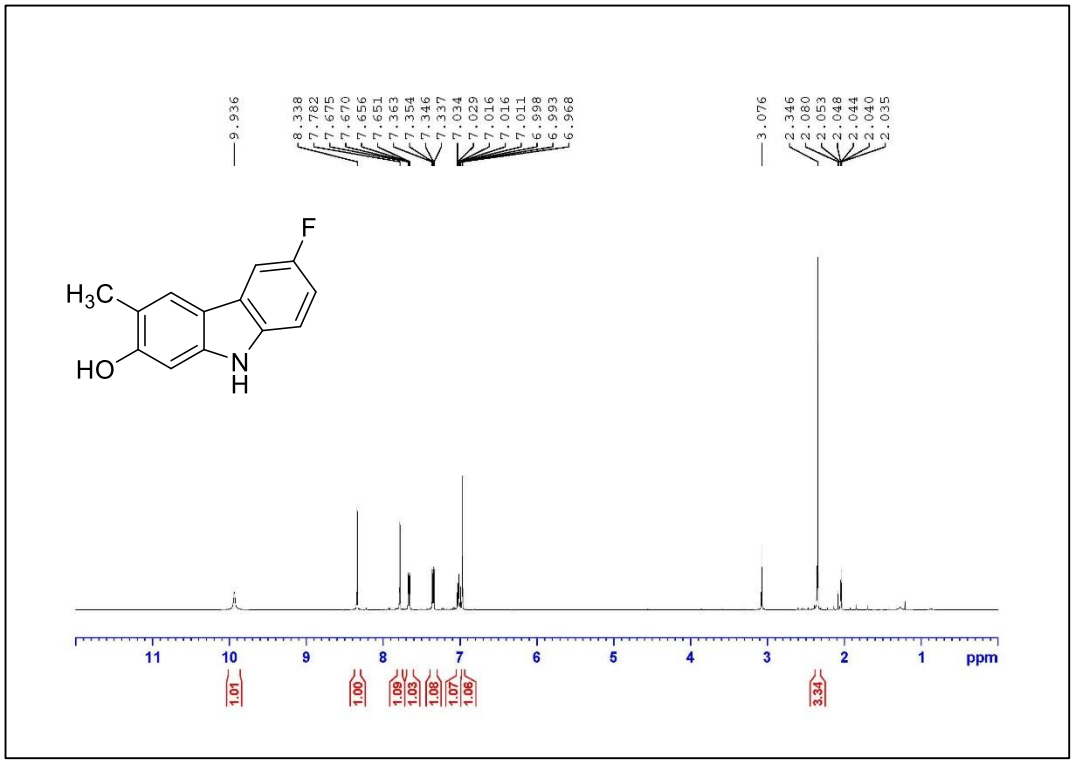

Figure A.15. ^{1}H NMR Spectrum of Compound **1.10f** (500 MHz, acetone-d_6)

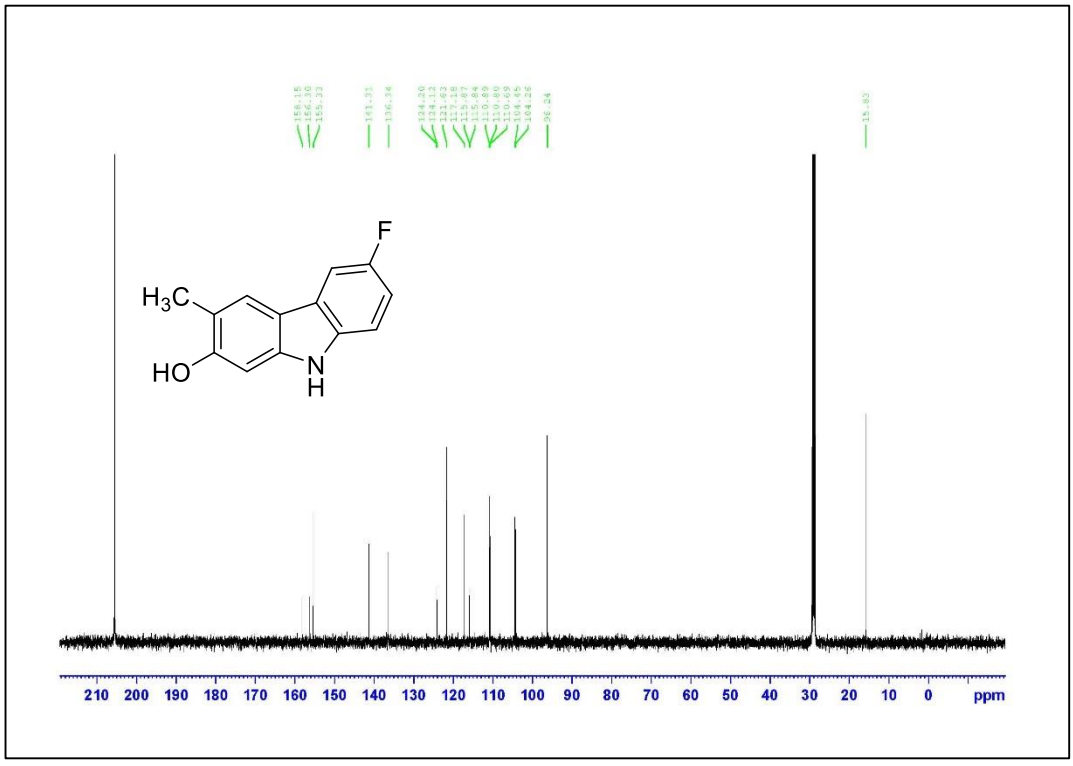

Figure A.16. ^{13}C NMR Spectrum of Compound **1.10f** (125 MHz, acetone-d_6)

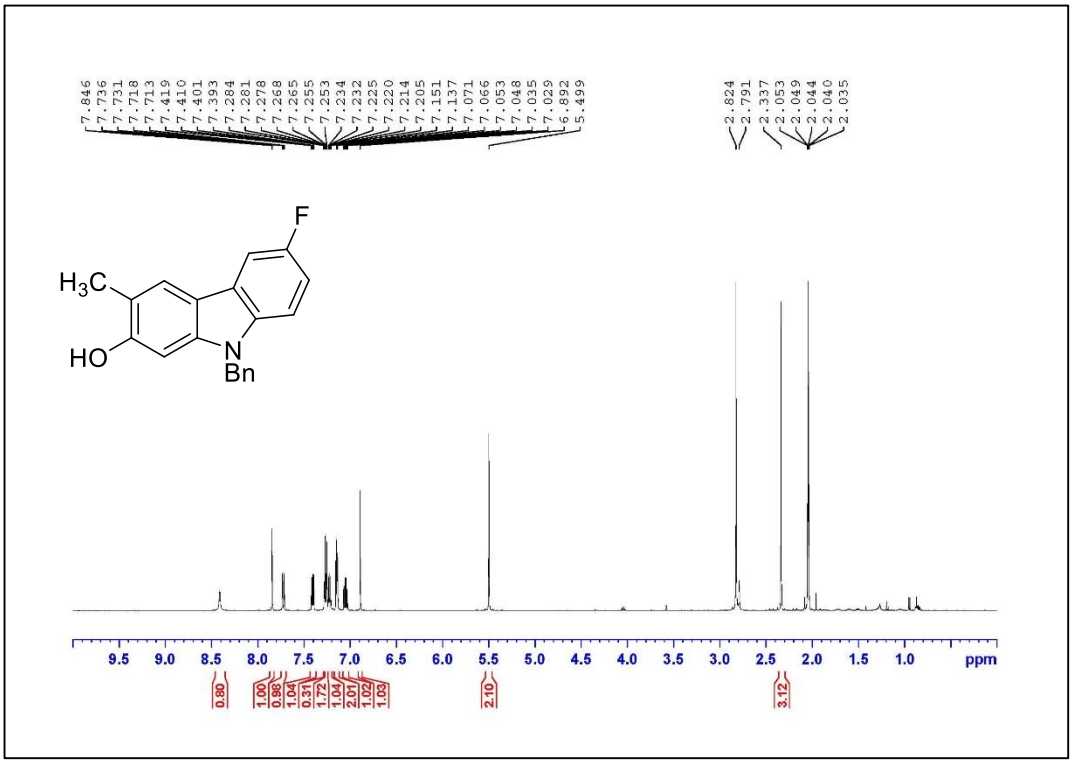

Figure A.17. ^{1}H NMR Spectrum of Compound **1.4f** (500 MHz, acetone-d_6)

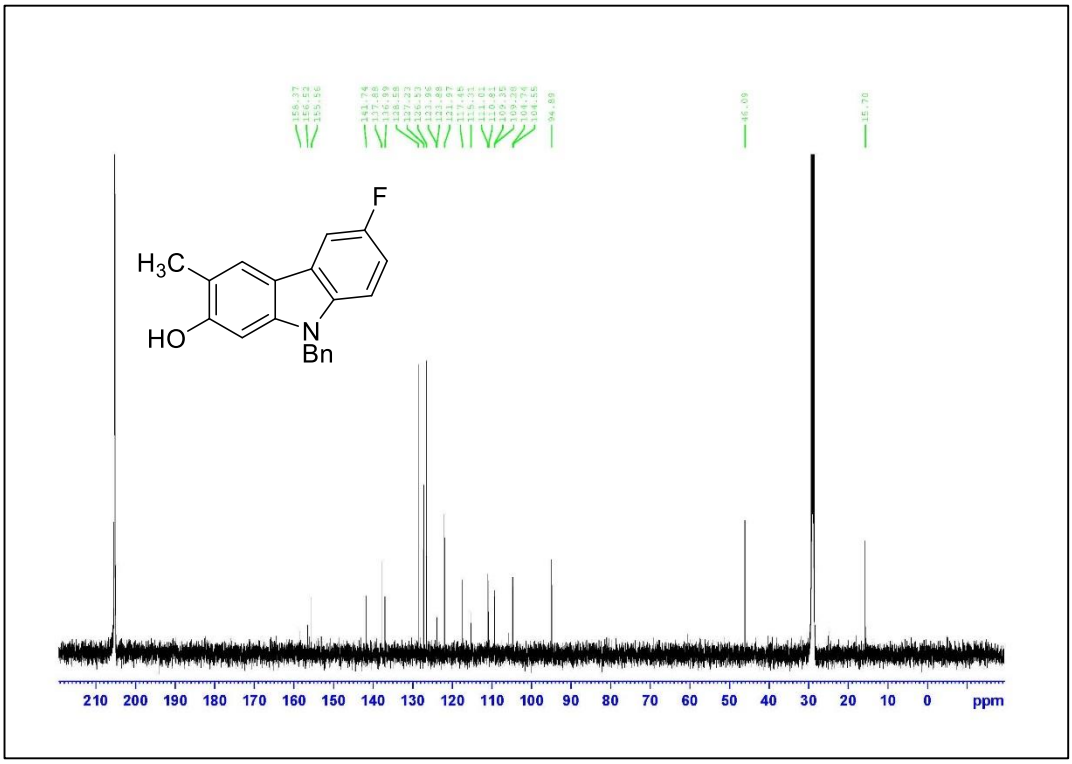

Figure A.18. ^{13}C NMR Spectrum of Compound **1.4f** (125 MHz, acetone-d_6)

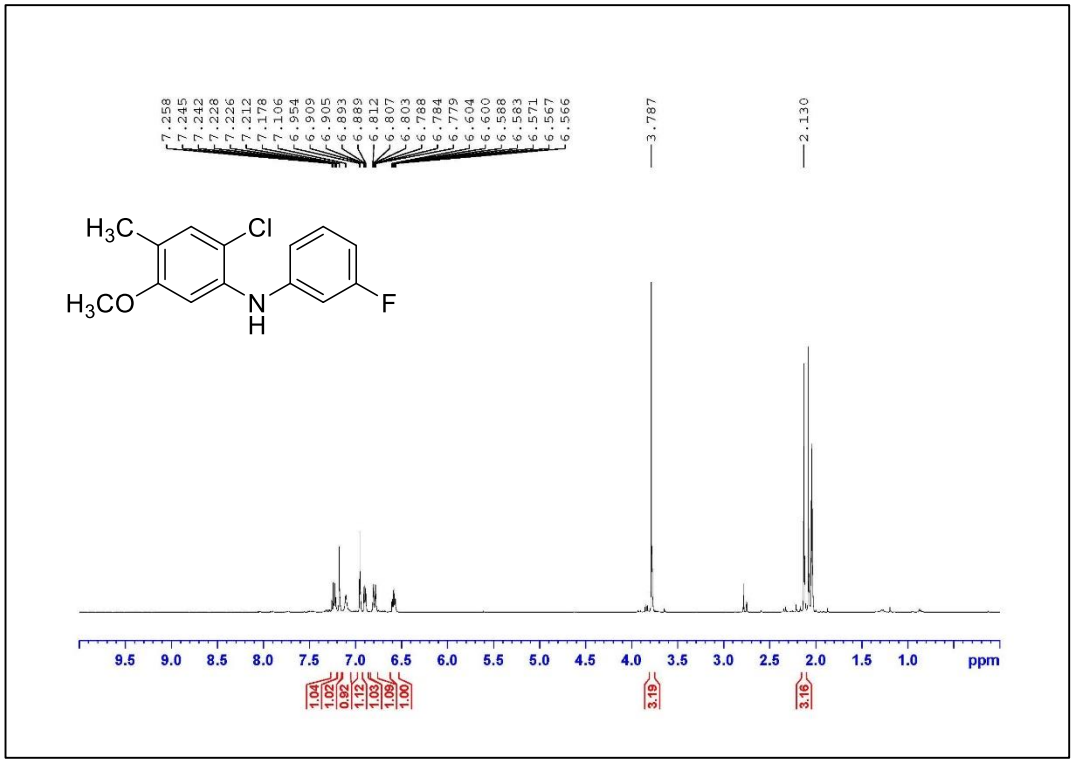

Figure A.19. ^{1}H NMR Spectrum of Compound **1.8g** (500 MHz, acetone-d_6)

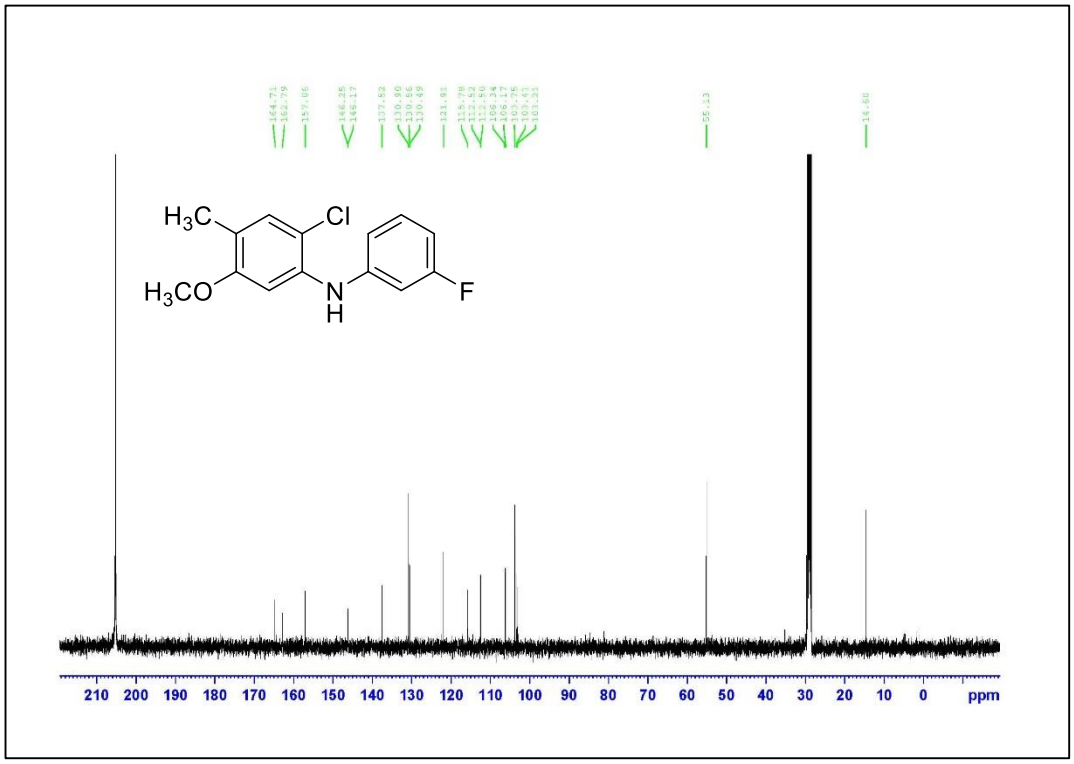

Figure A.20. ^{13}C NMR Spectrum of Compound **1.8g** (125 MHz, acetone-d_6)

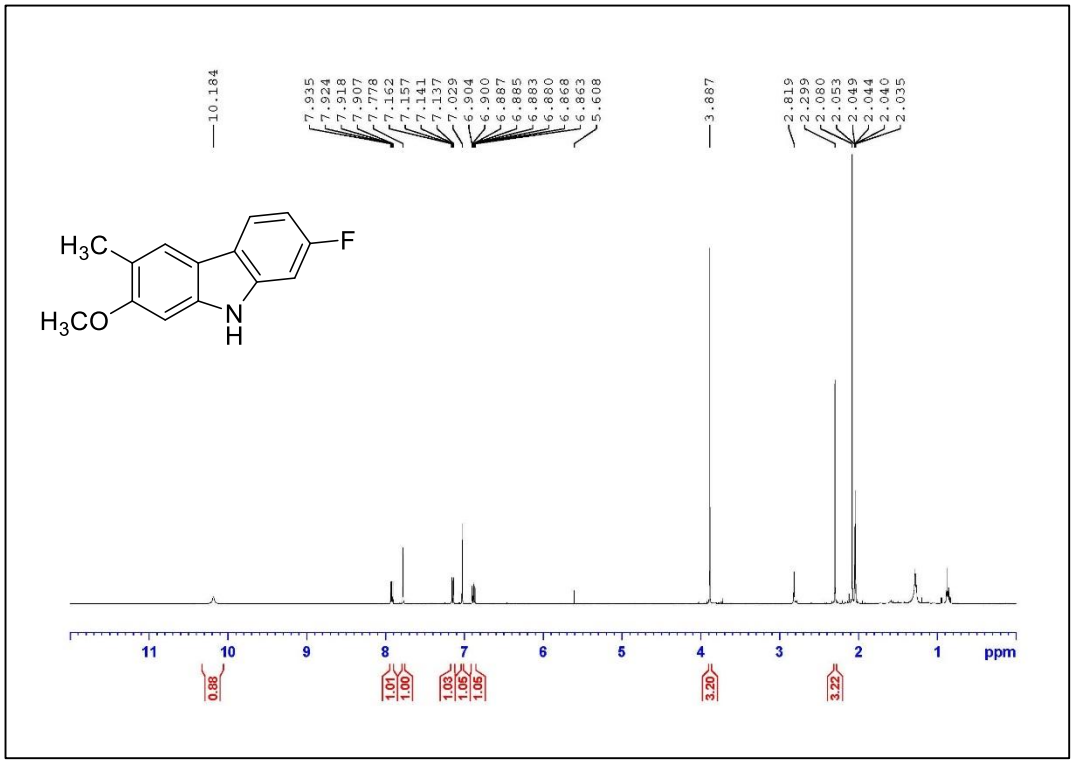

Figure A.21. ^{1}H NMR Spectrum of Compound **1.9g** (500 MHz, acetone-d_6)

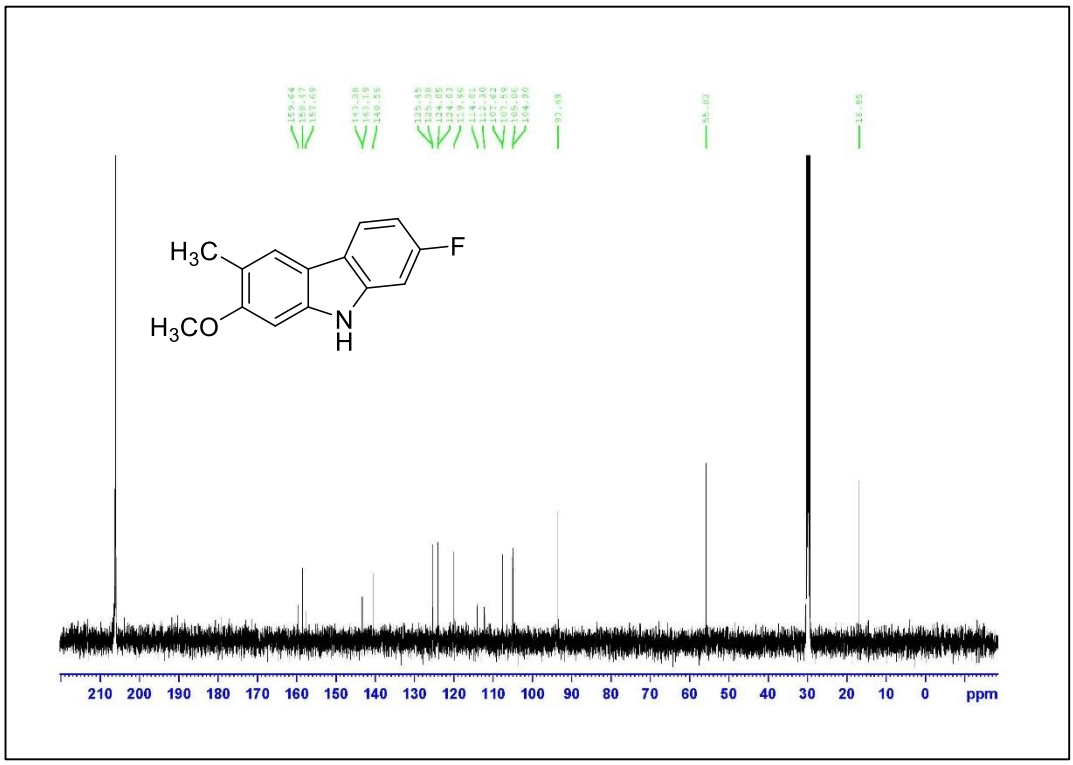

Figure A.22. ^{13}C NMR Spectrum of Compound **1.9g** (125 MHz, acetone-d_6)

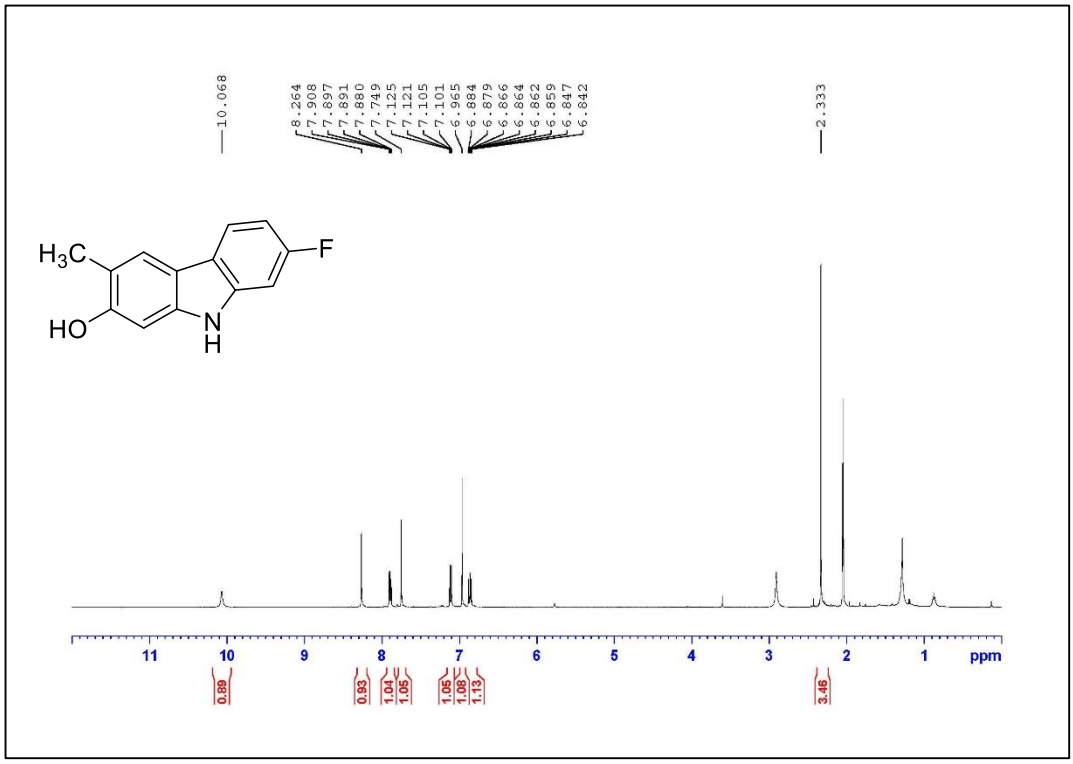

Figure A.23. ^{1}H NMR Spectrum of Compound **1.10g** (500 MHz, acetone-d_6)

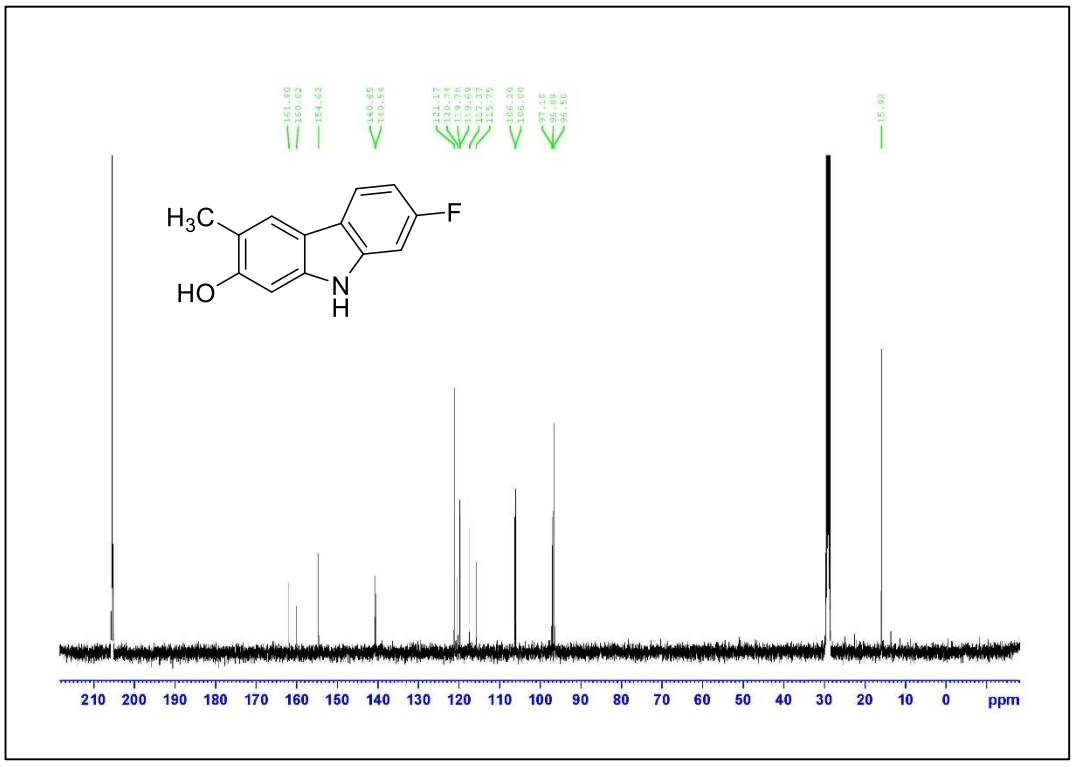

Figure A.24. ^{13}C NMR Spectrum of Compound **1.10g** (125 MHz, acetone-d_6)

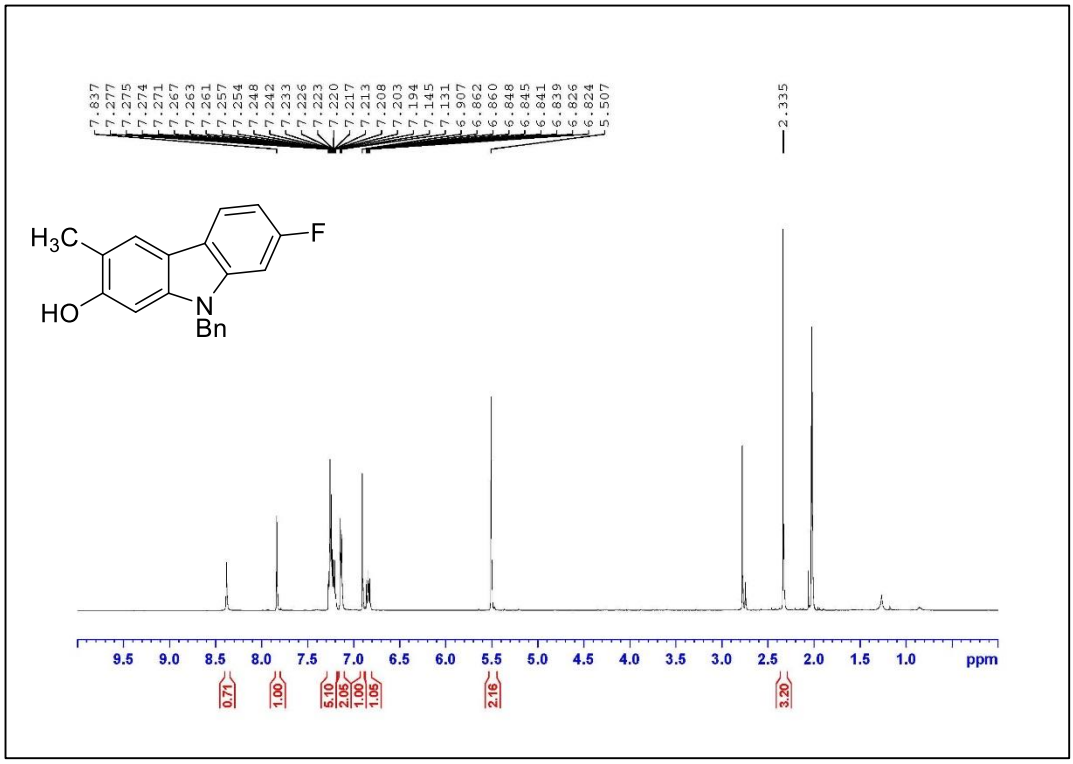

Figure A.25. ^{1}H NMR Spectrum of Compound **1.4g** (500 MHz, acetone-d_6)

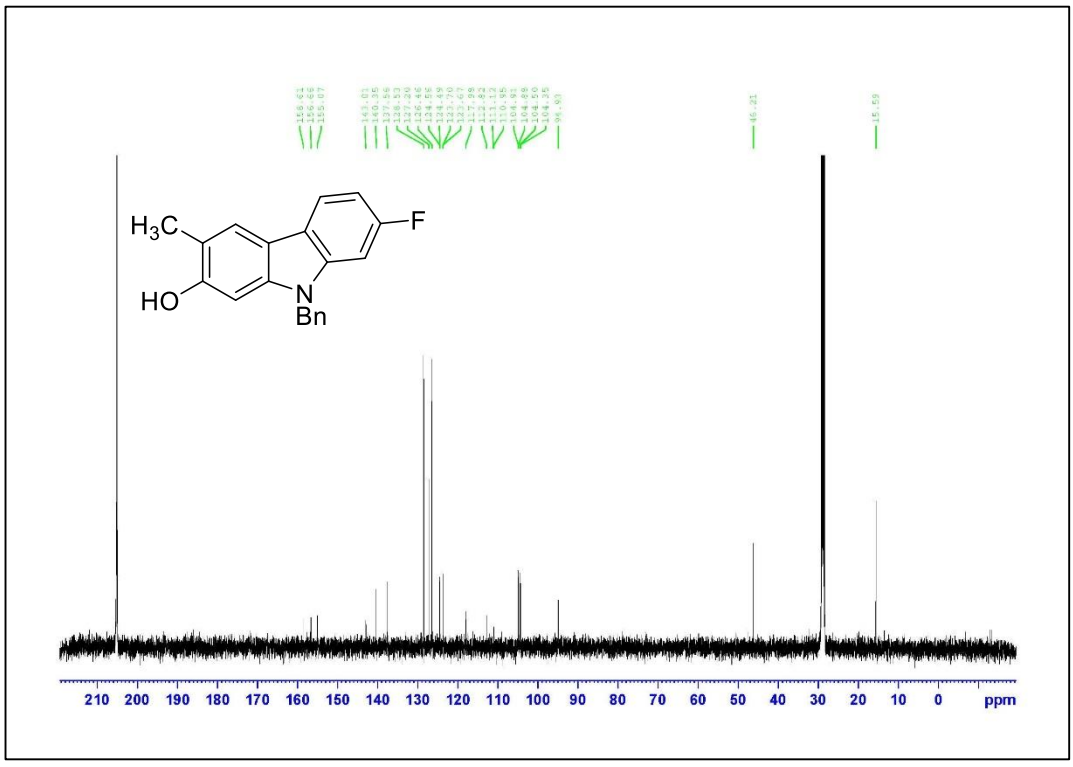

Figure A.26. ^{13}C NMR Spectrum of Compound **1.4g** (125 MHz, acetone-d_6)

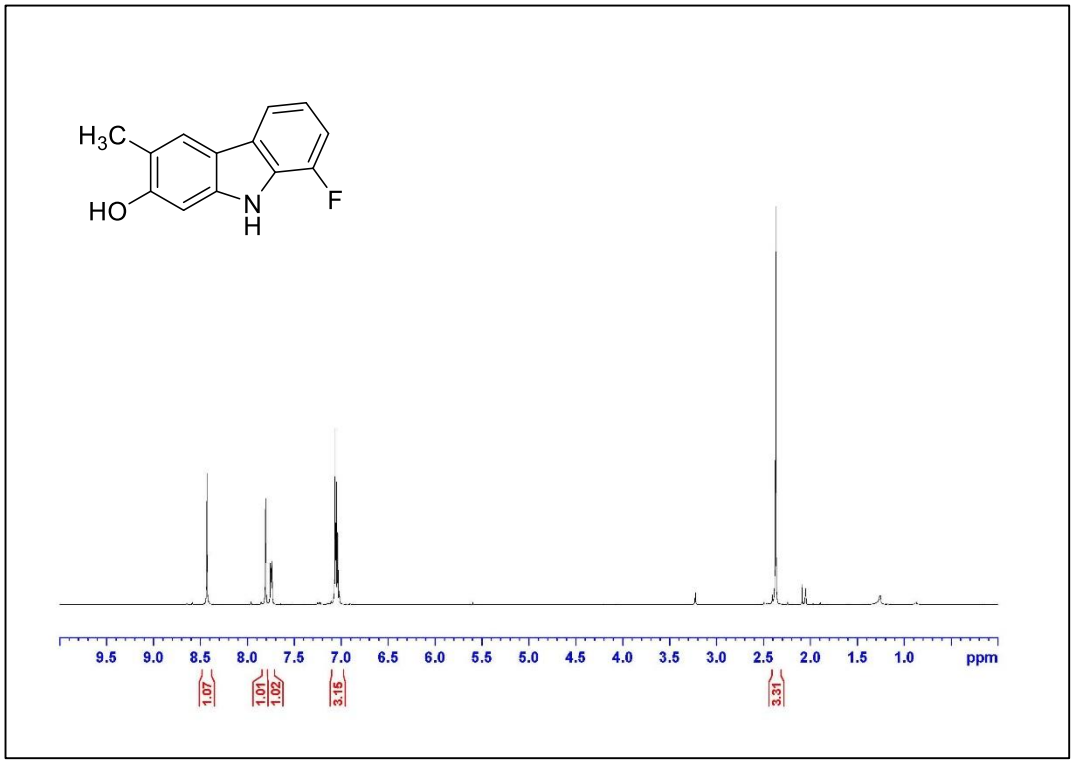

Figure A.27. ^{1}H NMR Spectrum of Compound **1.10h** (500 MHz, acetone-d_6)

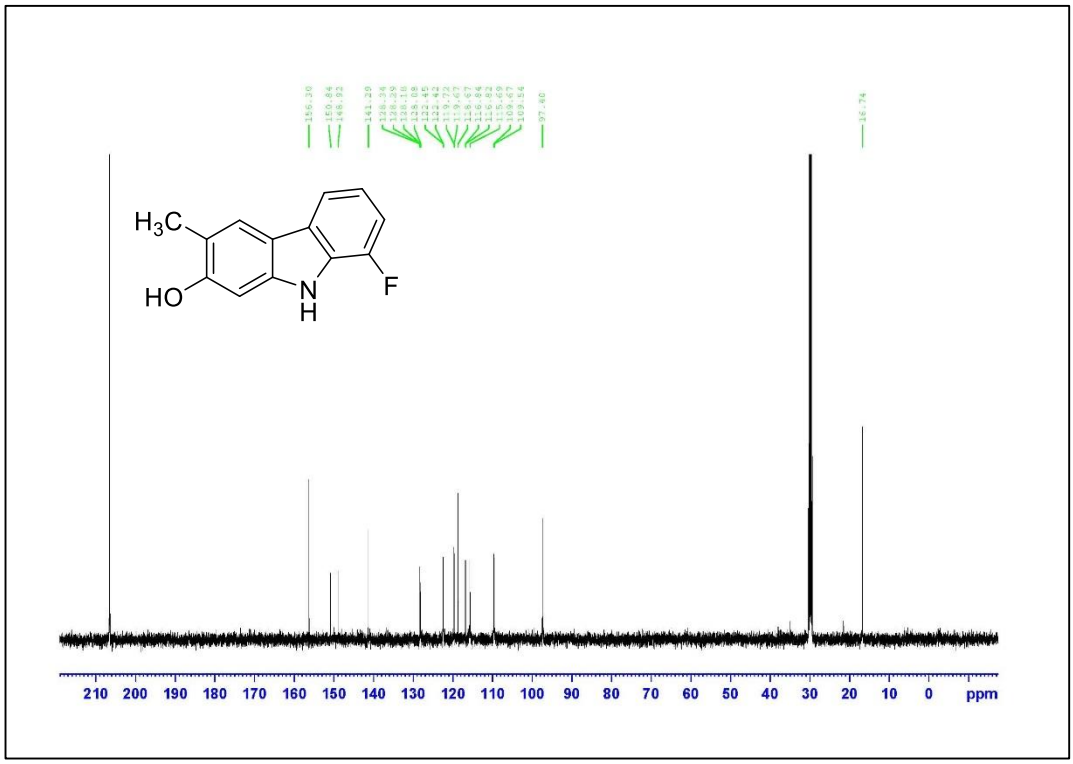

Figure A.28. ^{13}C NMR Spectrum of Compound **1.10h** (125 MHz, acetone-d_6)

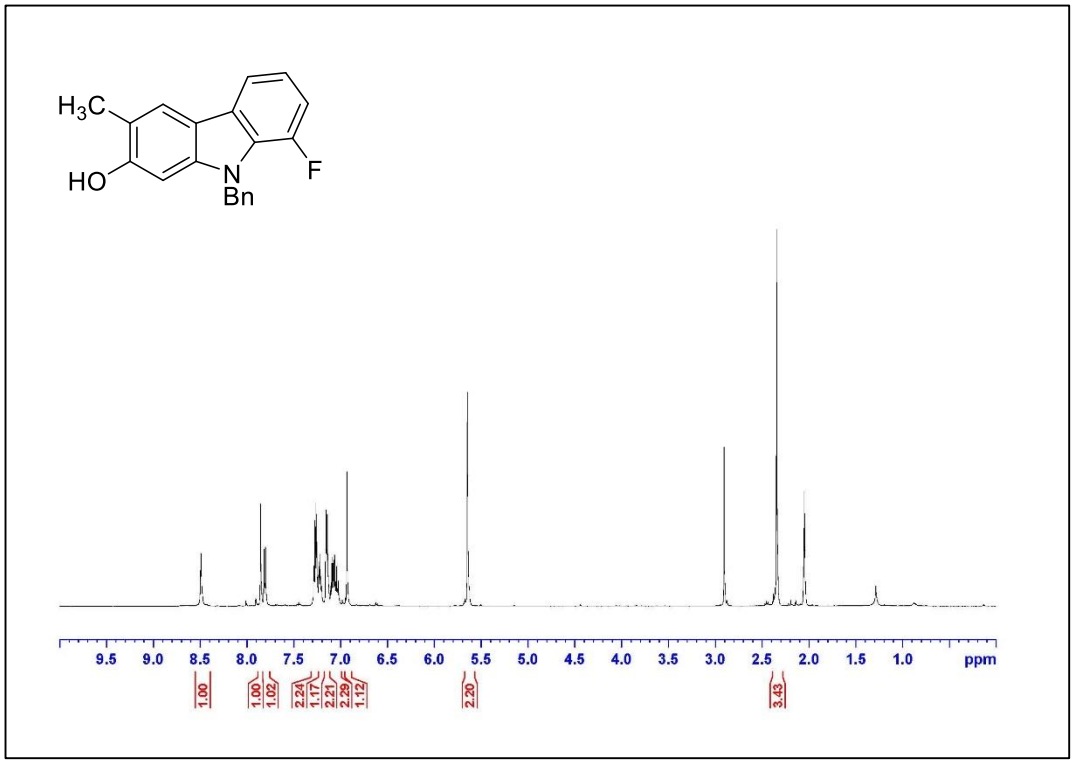

Figure A.29. ^{1}H NMR Spectrum of Compound **1.4h** (500 MHz, acetone-d_6)

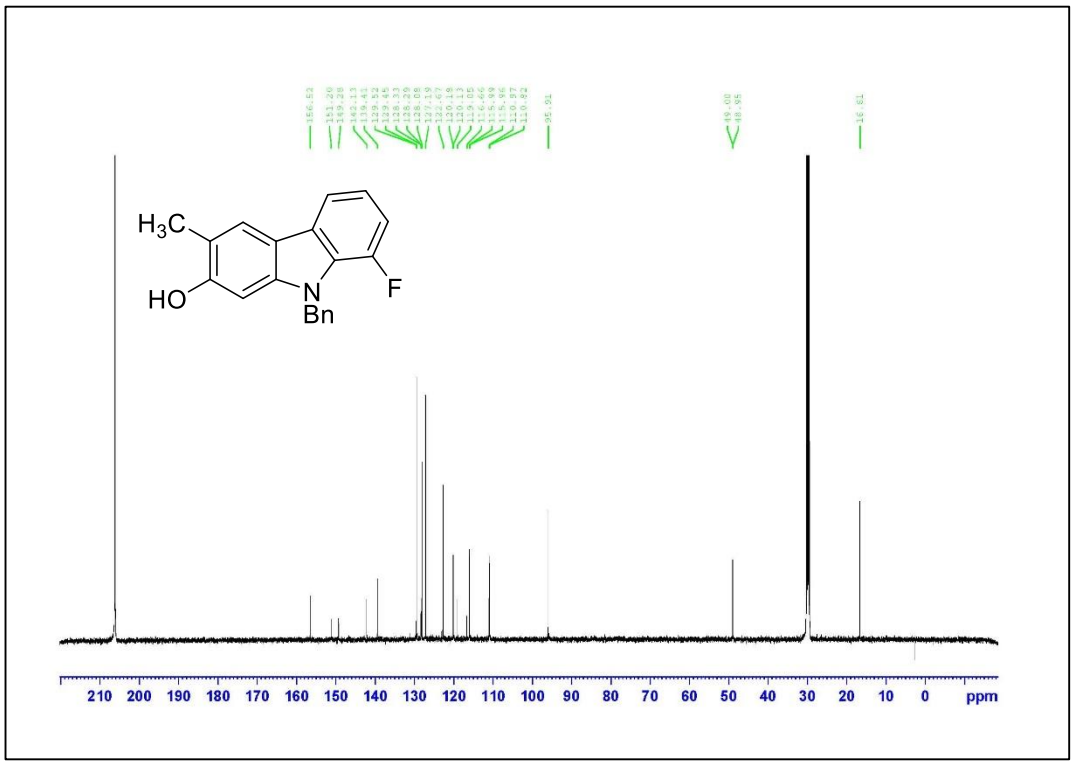

Figure A.30. ^{13}C NMR Spectrum of Compound **1.4h** (125 MHz, acetone-d_6)

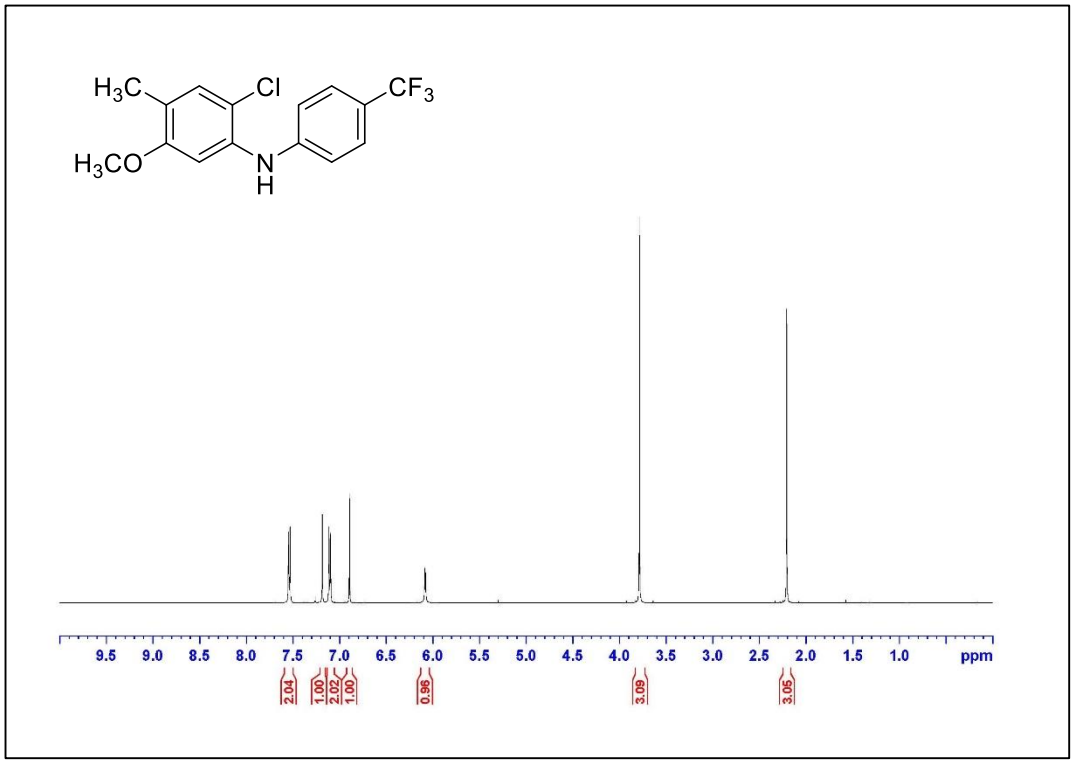

Figure A.31. ^{1}H NMR Spectrum of Compound **1.8i** (500 MHz, $CDCl_3$)

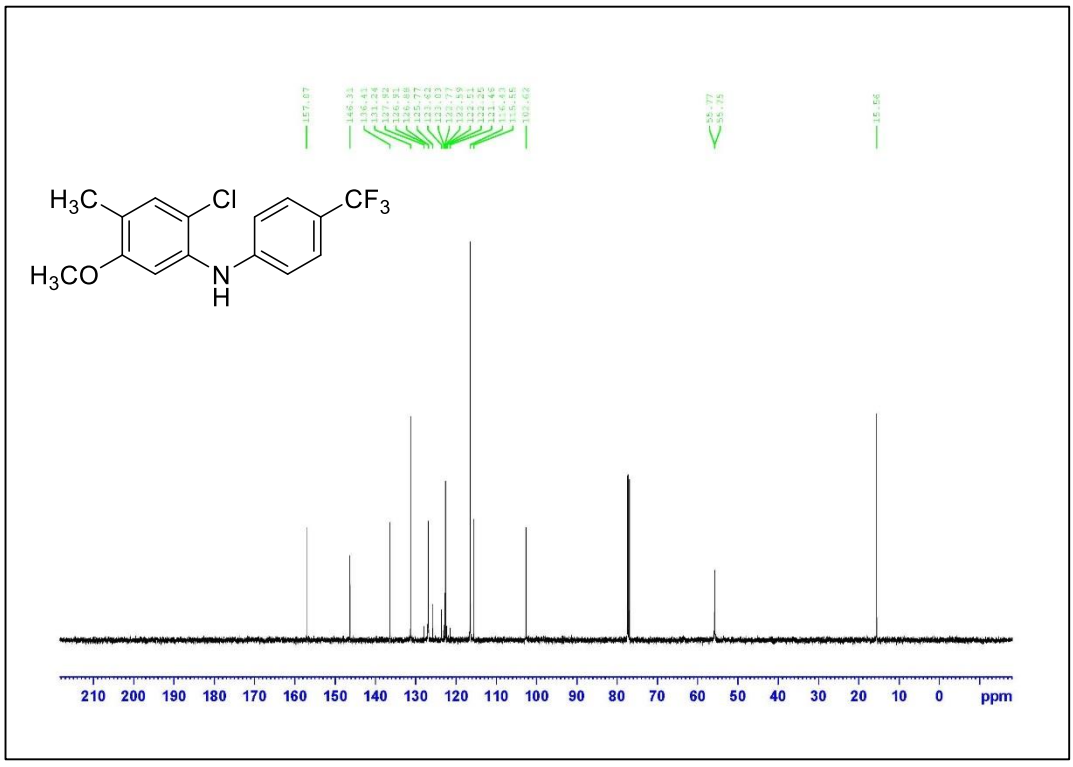

Figure A.32. ^{13}C NMR Spectrum of Compound **1.8i** (125 MHz, $CDCl_3$)

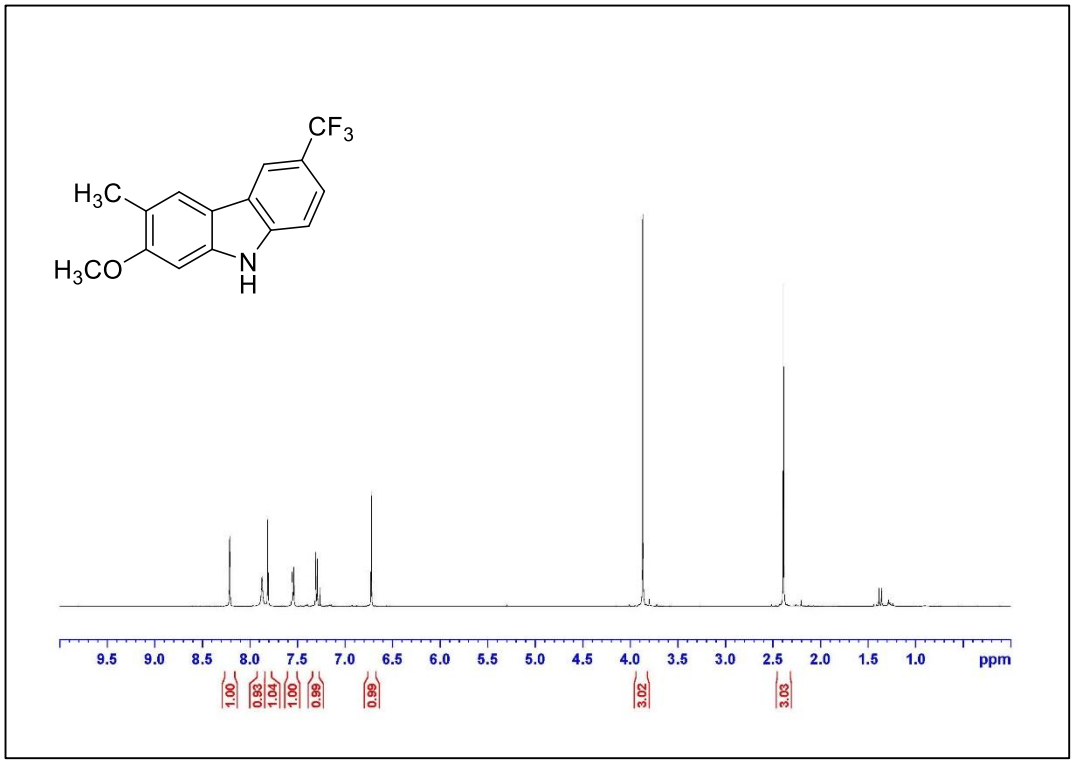

Figure A.33. ^{1}H NMR Spectrum of Compound **1.9i** (500 MHz, $CDCl_3$)

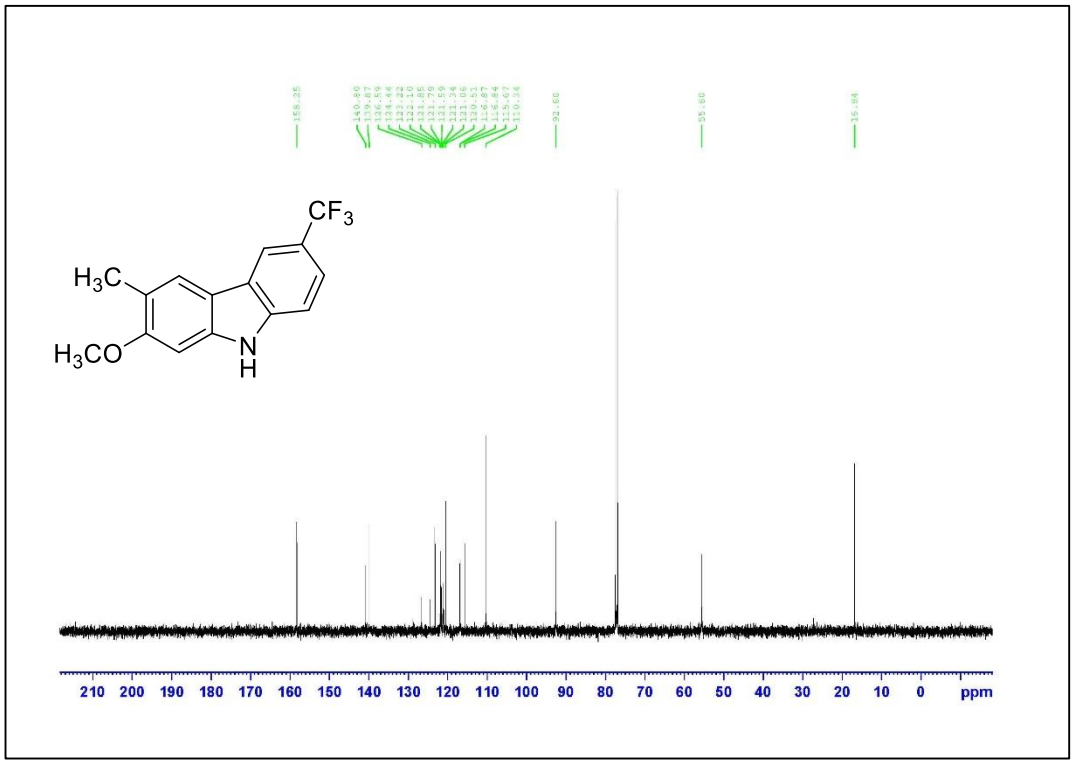

Figure A.34. ^{13}C NMR Spectrum of Compound **1.9i** (125 MHz, $CDCl_3$)

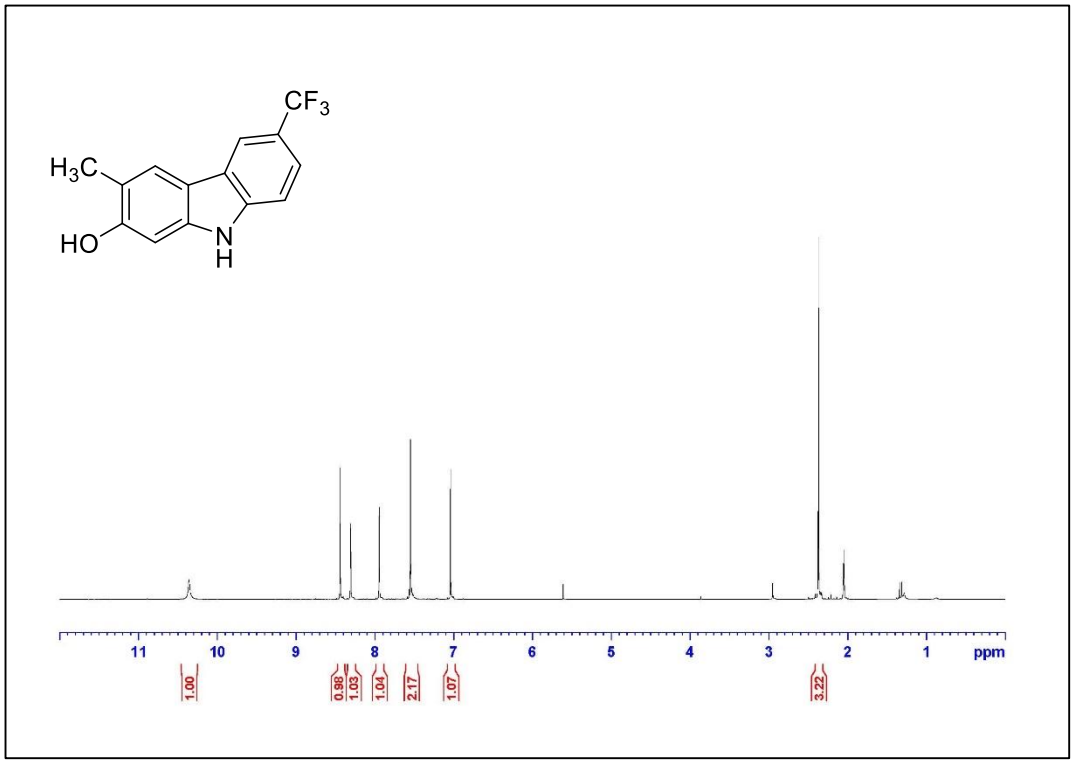

Figure A.35. ^{1}H NMR Spectrum of Compound **1.10i** (500 MHz, acetone-d_6)

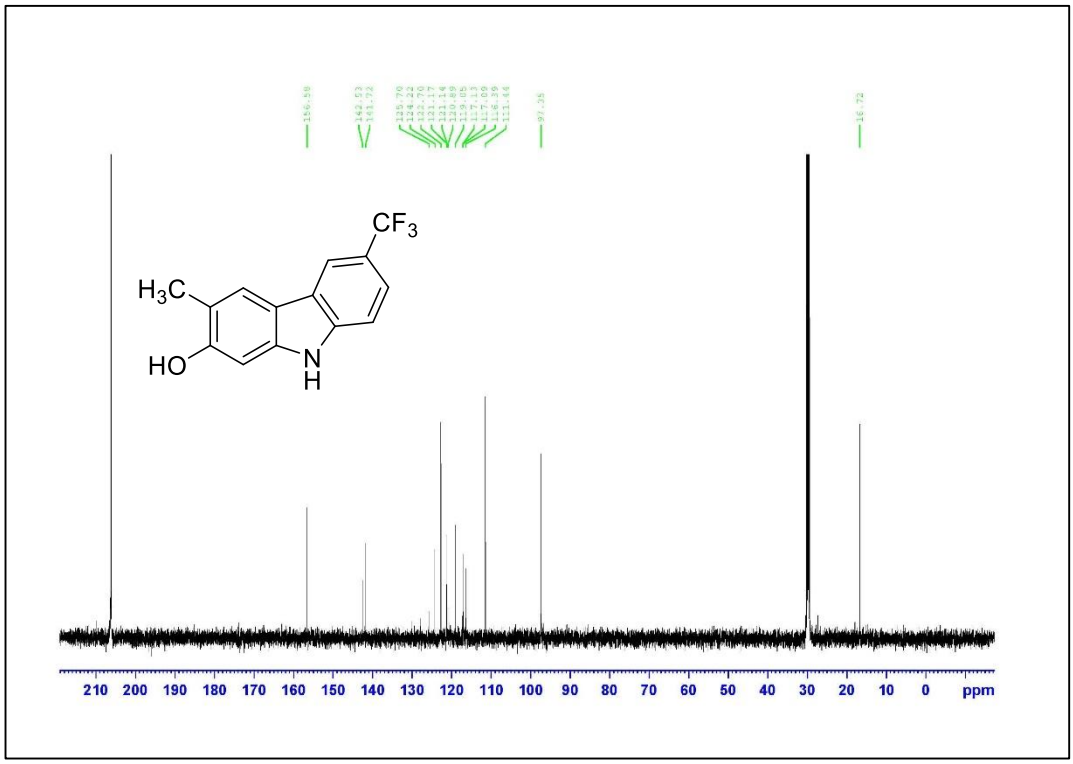

Figure A.36. ^{13}C NMR Spectrum of Compound **1.10i** (125 MHz, acetone-d_6)

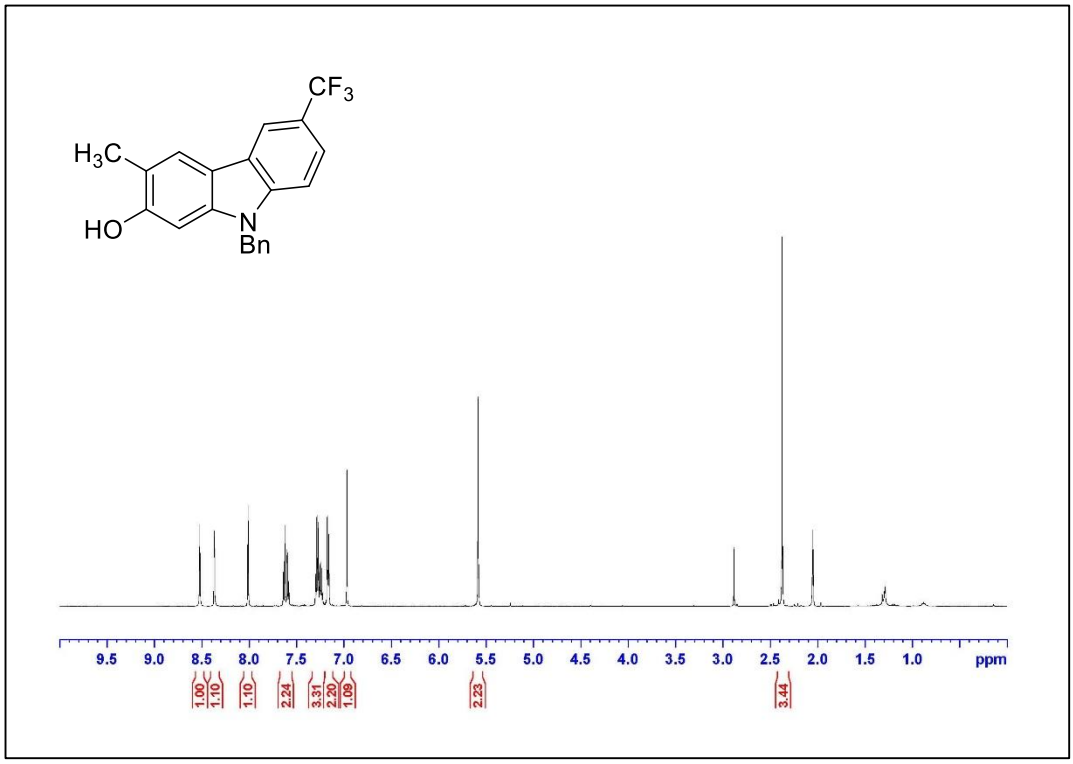

Figure A.37. ^{1}H NMR Spectrum of Compound **1.4i** (500 MHz, acetone-d_6)

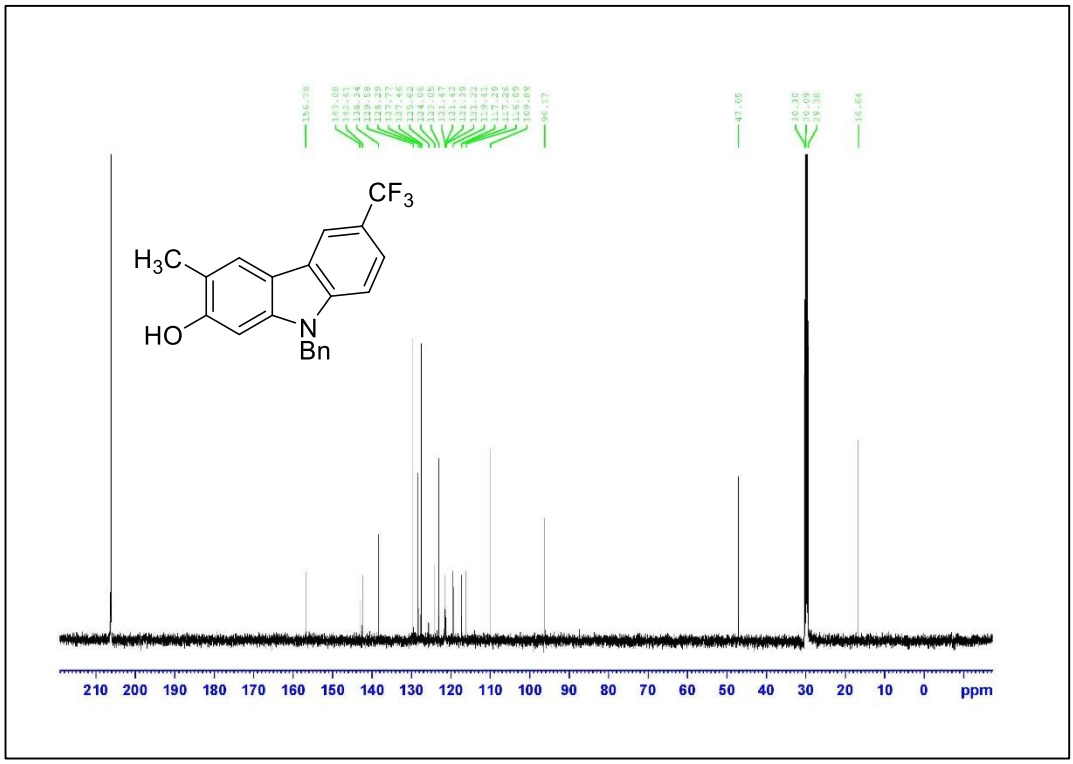

Figure A.38. ^{13}C NMR Spectrum of Compound **1.4i** (125 MHz, acetone-d_6)

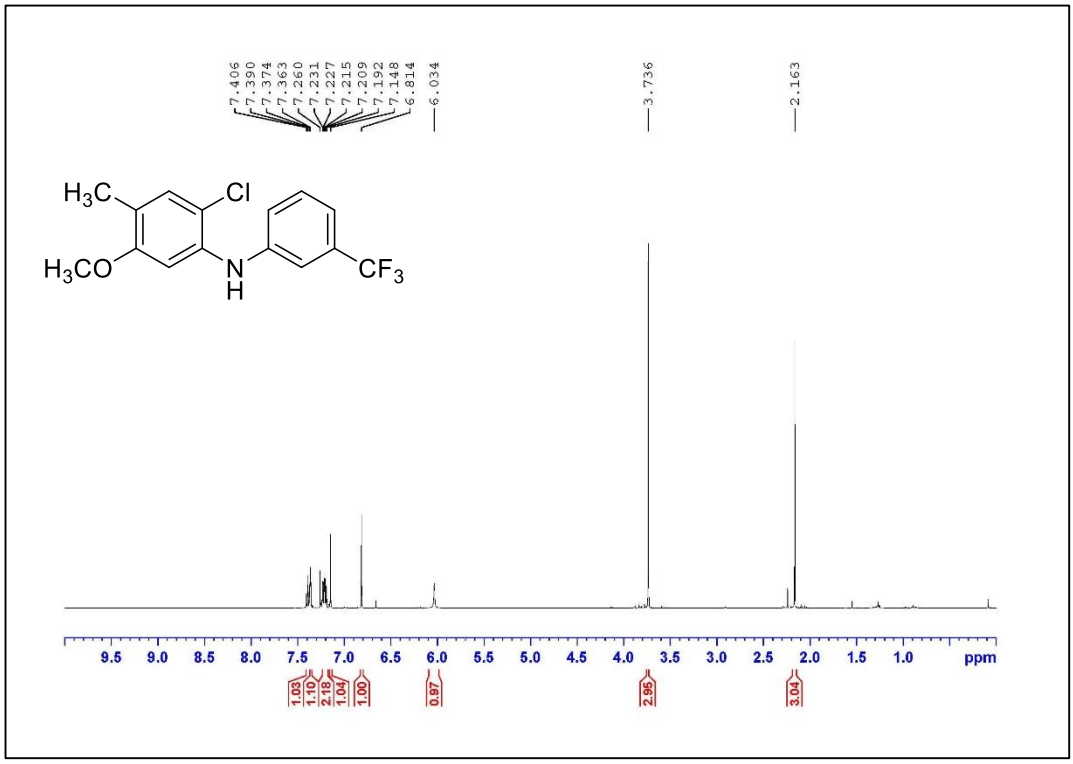

Figure A.39. ^{1}H NMR Spectrum of Compound **1.8j** (500 MHz, $CDCl_3$)

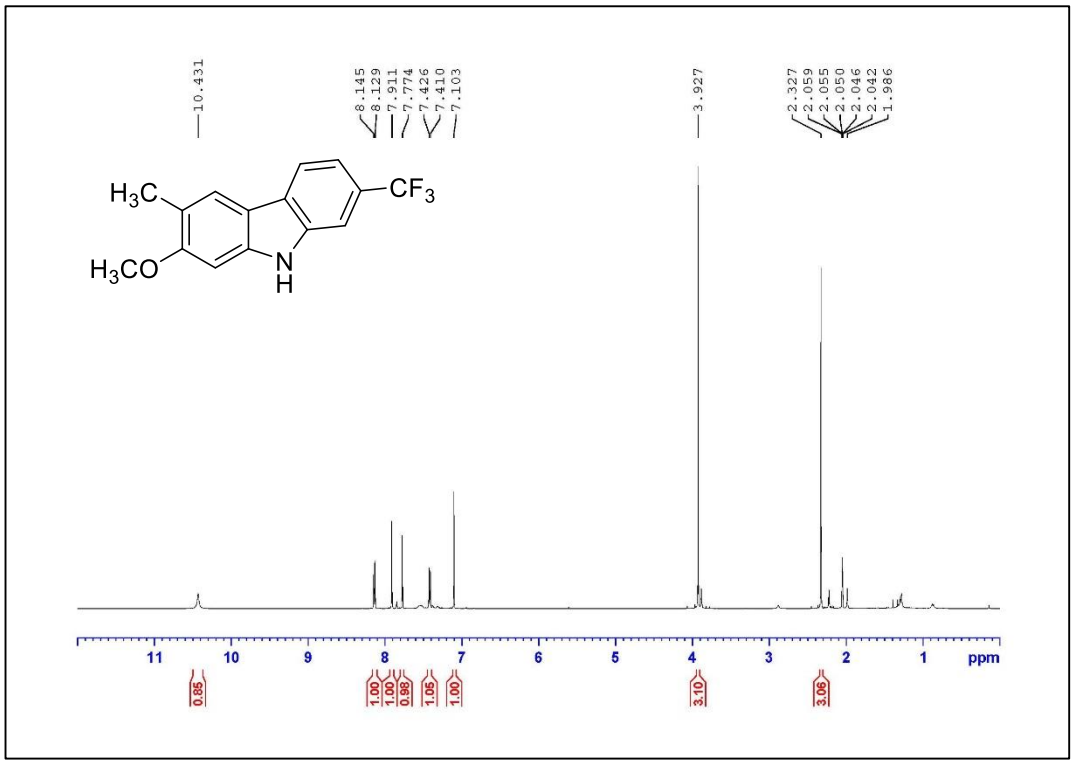

Figure A.40. ^{1}H NMR Spectrum of Compound **1.9j** (500 MHz, acetone-d_6)

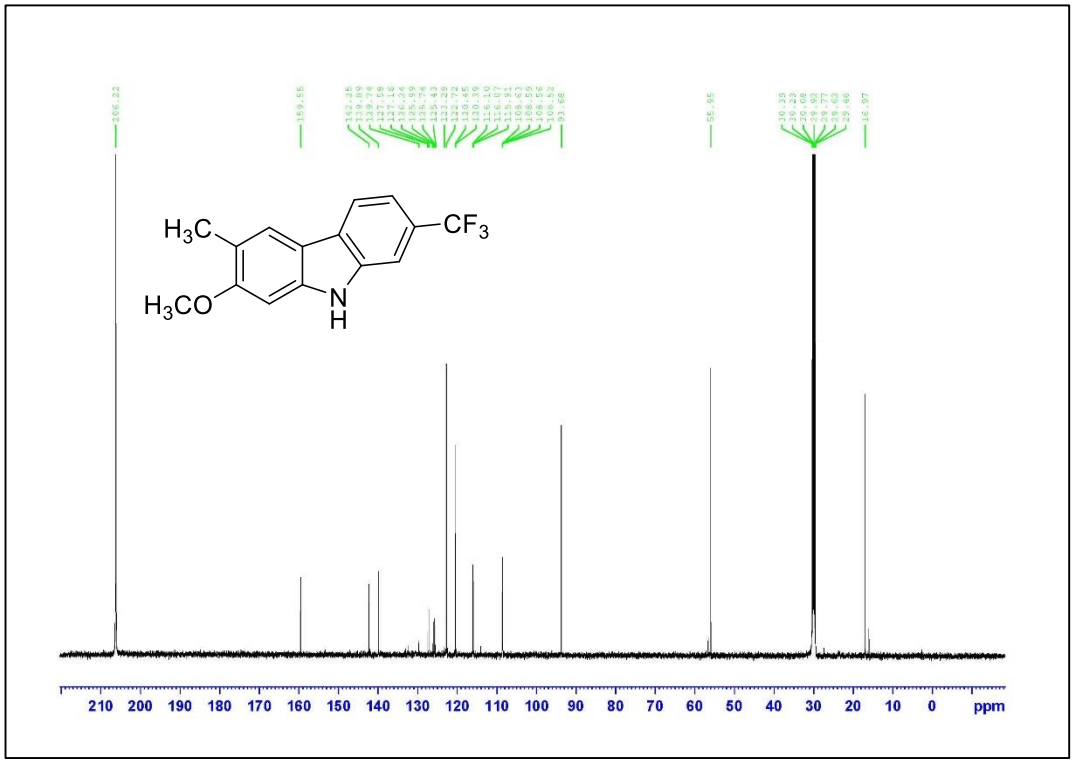

Figure A.41. ^{13}C NMR Spectrum of Compound **1.9j** (125 MHz, acetone-d_6)

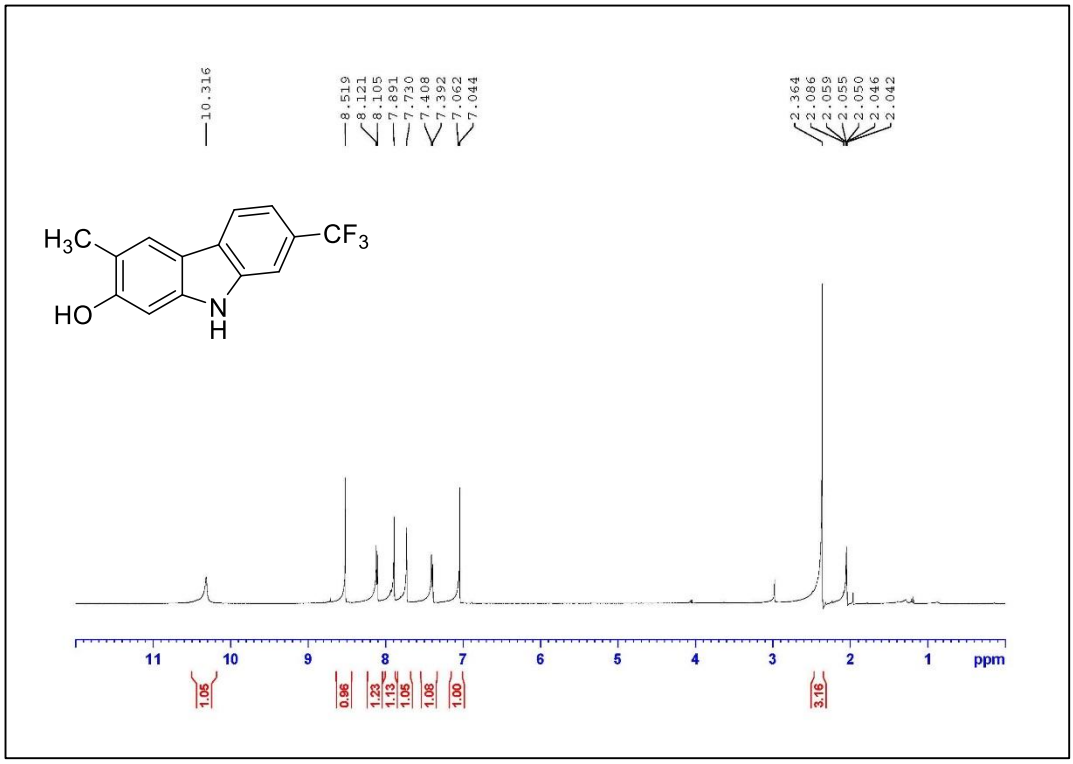

Figure A.42. ^{1}H NMR Spectrum of Compound **1.10j** (500 MHz, acetone-d_6)

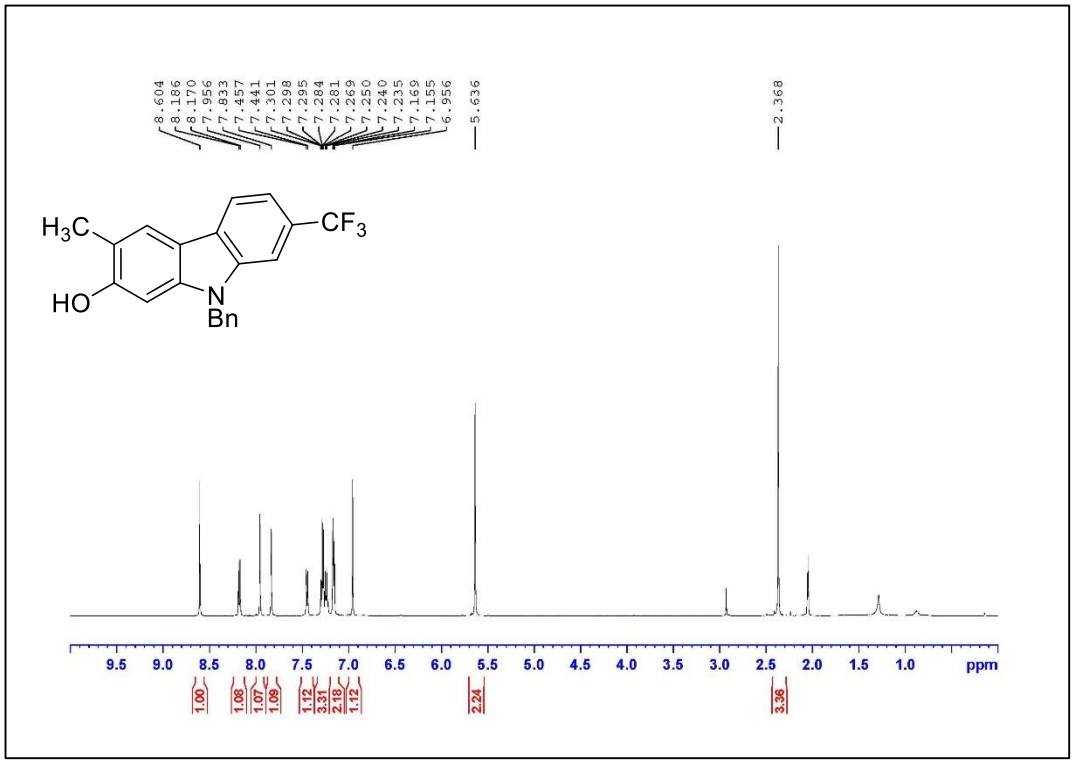

Figure A.43. ^{1}H NMR Spectrum of Compound **1.4j** (500 MHz, acetone-d_6)

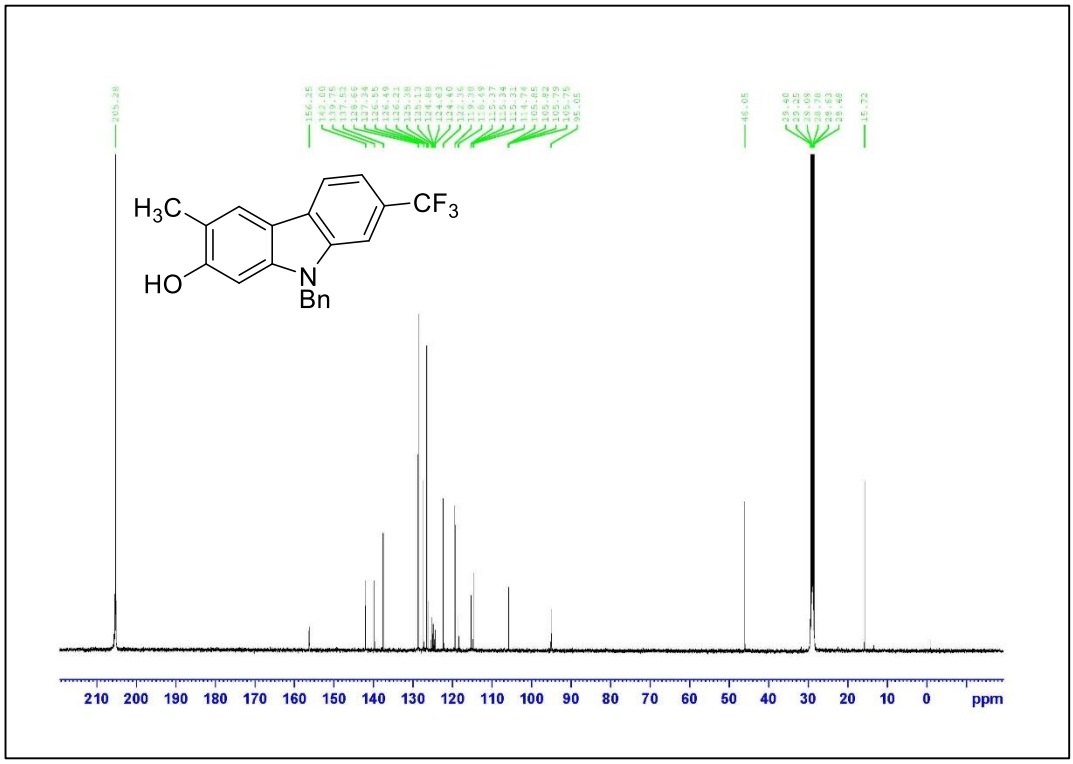

Figure A.44. ^{13}C NMR Spectrum of Compound **1.4j** (125 MHz, acetone-d_6)

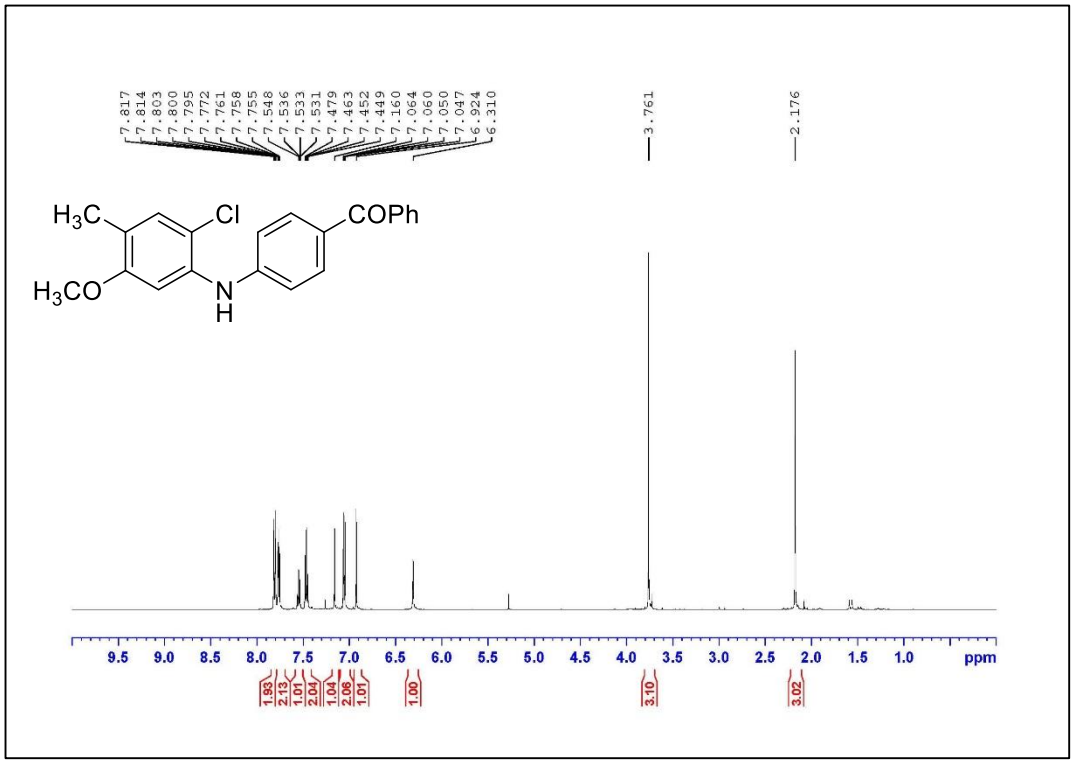

Figure A.45. ^{1}H NMR Spectrum of Compound **1.8k** (500 MHz, $CDCl_3$)

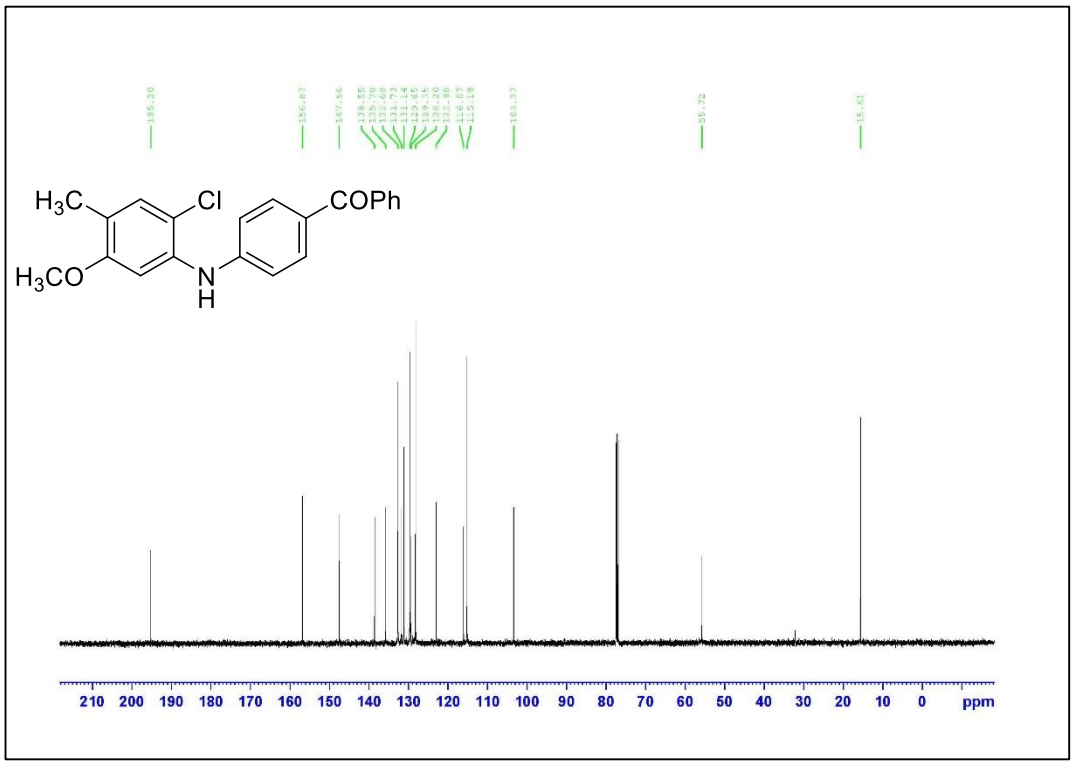

Figure A.46. ^{13}C NMR Spectrum of Compound **1.8k** (125 MHz, $CDCl_3$)

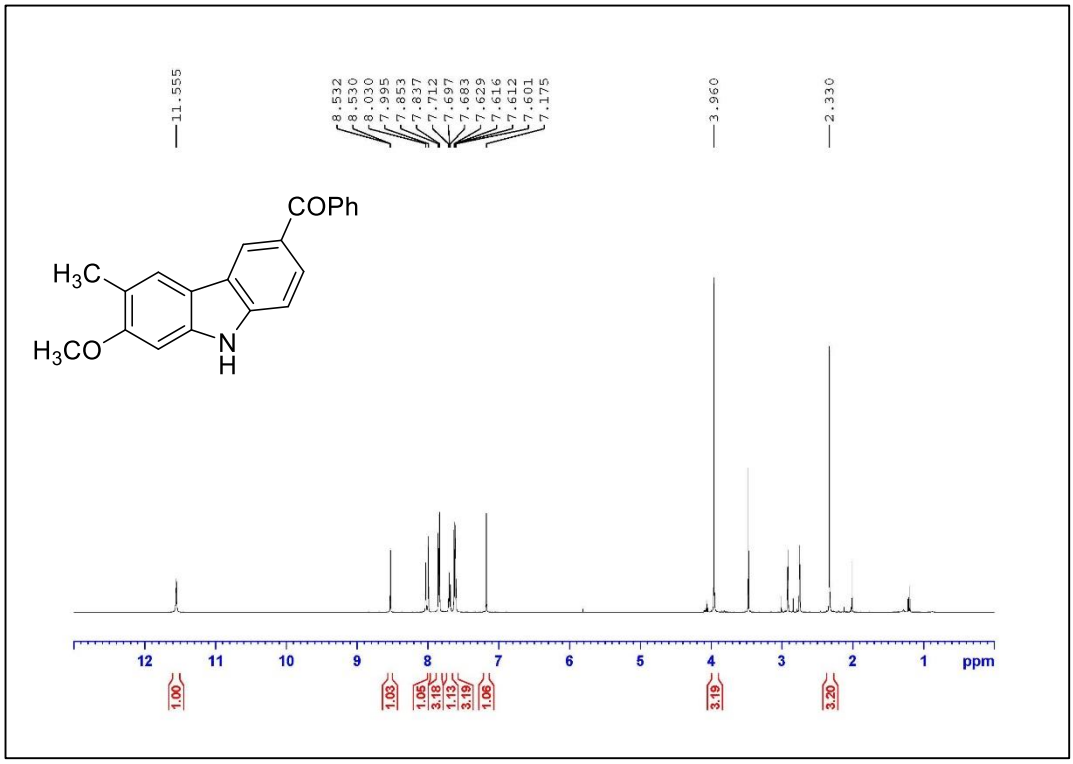

Figure A.47. ^{1}H NMR Spectrum of Compound **1.9k** (500 MHz, DMF-d_7)

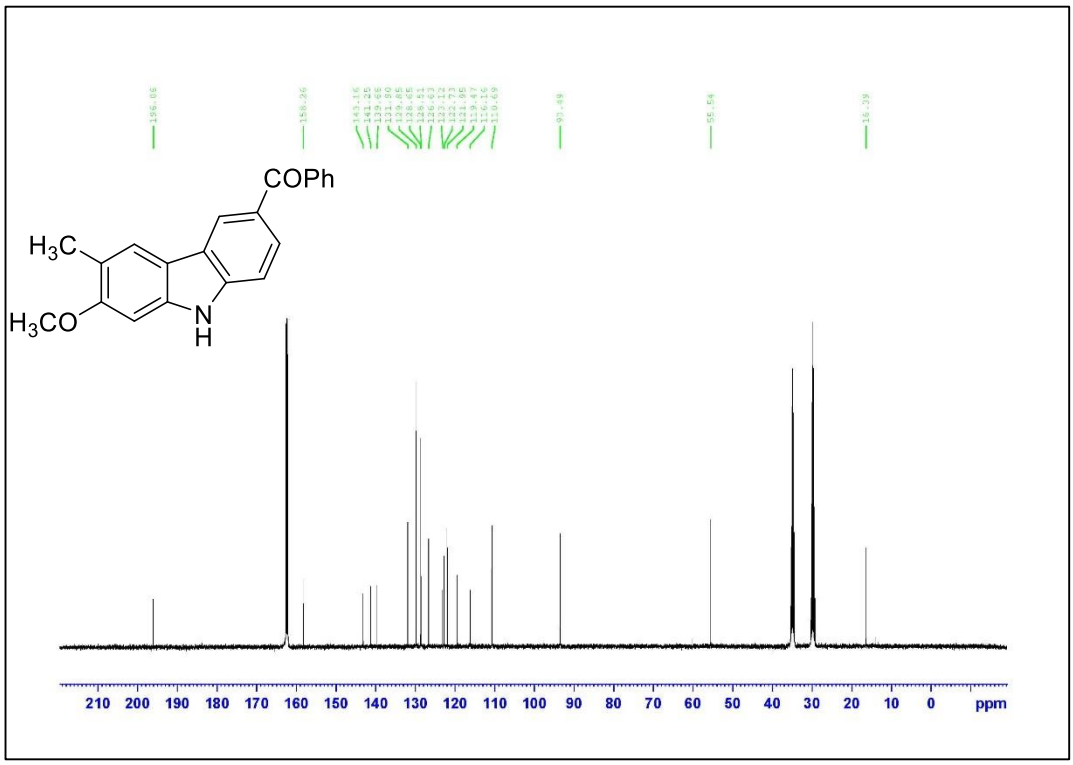

Figure A.48. ^{13}C NMR Spectrum of Compound **1.9k** (125 MHz, DMF-d_7)

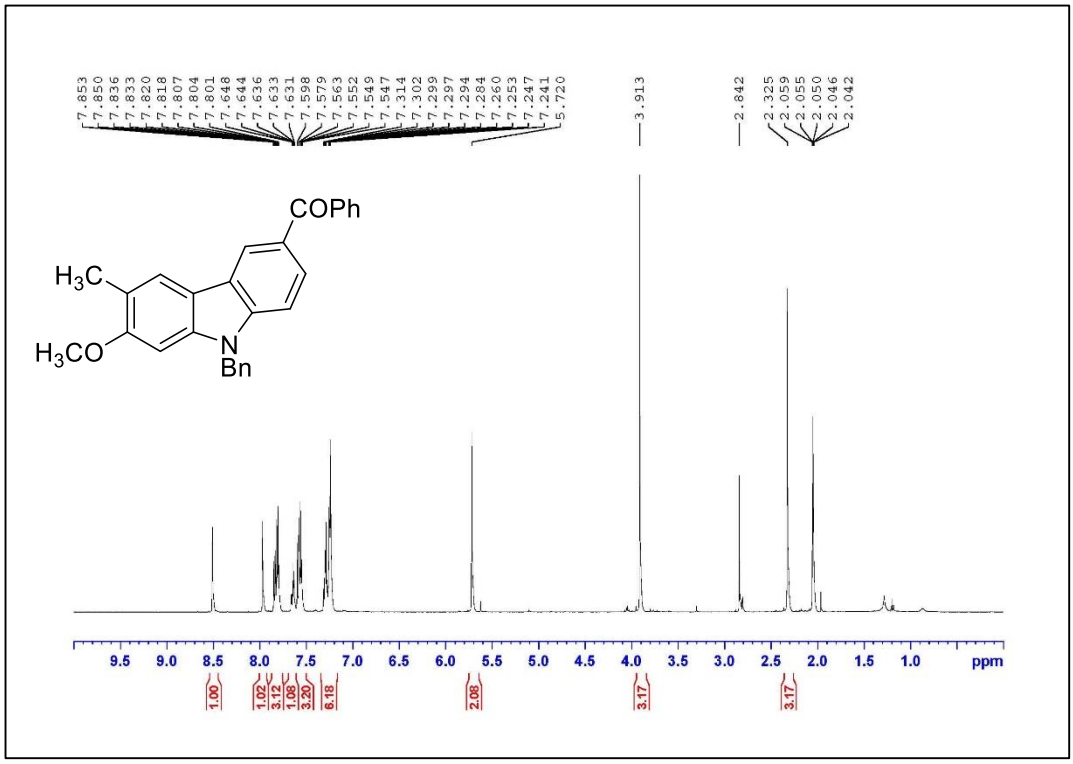

Figure A.49. ^{1}H NMR Spectrum of Compound **1.11k** (500 MHz, acetone-d_6)

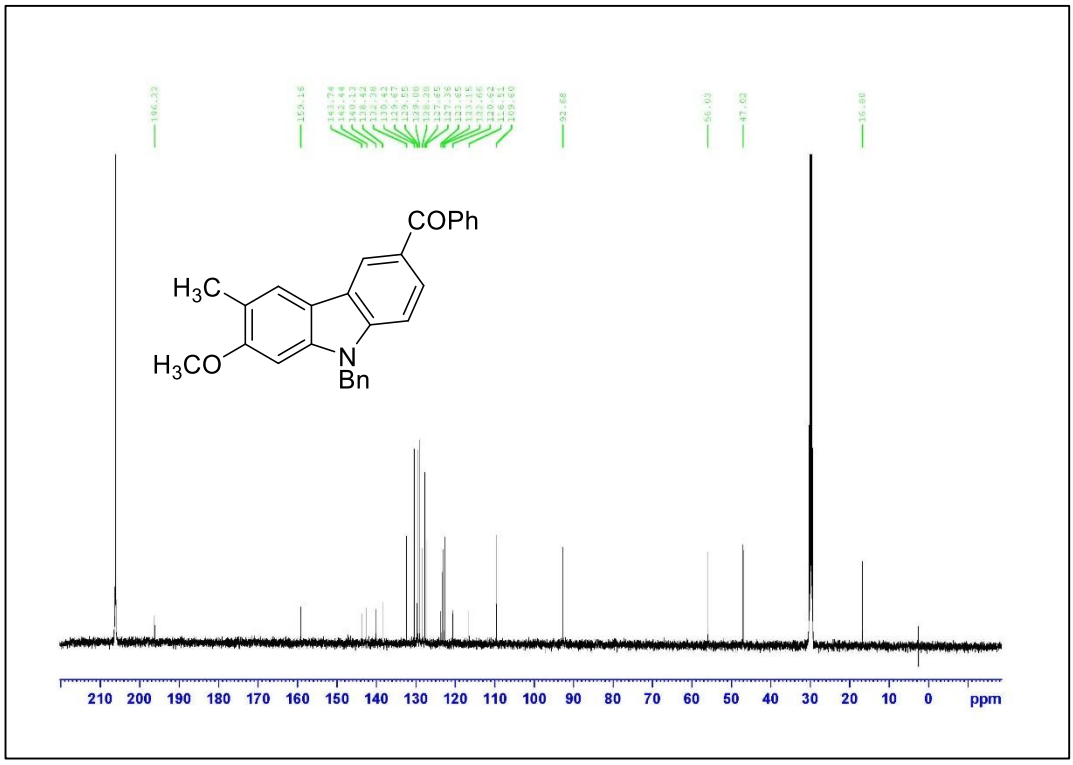

Figure A.50. ^{13}C NMR Spectrum of Compound **1.11k** (125 MHz, acetone-d_6)

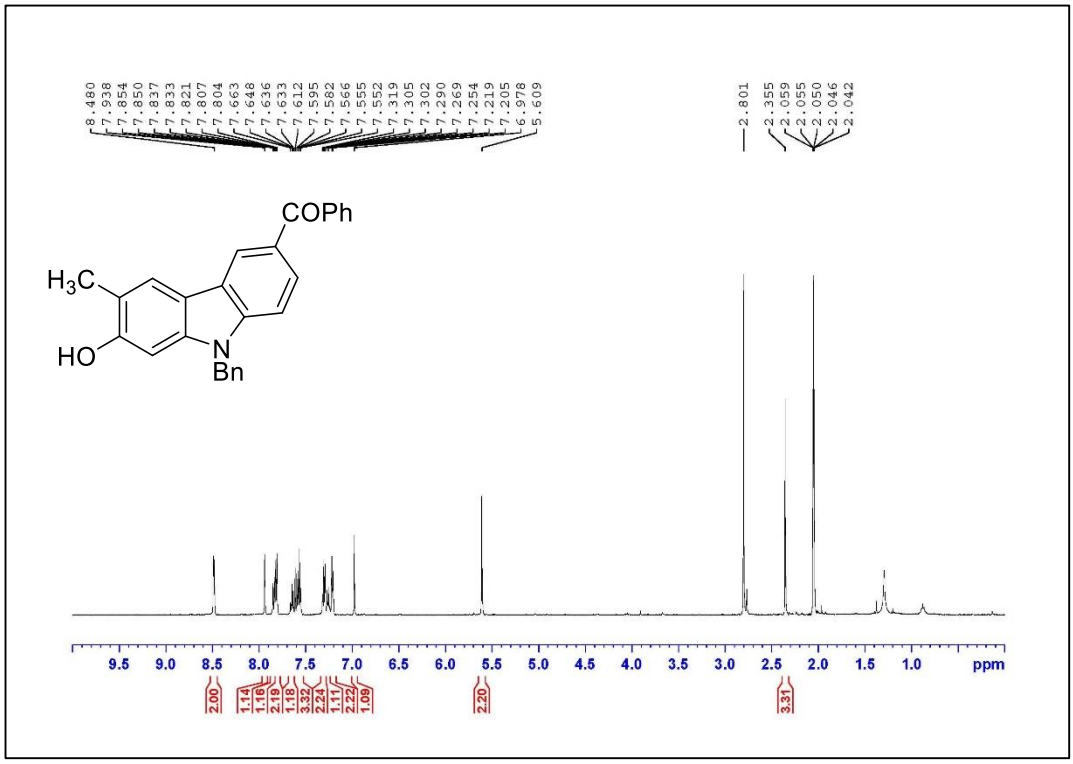

Figure A.51. ^{1}H NMR Spectrum of Compound **1.4k** (500 MHz, acetone-d_6)

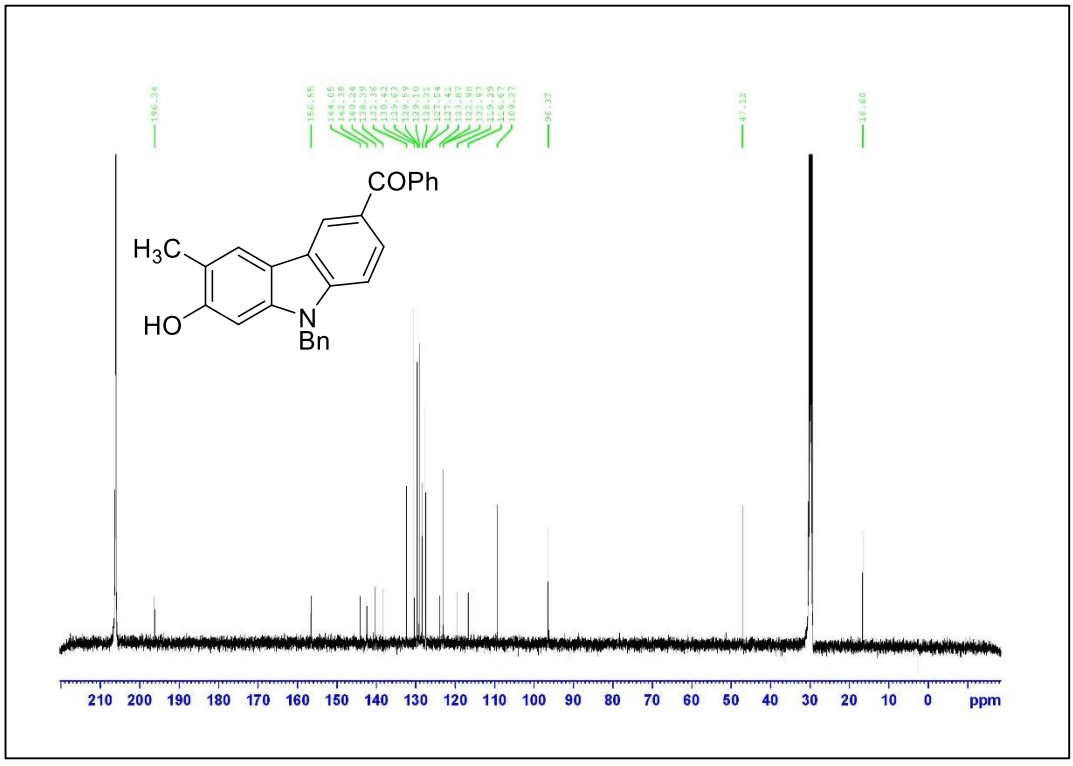

Figure A.52. ^{13}C NMR Spectrum of Compound **1.4k** (125 MHz, acetone-d_6)

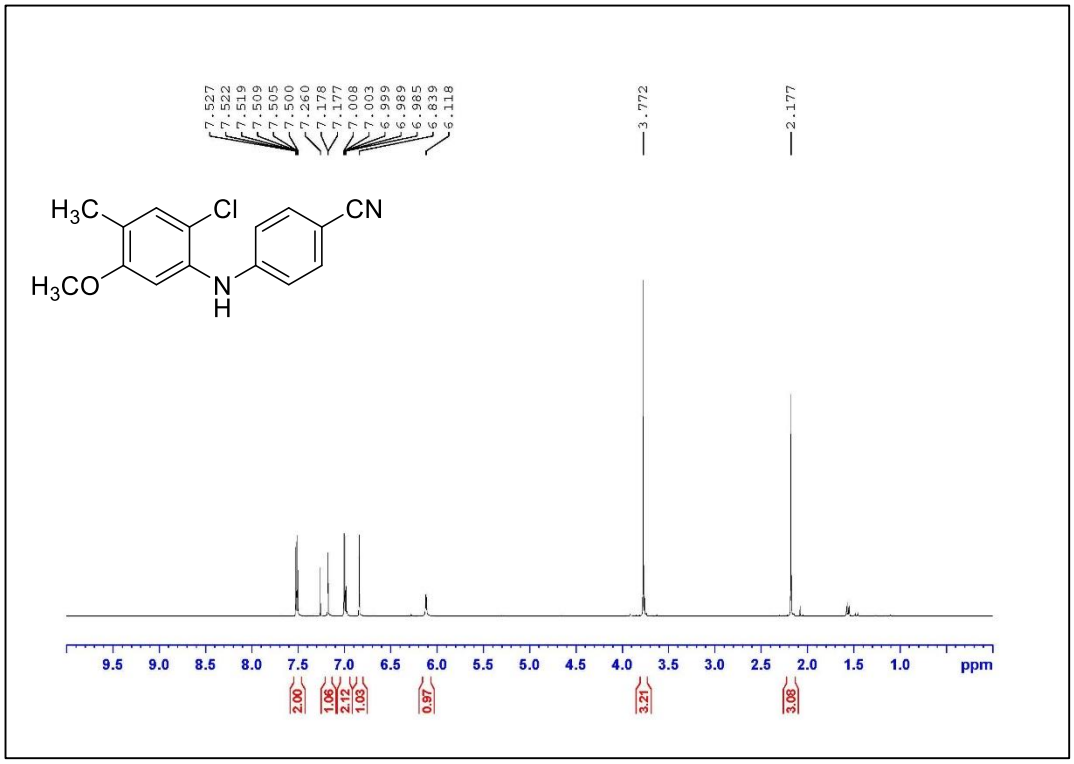

Figure A.53. ^{1}H NMR Spectrum of Compound **1.8l** (500 MHz, $CDCl_3$)

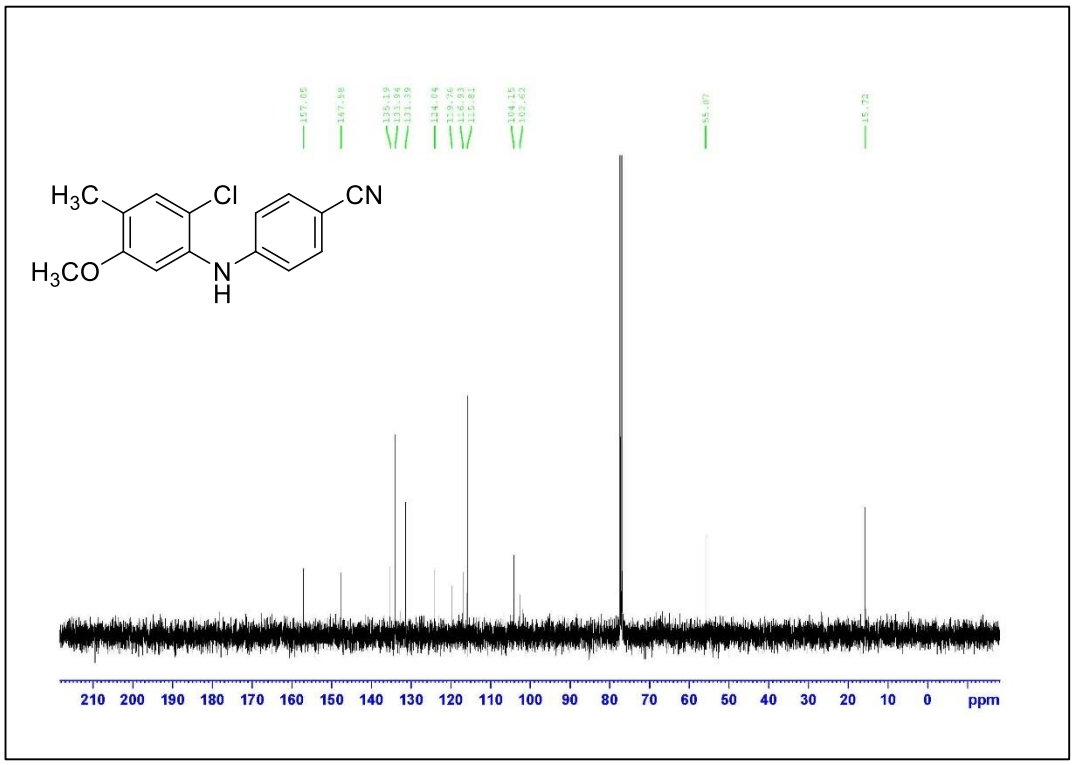

Figure A.54. ^{13}C NMR Spectrum of Compound **1.8l** (125 MHz, $CDCl_3$)

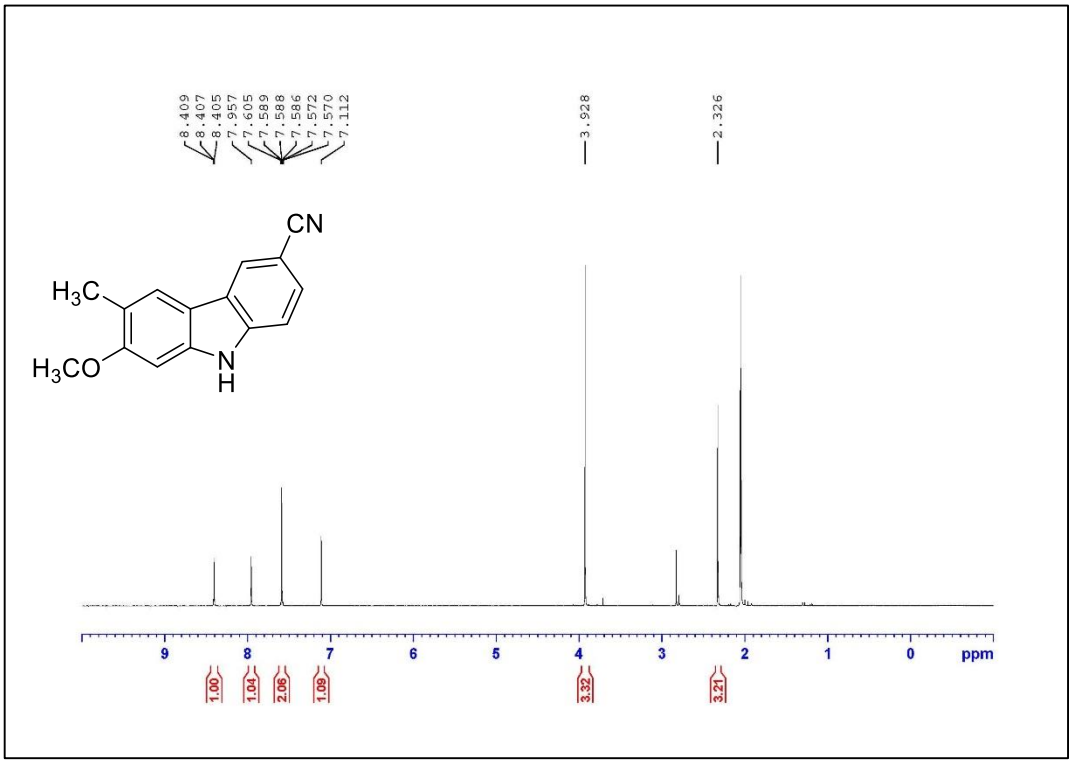

Figure A.55. ^{1}H NMR Spectrum of Compound **1.9l** (500 MHz, acetone-d_6)

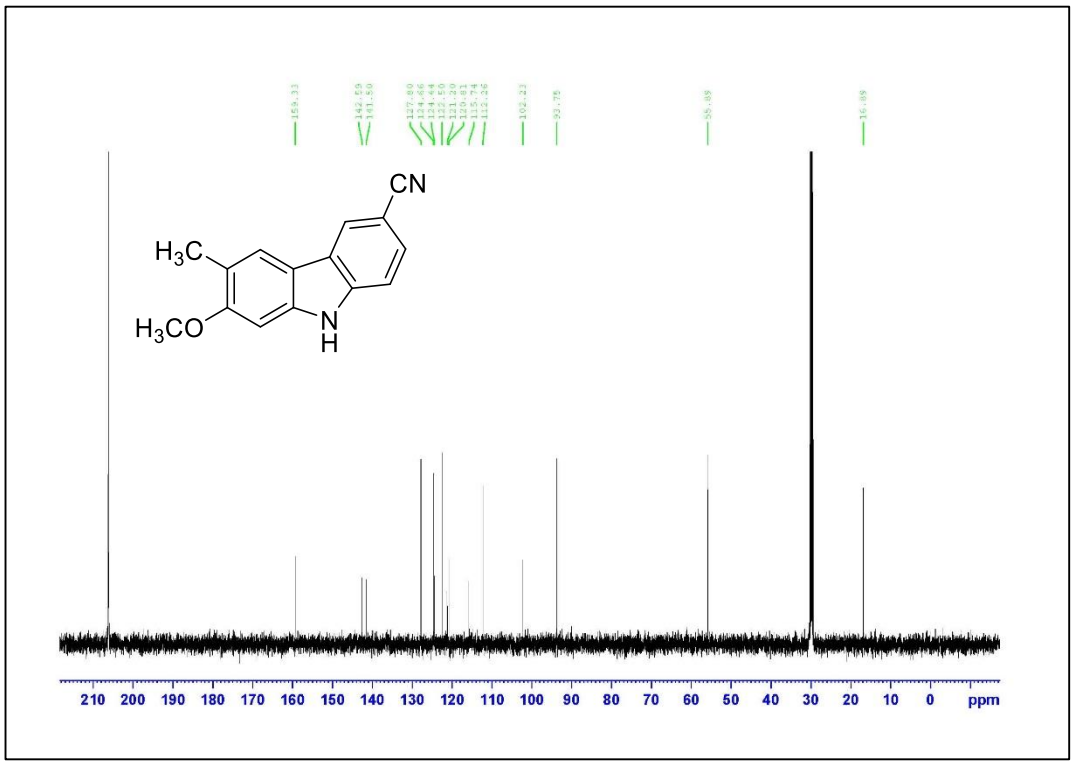

Figure A.56. ^{13}C NMR Spectrum of Compound **1.9l** (125 MHz, acetone-d_6)

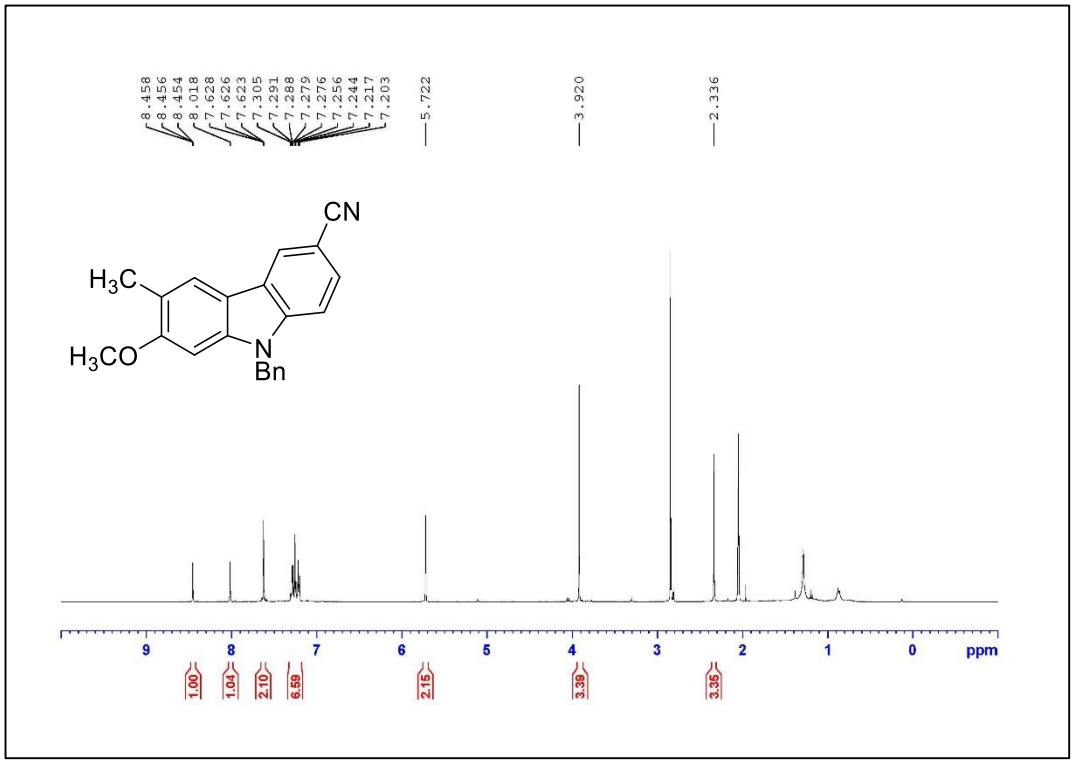

Figure A.57. ^{1}H NMR Spectrum of Compound **1.11l** (500 MHz, acetone-d_6)

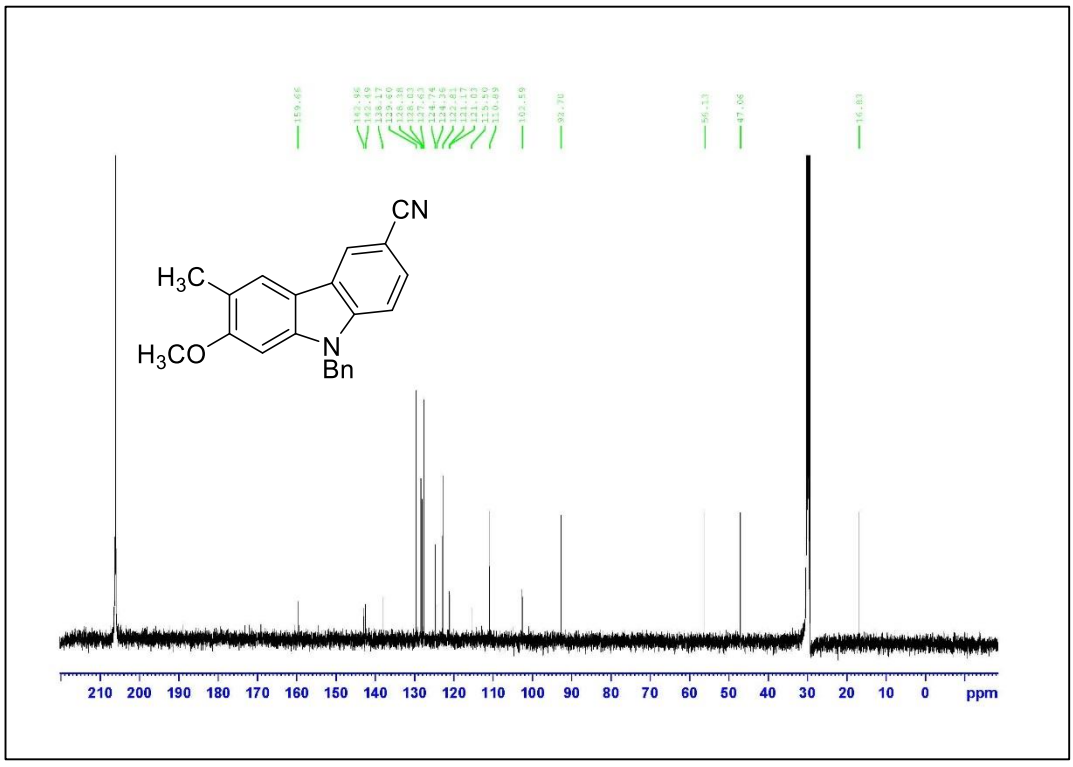

Figure A.58. ^{13}C NMR Spectrum of Compound **1.11l** (125 MHz, acetone-d_6)

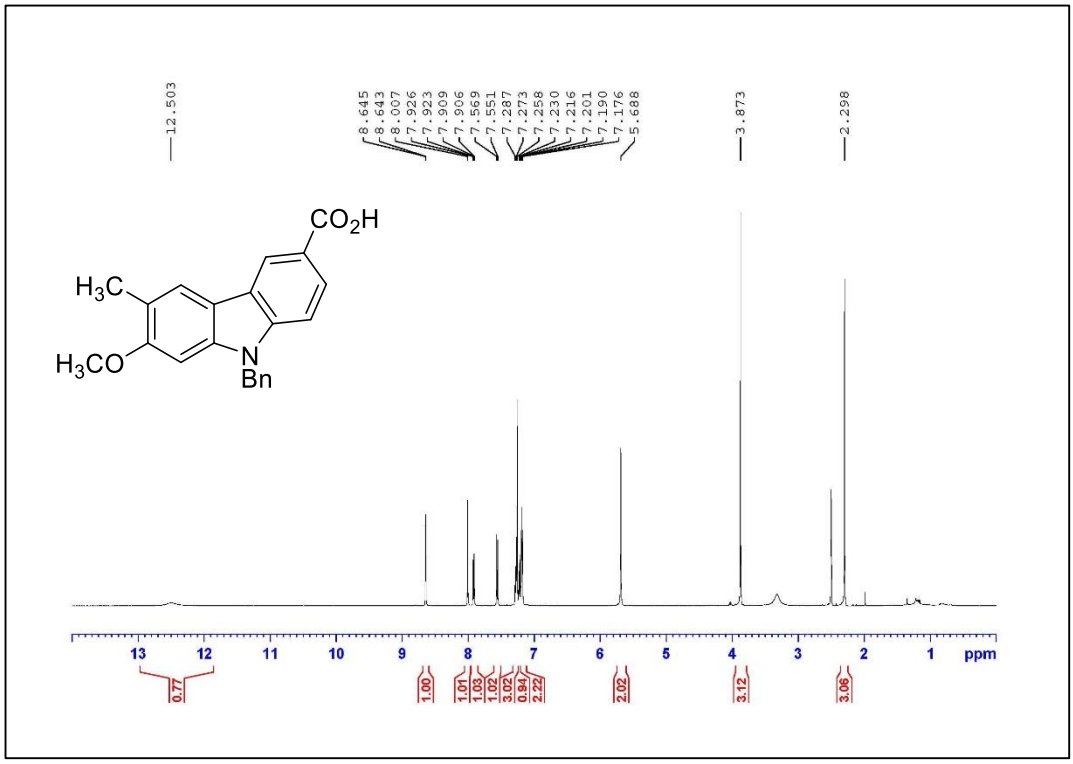

Figure A.59. ^{1}H NMR Spectrum of Compound **1.19** (500 MHz, DMSO-d_6)

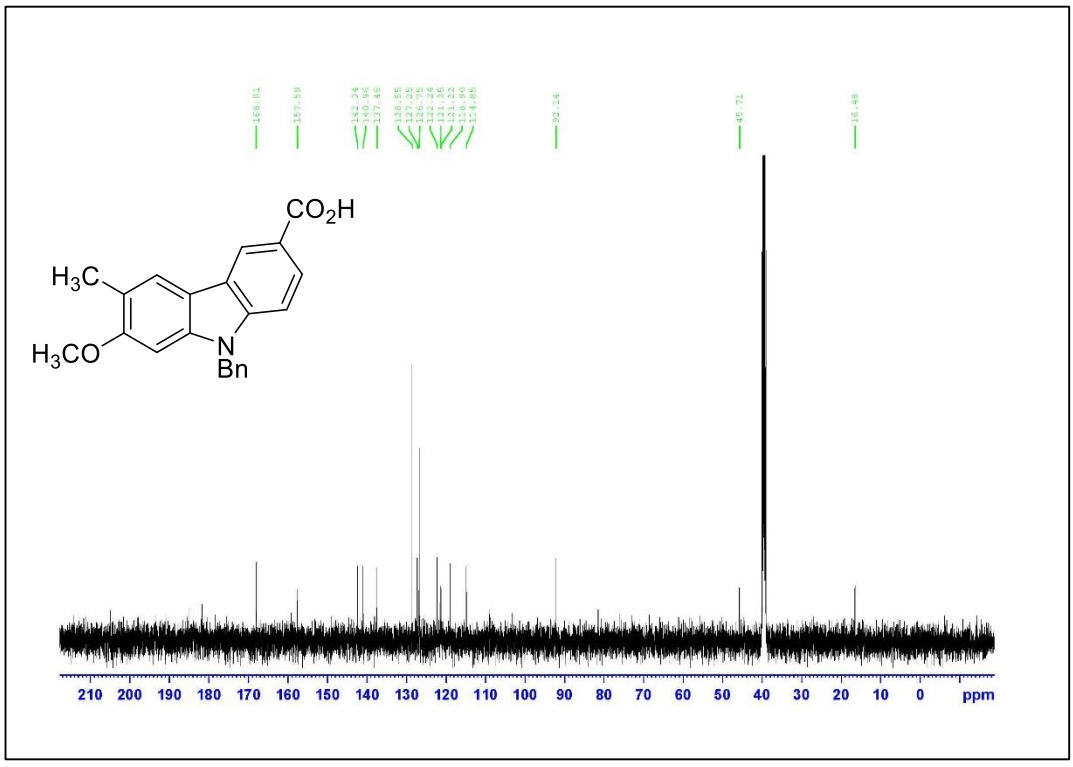

Figure A.60. ^{13}C NMR Spectrum of Compound **1.19** (125 MHz, DMSO-d_6)

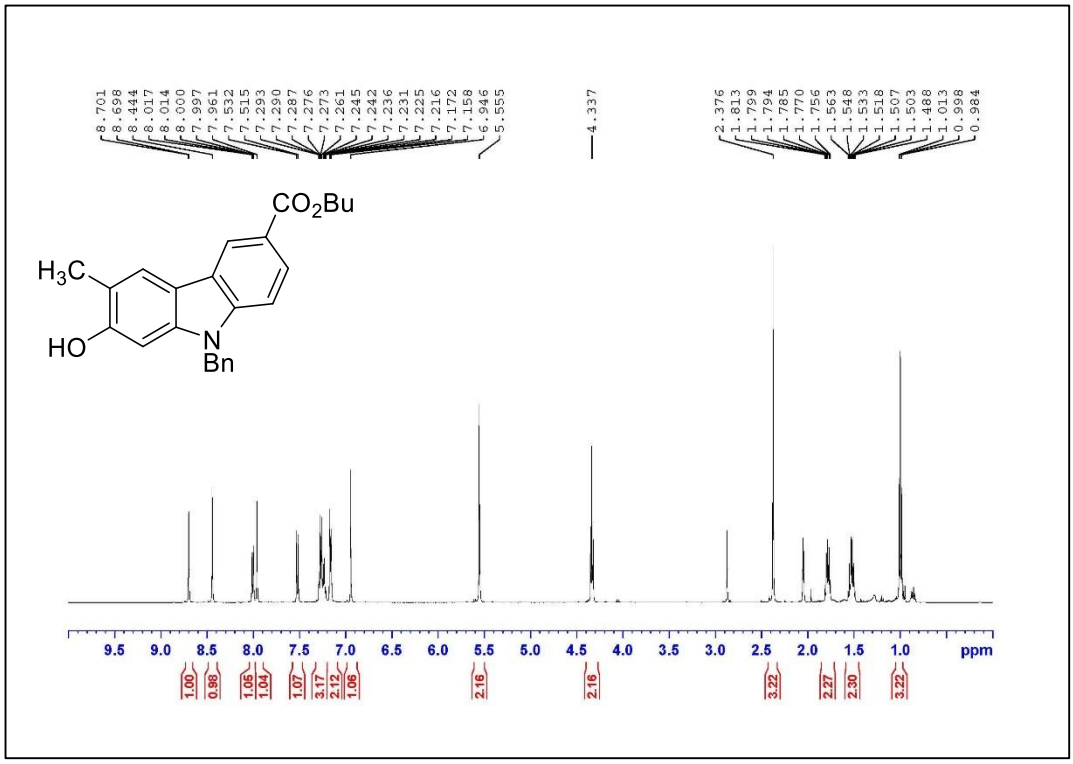

Figure A.61. ^{1}H NMR Spectrum of Compound **1.4l** (500 MHz, acetone-d_6)

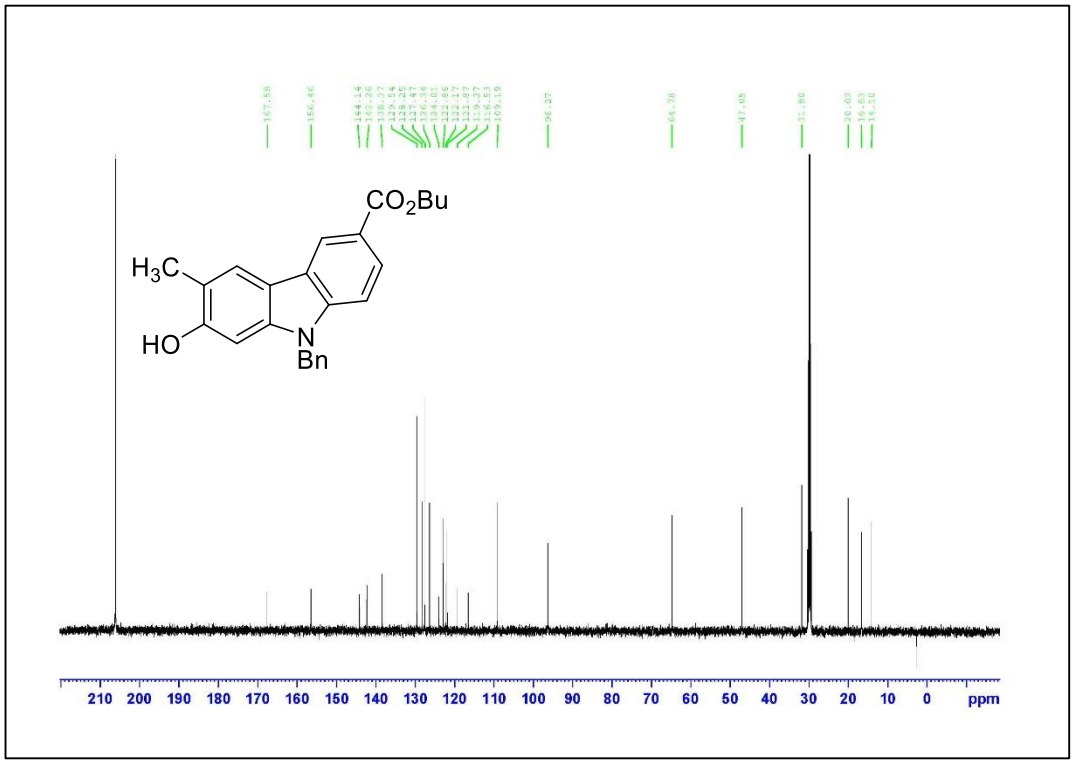

Figure A.62. ^{13}C NMR Spectrum of Compound **1.4l** (125 MHz, acetone-d_6)

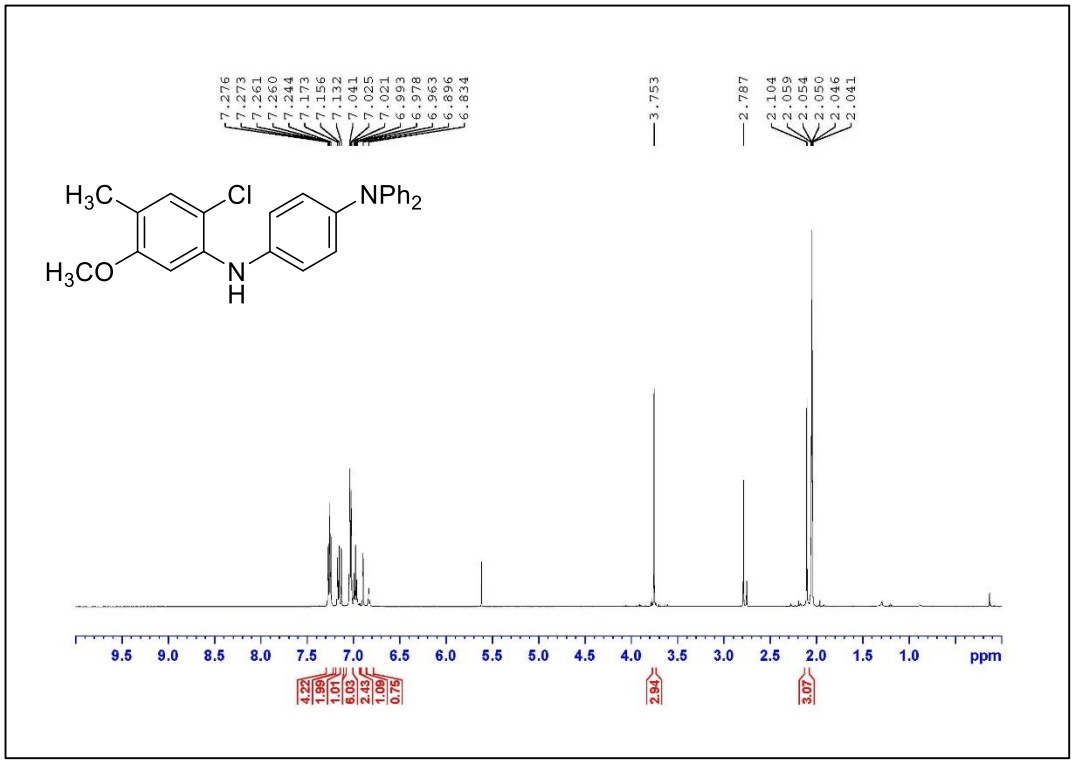

Figure A.63. ^{1}H NMR Spectrum of Compound **1.8m** (500 MHz, acetone-d_6)

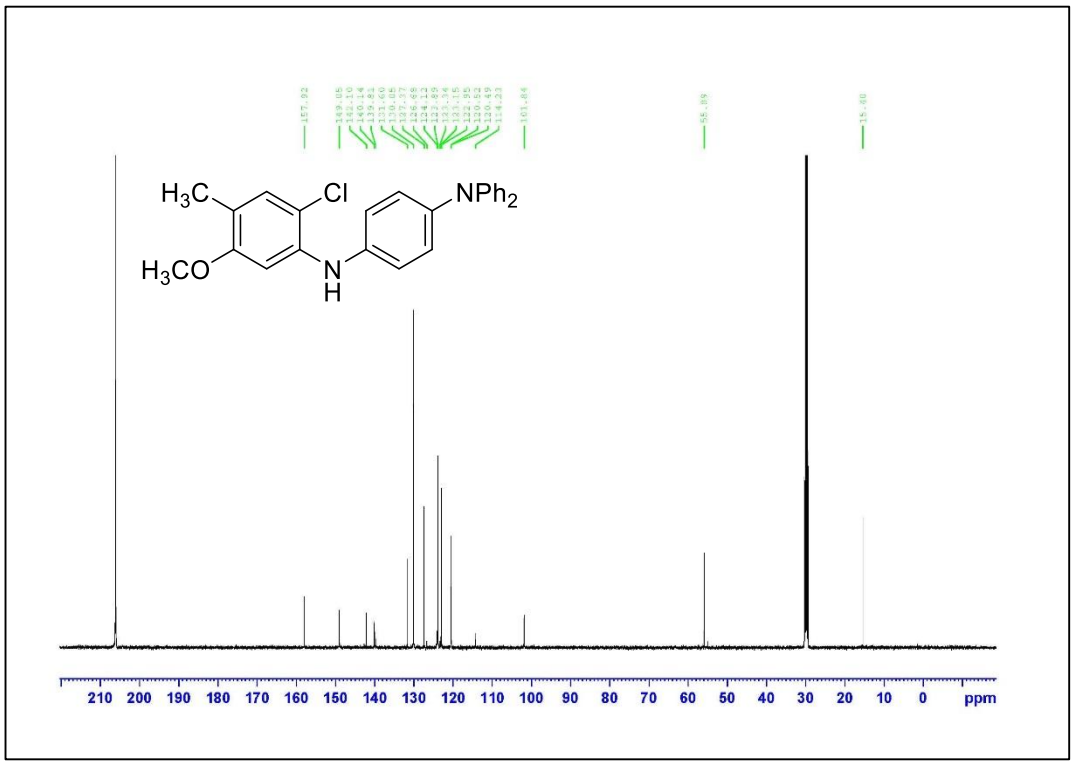

Figure A.64. ^{13}C NMR Spectrum of Compound **1.8m** (125 MHz, acetone-d_6)

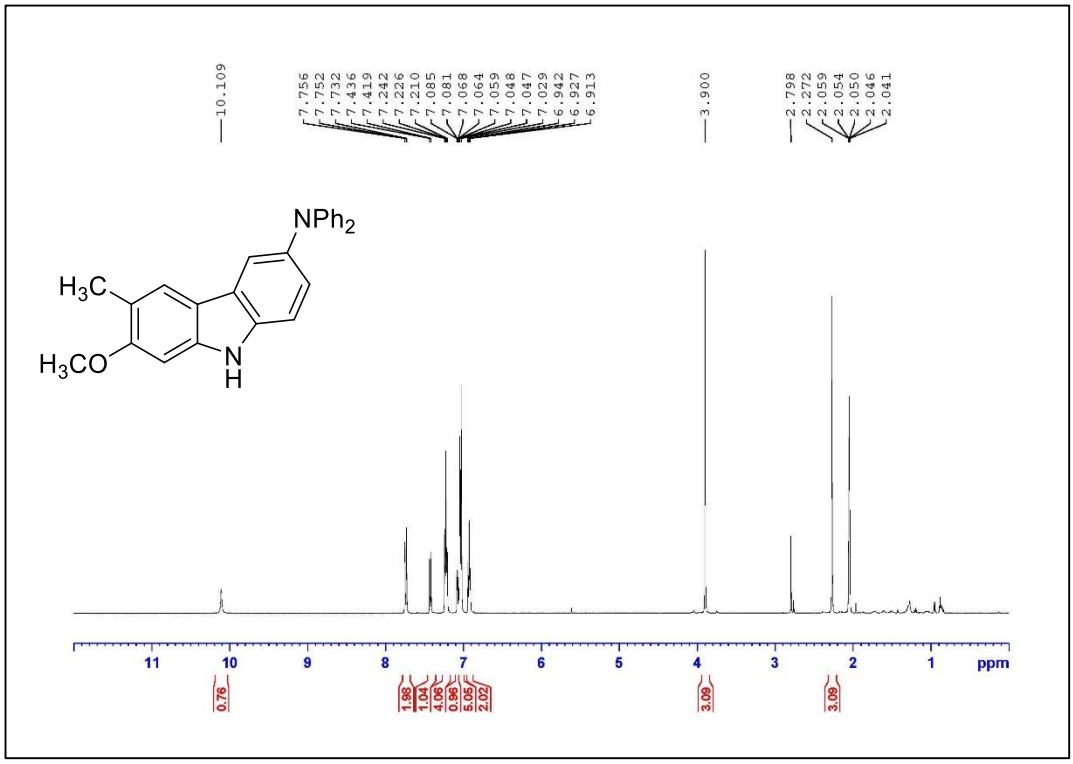

Figure A.65. ^{1}H NMR Spectrum of Compound **1.9m** (500 MHz, acetone-d_6)

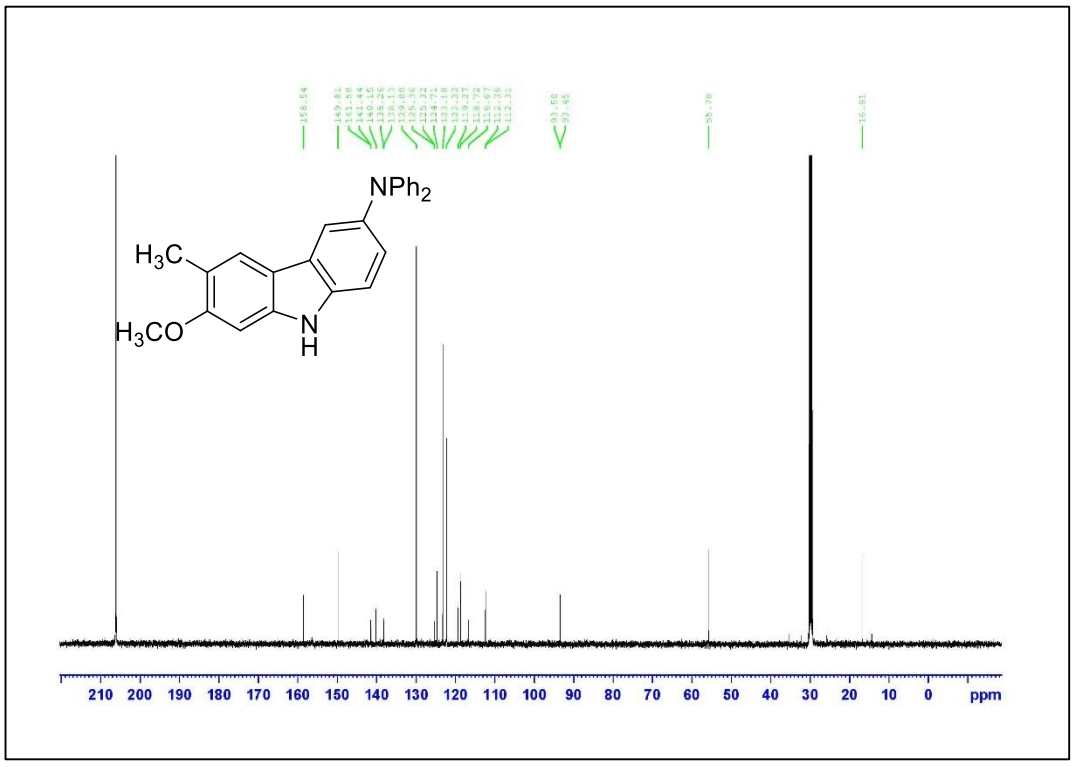

Figure A.66. ^{13}C NMR Spectrum of Compound **1.9m** (125 MHz, acetone-d_6)

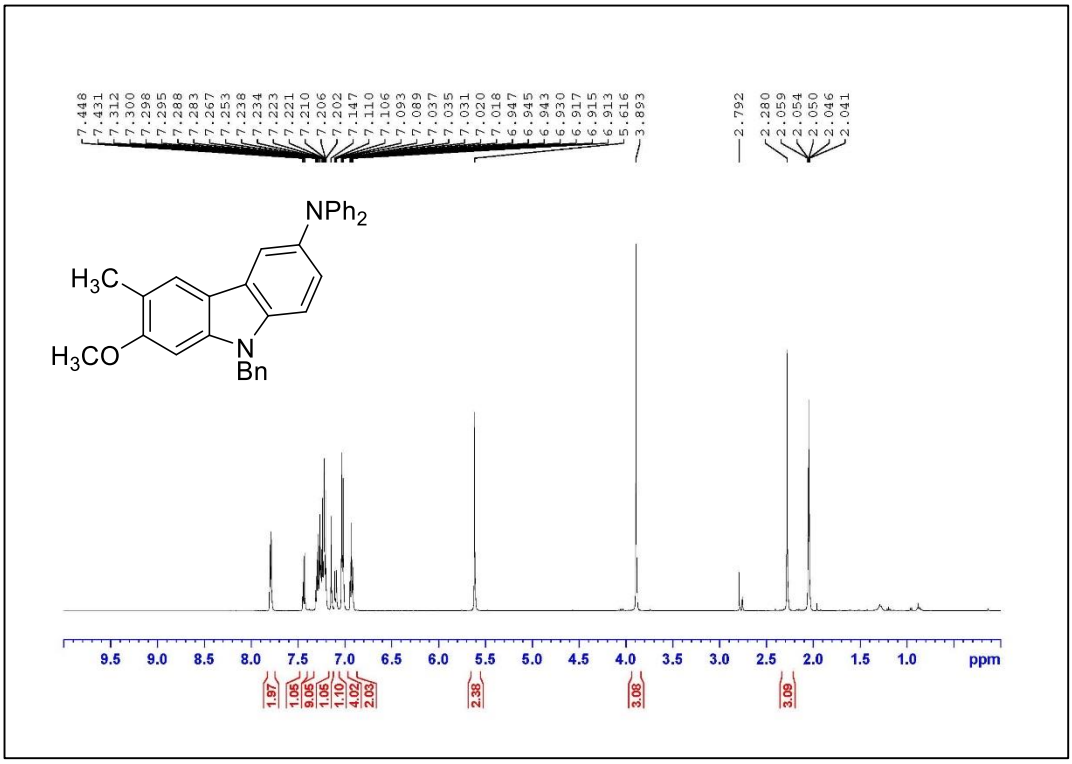

Figure A.67. ^{1}H NMR Spectrum of Compound **1.11m** (500 MHz, acetone-d_6)

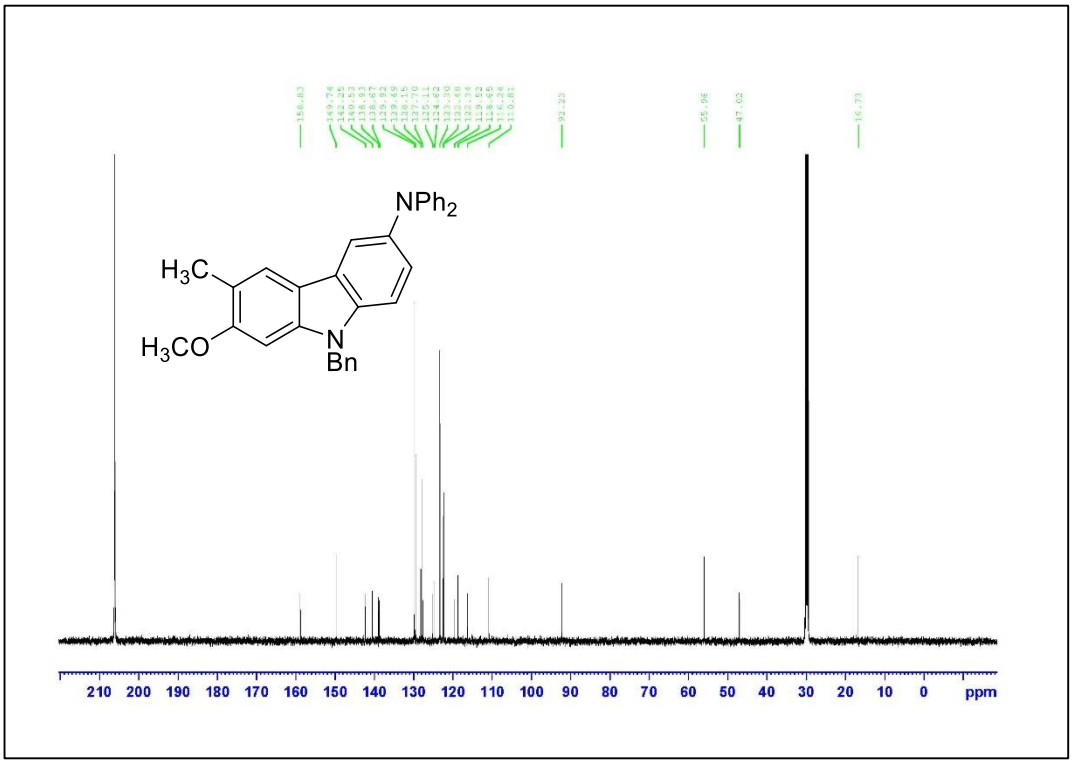

Figure A.68. ^{13}C NMR Spectrum of Compound **1.11m** (125 MHz, acetone-d_6)

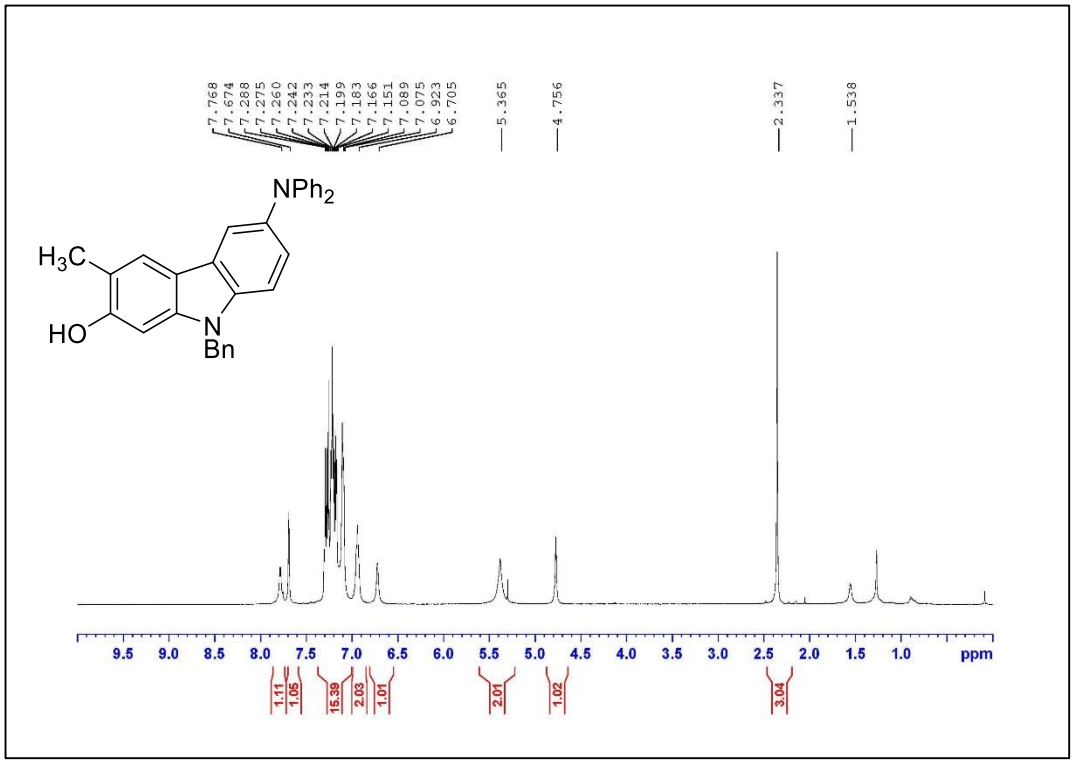

Figure A.69. ^{1}H NMR Spectrum of Compound **1.4m** (500 MHz, $CDCl_3$)

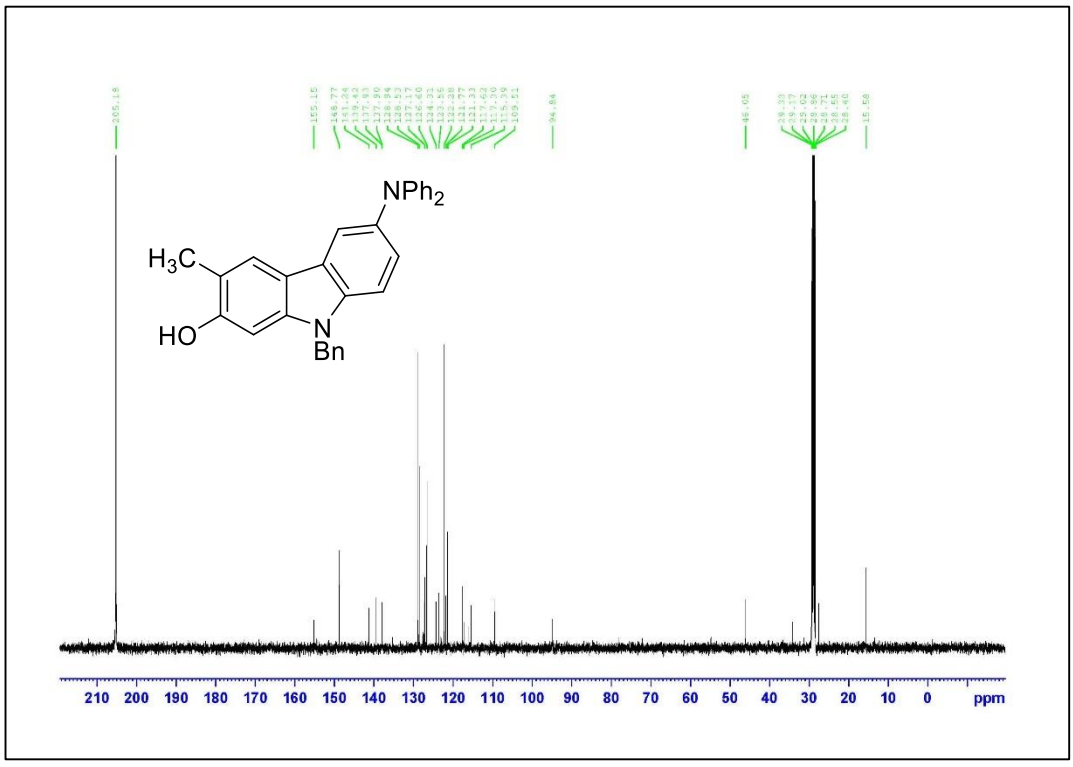

Figure A.70. ^{13}C NMR Spectrum of Compound **1.4m** (125 MHz, acetone-d_6)

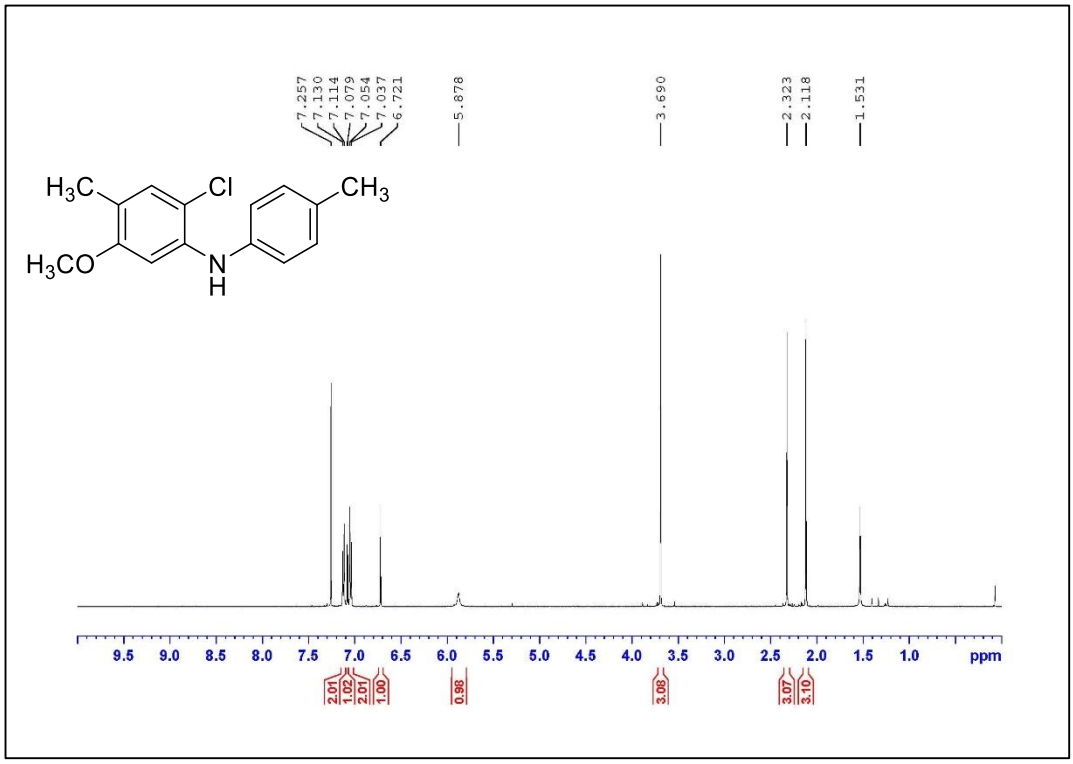

Figure A.71. ^{1}H NMR Spectrum of Compound **1.8n** (500 MHz, $CDCl_3$)

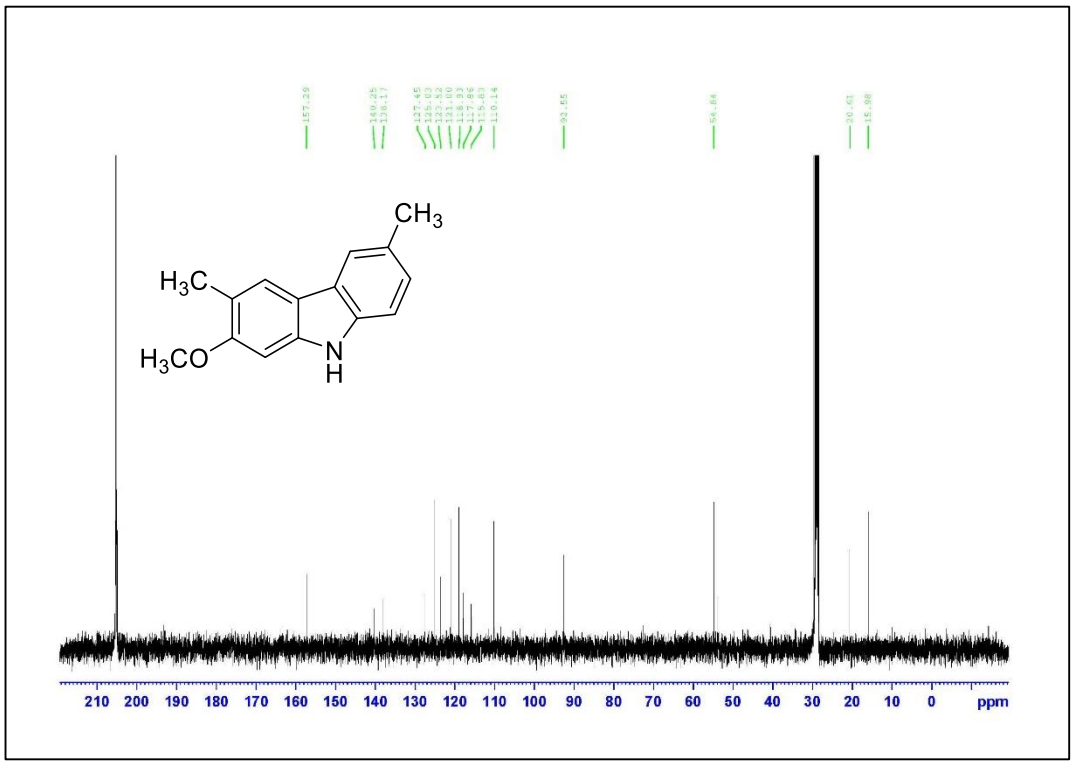

Figure A.72. ^{13}C NMR Spectrum of Compound **1.9n** (125 MHz, acetone-d_6)

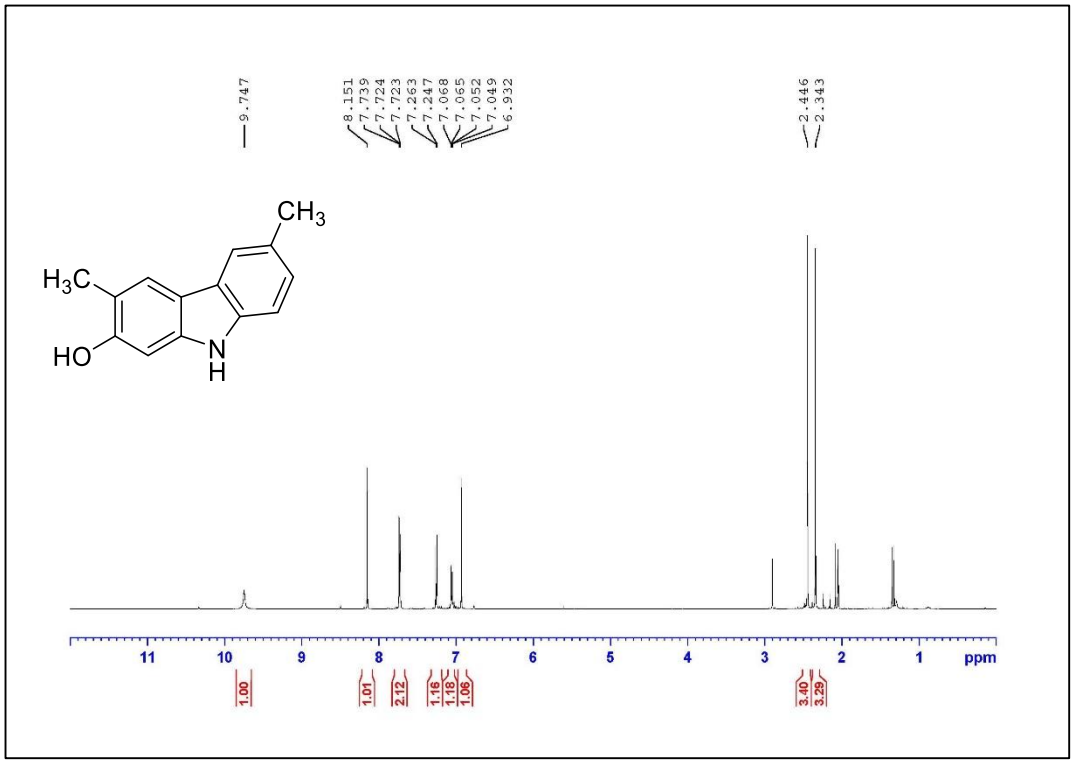

Figure A.73. ^{1}H NMR Spectrum of Compound **1.10n** (500 MHz, acetone-d_6)

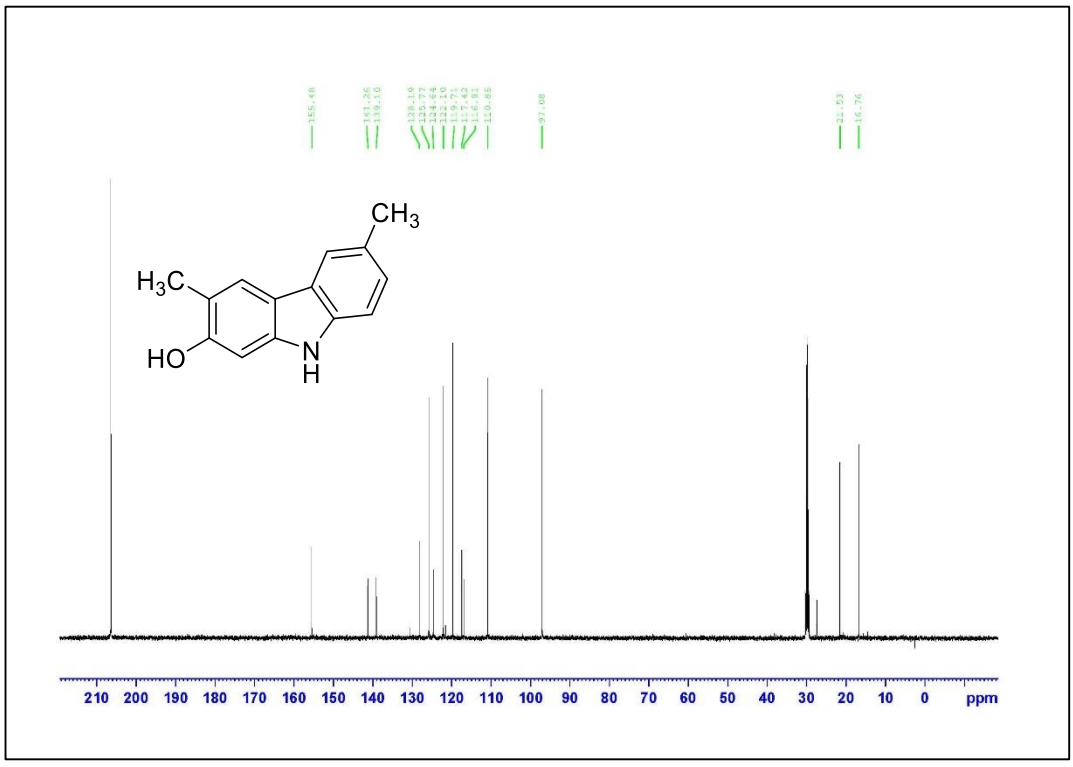

Figure A.74. ^{13}C NMR Spectrum of Compound **1.10n** (125 MHz, acetone-d_6)

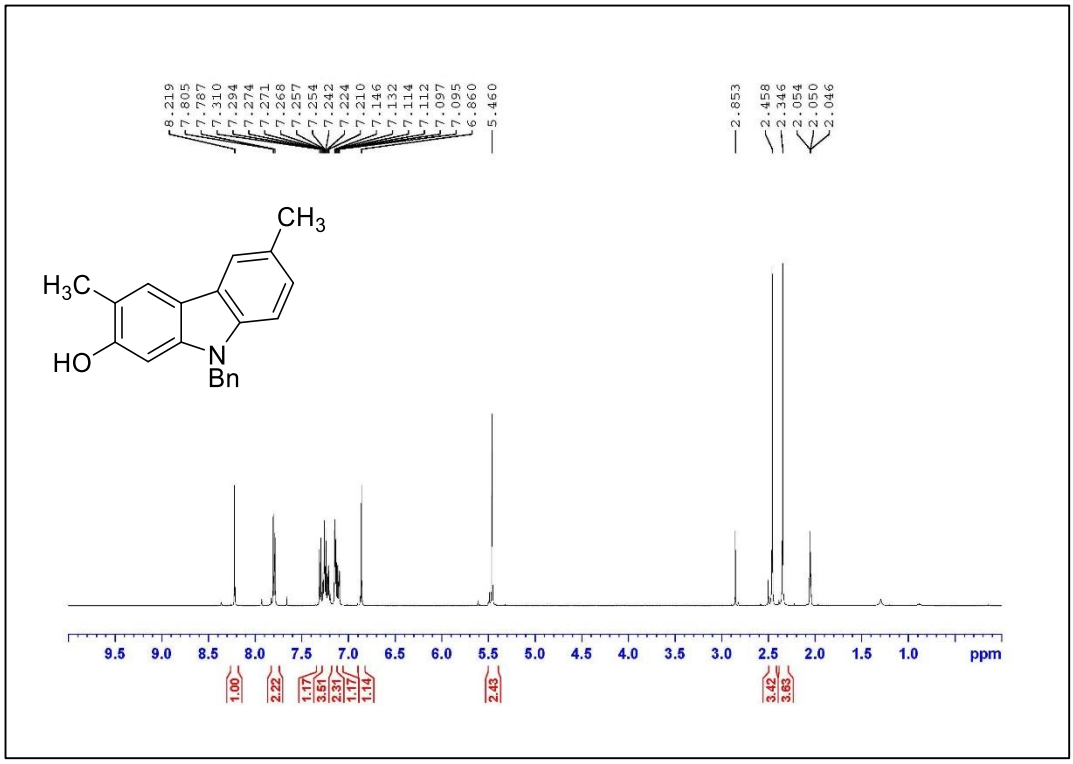

Figure A.75. ^{1}H NMR Spectrum of Compound **1.4n** (500 MHz, acetone-d_6)

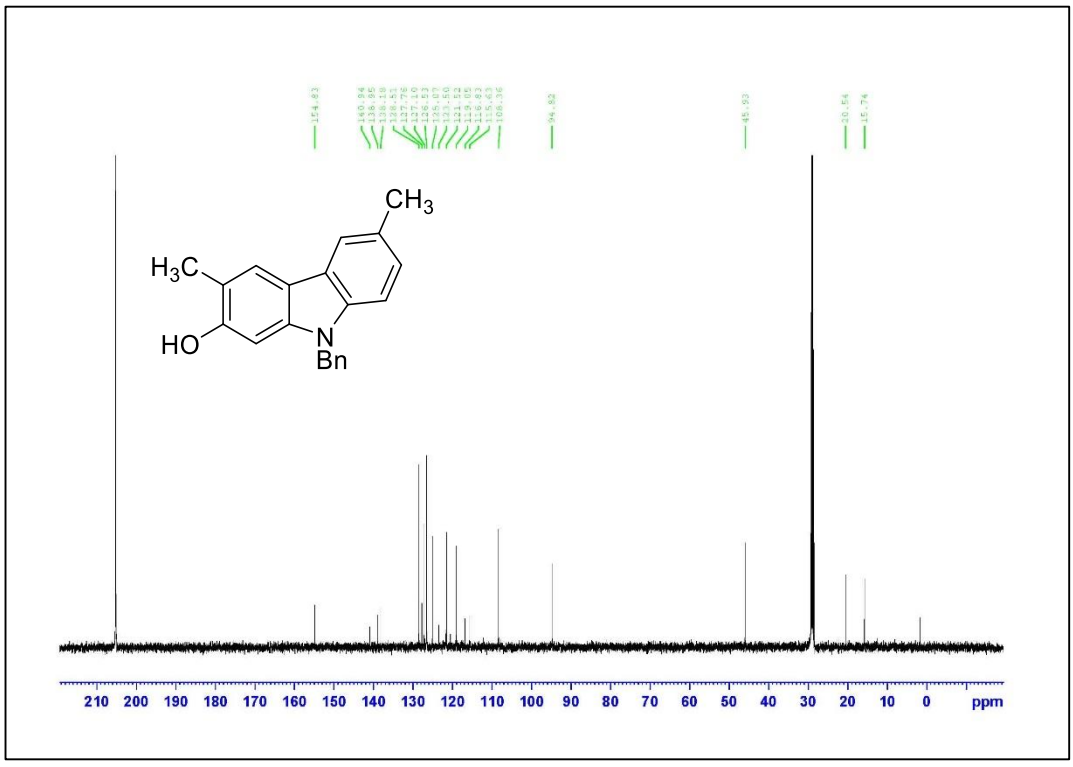

Figure A.76. ^{13}C NMR Spectrum of Compound **1.4n** (125 MHz, acetone-d_6)

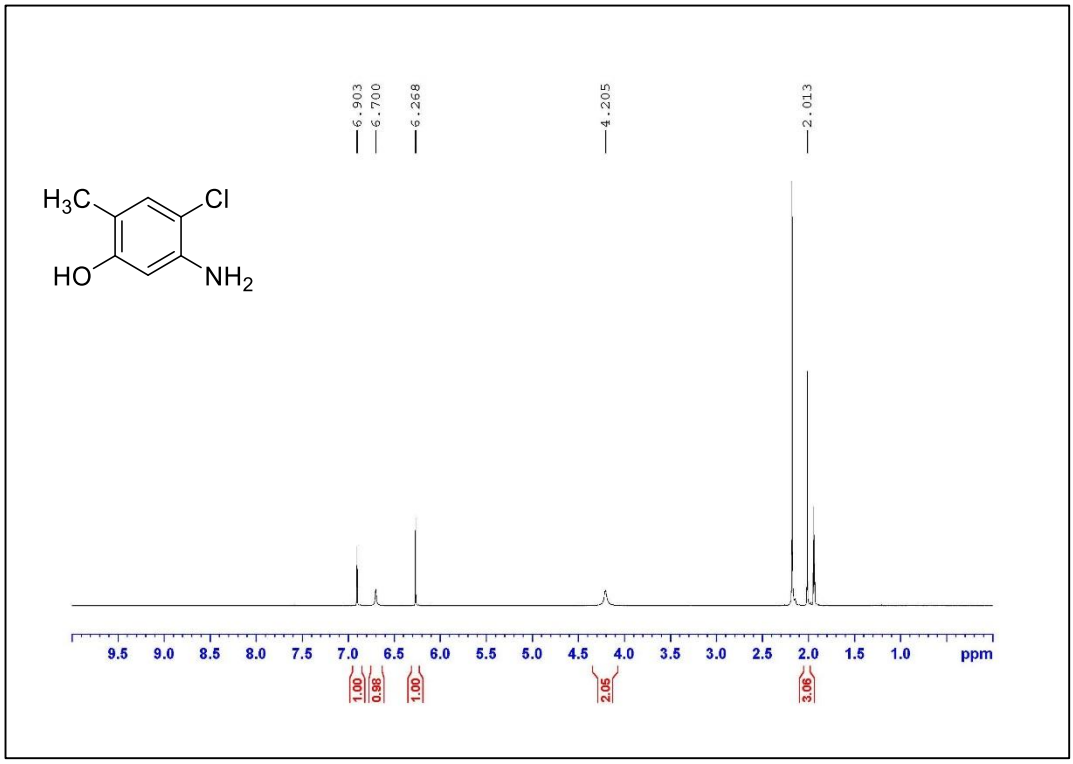

Figure A.77. ^{1}H NMR Spectrum of Compound **1.S1** (500 MHz, CD_3CN)

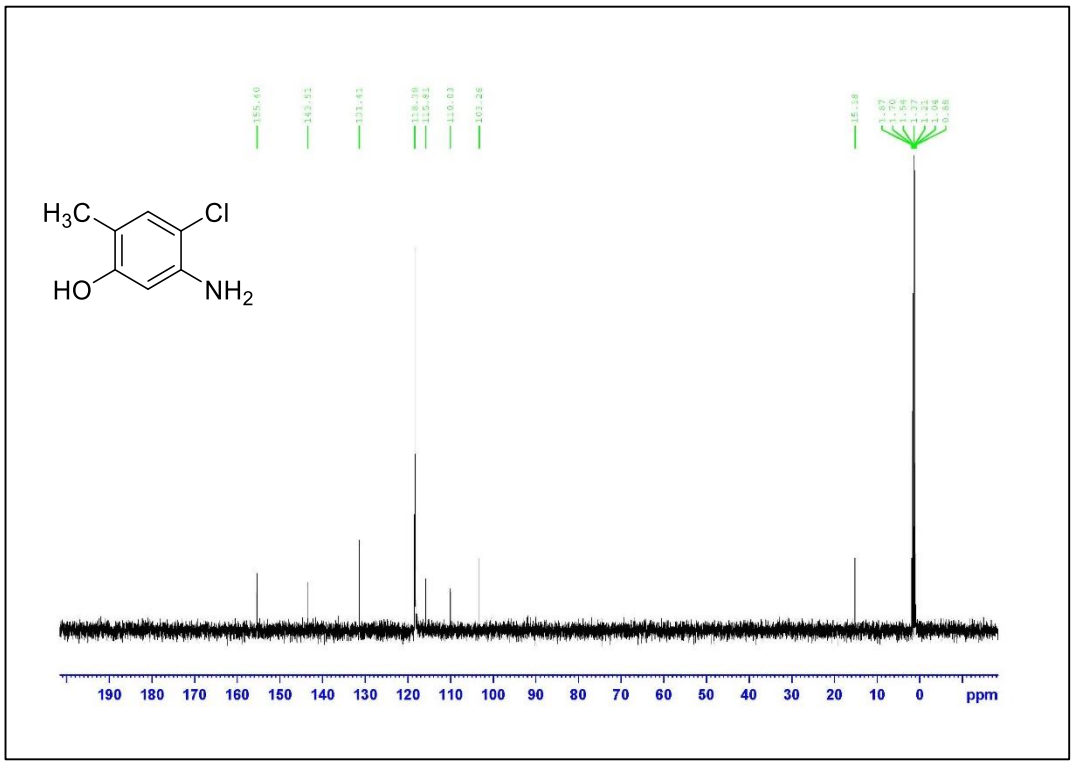

Figure A.78. ^{13}C NMR Spectrum of Compound **1.S1** (125 MHz, CD_3CN)

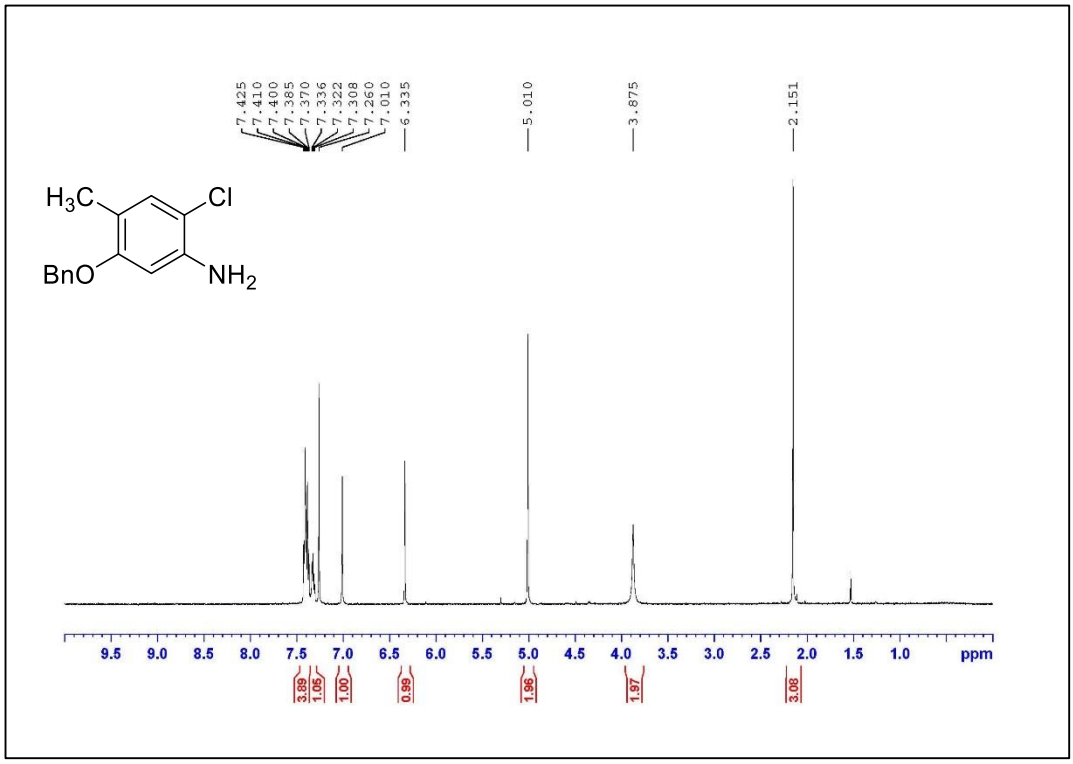

Figure A.79. ^{1}H NMR Spectrum of Compound **1.14** (500 MHz, $CDCl_3$)

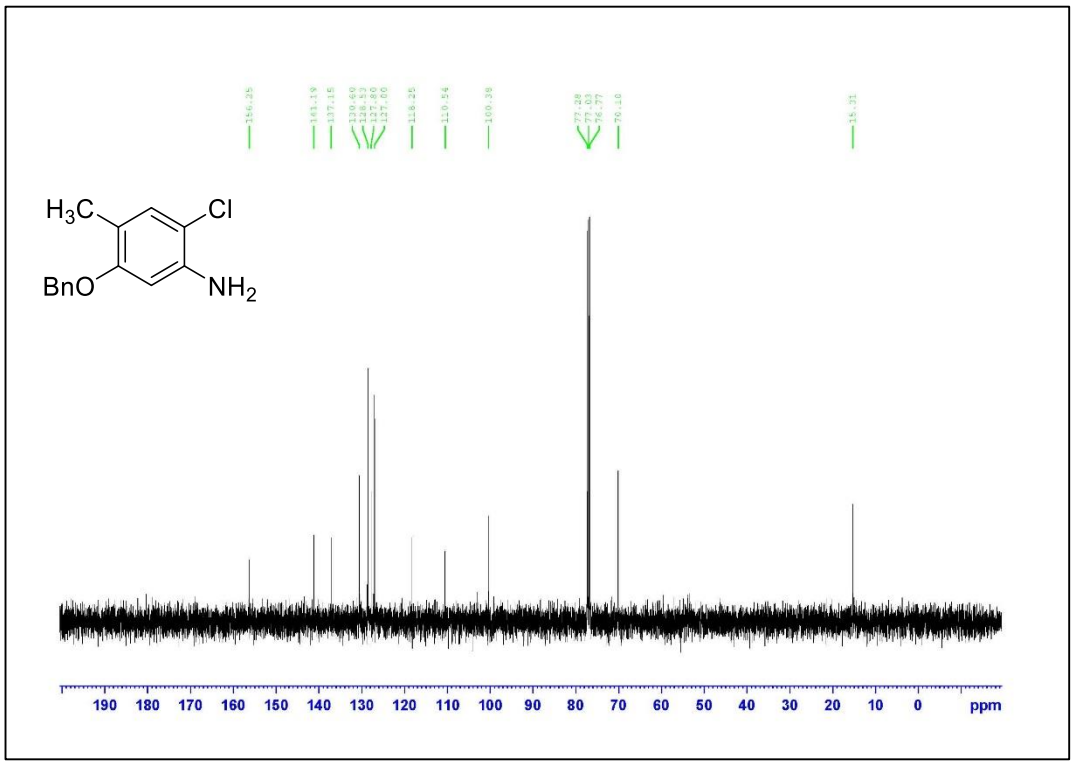

Figure A.80. ^{13}C NMR Spectrum of Compound **1.14** (125 MHz, $CDCl_3$)

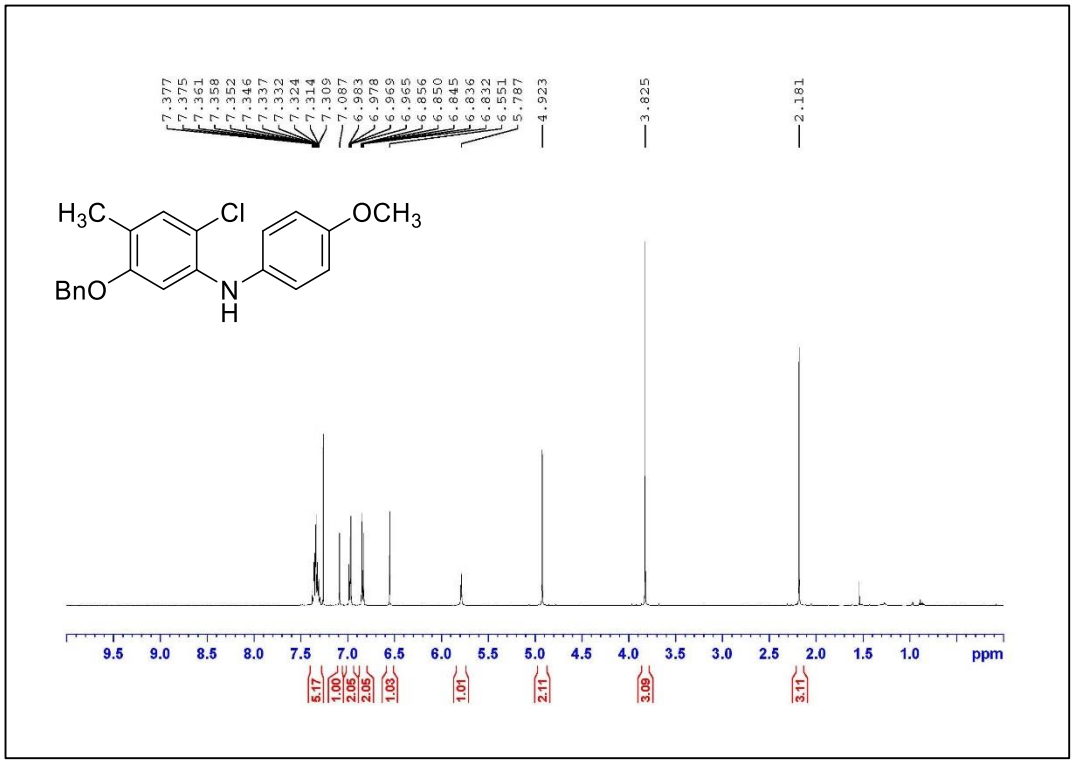

Figure A.81. ^{1}H NMR Spectrum of Compound **1.16** (500 MHz, $CDCl_3$)

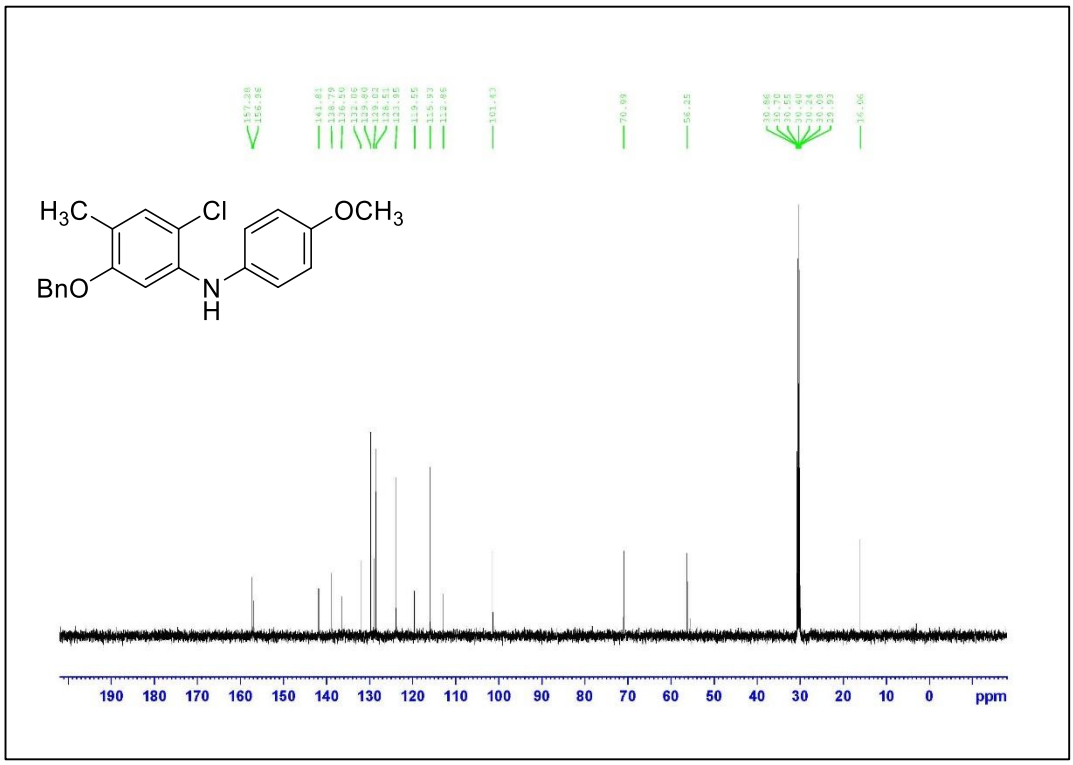

Figure A.82. ^{13}C NMR Spectrum of Compound **1.16** (125 MHz, acetone-d_6)

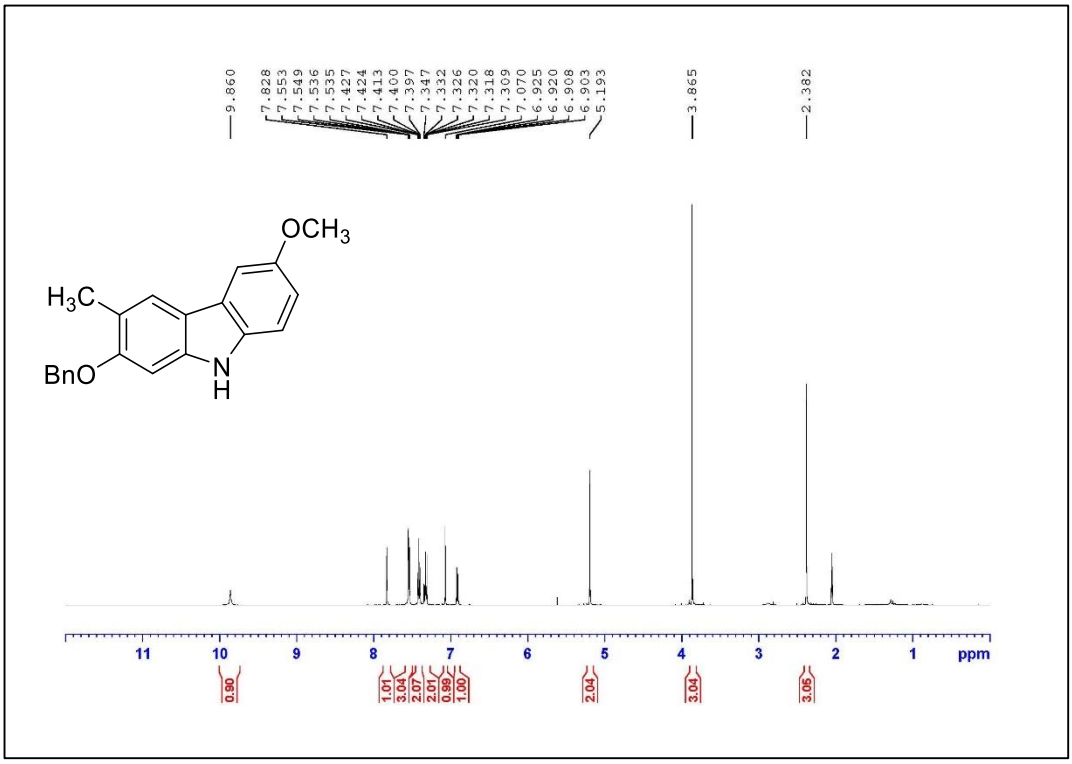

Figure A.83. ^{1}H NMR Spectrum of Compound **1.17** (500 MHz, acetone-d_6)

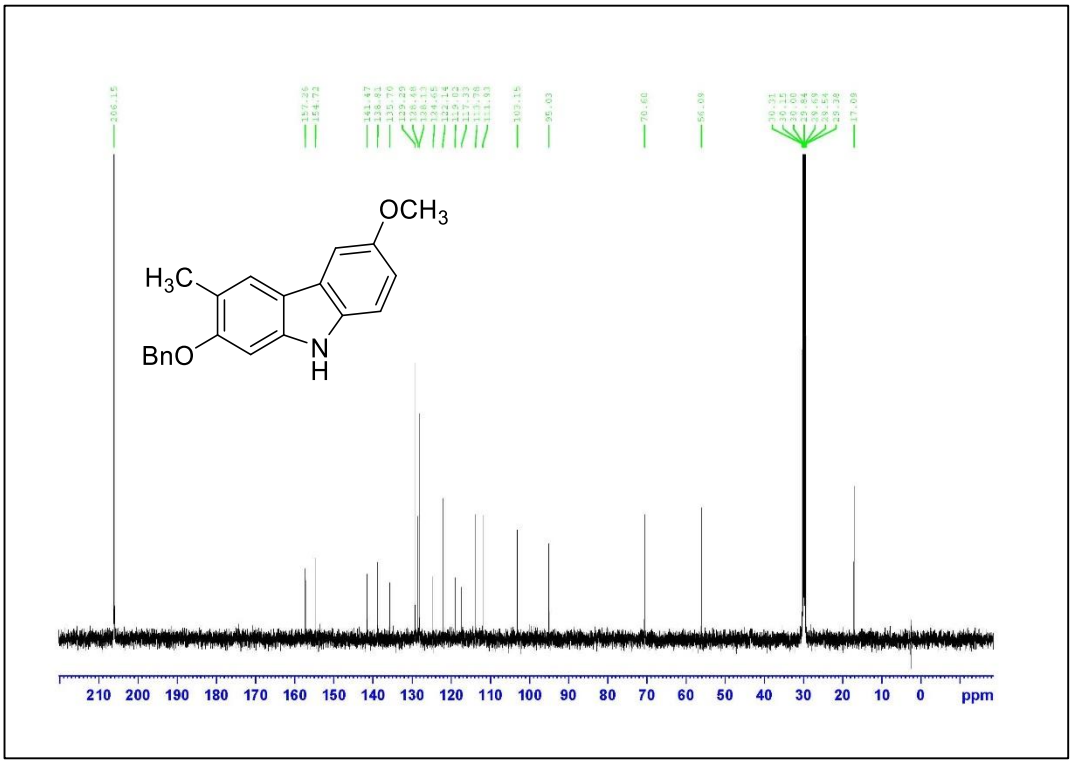

Figure A.84. ^{13}C NMR Spectrum of Compound **1.17** (125 MHz, acetone-d_6)

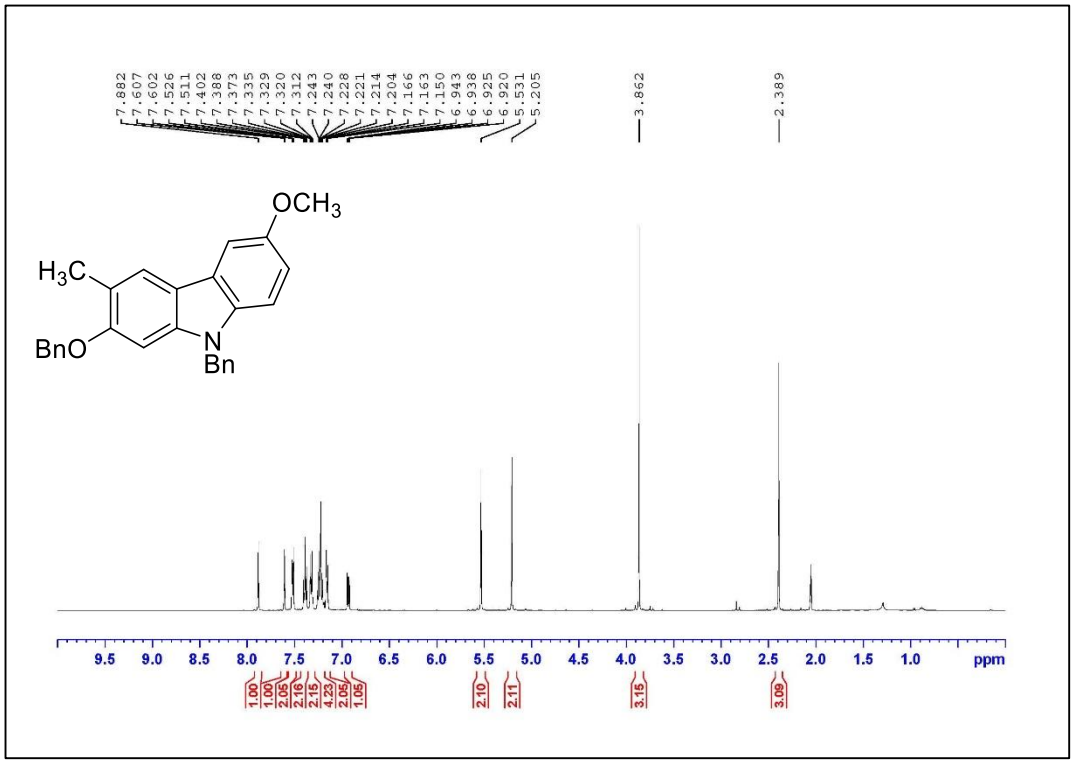

Figure A.85. ^{1}H NMR Spectrum of Compound **1.18** (500 MHz, acetone-d_6)

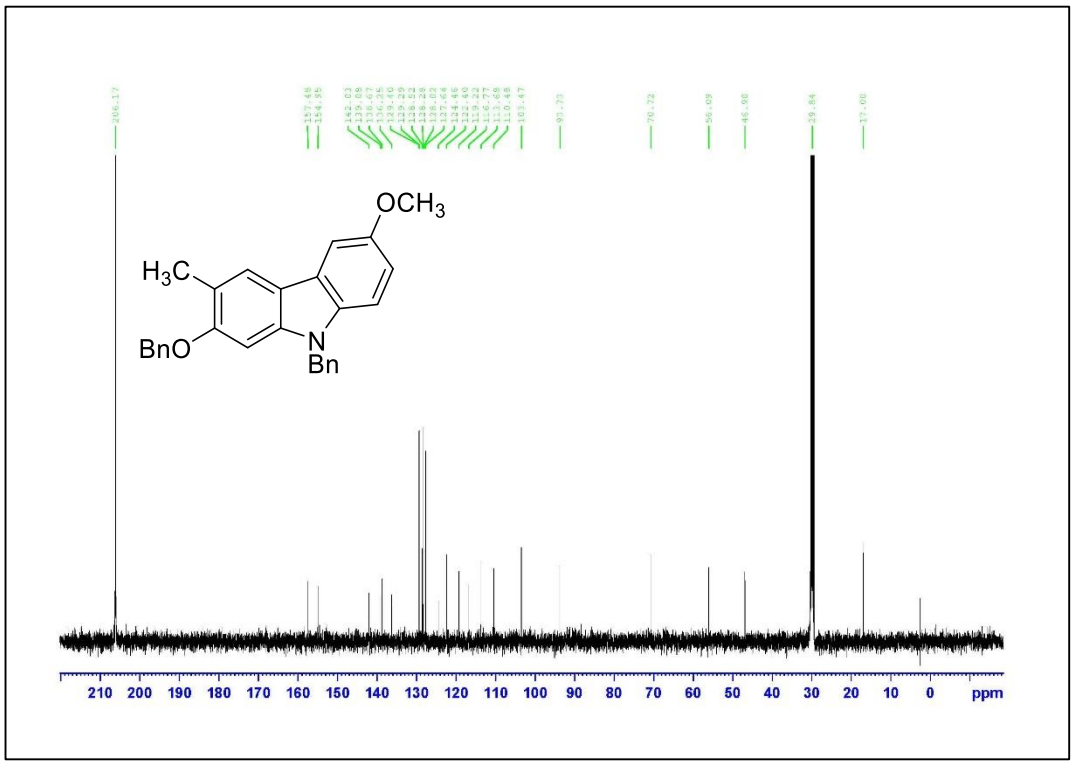

Figure A.86. ^{13}C NMR Spectrum of Compound **1.18** (125 MHz, acetone-d_6)

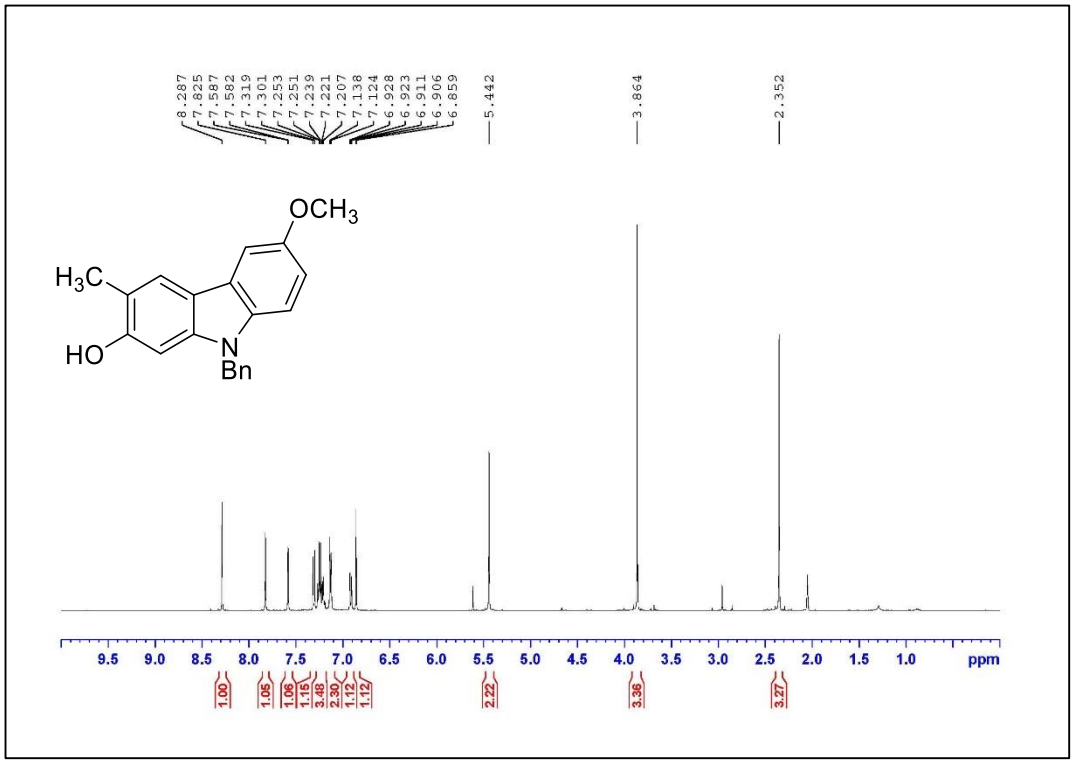

Figure A.87. ^{1}H NMR Spectrum of Compound **1.4o** (500 MHz, acetone-d_6)

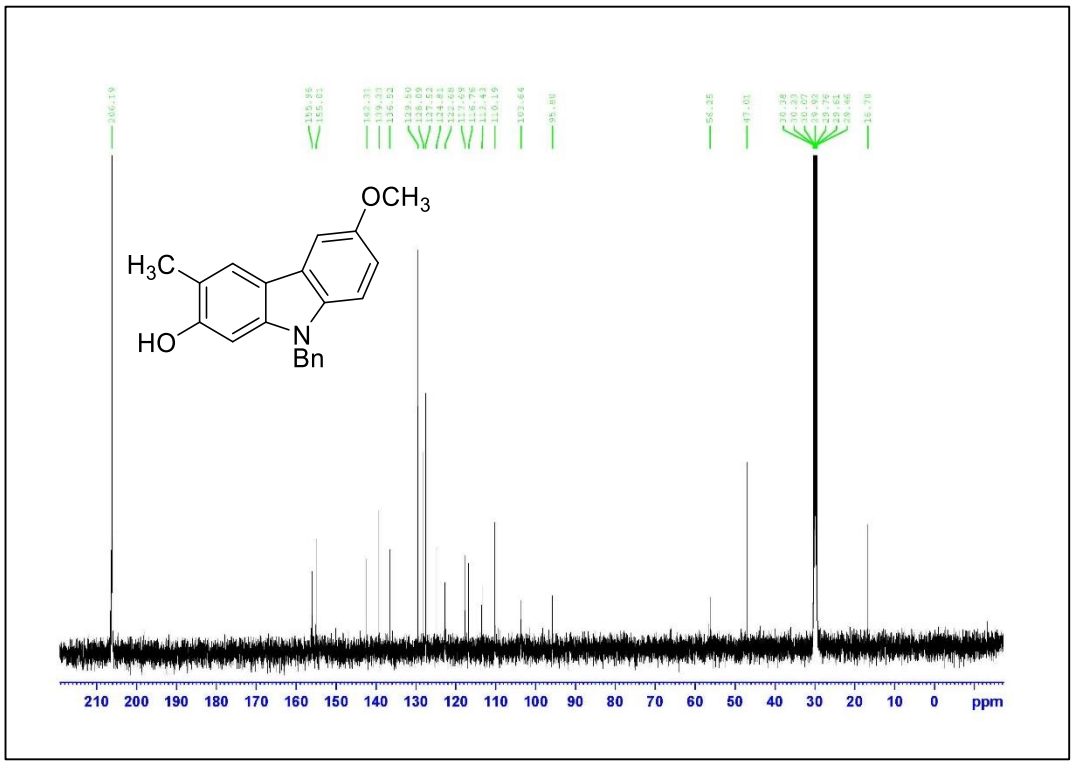

Figure A.88. ^{13}C NMR Spectrum of Compound **1.4o** (125 MHz, acetone-d_6)

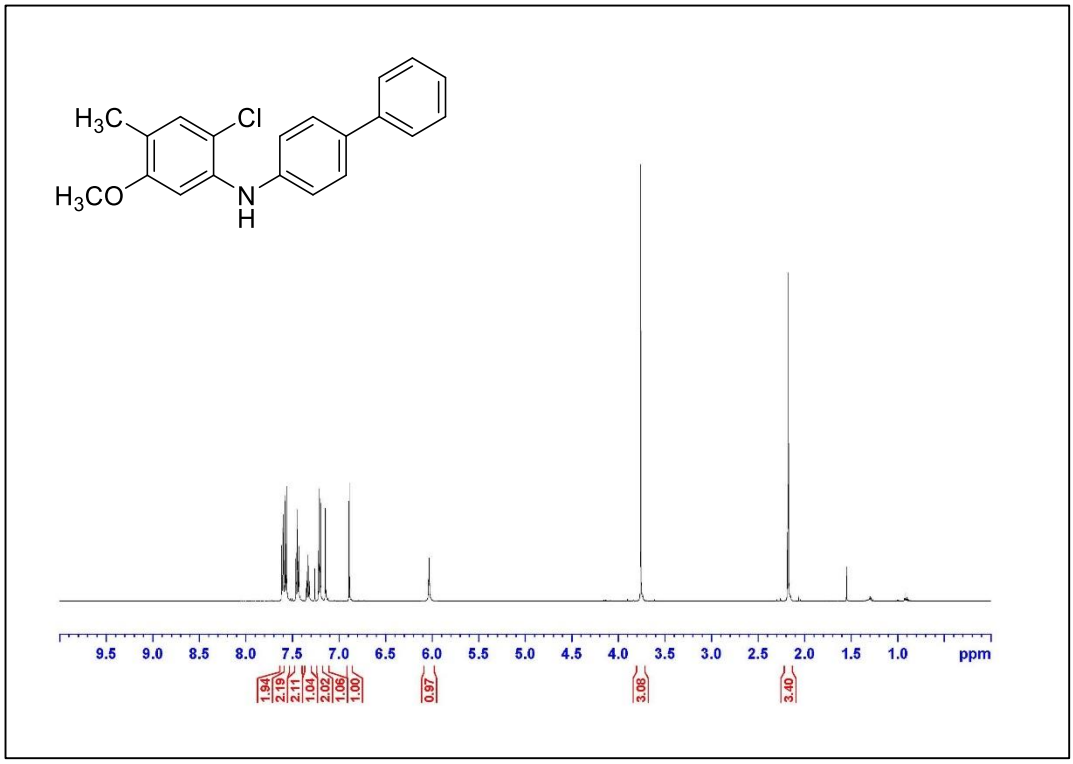

Figure A.89. ^{1}H NMR Spectrum of Compound **1.8p** (500 MHz, $CDCl_3$)

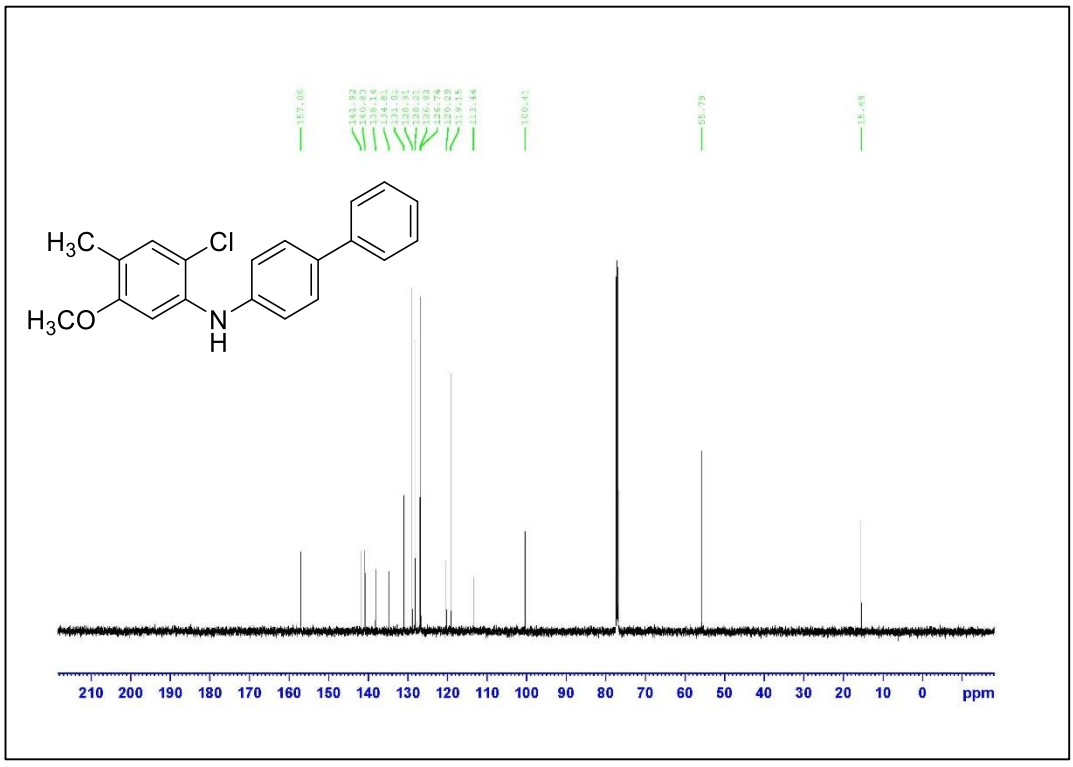

Figure A.90. ^{13}C NMR Spectrum of Compound **1.8p** (125 MHz, $CDCl_3$)

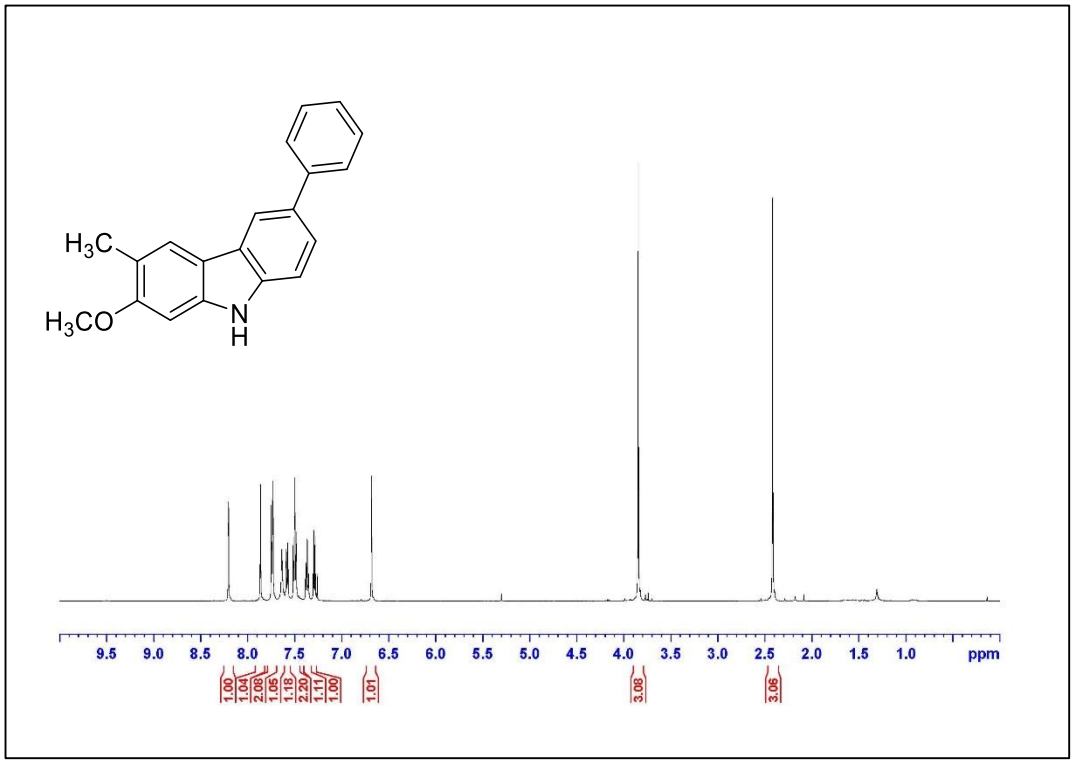

Figure A.91. ^{1}H NMR Spectrum of Compound **1.9p** (500 MHz, $CDCl_3$)

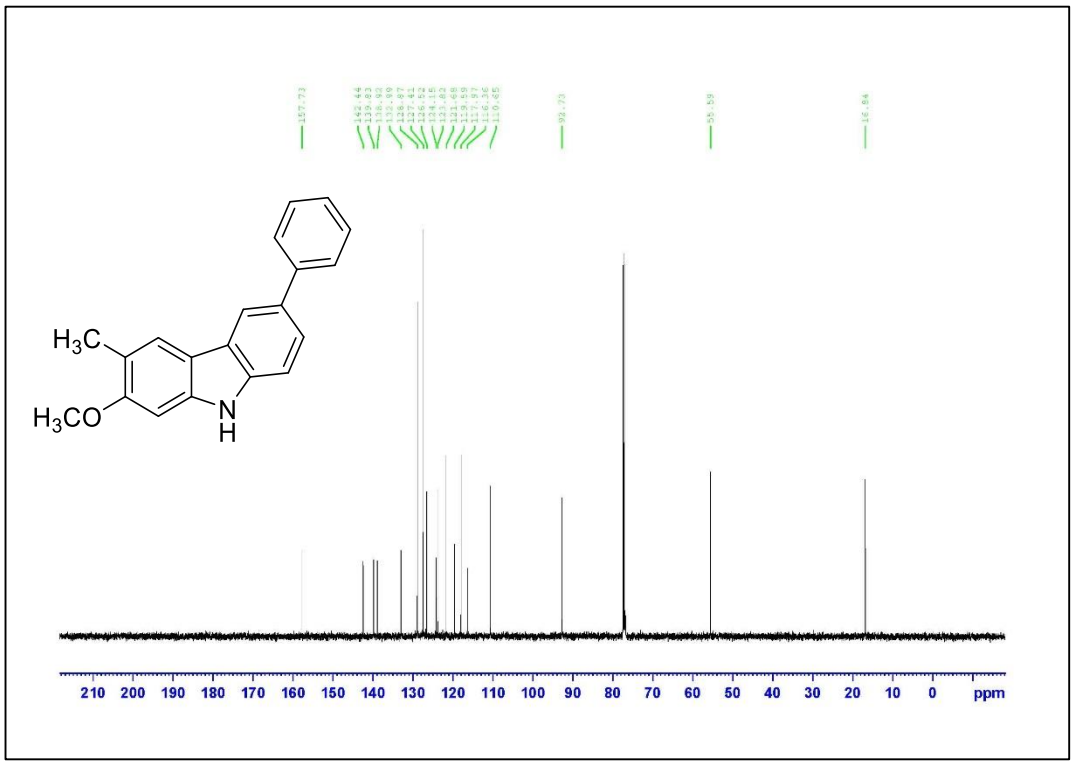

Figure A.92. ^{13}C NMR Spectrum of Compound **1.9p** (125 MHz, $CDCl_3$)

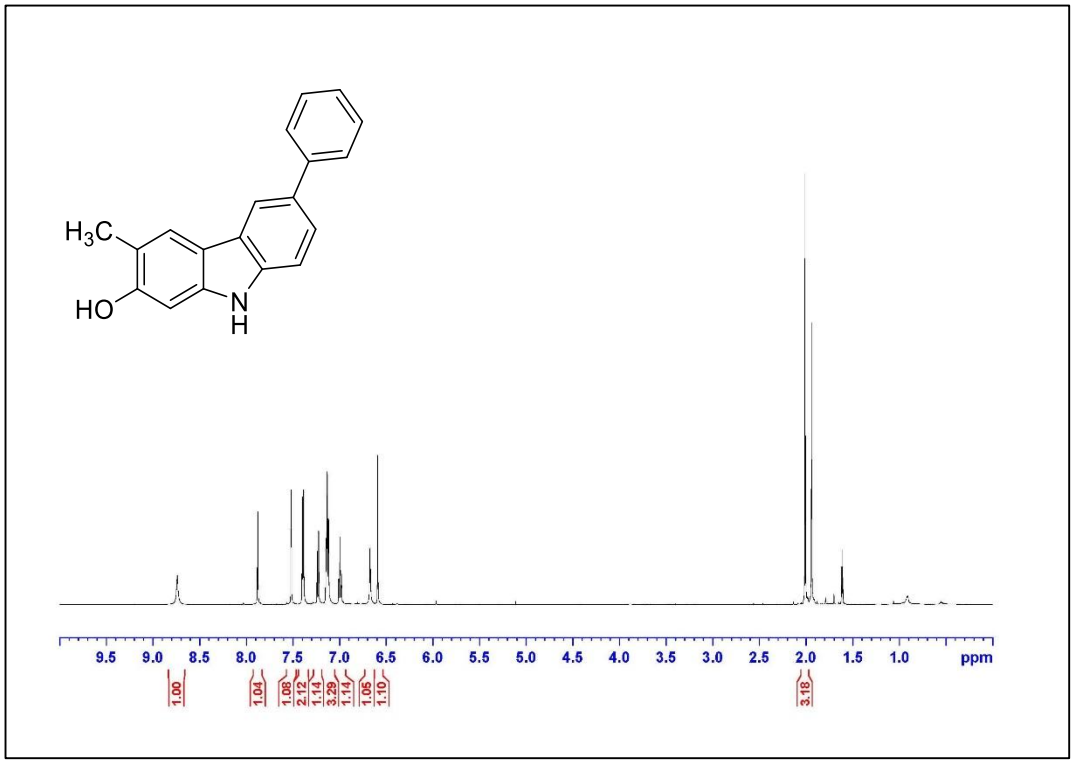

Figure A.93. ^{1}H NMR Spectrum of Compound **1.10p** (500 MHz, CD_3CN)

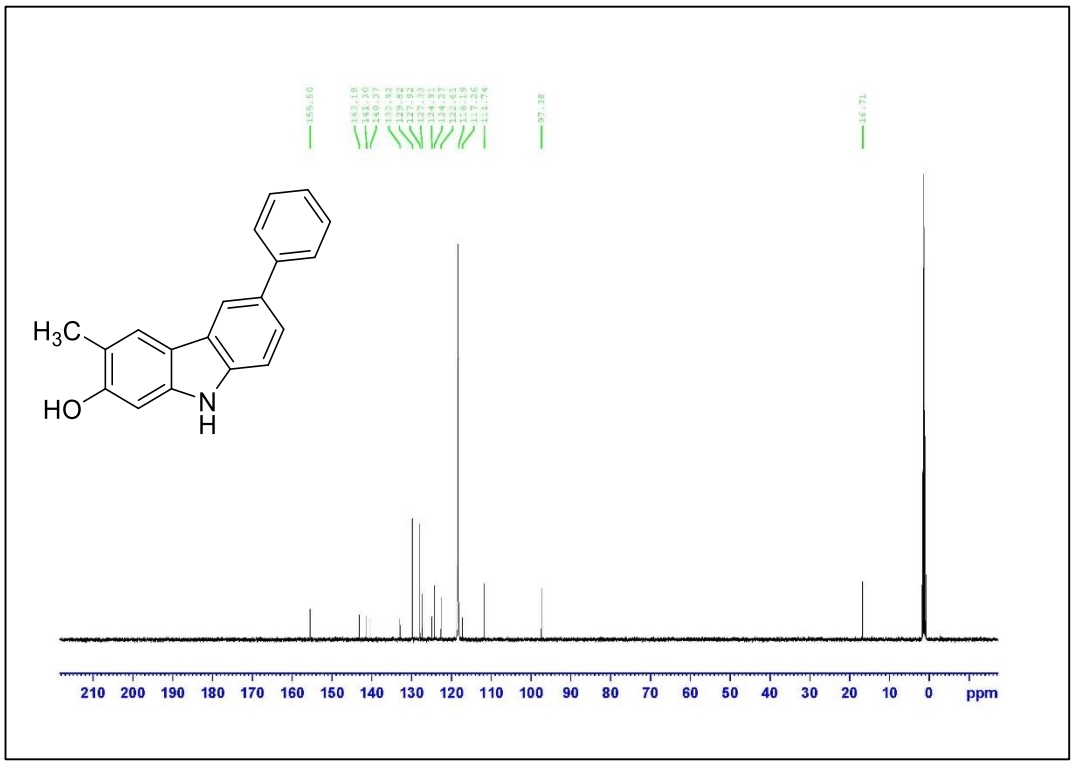

Figure A.94. ^{13}C NMR Spectrum of Compound **1.10p** (125 MHz, CD_3CN)

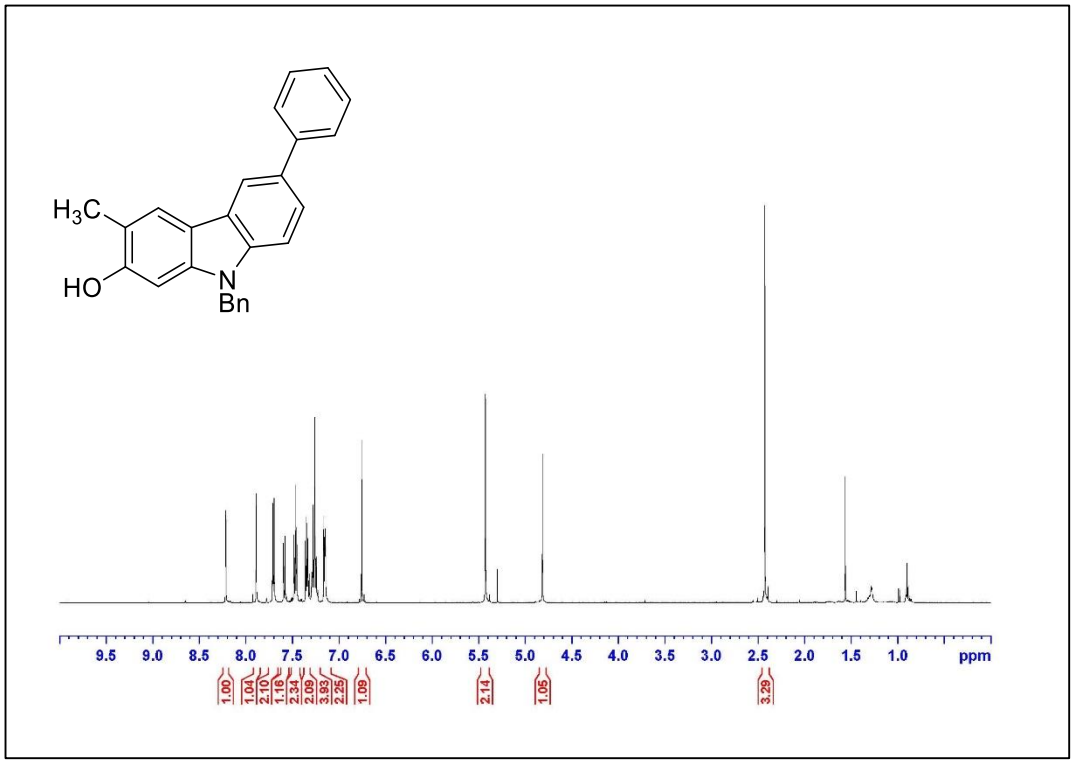

Figure A.95. ^{1}H NMR Spectrum of Compound **1.4p** (500 MHz, $CDCl_3$)

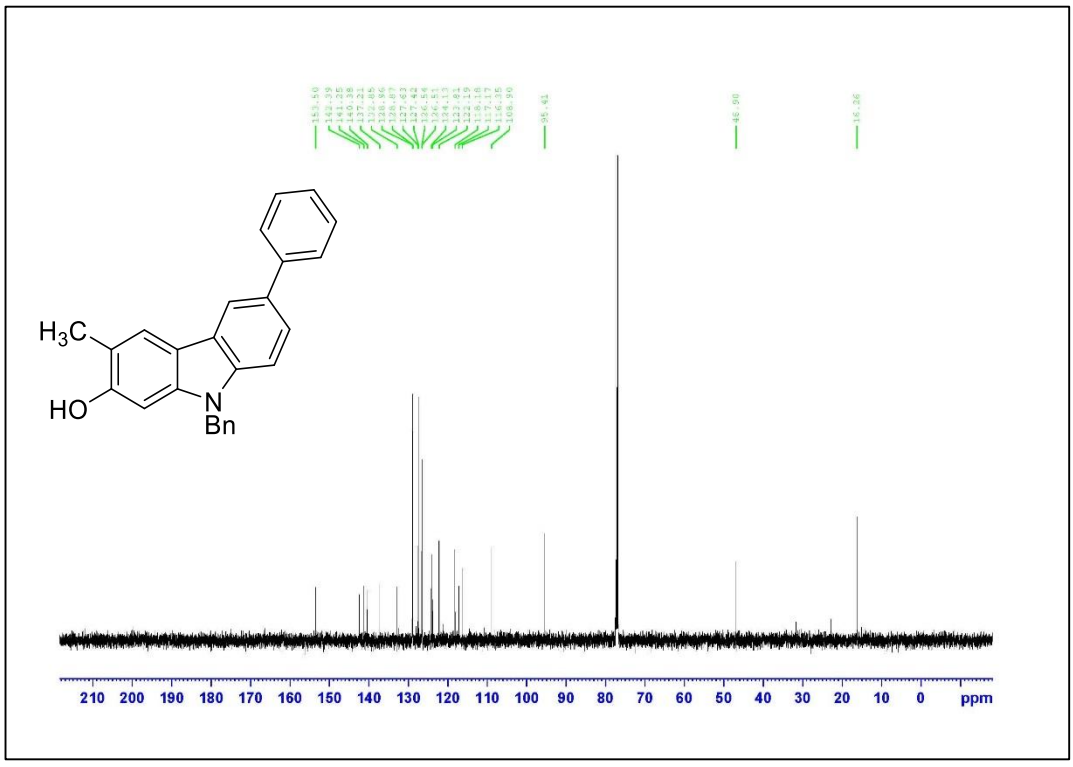

Figure A.96. ^{13}C NMR Spectrum of Compound **1.4p** (125 MHz, $CDCl_3$)

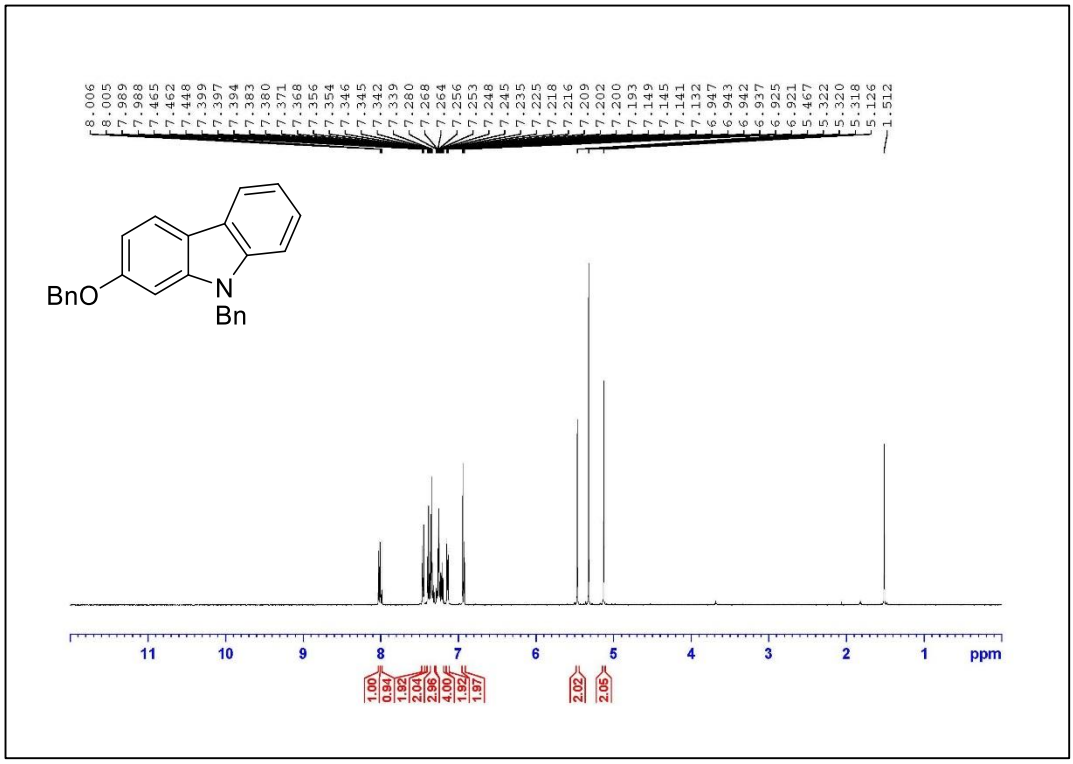

Figure A.97. ^{1}H NMR Spectrum of Compound **1.S2** (500 MHz, CD_2Cl_2)

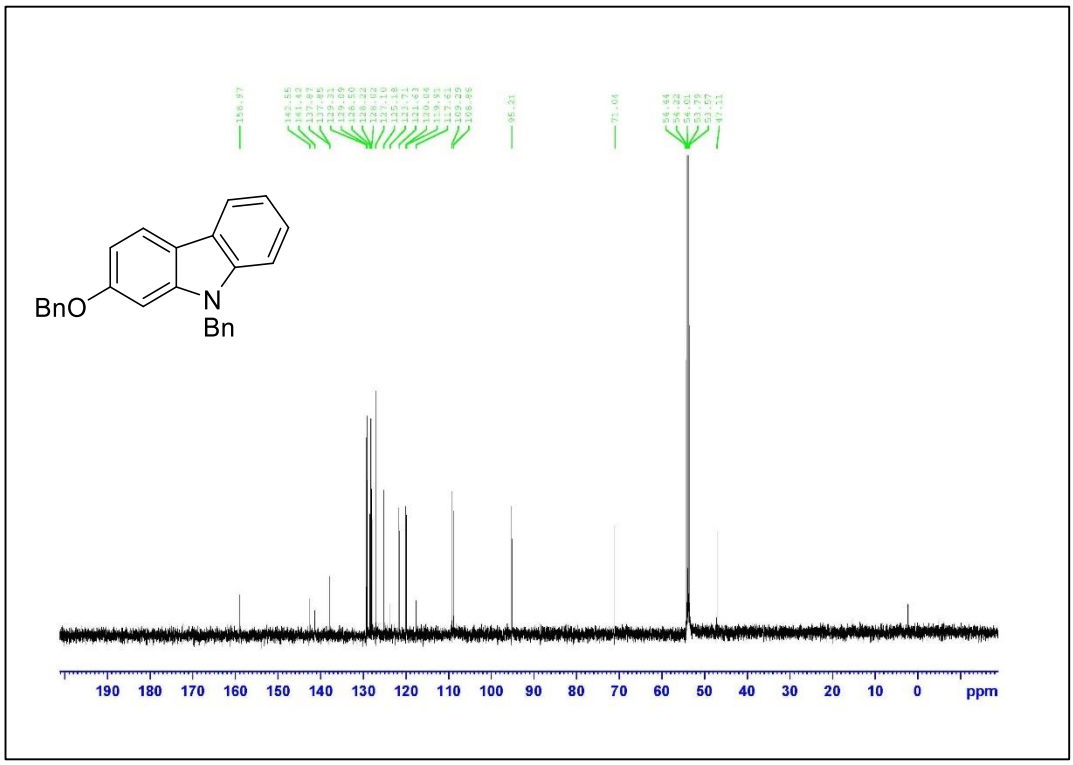

Figure A.98. ^{13}C NMR Spectrum of Compound **1.S2** (125 MHz, CD_2Cl_2)

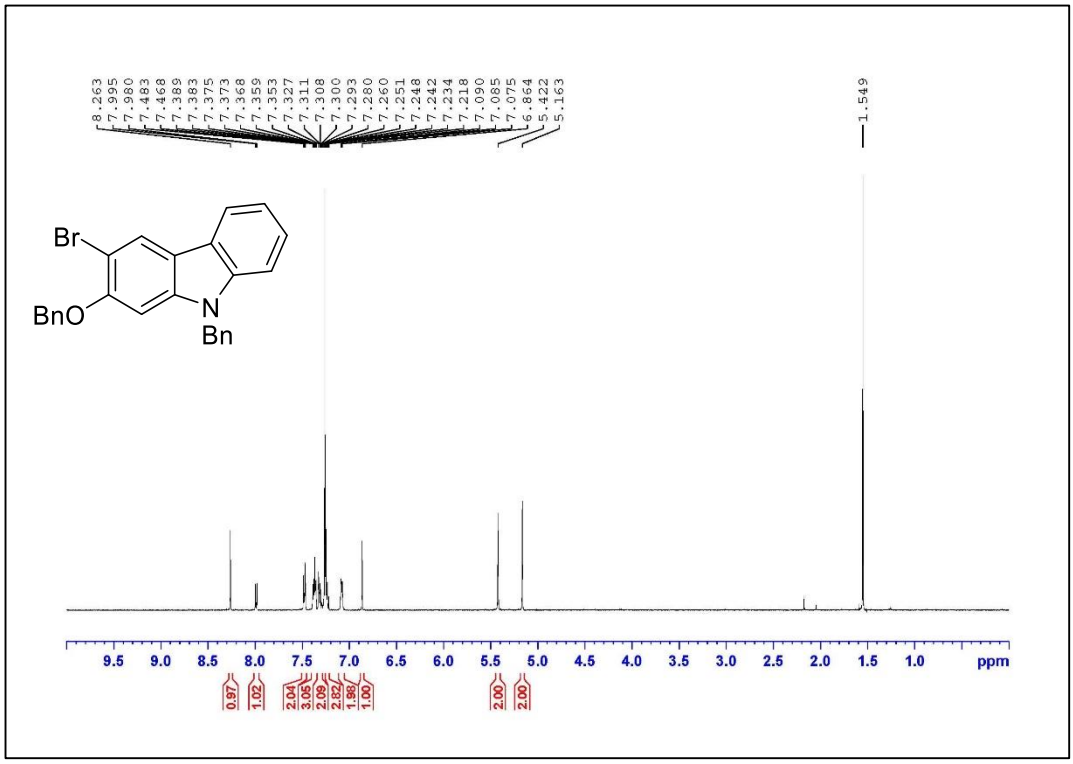

Figure A.99. ^{1}H NMR Spectrum of Compound **1.13** (500 MHz, $CDCl_3$)

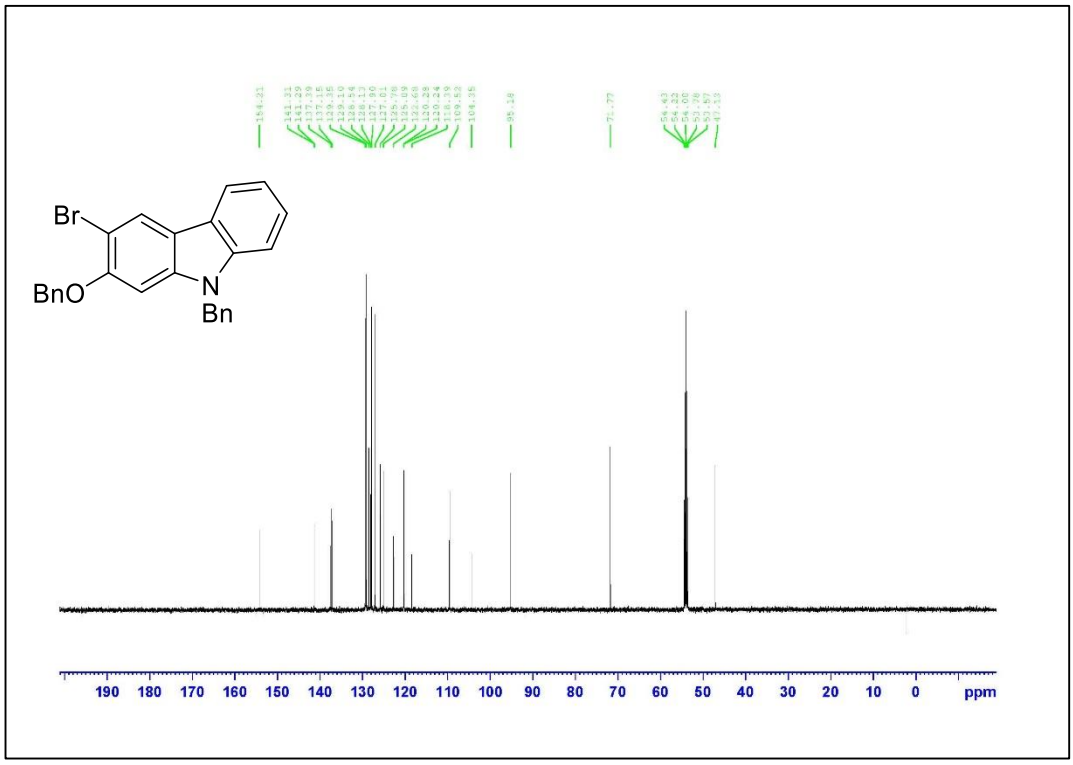

Figure A.100. ^{13}C NMR Spectrum of Compound **1.13** (125 MHz, CD_2Cl_2)

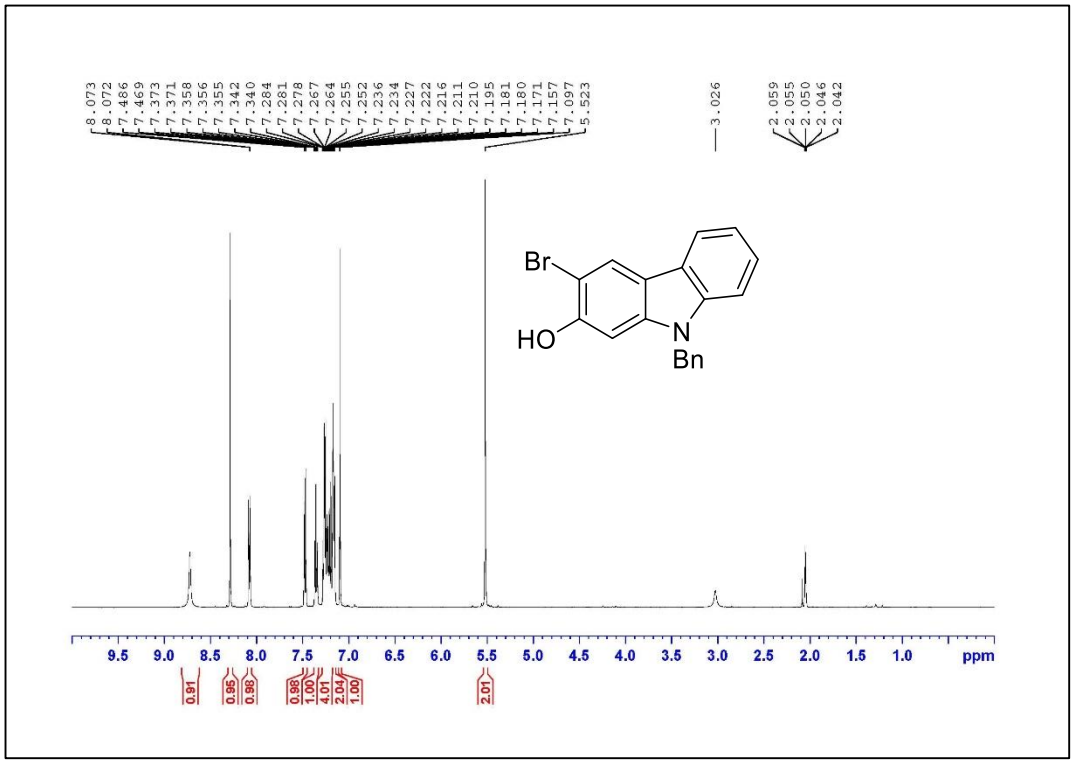

Figure A.101. ^{1}H NMR Spectrum of Compound **1.4q** (500 MHz, acetone-d_6)

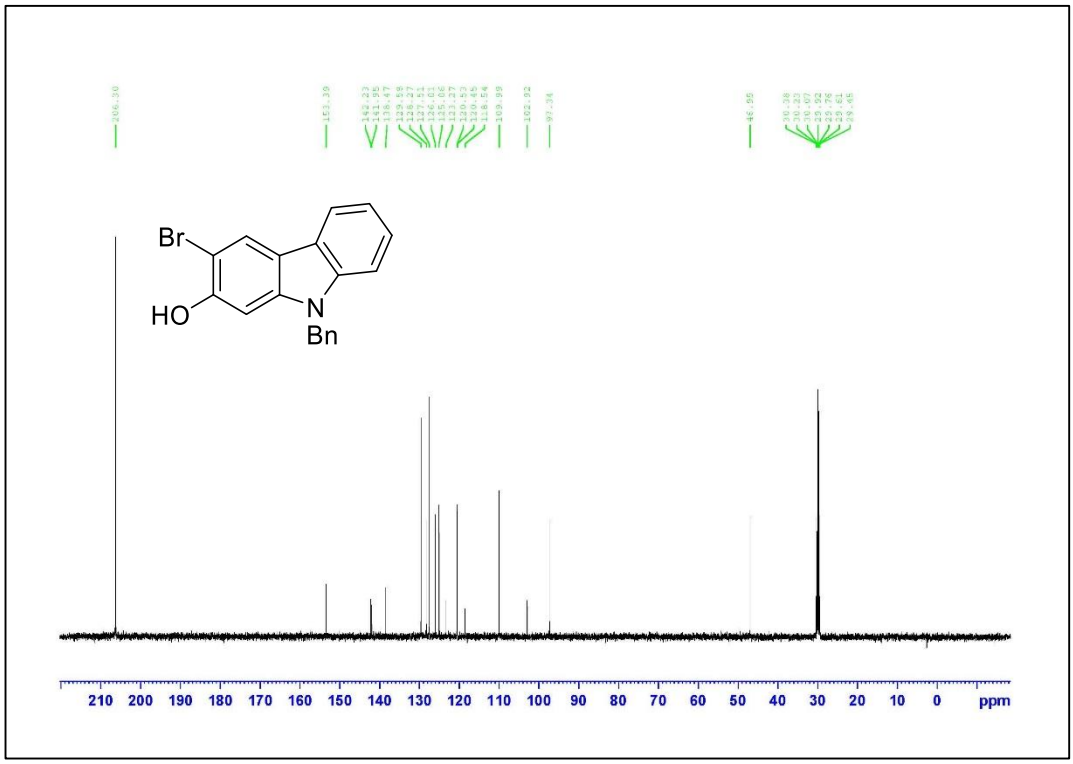

Figure A.102. ^{13}C NMR Spectrum of Compound **1.4q** (125 MHz, acetone-d_6)

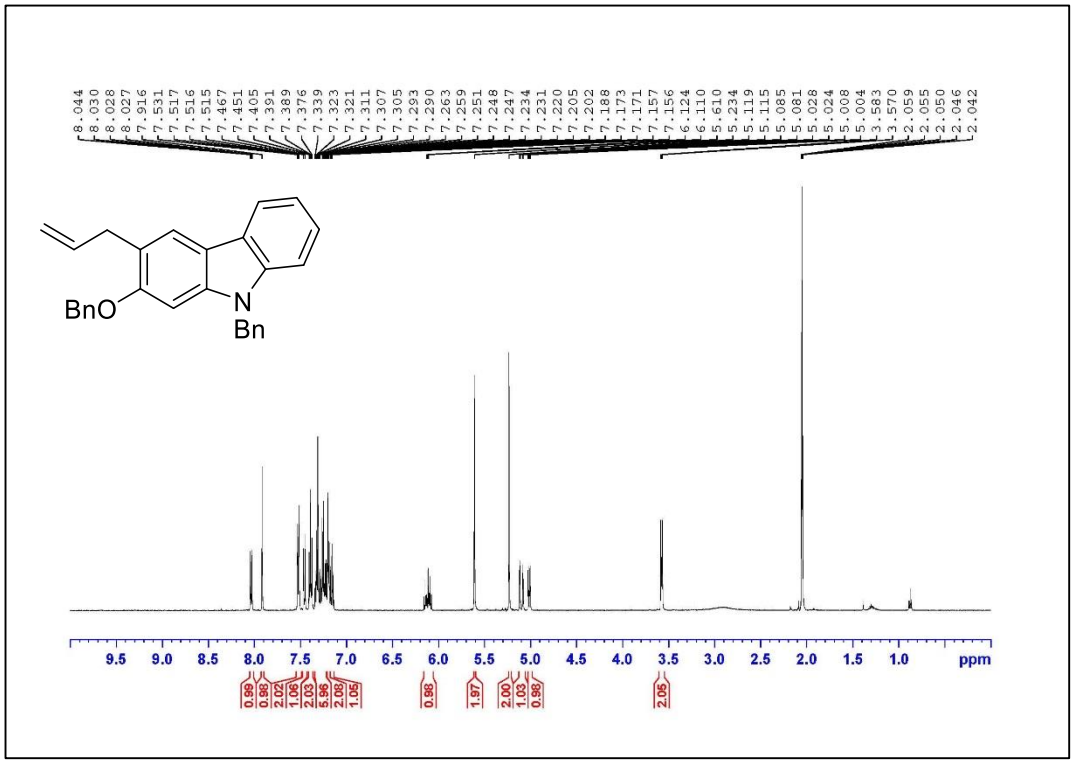

Figure A.103. ^{1}H NMR Spectrum of Compound **1.S3** (500 MHz, acetone-d_6)

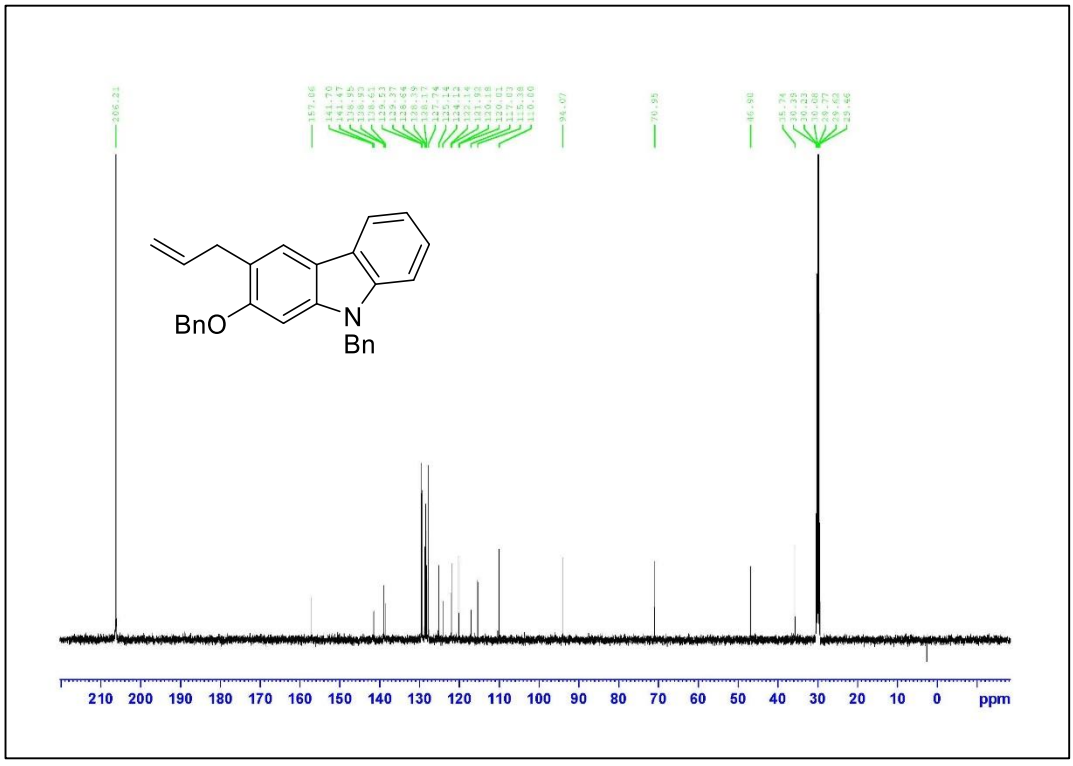

Figure A.104. ^{13}C NMR Spectrum of Compound **1.S3** (125 MHz, acetone-d_6)

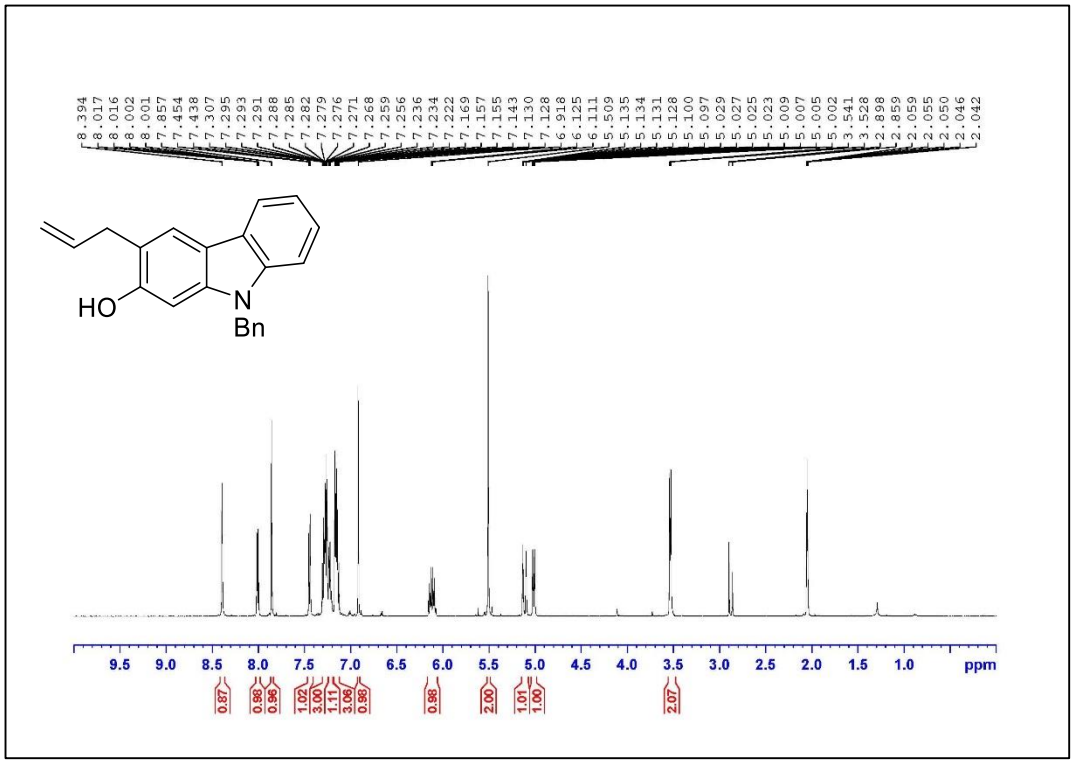

Figure A.105. ^{1}H NMR Spectrum of Compound **1.4r** (500 MHz, acetone-d_6)

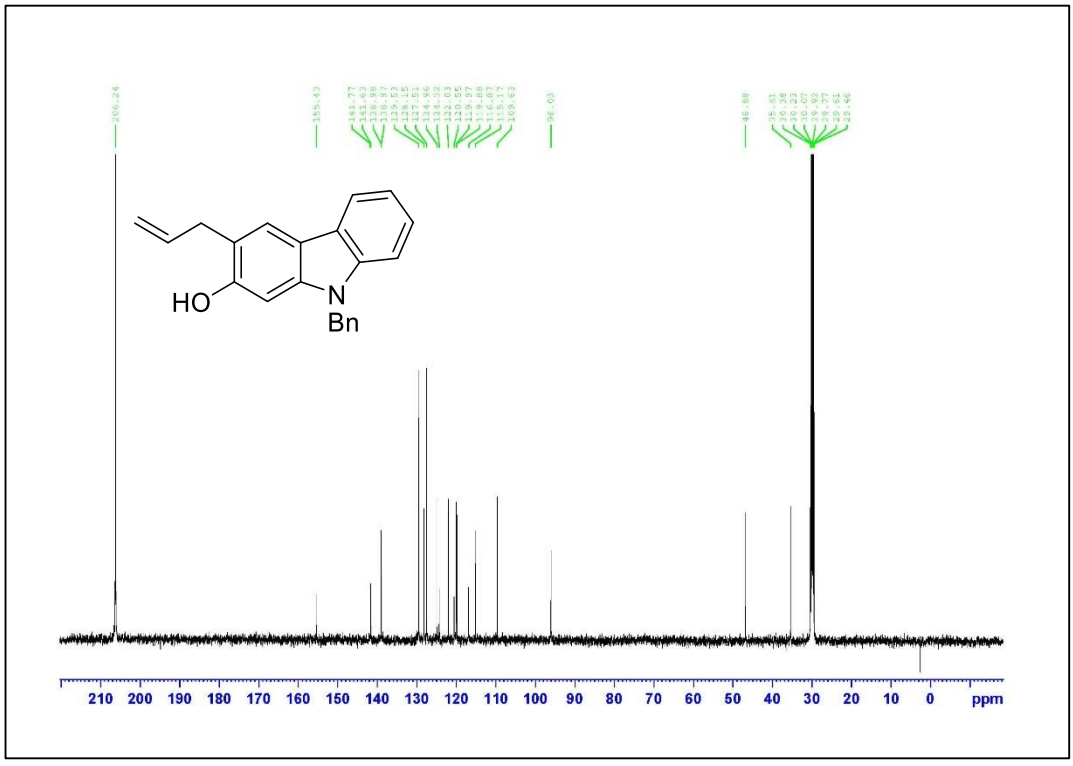

Figure A.106. ^{13}C NMR Spectrum of Compound **1.4r** (125 MHz, acetone-d_6)

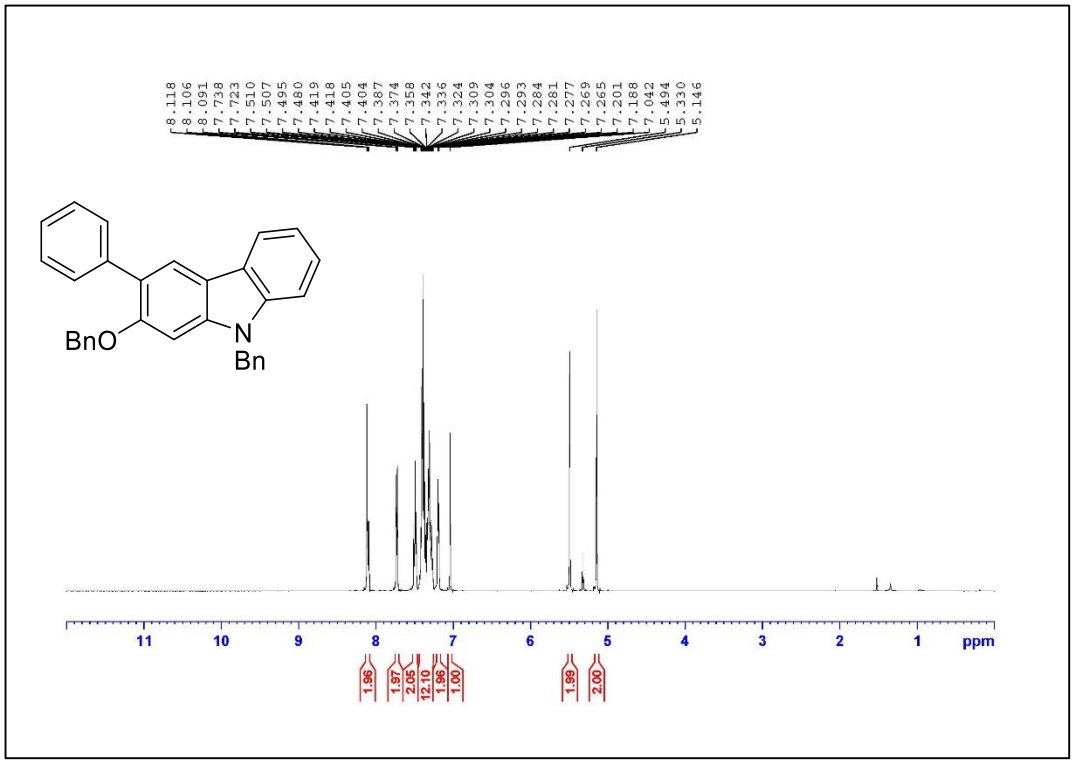

Figure A.107. ^{1}H NMR Spectrum of Compound **1.S4** (500 MHz, CD_2Cl_2)

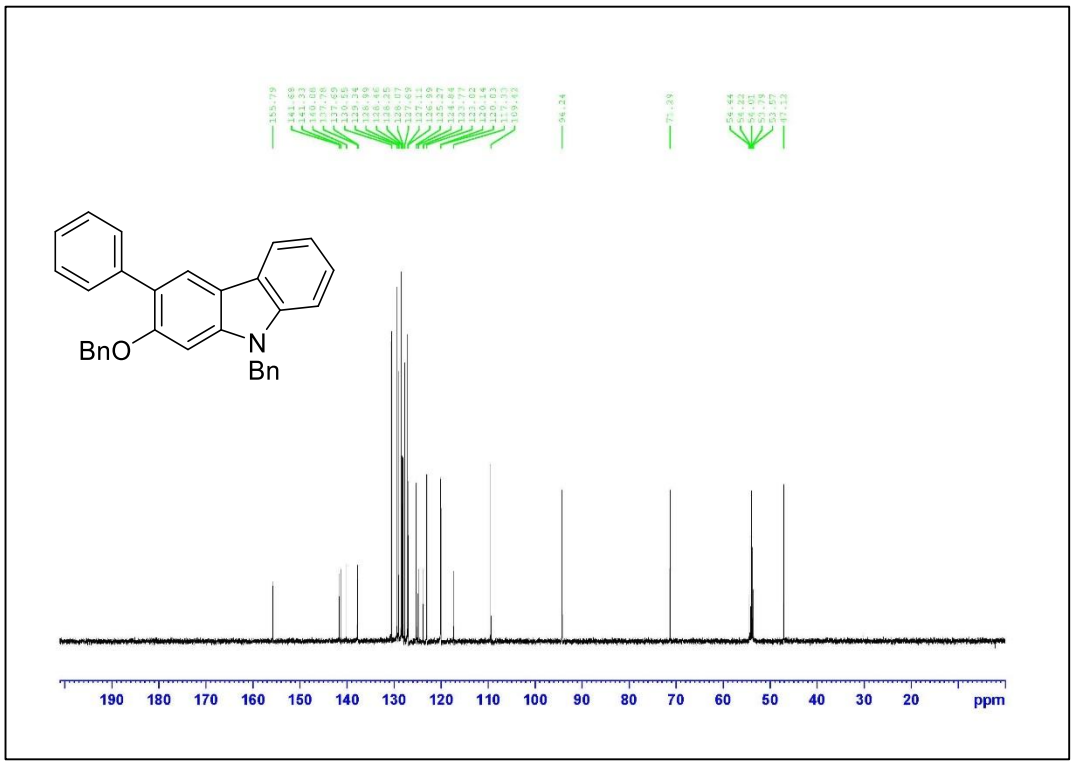

Figure A.108. ^{13}C NMR Spectrum of Compound **1.S4** (125 MHz, CD_2Cl_2)

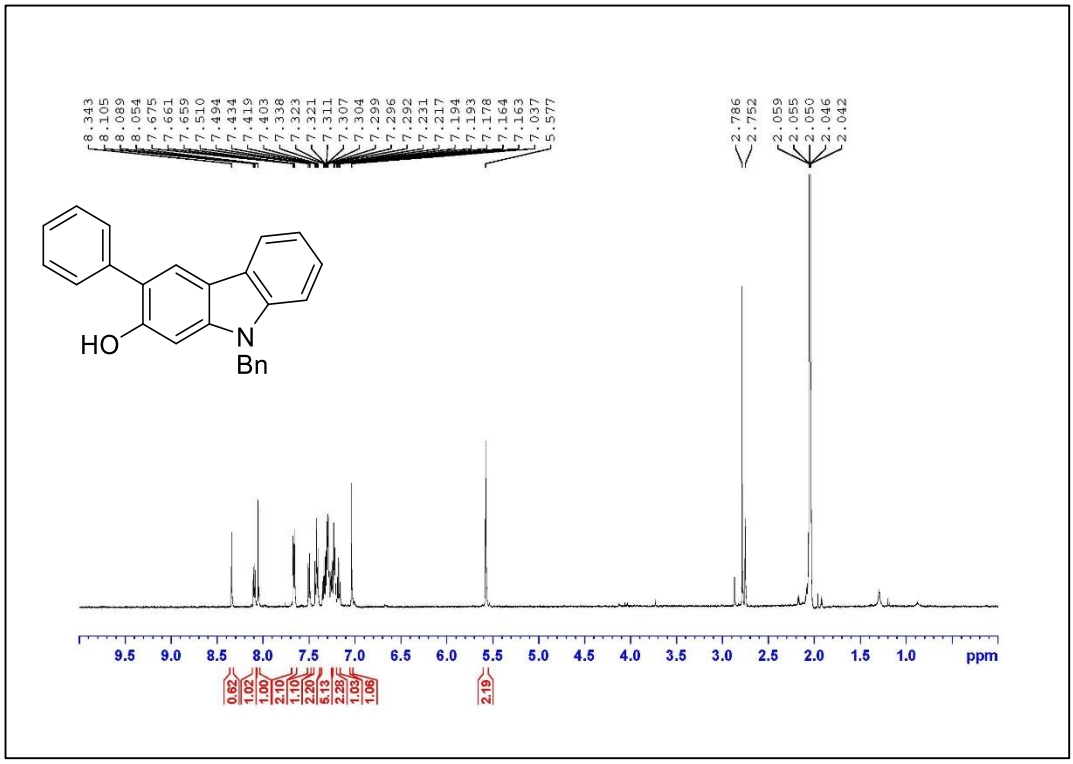

Figure A.109. ^{1}H NMR Spectrum of Compound **1.4s** (500 MHz, acetone-d_6)

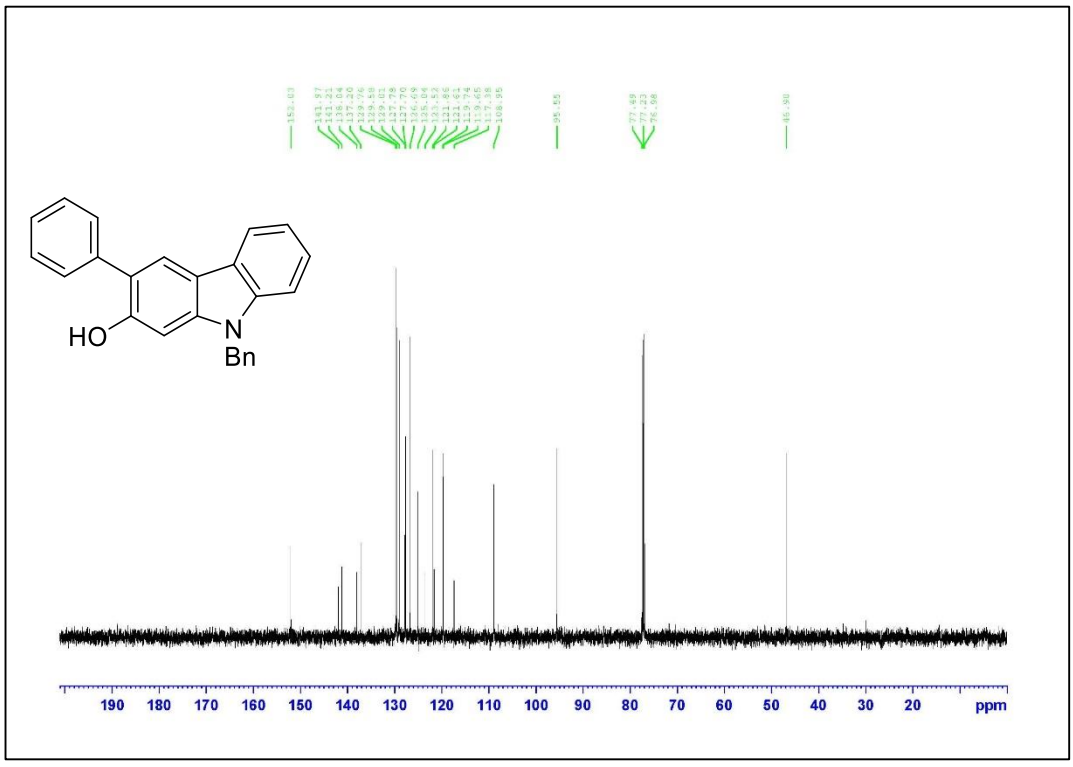

Figure A.110. ^{13}C NMR Spectrum of Compound **1.4s** (125 MHz, $CDCl_3$)

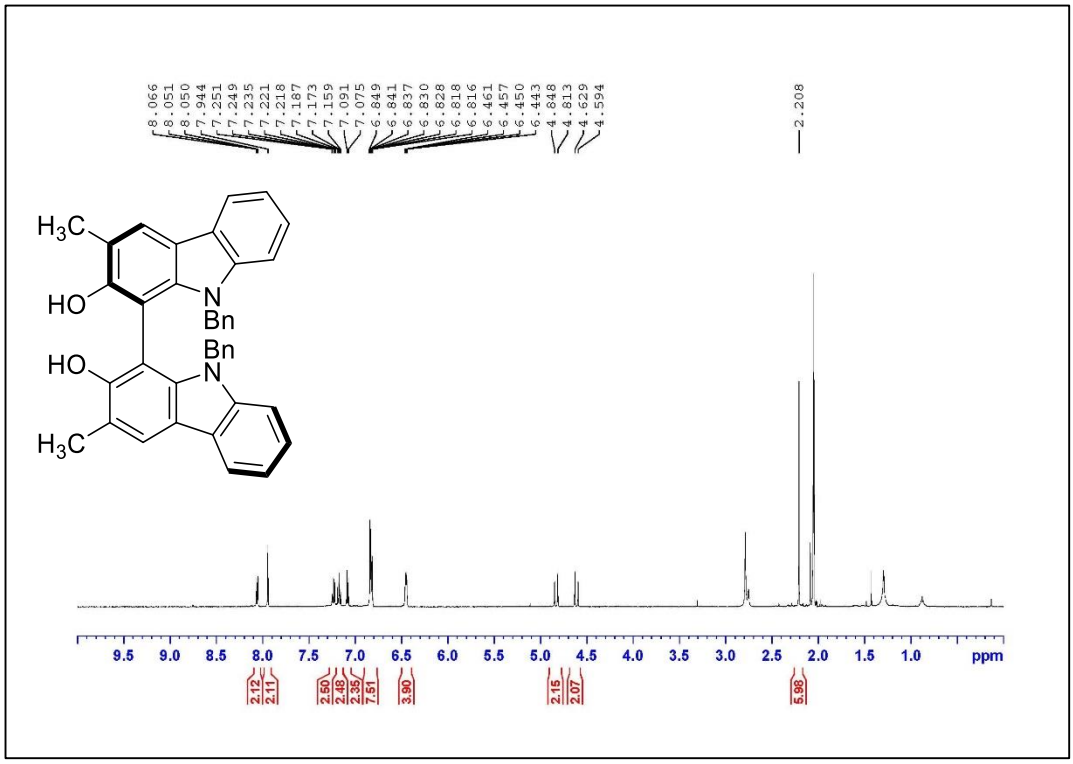

Figure A.111. ^{1}H NMR Spectrum of Compound **1.5a** (500 MHz, acetone-d_6)

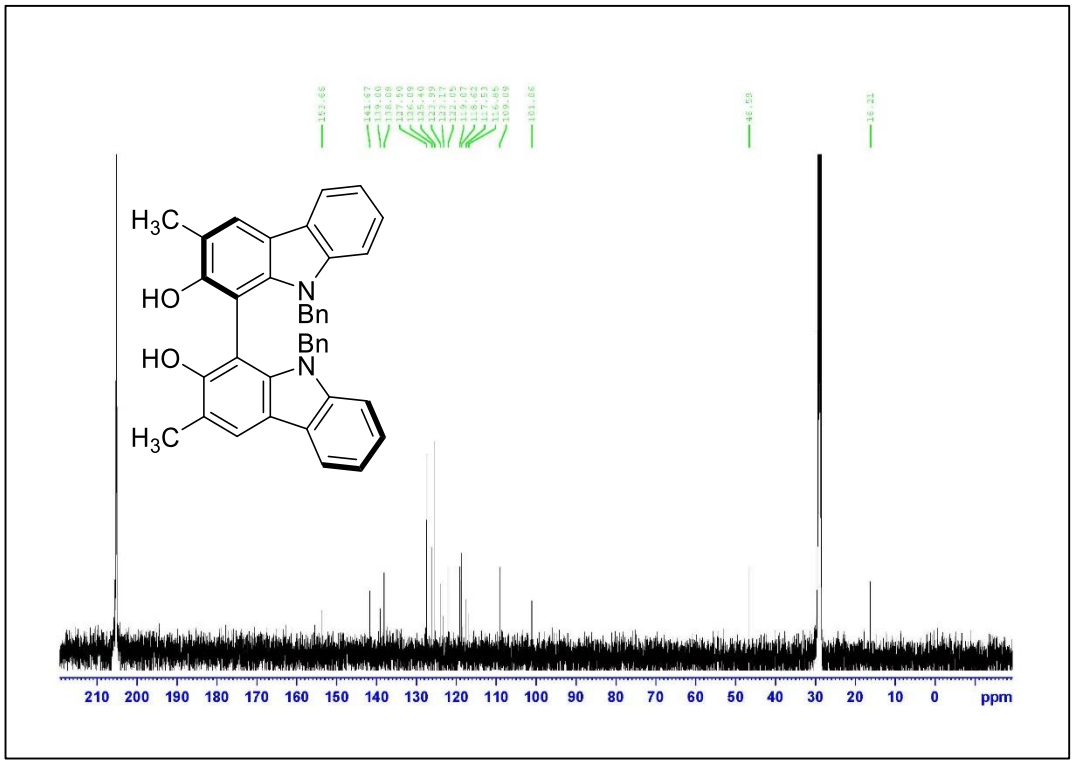

Figure A.112. ^{13}C NMR Spectrum of Compound **1.5a** (125 MHz, acetone-d_6)

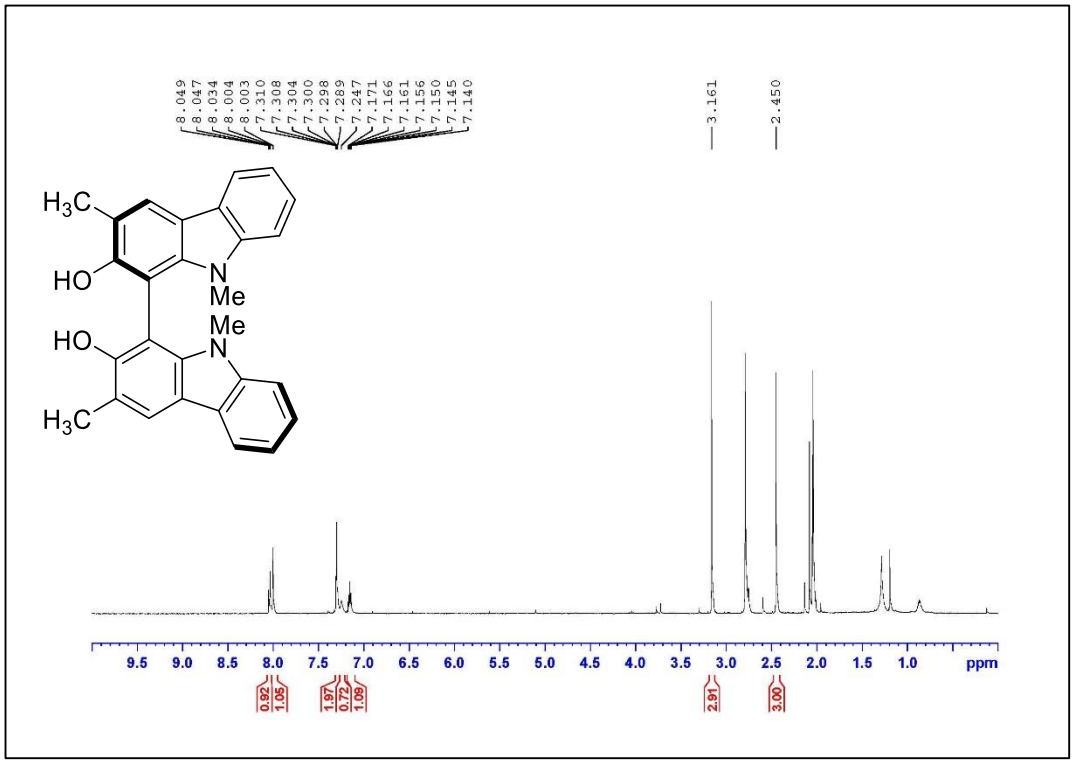

Figure A.113. ^{1}H NMR Spectrum of Compound **1.5b** (500 MHz, acetone-d_6)

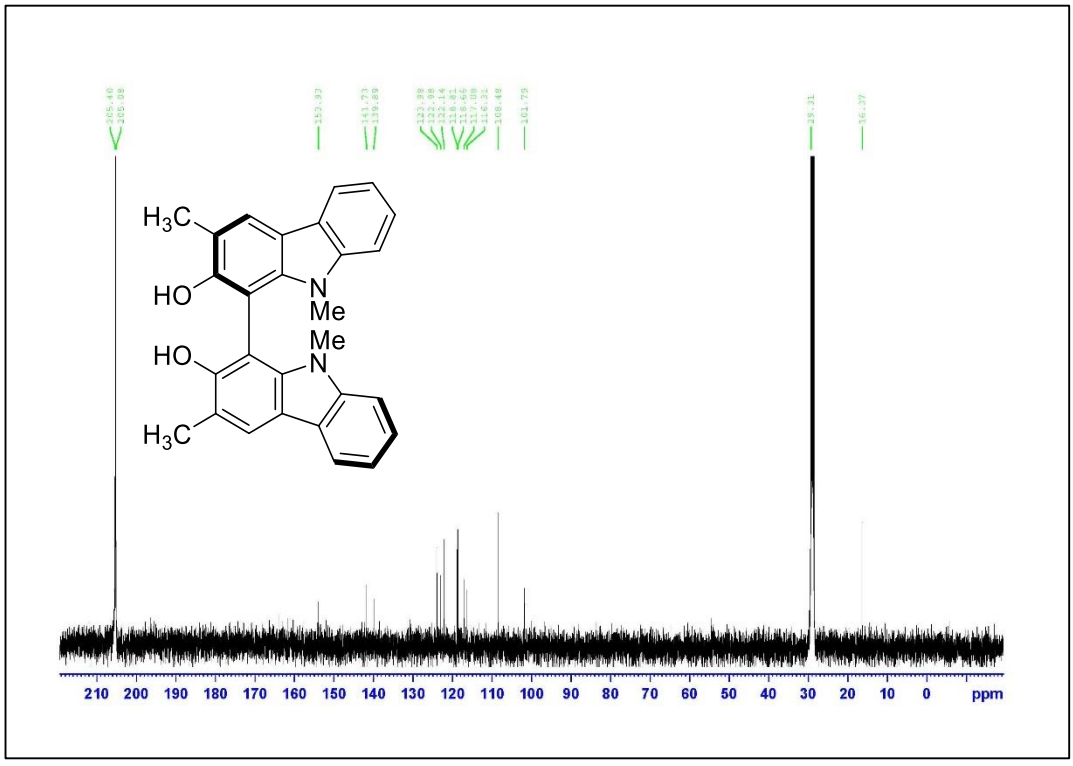

Figure A.114. ^{13}C NMR Spectrum of Compound **1.5b** (125 MHz, acetone-d_6)

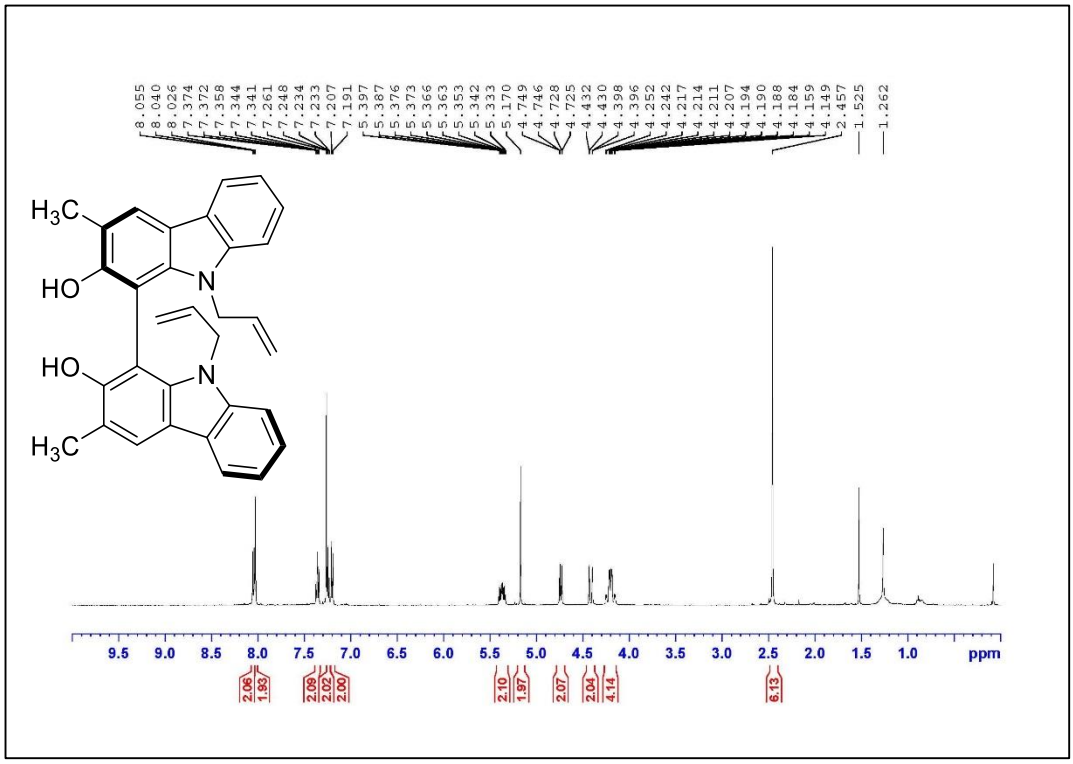

Figure A.115. ^{1}H NMR Spectrum of Compound **1.5c** (500 MHz, $CDCl_3$)

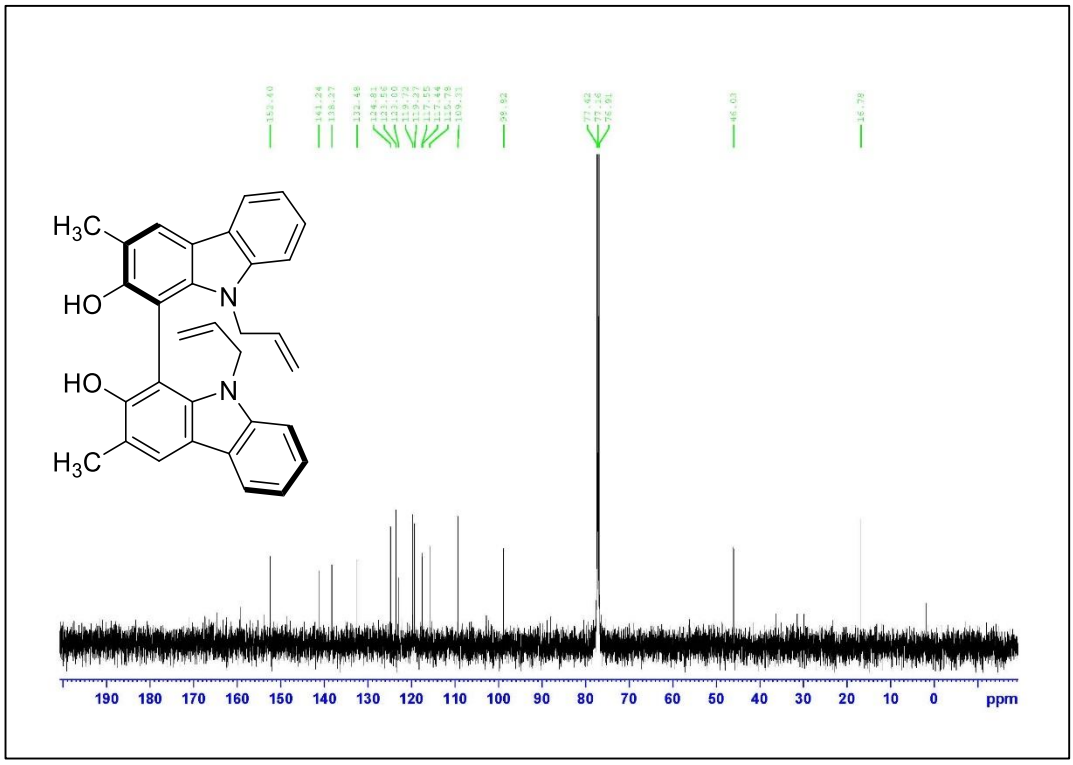

Figure A.116. ^{13}C NMR Spectrum of Compound **1.5c** (125 MHz, $CDCl_3$)

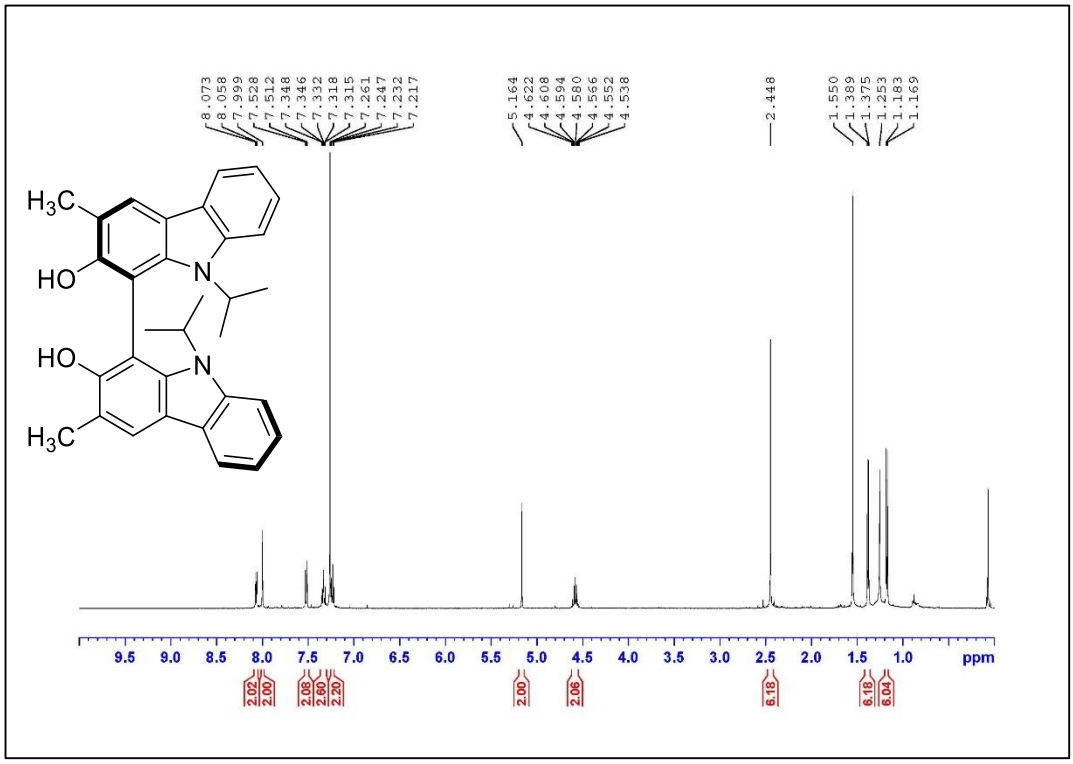

Figure A.117. ^{1}H NMR Spectrum of Compound **1.5d** (500 MHz, $CDCl_3$)

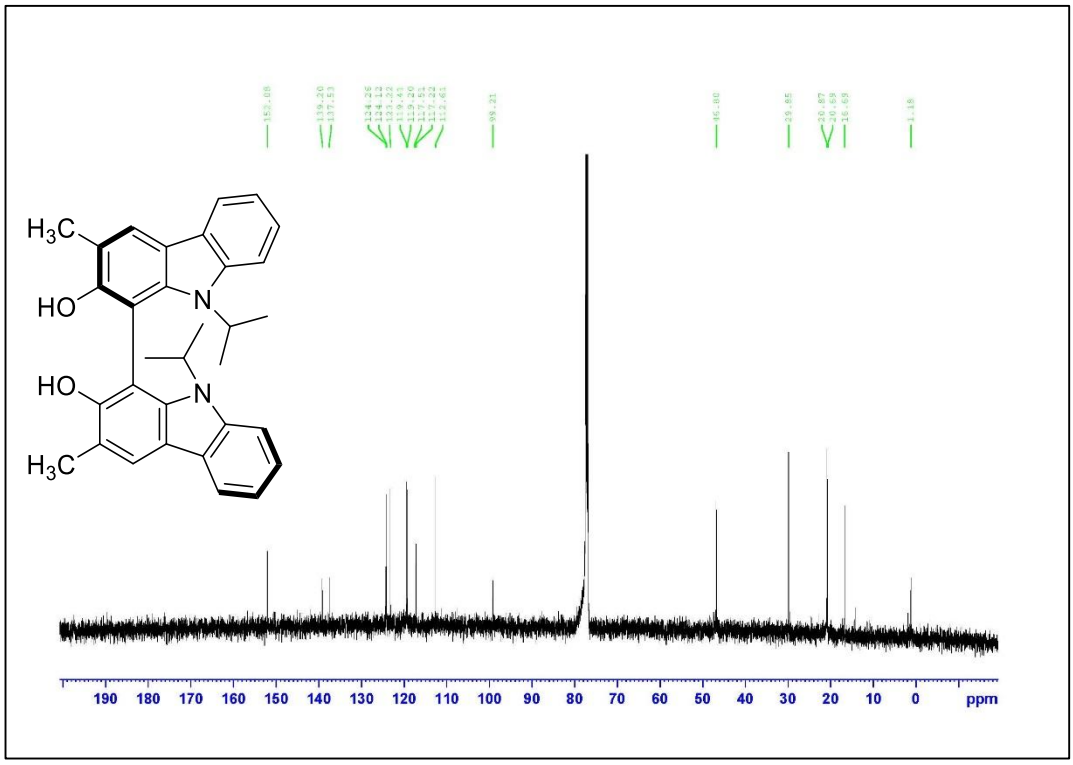

Figure A.118. ^{13}C NMR Spectrum of Compound **1.5d** (125 MHz, $CDCl_3$)

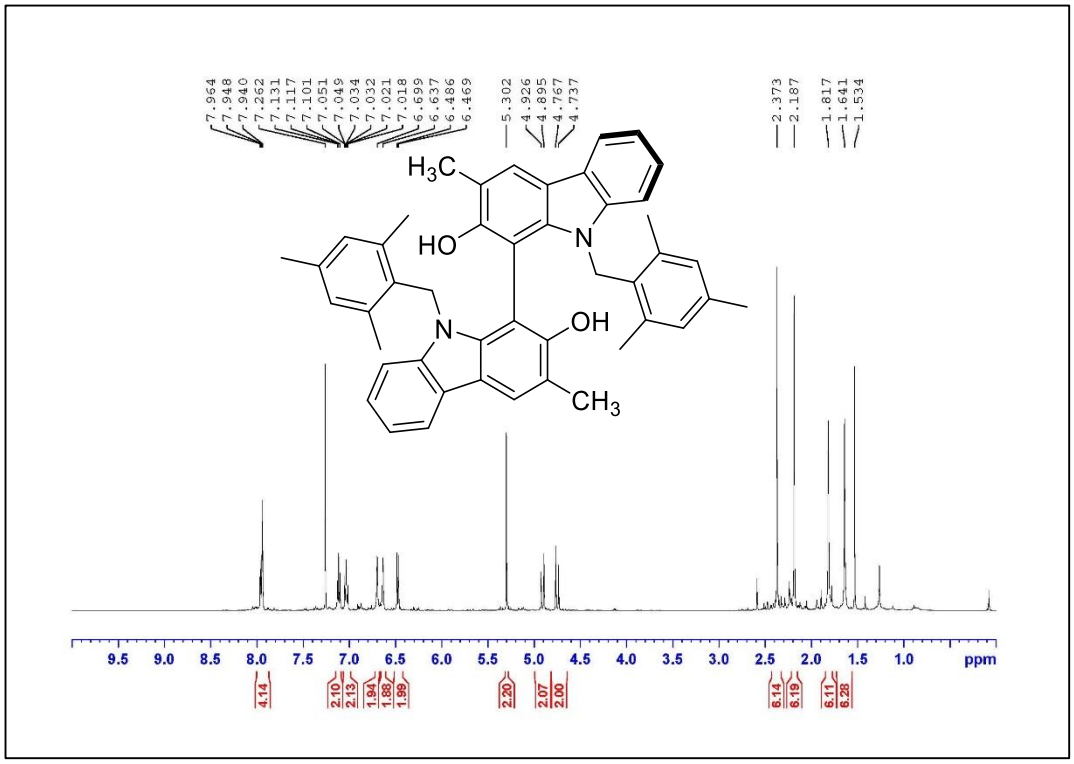

Figure A.119. ^{1}H NMR Spectrum of Compound **1.5e** (500 MHz, $CDCl_3$)

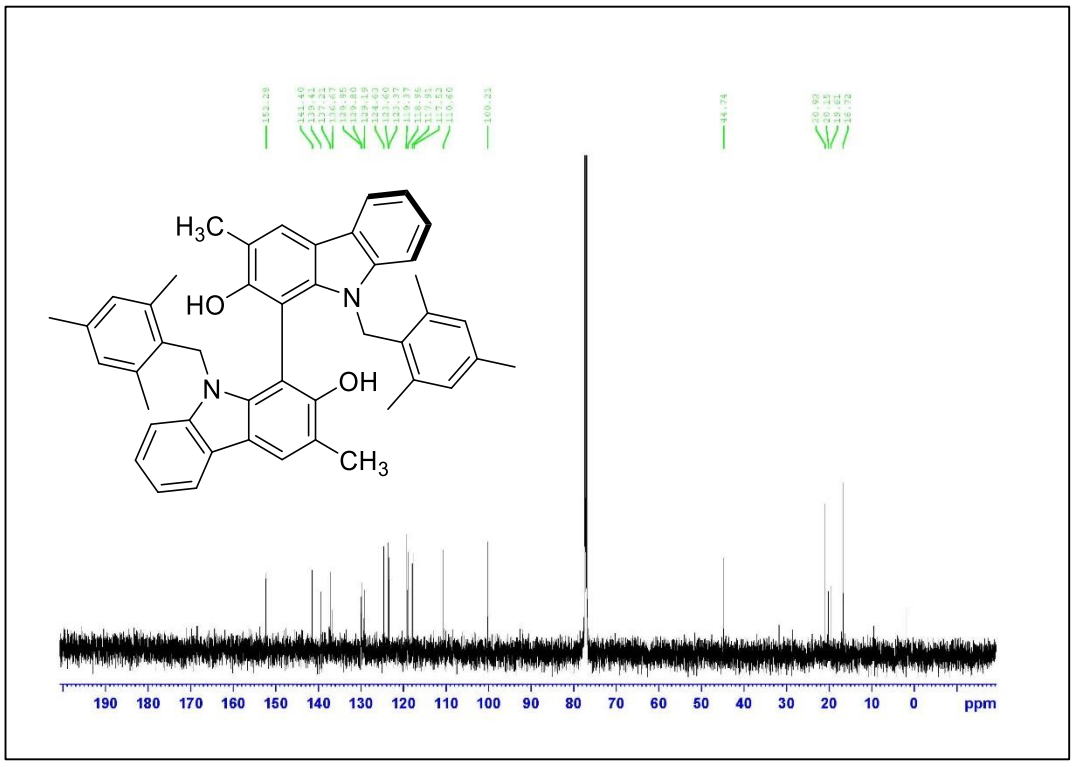

Figure A.120. ^{13}C NMR Spectrum of Compound **1.5e** (125 MHz, $CDCl_3$)

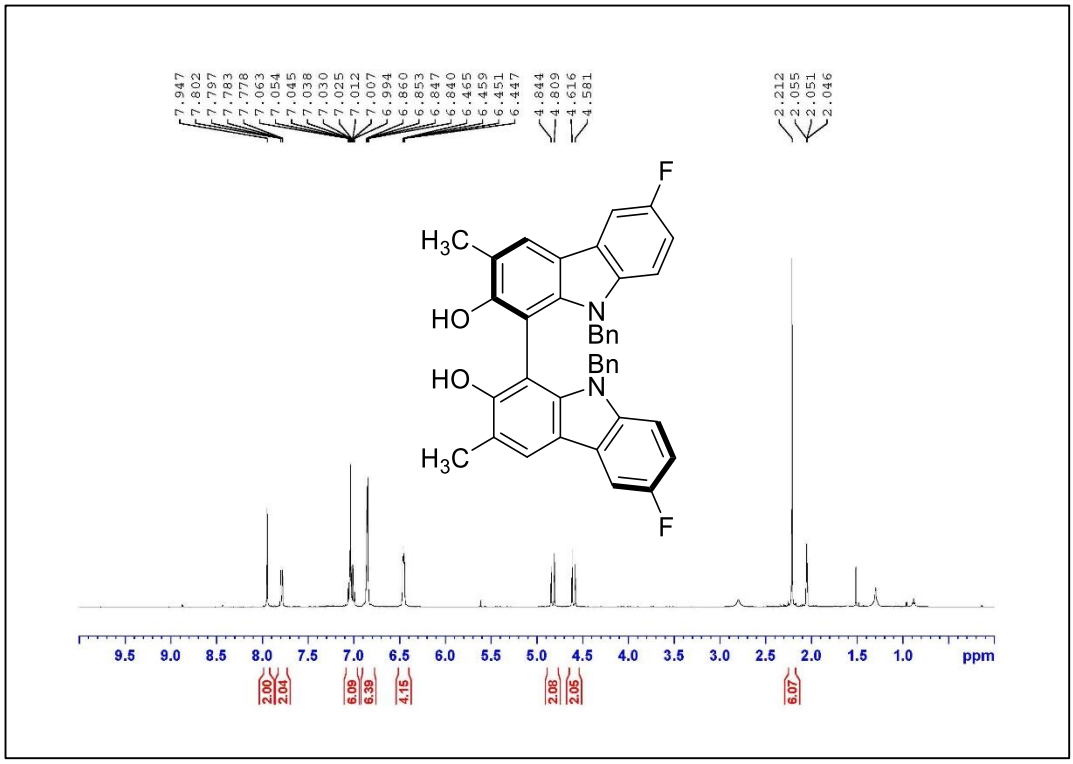

Figure A.121. ^{1}H NMR Spectrum of Compound **1.5f** (500 MHz, acetone-d_6)

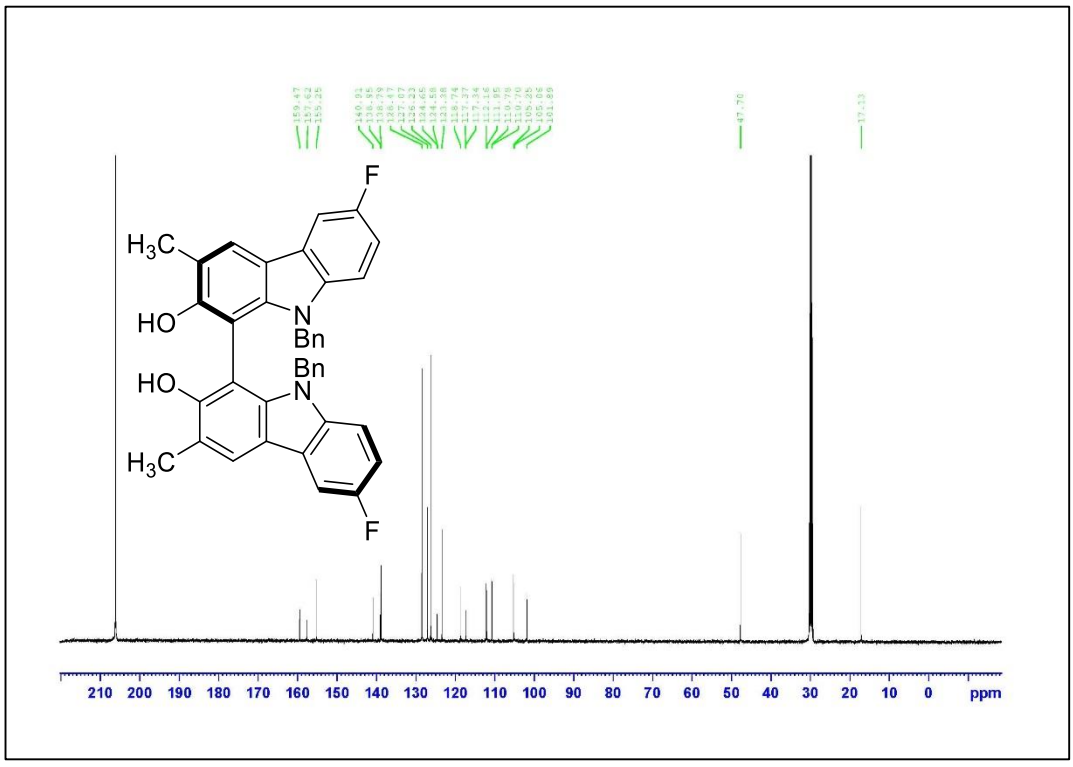

Figure A.122. ^{13}C NMR Spectrum of Compound **1.5f** (125 MHz, acetone-d_6)

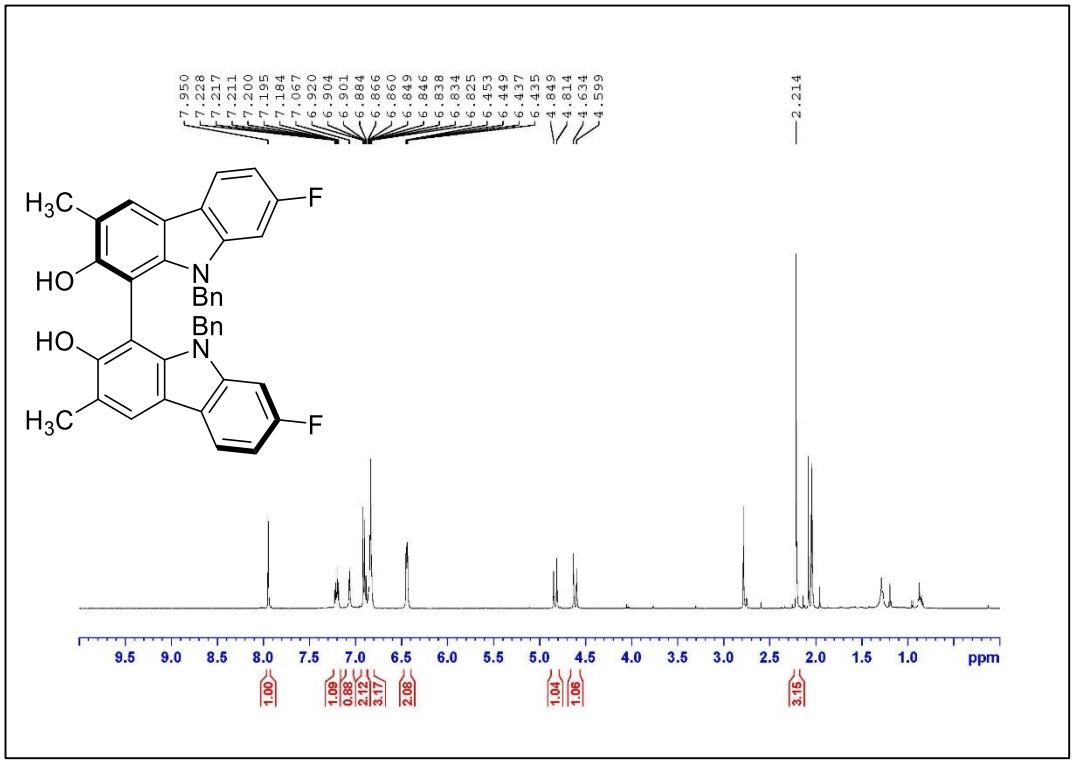

Figure A.123. ^{1}H NMR Spectrum of Compound **1.5g** (500 MHz, acetone-d_6)

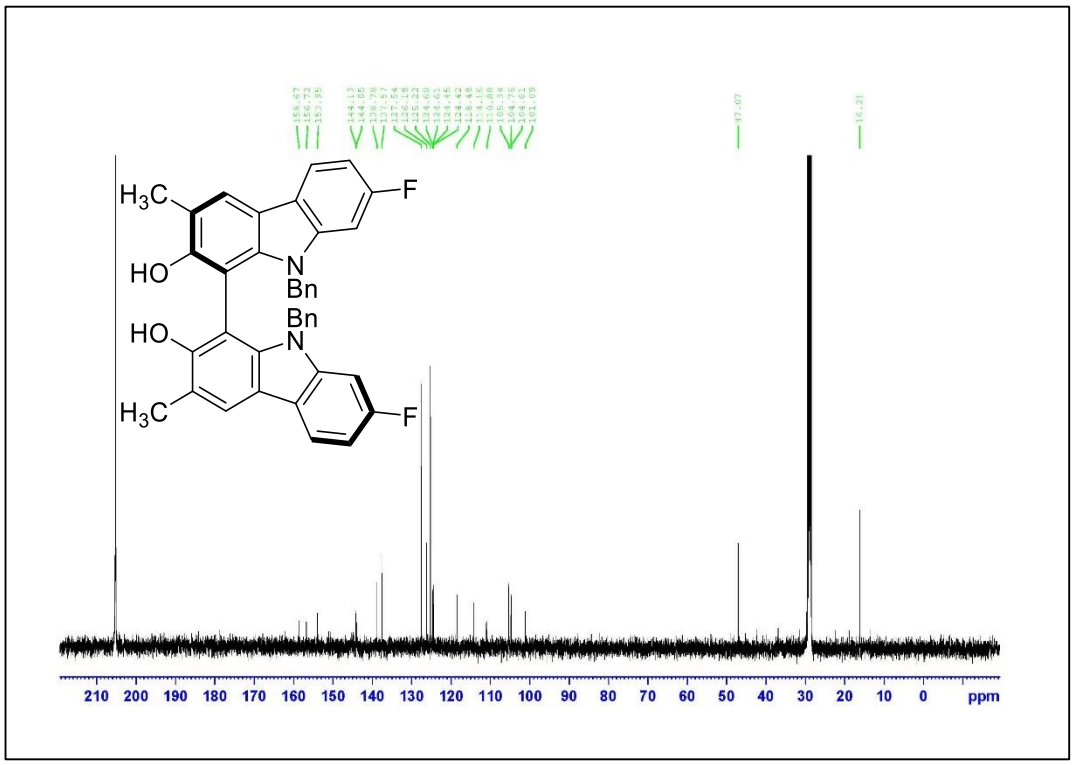

Figure A.124. ^{13}C NMR Spectrum of Compound **1.5g** (125 MHz, acetone-d_6)

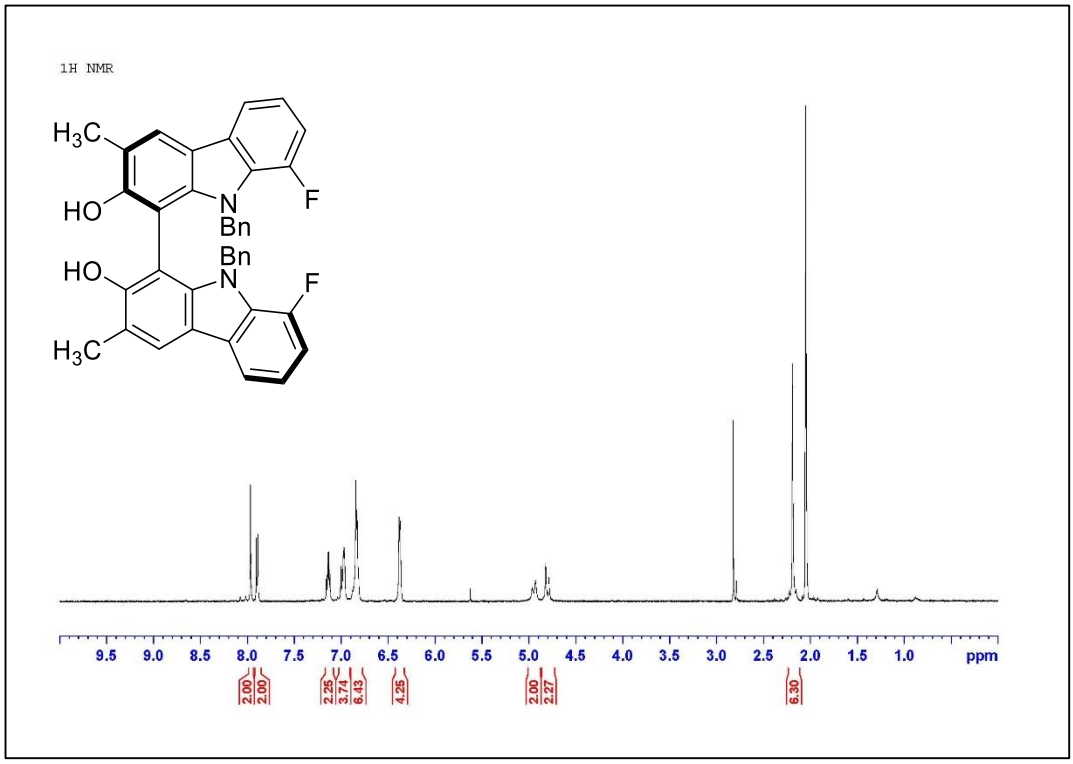

Figure A.125. ^{1}H NMR Spectrum of Compound **1.5h** (500 MHz, acetone-d_6)

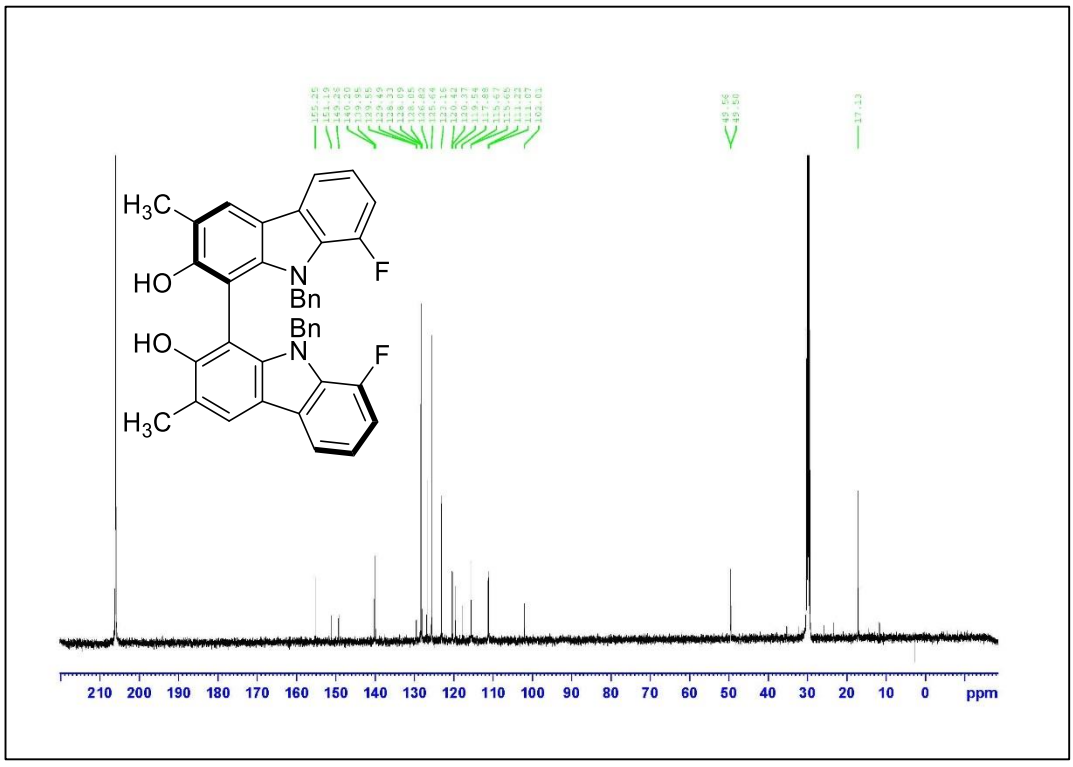

Figure A.126. ^{13}C NMR Spectrum of Compound **1.5h** (125 MHz, acetone-d_6)

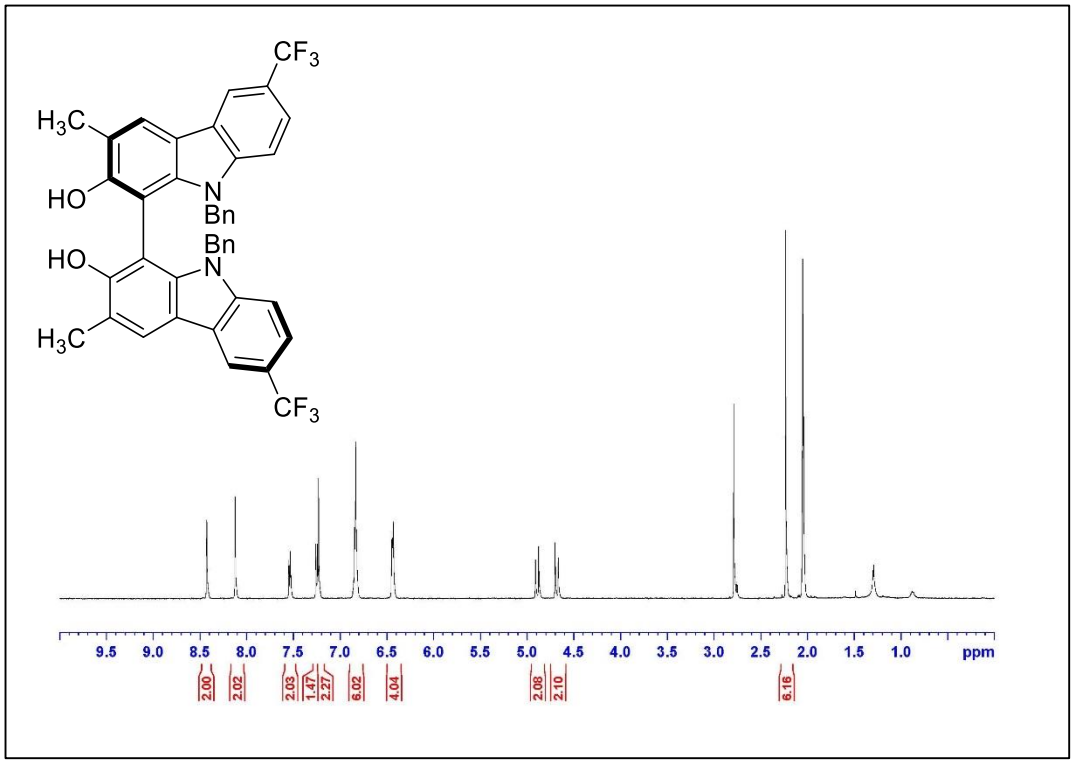

Figure A.127. ^{1}H NMR Spectrum of Compound **1.5i** (500 MHz, acetone-d_6)

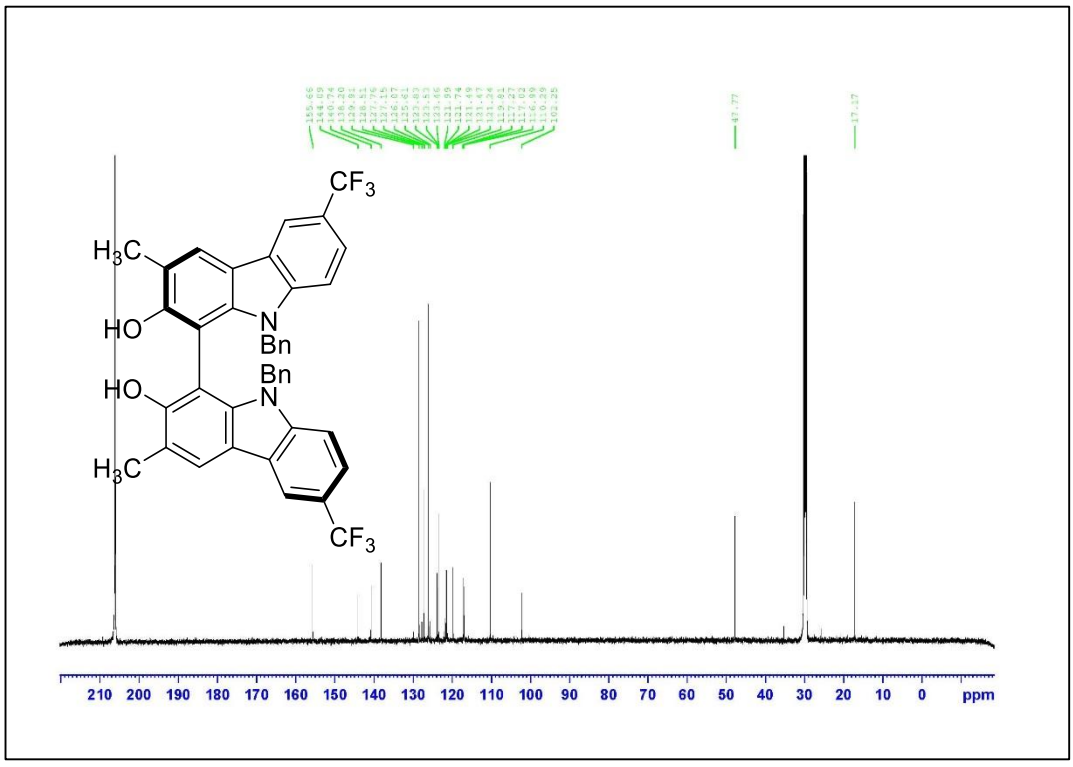

Figure A.128. ^{13}C NMR Spectrum of Compound **1.5i** (125 MHz, acetone-d_6)

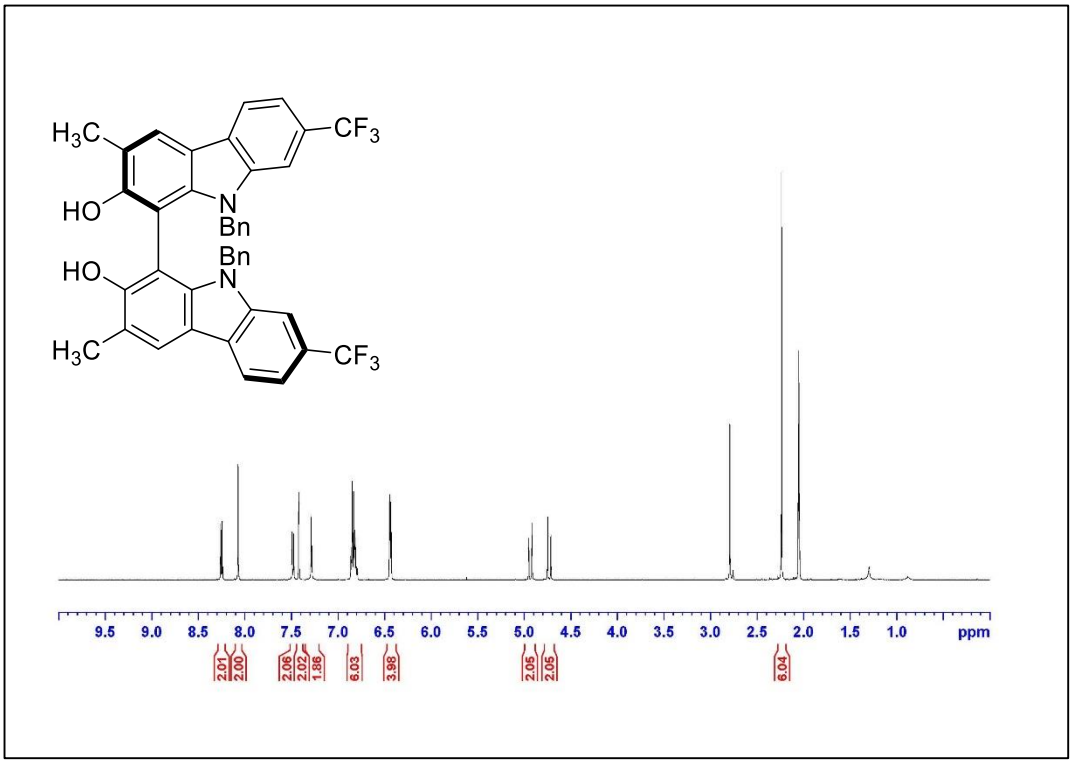

Figure A.129. ^{1}H NMR Spectrum of Compound **1.5j** (500 MHz, acetone-d_6)

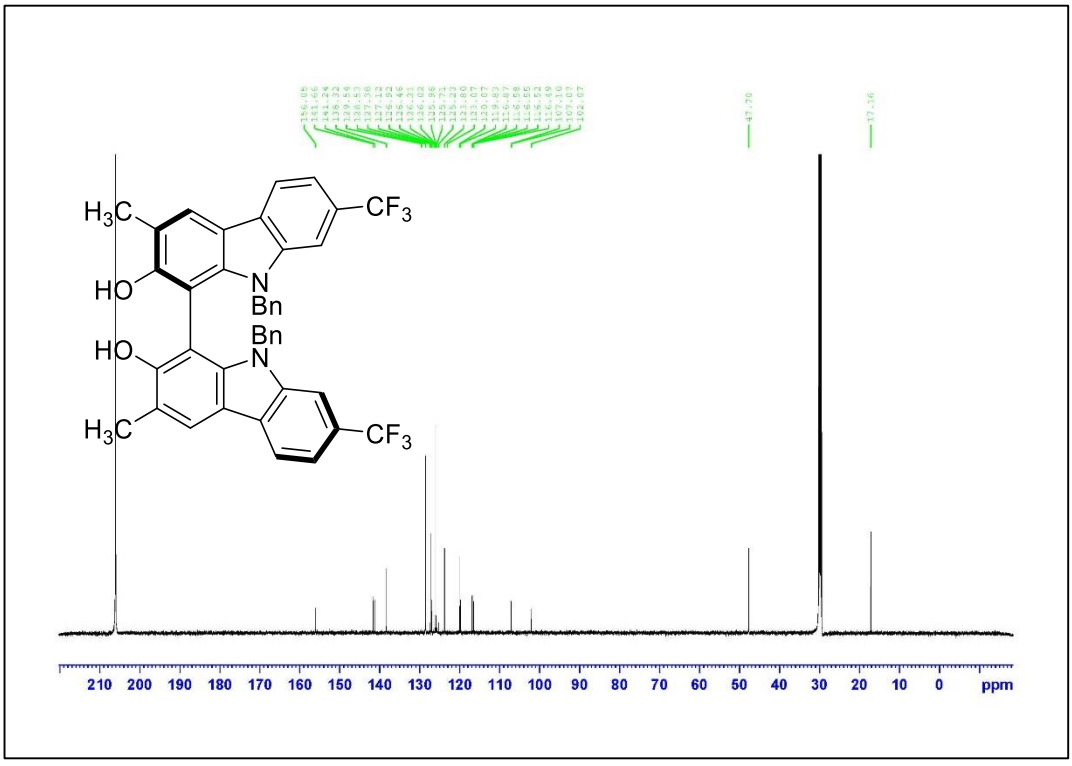

Figure A.130. ^{13}C NMR Spectrum of Compound **1.5j** (125 MHz, acetone-d_6)

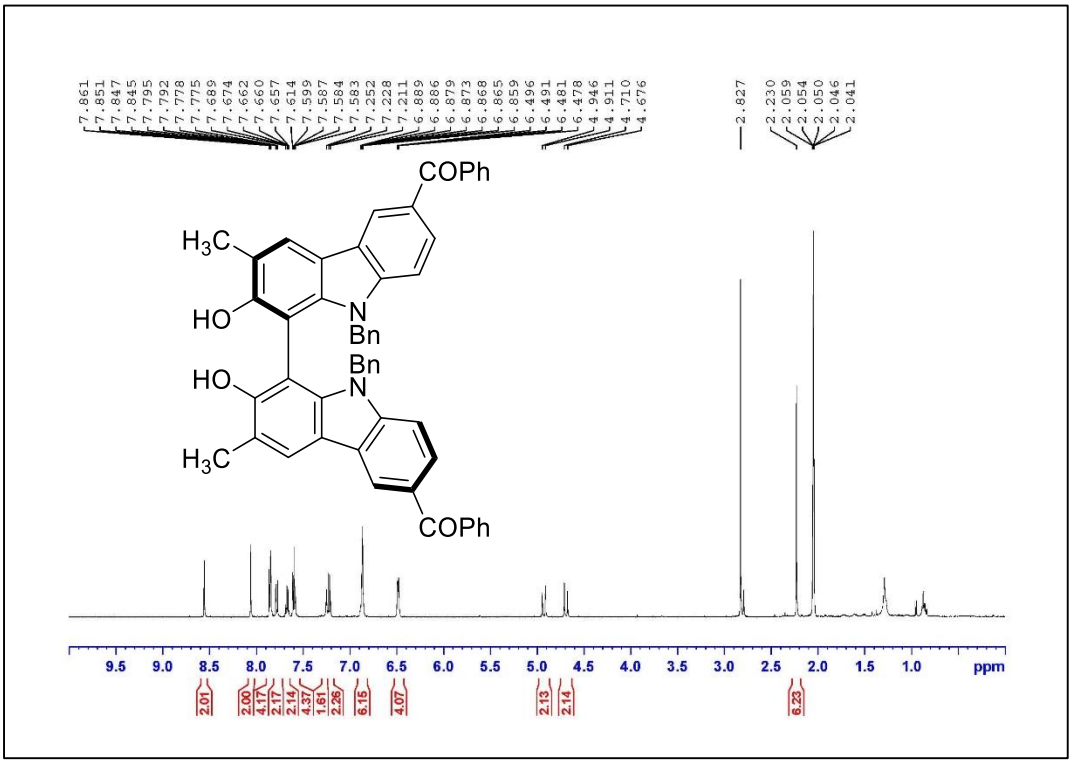

Figure A.131. ^{1}H NMR Spectrum of Compound **1.5k** (500 MHz, acetone-d_6)

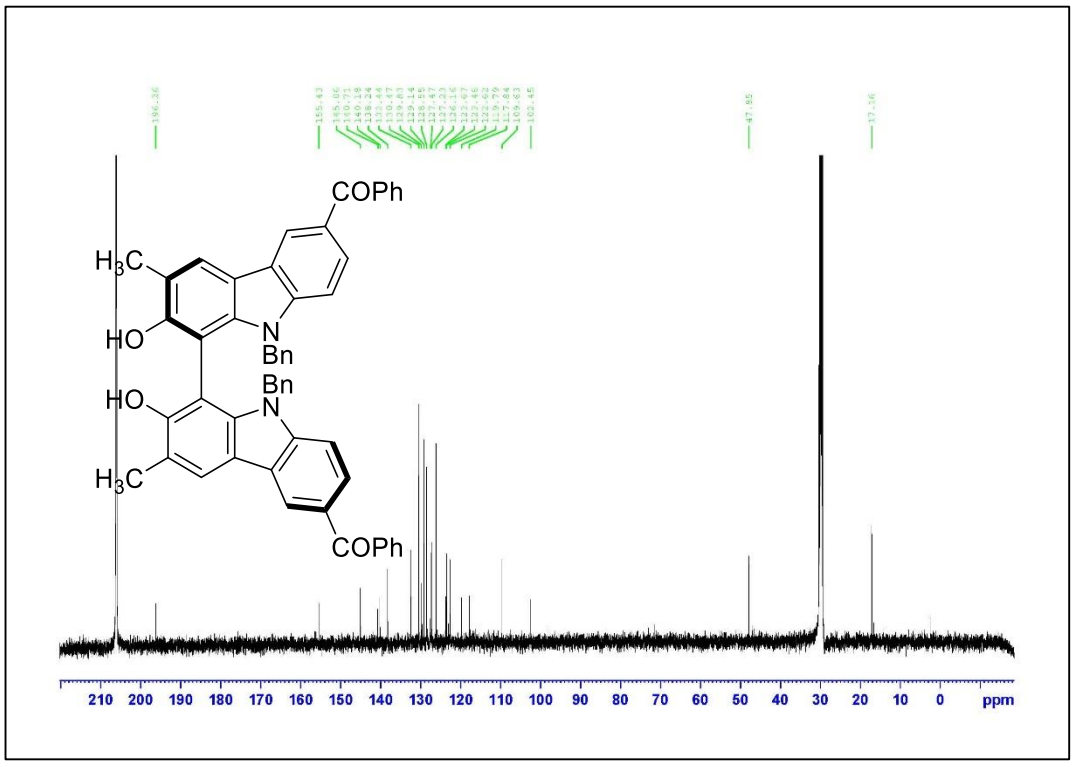

Figure A.132. ^{13}C NMR Spectrum of Compound **1.5k** (125 MHz, acetone-d_6)

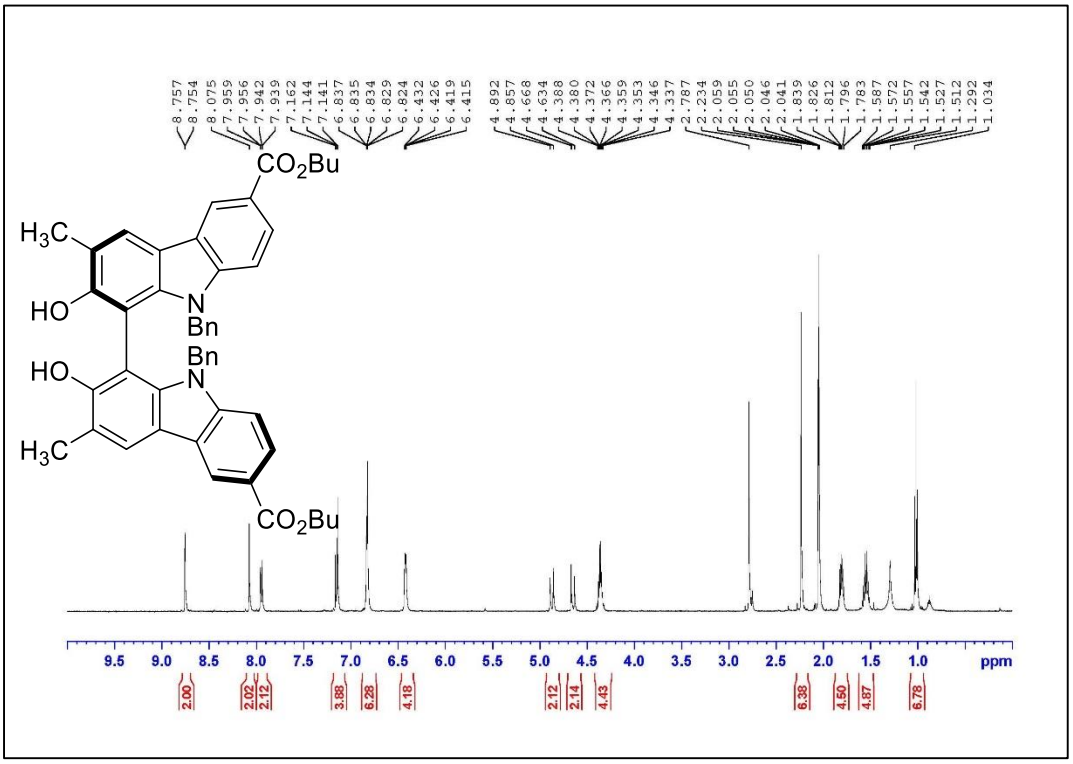

Figure A.133. ^{1}H NMR Spectrum of Compound **1.5l** (500 MHz, acetone-d_6)

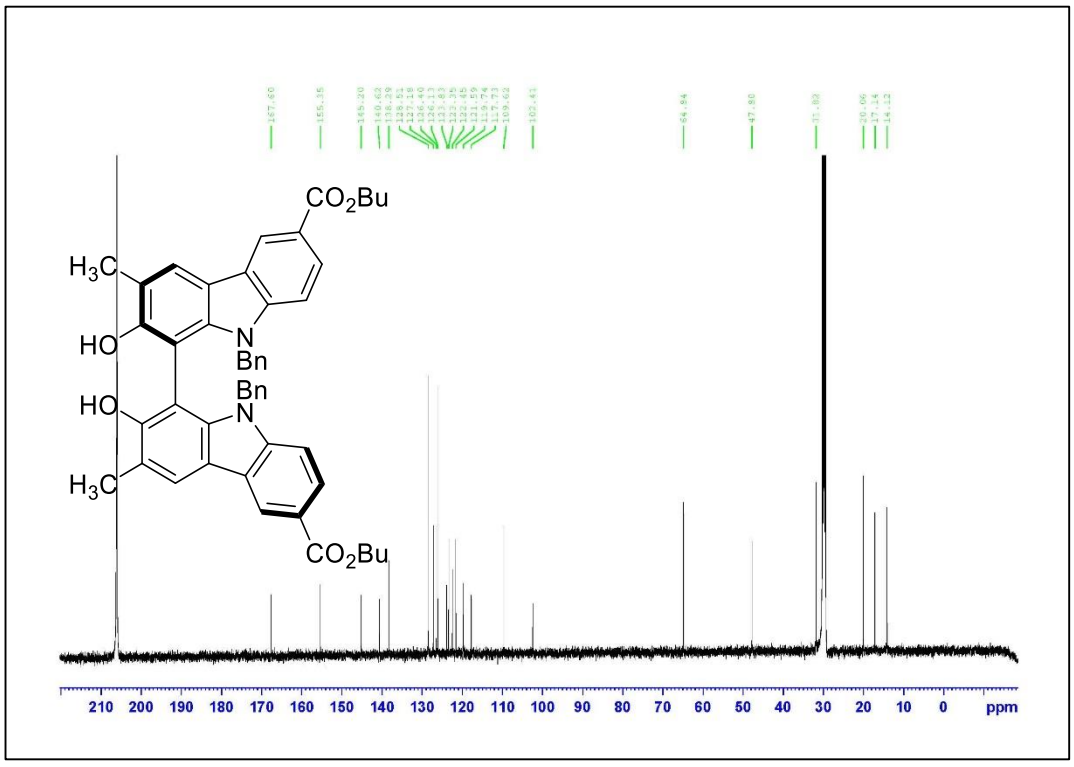

Figure A.134. ^{13}C NMR Spectrum of Compound **1.5l** (125 MHz, acetone-d_6)

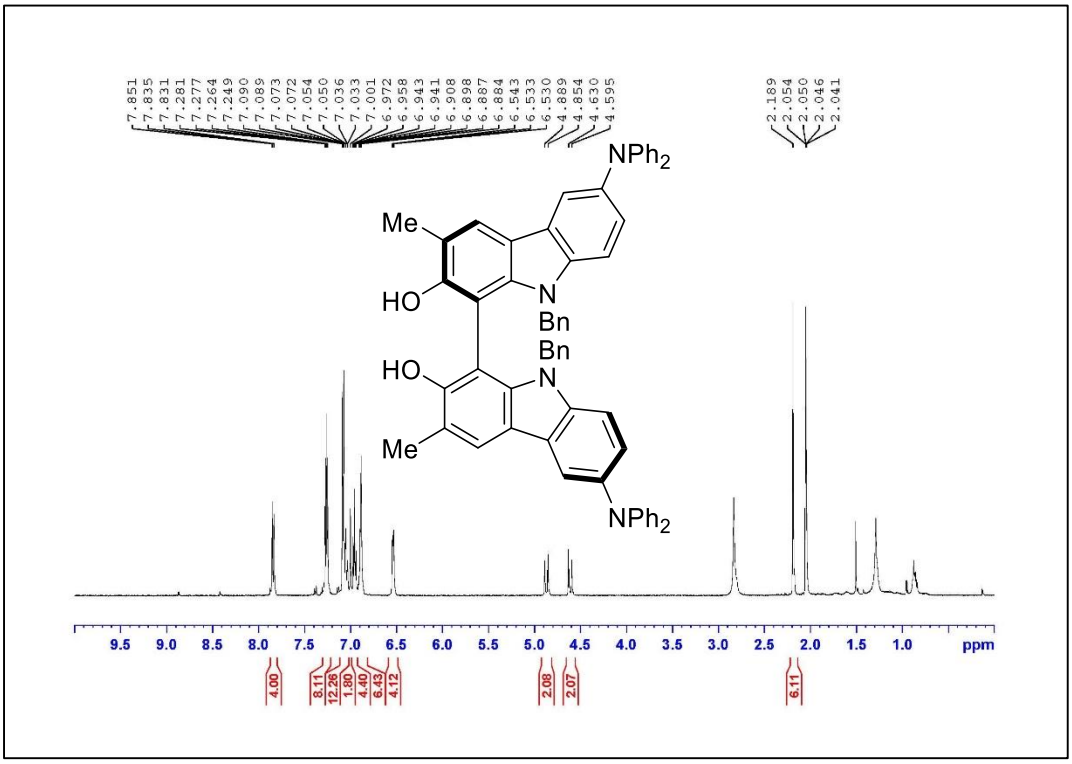

Figure A.135. ^{1}H NMR Spectrum of Compound **1.5m** (500 MHz, acetone-d_6)

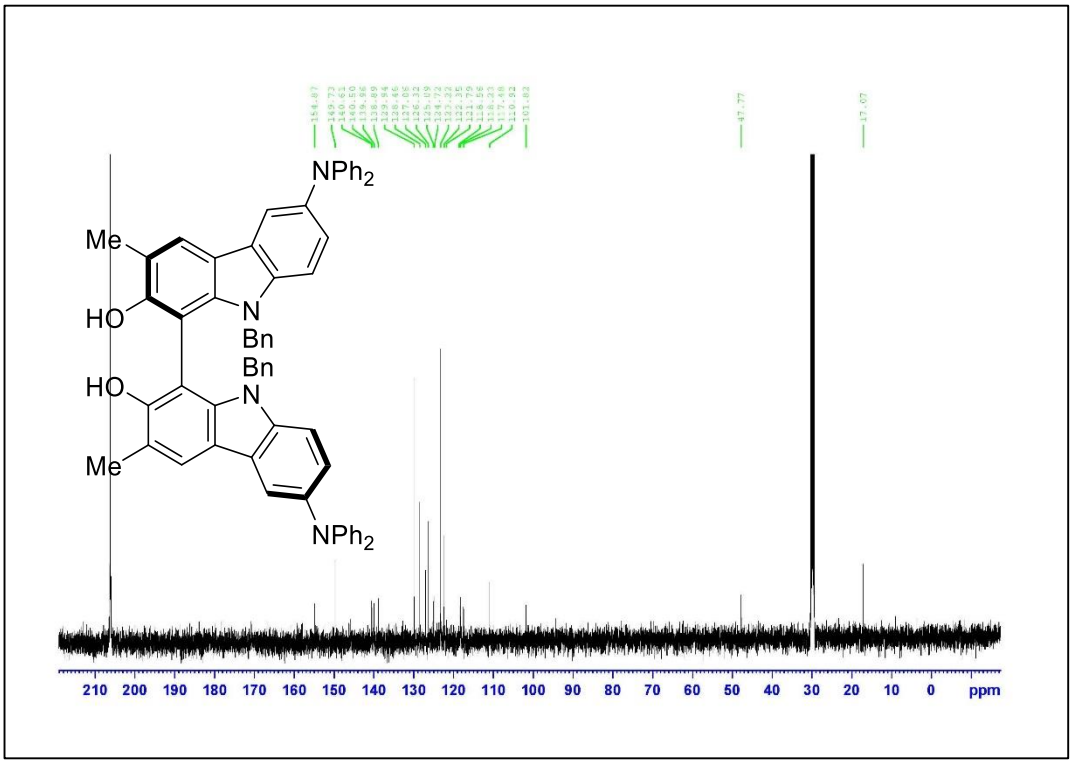

Figure A.136. ^{13}C NMR Spectrum of Compound **1.5m** (125 MHz, acetone-d_6)

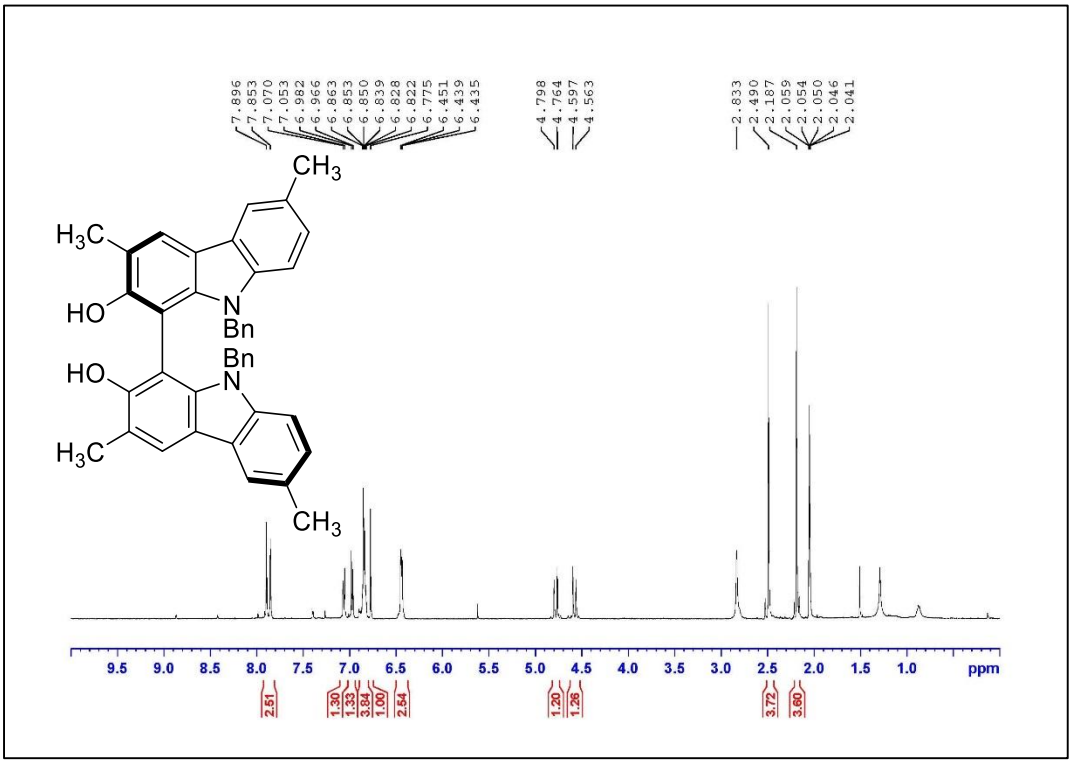

Figure A.137. ^{1}H NMR Spectrum of Compound **1.5n** (500 MHz, acetone-d_6)

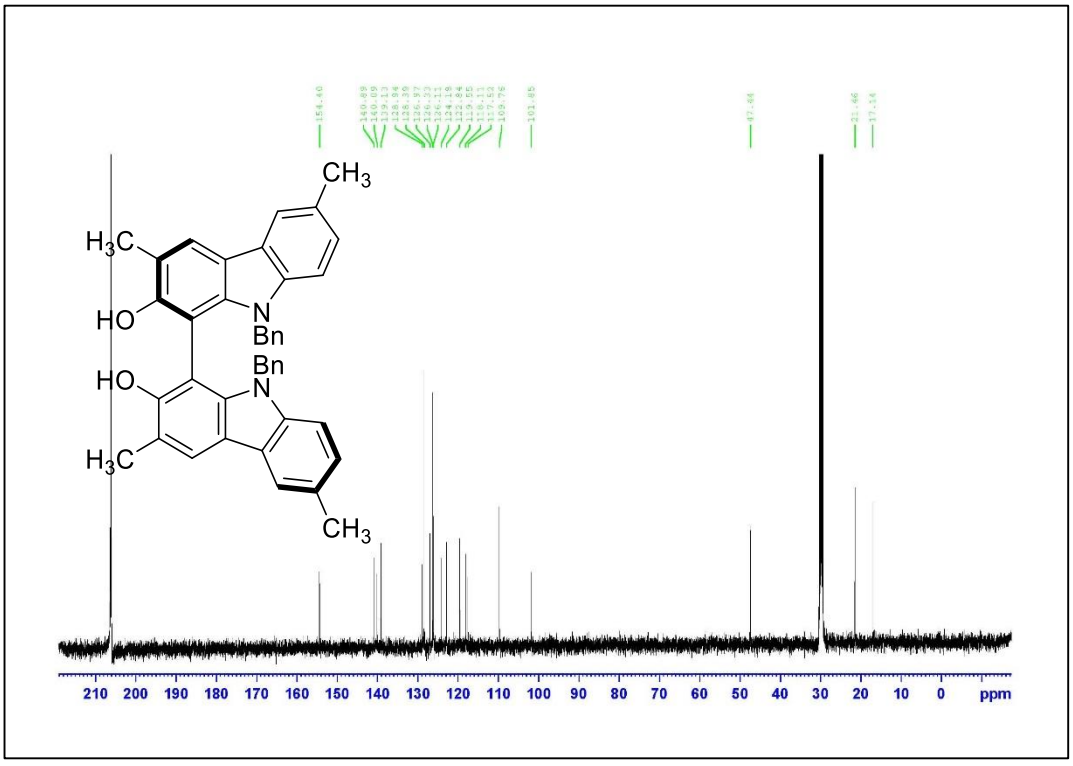

Figure A.138. ^{13}C NMR Spectrum of Compound **1.5n** (125 MHz, acetone-d_6)

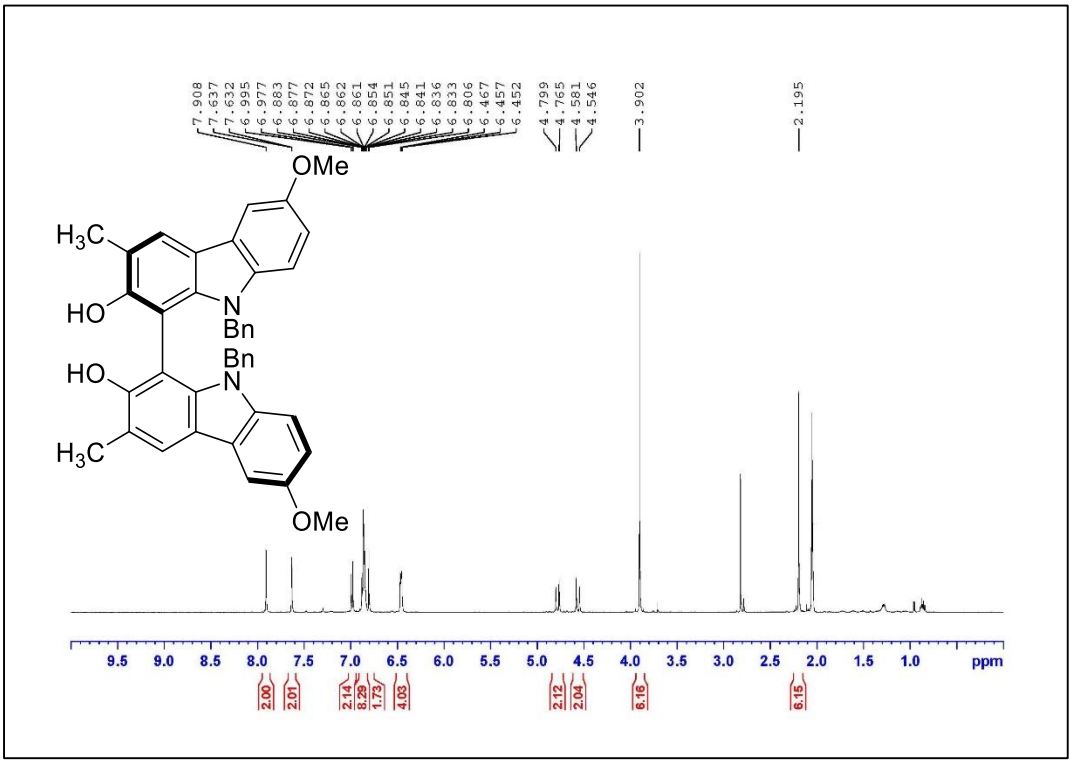

Figure A.139. ^{1}H NMR Spectrum of Compound **1.5o** (500 MHz, acetone-d_6)

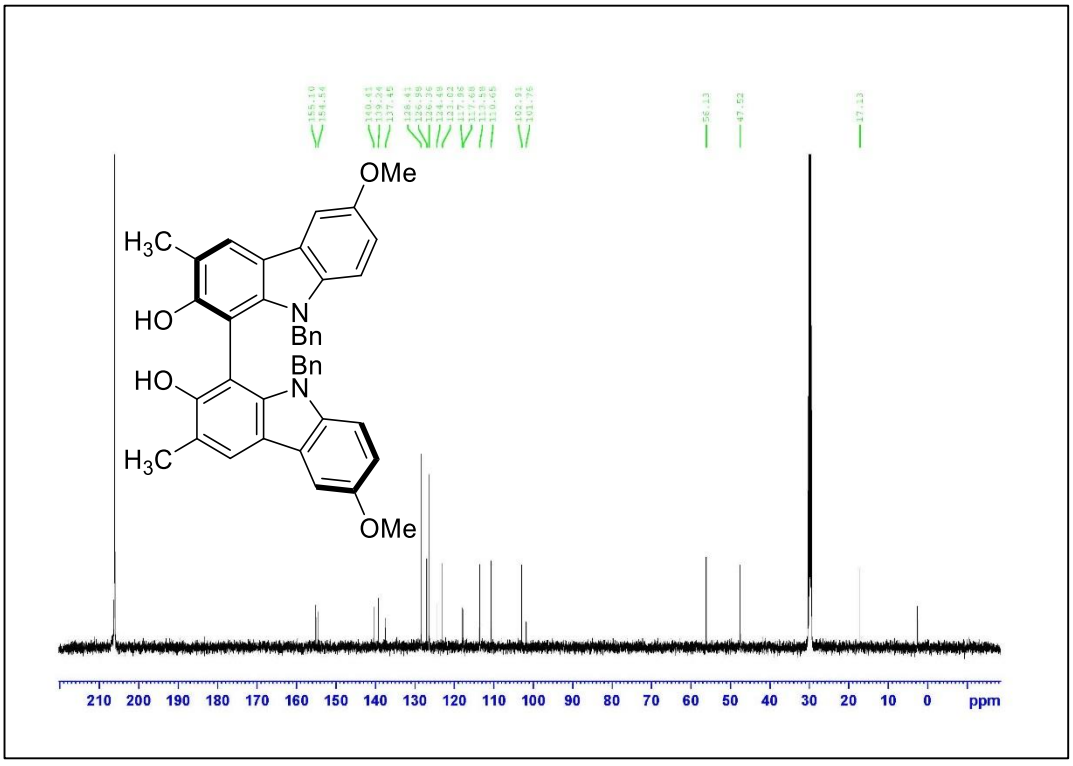

Figure A.140. ^{13}C NMR Spectrum of Compound **1.5o** (125 MHz, acetone-d_6)

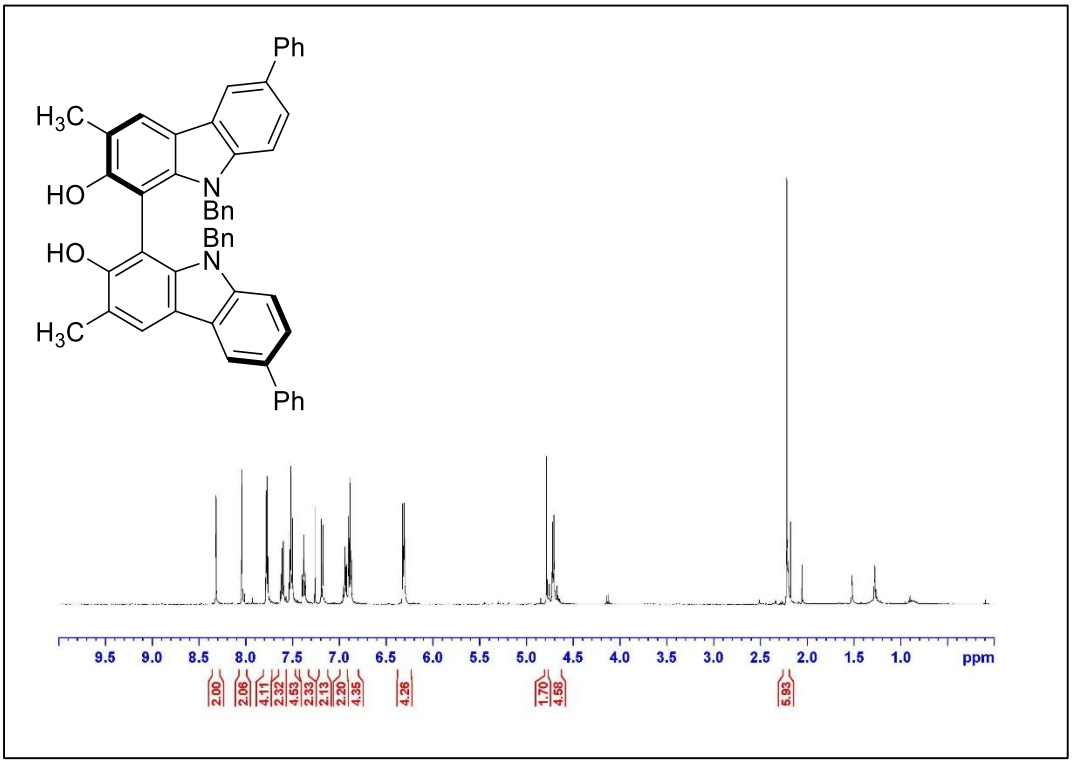

Figure A.141. ^{1}H NMR Spectrum of Compound **1.5p** (500 MHz, $CDCl_3$)

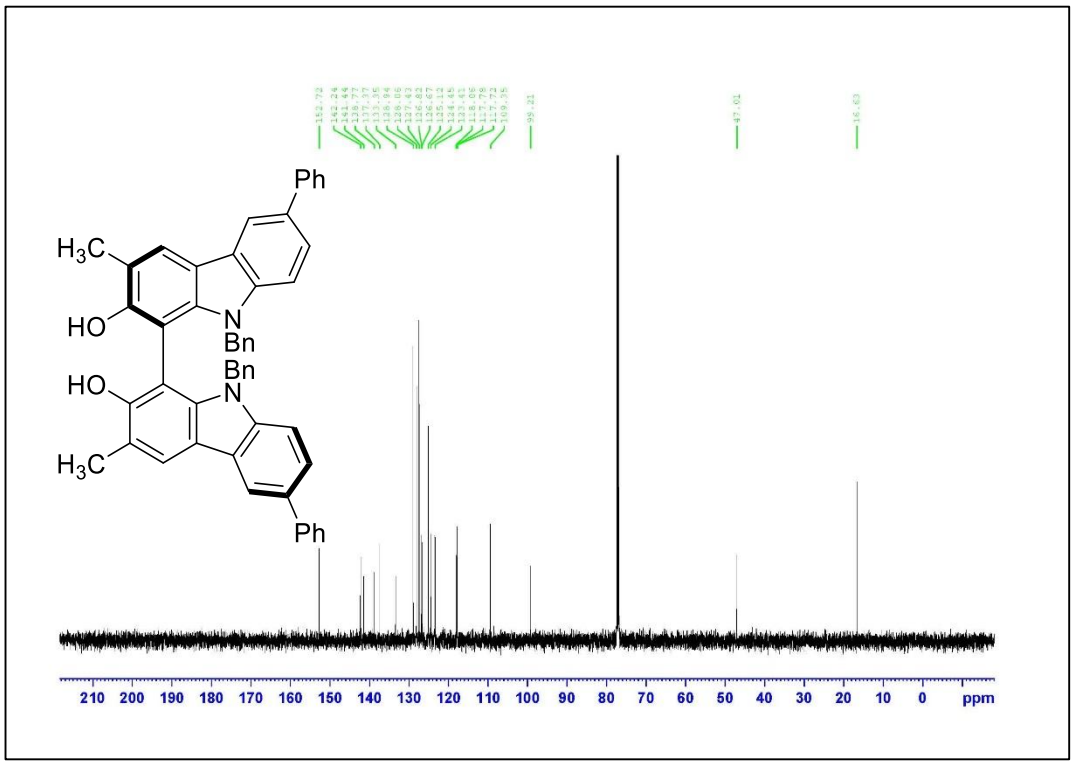

Figure A.142. ^{13}C NMR Spectrum of Compound **1.5p** (125 MHz, $CDCl_3$)

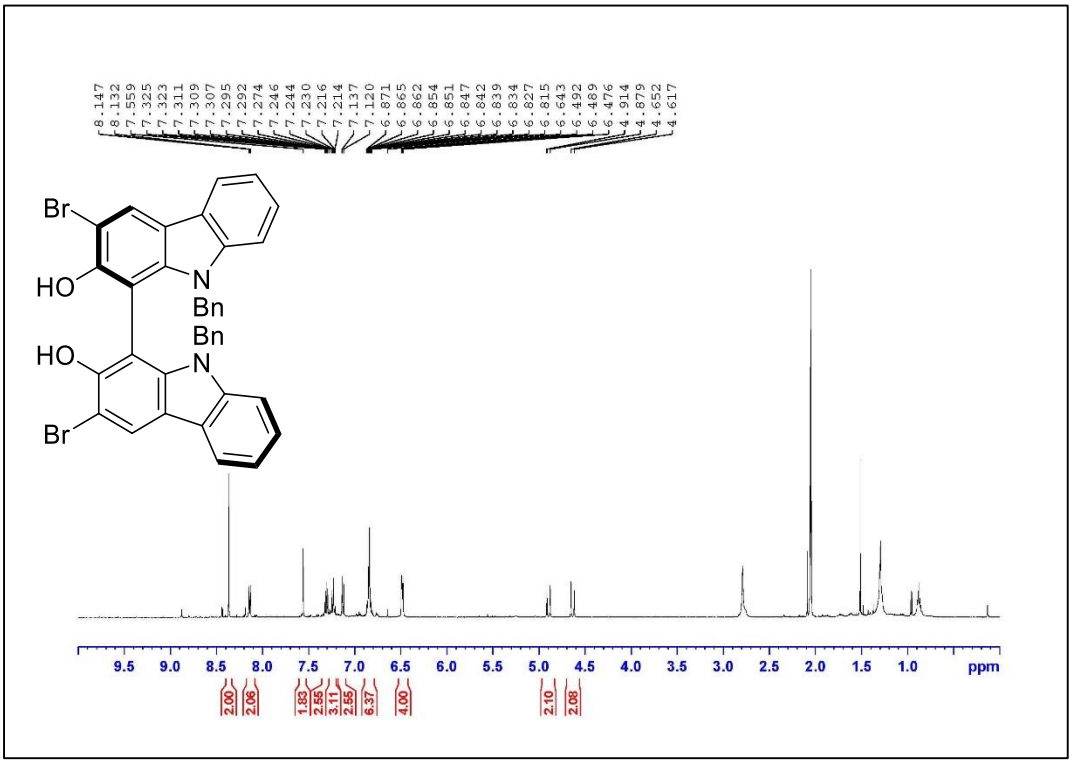

Figure A.143. ^{1}H NMR Spectrum of Compound **1.5q** (500 MHz, acetone-d_6)

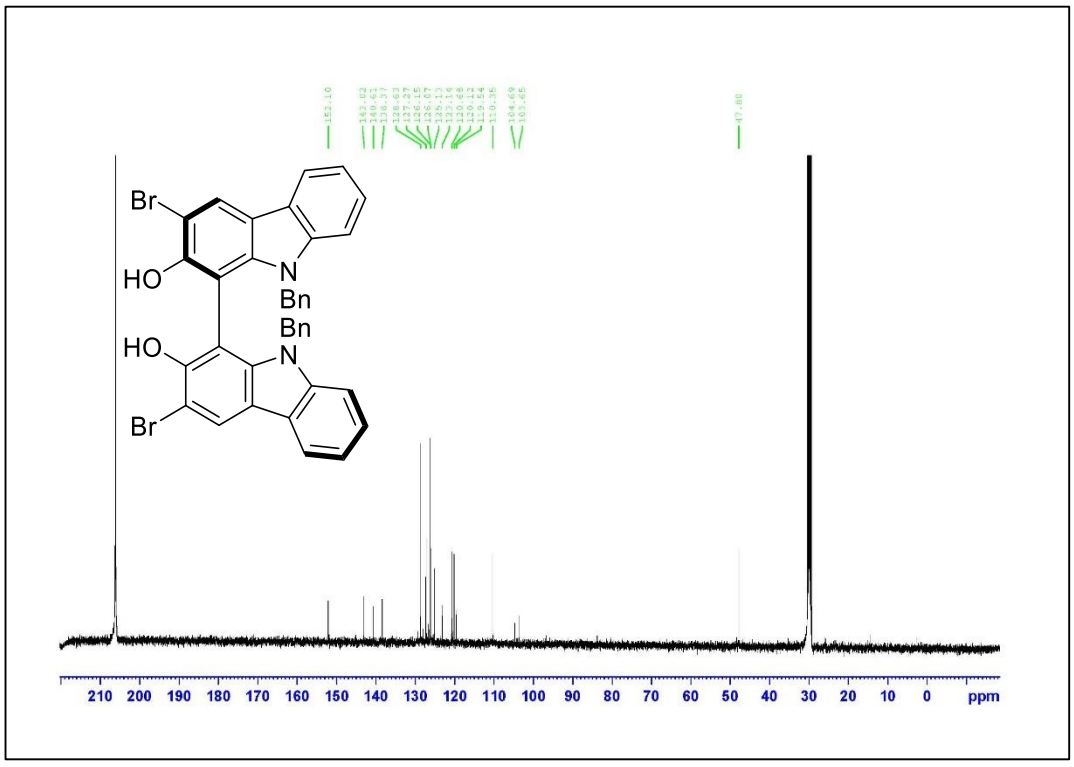

Figure A.144. ^{13}C NMR Spectrum of Compound **1.5q** (125 MHz, acetone-d_6)

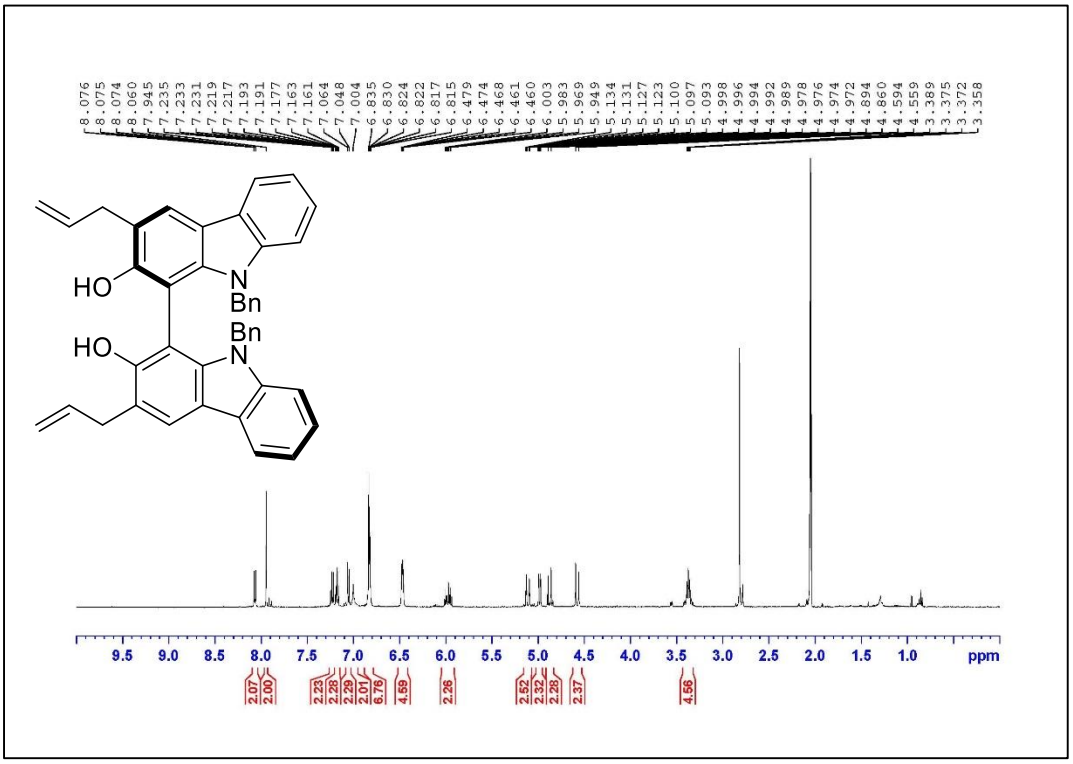

Figure A.145. ^{1}H NMR Spectrum of Compound **1.5r** (500 MHz, acetone-d_6)

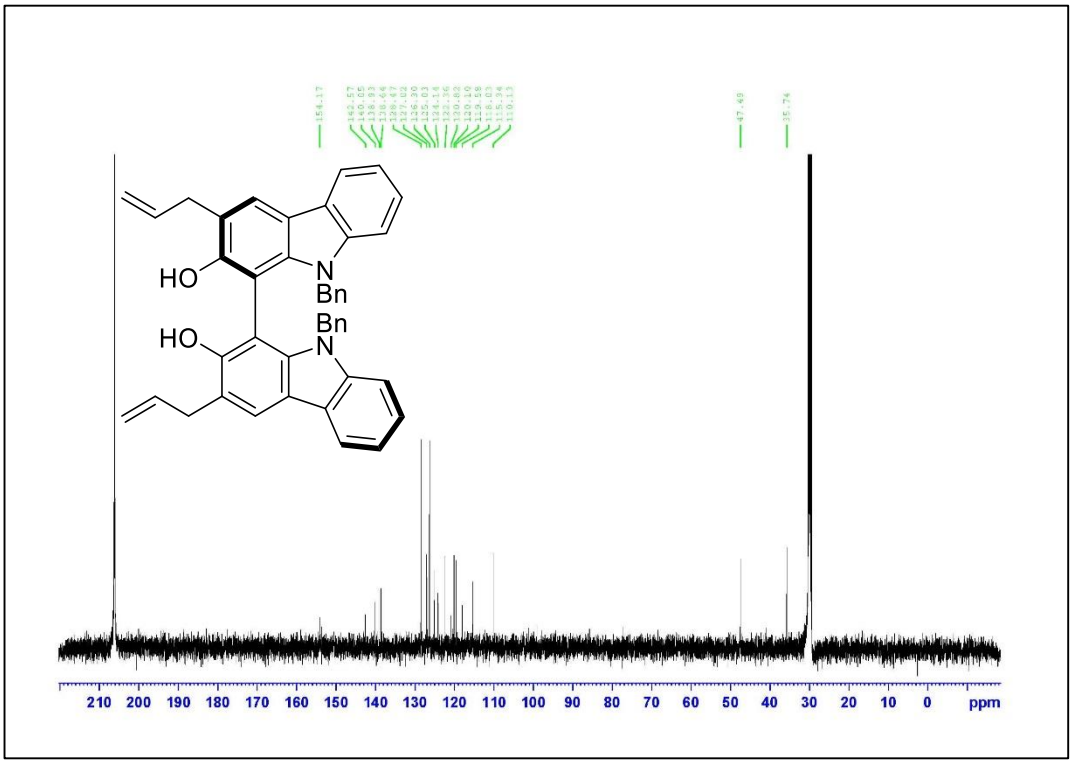

Figure A.146. ^{13}C NMR Spectrum of Compound **1.5r** (125 MHz, acetone-d_6)

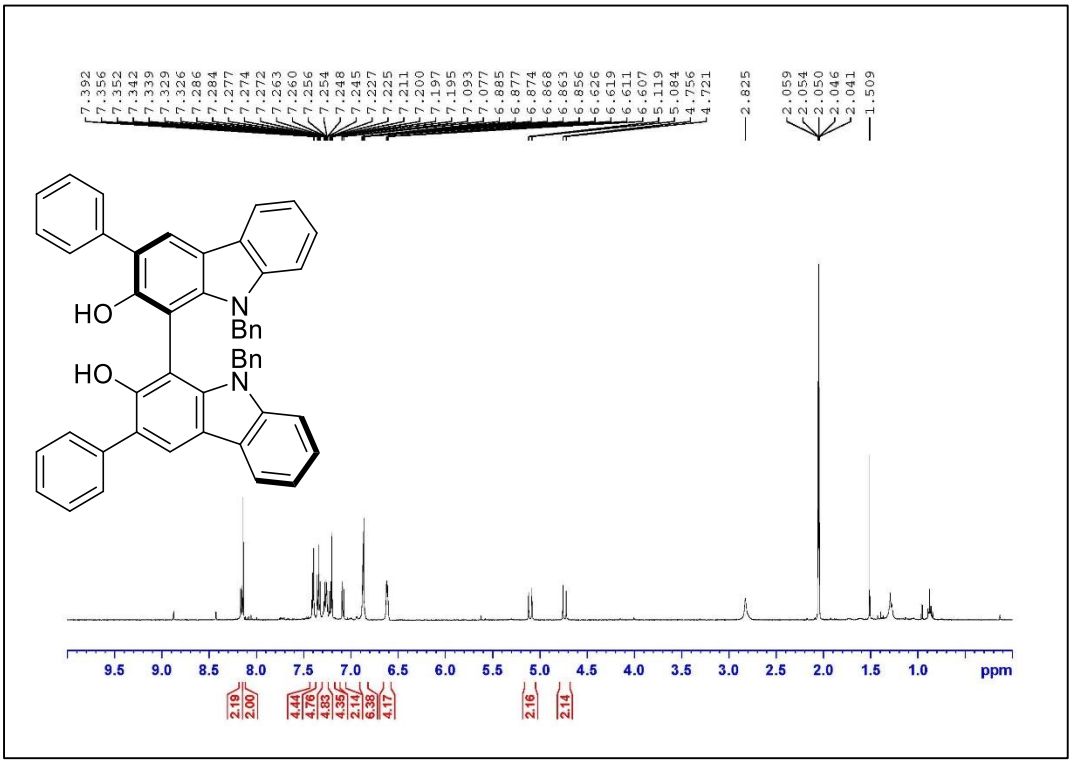

Figure A.147. ^{1}H NMR Spectrum of Compound **1.5s** (500 MHz, acetone-d_6)

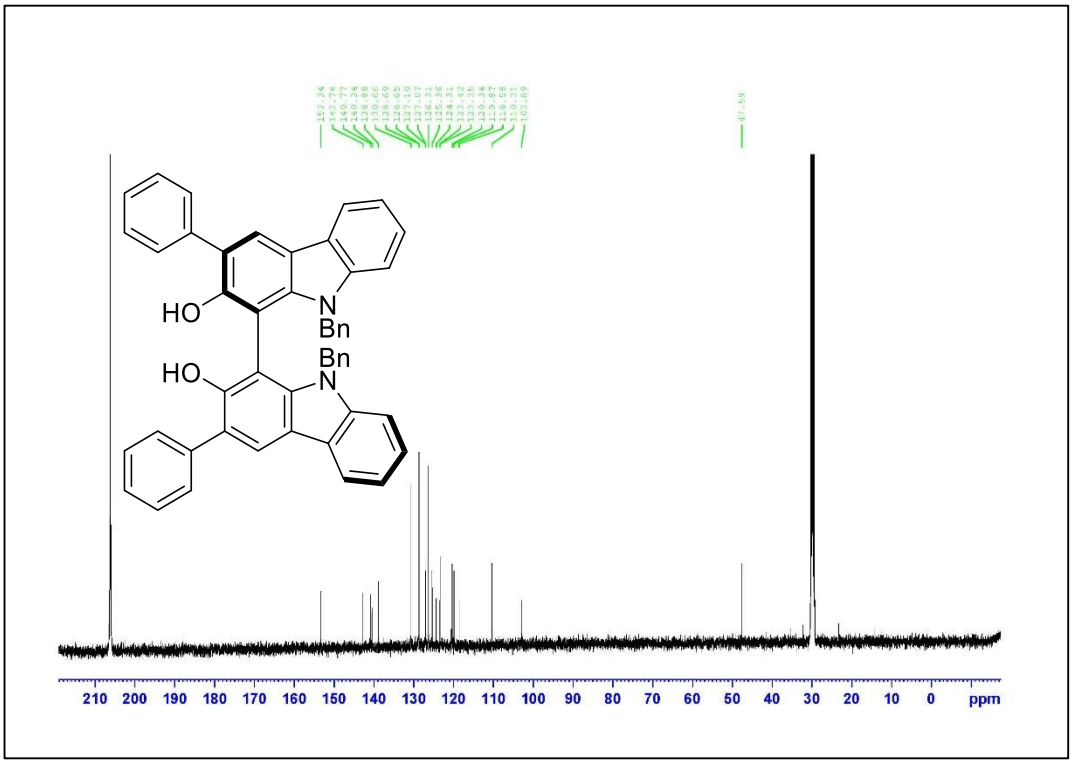

Figure A.148. ^{13}C NMR Spectrum of Compound **1.5s** (125 MHz, acetone-d_6)

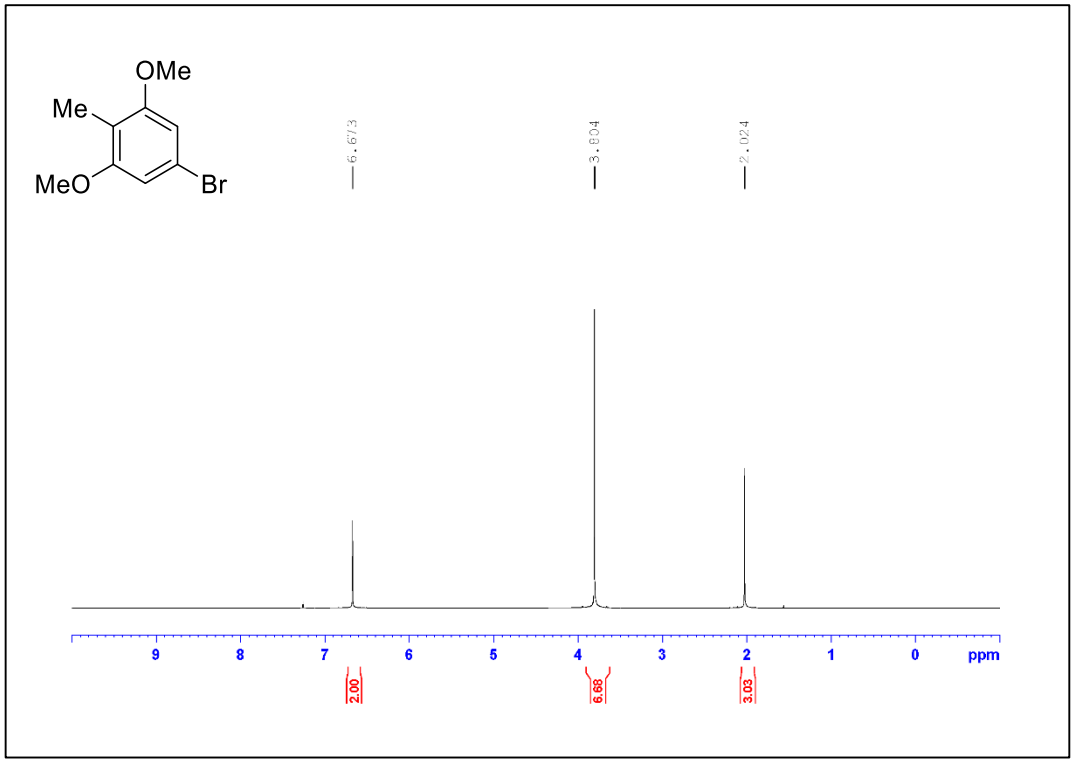

Figure A.149. ^{1}H NMR Spectrum of Compound **2.13** (500 MHz, $CDCl_3$)

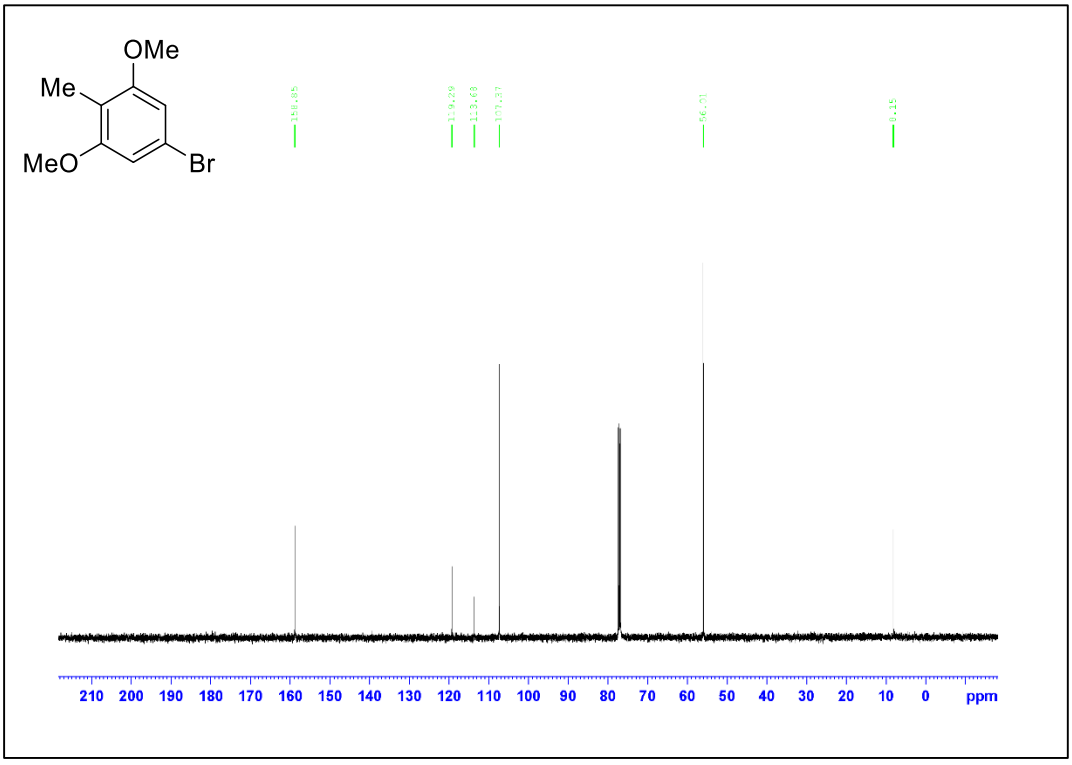

Figure A.150. ^{13}C NMR Spectrum of Compound **2.13** (125 MHz, $CDCl_3$)

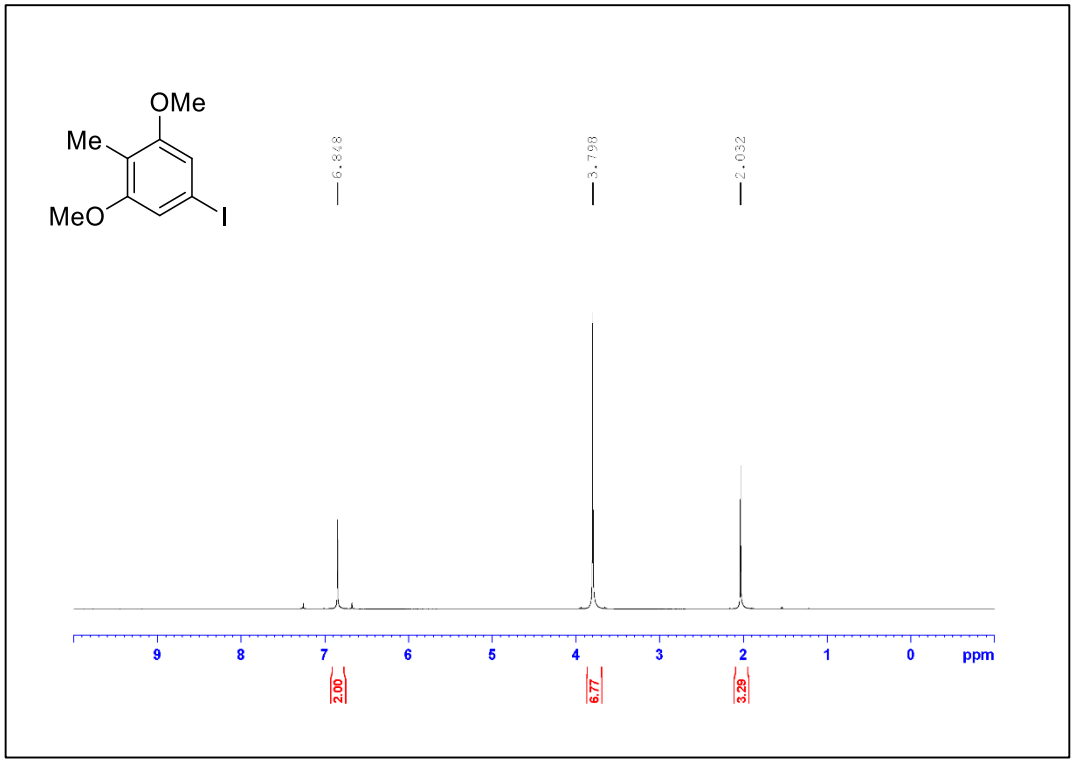

Figure A.151. ^{1}H NMR Spectrum of Compound **2.S1** (500 MHz, $CDCl_3$)

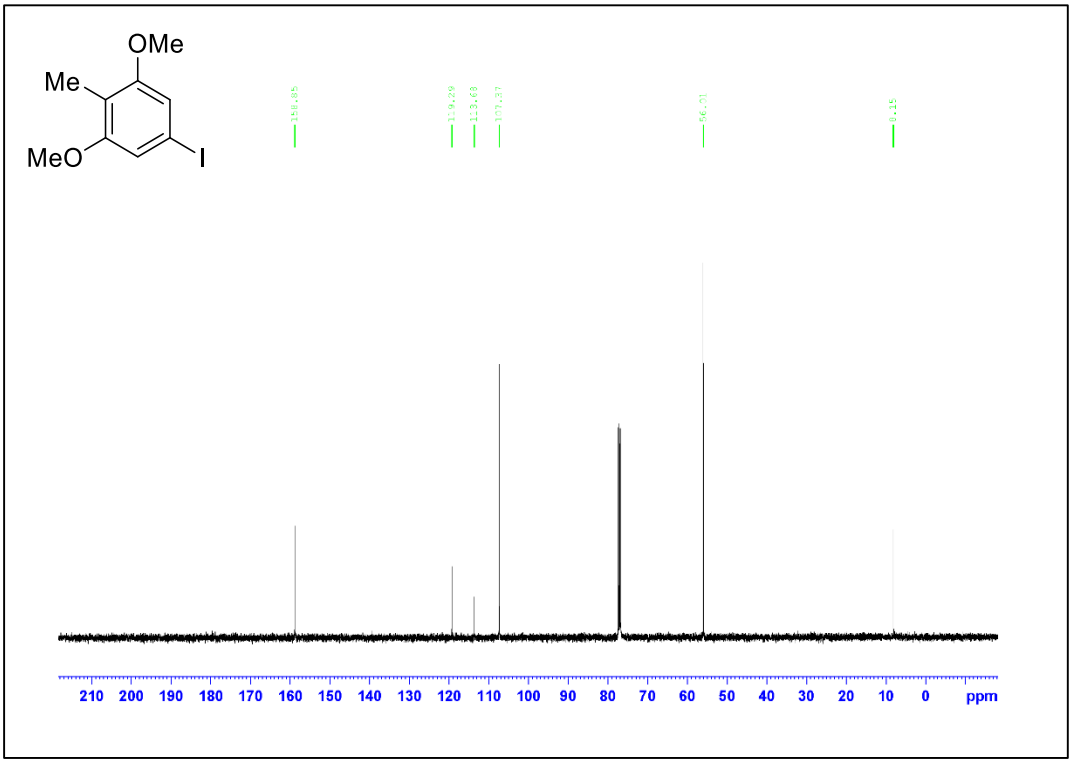

Figure A.152. ^{13}C NMR Spectrum of Compound **2.S1** (125 MHz, $CDCl_3$)

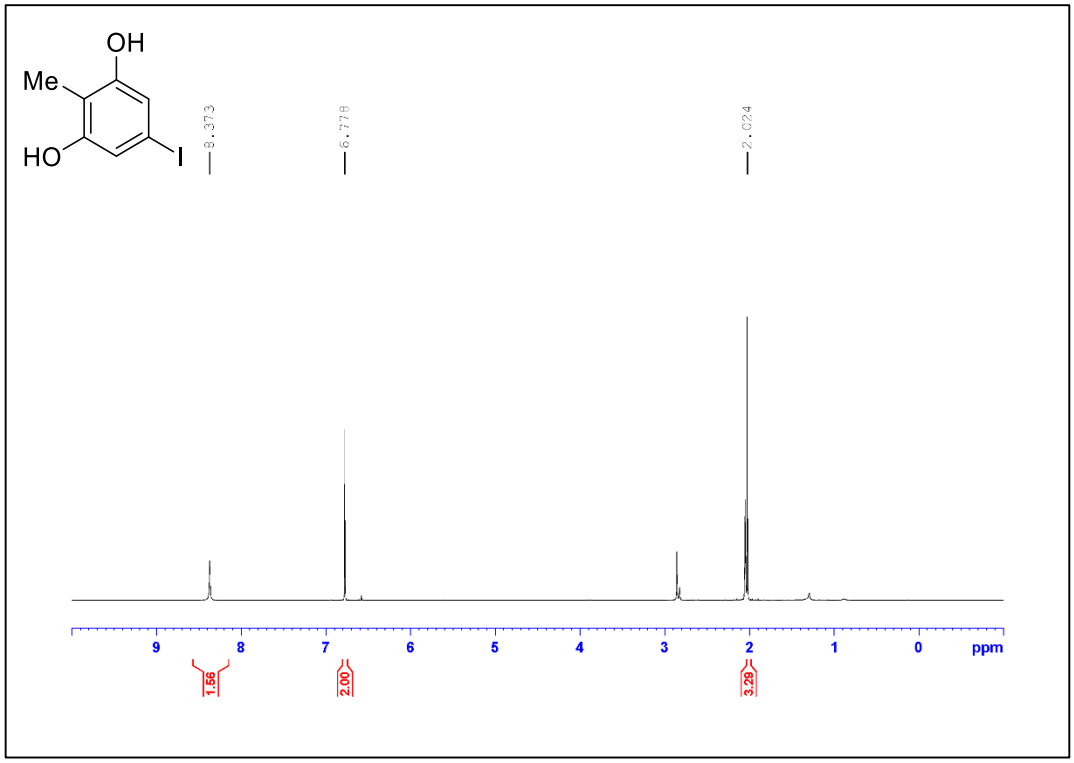

Figure A.153. ^{1}H NMR Spectrum of Compound **2.9** (500 MHz, acetone-d_6)

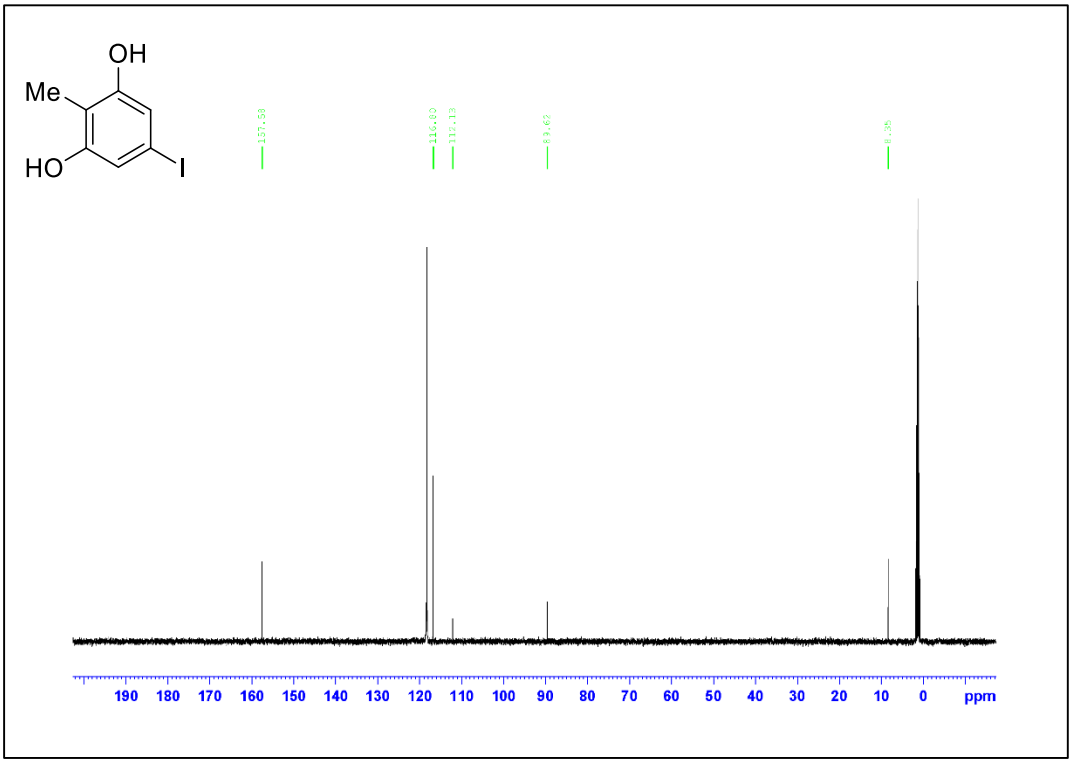

Figure A.154. ^{13}C NMR Spectrum of Compound **2.9** (125 MHz, CD_3CN)

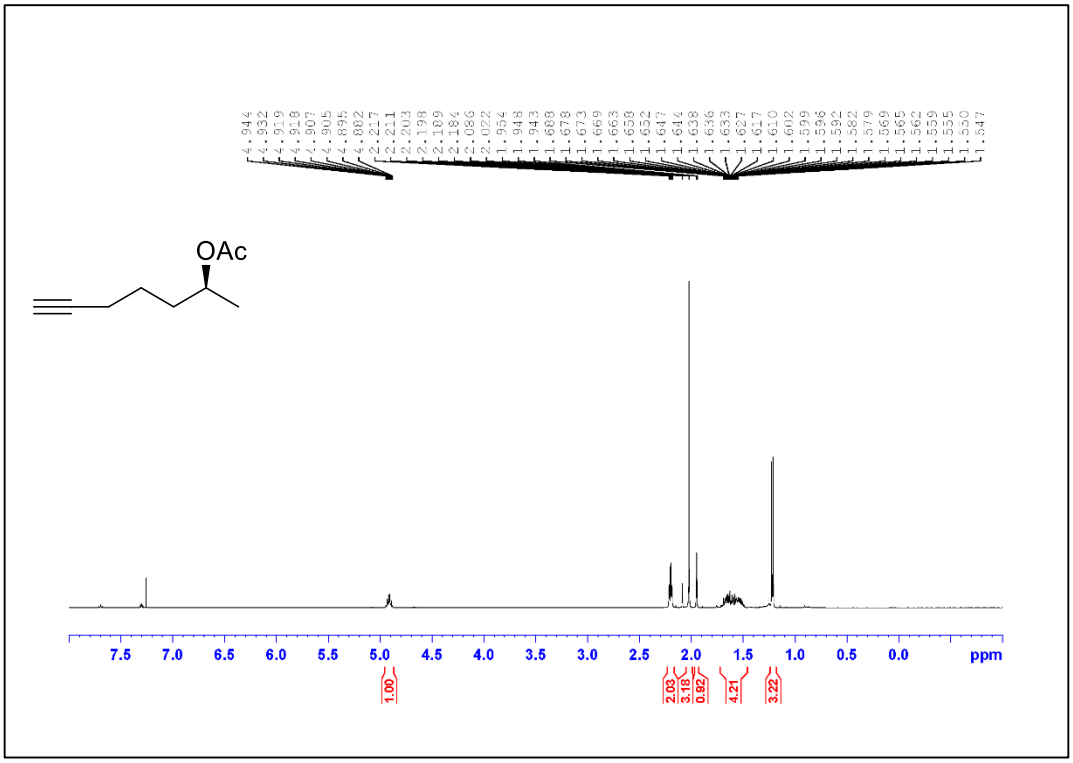

Figure A.155. ^{1}H NMR Spectrum of Compound **2.10** (500 MHz, $CDCl_3$)

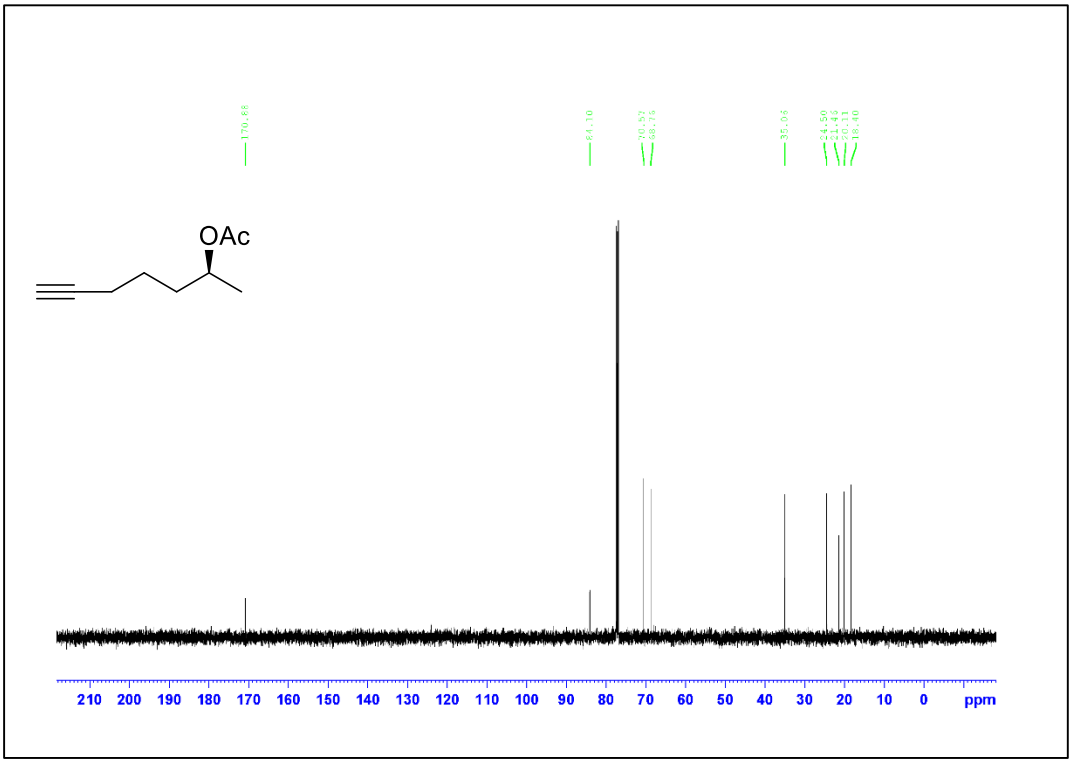

Figure A.156. ^{13}C NMR Spectrum of Compound **2.10** (125 MHz, $CDCl_3$)

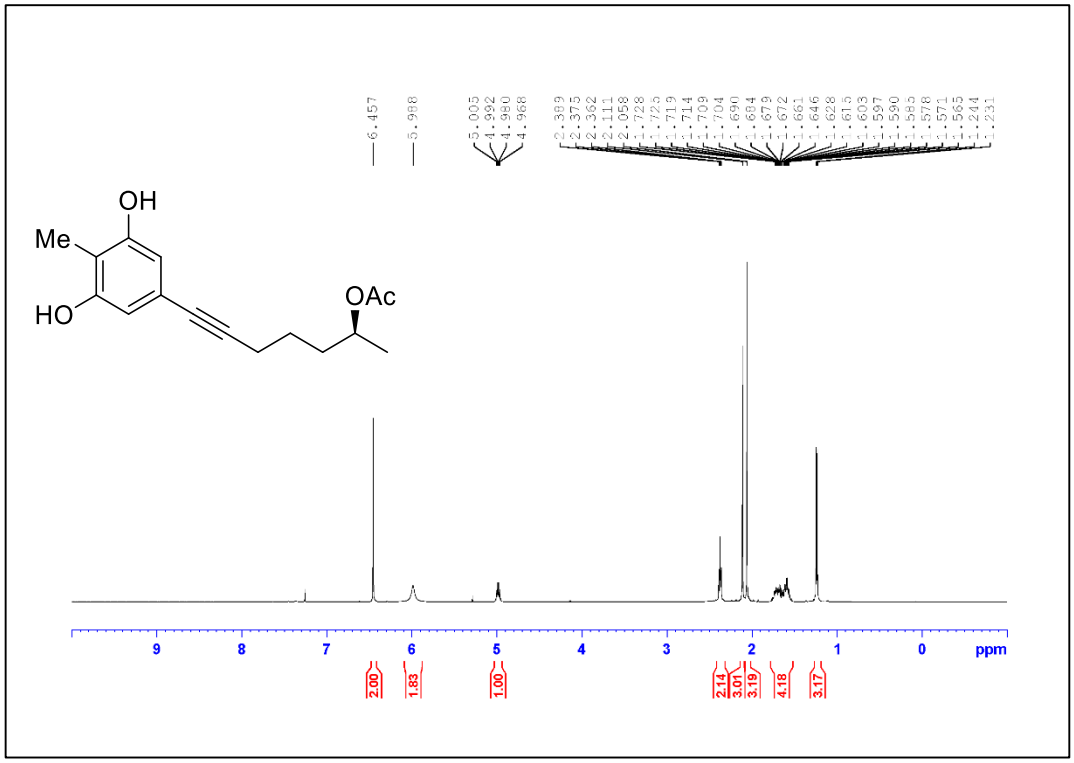

Figure A.157. ^{1}H NMR Spectrum of Compound **2.8** (500 MHz, $CDCl_3$)

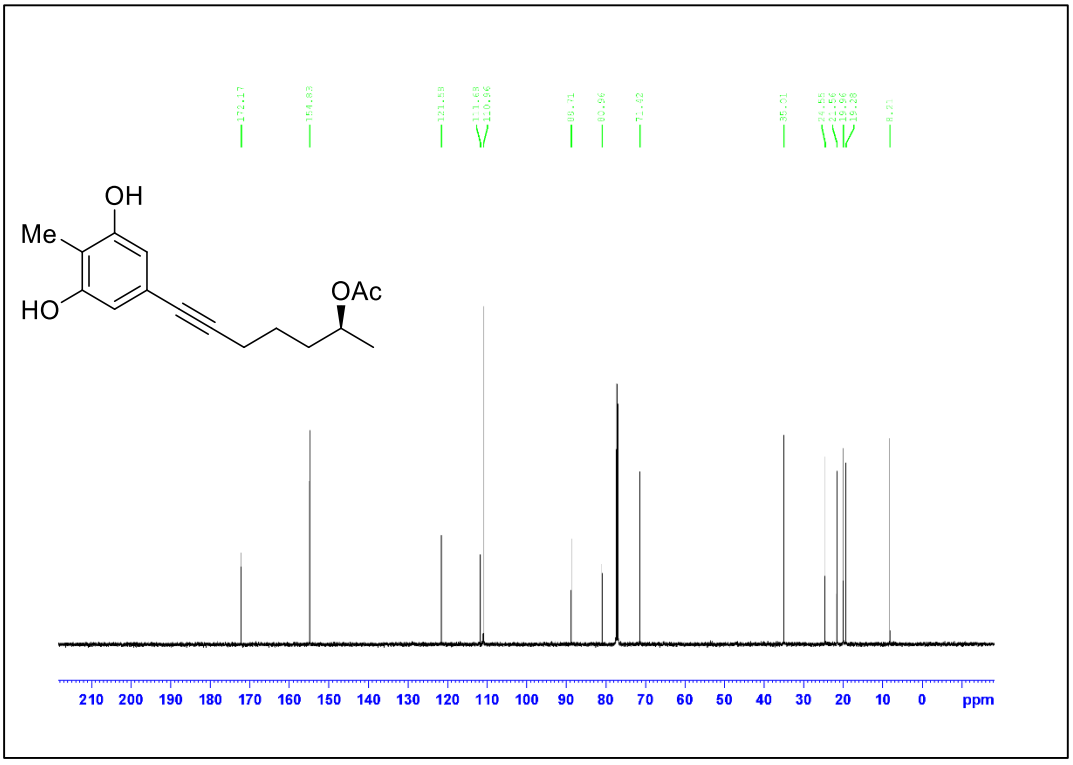

Figure A.158. ^{13}C NMR Spectrum of Compound **2.8** (125 MHz, $CDCl_3$)

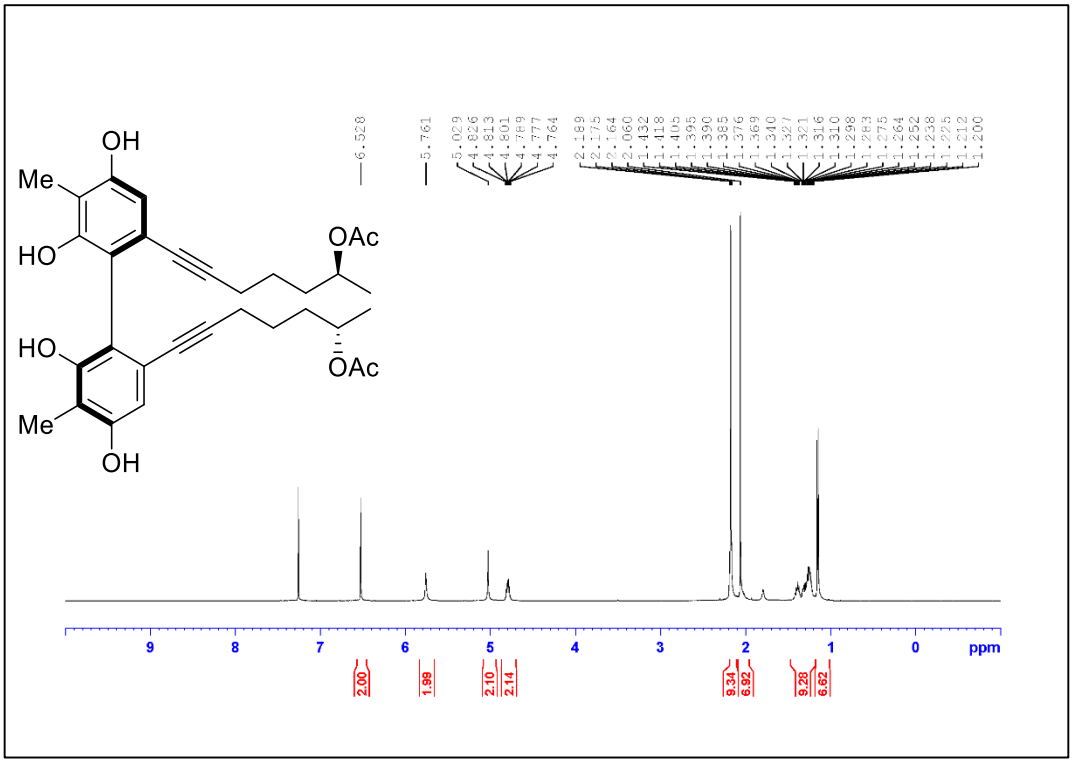

Figure A.159. ^{1}H NMR Spectrum of Compound **2.7** (500 MHz, $CDCl_3$)

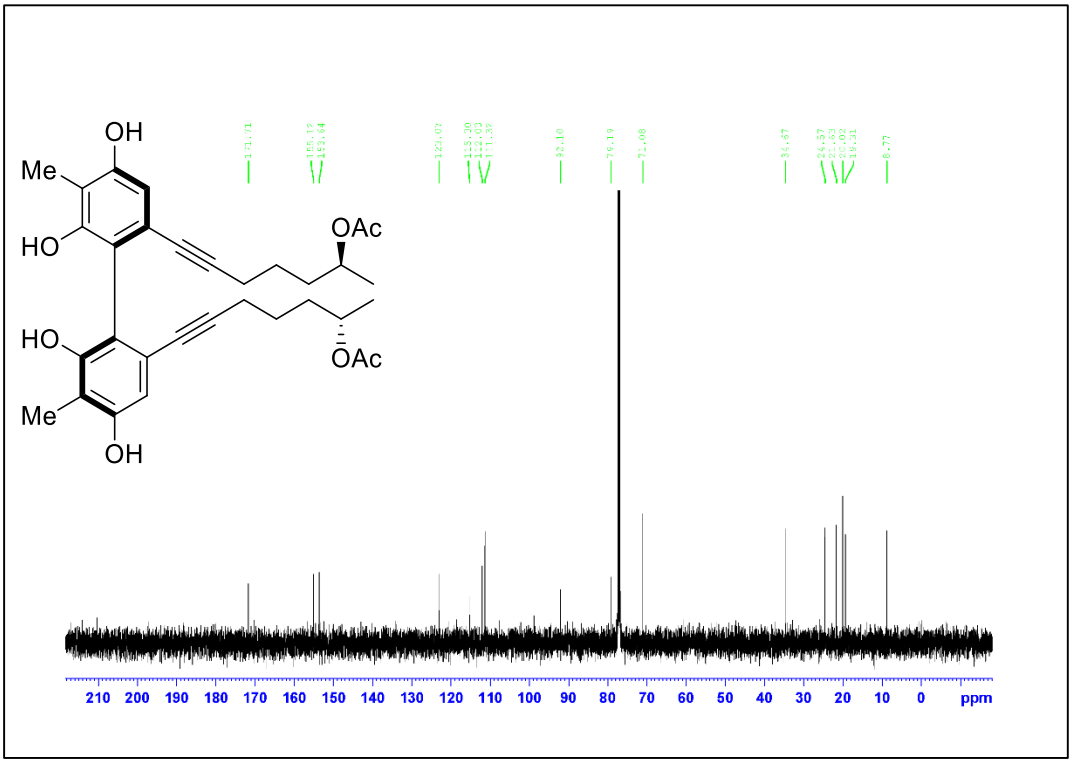

Figure A.160. ^{13}C NMR Spectrum of Compound **2.7** (125 MHz, $CDCl_3$)

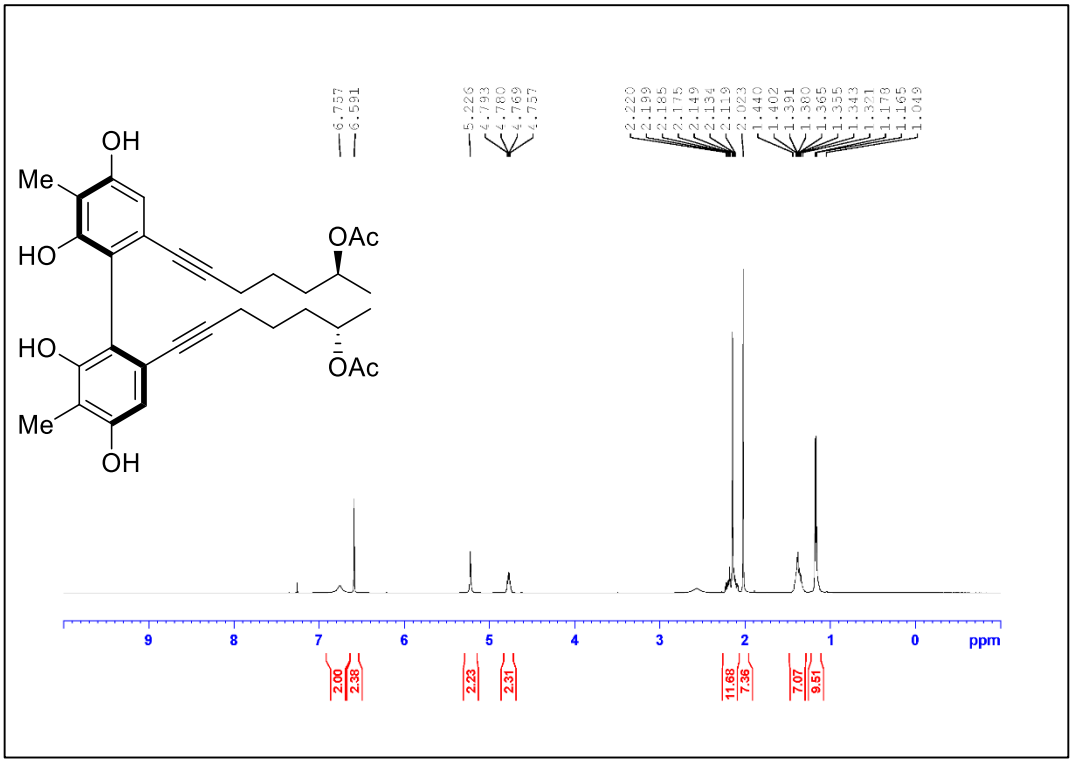

Figure A.161. ^{1}H NMR Spectrum of Compound (*P*)-**2.7** (500 MHz, $CDCl_3$)

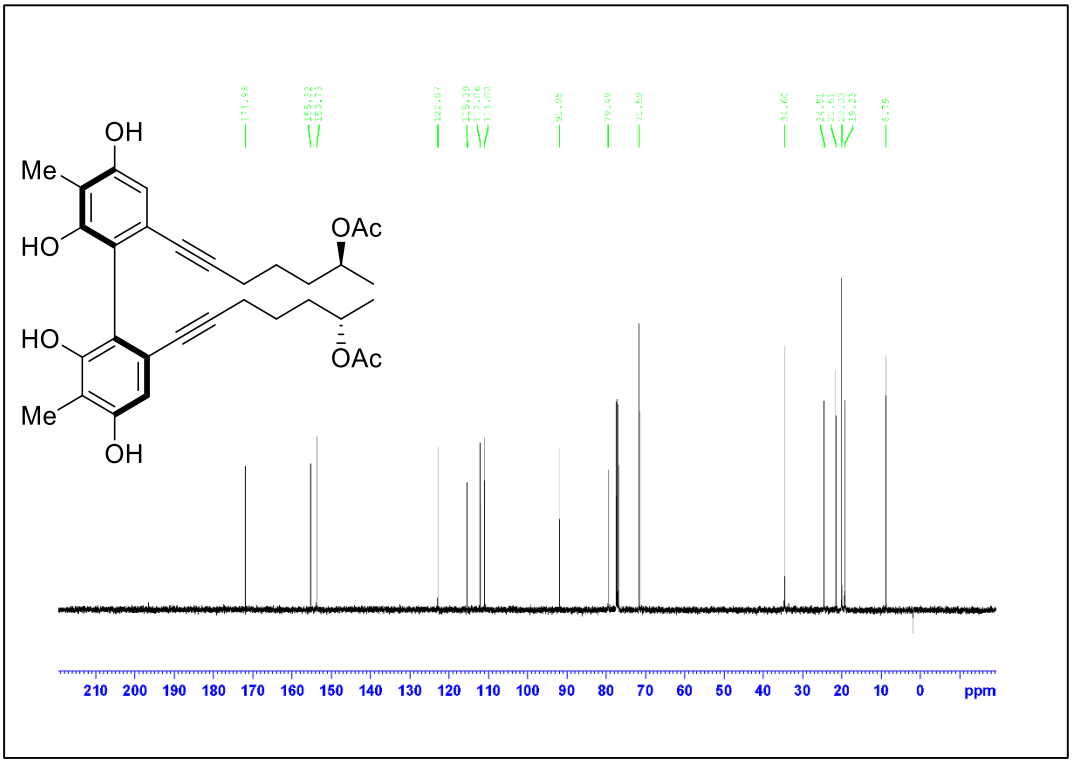

Figure A.162. ^{13}C NMR Spectrum of Compound (*P*)-**2.7** (125 MHz, $CDCl_3$)

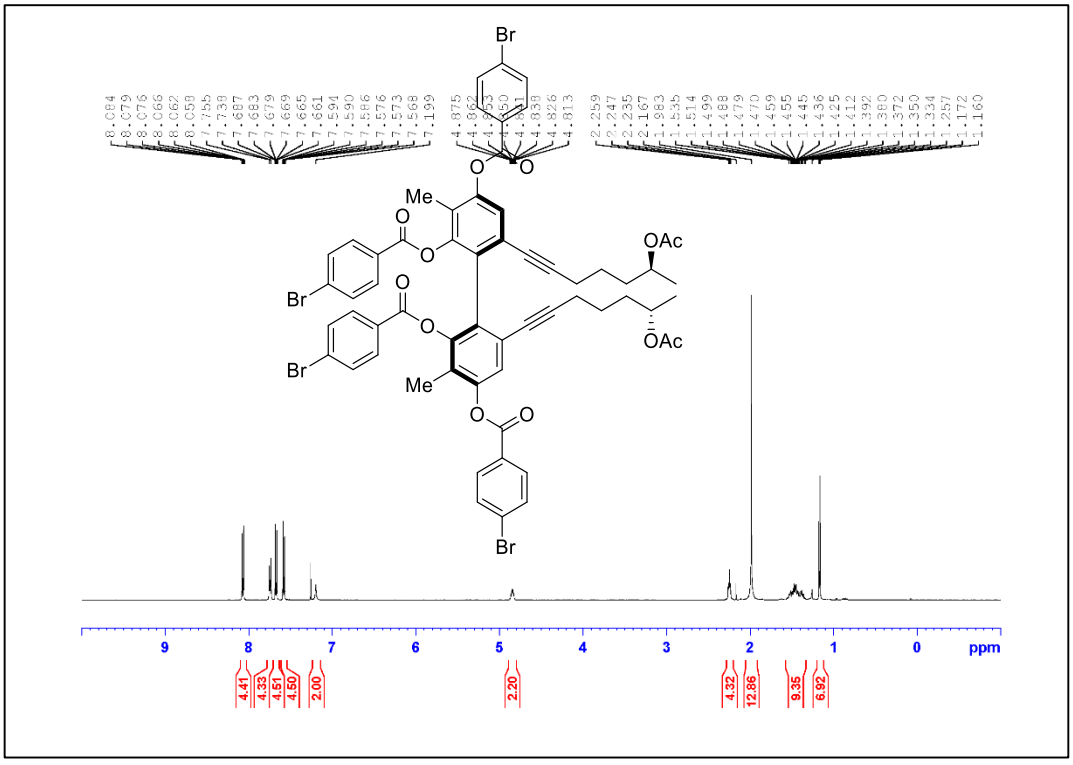

Figure A.163. ^{1}H NMR Spectrum of Compound **2.19** (500 MHz, $CDCl_3$)

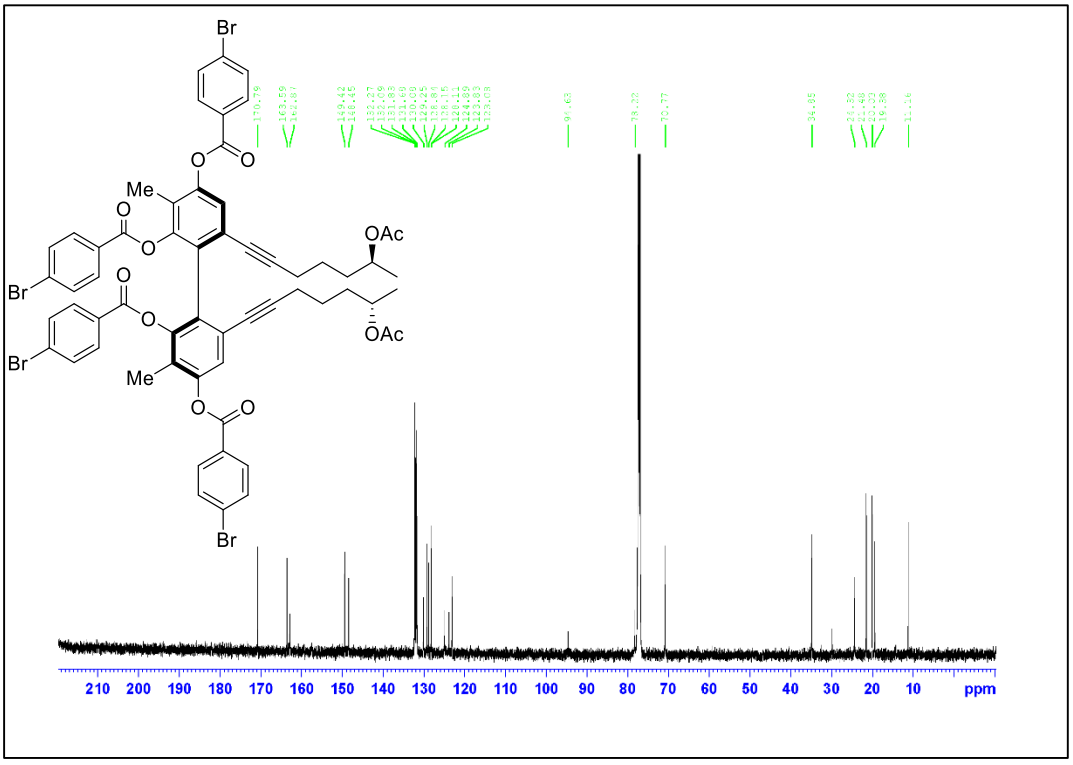

Figure A.164. ^{13}C NMR Spectrum of Compound **2.19** (125 MHz, $CDCl_3$)

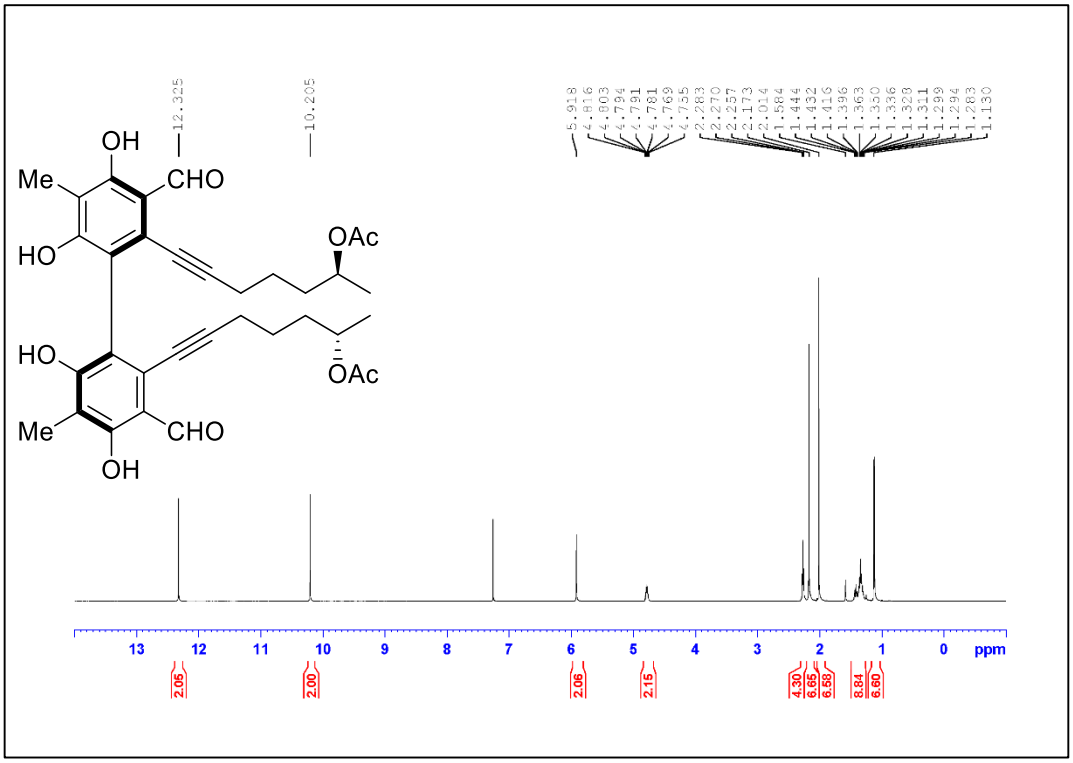

Figure A.165. ^{1}H NMR Spectrum of Compound **2.6** (500 MHz, $CDCl_3$)

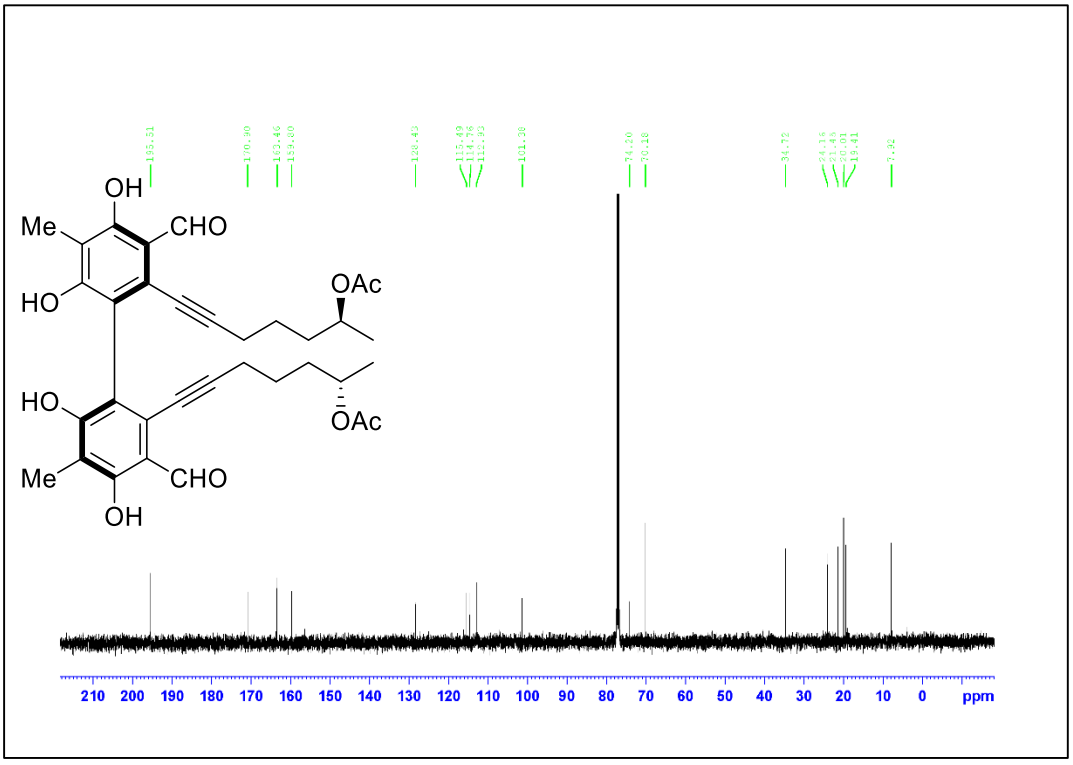

Figure A.166. ^{13}C NMR Spectrum of Compound **2.6** (125 MHz, $CDCl_3$)

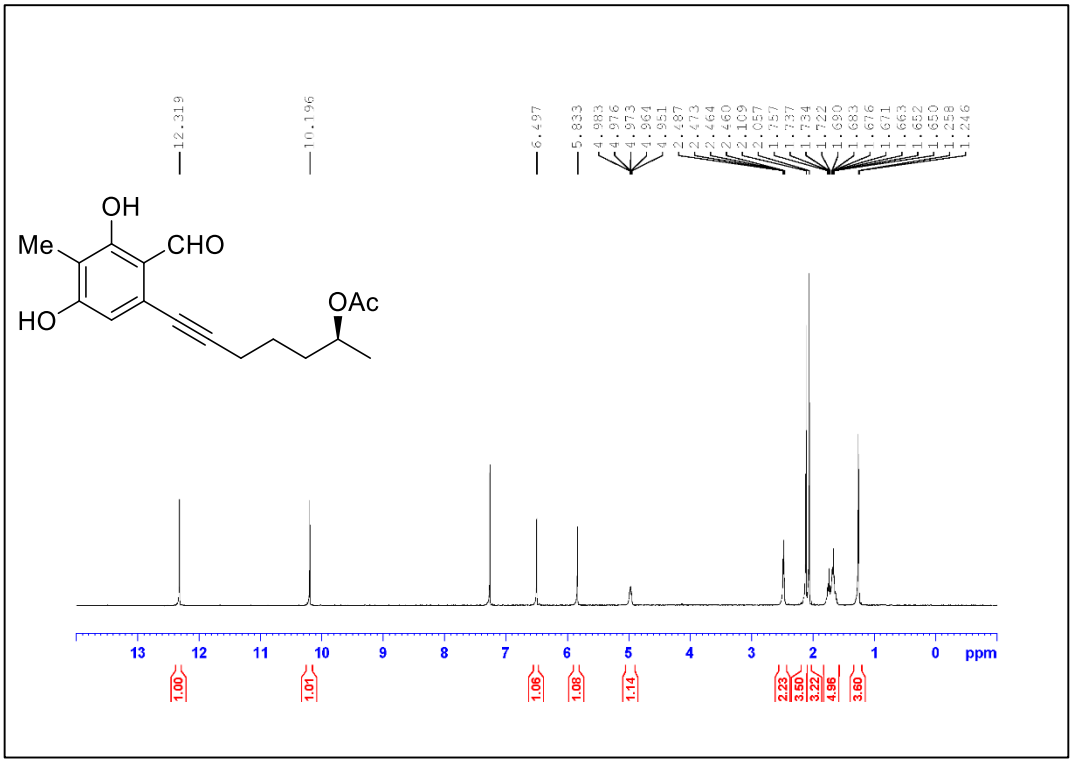

Figure A.167. ^{1}H NMR Spectrum of Compound **2.20** (500 MHz, $CDCl_3$)

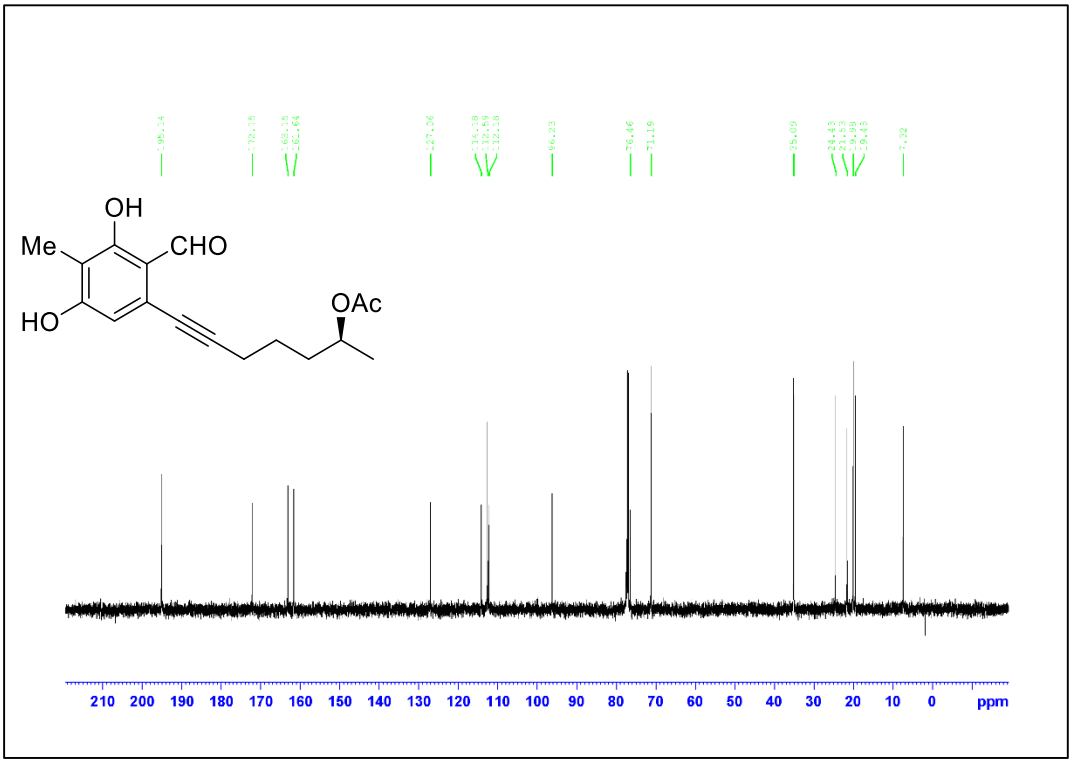

Figure A.168. ^{13}C NMR Spectrum of Compound **2.20** (125 MHz, $CDCl_3$)

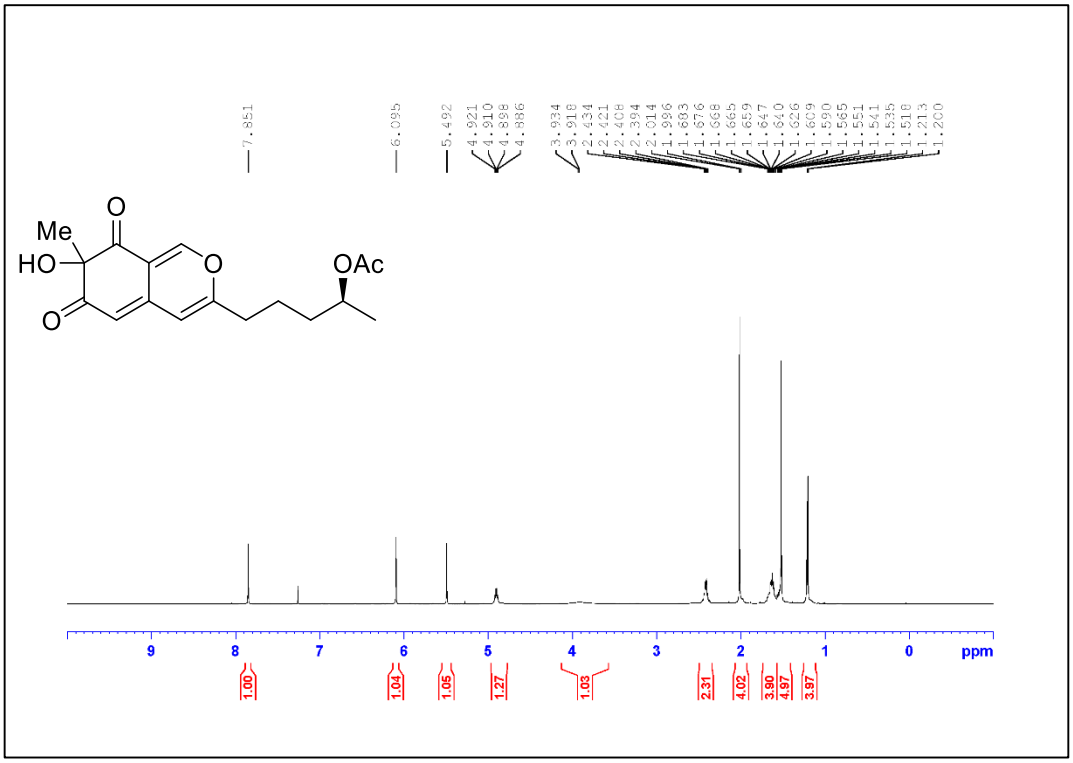

Figure A.169. ^{1}H NMR Spectrum of Compound **2.21** (500 MHz, $CDCl_3$)

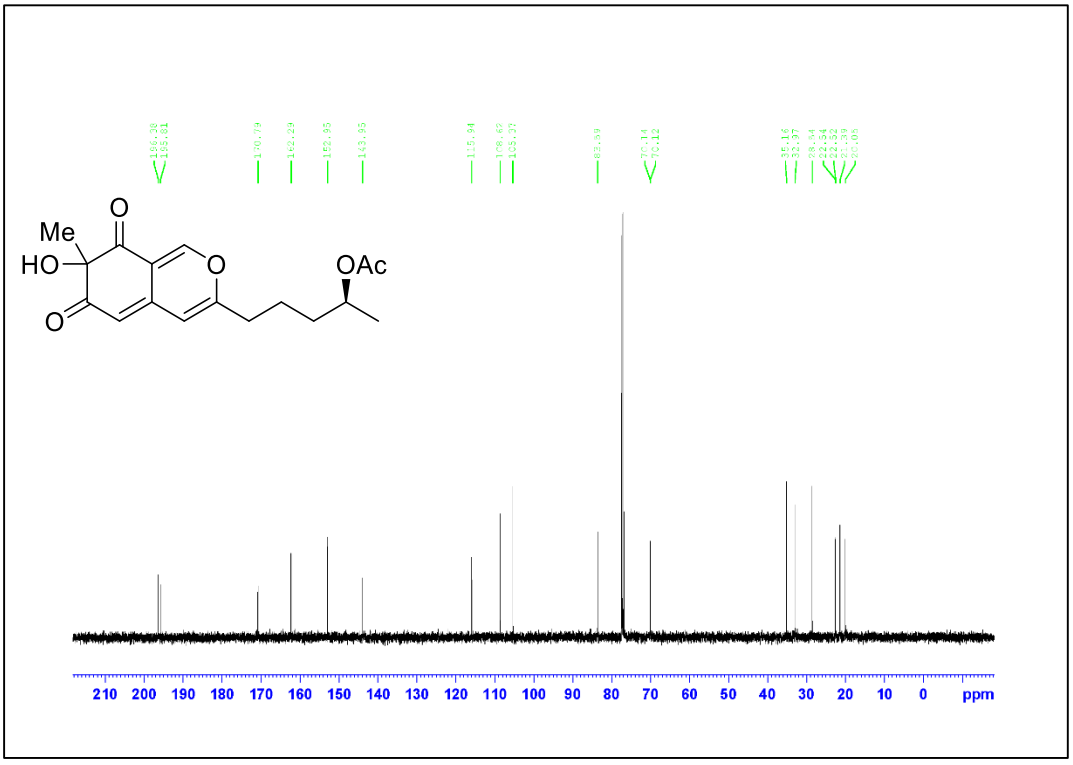

Figure A.170. ^{13}C NMR Spectrum of Compound **2.21** (125 MHz, $CDCl_3$)

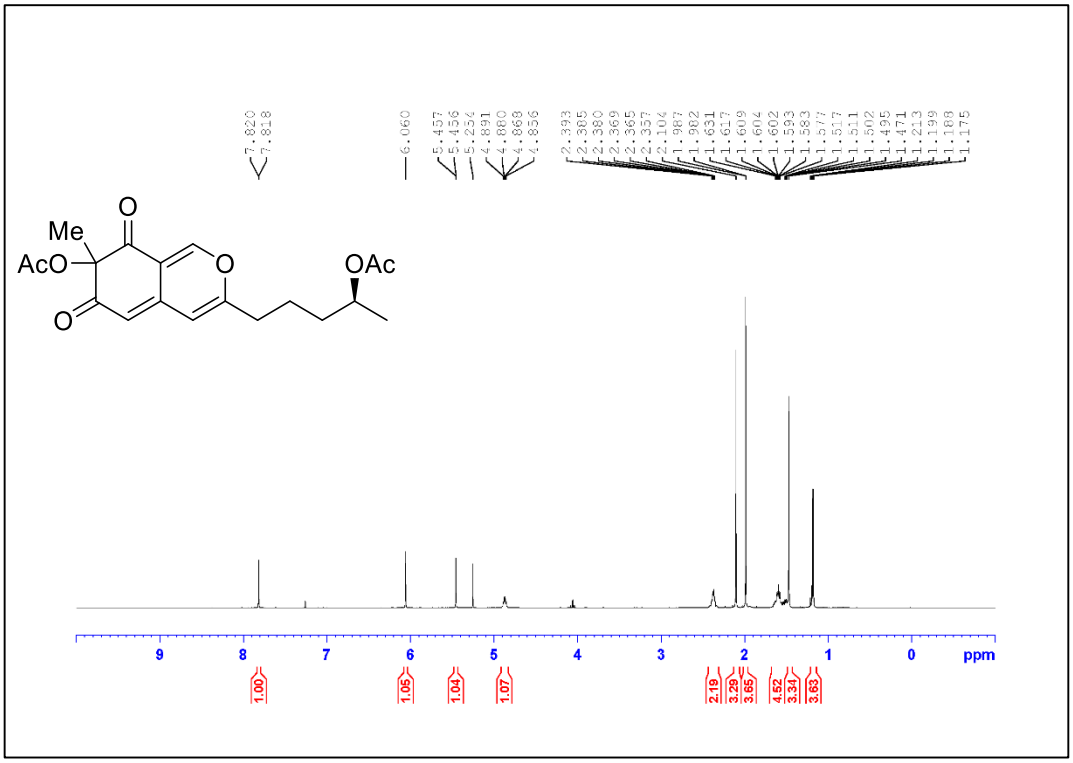

Figure A.171. ^{1}H NMR Spectrum of Compound **2.22** (500 MHz, $CDCl_3$)

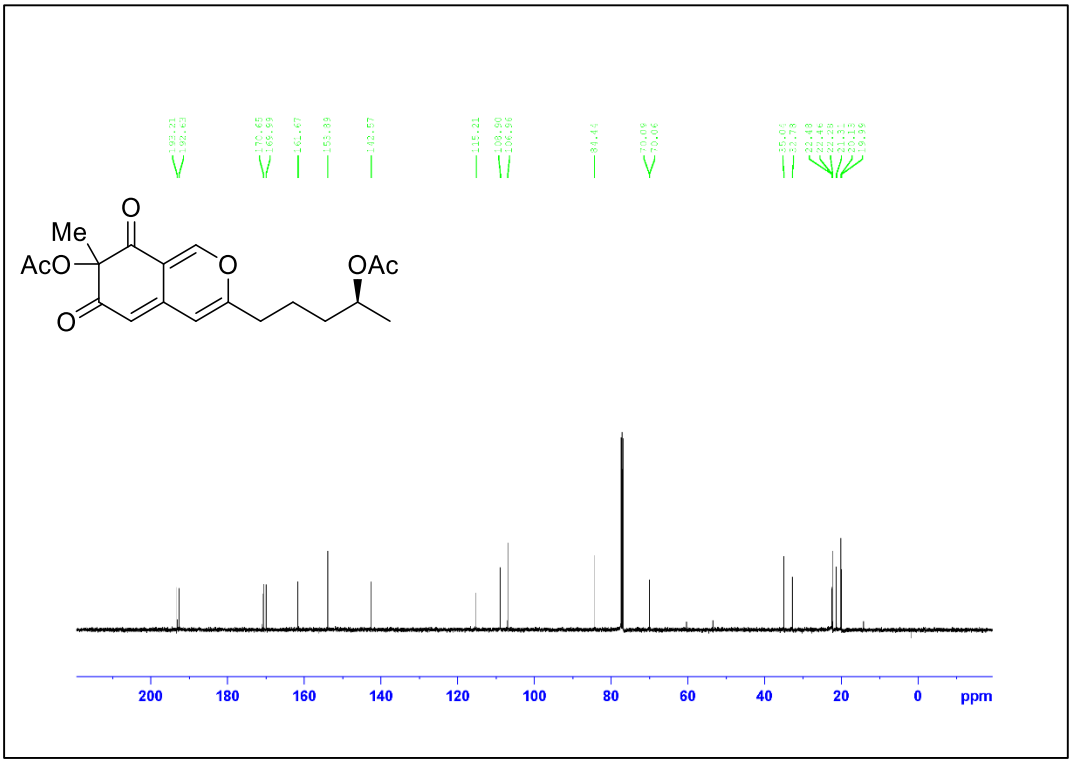

Figure A.172. ^{13}C NMR Spectrum of Compound **2.22** (125 MHz, $CDCl_3$)

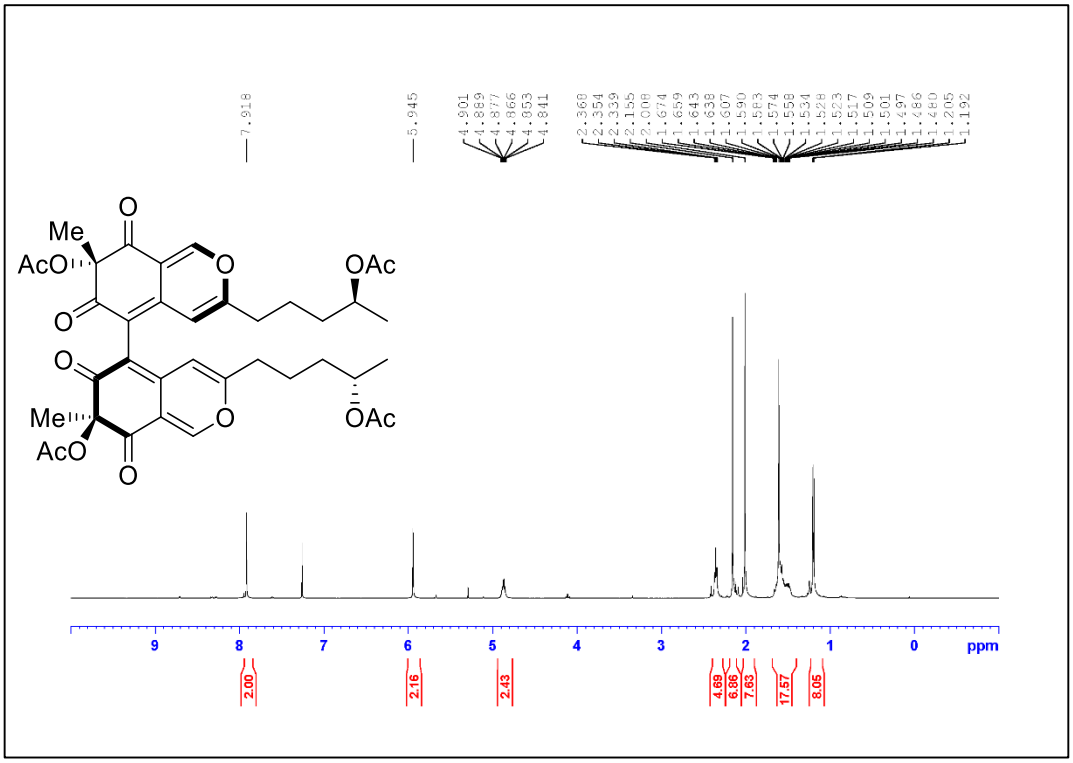

Figure A.173. ^{1}H NMR Spectrum of Compound **2.23** (500 MHz, $CDCl_3$)

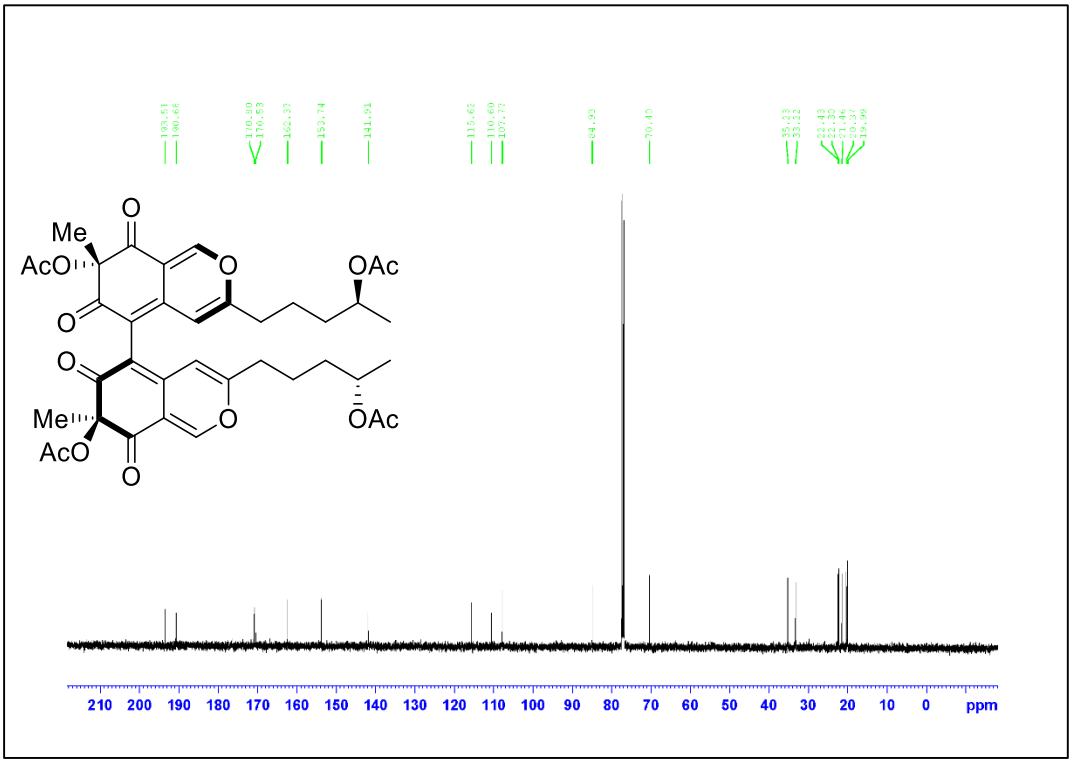

Figure A.174. ^{13}C NMR Spectrum of Compound **2.23** (125 MHz, $CDCl_3$)

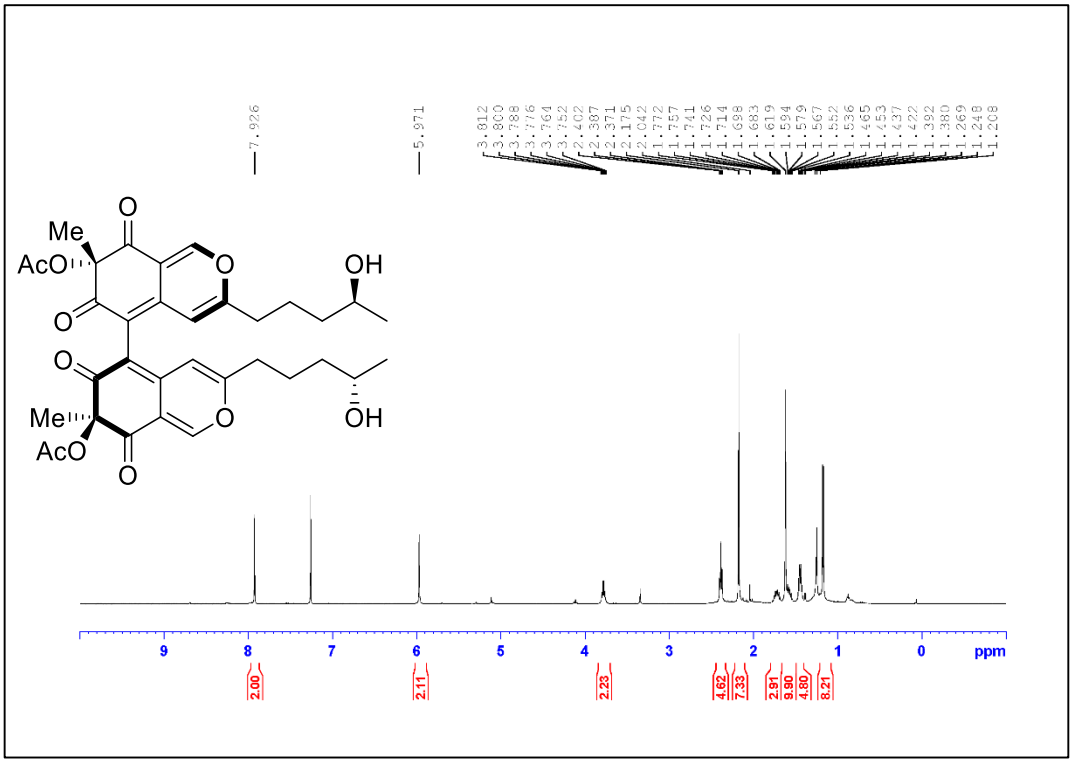

Figure A.175. ^{1}H NMR Spectrum of Compound **2.24** (500 MHz, $CDCl_3$)

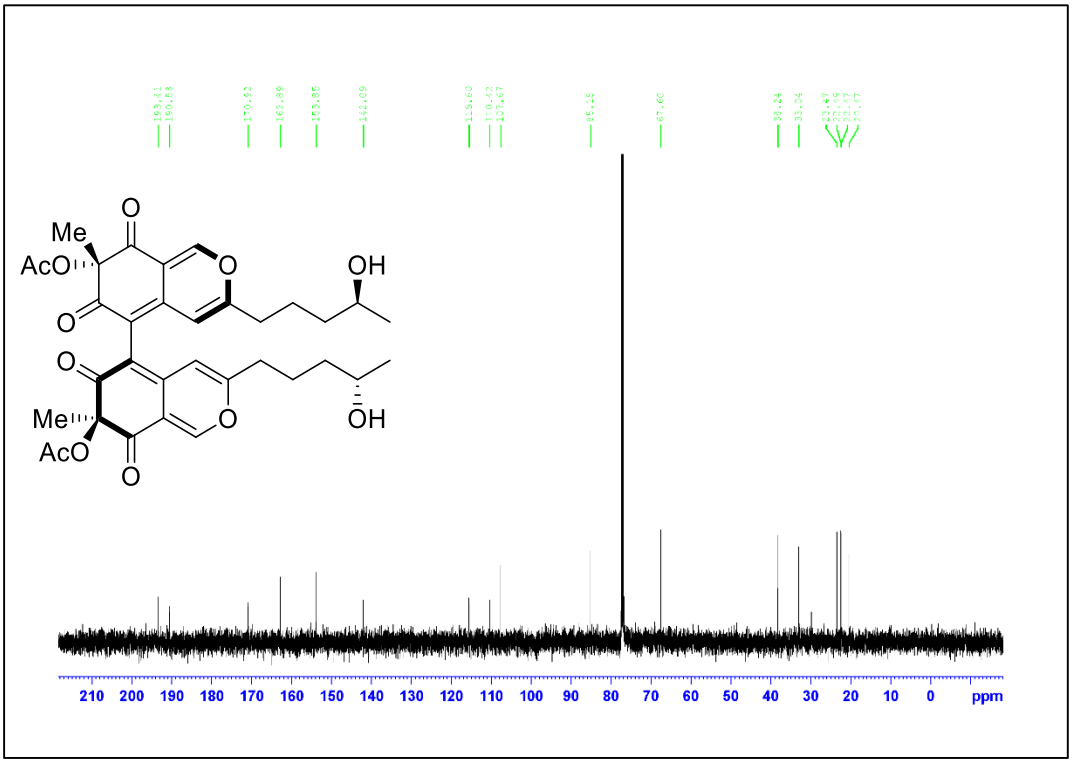

Figure A.176. ^{13}C NMR Spectrum of Compound **2.24** (125 MHz, $CDCl_3$)

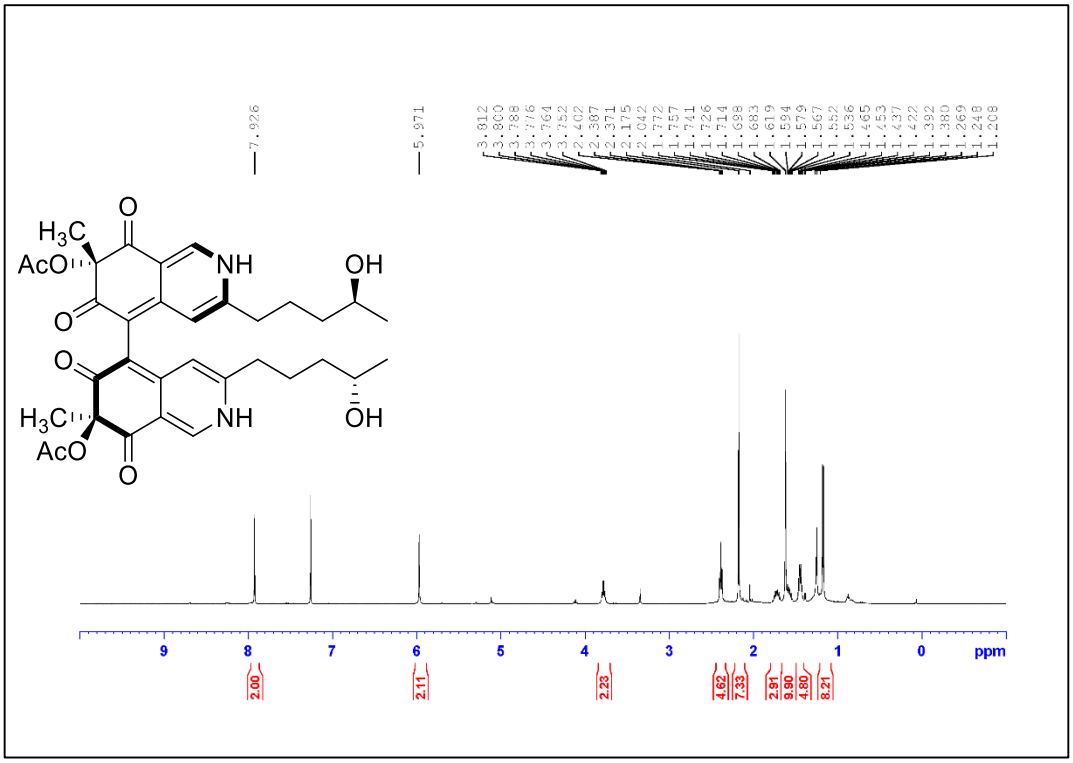

Figure A.177. ^{1}H NMR Spectrum of Compound **2.1** (500 MHz, CD_3OD)

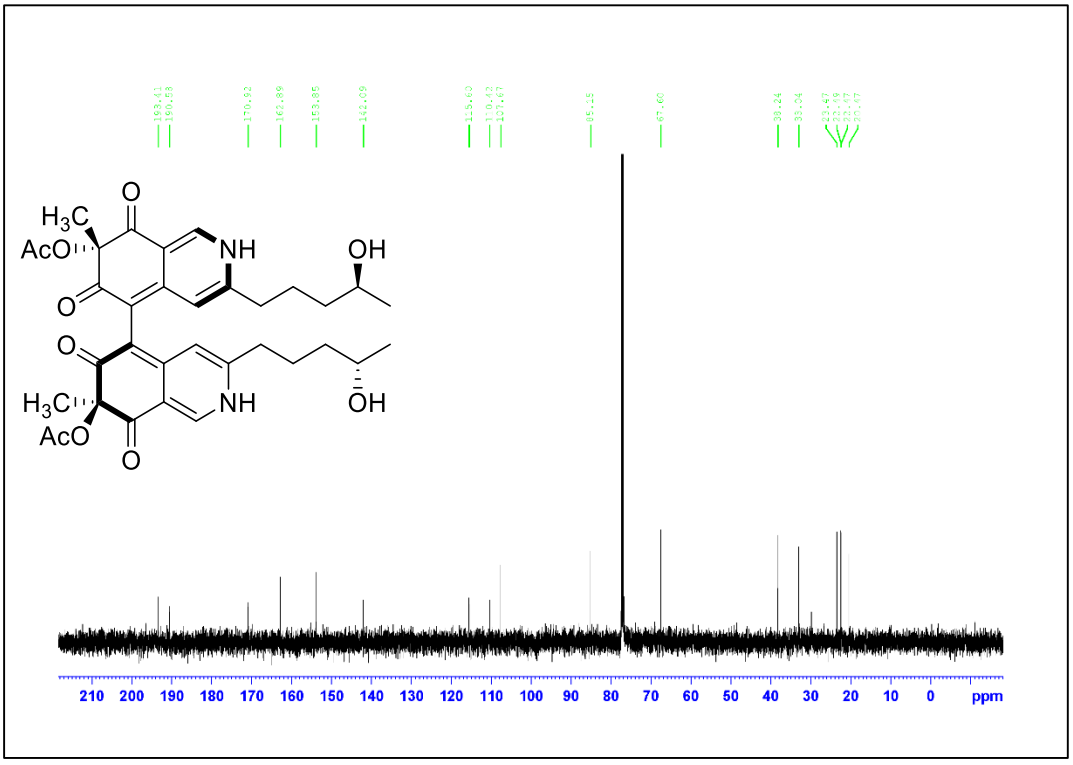

Figure A.178. ^{13}C NMR Spectrum of Compound **2.1** (125 MHz, CD_3OD)

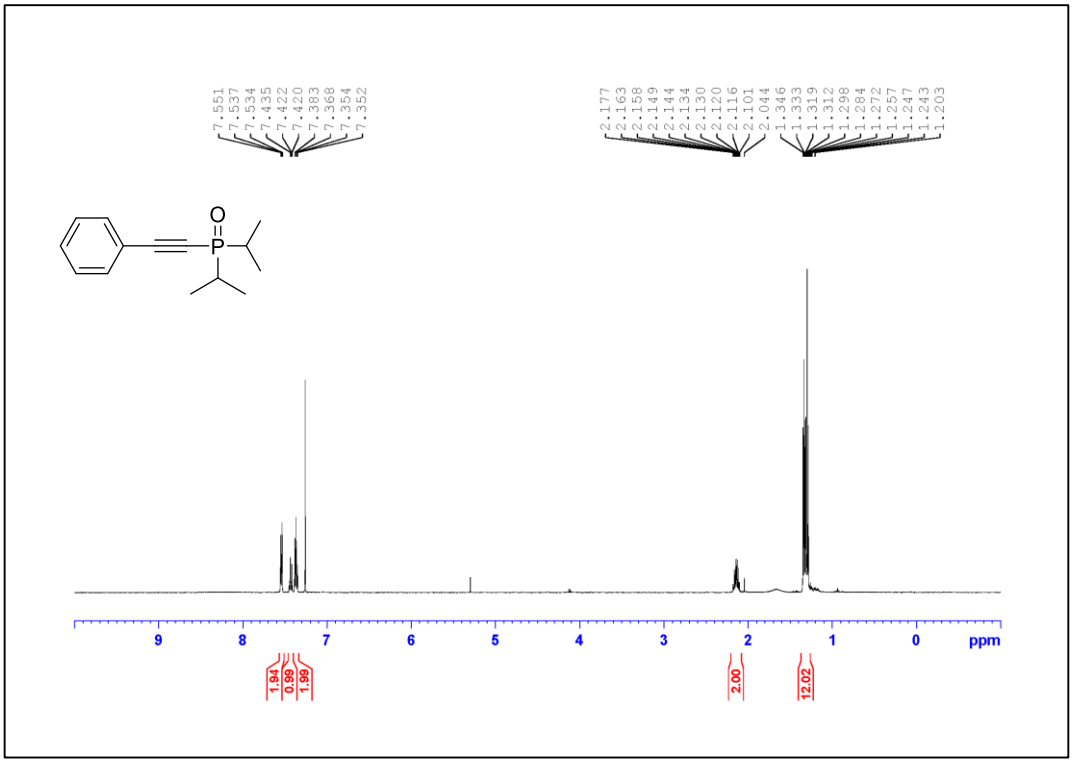

Figure A.179. ^{1}H NMR Spectrum of Compound **3.3a** (500 MHz, $CDCl_3$)

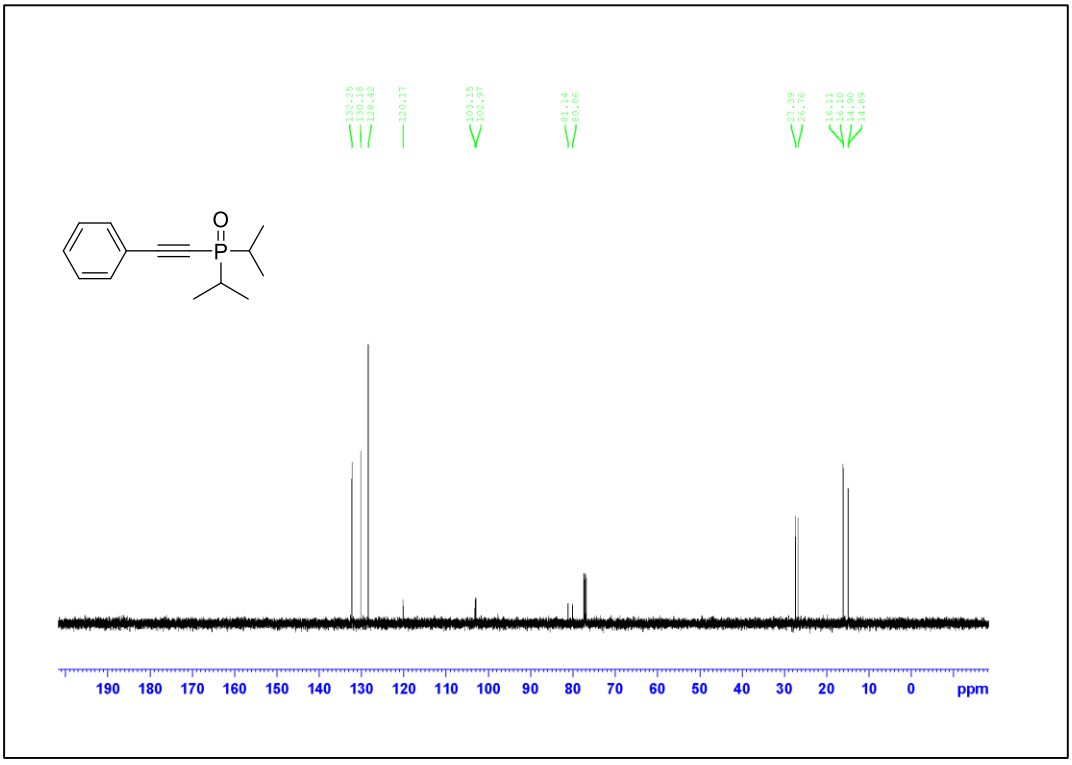

Figure A.180. ^{13}C NMR Spectrum of Compound **3.3a** (125 MHz, $CDCl_3$)

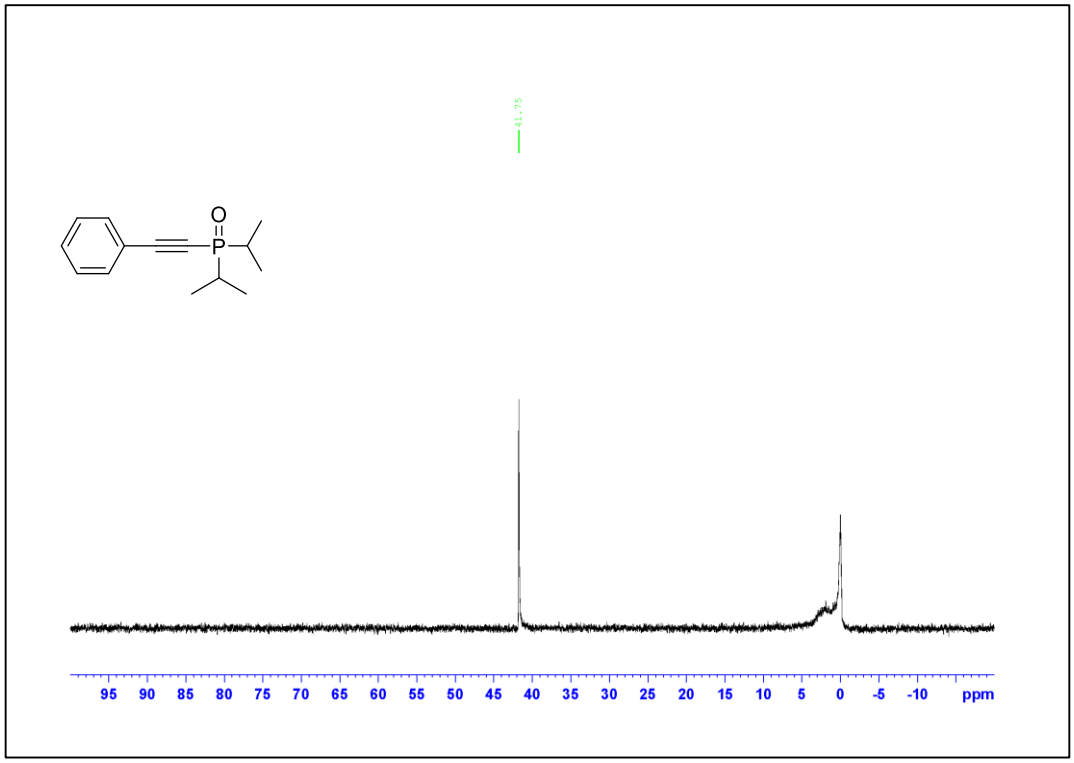

Figure A.181. ^{31}P NMR Spectrum of Compound **3.3a**

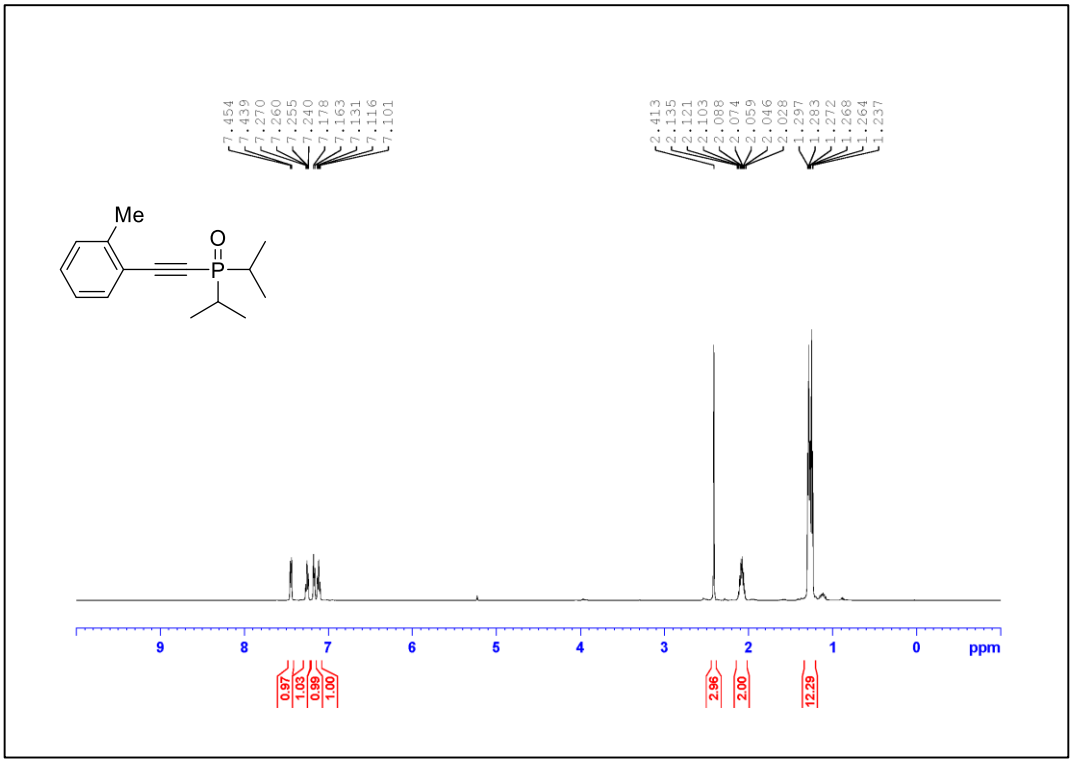

Figure A.182. ^{1}H NMR Spectrum of Compound **3.3b** (500 MHz, $CDCl_3$)

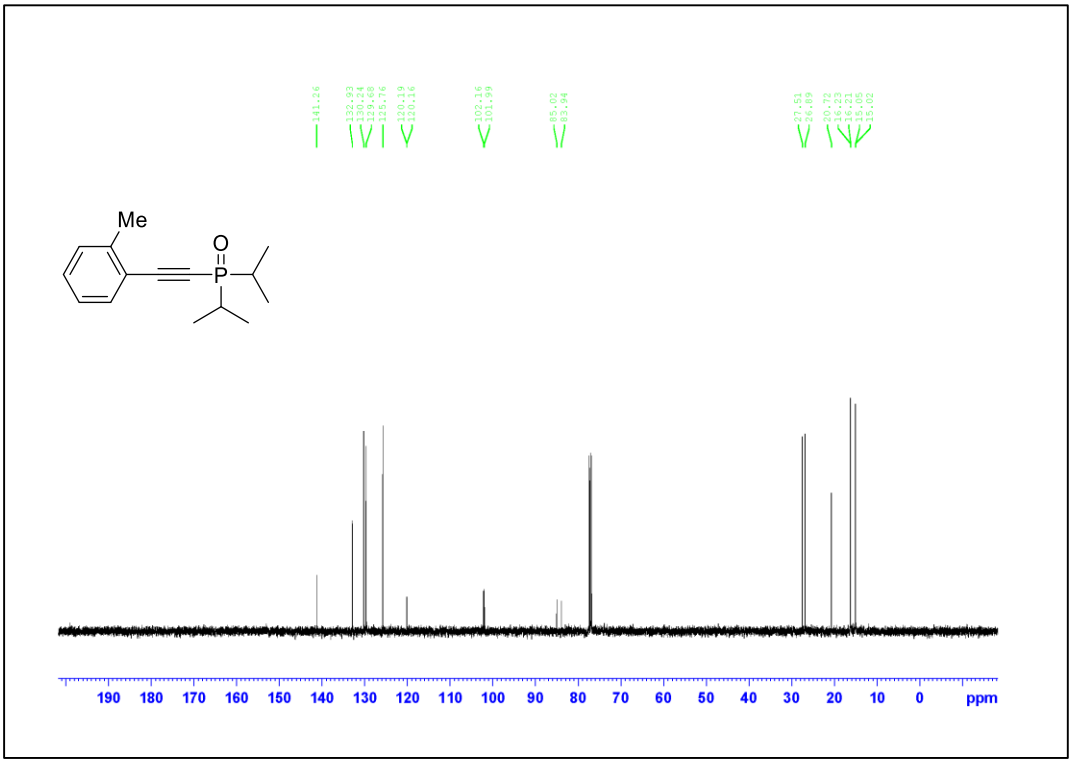

Figure A.183. ^{13}C NMR Spectrum of Compound **3.3b** (125 MHz, $CDCl_3$)

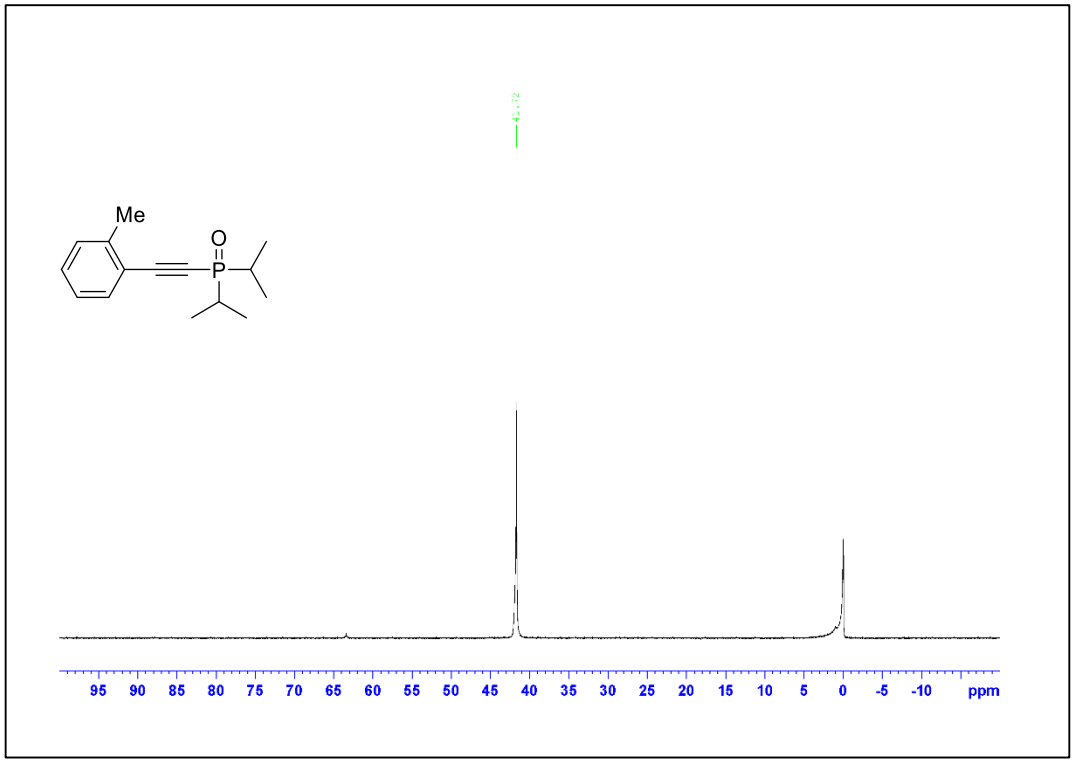

Figure A.184. ^{31}P NMR Spectrum of Compound **3.3b**

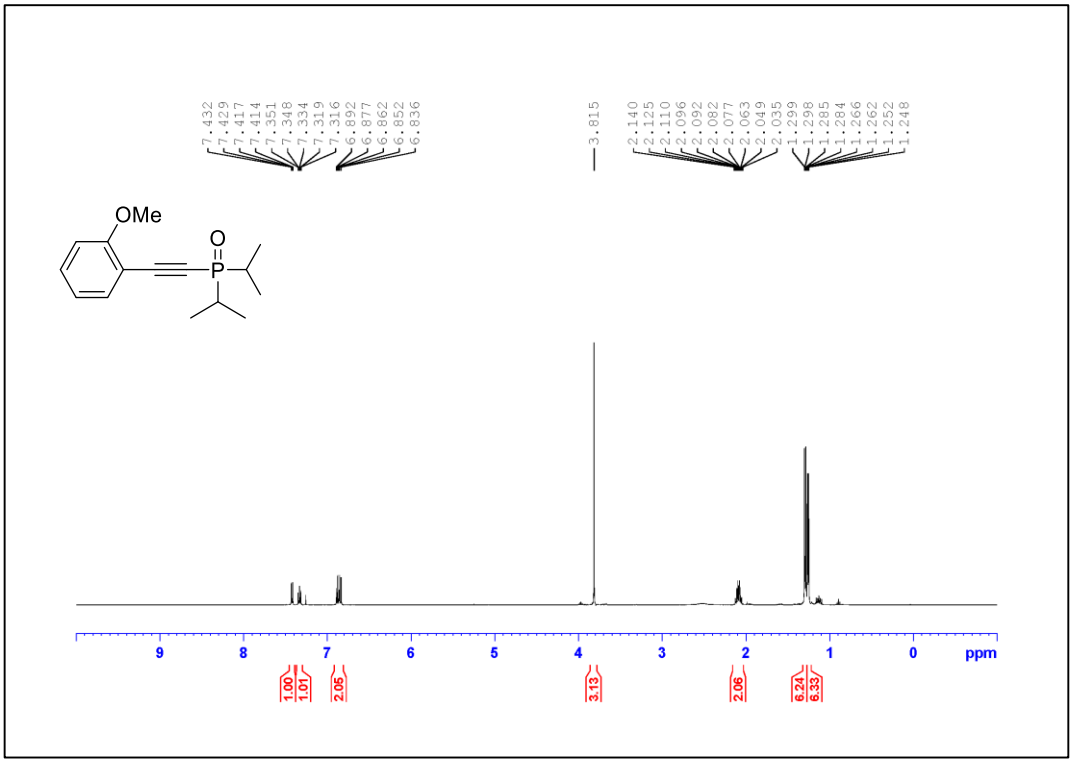

Figure A.185. ^{1}H NMR Spectrum of Compound **3.3c** (500 MHz, $CDCl_3$)

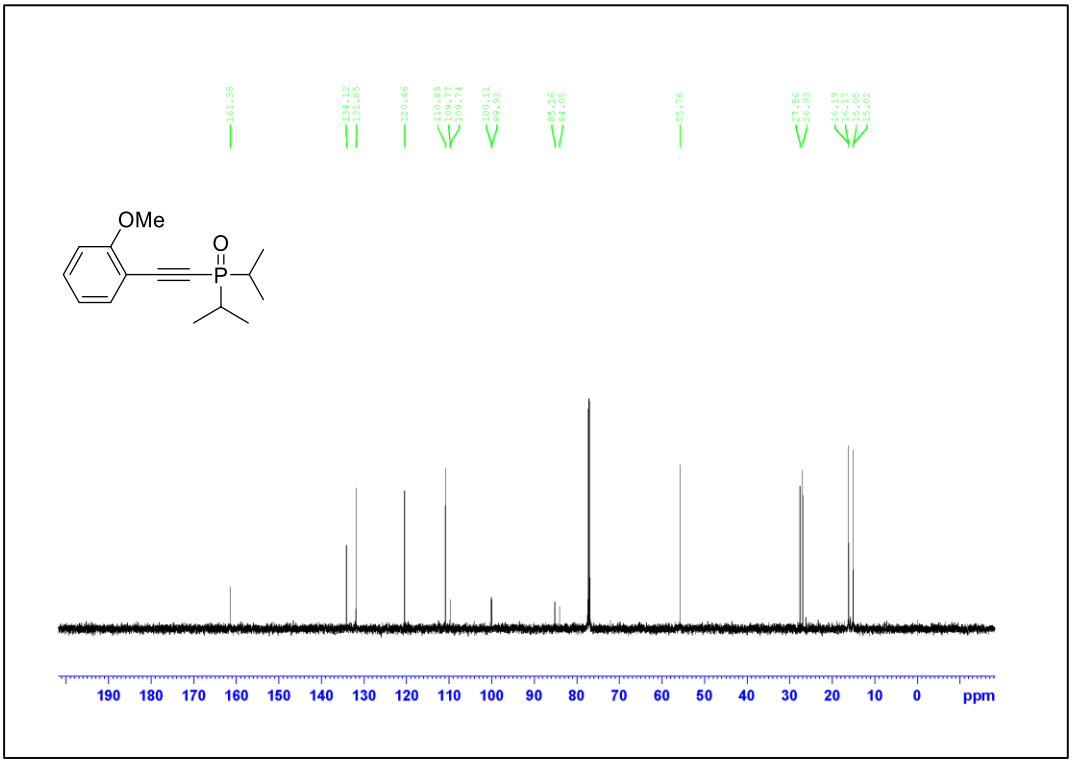

Figure A.186. ^{13}C NMR Spectrum of Compound **3.3c** (125 MHz, $CDCl_3$)

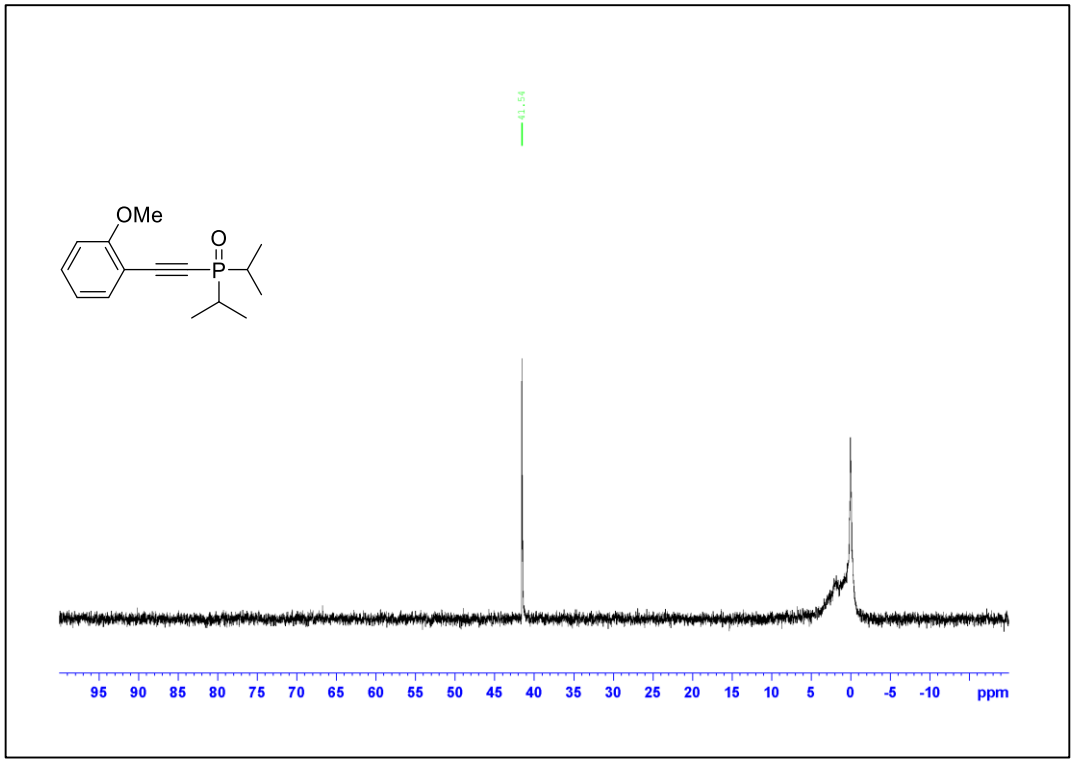

Figure A.187. ^{31}P NMR Spectrum of Compound **3.3c**

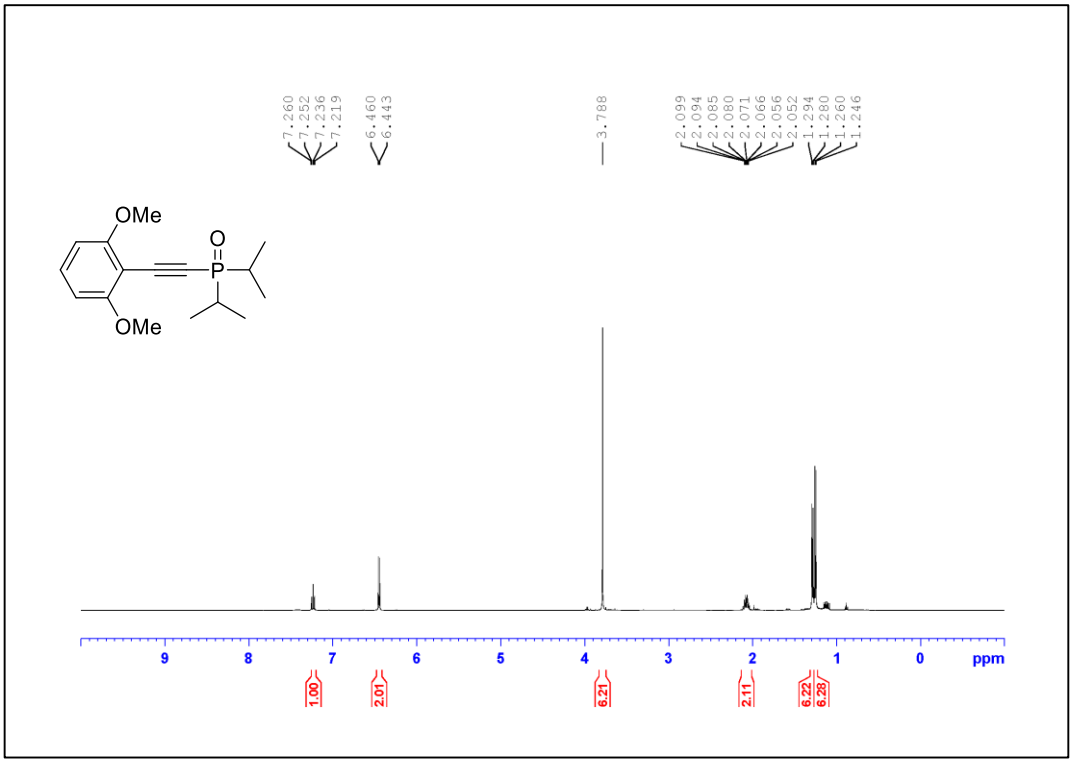

Figure A.188. ^{1}H NMR Spectrum of Compound **3.3d** (500 MHz, $CDCl_3$)

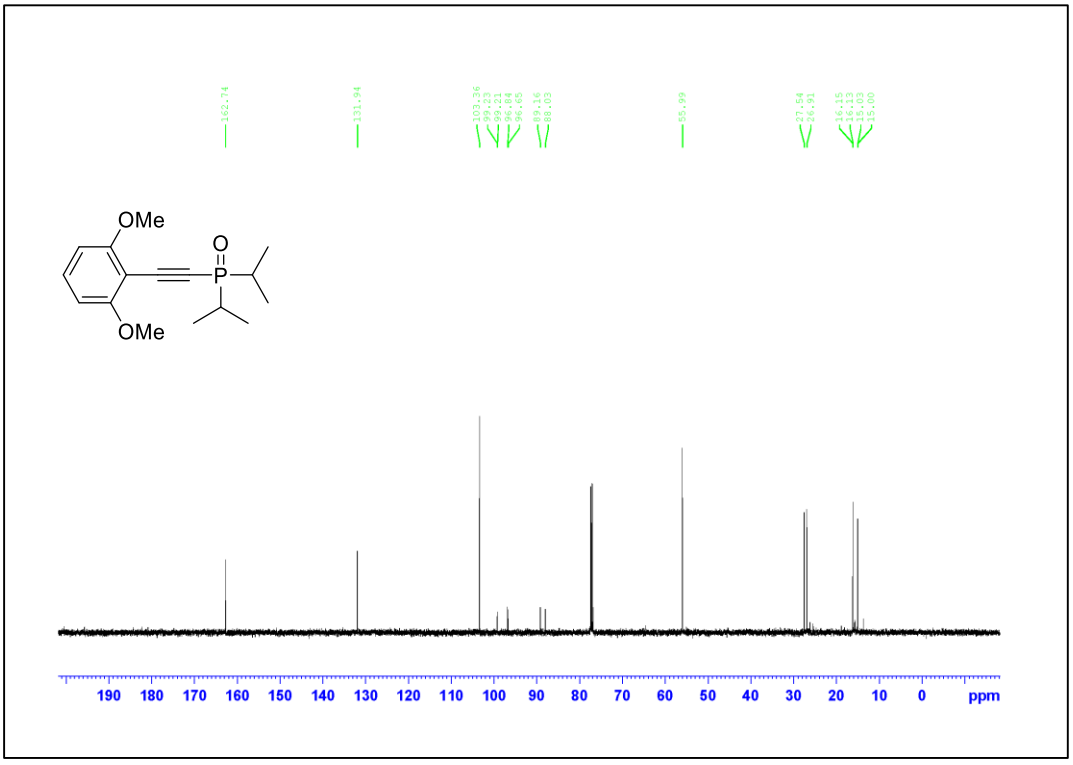

Figure A.189. ^{13}C NMR Spectrum of Compound **3.3d** (125 MHz, $CDCl_3$)

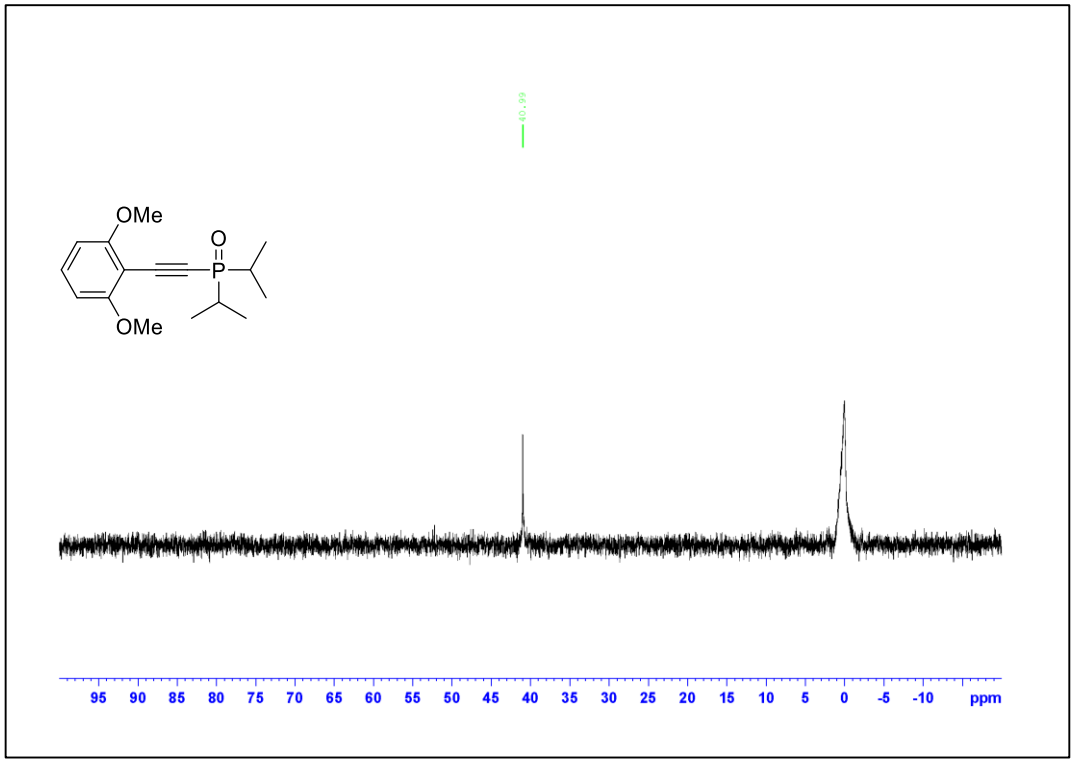

Figure A.190. ^{31}P NMR Spectrum of Compound **3.3d**

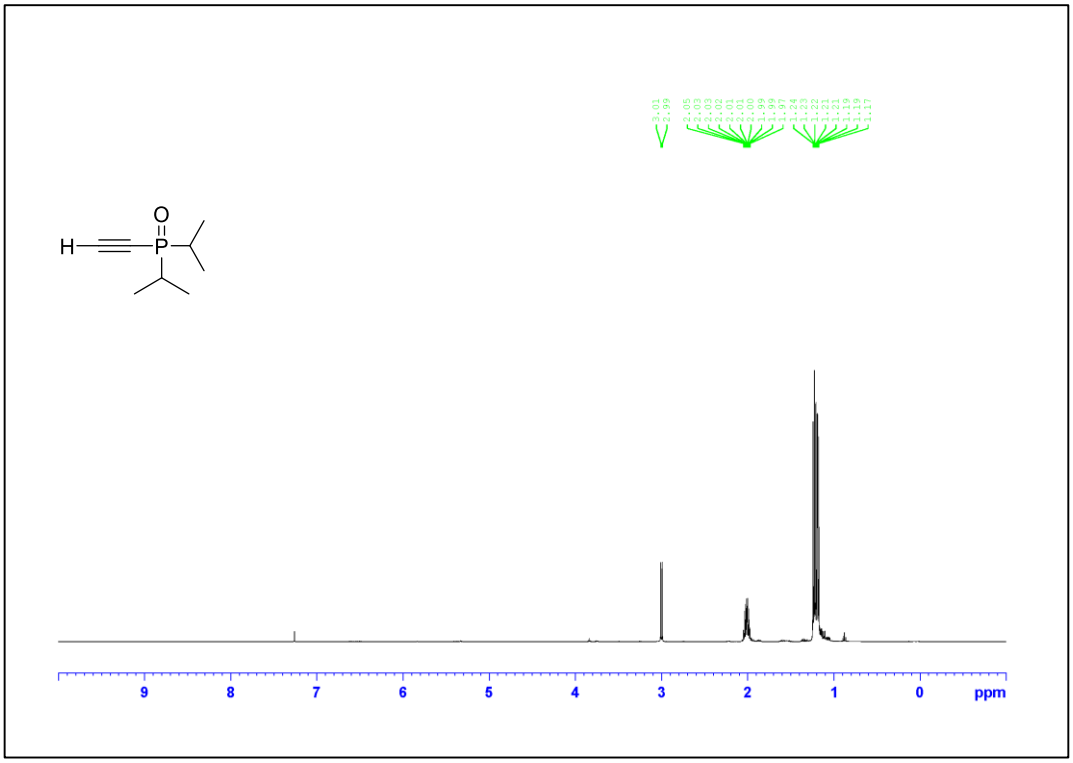

Figure A.191. ^{1}H NMR Spectrum of Compound **3.3e** (500 MHz, $CDCl_3$)

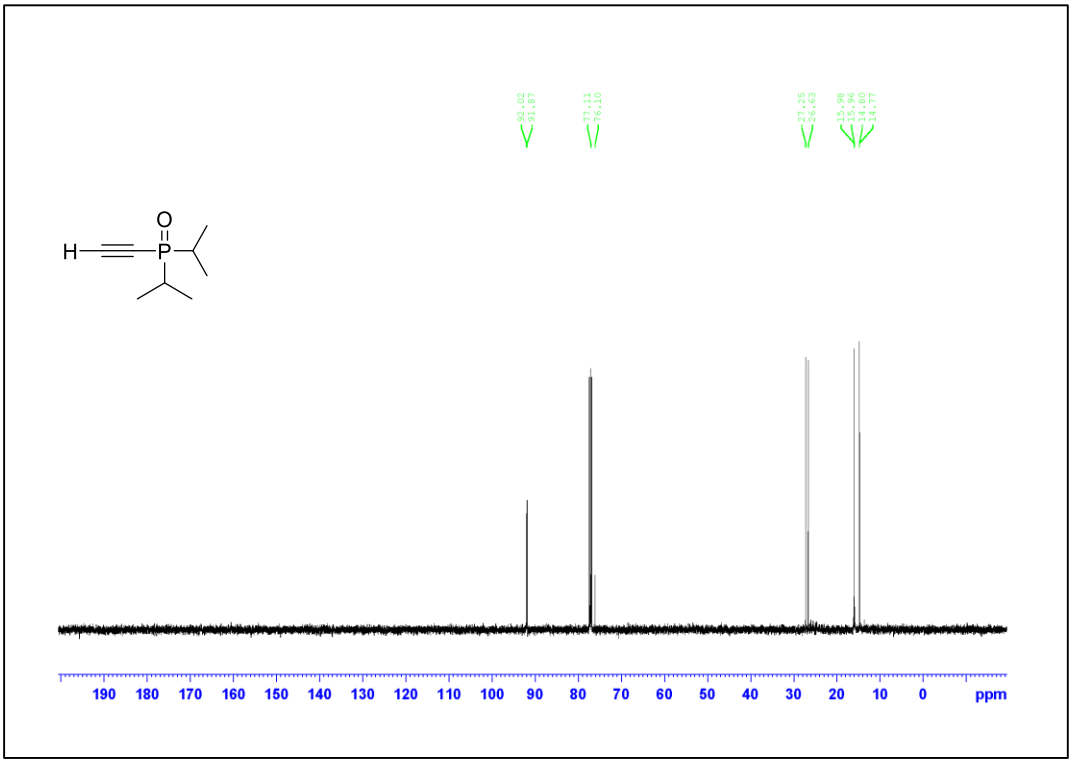

Figure A.192. ^{13}C NMR Spectrum of Compound **3.3e** (125 MHz, $CDCl_3$)

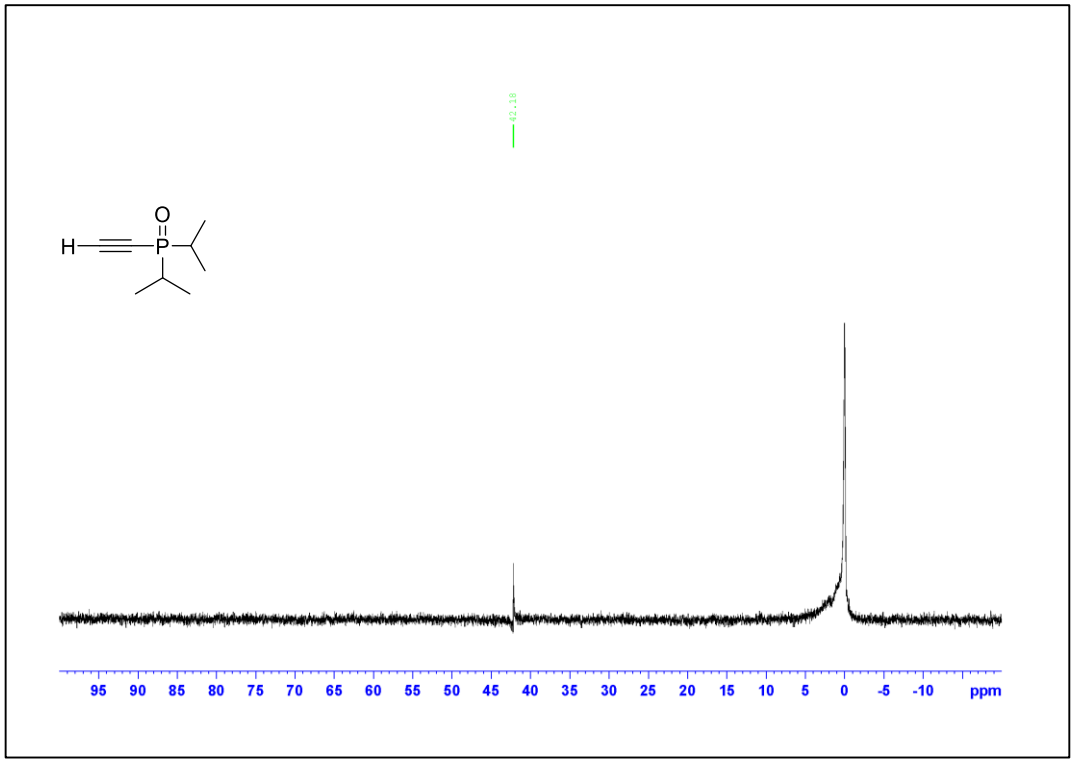

Figure A.193. ^{31}P NMR Spectrum of Compound **3.3e**

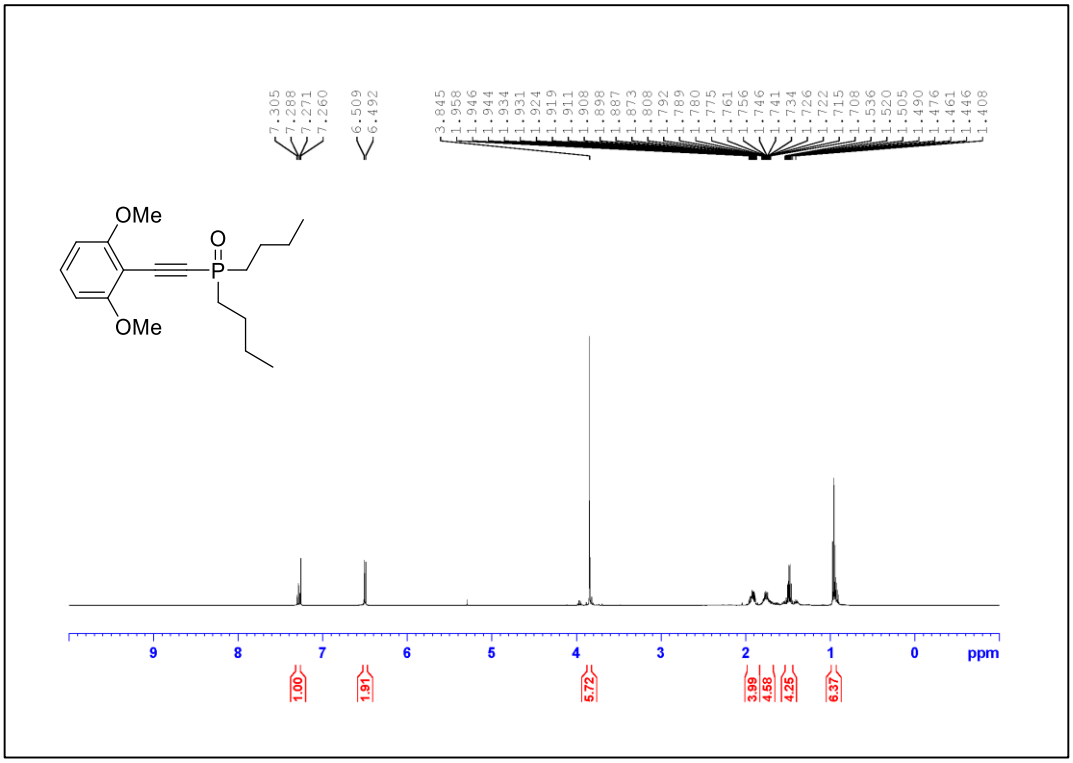

Figure A.194. ^{1}H NMR Spectrum of Compound **3.3d_*n*Bu** (500 MHz, $CDCl_3$)

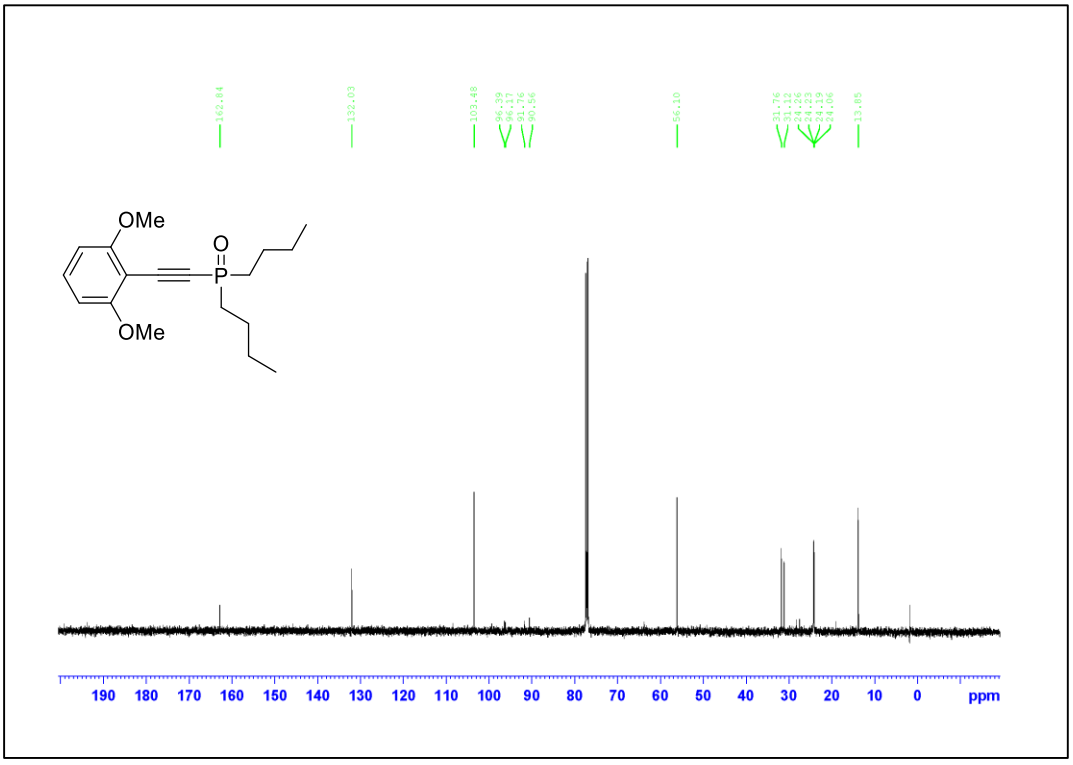

Figure A.195. ^{13}C NMR Spectrum of Compound **3.3d_*n*Bu** (125 MHz, $CDCl_3$)

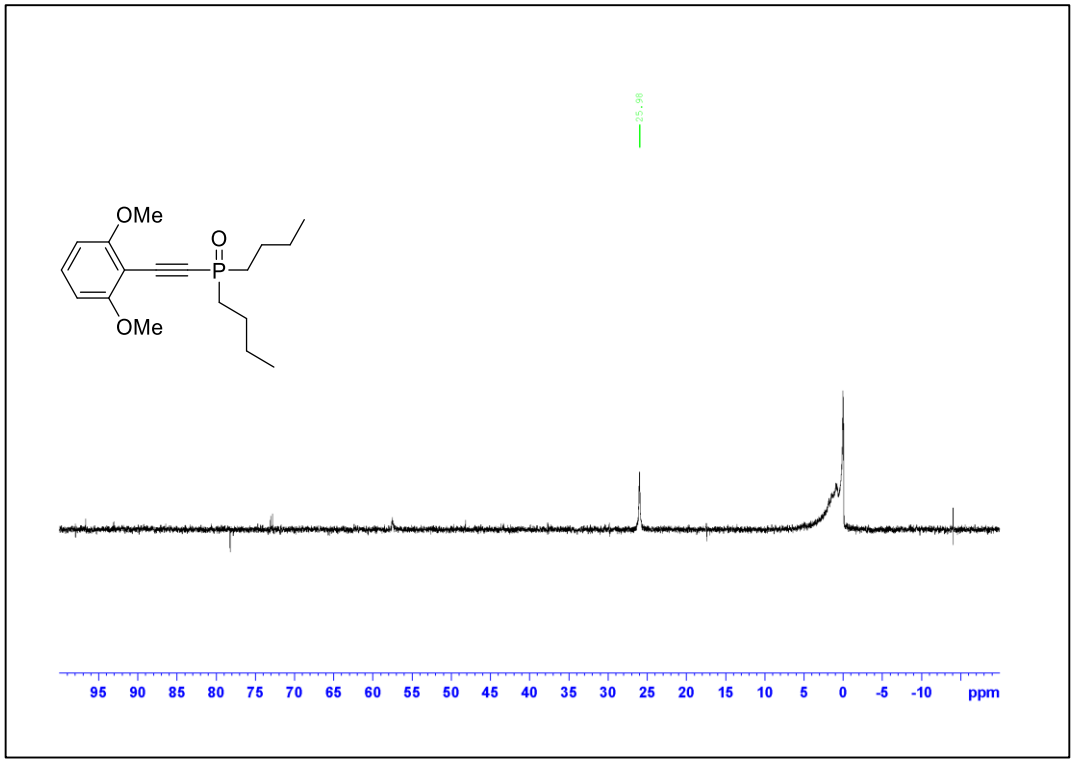

Figure A.196. ^{31}P NMR Spectrum of Compound **3.3d_*n*Bu**

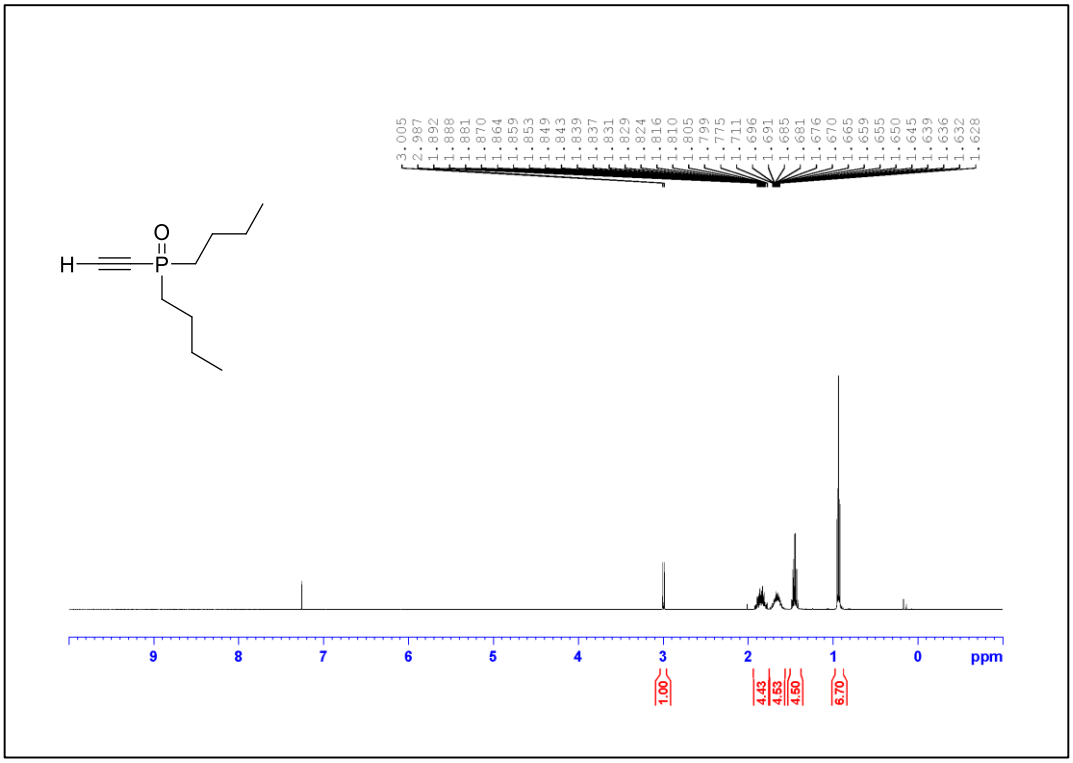

Figure A.197. ^{1}H NMR Spectrum of Compound **3.3e_*n*Bu** (500 MHz, $CDCl_3$)

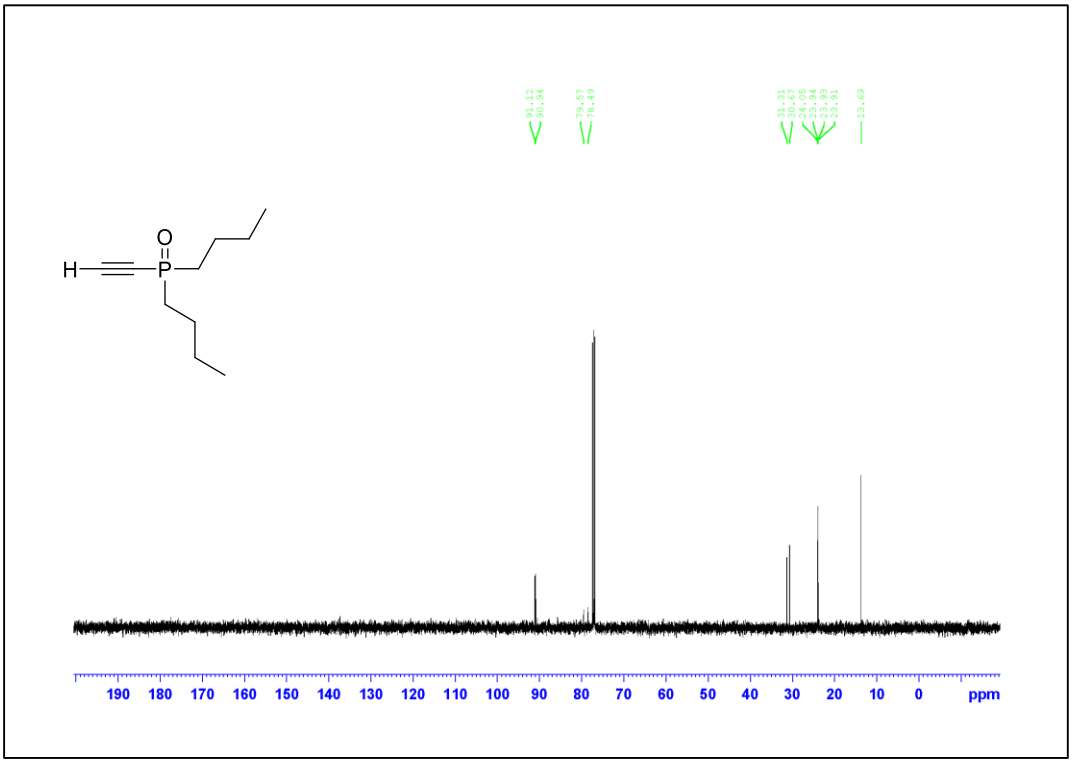

Figure A.198. ^{13}C NMR Spectrum of Compound **3.3e_*n*Bu** (125 MHz, $CDCl_3$)

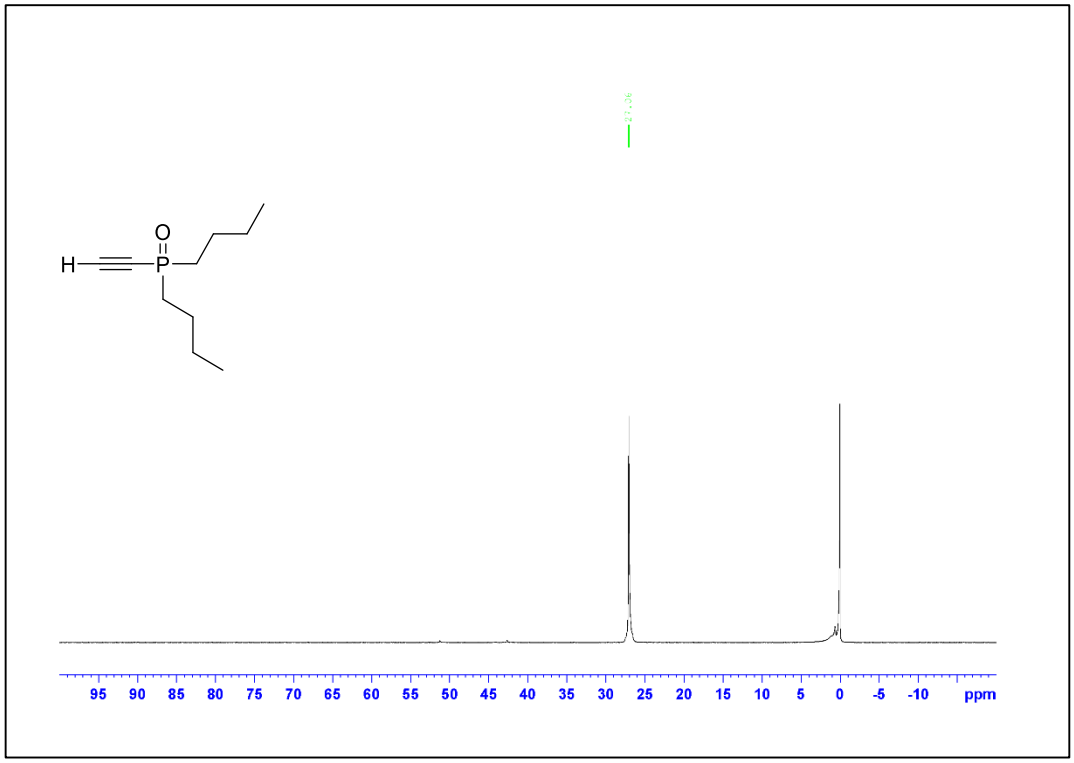

Figure A.199. ^{31}P NMR Spectrum of Compound **3.3e_*n*Bu**

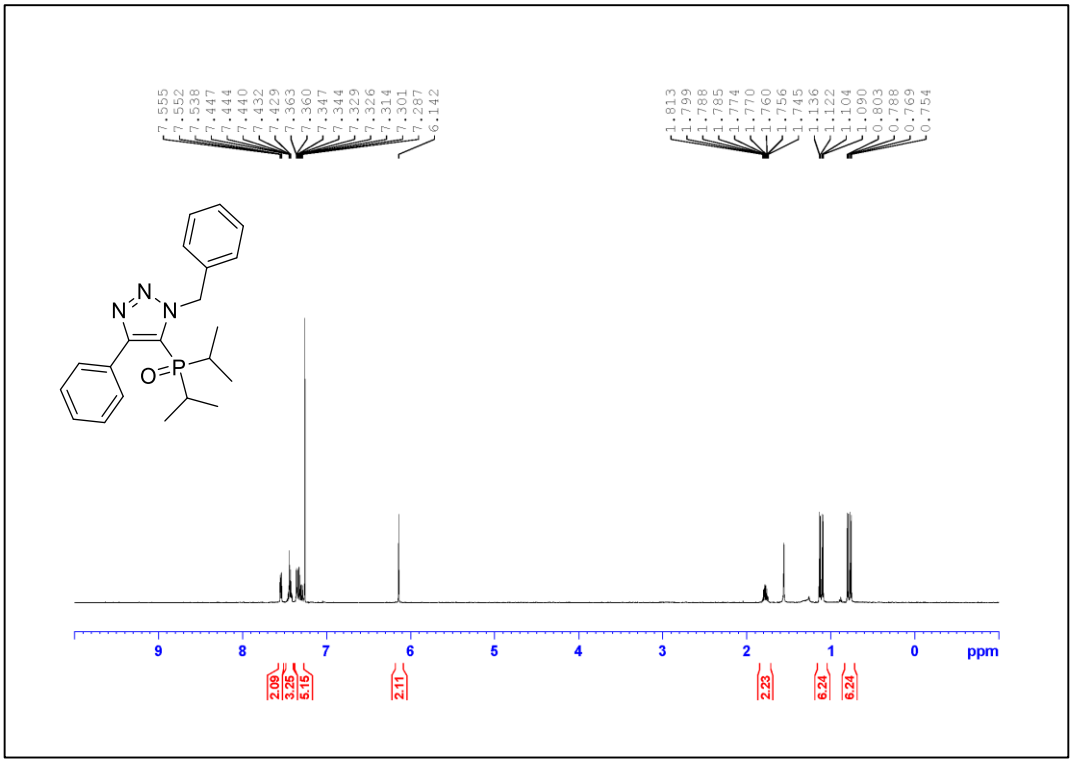

Figure A.200. ^{1}H NMR Spectrum of Compound **3.5a** (500 MHz, $CDCl_3$)

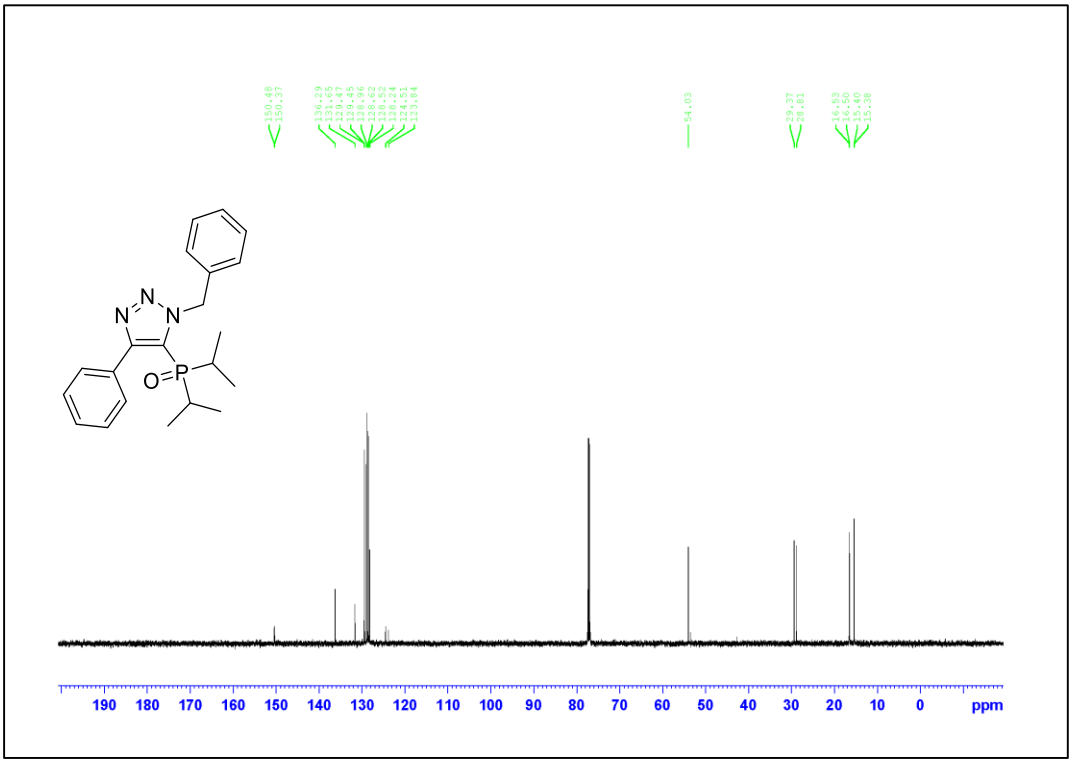

Figure A.201. ^{13}C NMR Spectrum of Compound **3.5a** (125 MHz, $CDCl_3$)

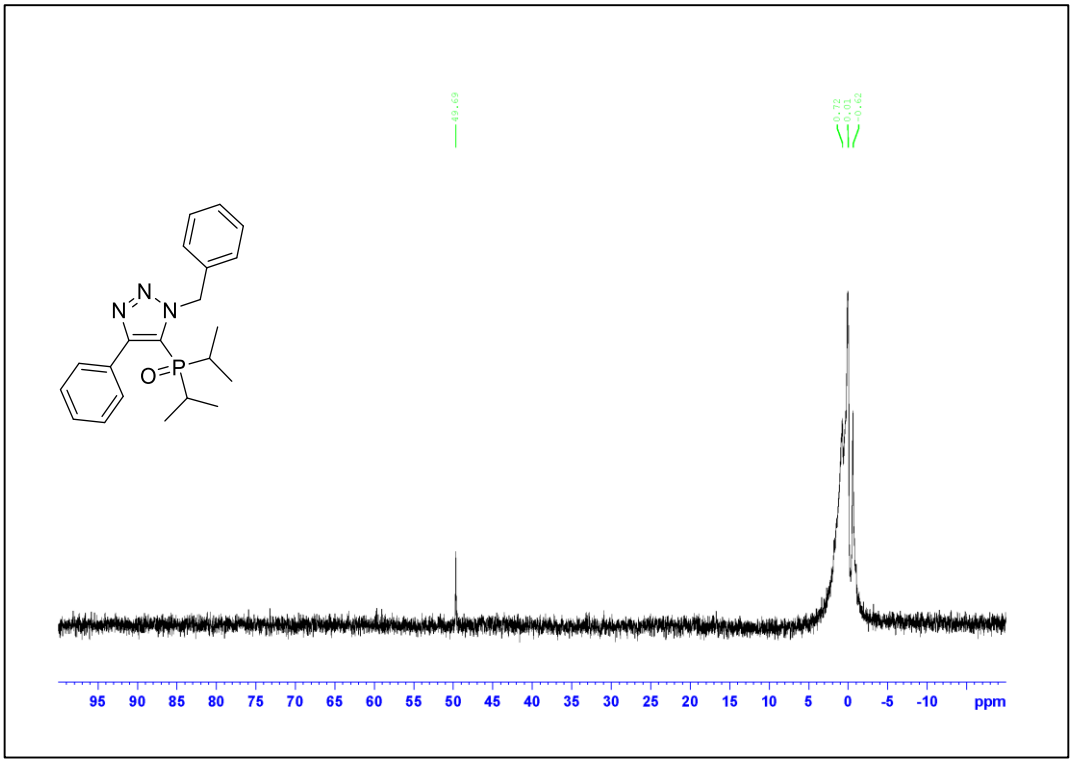

Figure A.202. ^{31}P NMR Spectrum of Compound **3.5a**

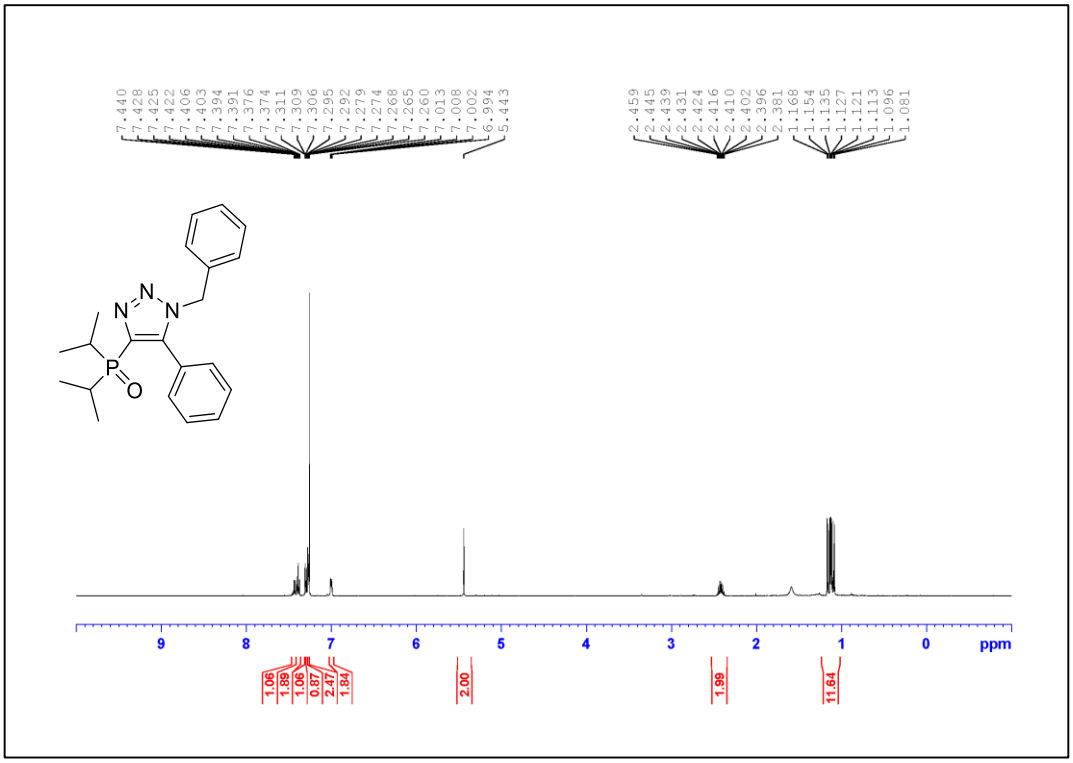

Figure A.203. ^{1}H NMR Spectrum of Compound **3.6a** (500 MHz, $CDCl_3$)

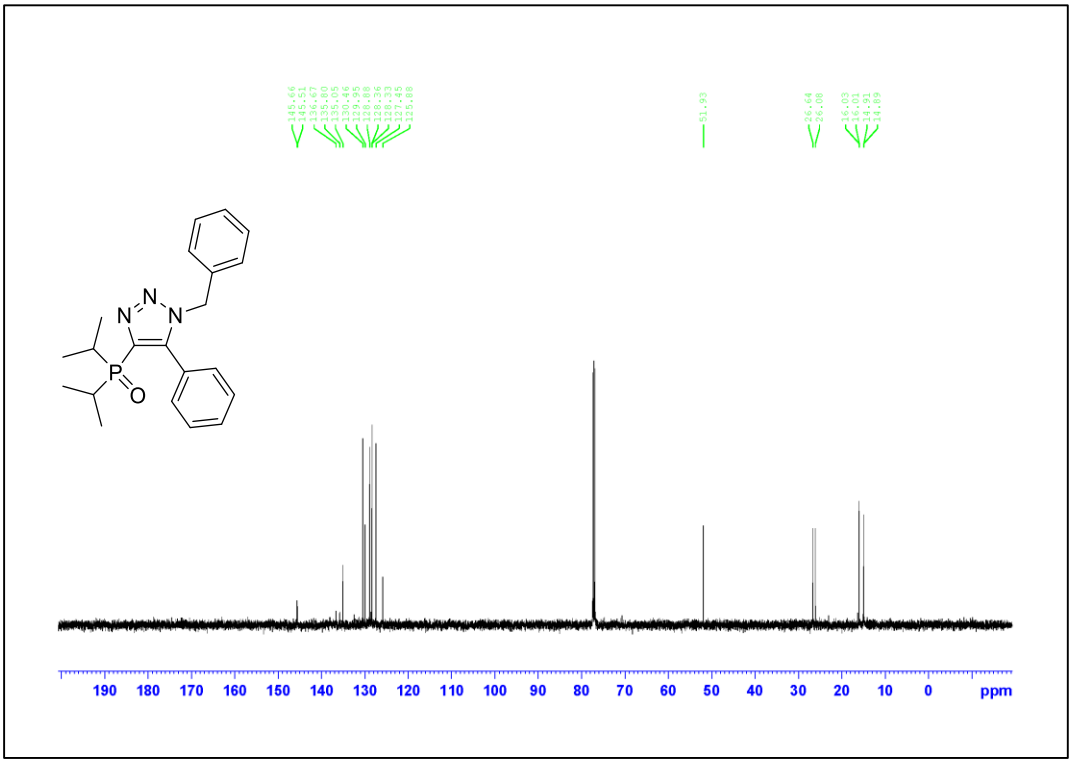

Figure A.204. ^{13}C NMR Spectrum of Compound **3.6a** (125 MHz, $CDCl_3$)

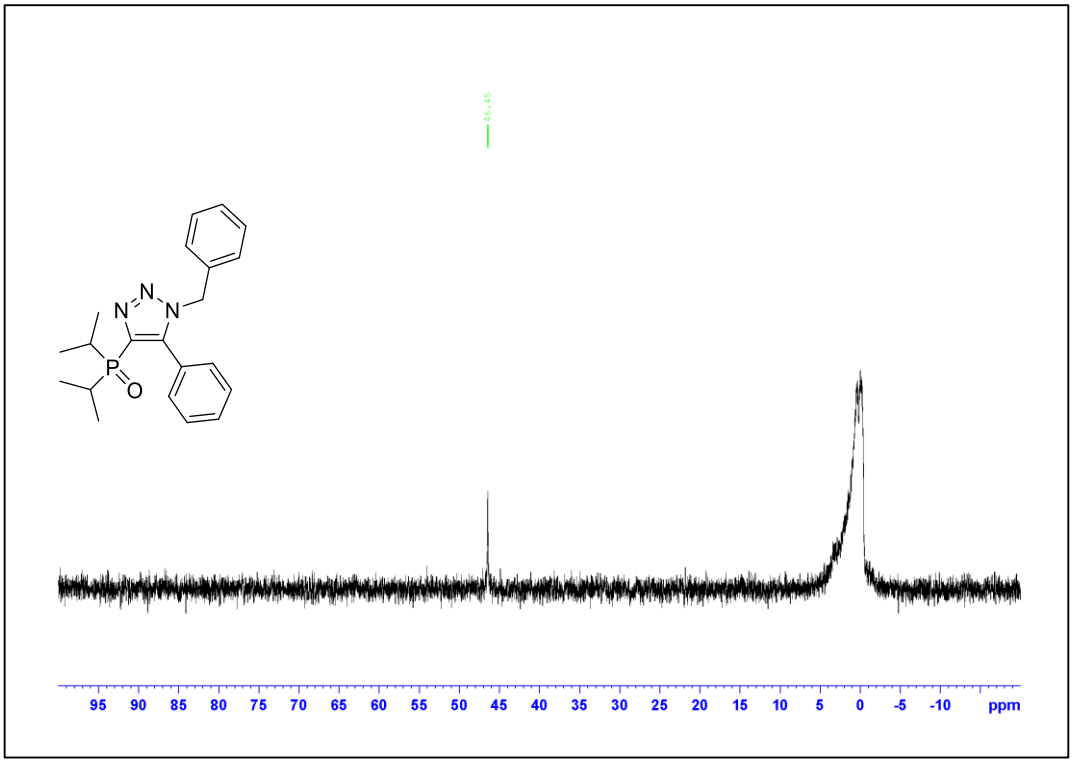

Figure A.205. ^{31}P NMR Spectrum of Compound **3.6a**

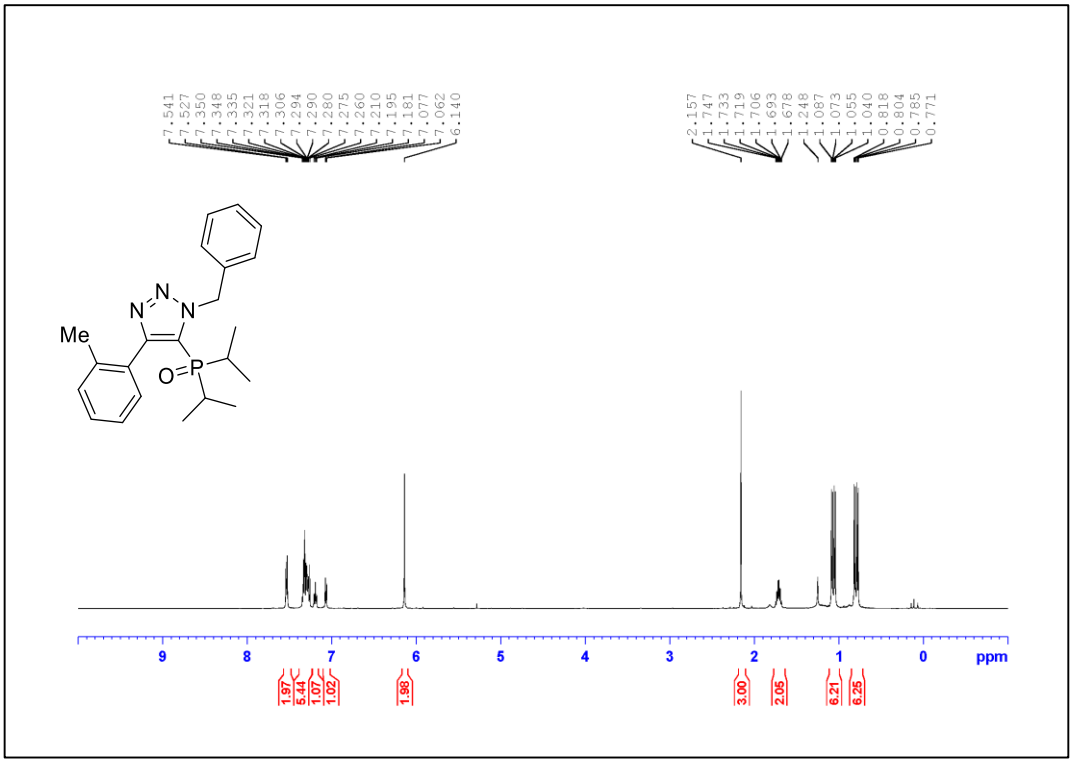

Figure A.206. ^{1}H NMR Spectrum of Compound **3.5b** (500 MHz, $CDCl_3$)

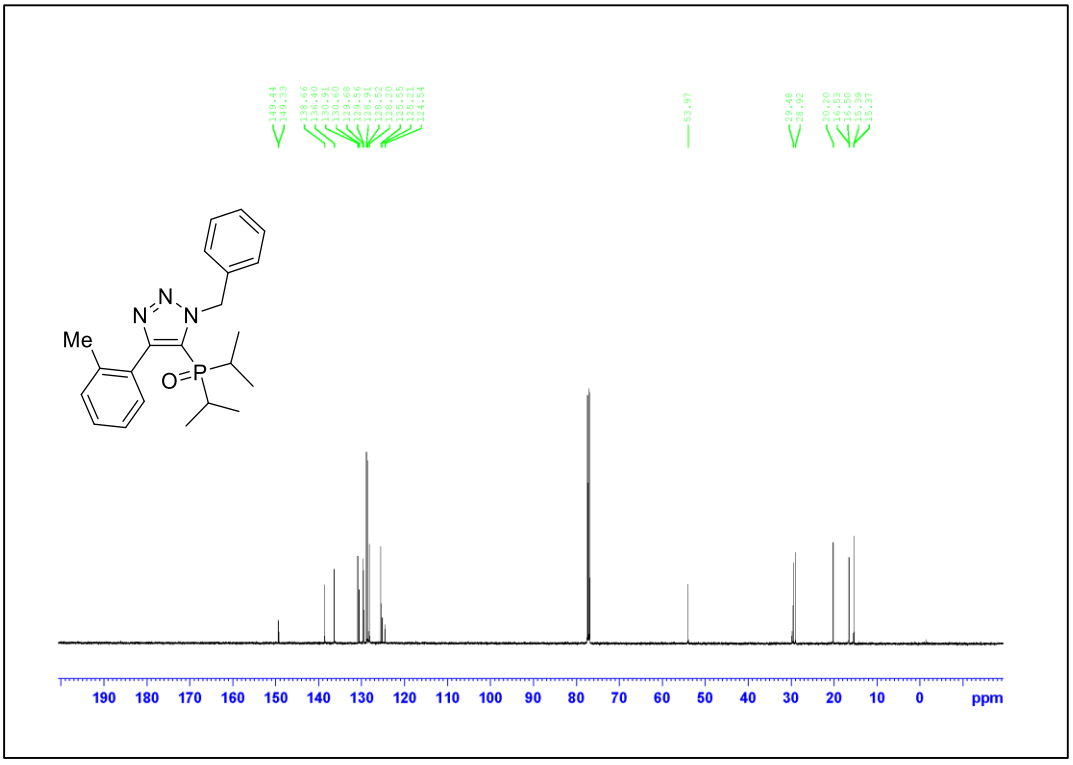

Figure A.207. ^{13}C NMR Spectrum of Compound **3.5b** (125 MHz, $CDCl_3$)

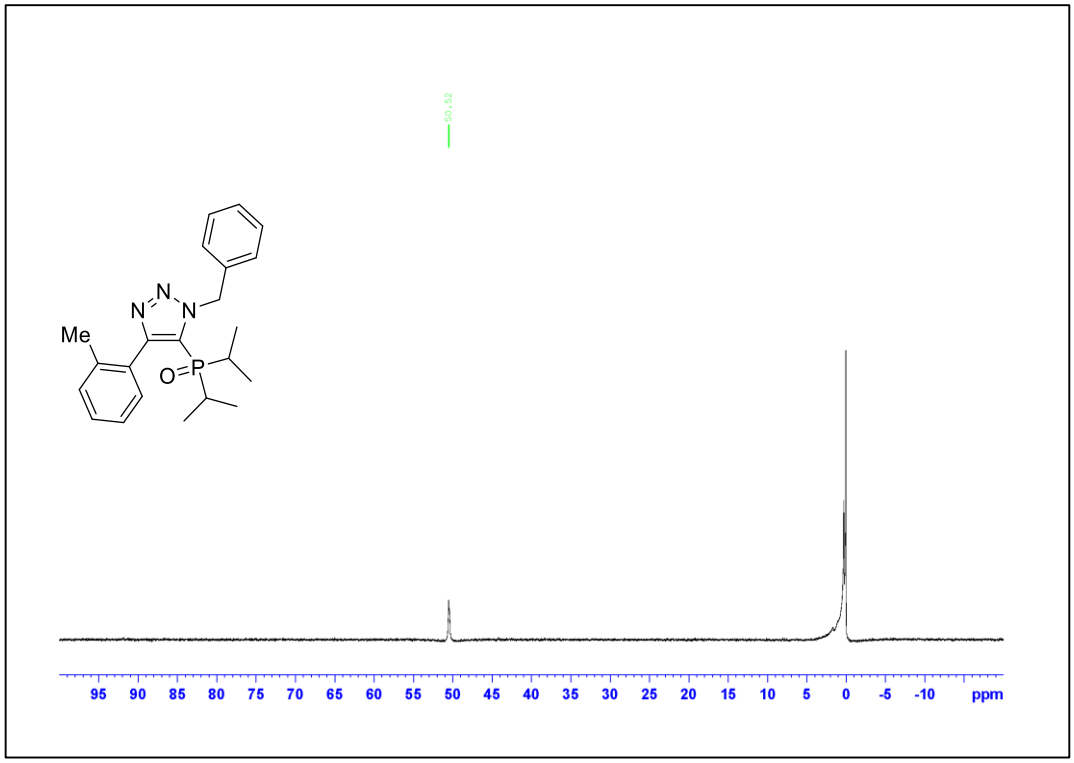

Figure A.208. ^{31}P NMR Spectrum of Compound **3.5b**

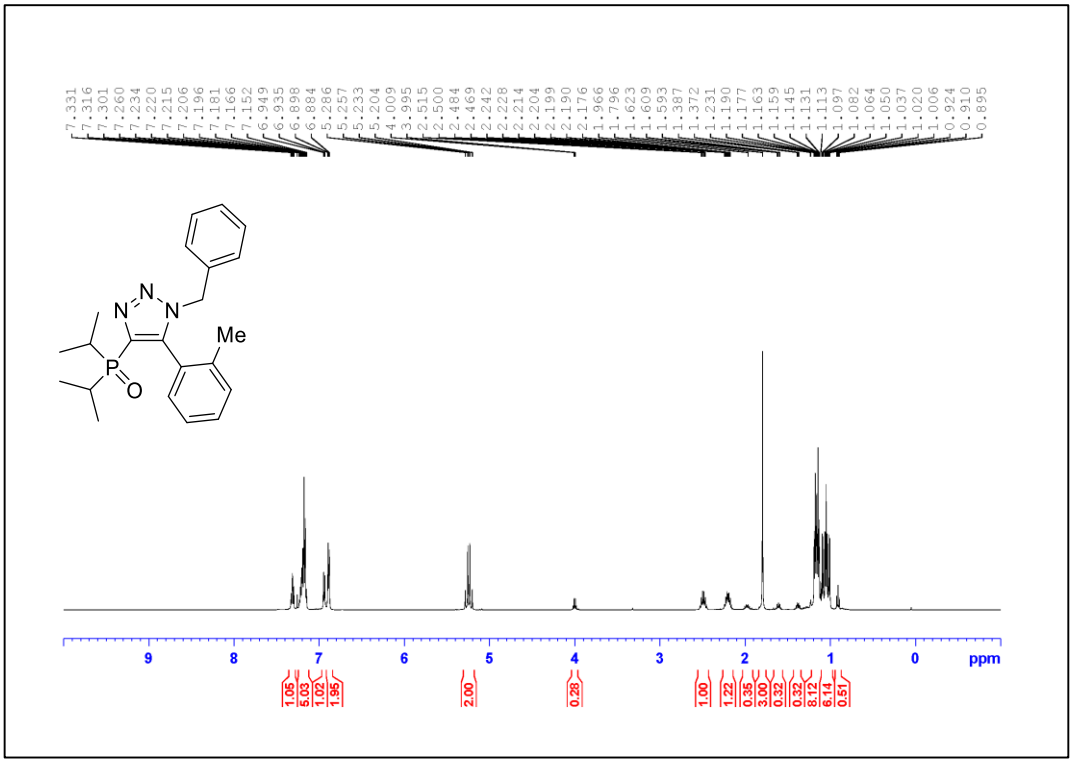

Figure A.209. ^{1}H NMR Spectrum of Compound **3.6b** (500 MHz, $CDCl_3$)

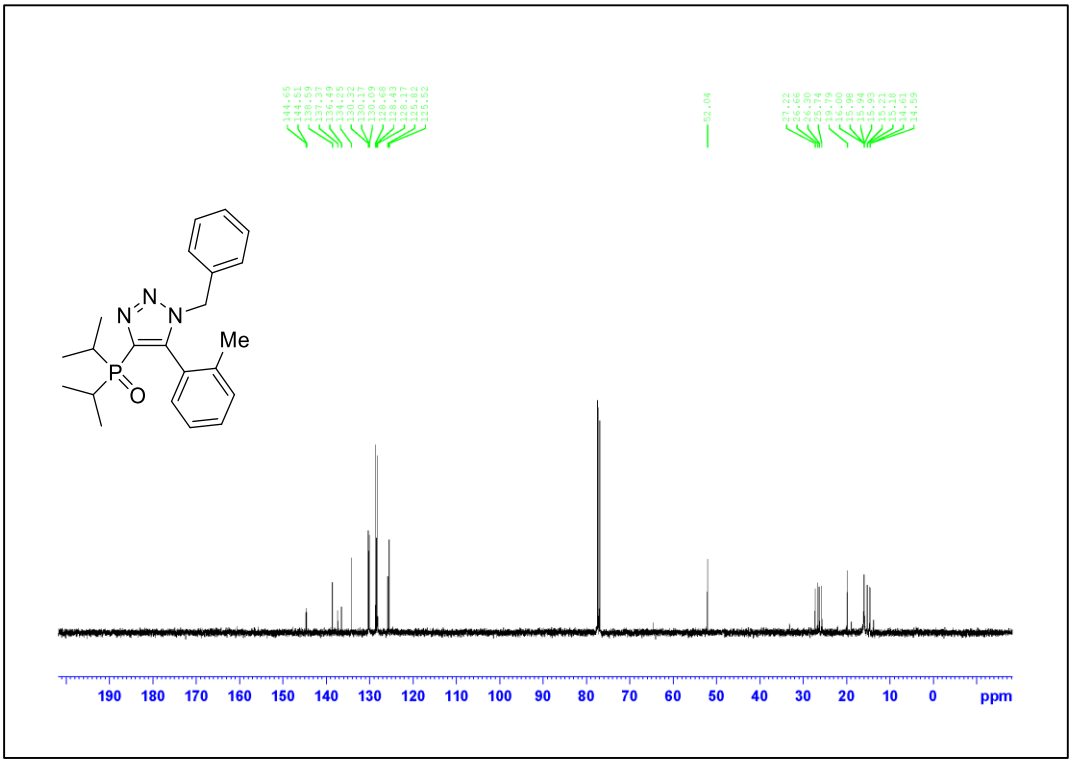

Figure A.210. ^{13}C NMR Spectrum of Compound **3.6b** (125 MHz, $CDCl_3$)

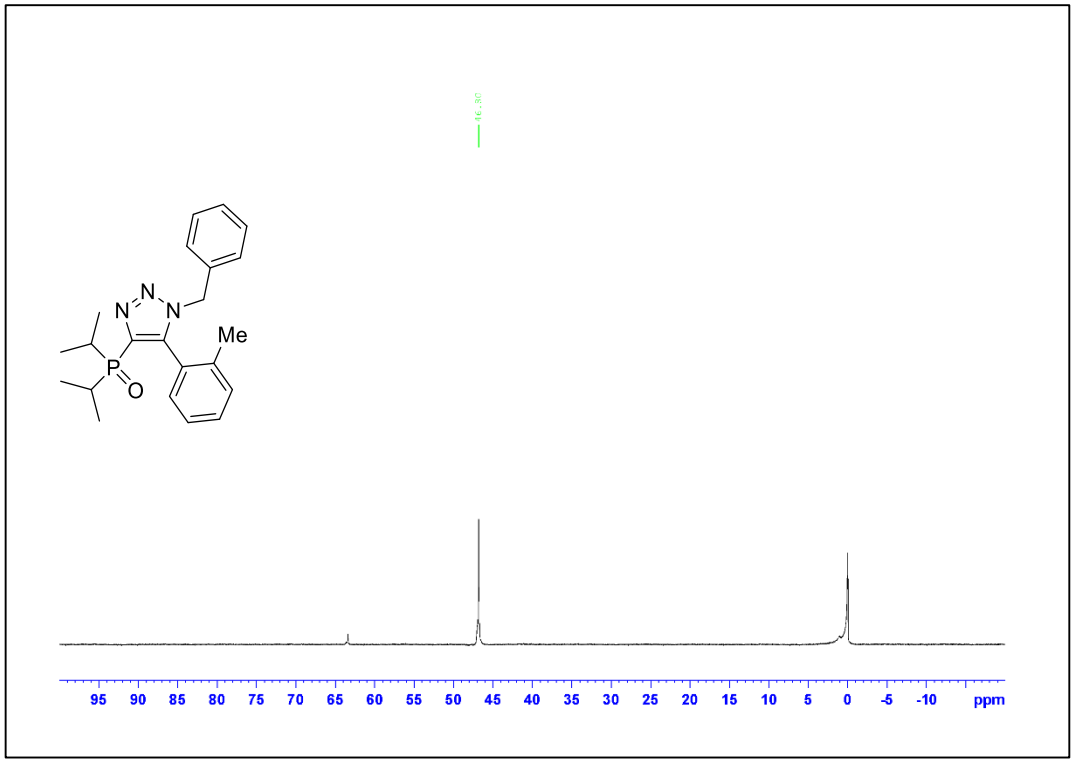

Figure A.211. ^{31}P NMR Spectrum of Compound **3.6b**

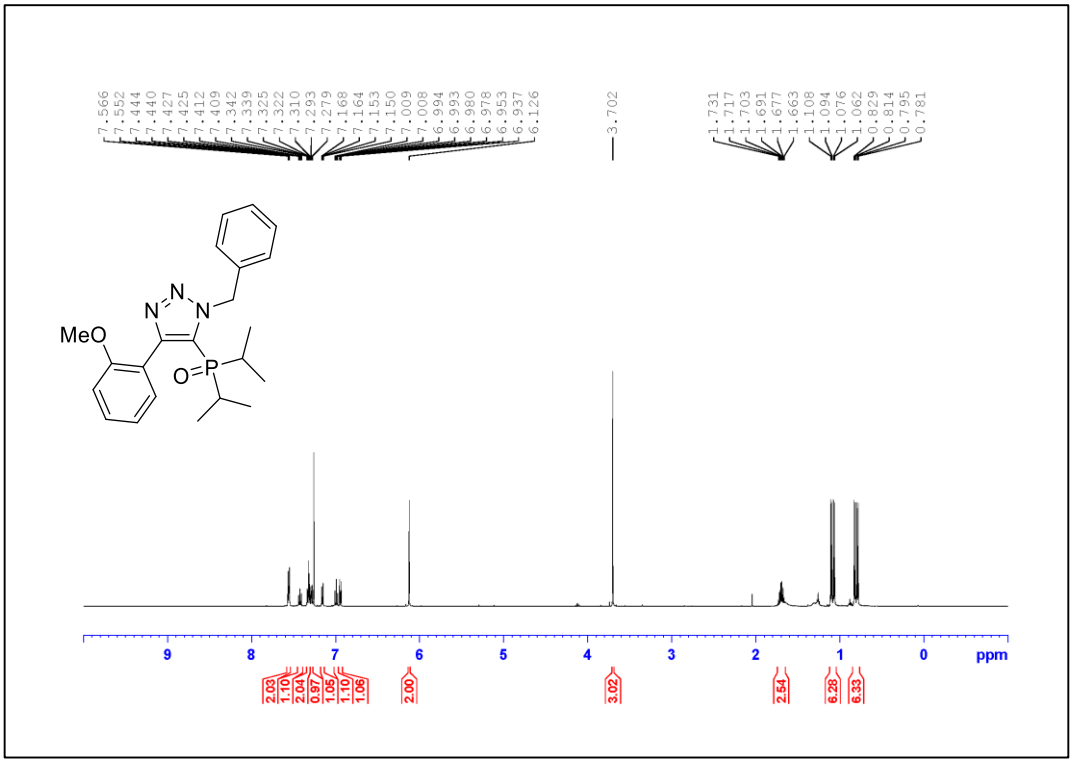

Figure A.212. ^{1}H NMR Spectrum of Compound **3.5c** (500 MHz, $CDCl_3$)

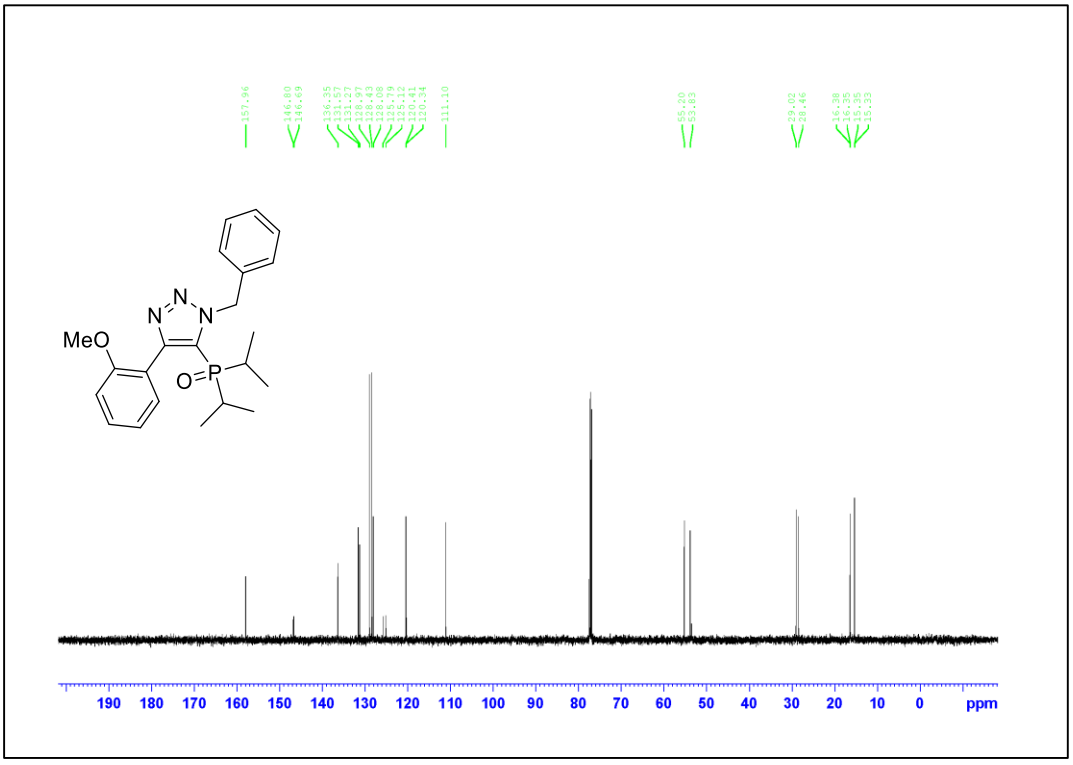

Figure A.213. ^{13}C NMR Spectrum of Compound **3.5c** (125 MHz, $CDCl_3$)

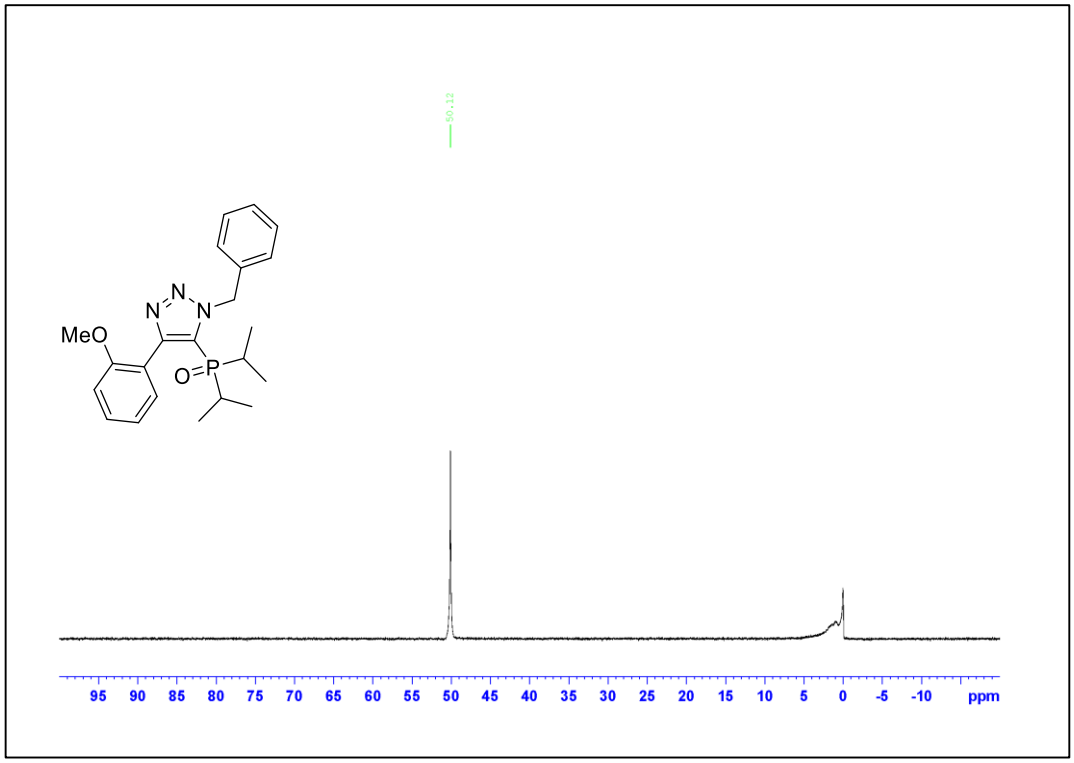

Figure A.214. ^{31}P NMR Spectrum of Compound **3.5c**

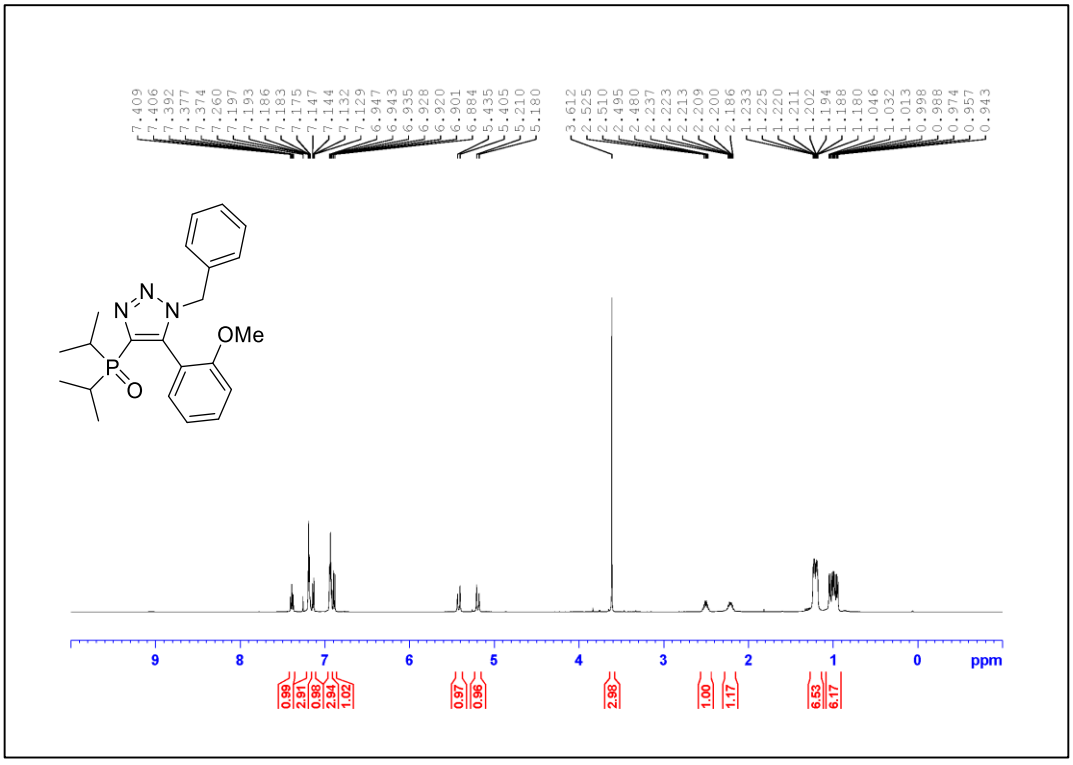

Figure A.215. ^{1}H NMR Spectrum of Compound **3.6c** (500 MHz, $CDCl_3$)

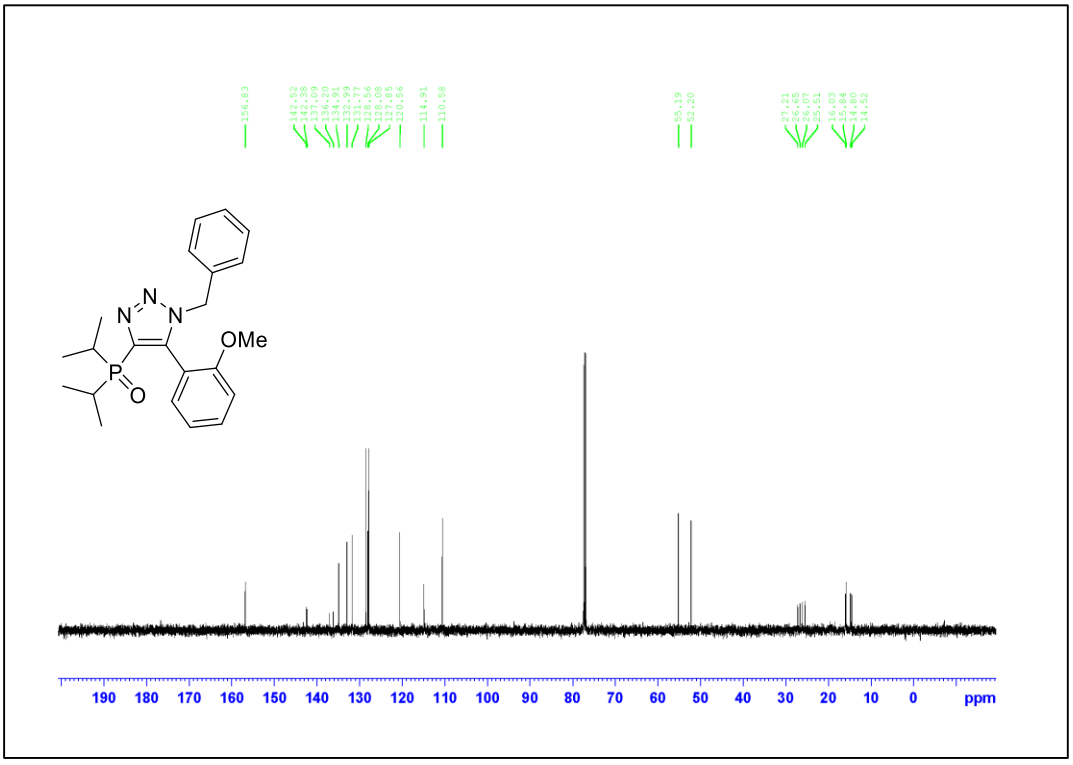

Figure A.216. ^{13}C NMR Spectrum of Compound **3.6c** (125 MHz, $CDCl_3$)

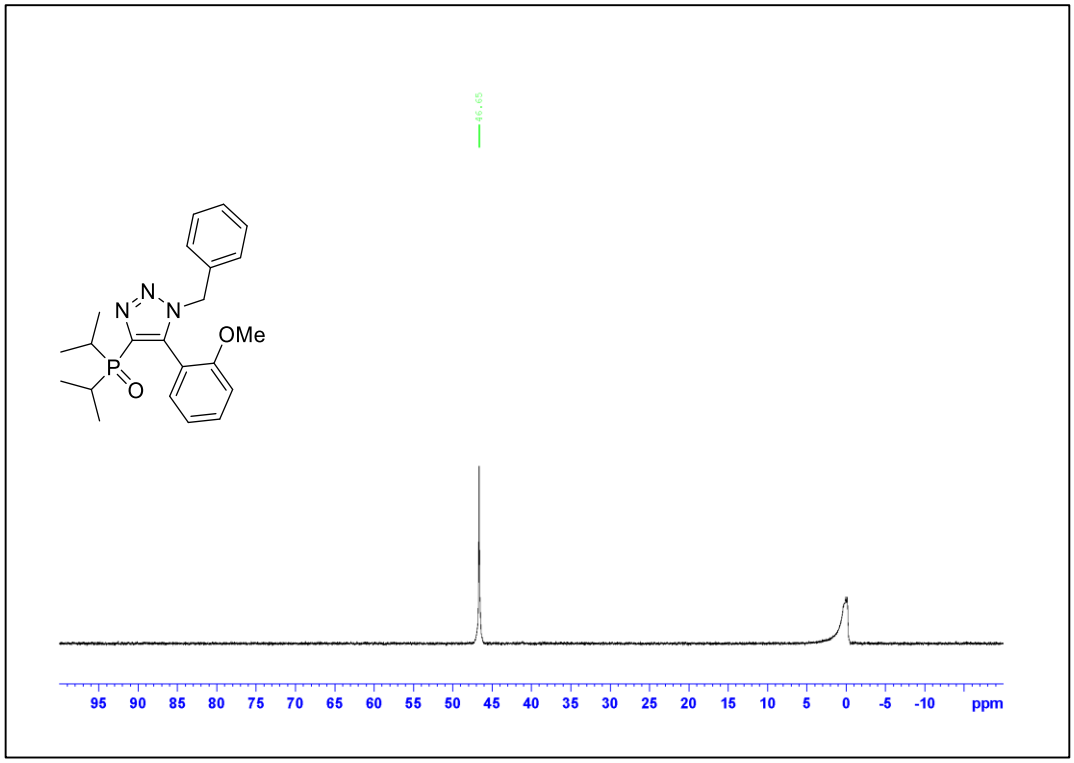

Figure A.217. ^{31}P NMR Spectrum of Compound **3.6c**

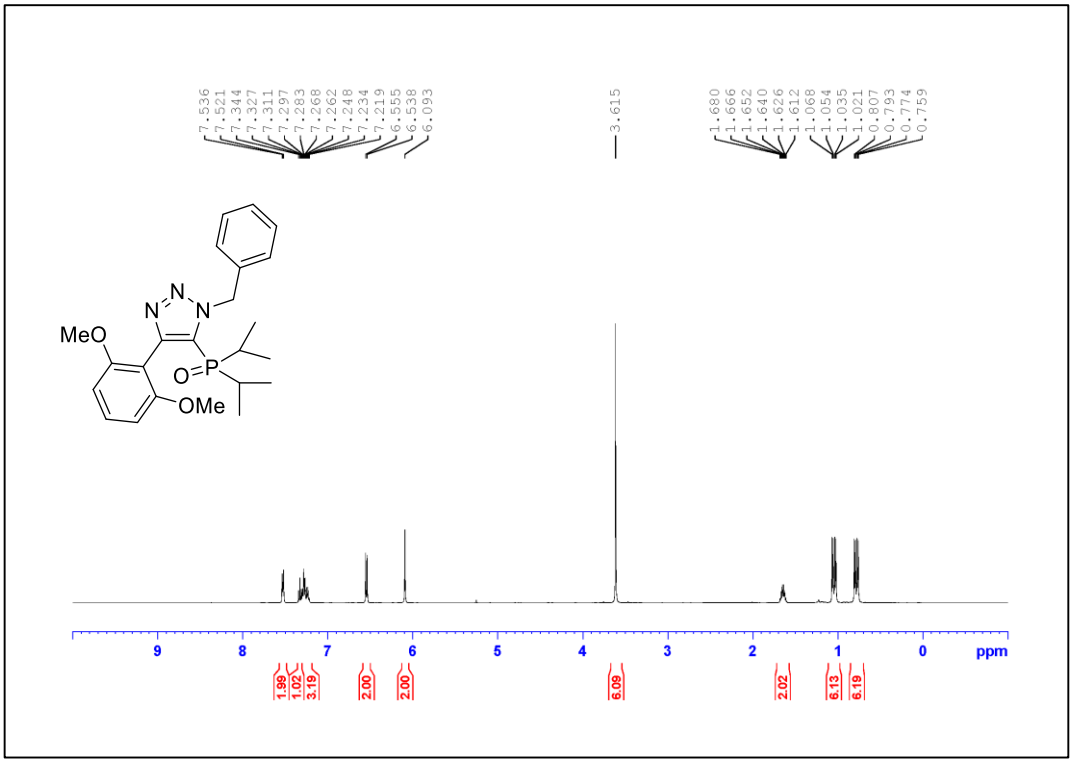

Figure A.218. ^{1}H NMR Spectrum of Compound **3.5d** (500 MHz, $CDCl_3$)

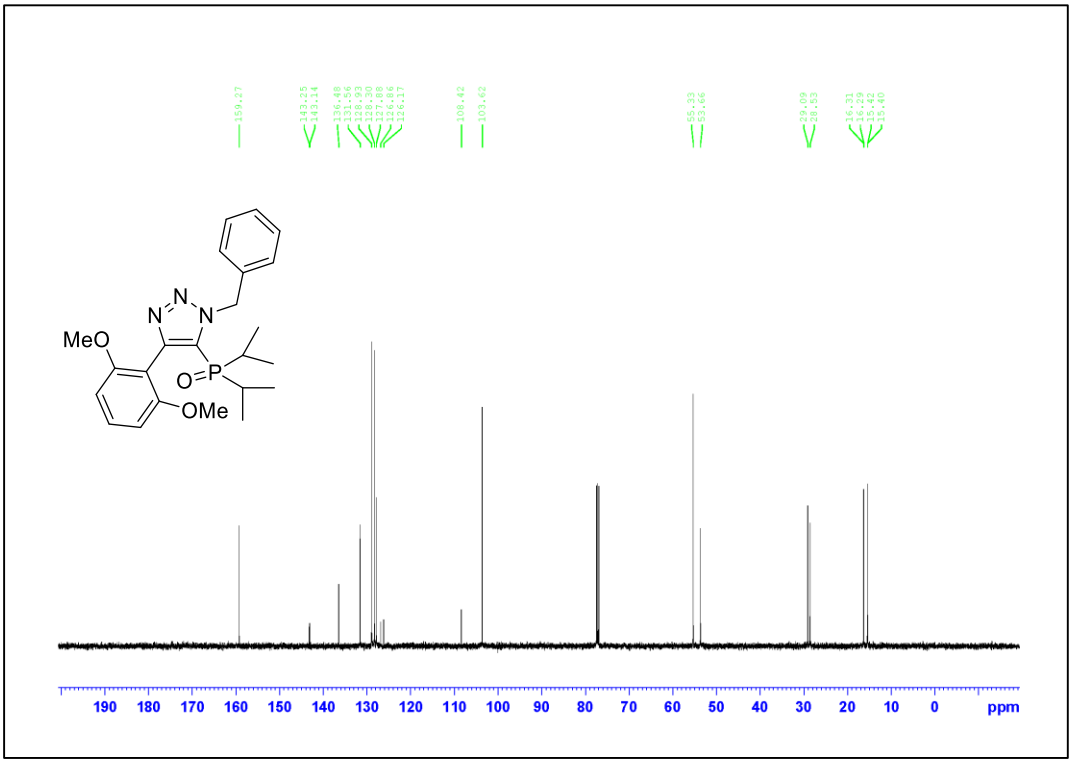

Figure A.219. ^{13}C NMR Spectrum of Compound **3.5d** (125 MHz, $CDCl_3$)

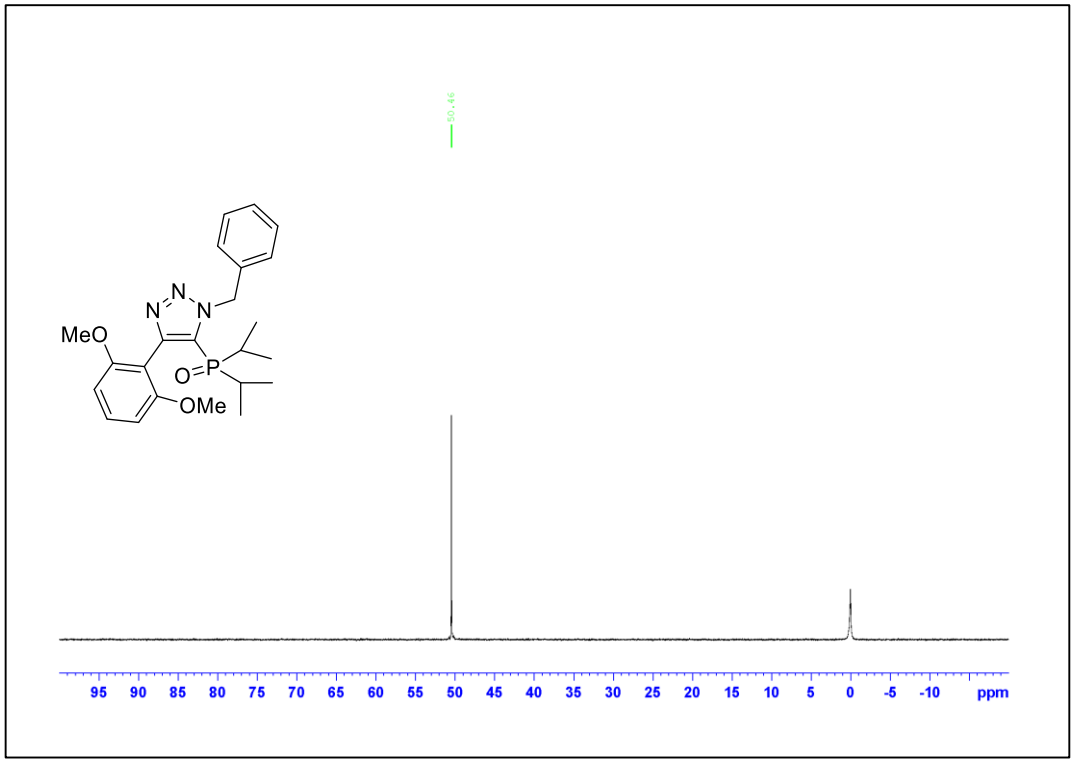

Figure A.220. ^{31}P NMR Spectrum of Compound **3.5d**

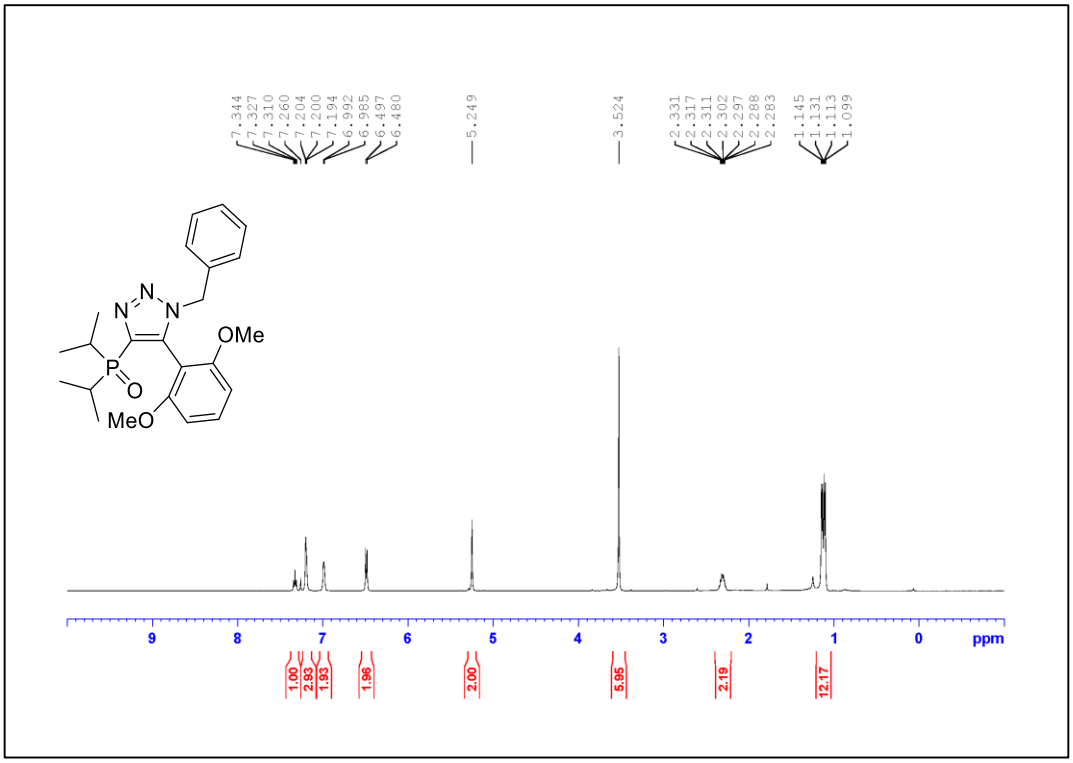

Figure A.221. ^{1}H NMR Spectrum of Compound **3.6d** (500 MHz, $CDCl_3$)

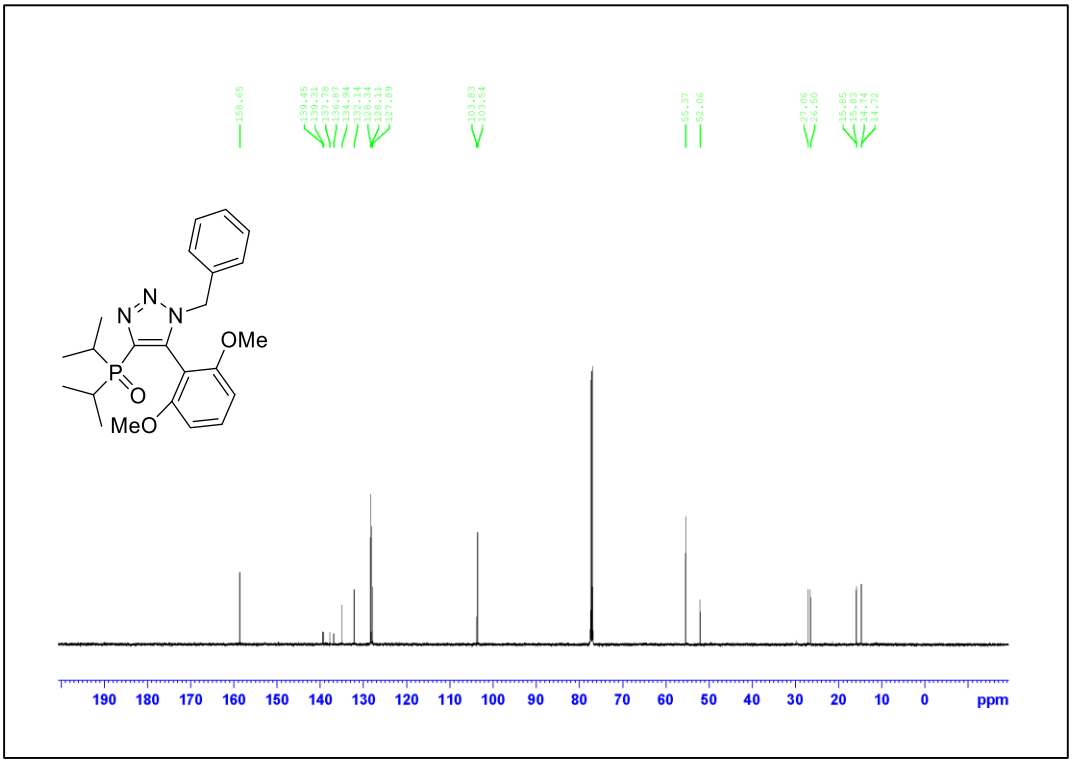

Figure A.222. ^{13}C NMR Spectrum of Compound **3.6d** (125 MHz, $CDCl_3$)

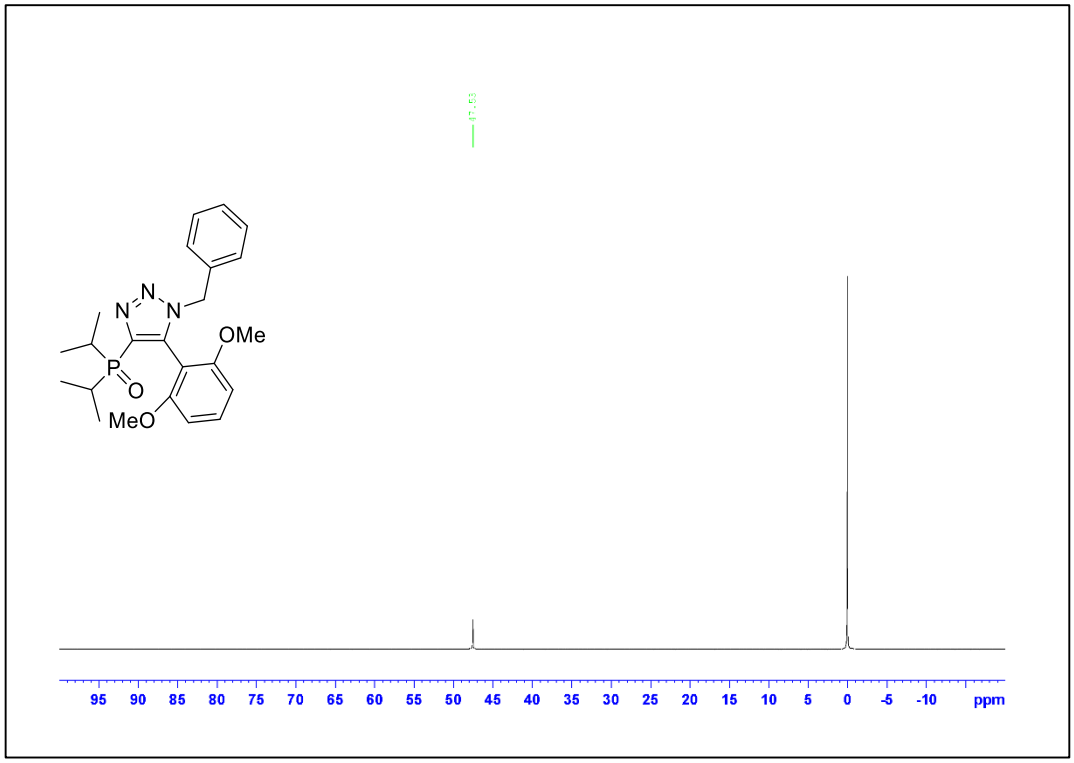

Figure A.223. ^{31}P NMR Spectrum of Compound **3.6d**

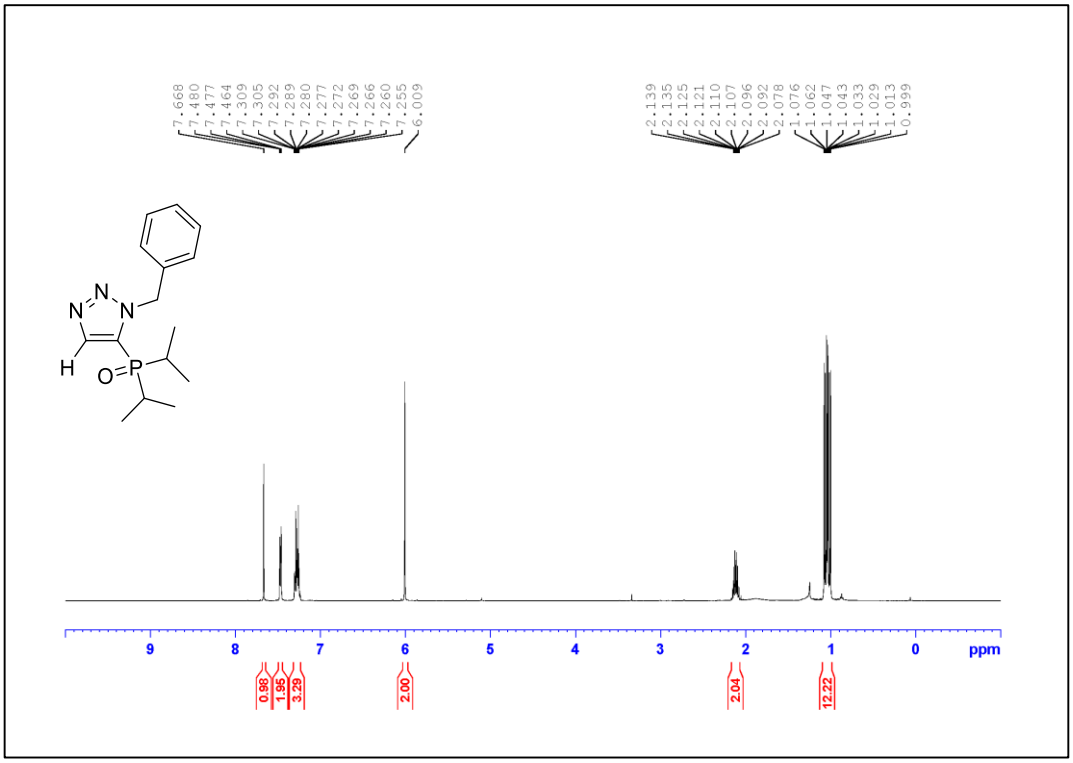

Figure A.224. ^{1}H NMR Spectrum of Compound **3.5e** (500 MHz, $CDCl_3$)

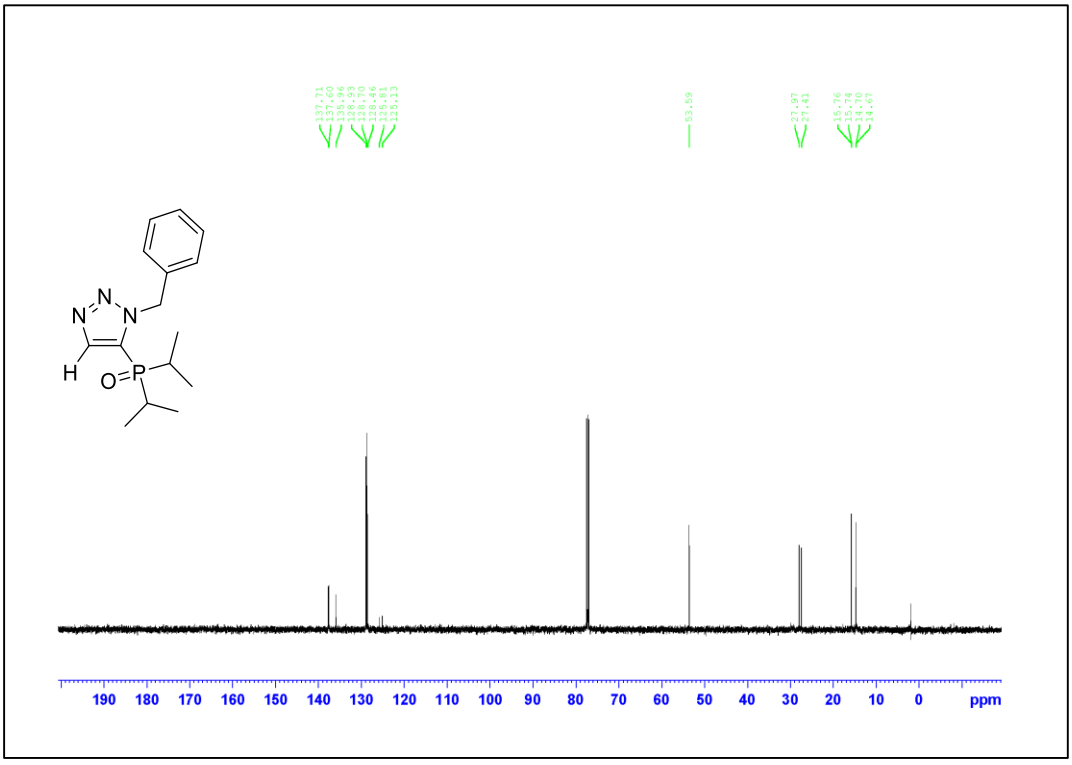

Figure A.225. ^{13}C NMR Spectrum of Compound **3.5e** (125 MHz, $CDCl_3$)

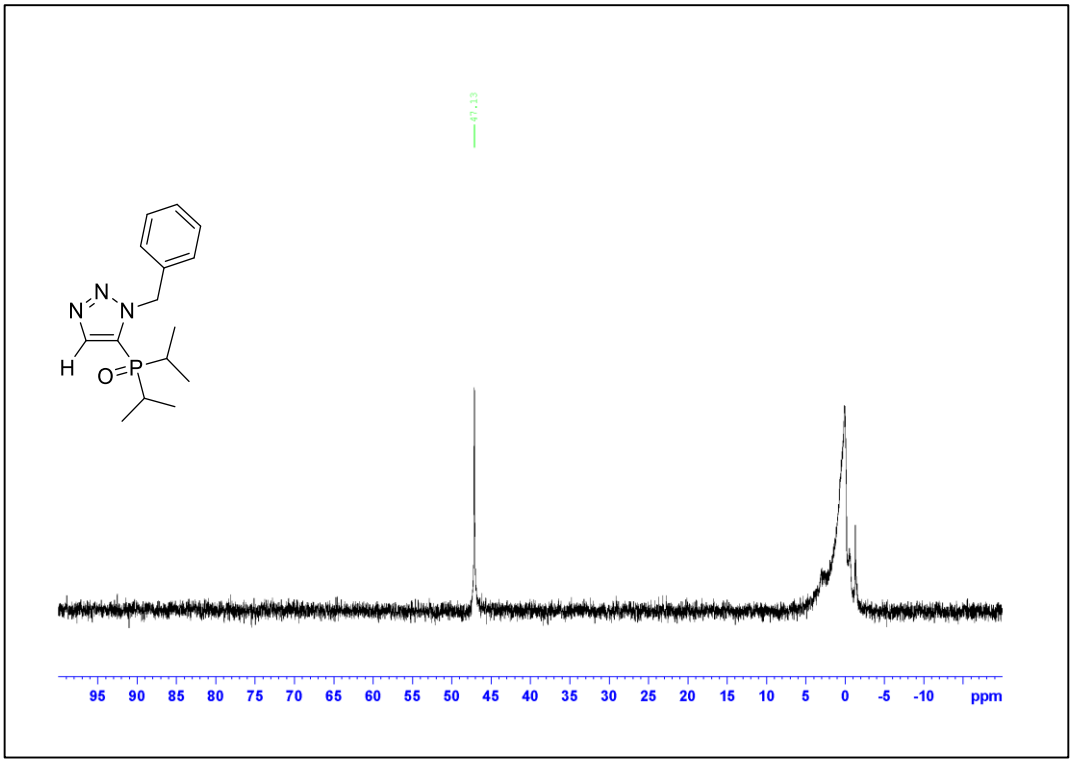

Figure A.226. ^{31}P NMR Spectrum of Compound **3.5e**

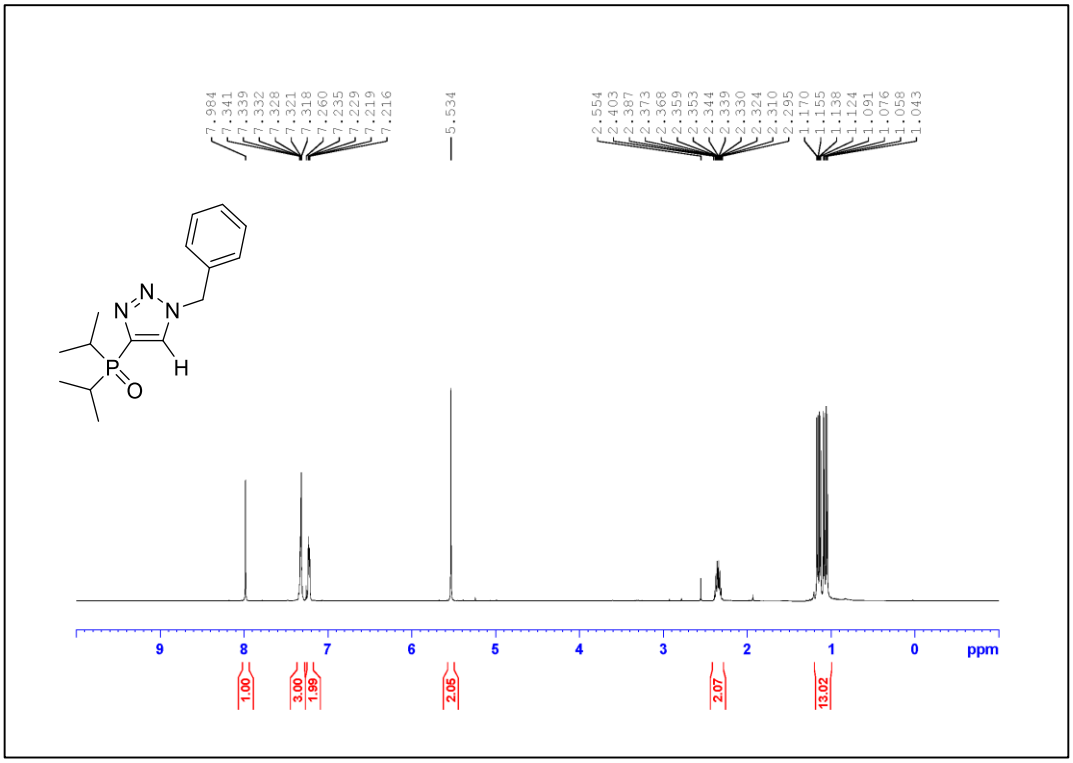

Figure A.227. ^{1}H NMR Spectrum of Compound **3.6e** (500 MHz, $CDCl_3$)

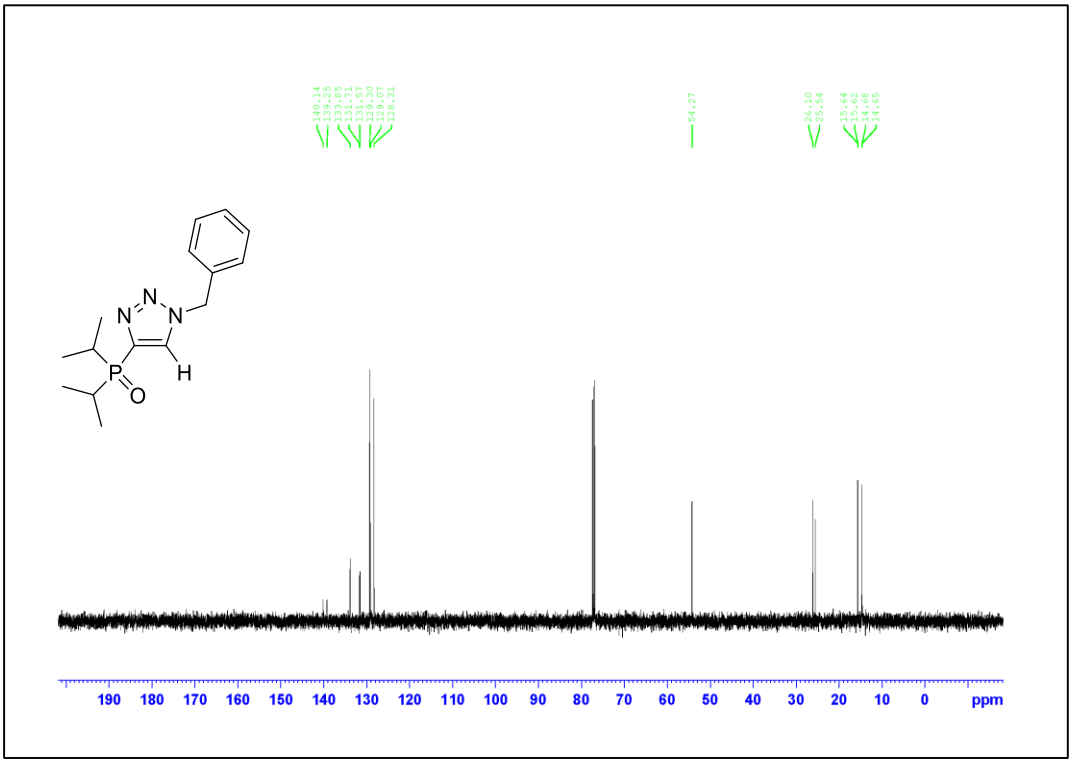

Figure A.228. ^{13}C NMR Spectrum of Compound **3.6e** (125 MHz, $CDCl_3$)

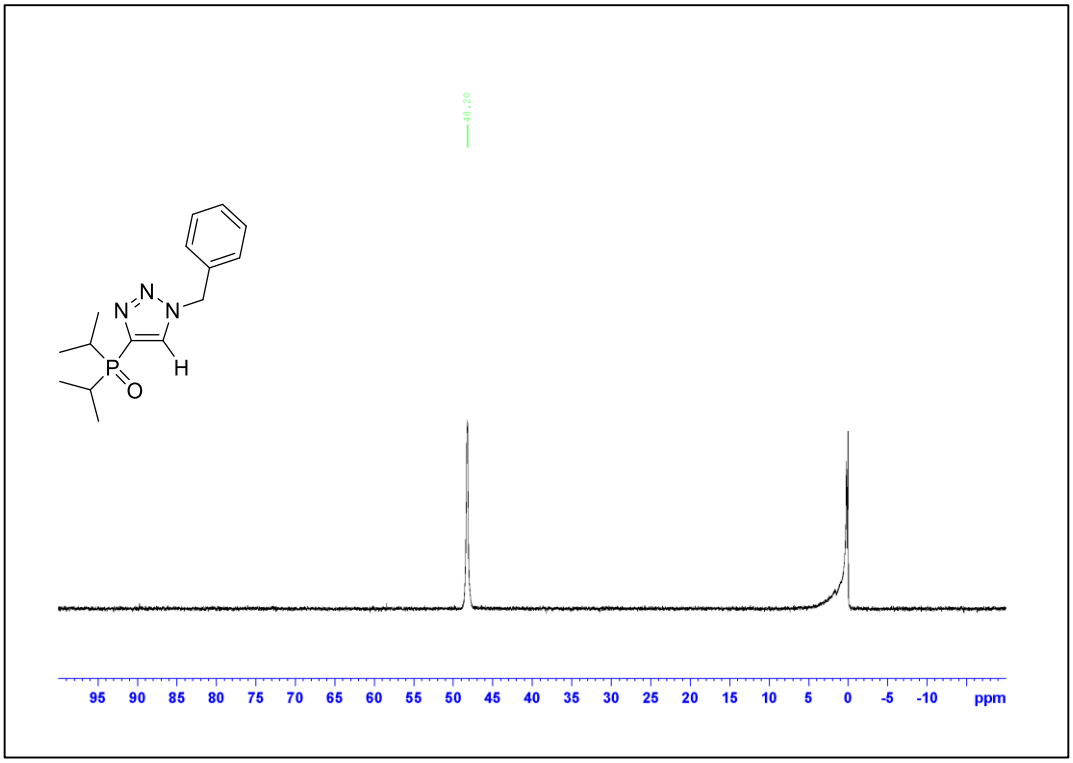

Figure A.229. ^{31}P NMR Spectrum of Compound **3.6e**

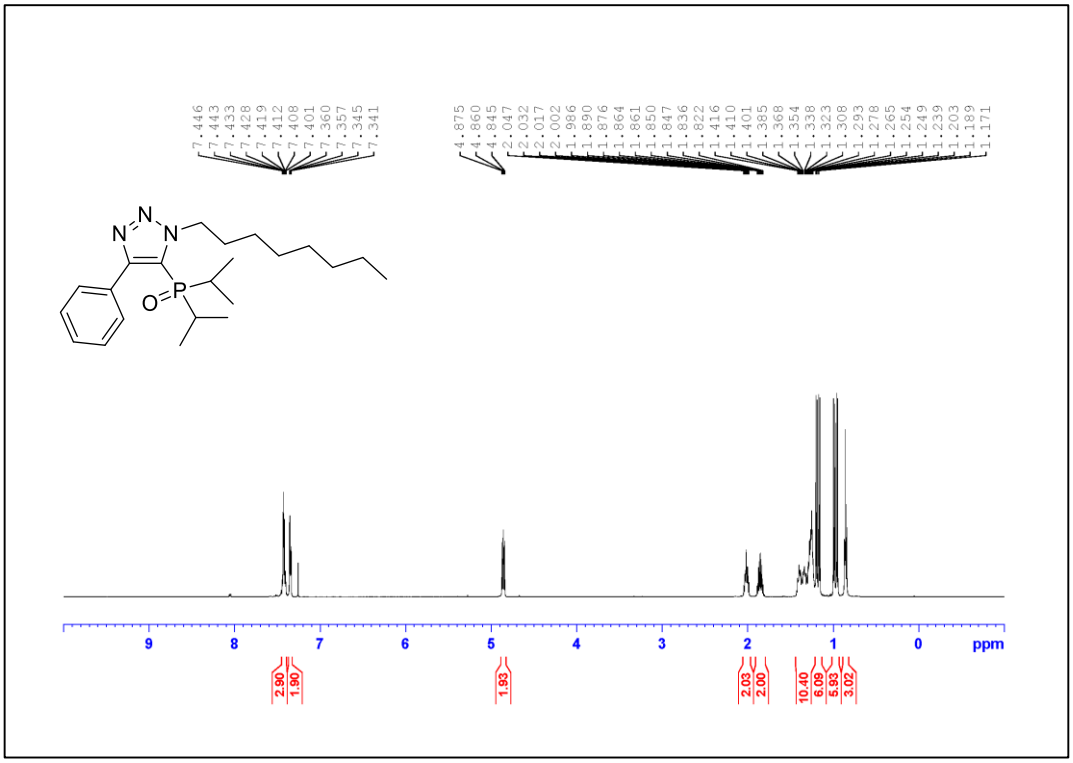

Figure A.230. ^{1}H NMR Spectrum of Compound **3.5f** (500 MHz, $CDCl_3$)

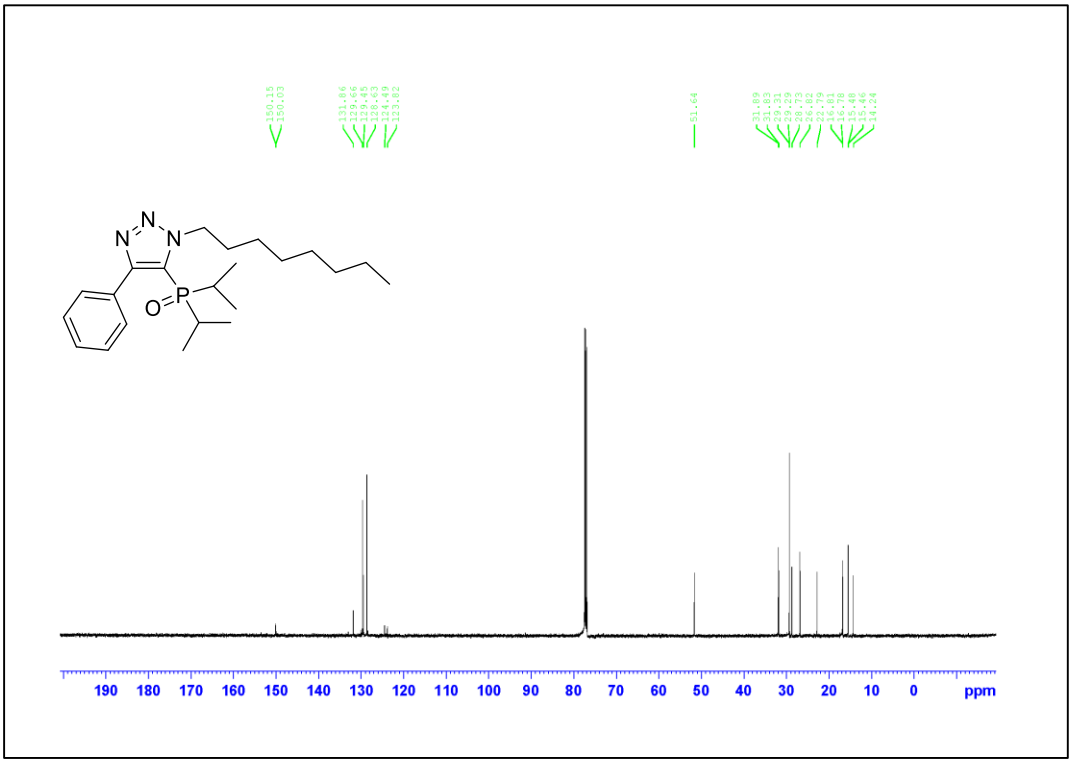

Figure A.231. ^{13}C NMR Spectrum of Compound **3.5f** (125 MHz, $CDCl_3$)

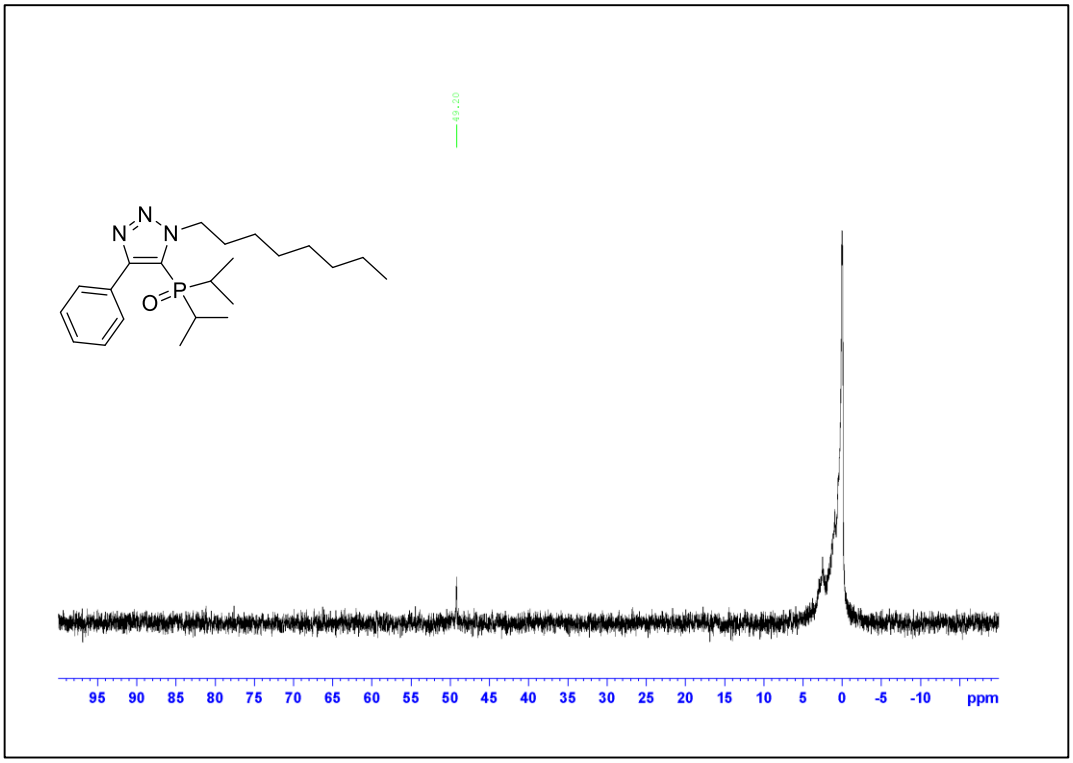

Figure A.232. ^{31}P NMR Spectrum of Compound **3.5f**

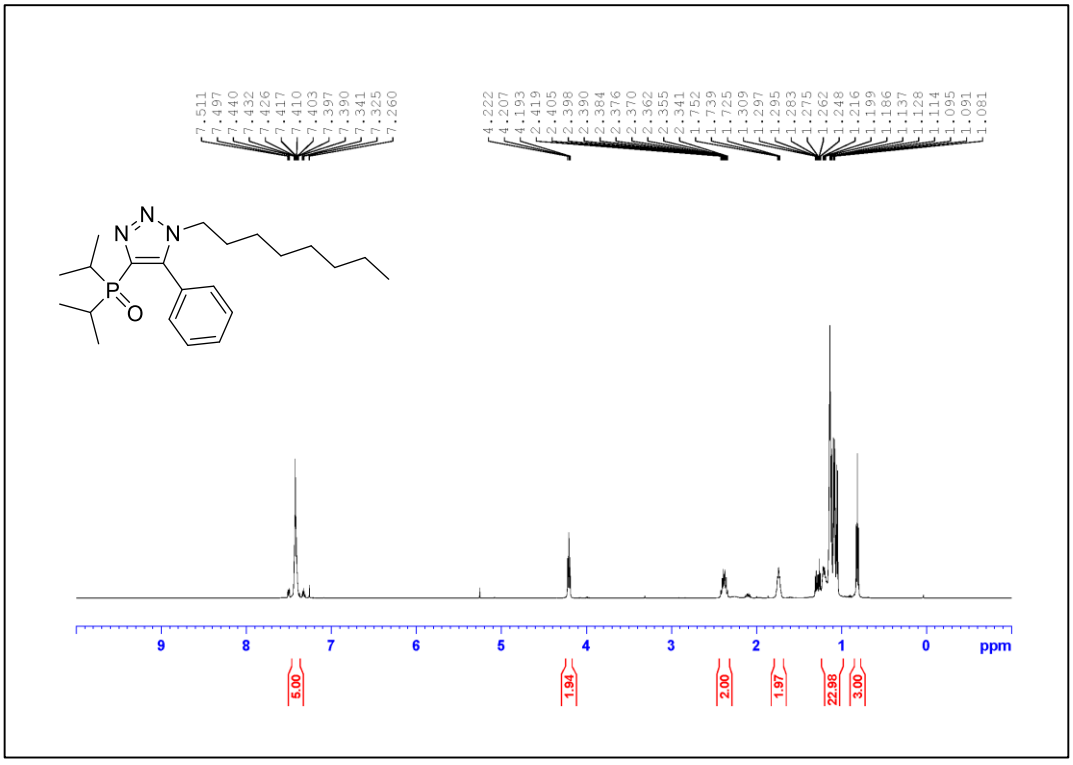

Figure A.233. ^{1}H NMR Spectrum of Compound **3.6f** (500 MHz, $CDCl_3$)

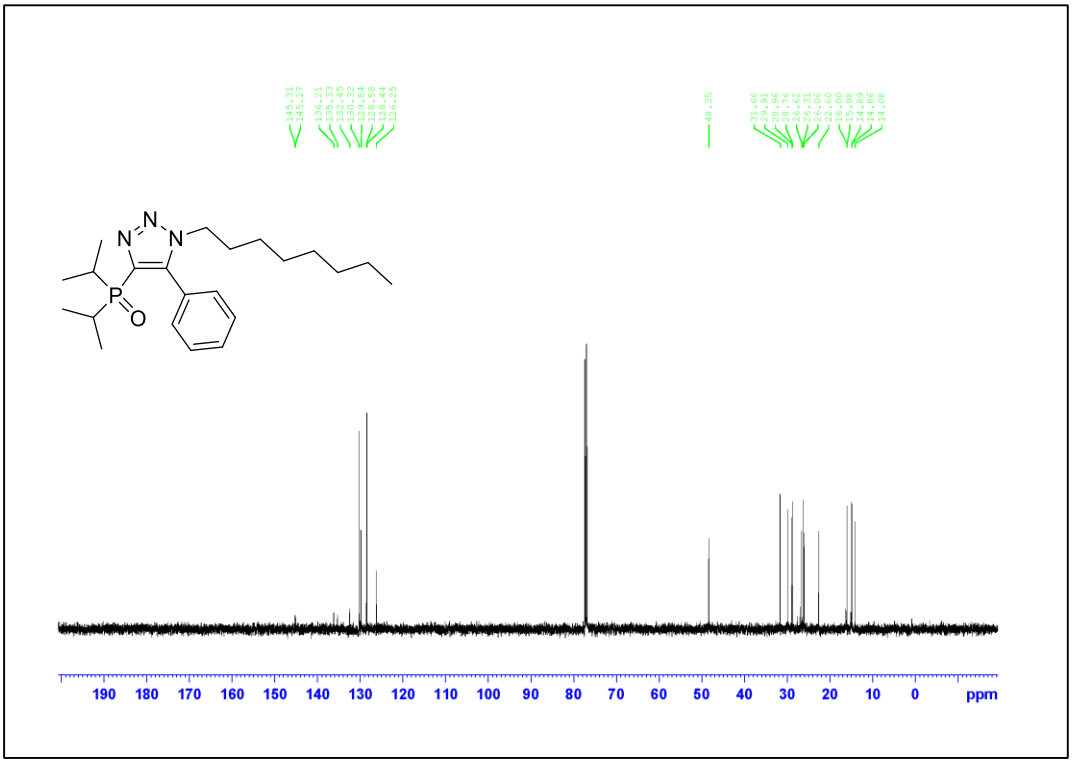

Figure A.234. ^{13}C NMR Spectrum of Compound **3.6f** (125 MHz, $CDCl_3$)

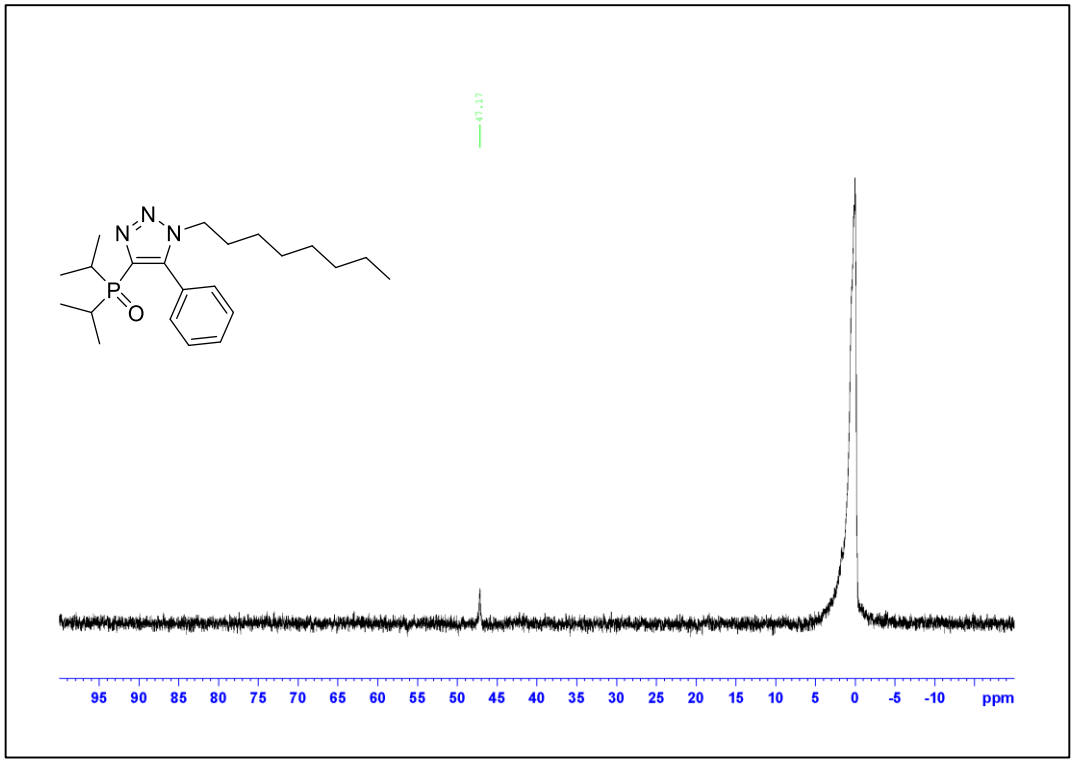

Figure A.235. ^{31}P NMR Spectrum of Compound **3.6f**

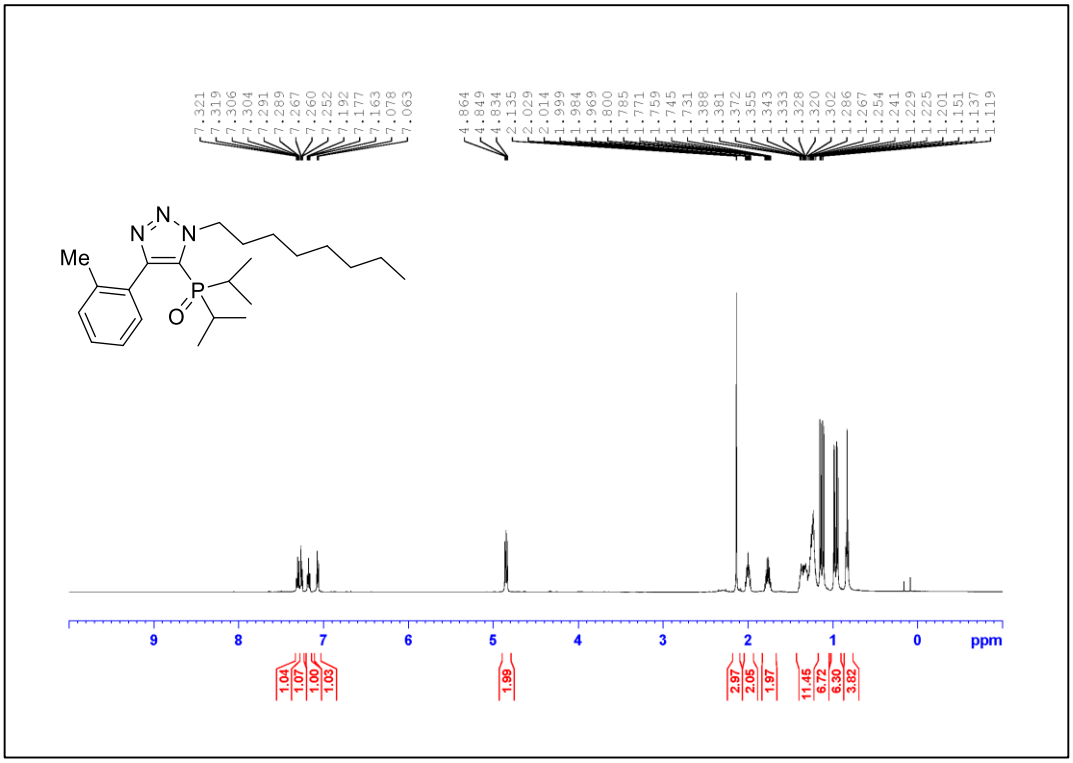

Figure A.236. ^{1}H NMR Spectrum of Compound **3.5g** (500 MHz, $CDCl_3$)

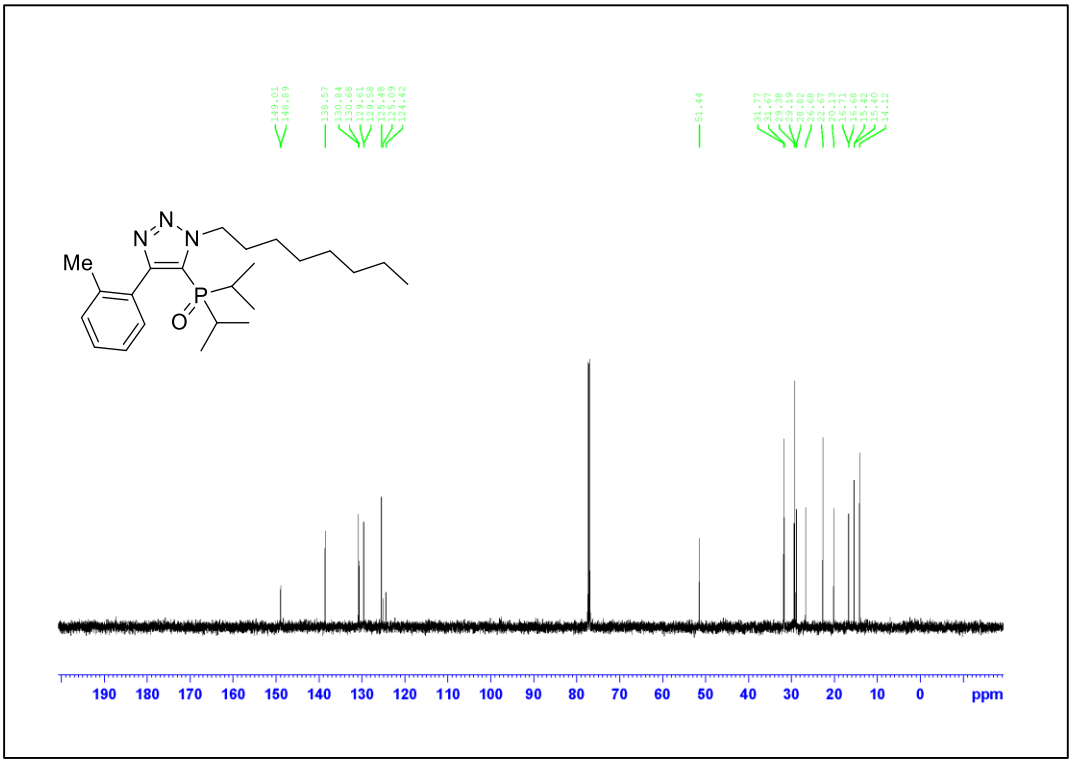

Figure A.237. ^{13}C NMR Spectrum of Compound **3.5g** (125 MHz, $CDCl_3$)

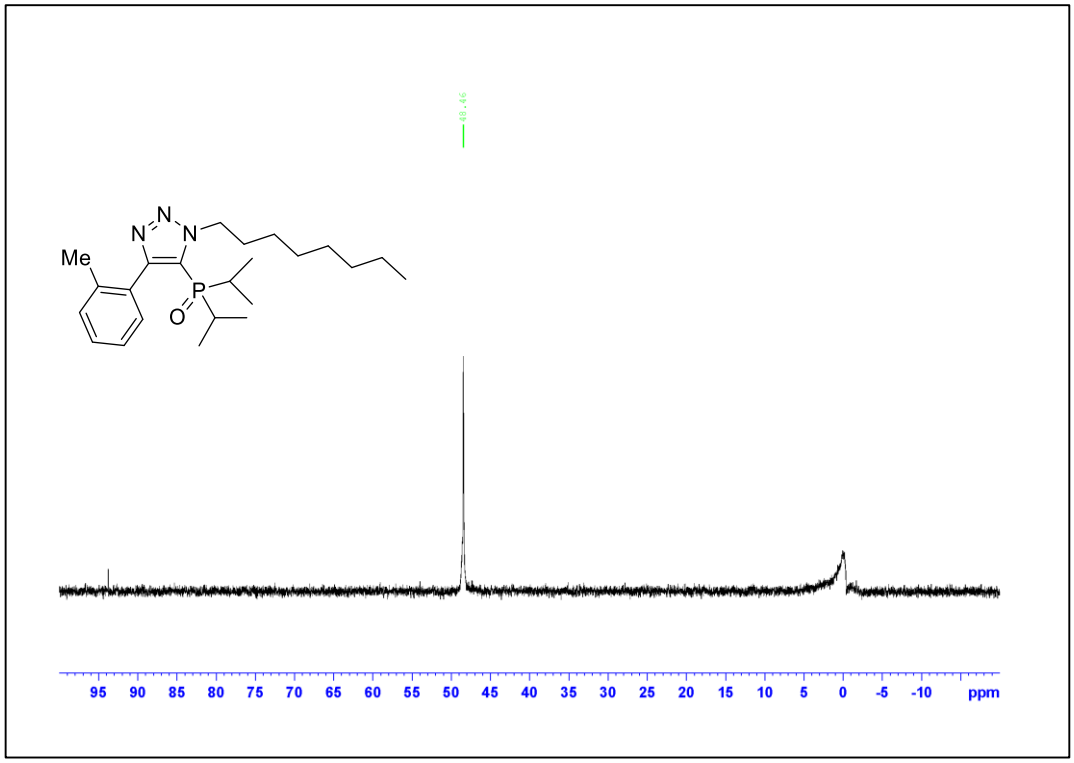

Figure A.238. ^{31}P NMR Spectrum of Compound **3.5g**

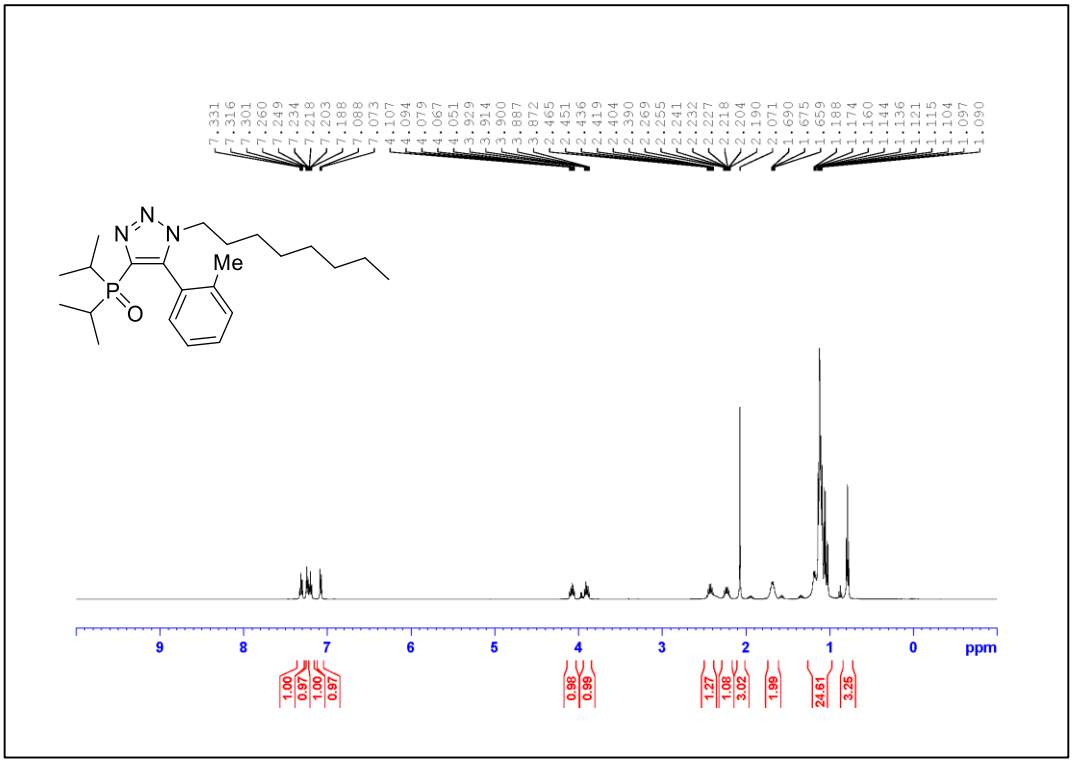

Figure A.239. ^{1}H NMR Spectrum of Compound **3.6g** (500 MHz, $CDCl_3$)

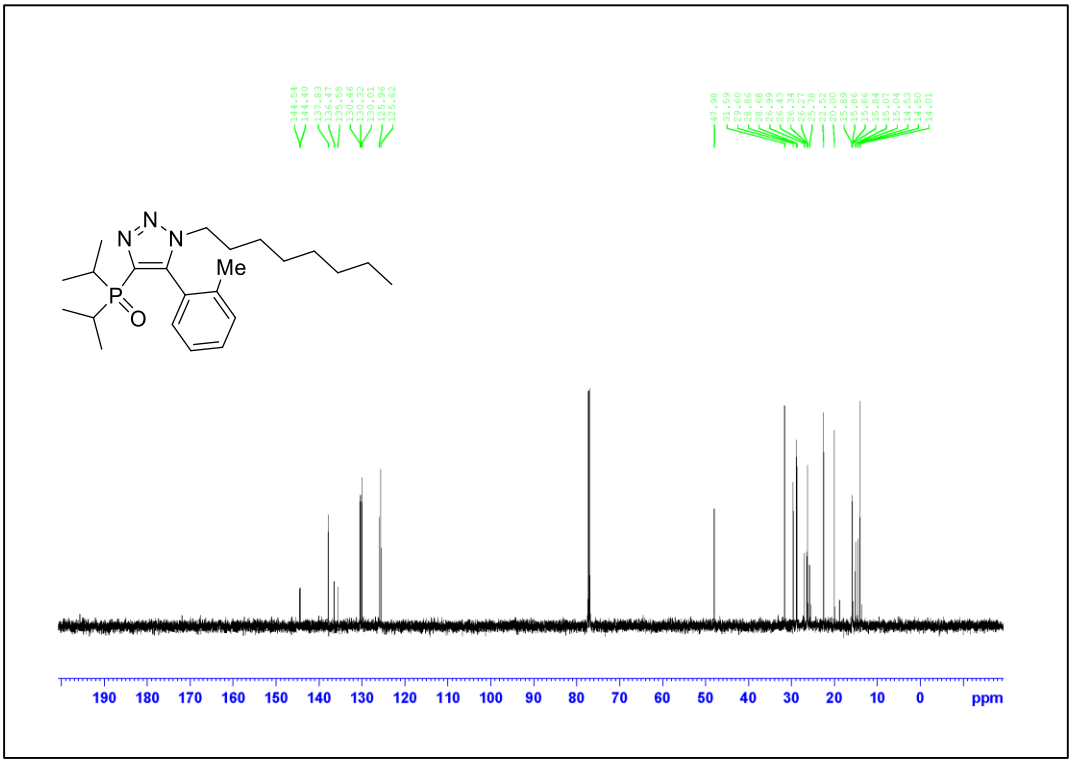

Figure A.240. ^{13}C NMR Spectrum of Compound **3.6g** (125 MHz, $CDCl_3$)

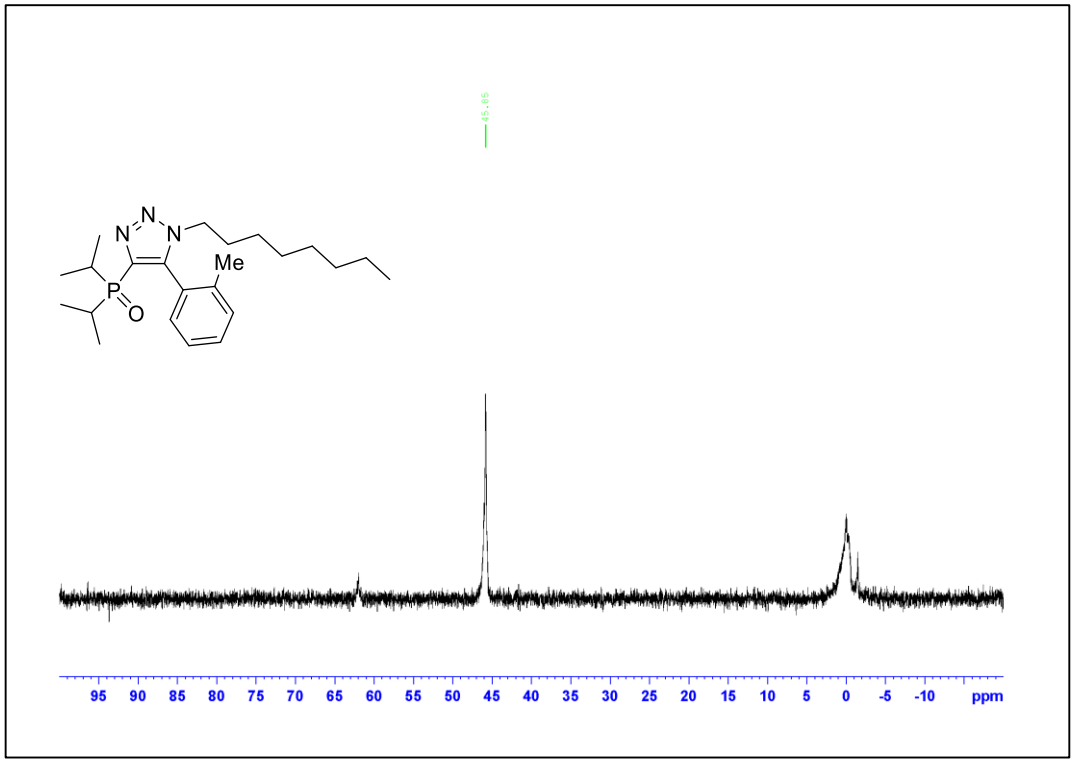

Figure A.241. ^{31}P NMR Spectrum of Compound **3.6g**

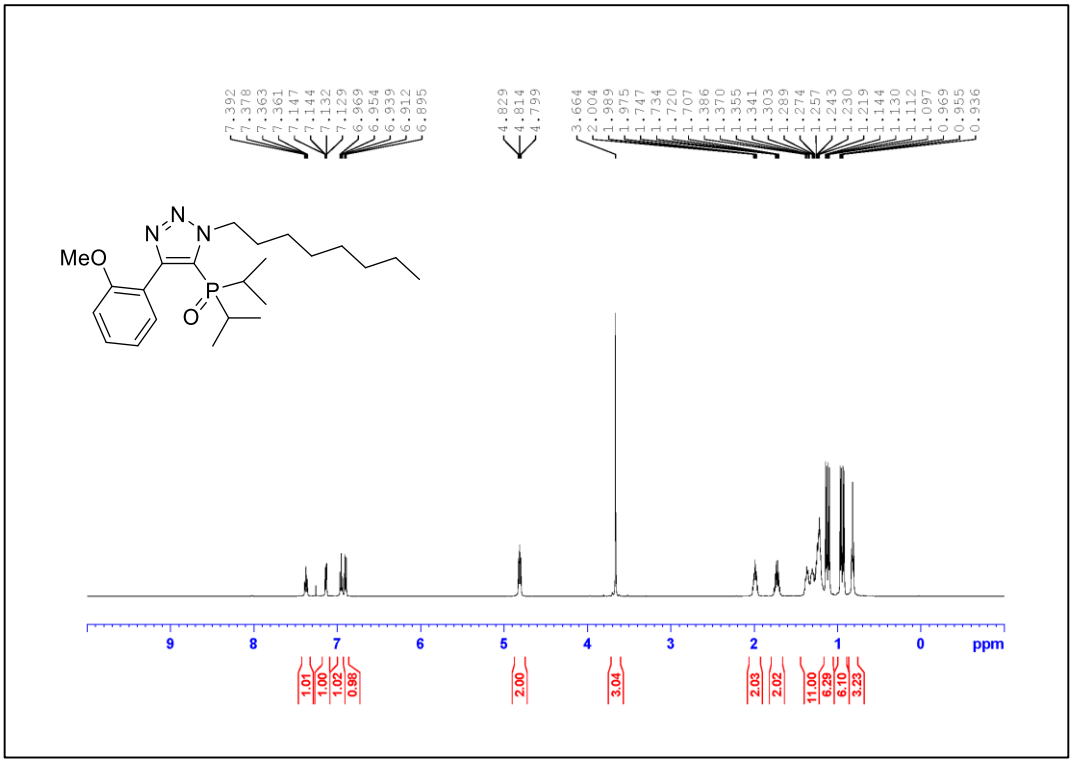

Figure A.242. ^{1}H NMR Spectrum of Compound **3.5h** (500 MHz, $CDCl_3$)

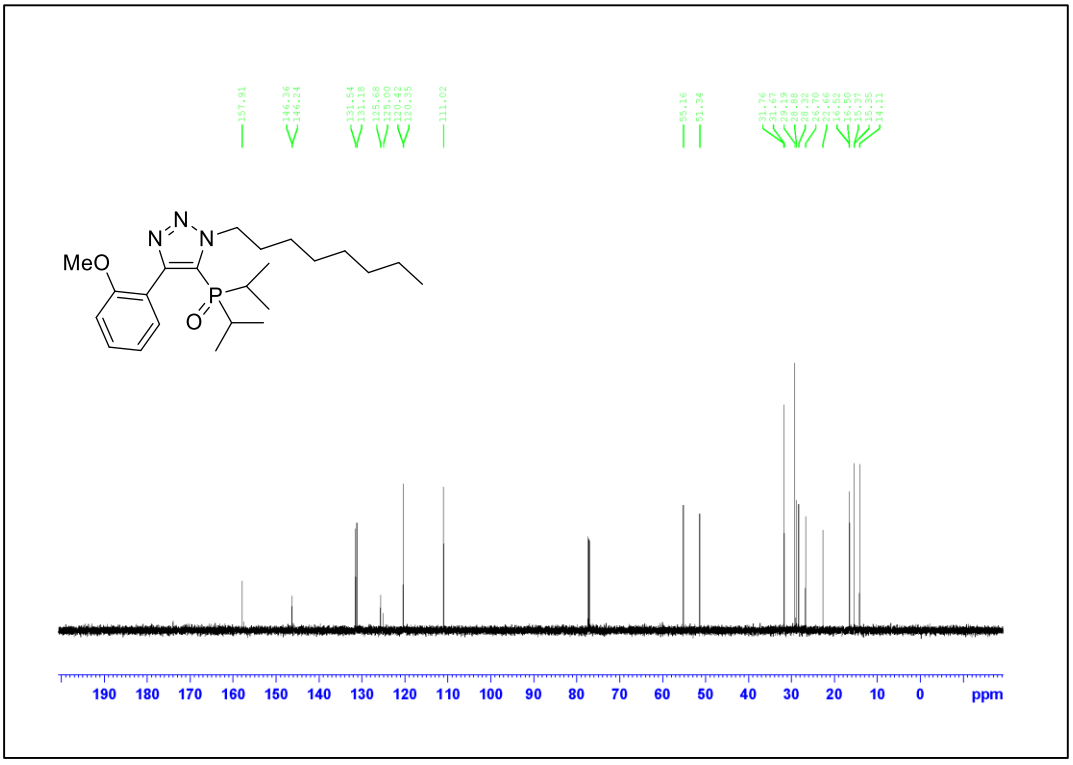

Figure A.243. ^{13}C NMR Spectrum of Compound **3.5h** (125 MHz, $CDCl_3$)

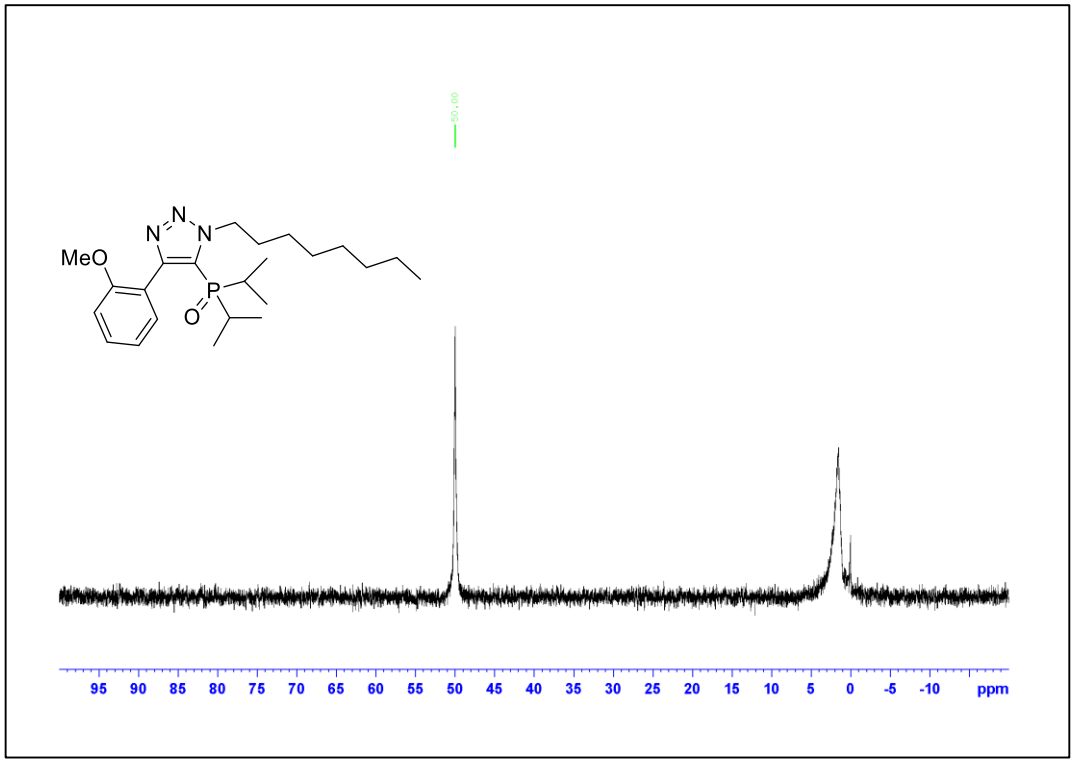

Figure A.244. ^{31}P NMR Spectrum of Compound **3.5h**

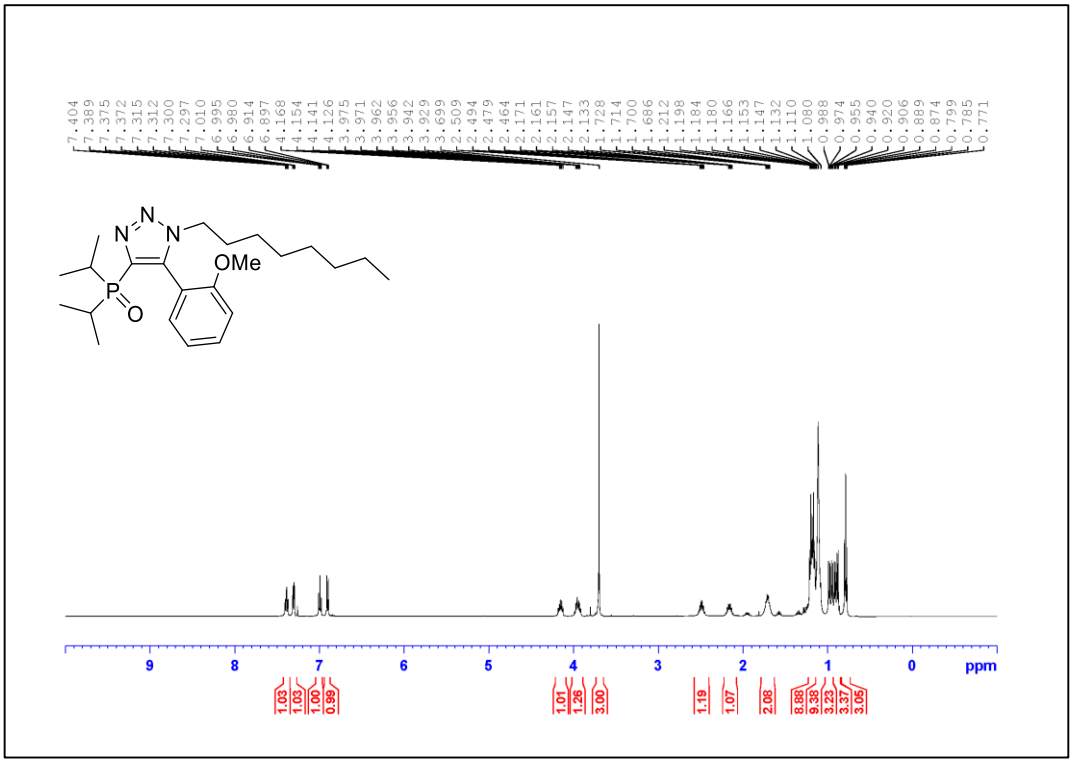

Figure A.245. ^{1}H NMR Spectrum of Compound **3.6h** (500 MHz, $CDCl_3$)

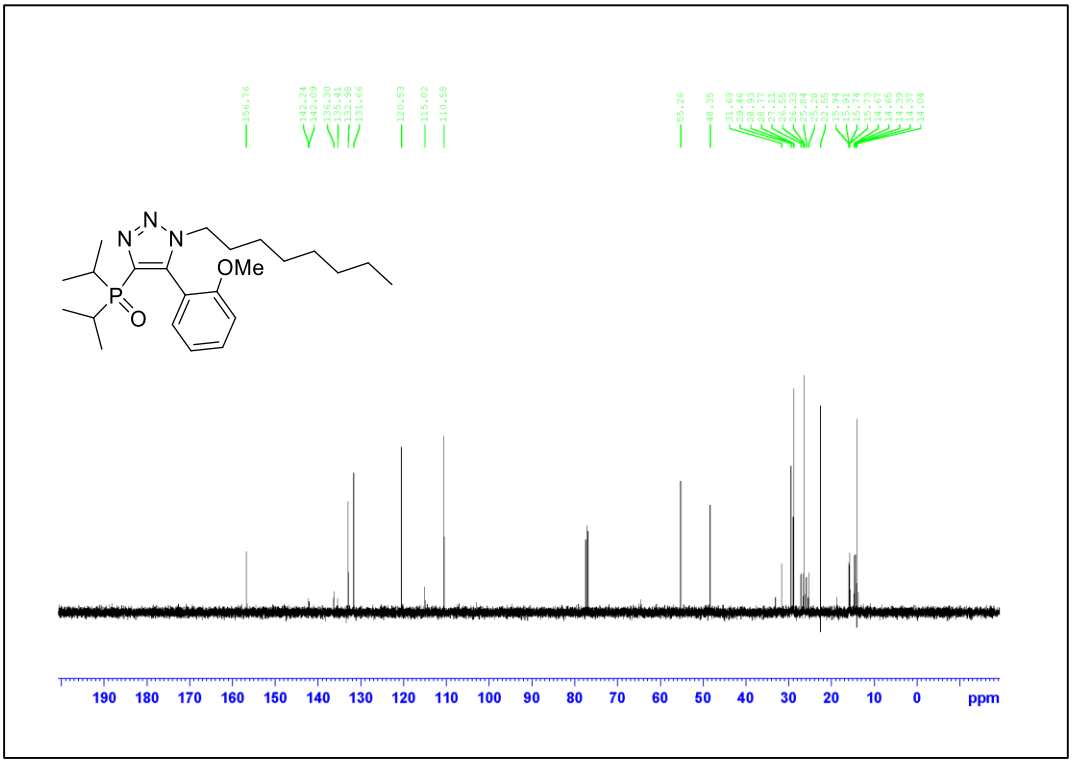

Figure A.246. ^{13}C NMR Spectrum of Compound **3.6h** (125 MHz, $CDCl_3$)

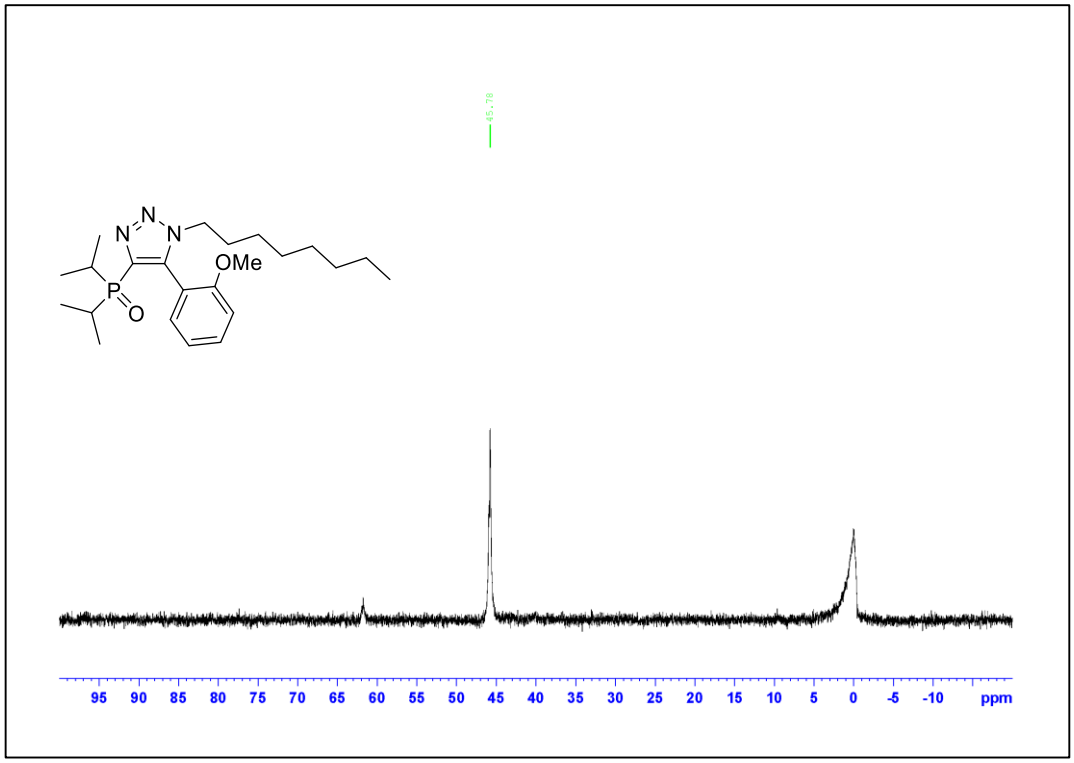

Figure A.247. ^{31}P NMR Spectrum of Compound **3.6h**

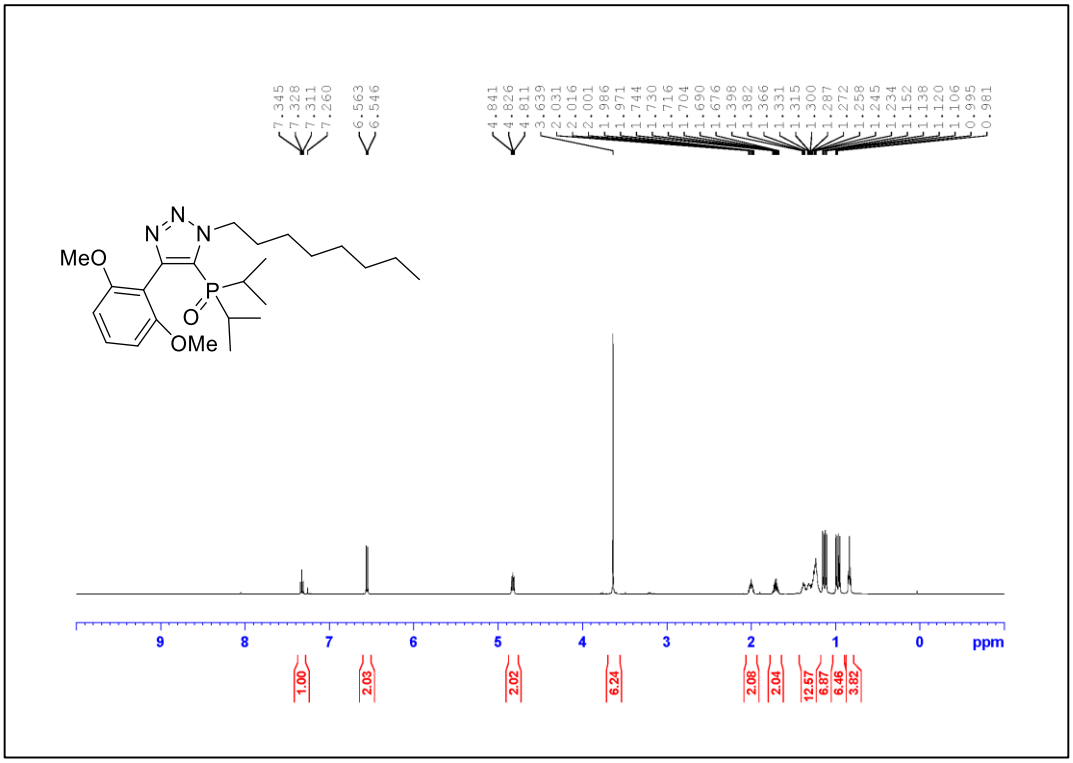

Figure A.248. ^{1}H NMR Spectrum of Compound **3.5i** (500 MHz, $CDCl_3$)

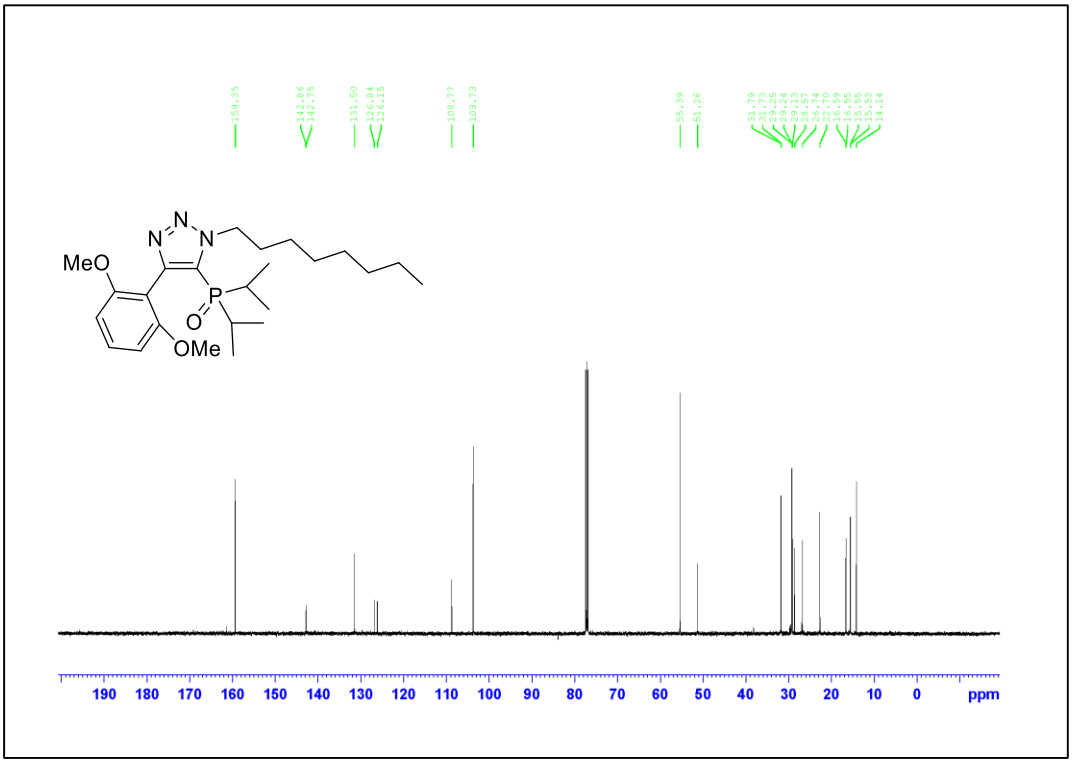

Figure A.249. ^{13}C NMR Spectrum of Compound **3.5i** (125 MHz, $CDCl_3$)

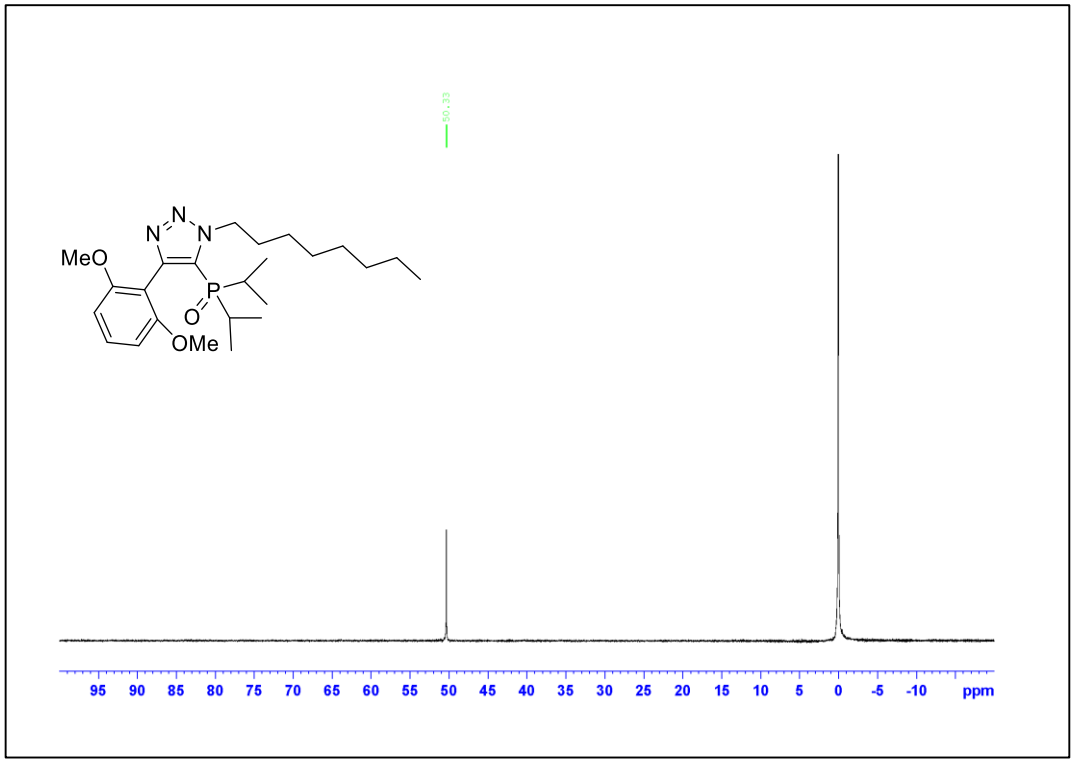

Figure A.250. ^{31}P NMR Spectrum of Compound **3.5i**

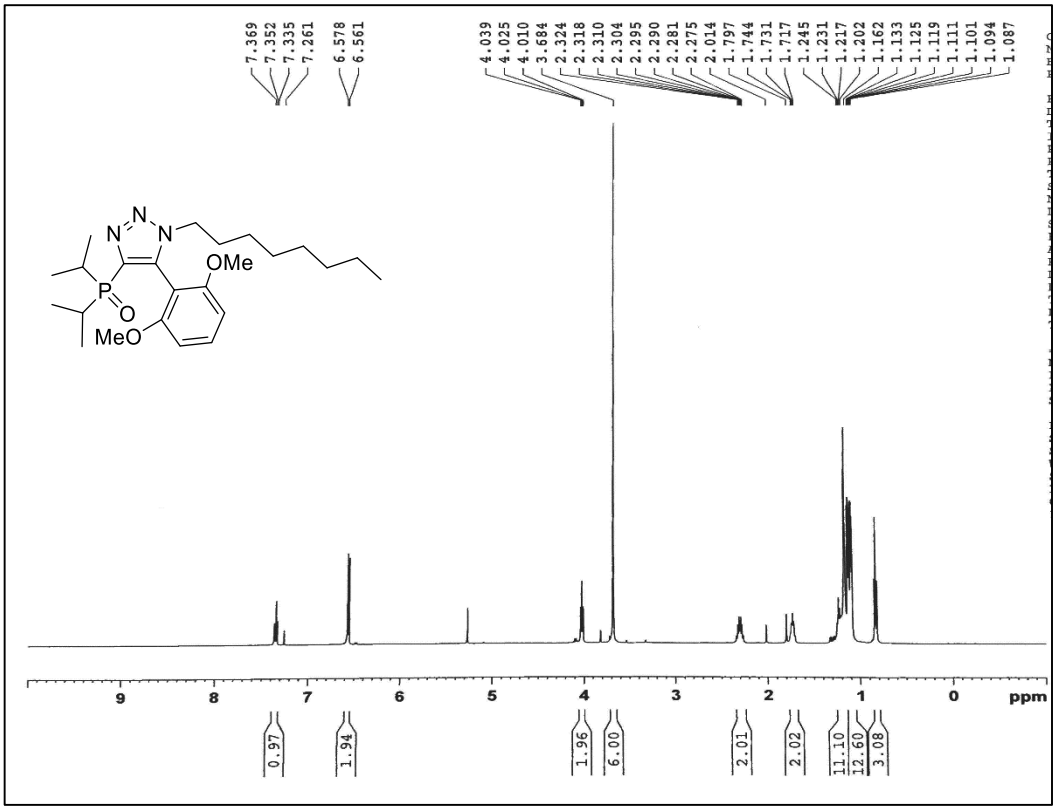

Figure A.251. ^{1}H NMR Spectrum of Compound **3.6i** (500 MHz, $CDCl_3$)

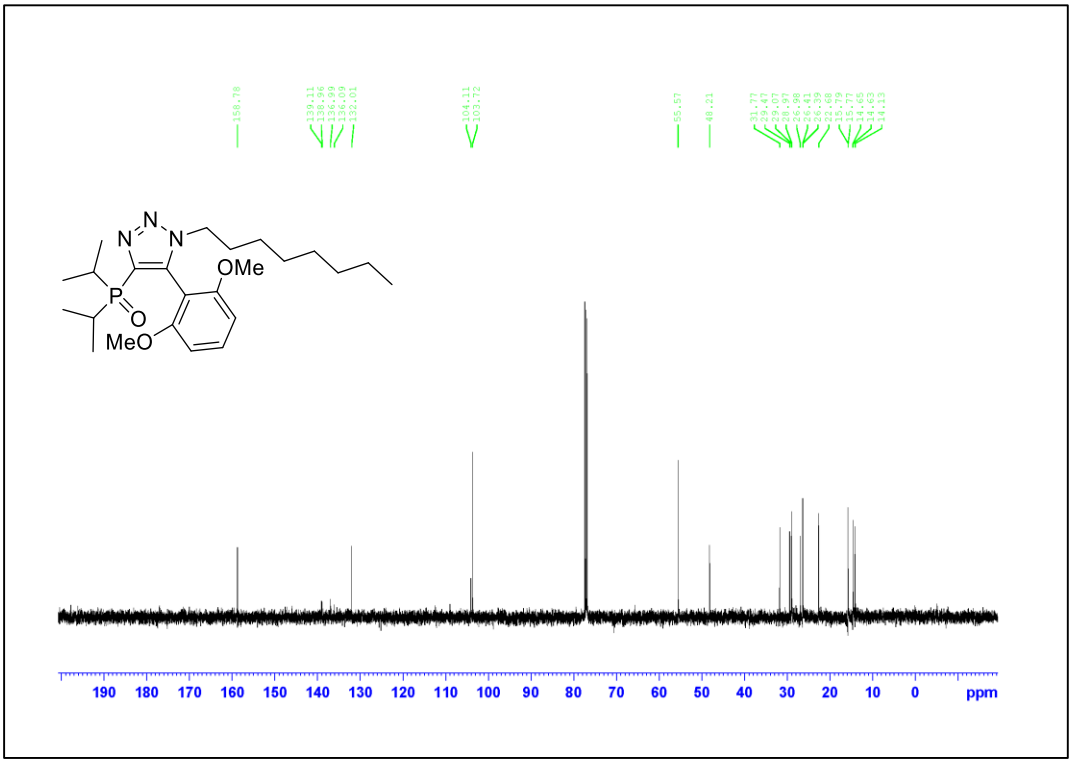

Figure A.252. ^{13}C NMR Spectrum of Compound **3.6i** (125 MHz, $CDCl_3$)

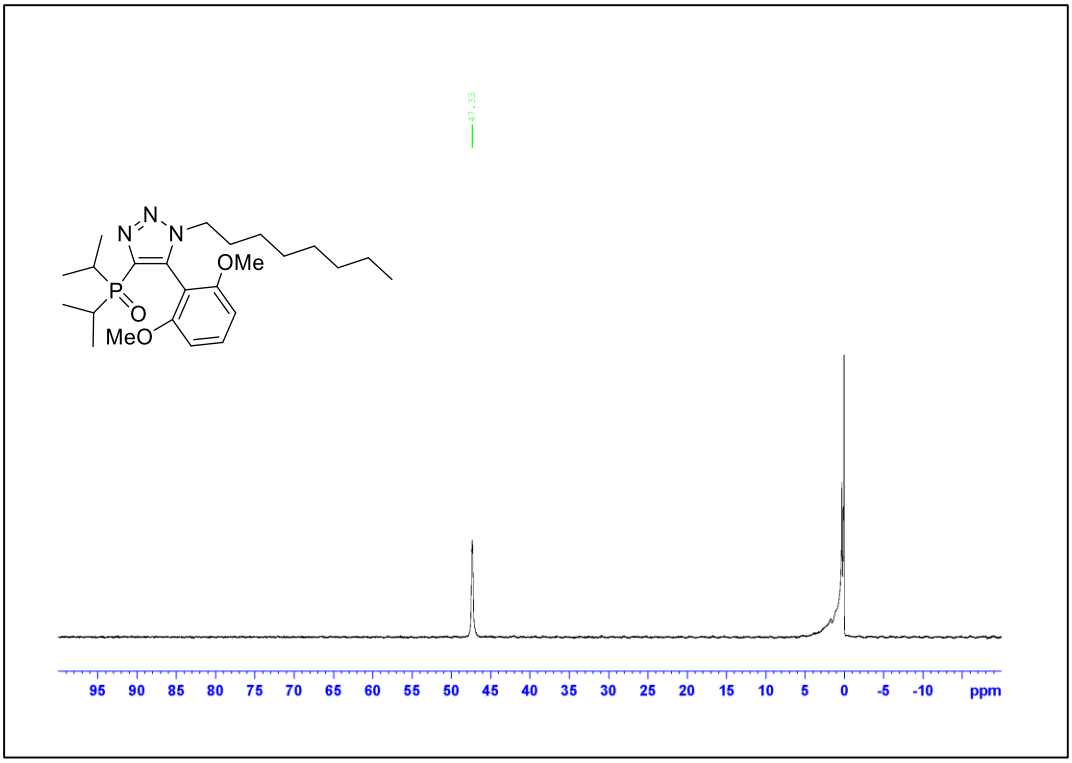

Figure A.253. ^{31}P NMR Spectrum of Compound **3.6i**

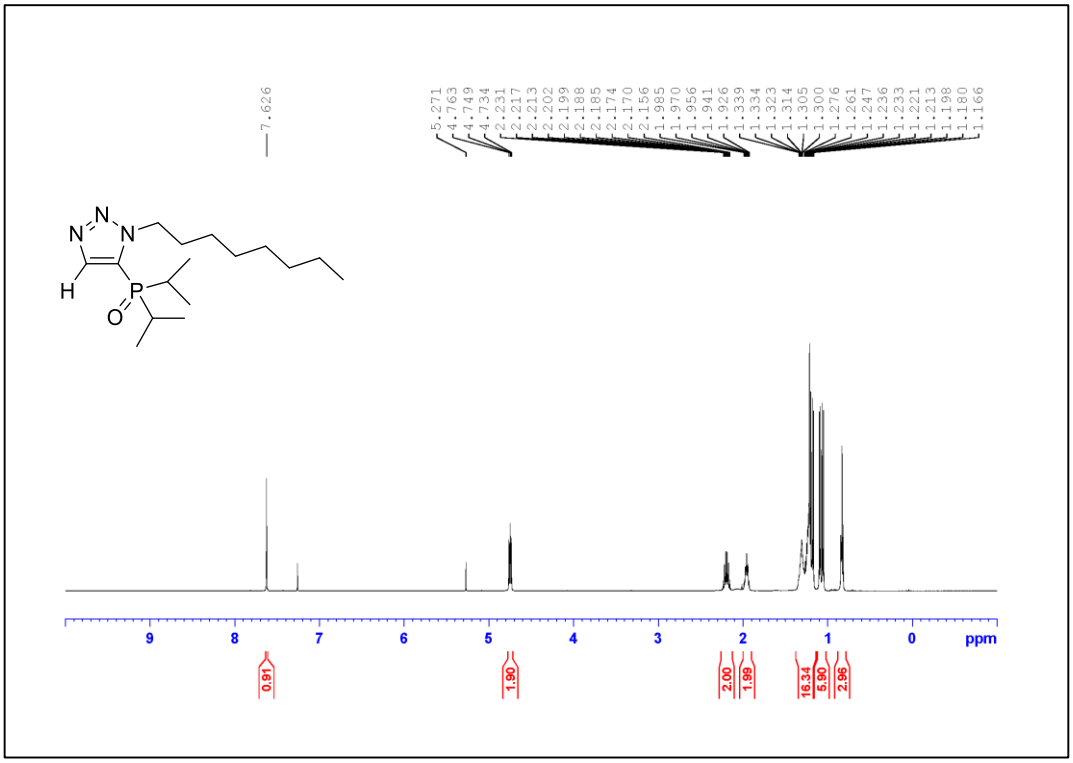

Figure A.254. ^{1}H NMR Spectrum of Compound **3.5j** (500 MHz, $CDCl_3$)

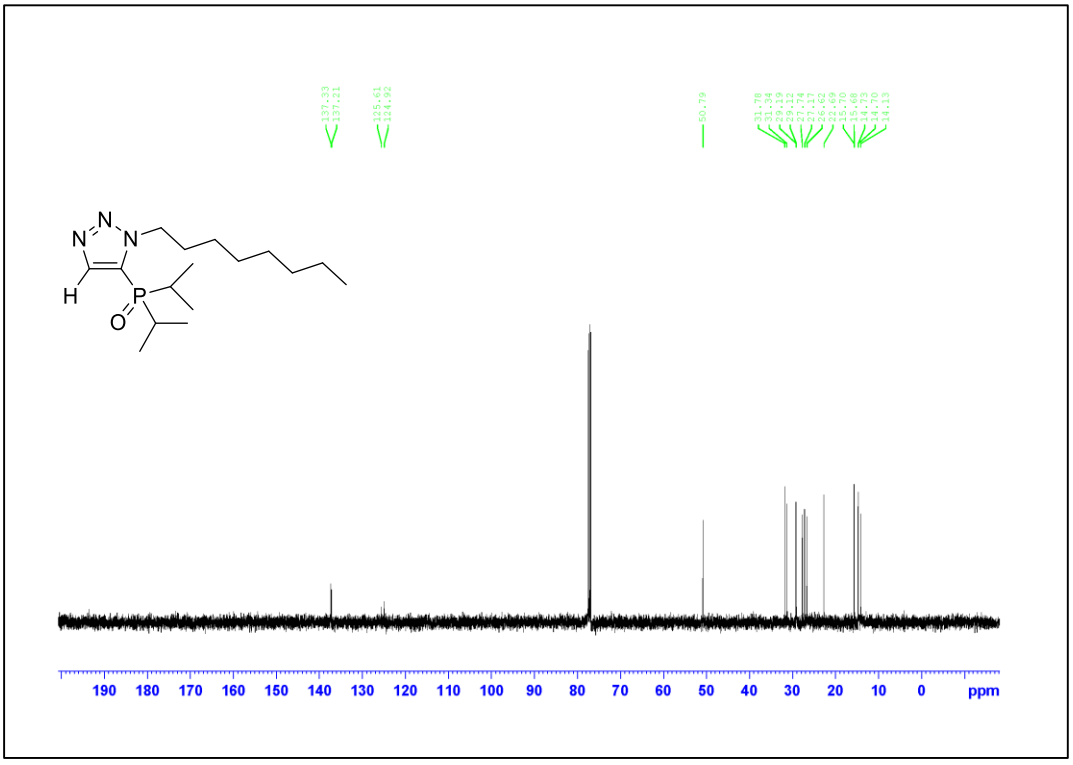

Figure A.255. ^{13}C NMR Spectrum of Compound **3.5j** (125 MHz, $CDCl_3$)

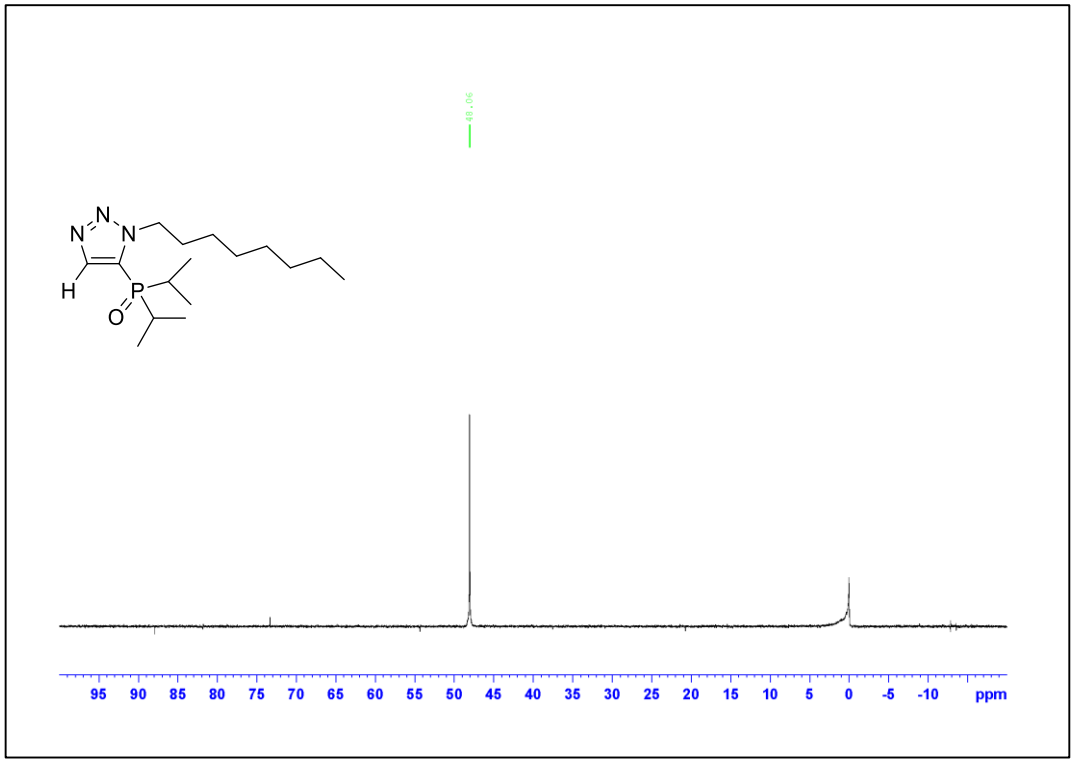

Figure A.256. ^{31}P NMR Spectrum of Compound **3.5j**

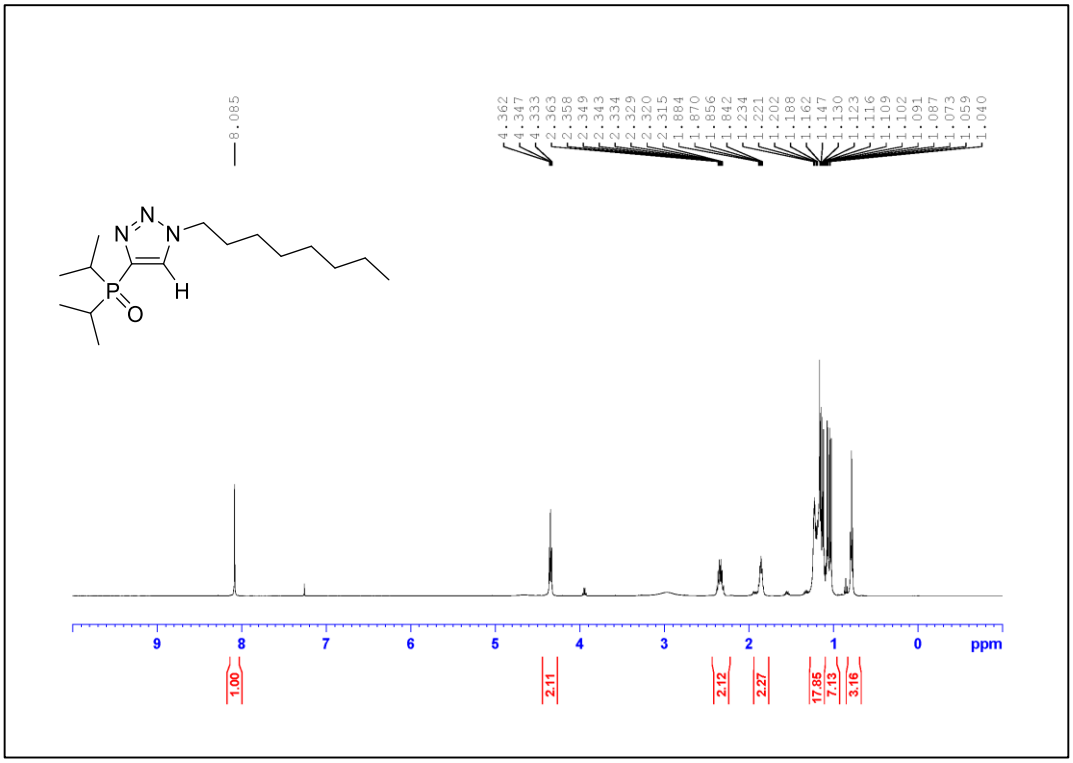

Figure A.257. ^{1}H NMR Spectrum of Compound **3.6j** (500 MHz, $CDCl_3$)

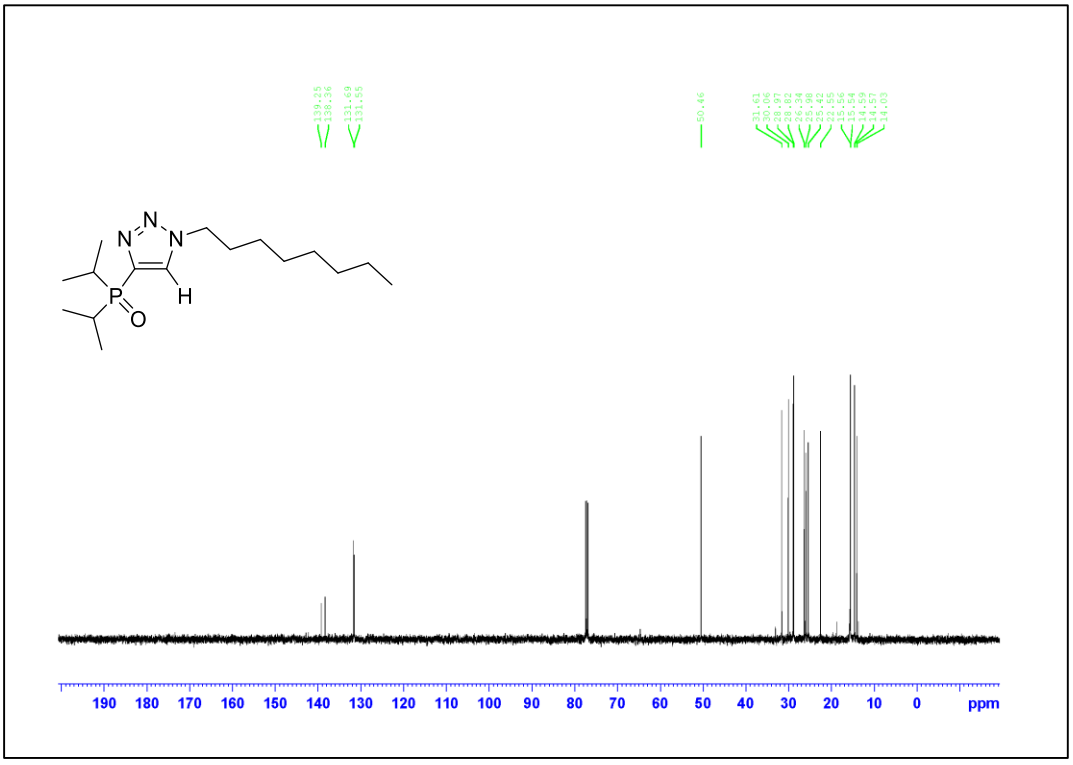

Figure A.258. ^{13}C NMR Spectrum of Compound **3.6j** (125 MHz, $CDCl_3$)

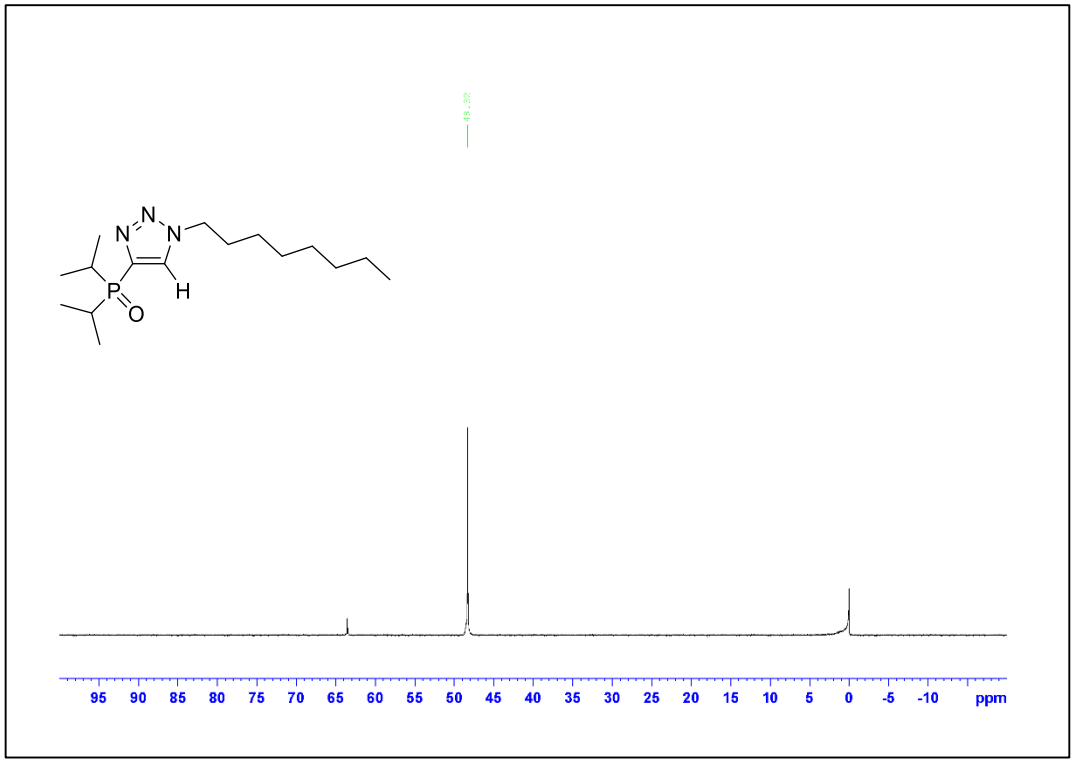

Figure A.259. ^{31}P NMR Spectrum of Compound **3.6j**

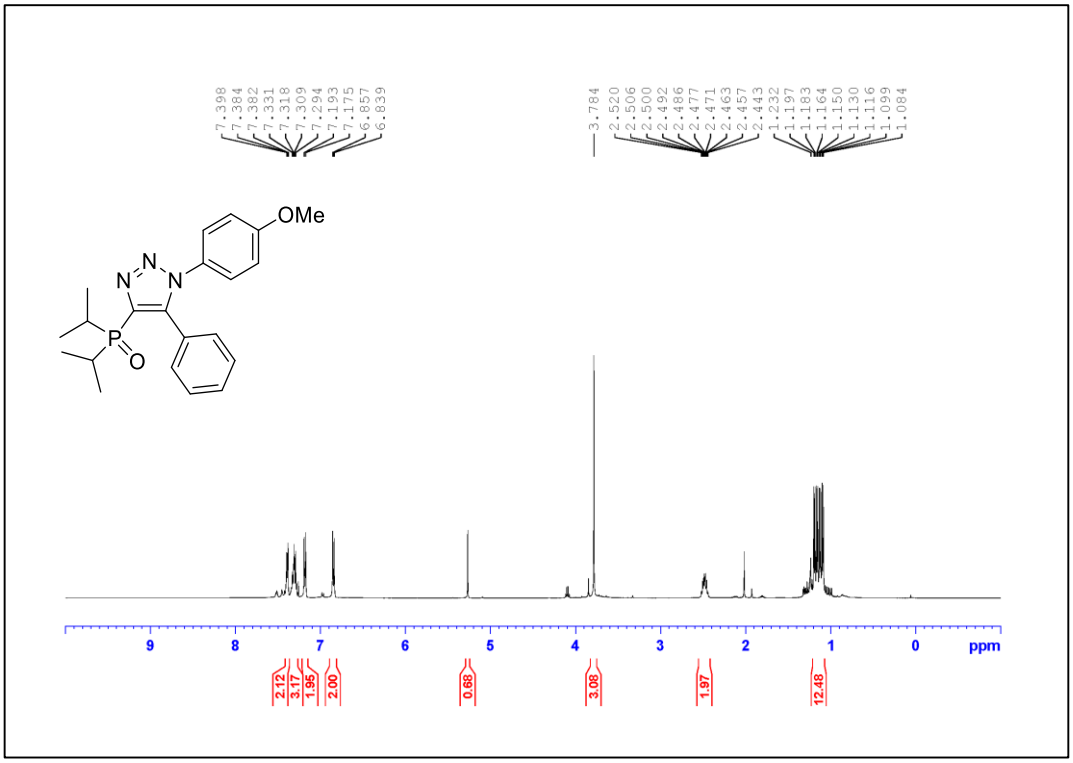

Figure A.260. ^{1}H NMR Spectrum of Compound **3.6k** (500 MHz, $CDCl_3$)

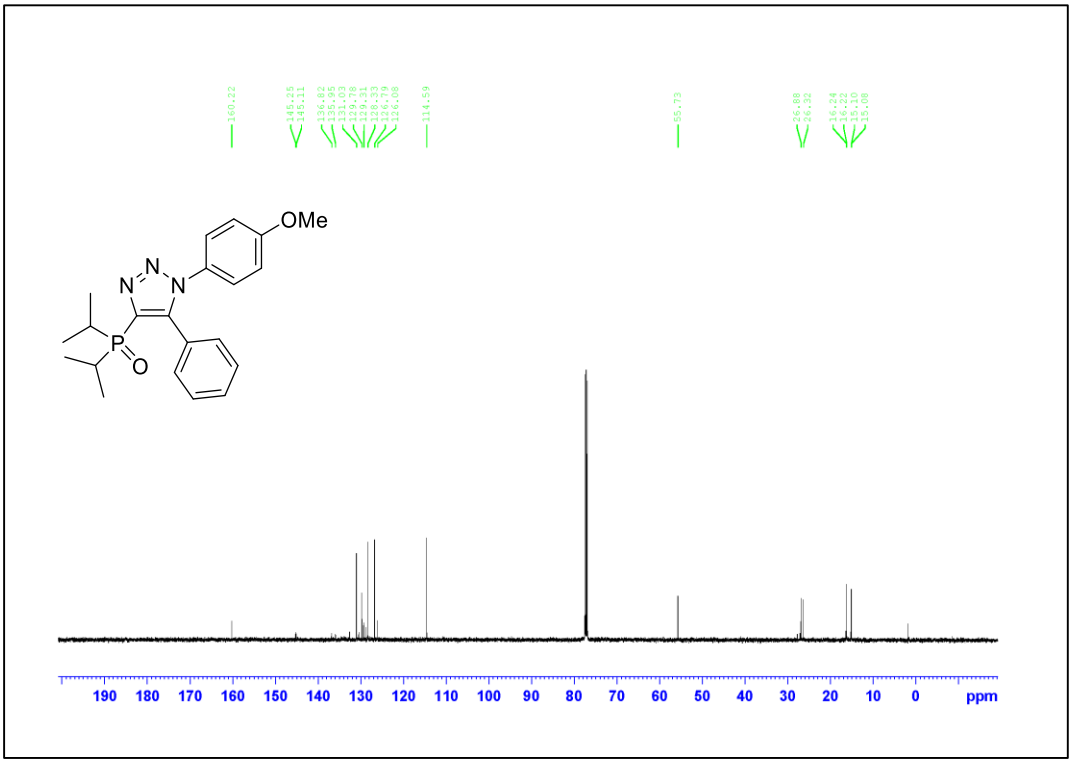

Figure A.261. ^{13}C NMR Spectrum of Compound **3.6k** (125 MHz, $CDCl_3$)

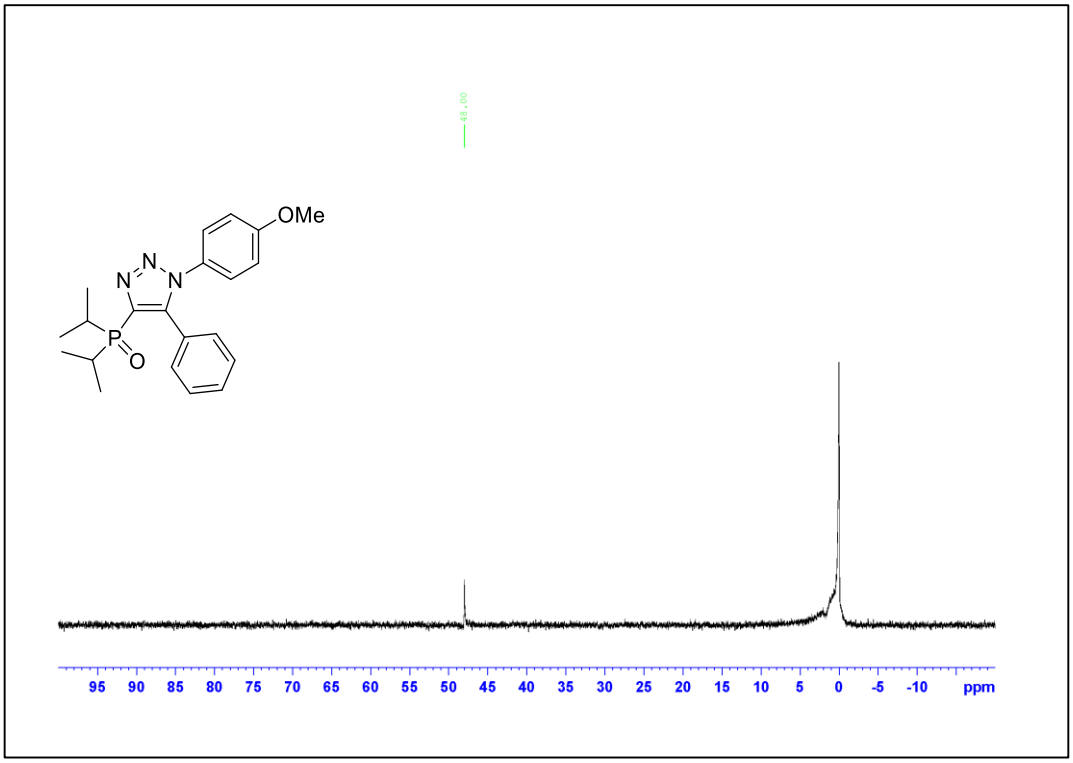

Figure A.262. ^{31}P NMR Spectrum of Compound **3.6k**

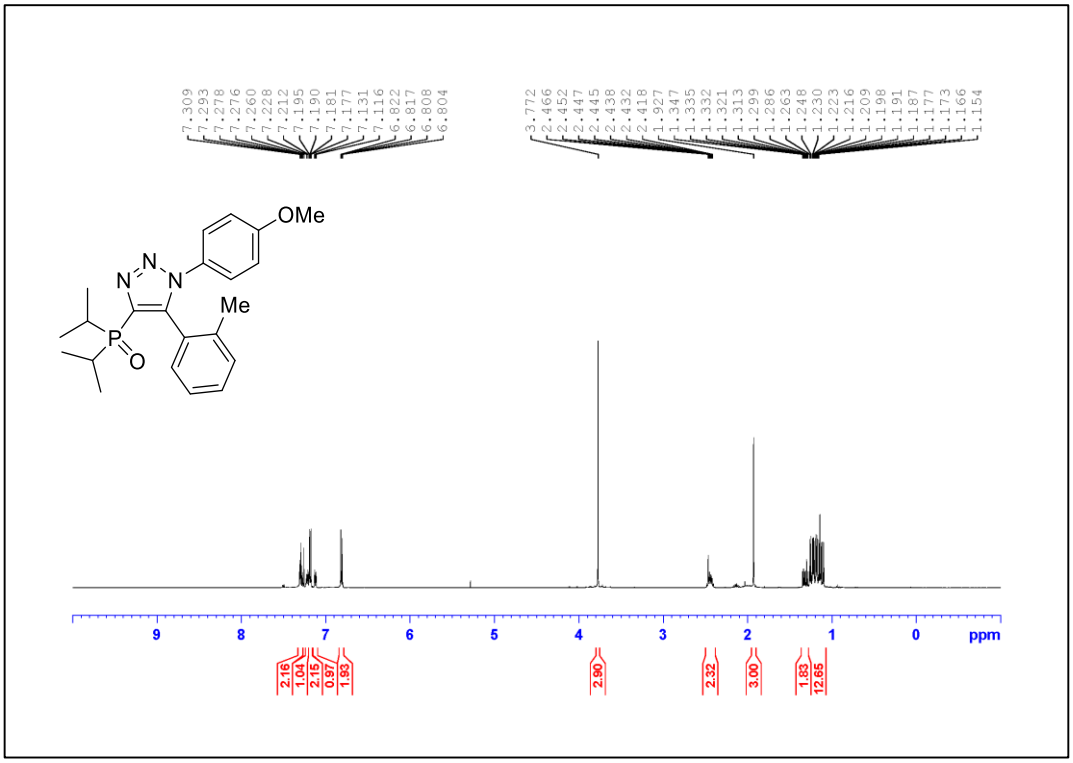

Figure A.263. ^{1}H NMR Spectrum of Compound **3.6l** (500 MHz, $CDCl_3$)

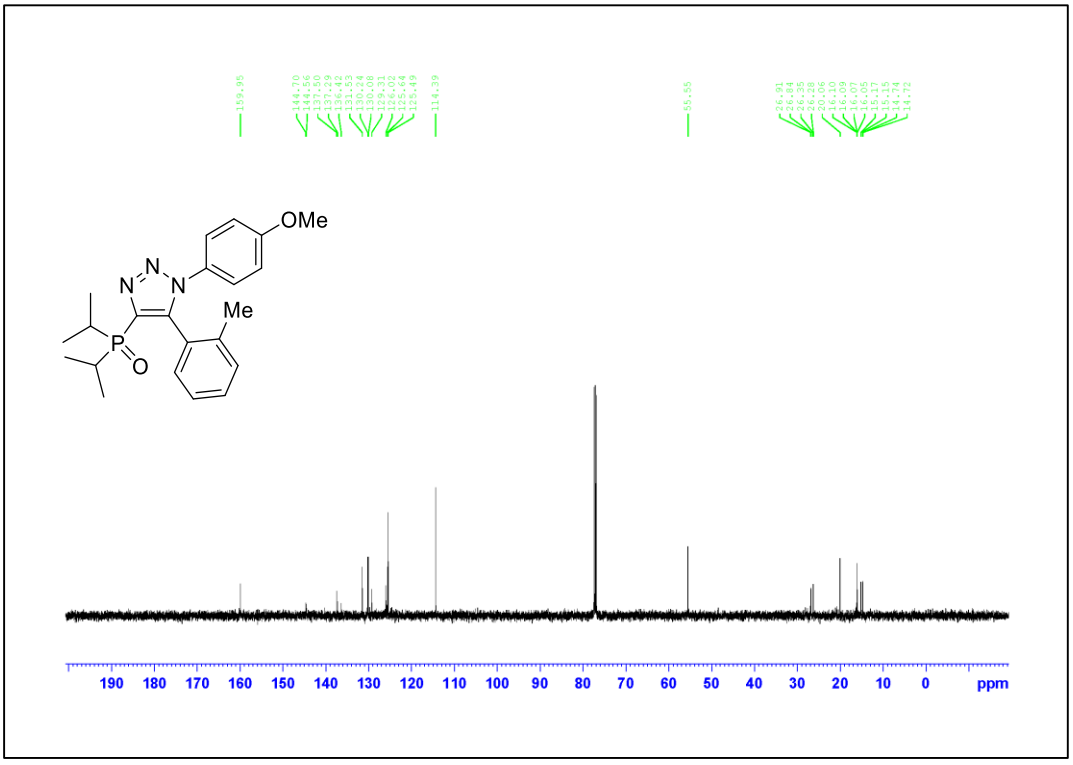

Figure A.264. ^{13}C NMR Spectrum of Compound **3.6l** (125 MHz, $CDCl_3$)

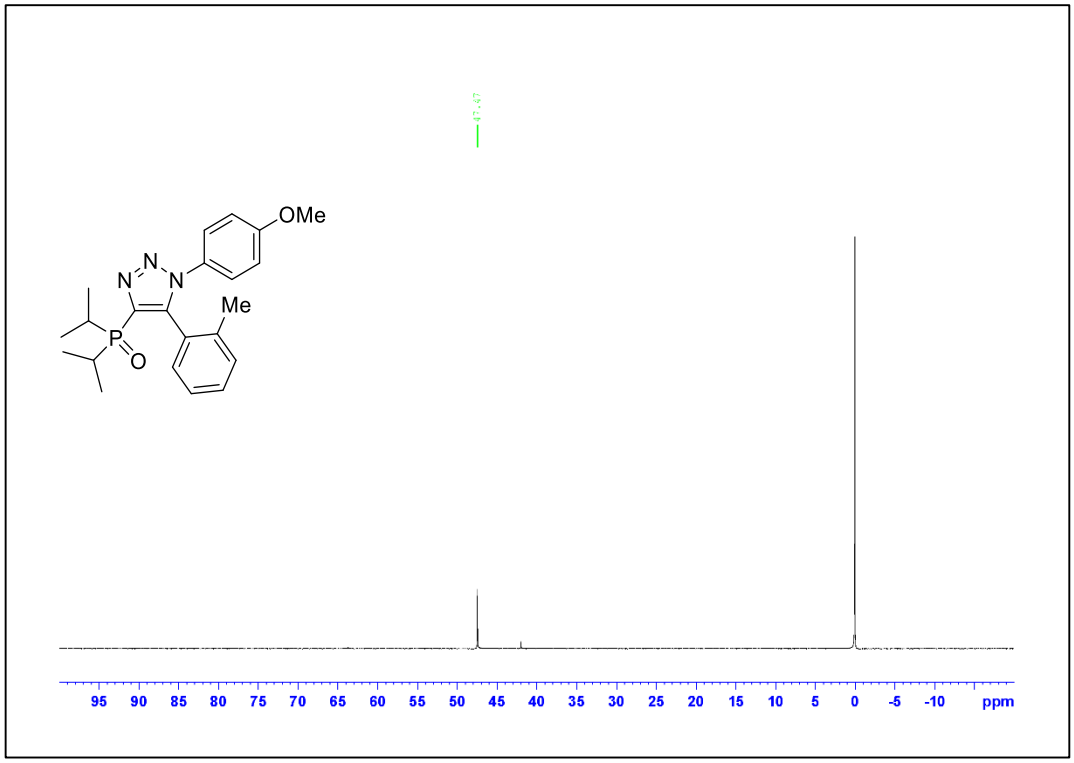

Figure A.265. ^{31}P NMR Spectrum of Compound **3.6l**

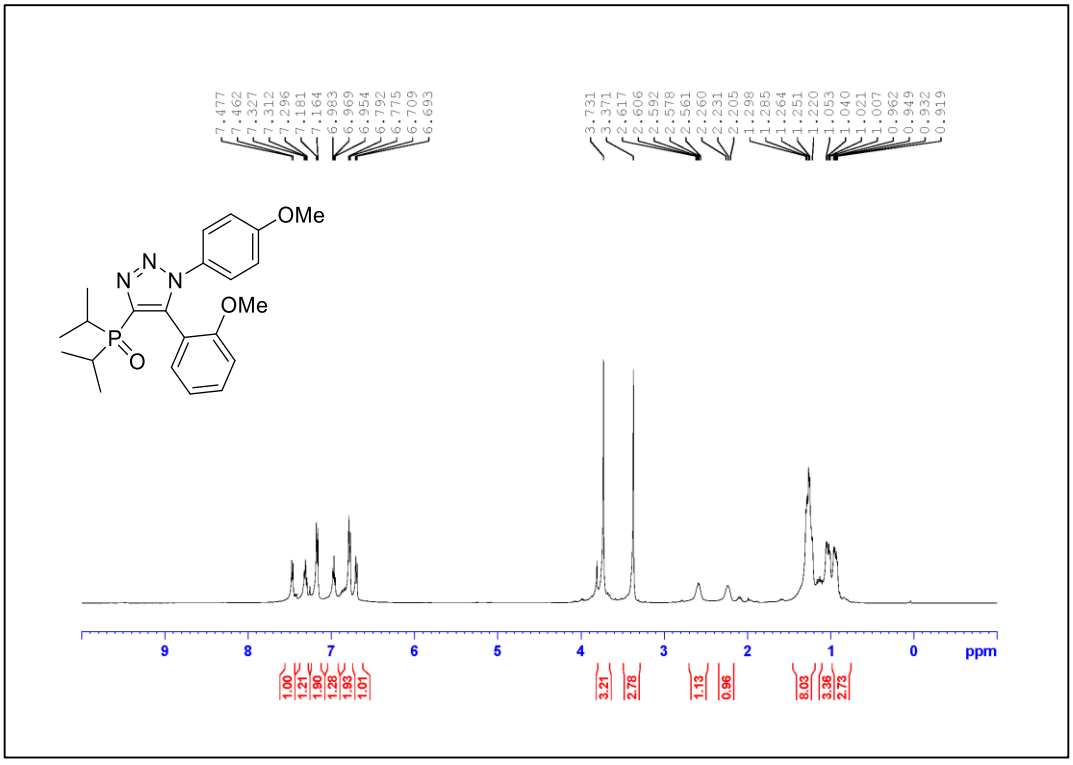

Figure A.266. ^{1}H NMR Spectrum of Compound **3.6m** (500 MHz, $CDCl_3$)

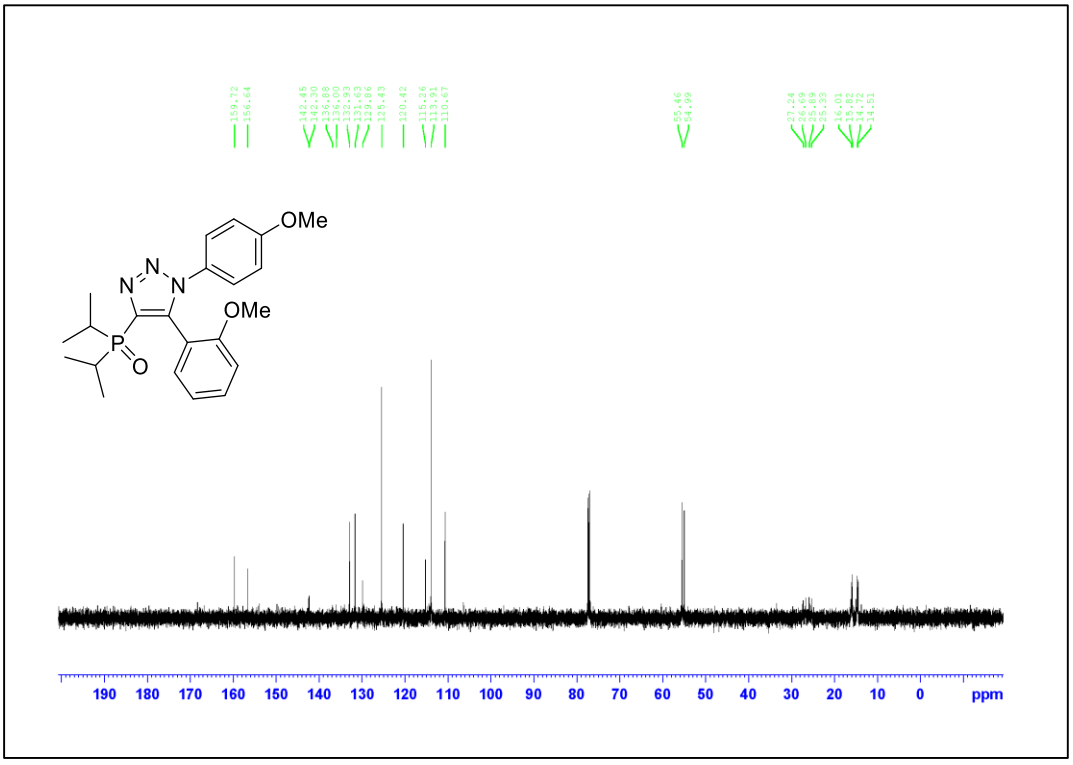

Figure A.267. ^{13}C NMR Spectrum of Compound **3.6m** (125 MHz, $CDCl_3$)

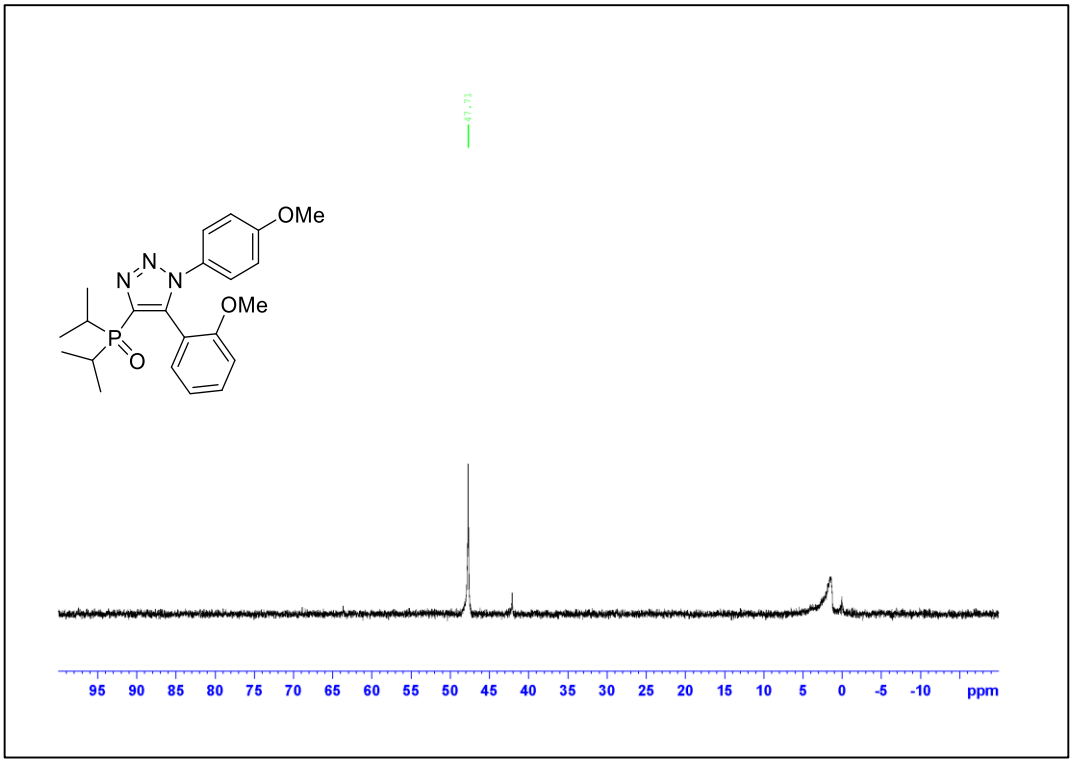

Figure A.268. ^{31}P NMR Spectrum of Compound **3.6m**

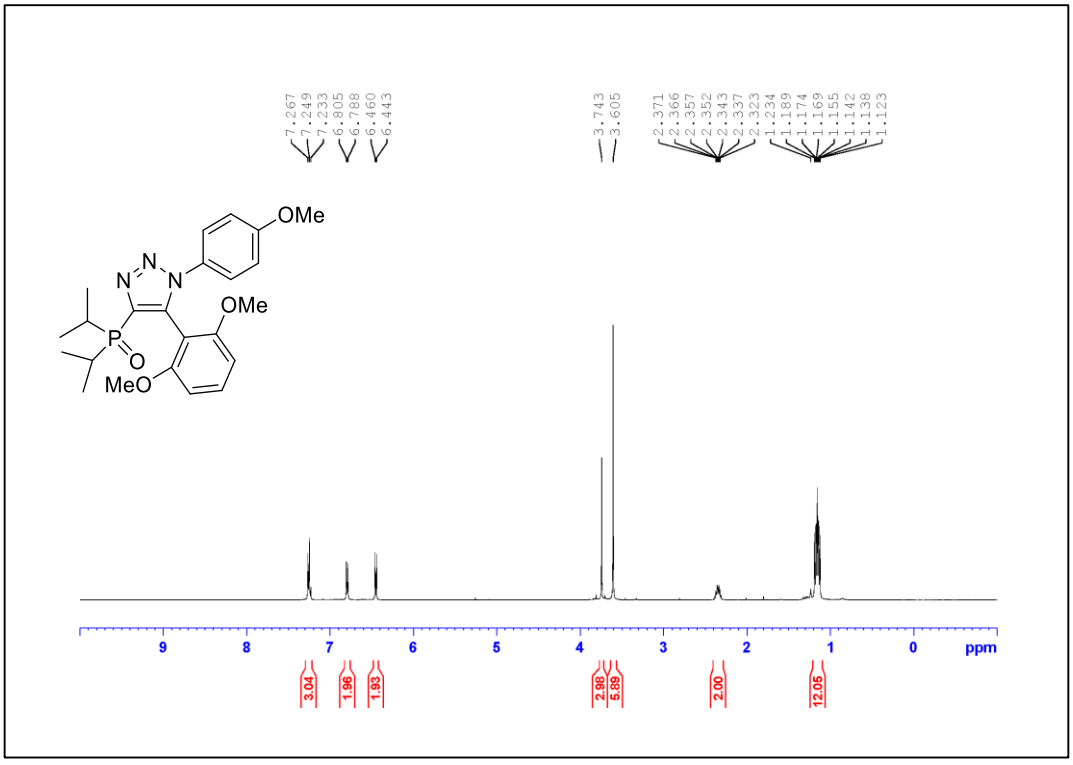

Figure A.269. ^{1}H NMR Spectrum of Compound **3.6n** (500 MHz, $CDCl_3$)

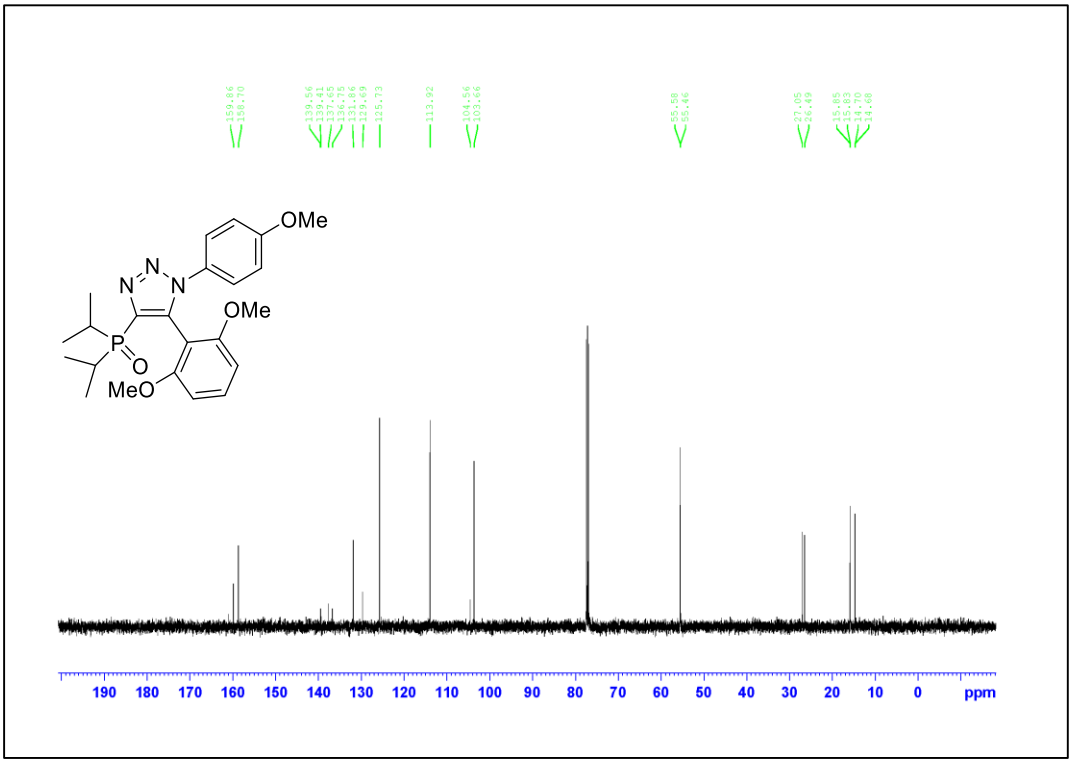

Figure A.270. ^{13}C NMR Spectrum of Compound **3.6n** (125 MHz, $CDCl_3$)

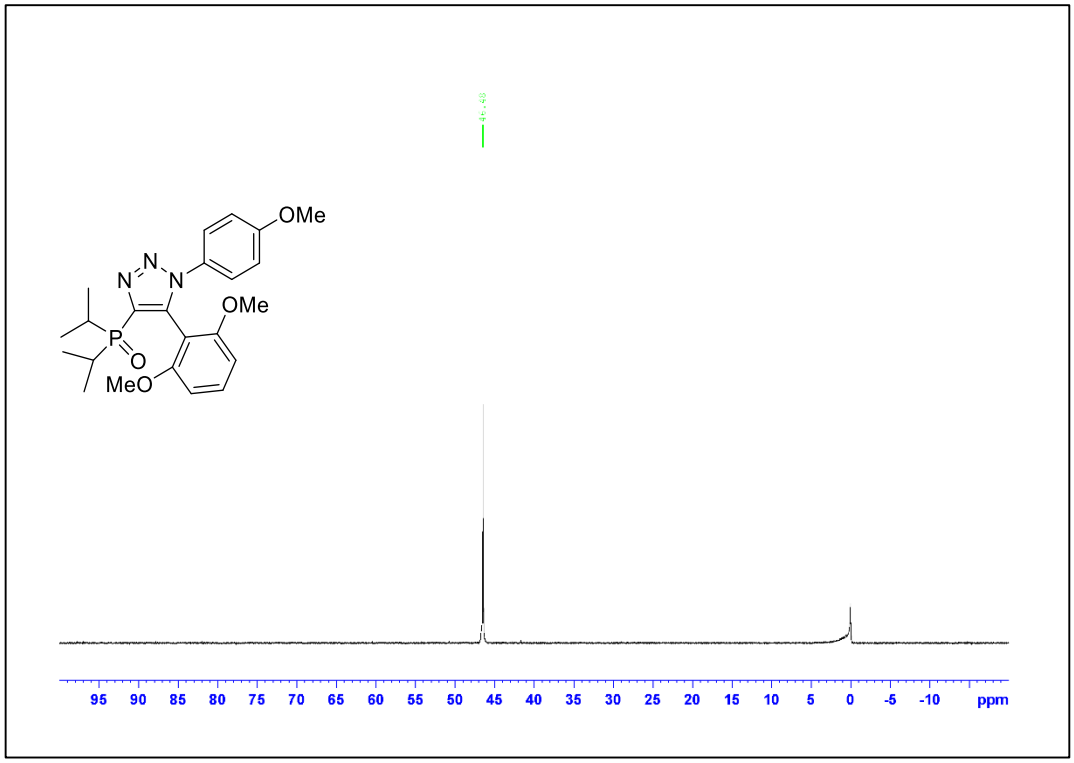

Figure A.271. ^{31}P NMR Spectrum of Compound **3.6n**

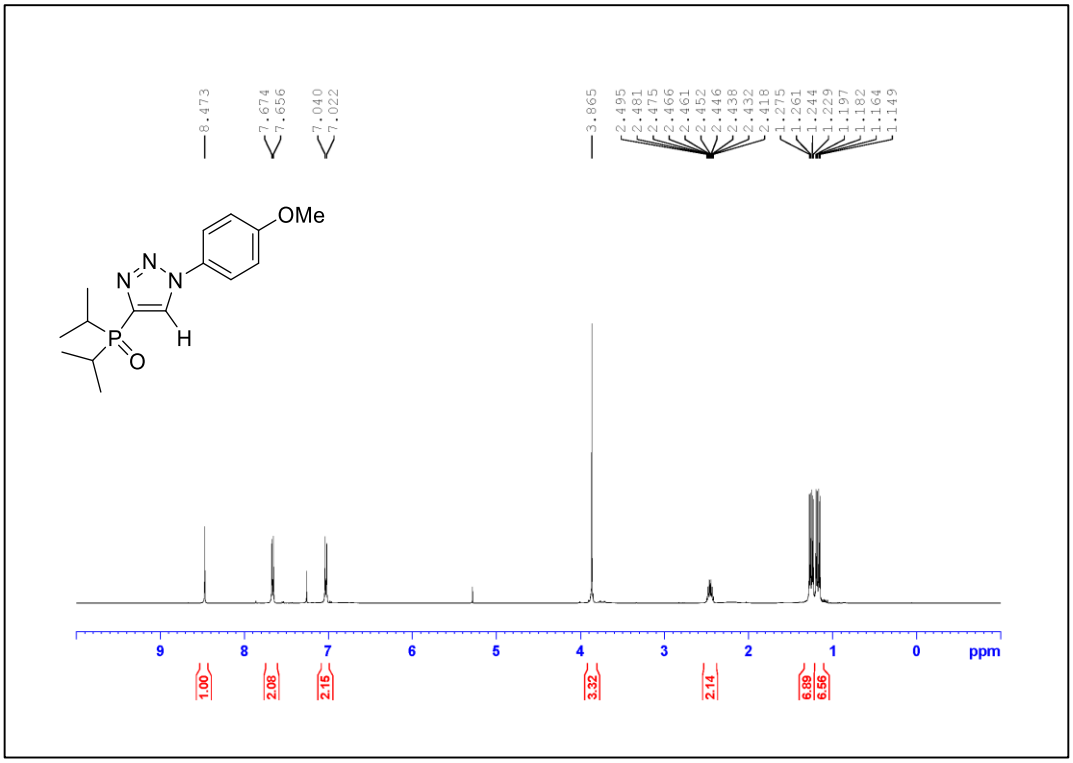

Figure A.272. ^{1}H NMR Spectrum of Compound **3.6o** (500 MHz, $CDCl_3$)

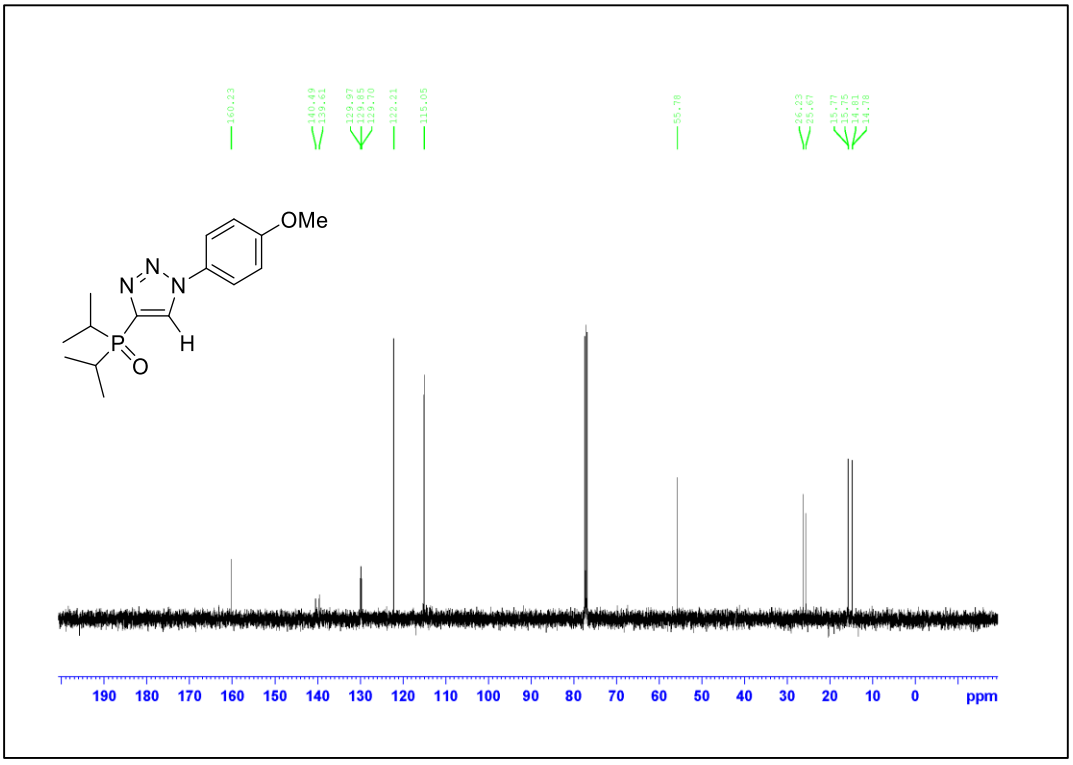

Figure A.273. ^{13}C NMR Spectrum of Compound **3.6o** (125 MHz, $CDCl_3$)

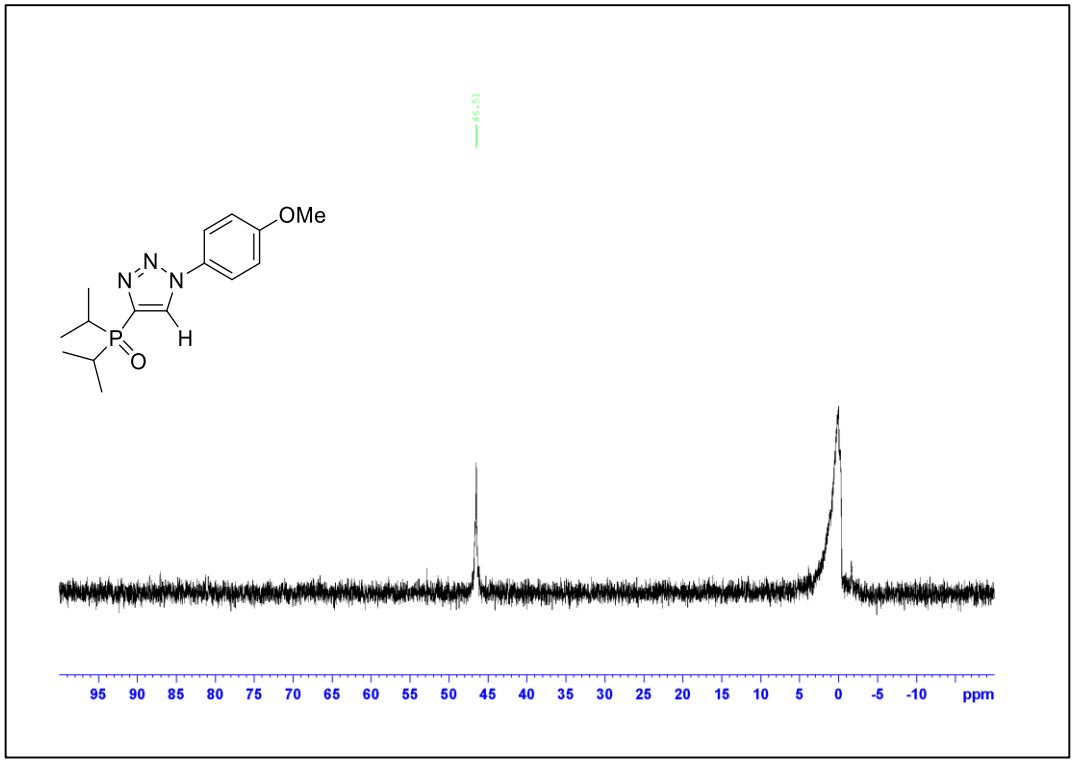

Figure A.274. ^{31}P NMR Spectrum of Compound **3.6o**

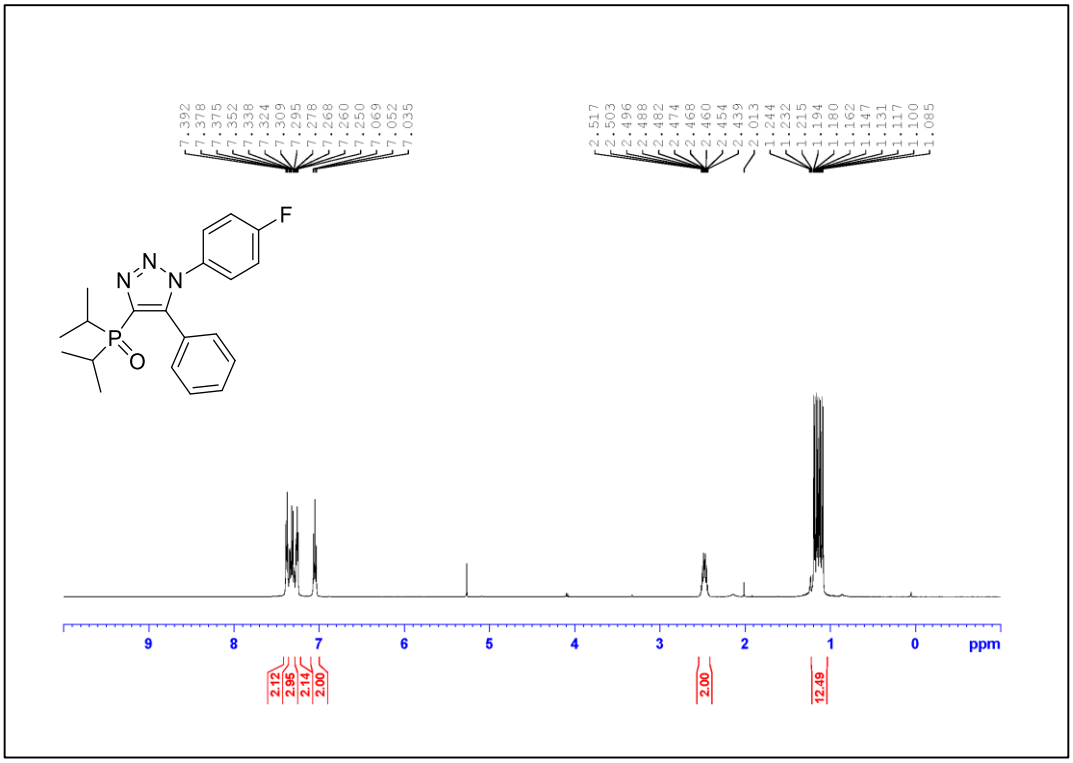

Figure A.275. ^{1}H NMR Spectrum of Compound **3.6p** (500 MHz, $CDCl_3$)

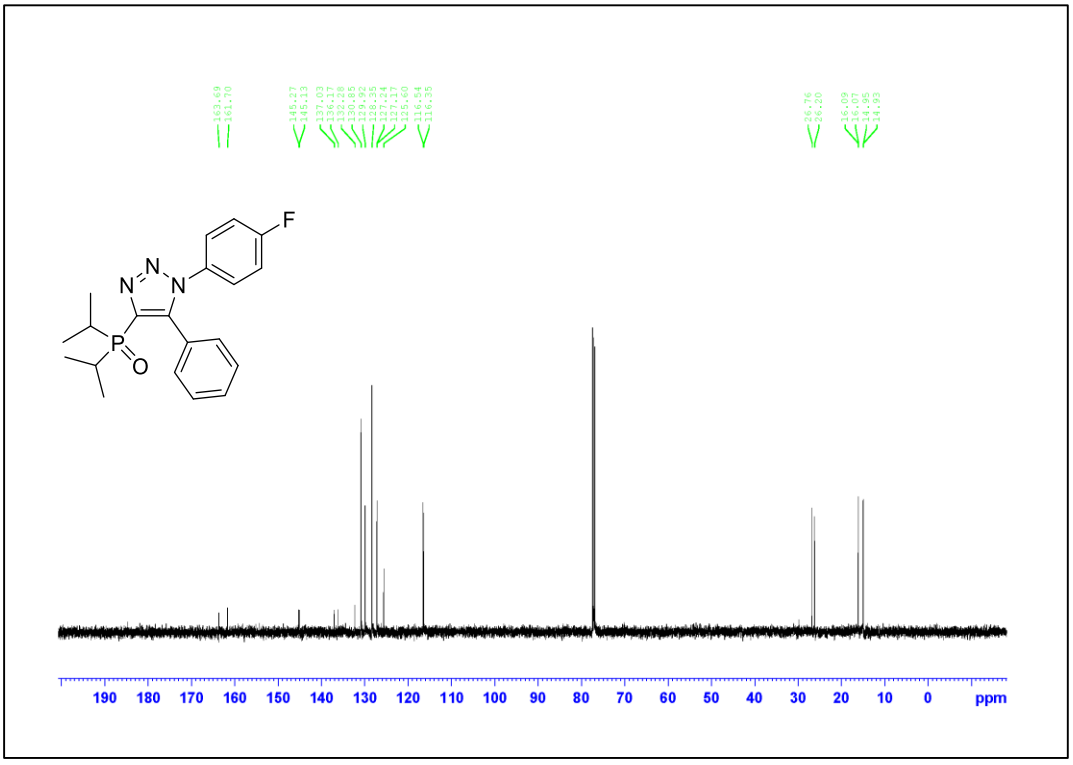

Figure A.276. ^{13}C NMR Spectrum of Compound **3.6p** (125 MHz, $CDCl_3$)

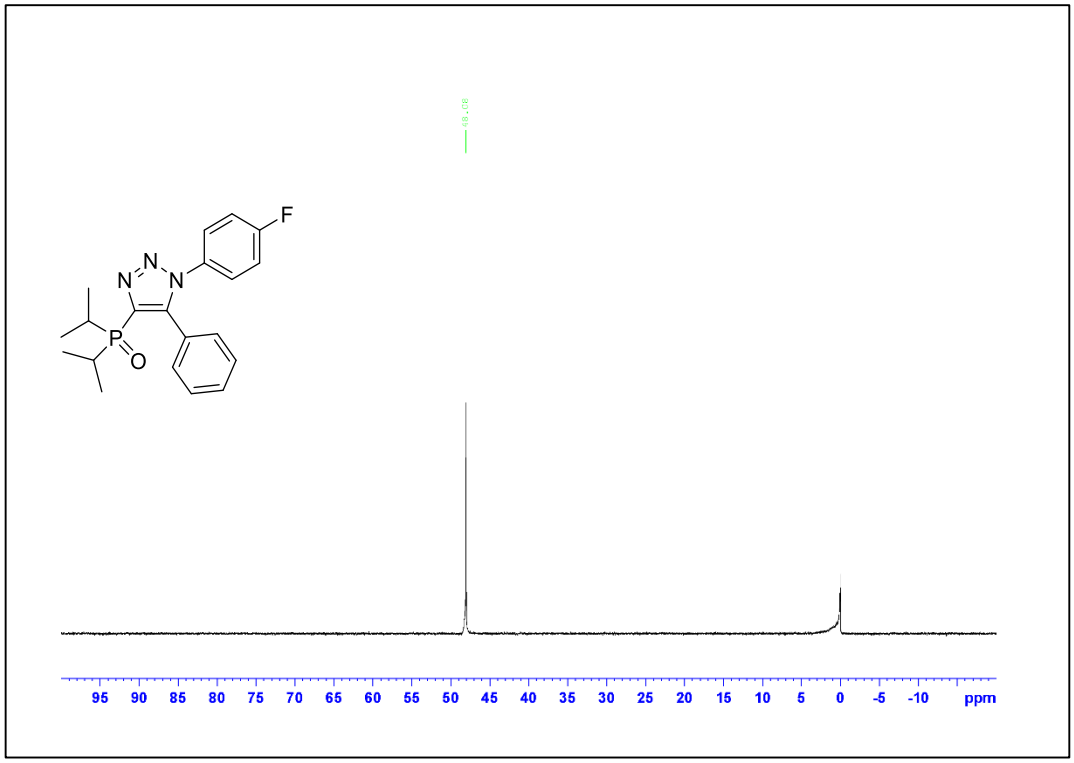

Figure A.277. ^{31}P NMR Spectrum of Compound **3.6p**

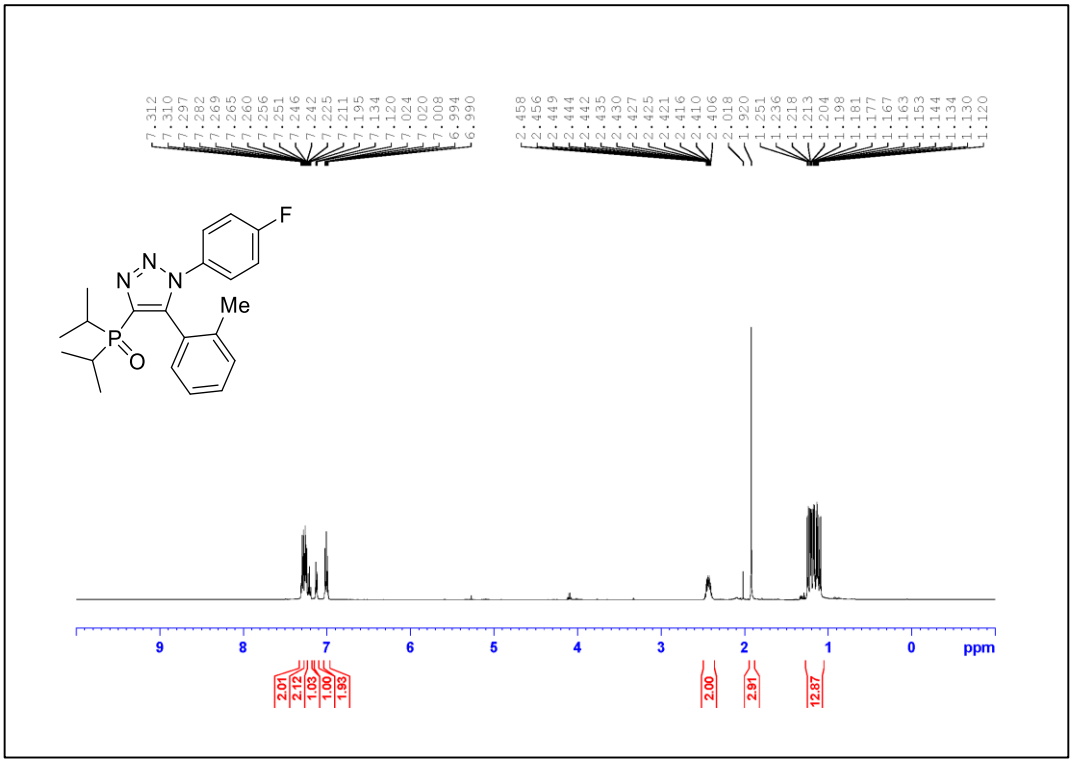

Figure A.278. ^{1}H NMR Spectrum of Compound **3.6q** (500 MHz, $CDCl_3$)

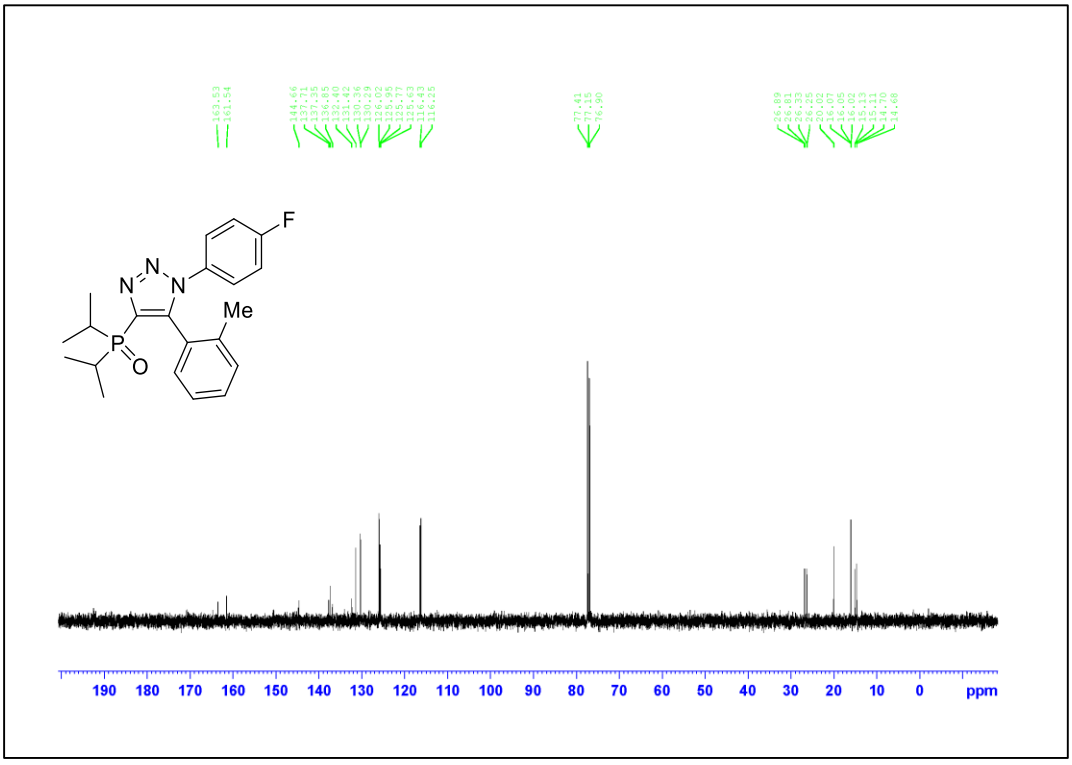

Figure A.279. ^{13}C NMR Spectrum of Compound **3.6q** (125 MHz, $CDCl_3$)

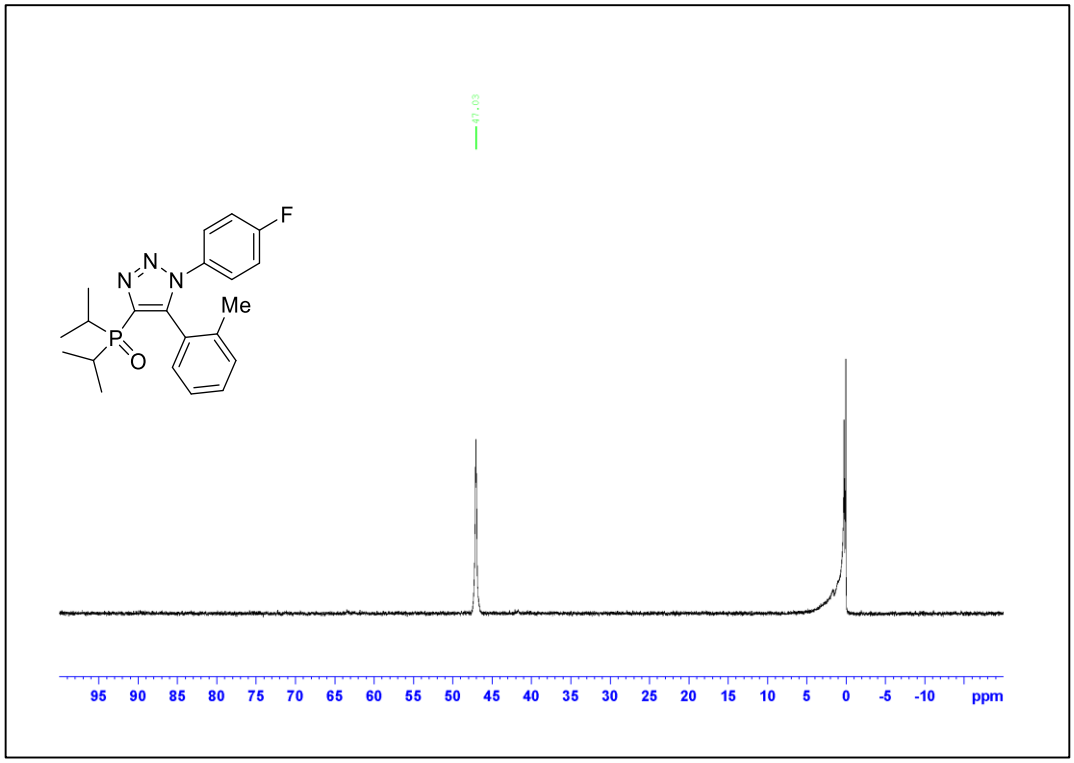

Figure A.280. ^{31}P NMR Spectrum of Compound **3.6q**

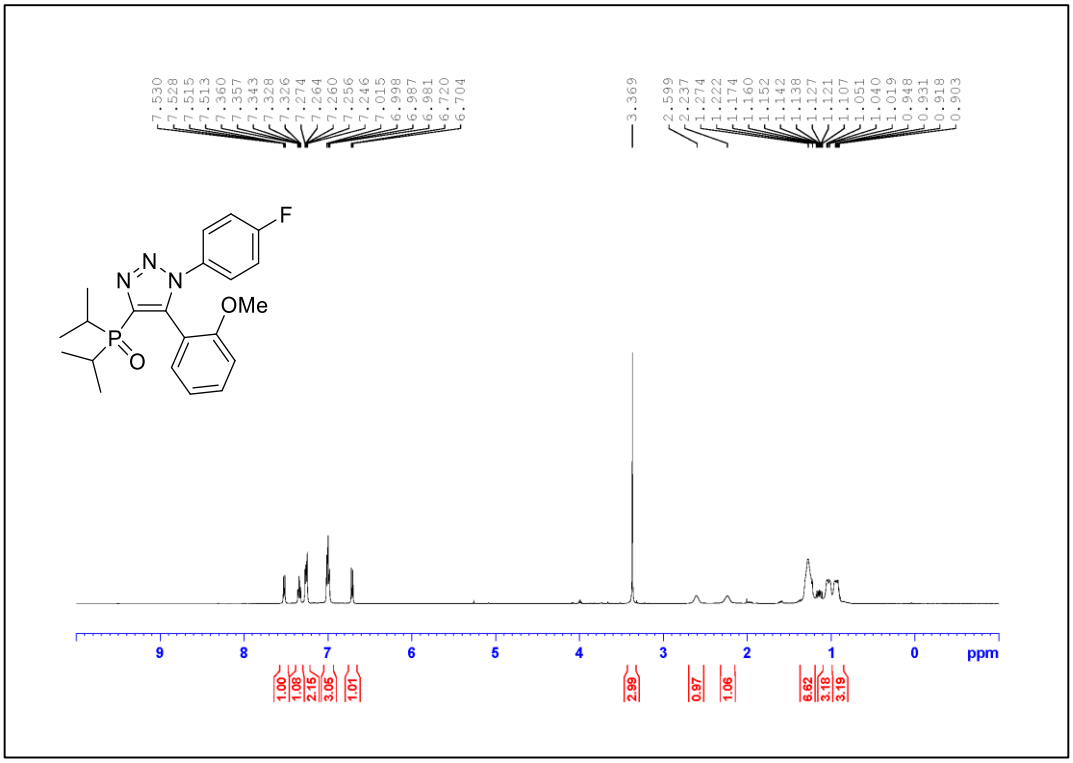

Figure A.281. ^{1}H NMR Spectrum of Compound **3.6r** (500 MHz, $CDCl_3$)

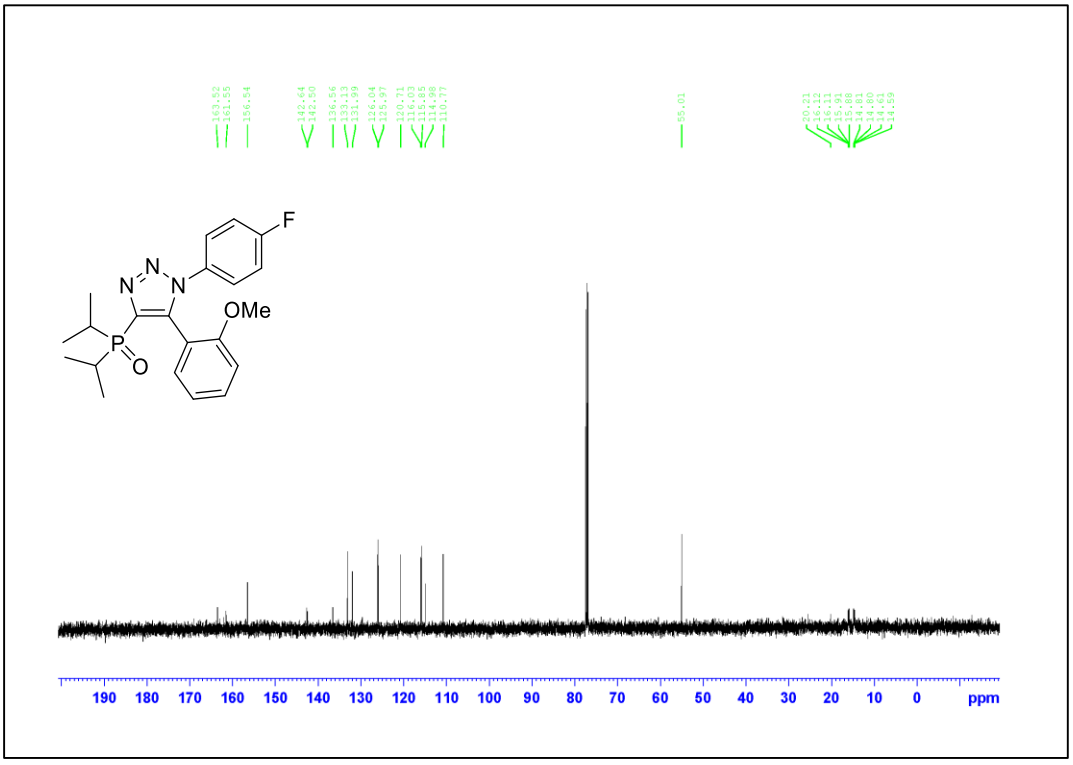

Figure A.282. ^{13}C NMR Spectrum of Compound **3.6r** (125 MHz, $CDCl_3$)

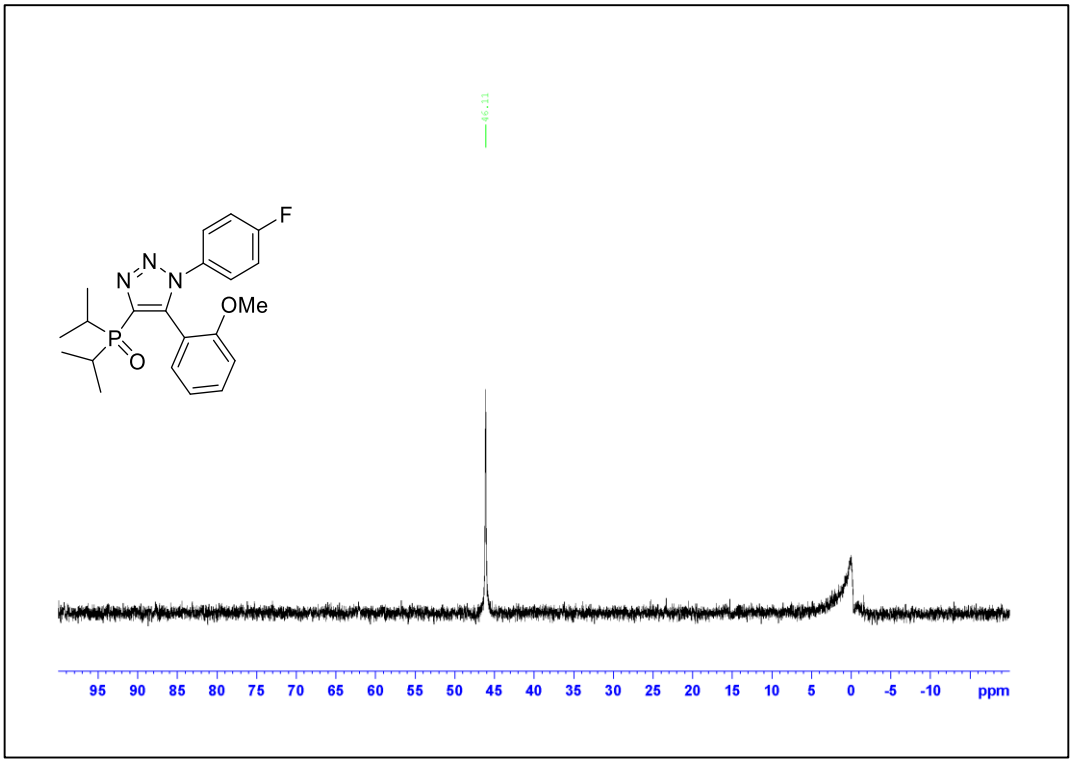

Figure A.283. ^{31}P NMR Spectrum of Compound **3.6r**

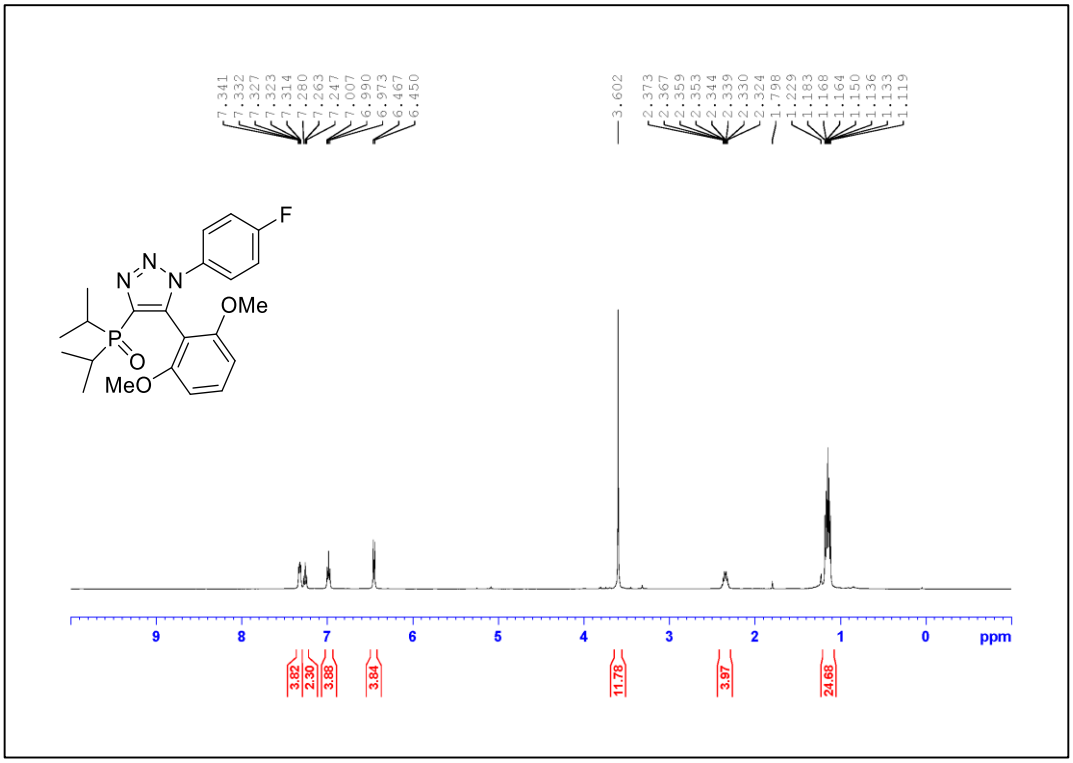

Figure A.284. ^{1}H NMR Spectrum of Compound **3.6s** (500 MHz, $CDCl_3$)

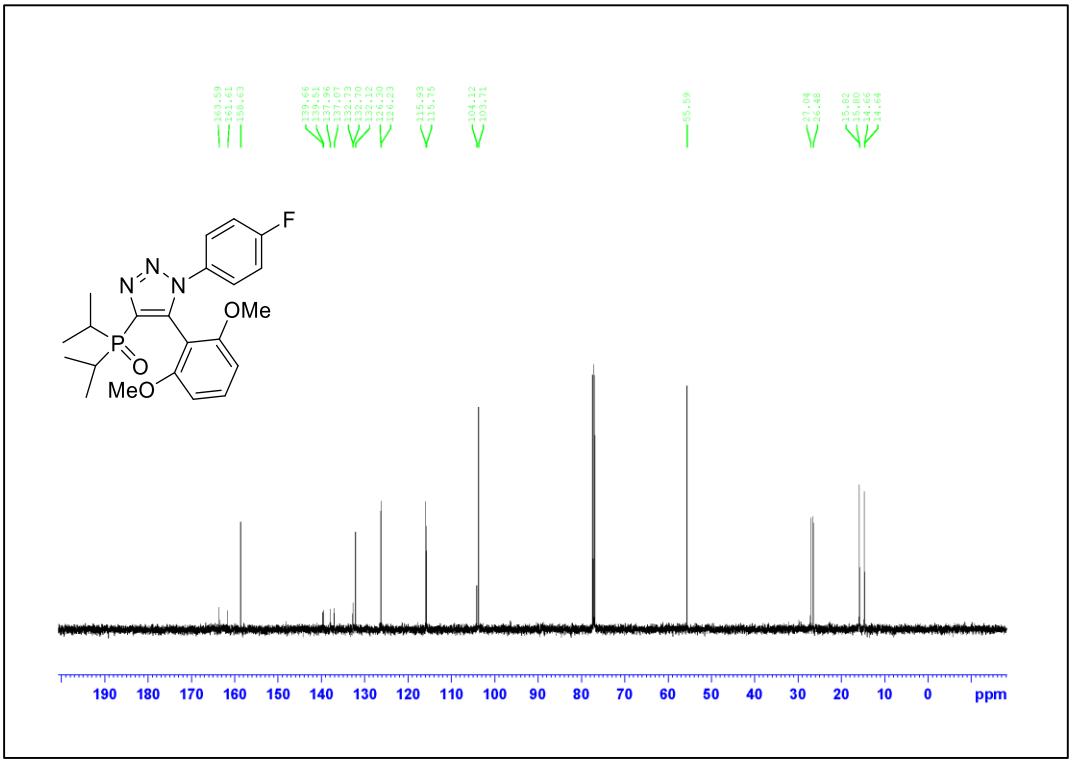

Figure A.285. ^{13}C NMR Spectrum of Compound **3.6s** (125 MHz, $CDCl_3$)

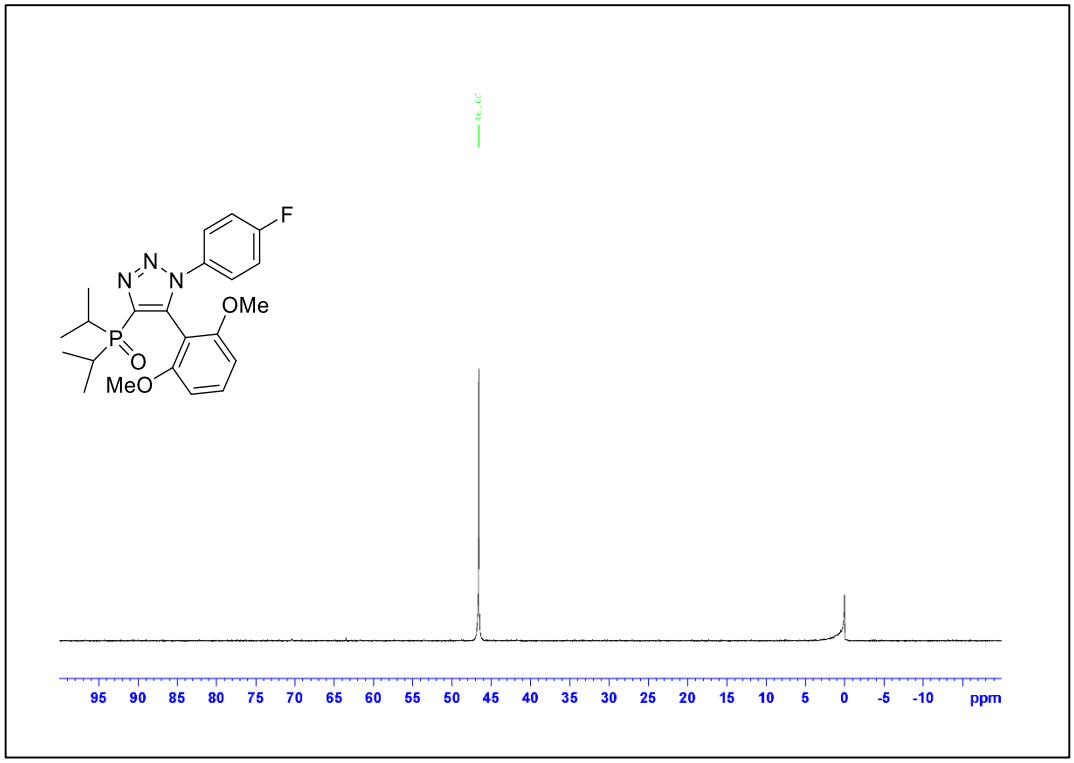

Figure A.286. ^{31}P NMR Spectrum of Compound **3.6s**

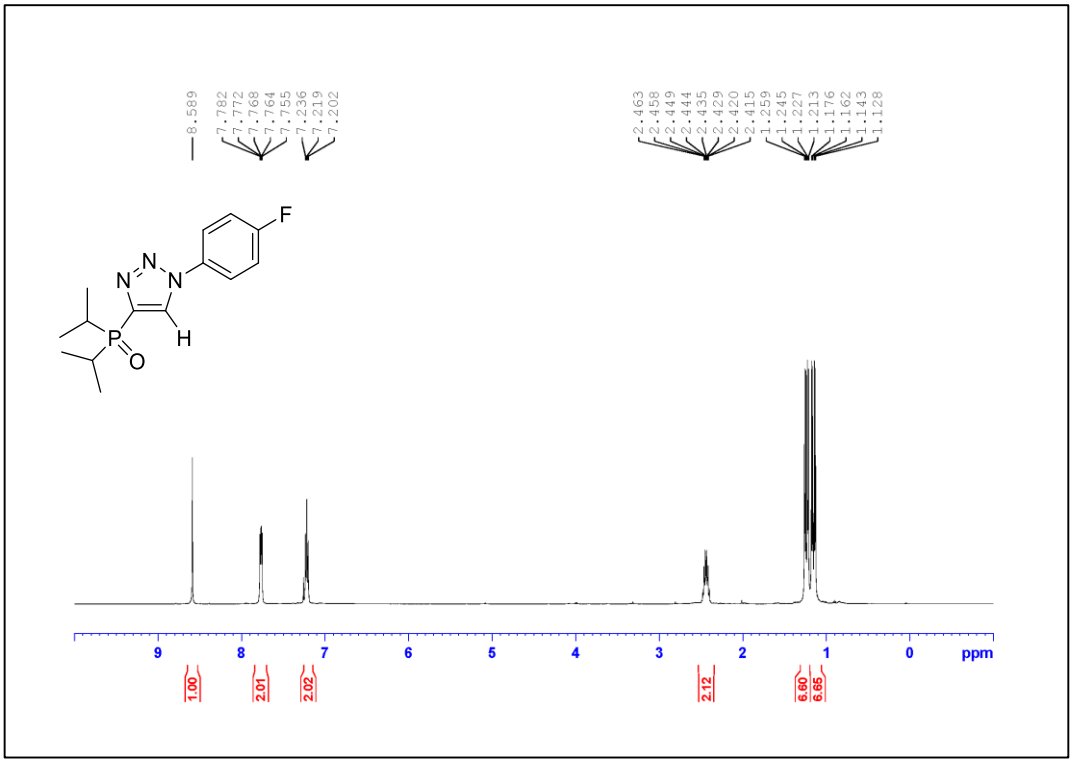

Figure A.287. ^{1}H NMR Spectrum of Compound **3.6t** (500 MHz, $CDCl_3$)

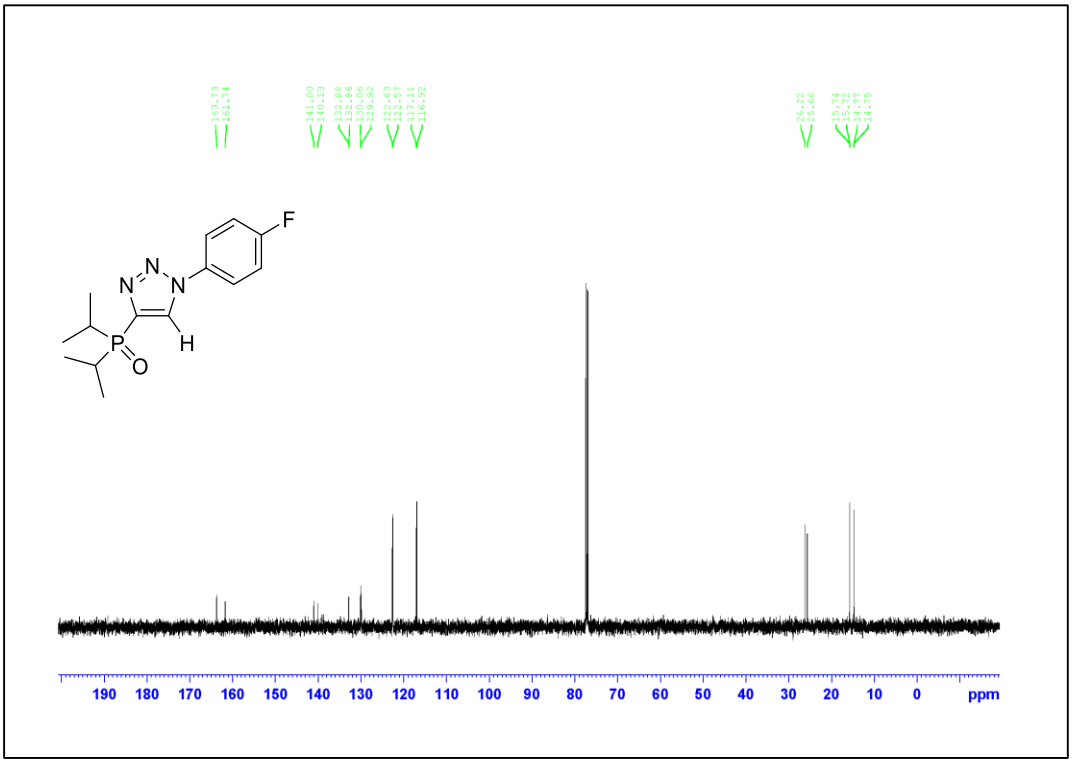

Figure A.288. ^{13}C NMR Spectrum of Compound **3.6t** (125 MHz, $CDCl_3$)

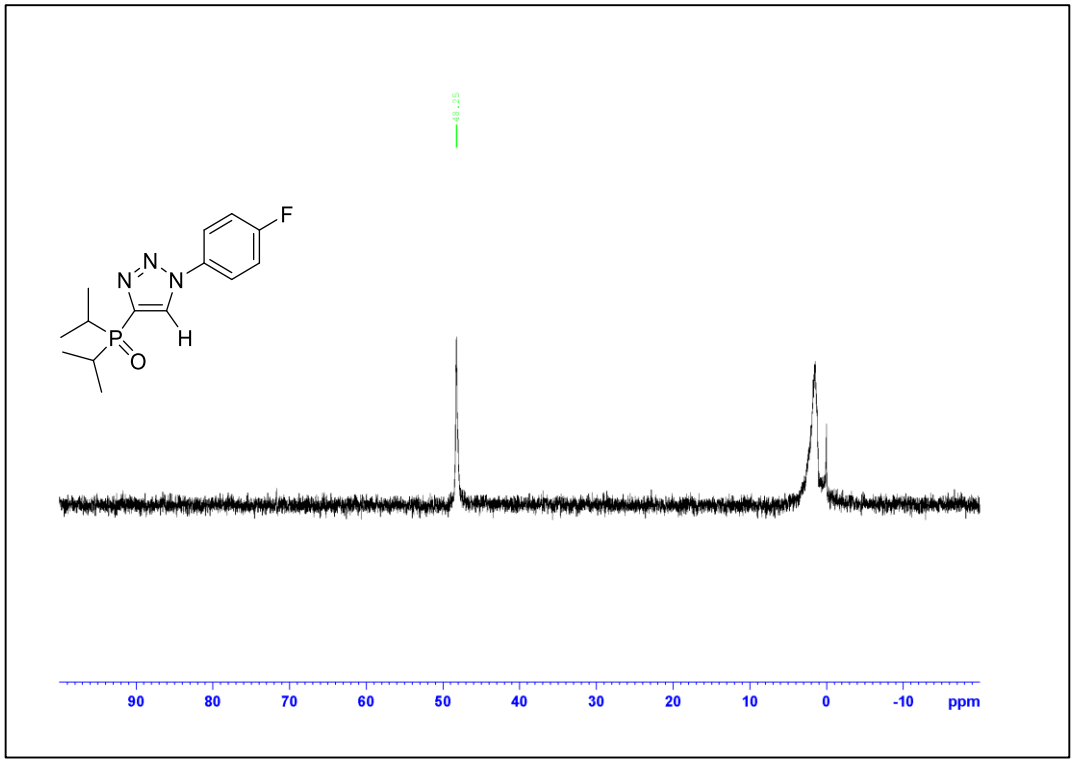

Figure A.289. ^{31}P NMR Spectrum of Compound **3.6t**

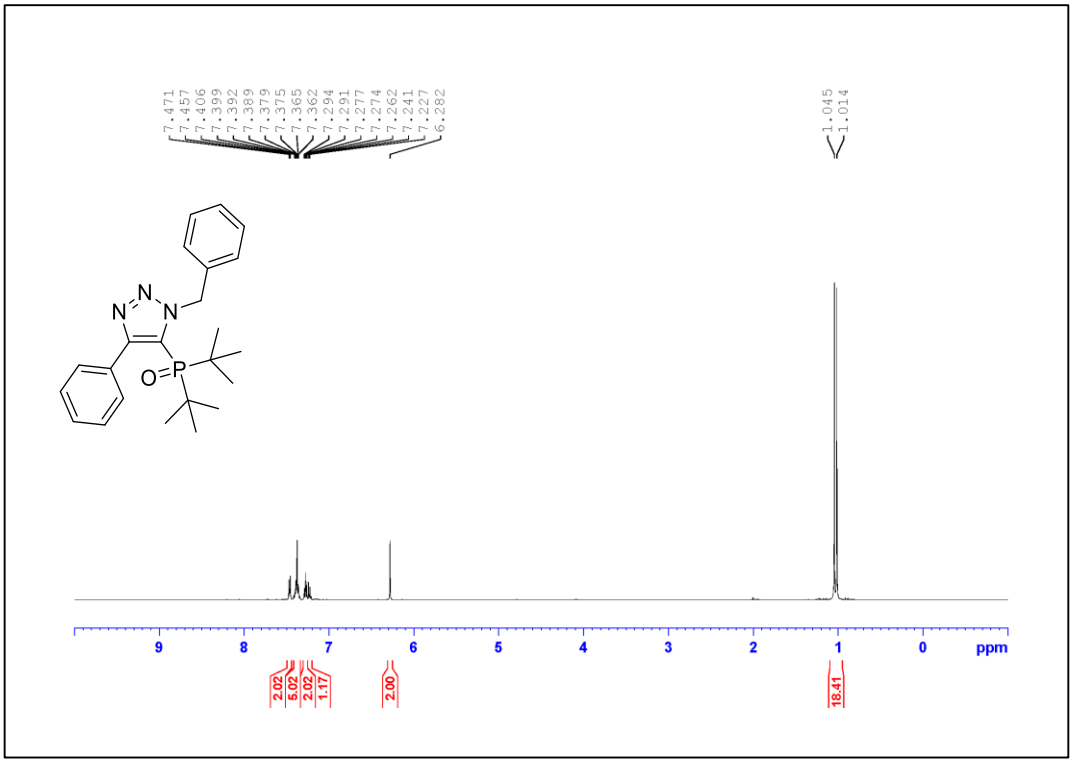

Figure A.290. ^{1}H NMR Spectrum of Compound **3.5a_*t*Bu** (500 MHz, $CDCl_3$)

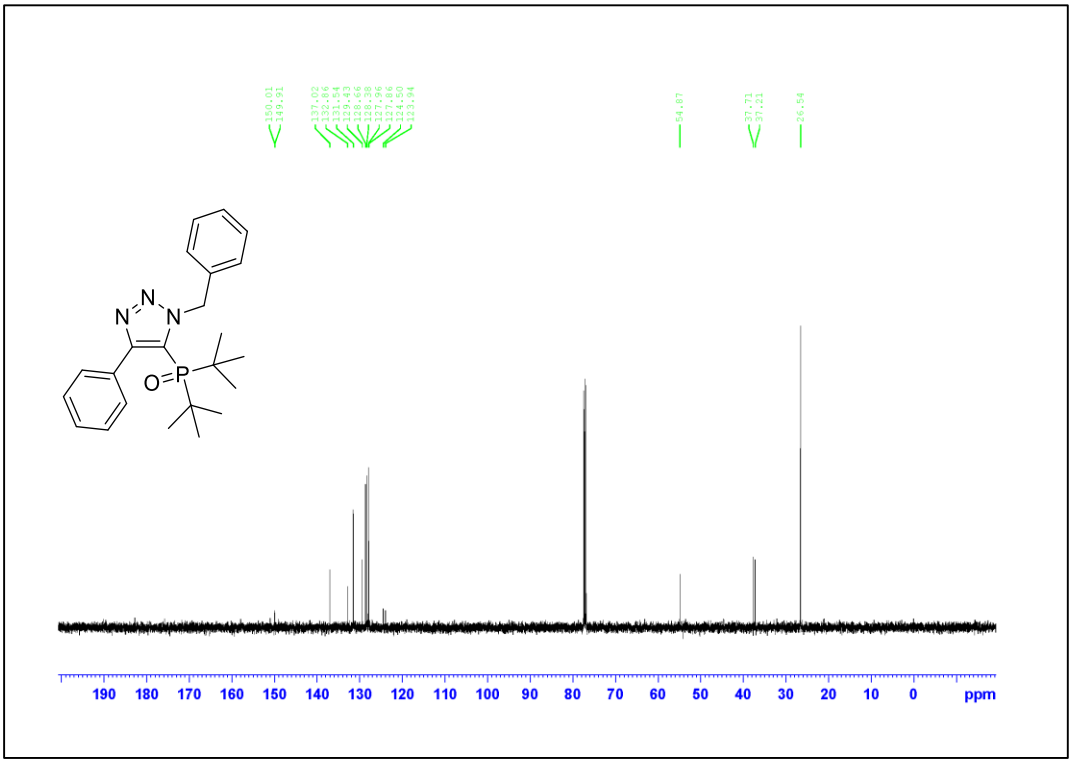

Figure A.291. ^{13}C NMR Spectrum of Compound **3.5a_*t*Bu** (125 MHz, $CDCl_3$)

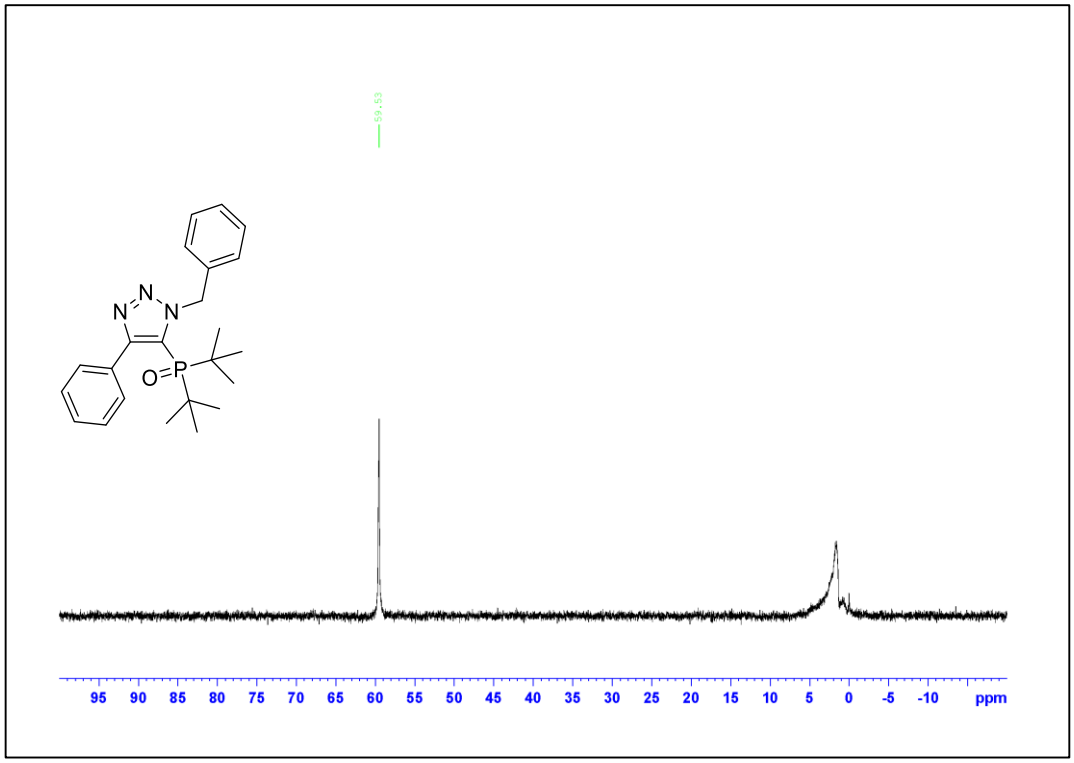

Figure A.292. ^{31}P NMR Spectrum of Compound **3.5a_*t*Bu**

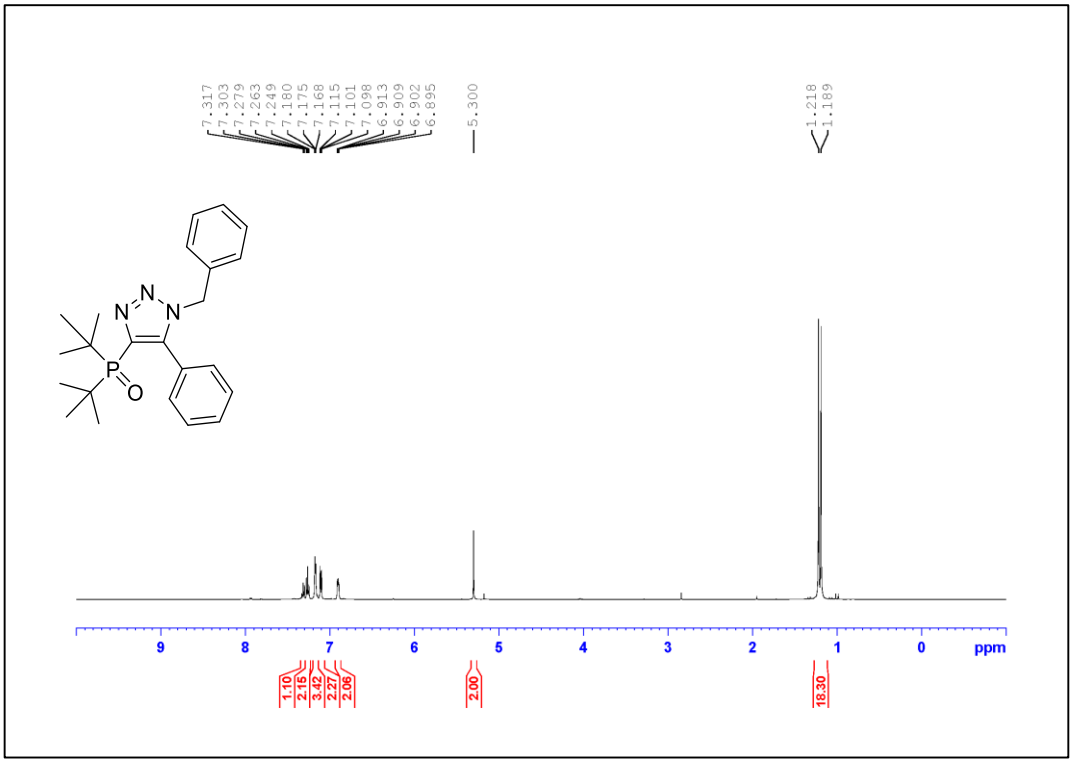

Figure A.293. ^{1}H NMR Spectrum of Compound **3.6a_*t*Bu** (500 MHz, $CDCl_3$)

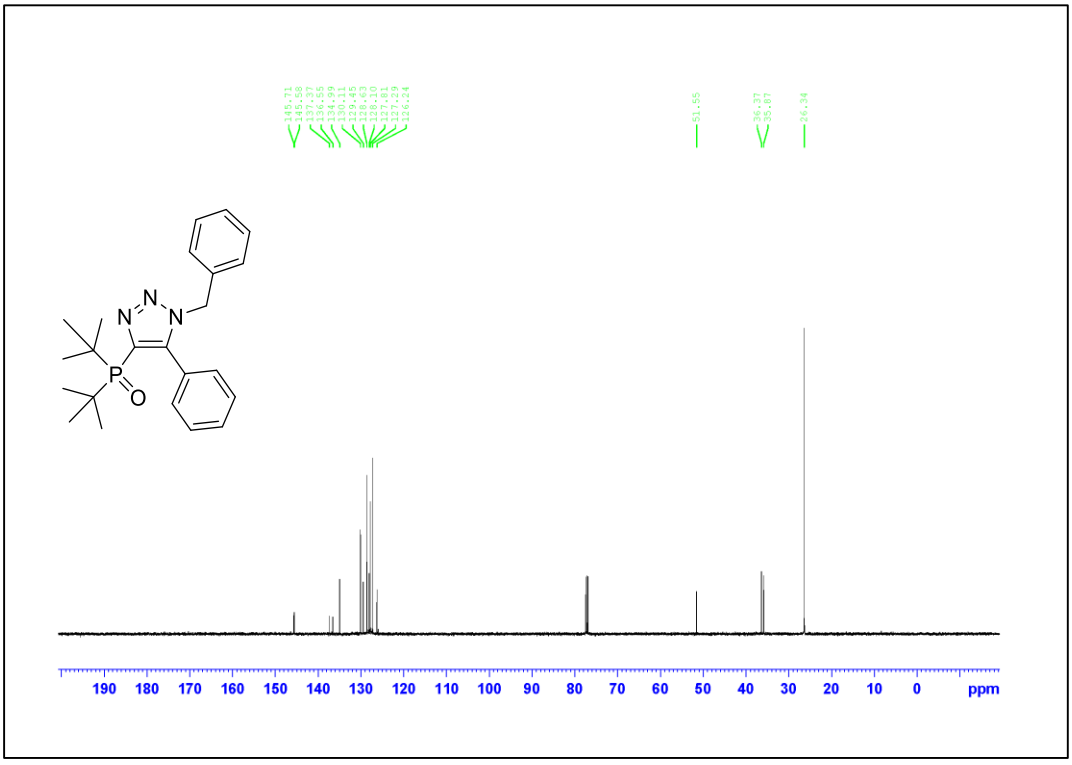

Figure A.294. ^{13}C NMR Spectrum of Compound **3.6a_*t*Bu** (125 MHz, $CDCl_3$)

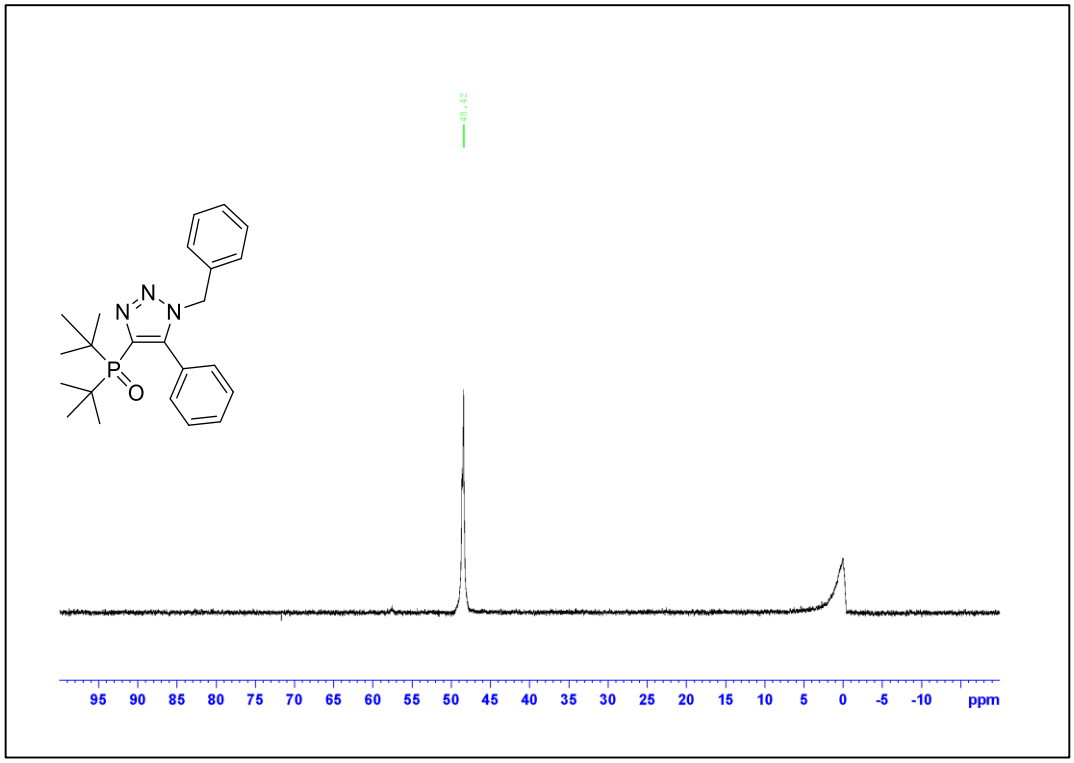

Figure A.295. ^{31}P NMR Spectrum of Compound **3.6a_*t*Bu**

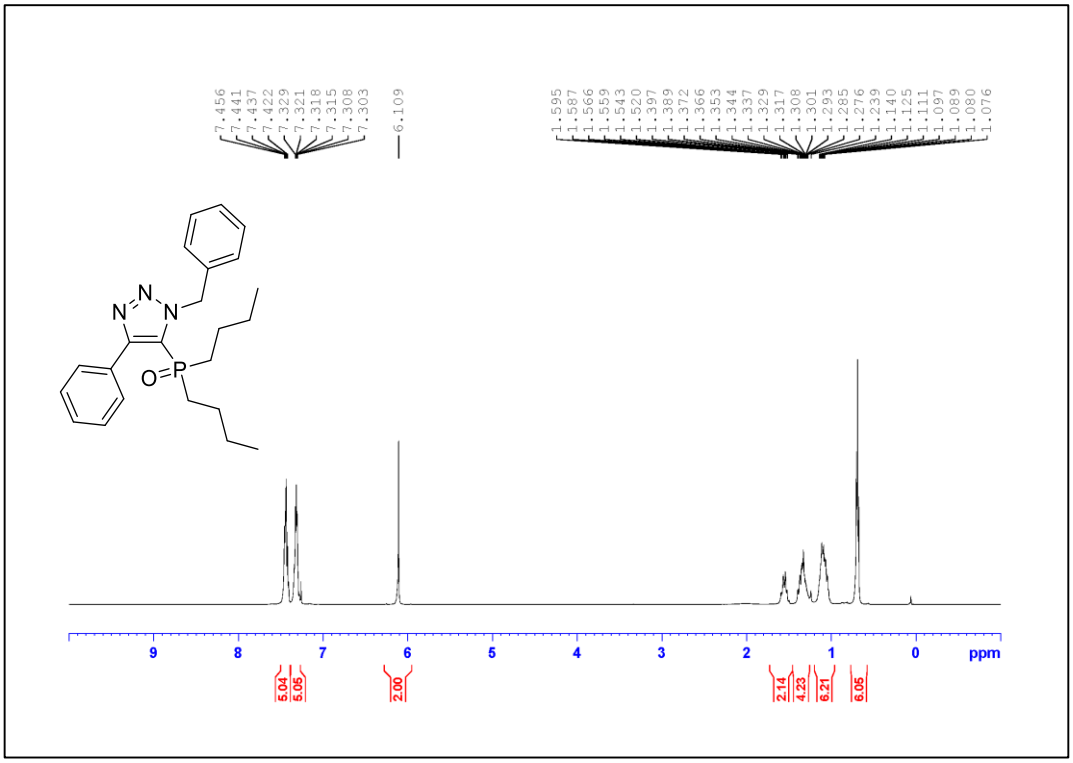

Figure A.296. ^{1}H NMR Spectrum of Compound **3.5a-*n*Bu** (500 MHz, $CDCl_3$)

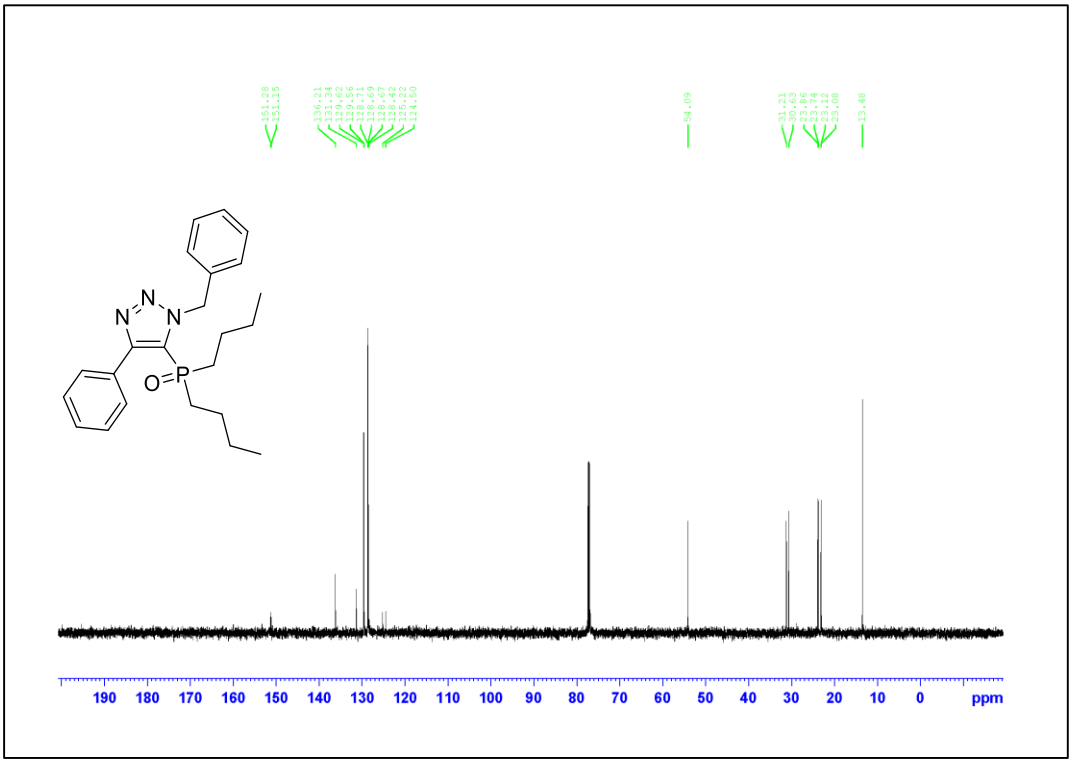

Figure A.297. ^{13}C NMR Spectrum of Compound **3.5a-*n*Bu** (125 MHz, $CDCl_3$)

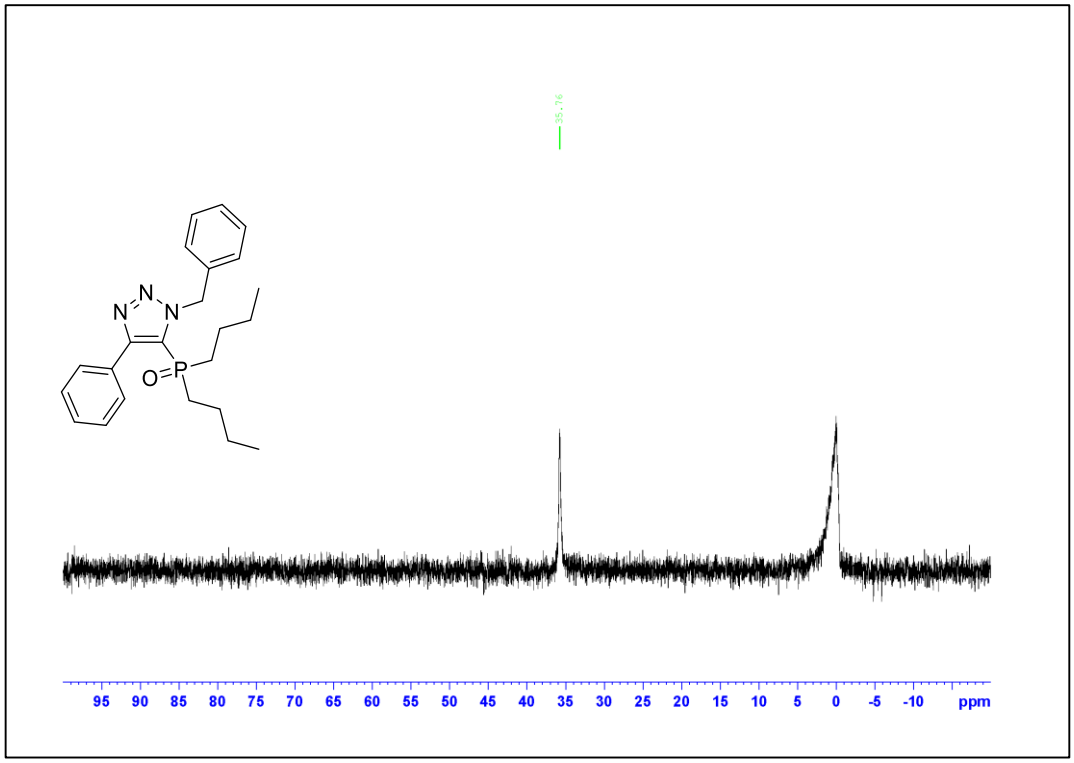

Figure A.298. ^{31}P NMR Spectrum of Compound **3.5a-*n*Bu**

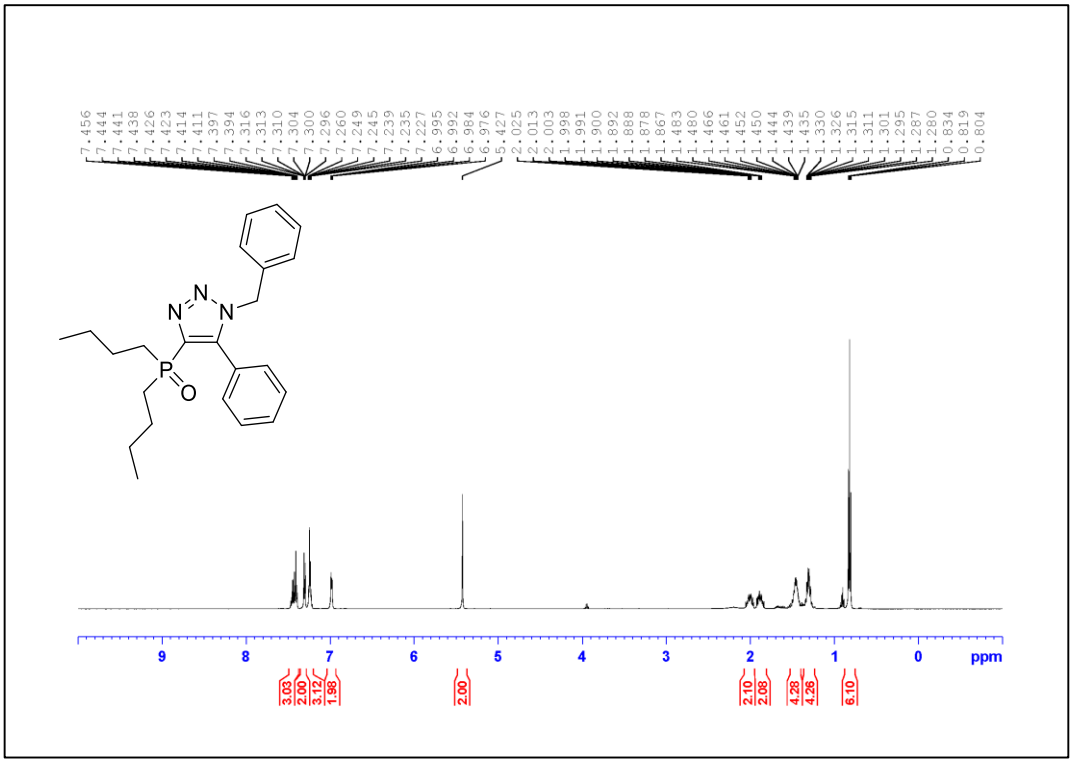

Figure A.299. ^{1}H NMR Spectrum of Compound **3.6a-*n*Bu** (500 MHz, $CDCl_3$)

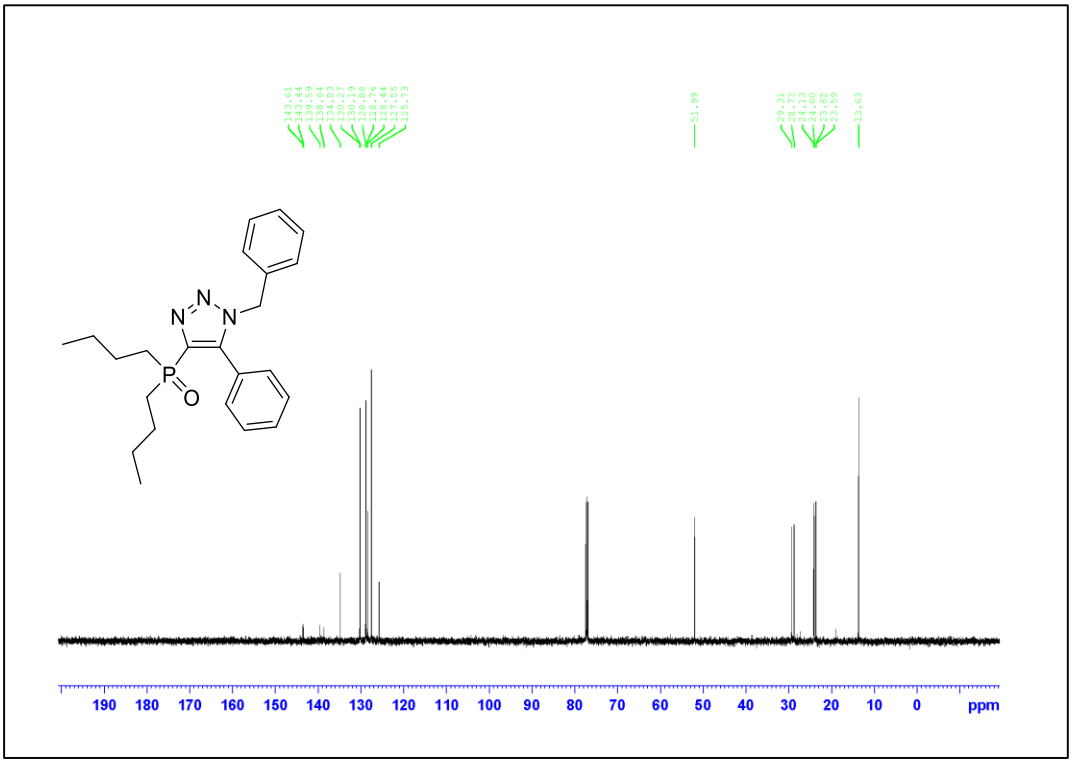

Figure A.300. ^{13}C NMR Spectrum of Compound **3.6a-*n*Bu** (125 MHz, $CDCl_3$)

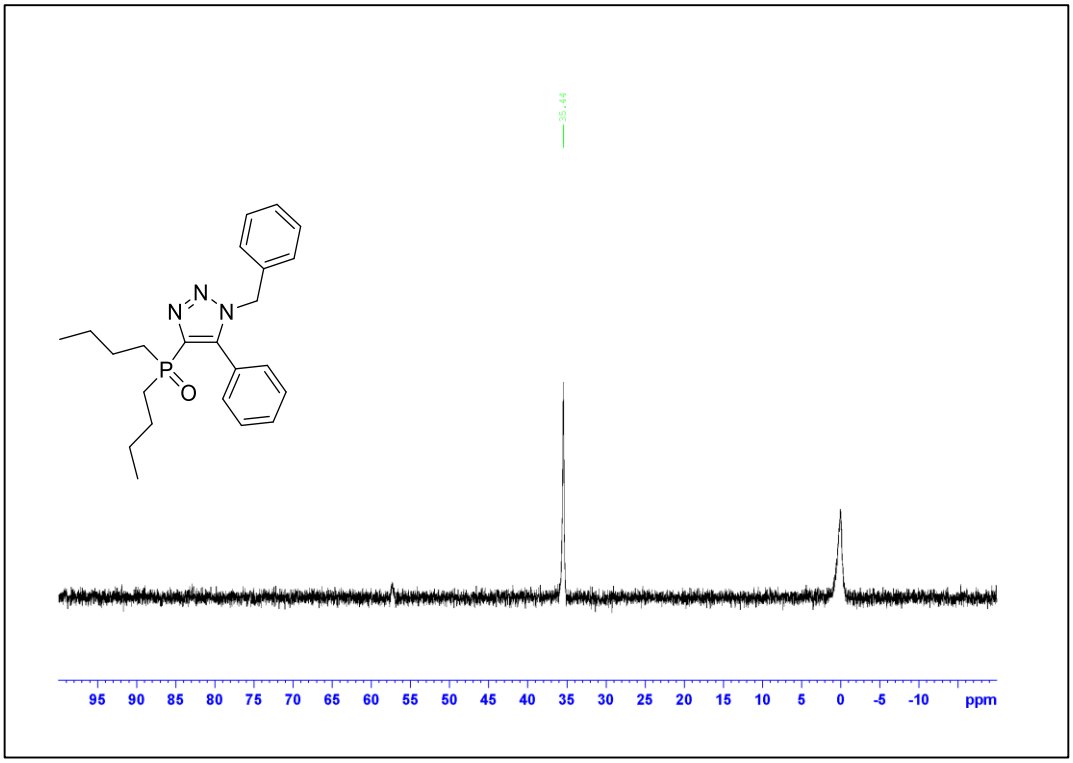

Figure A.301. ^{31}P NMR Spectrum of Compound **3.6a-*n*Bu**

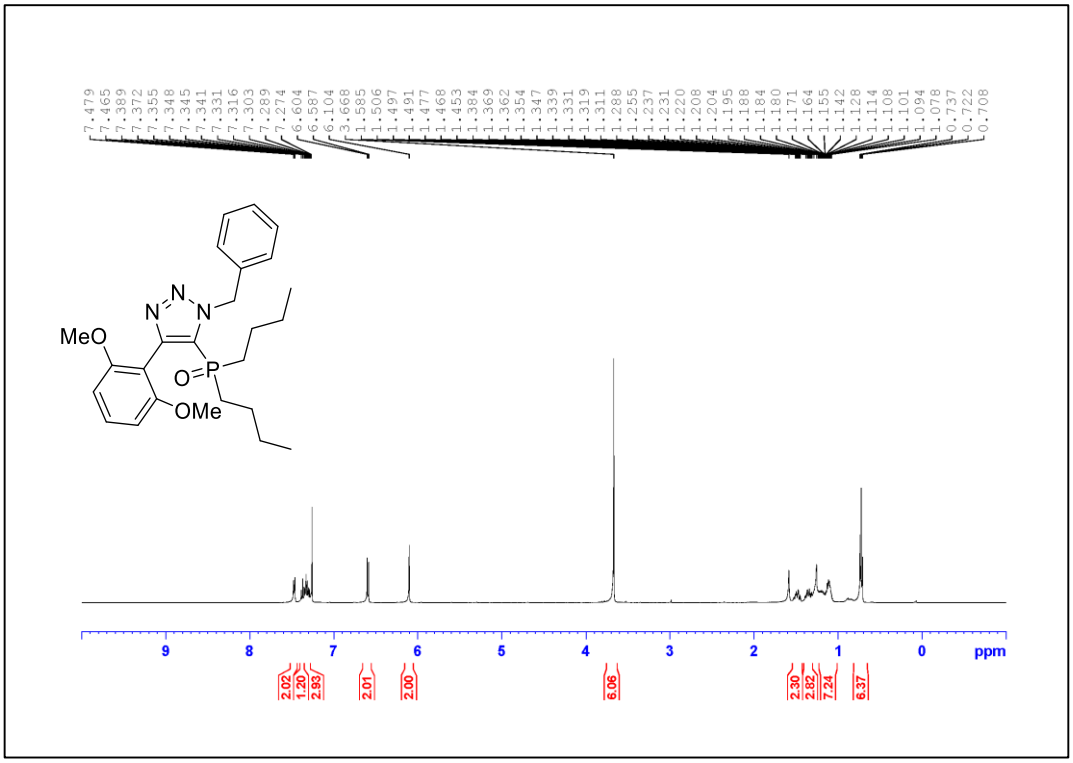

Figure A.302. ^{1}H NMR Spectrum of Compound **3.5d-*n*Bu** (500 MHz, $CDCl_3$)

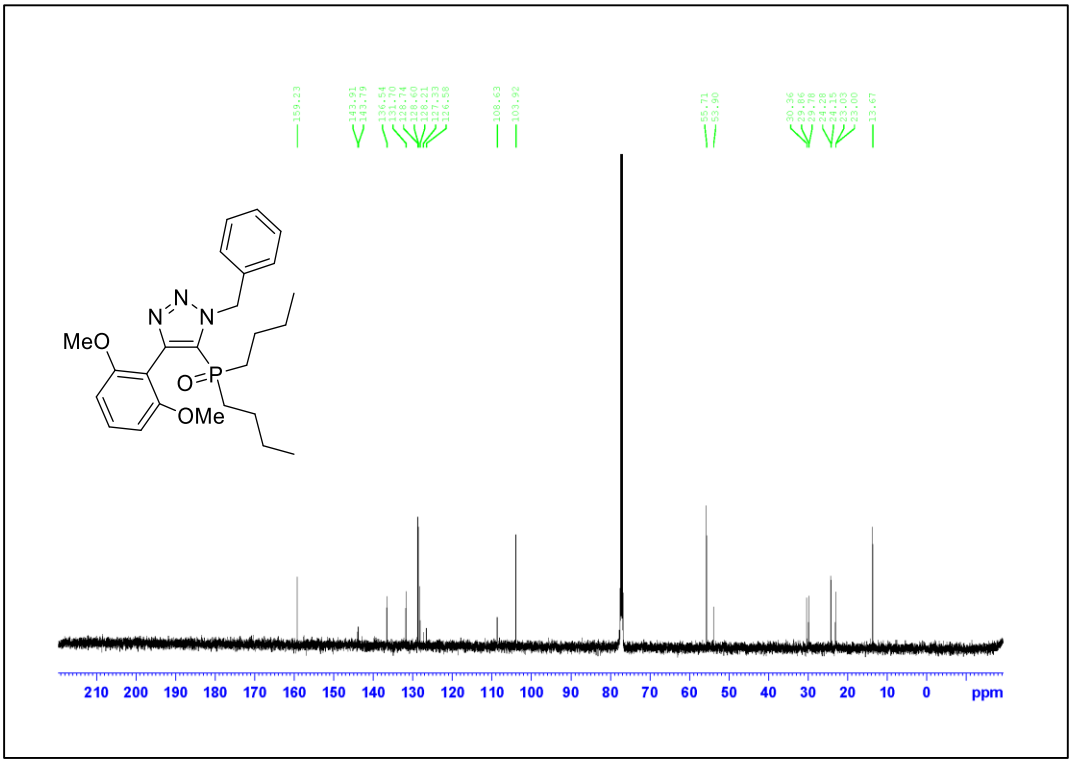

Figure A.303. ^{13}C NMR Spectrum of Compound **3.5d-*n*Bu** (125 MHz, $CDCl_3$)

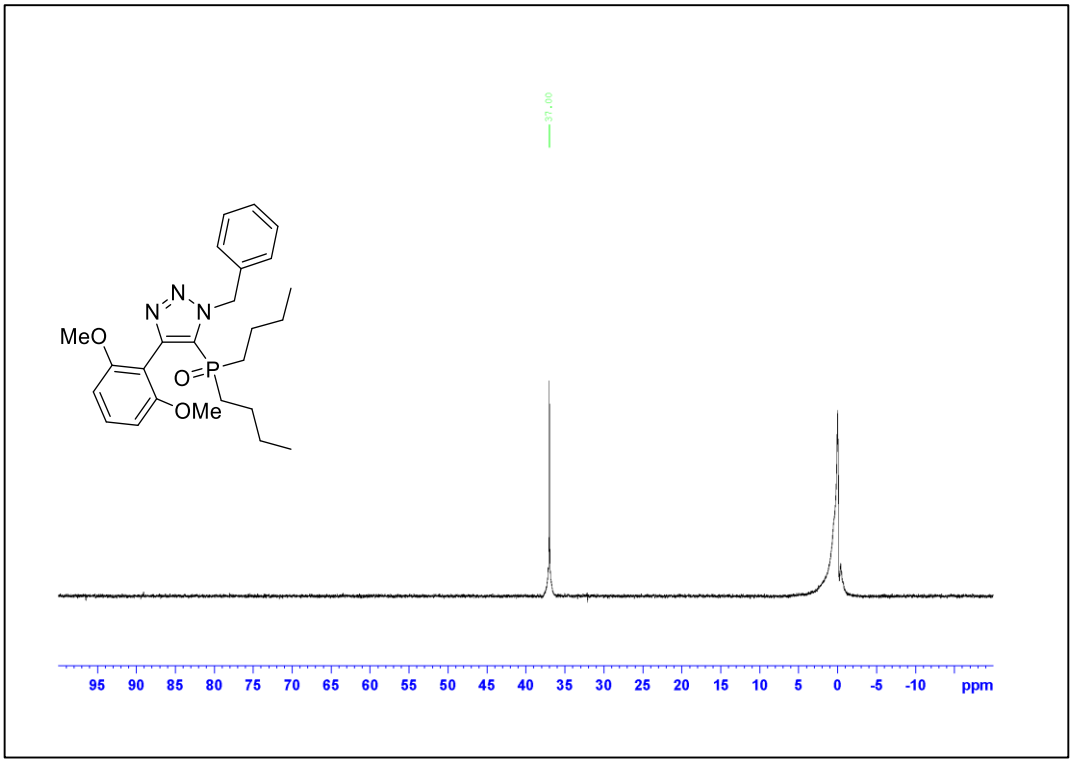

Figure A.304. ^{31}P NMR Spectrum of Compound **3.5d-*n*Bu**

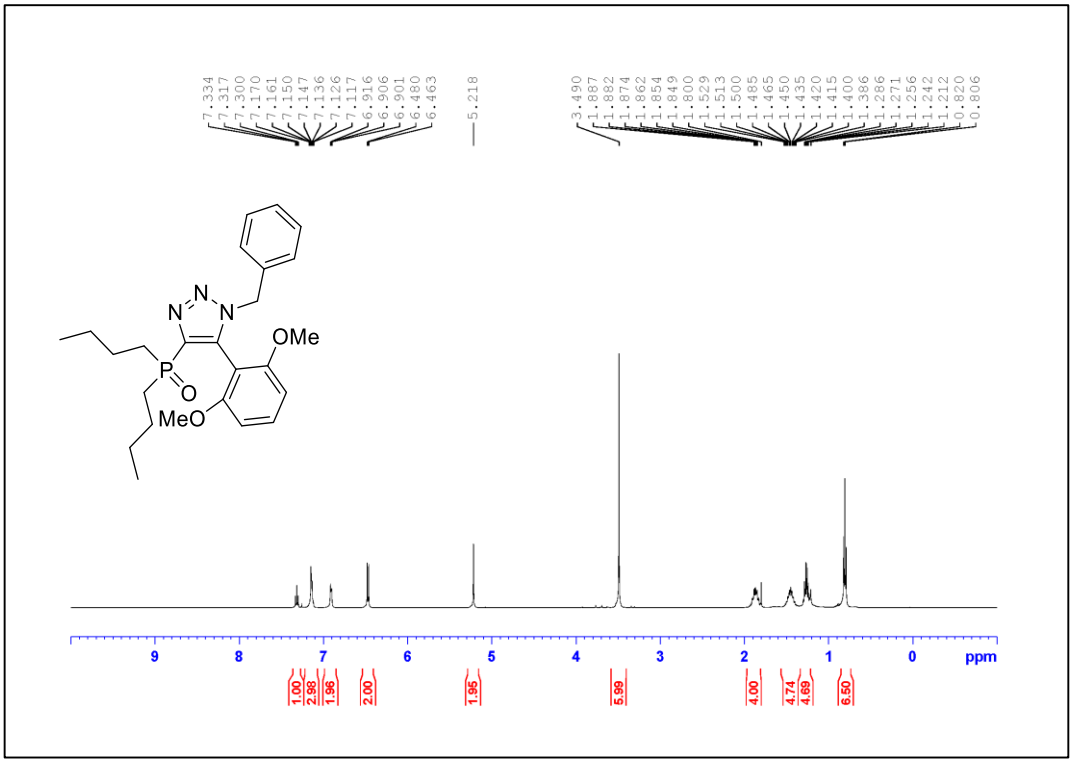

Figure A.305. ^{1}H NMR Spectrum of Compound **3.6d-*n*Bu** (500 MHz, $CDCl_3$)

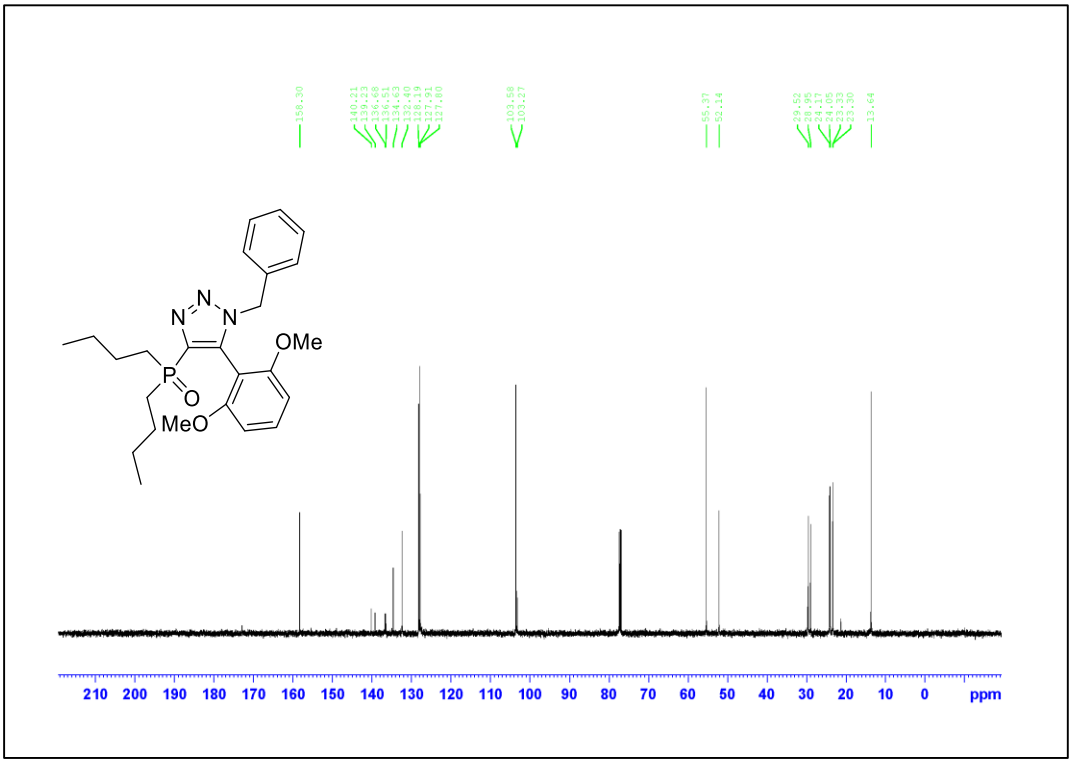

Figure A.306. ^{13}C NMR Spectrum of Compound **3.6d-*n*Bu** (125 MHz, $CDCl_3$)

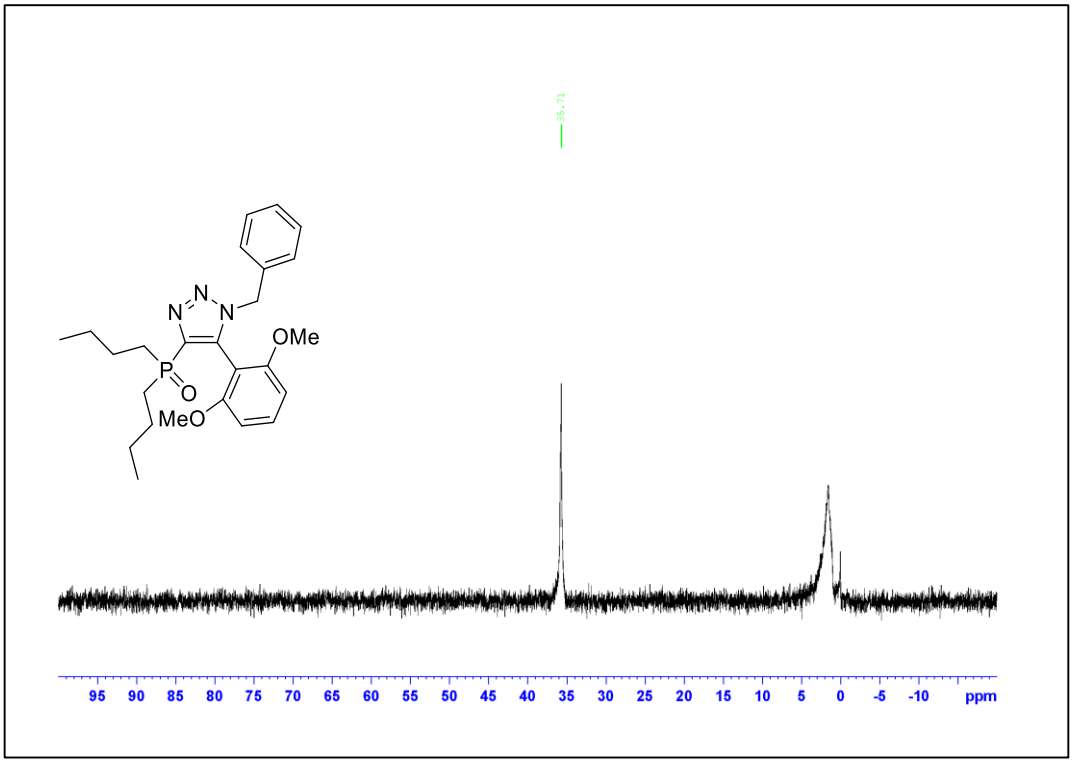

Figure A.307. ^{31}P NMR Spectrum of Compound **3.6d-*n*Bu**

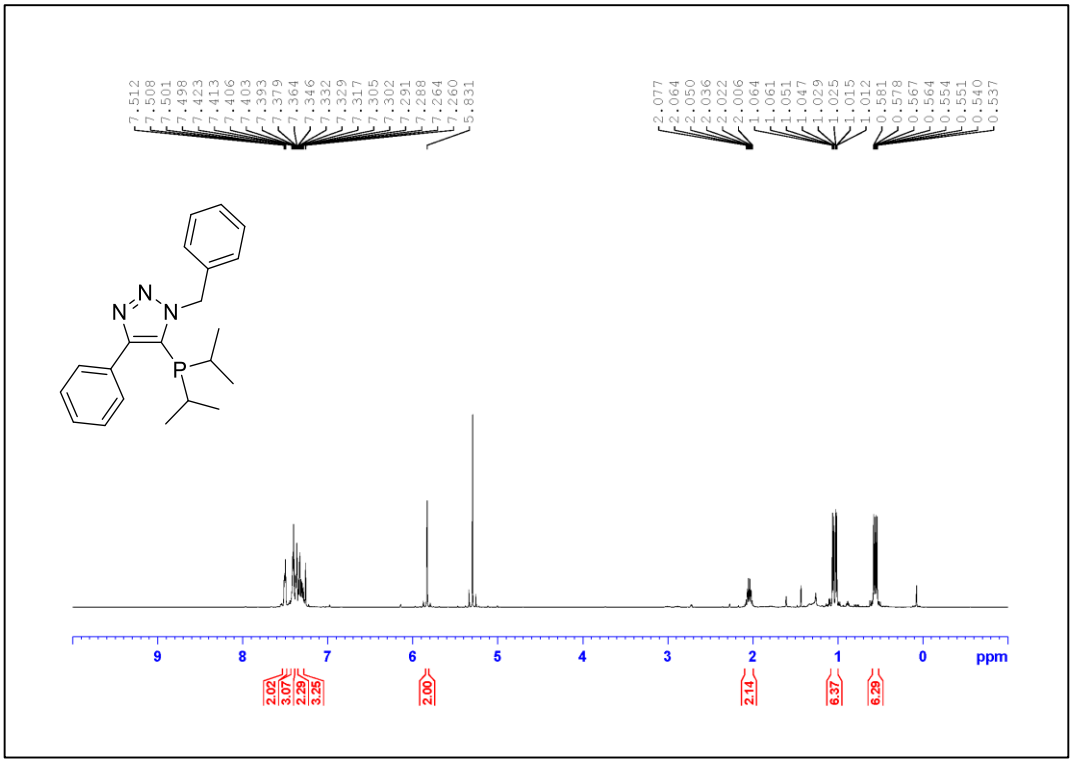

Figure A.308. ^{1}H NMR Spectrum of Compound **3.7a** (500 MHz, $CDCl_3$)

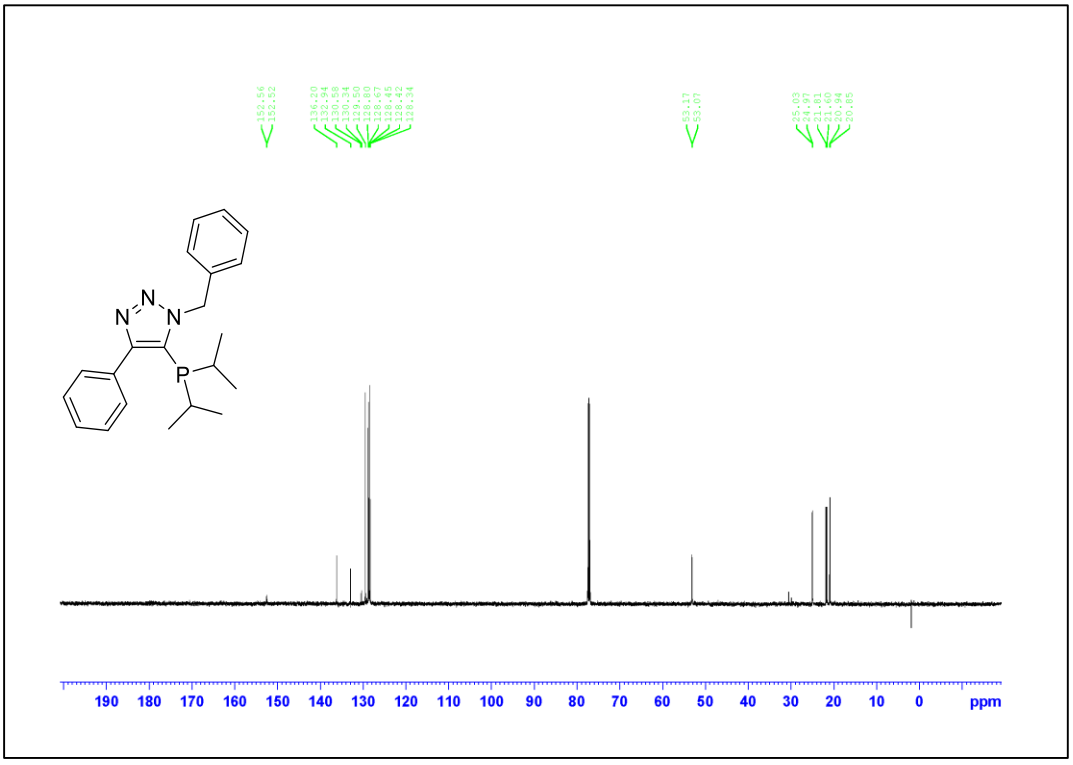

Figure A.309. ^{13}C NMR Spectrum of Compound **3.7a** (125 MHz, $CDCl_3$)

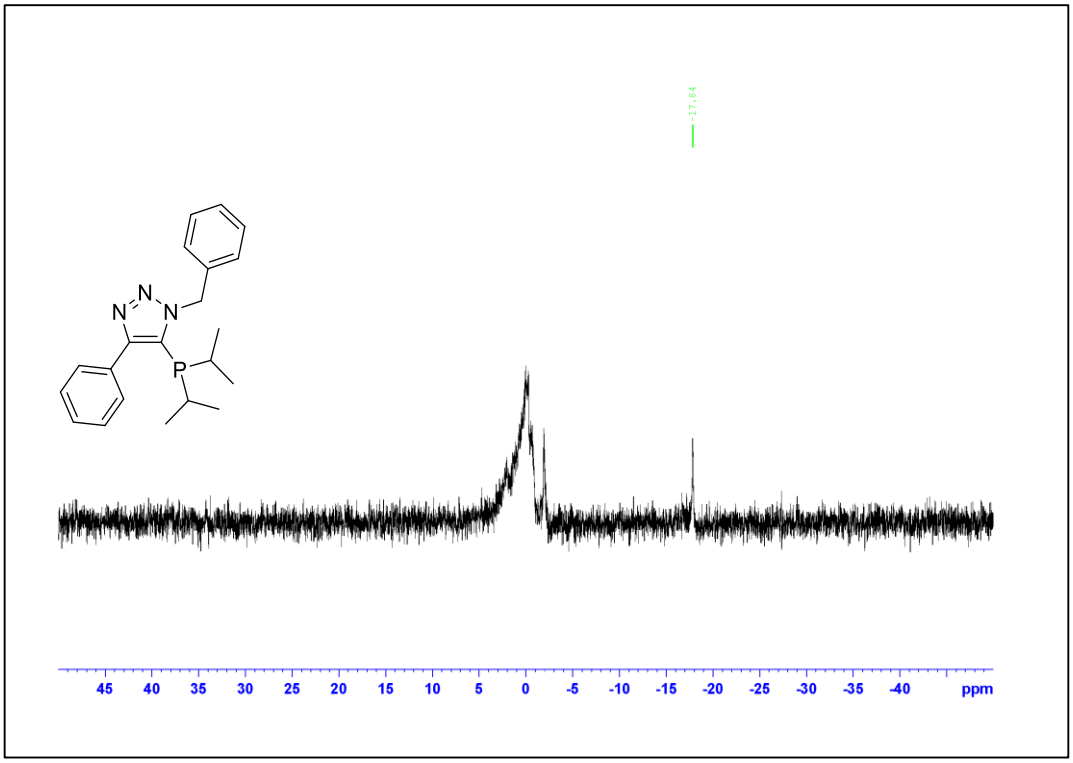

Figure A.310. ^{31}P NMR Spectrum of Compound **3.7a**

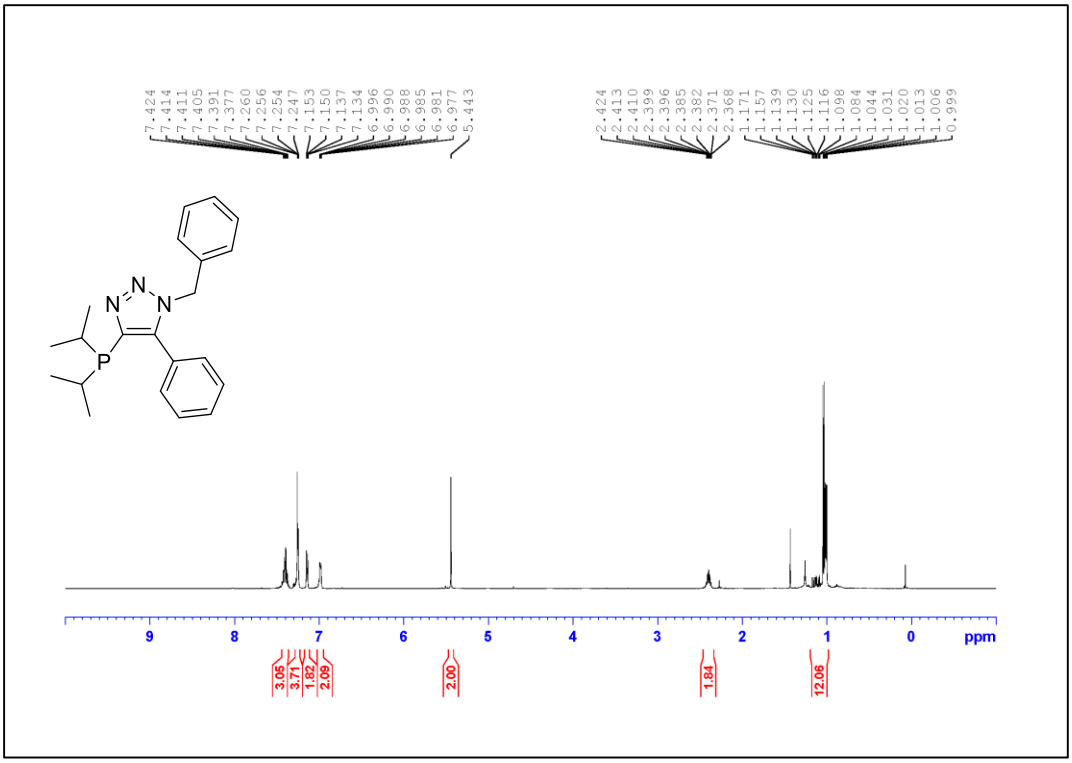

Figure A.311. ^{1}H NMR Spectrum of Compound **3.8a** (500 MHz, $CDCl_3$)

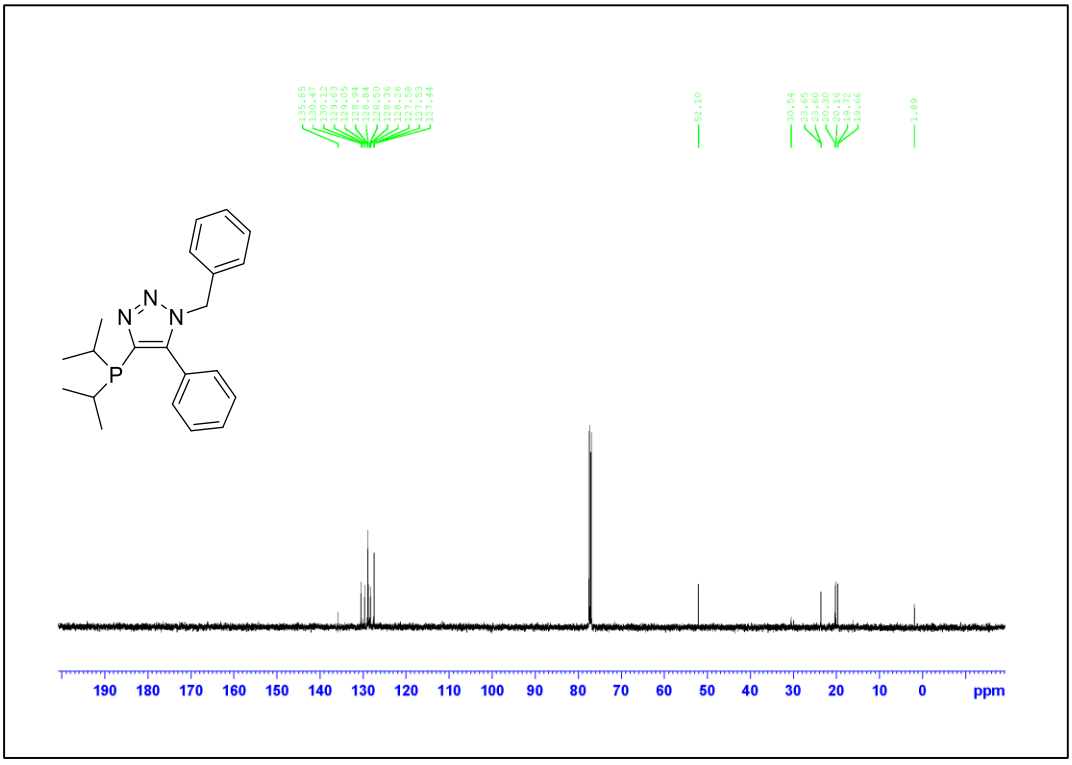

Figure A.312. ^{13}C NMR Spectrum of Compound **3.8a** (125 MHz, $CDCl_3$)

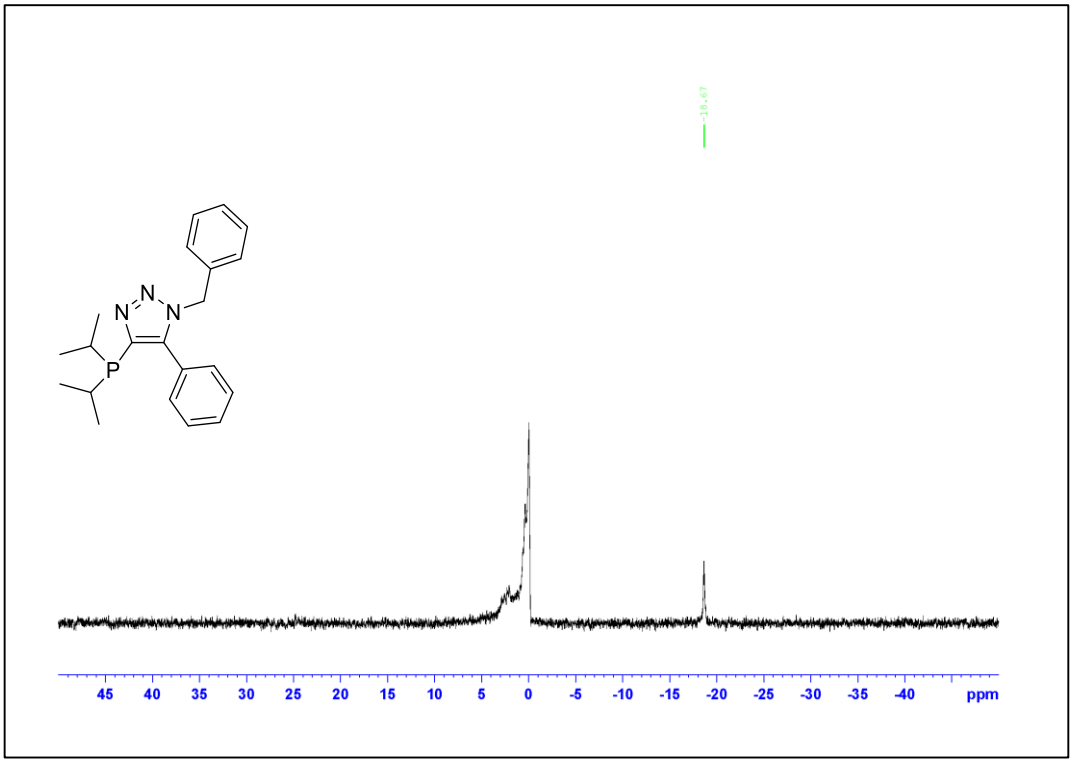

Figure A.313. ^{31}P NMR Spectrum of Compound **3.8a**

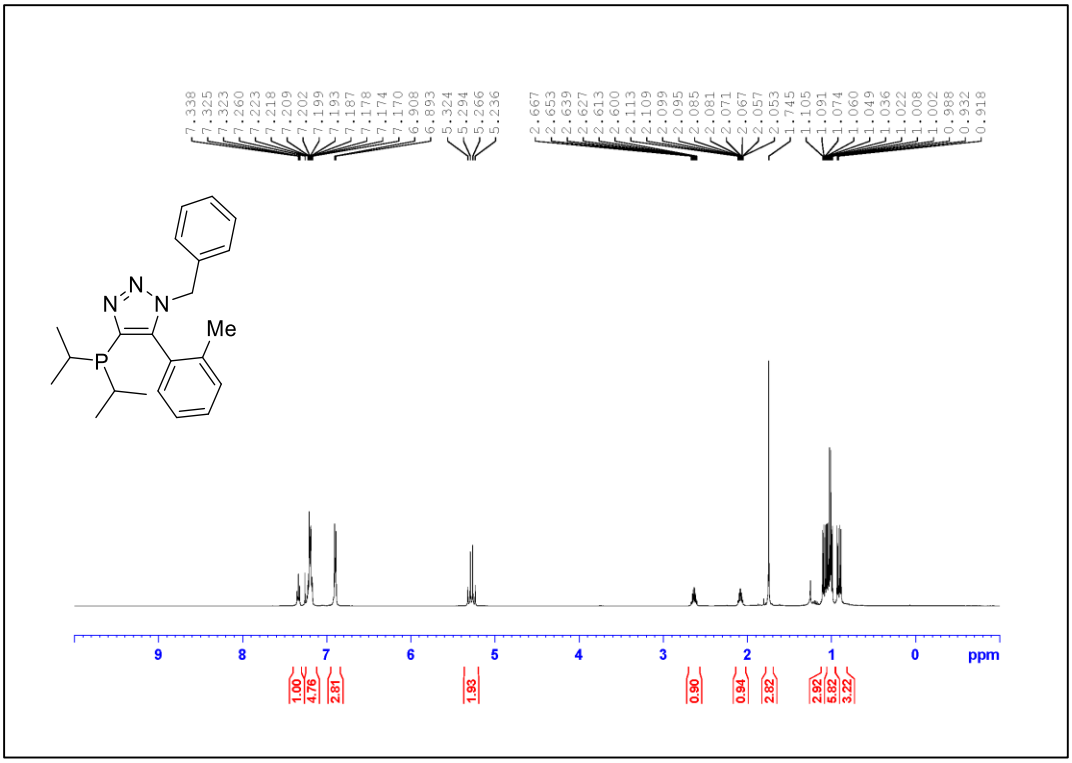

Figure A.314. ^{1}H NMR Spectrum of Compound **3.8b** (500 MHz, $CDCl_3$)

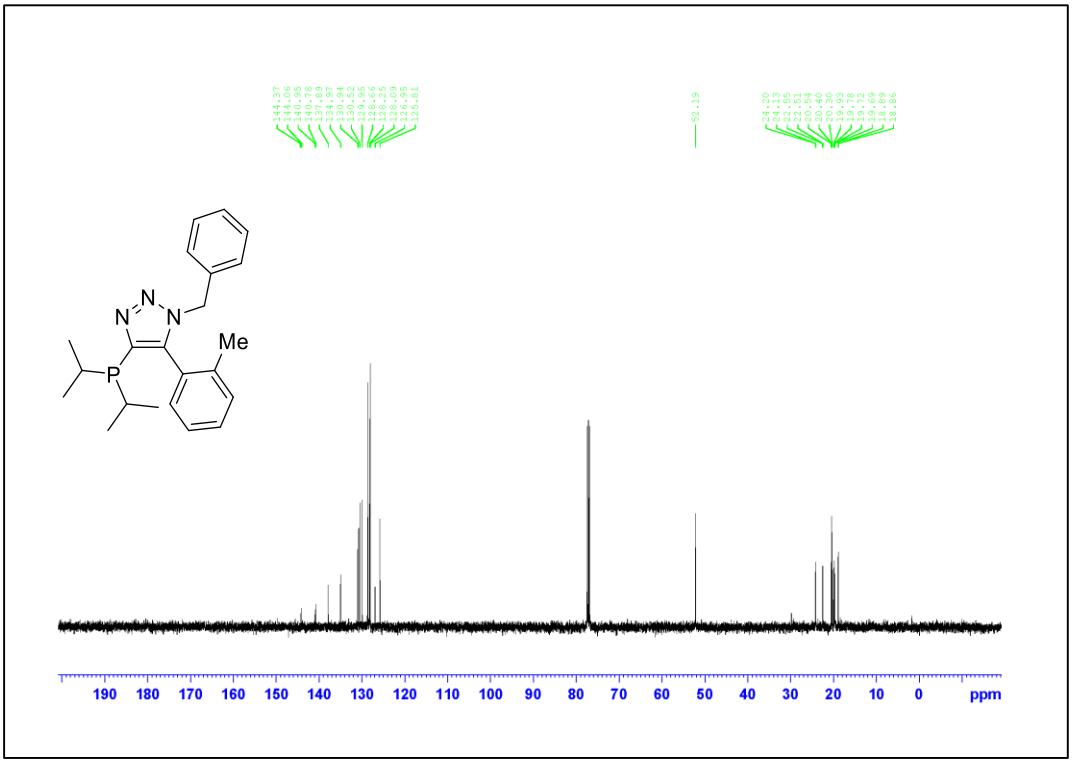

Figure A.315. ^{13}C NMR Spectrum of Compound **3.8b** (125 MHz, $CDCl_3$)

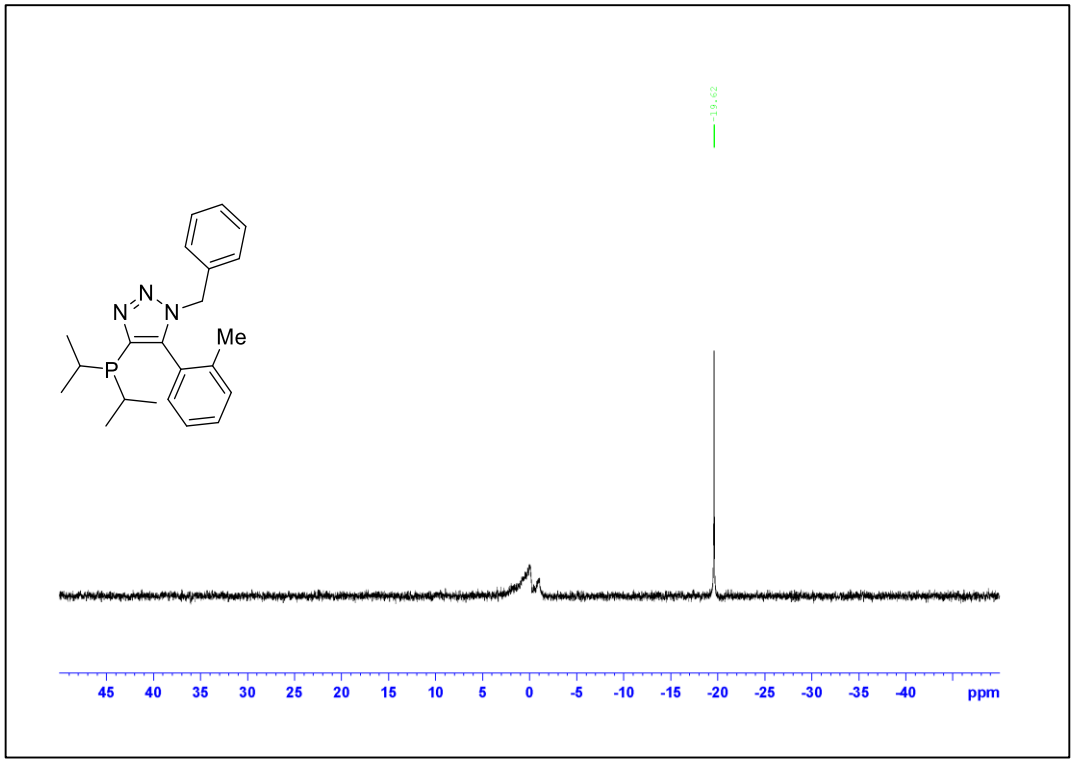

Figure A.316. ^{31}P NMR Spectrum of Compound **3.8b**

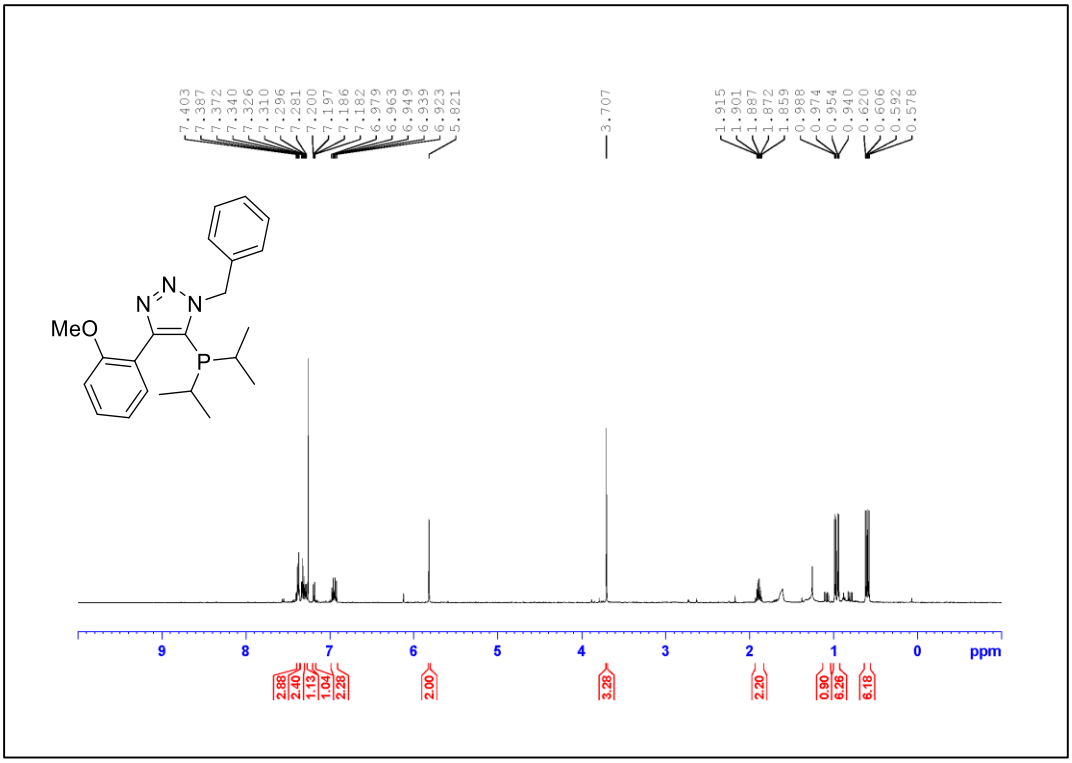

Figure A.317. ^{1}H NMR Spectrum of Compound **3.7c** (500 MHz, $CDCl_3$)

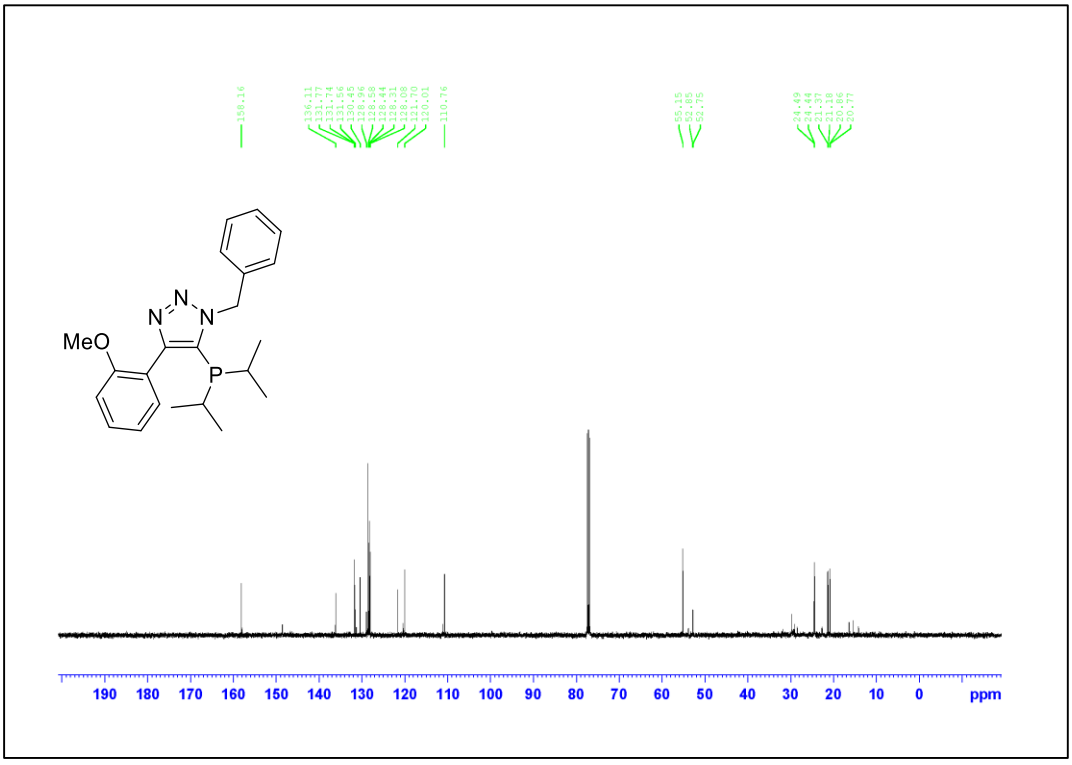

Figure A.318. ^{13}C NMR Spectrum of Compound **3.7c** (125 MHz, $CDCl_3$)

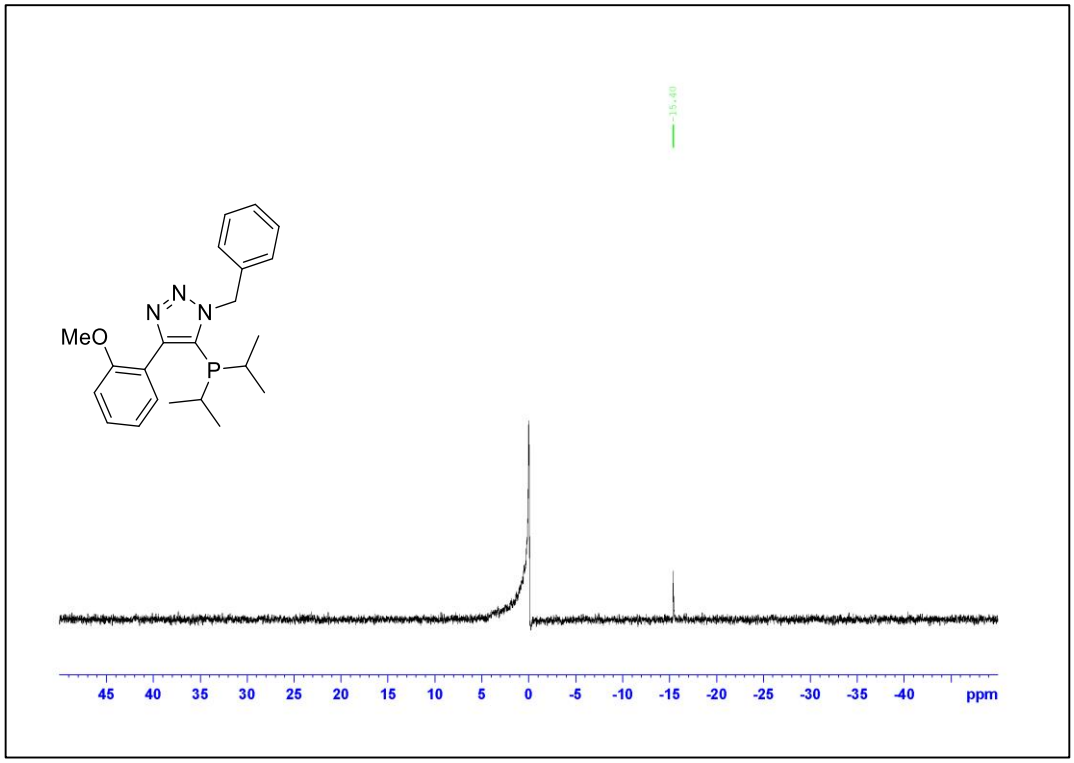

Figure A.319. ^{31}P NMR Spectrum of Compound **3.7c**

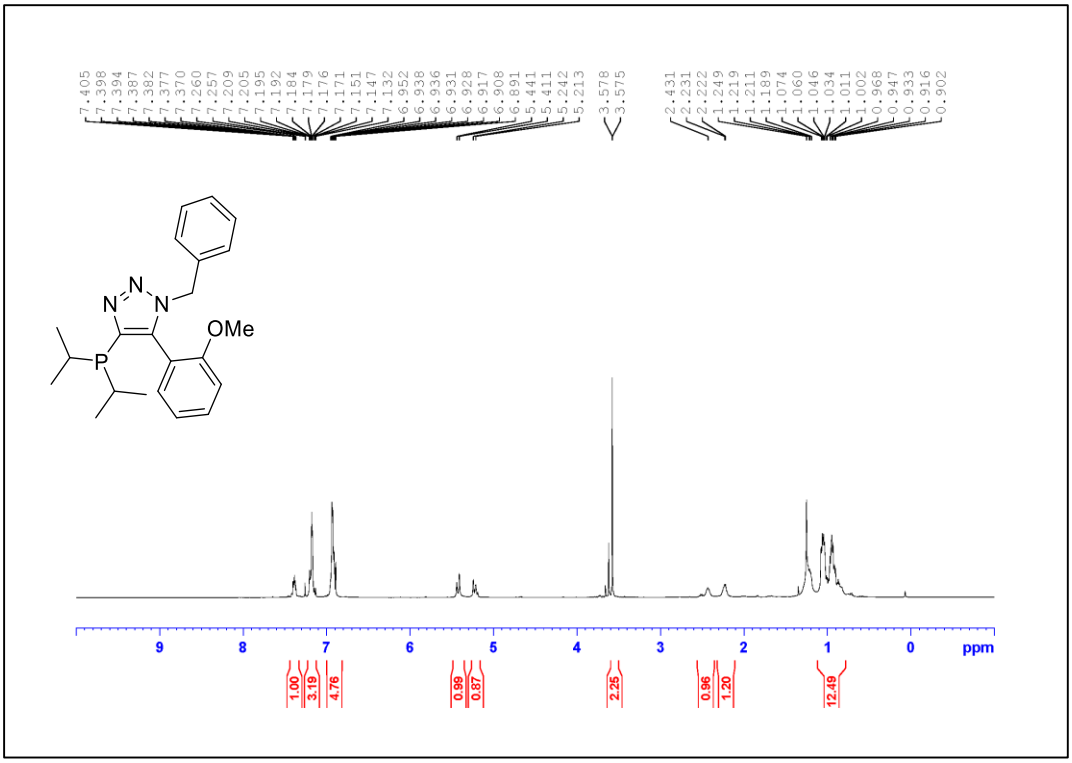

Figure A.320. ^{1}H NMR Spectrum of Compound **3.8c** (500 MHz, $CDCl_3$)

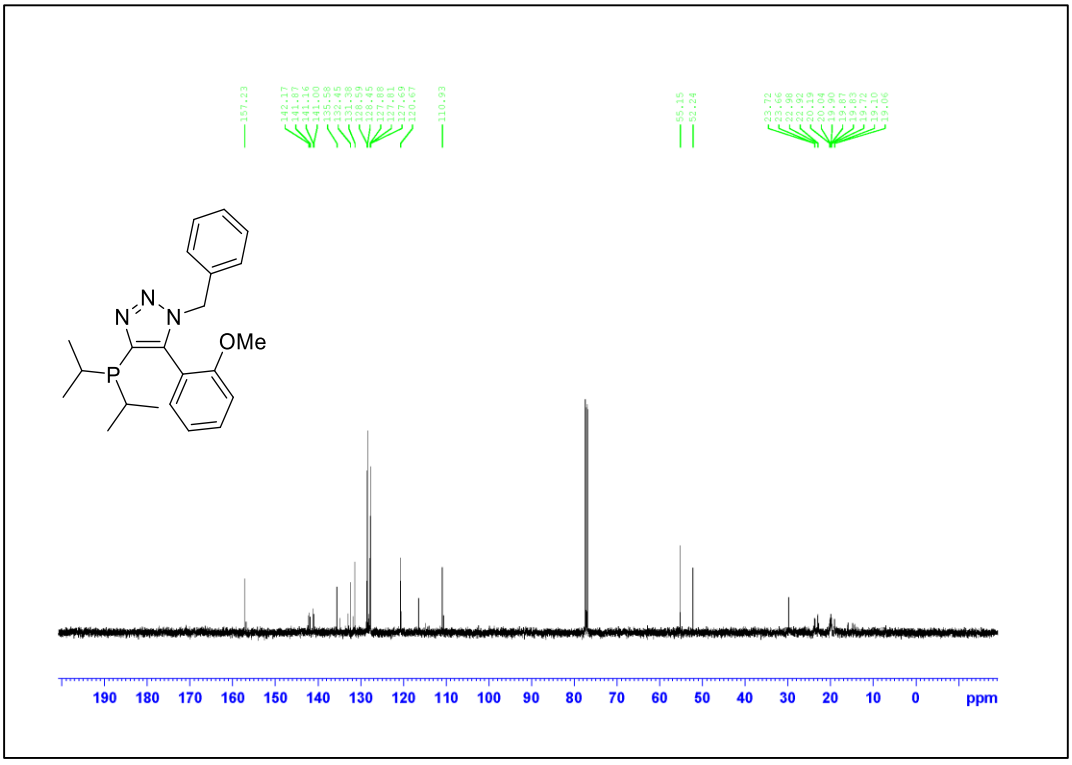

Figure A.321. ^{13}C NMR Spectrum of Compound **3.8c** (125 MHz, $CDCl_3$)

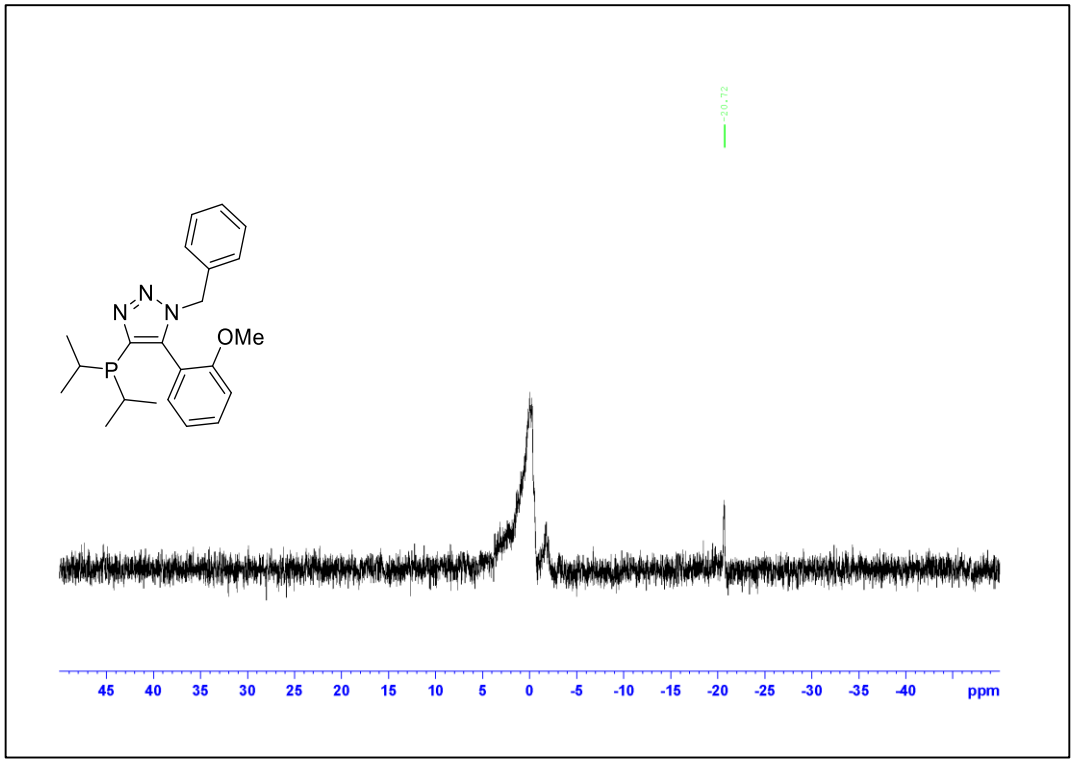

Figure A.322. ^{31}P NMR Spectrum of Compound **3.8c**

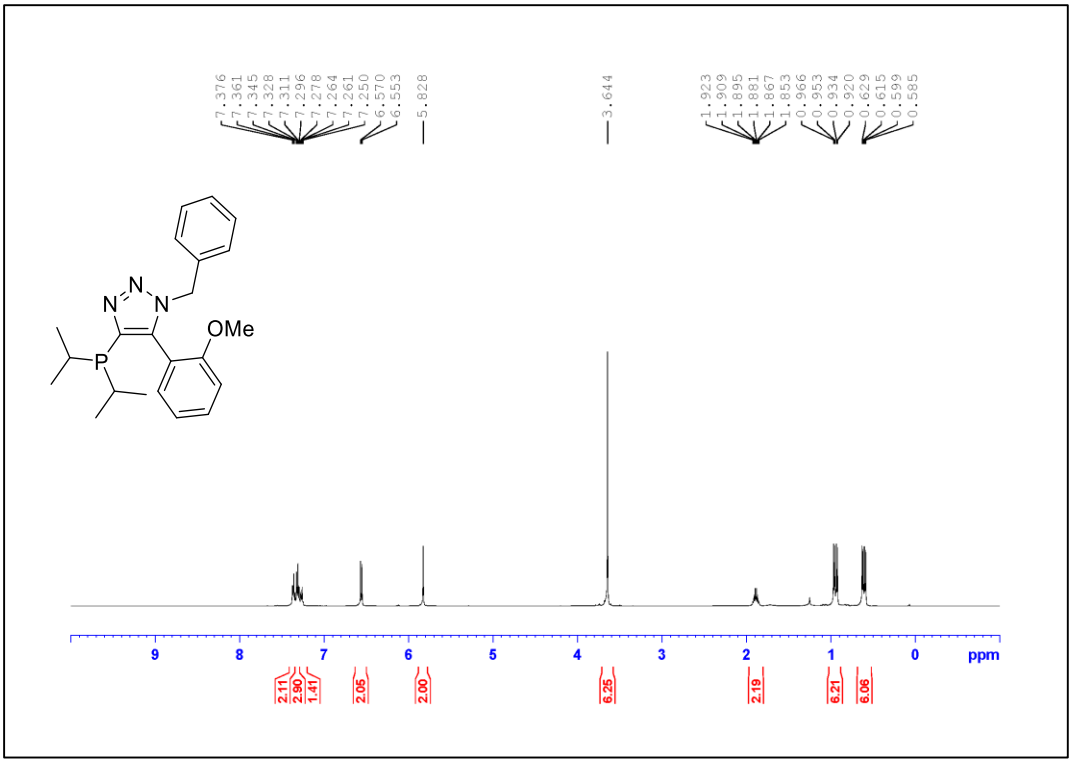

Figure A.323. ^{1}H NMR Spectrum of Compound **3.7d** (500 MHz, $CDCl_3$)

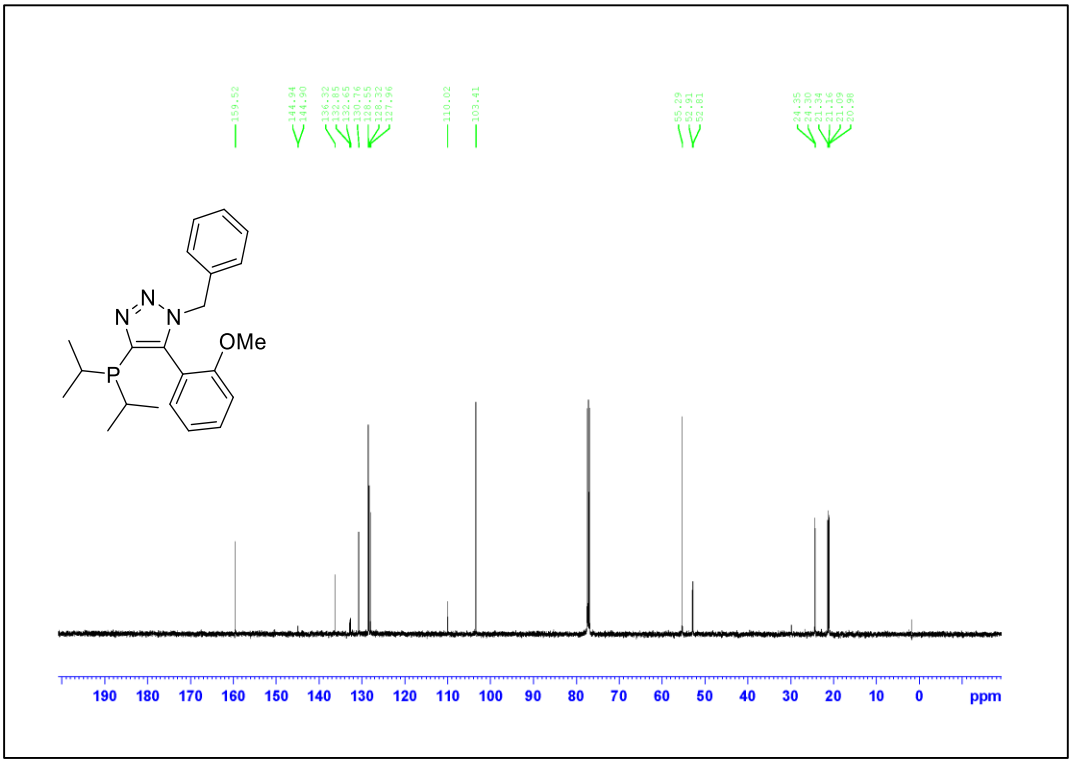

Figure A.324. ^{13}C NMR Spectrum of Compound **3.7d** (125 MHz, $CDCl_3$)

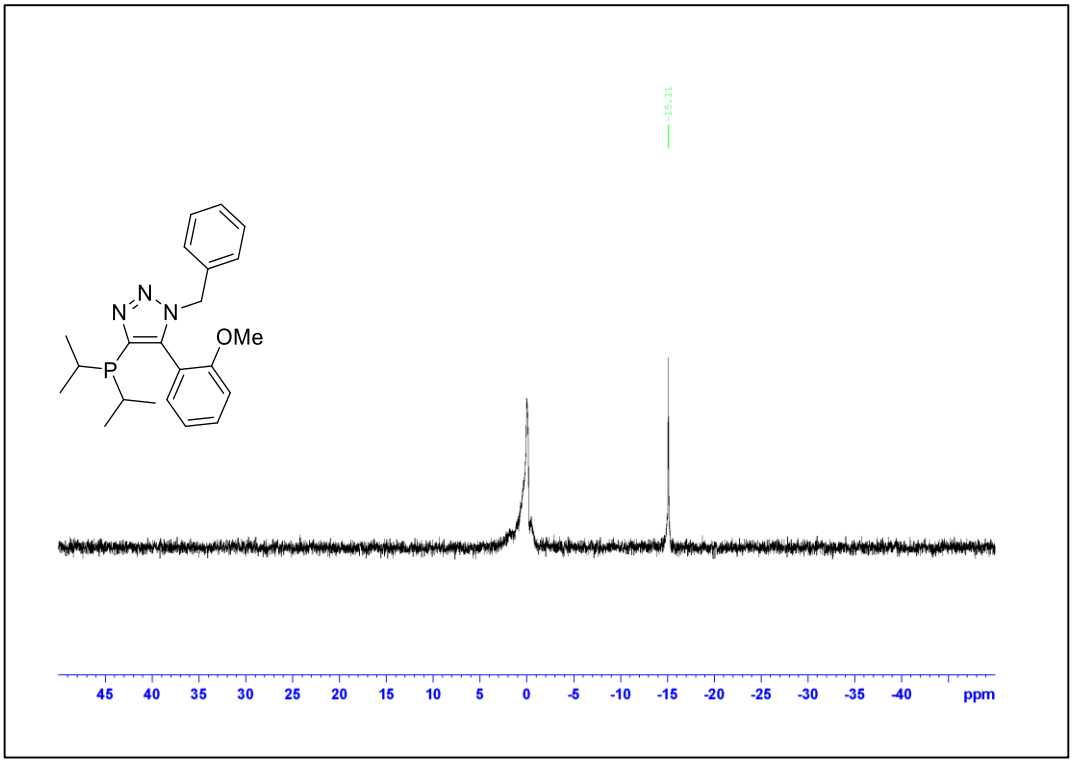

Figure A.325. ^{31}P NMR Spectrum of Compound **3.7d**

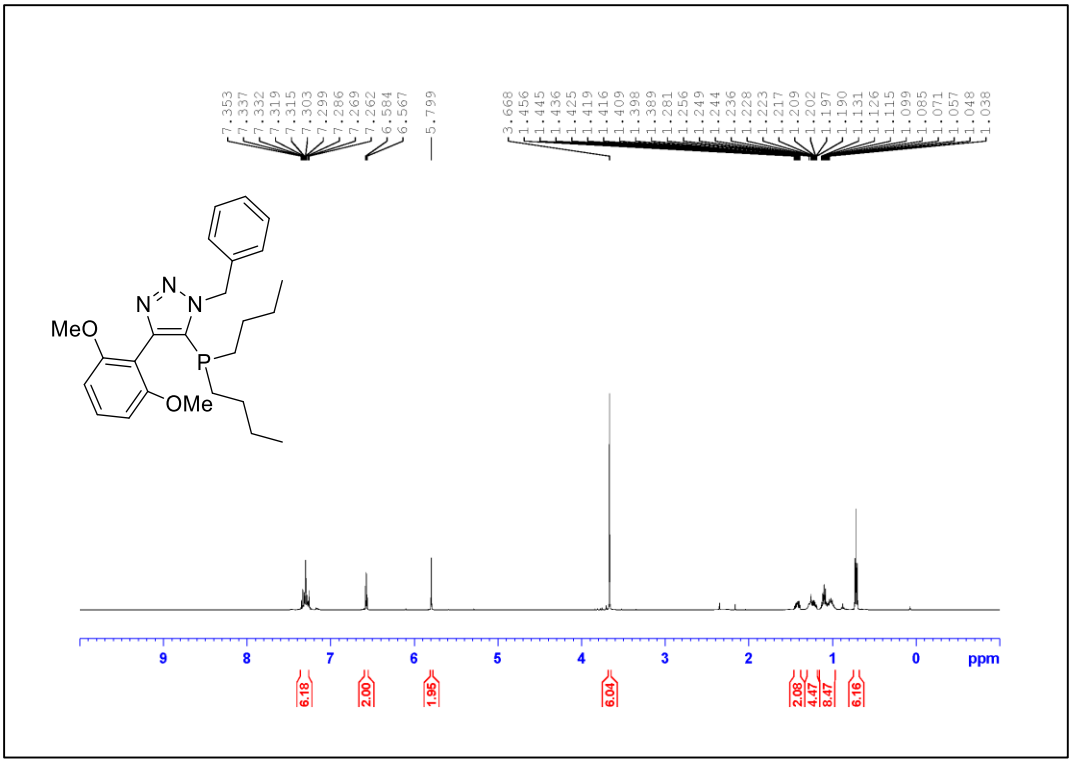

Figure A.326. ^{1}H NMR Spectrum of Compound **3.7d-*n*Bu** (500 MHz, $CDCl_3$)

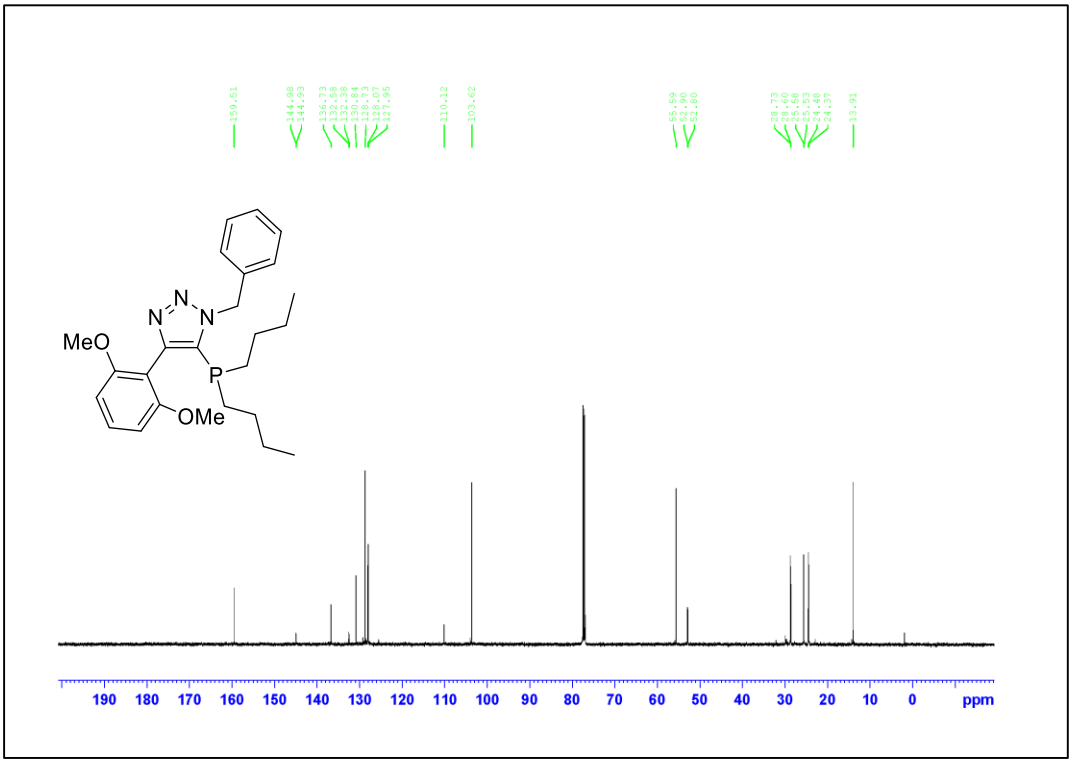

Figure A.327. ^{13}C NMR Spectrum of Compound **3.7d-*n*Bu** (125 MHz, $CDCl_3$)

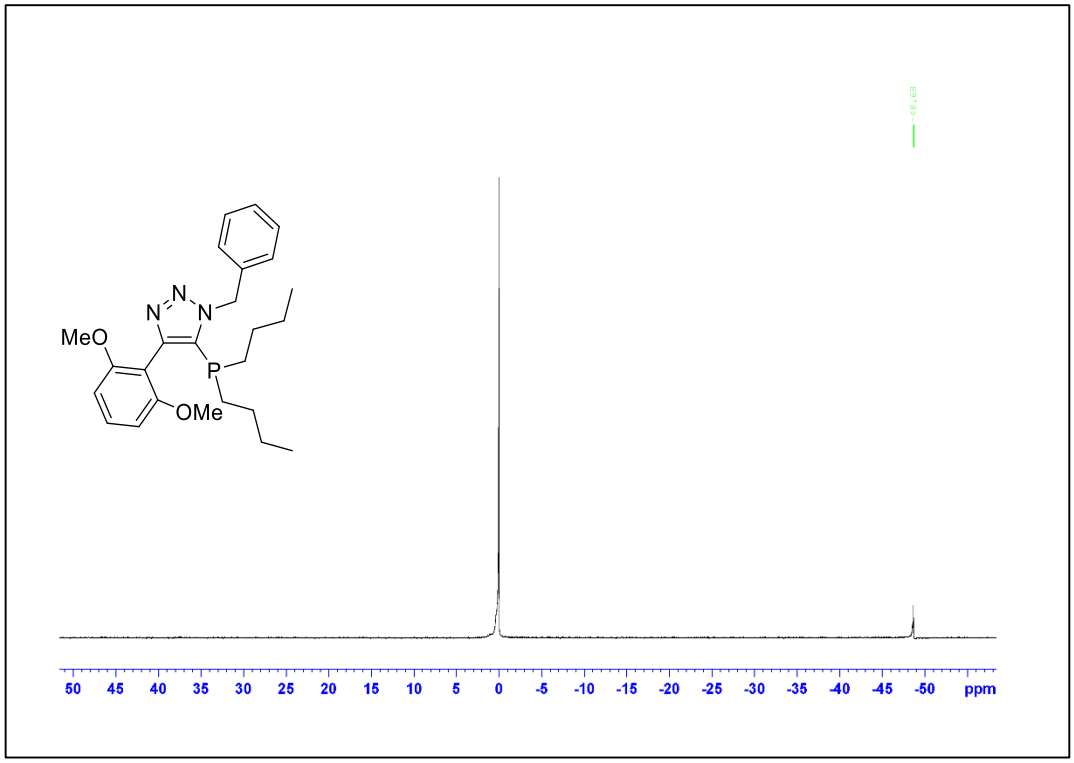

Figure A.328. ^{31}P NMR Spectrum of Compound **3.7d-*n*Bu**

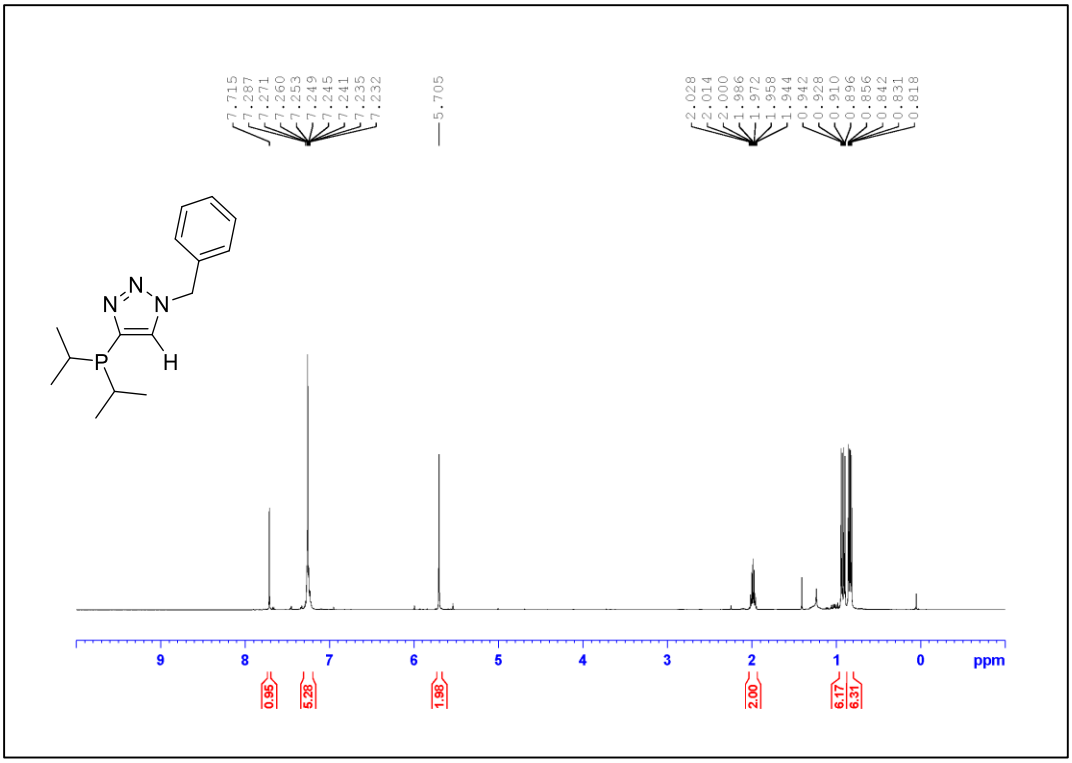

Figure A.329. ^{1}H NMR Spectrum of Compound **3.8e** (500 MHz, $CDCl_3$)

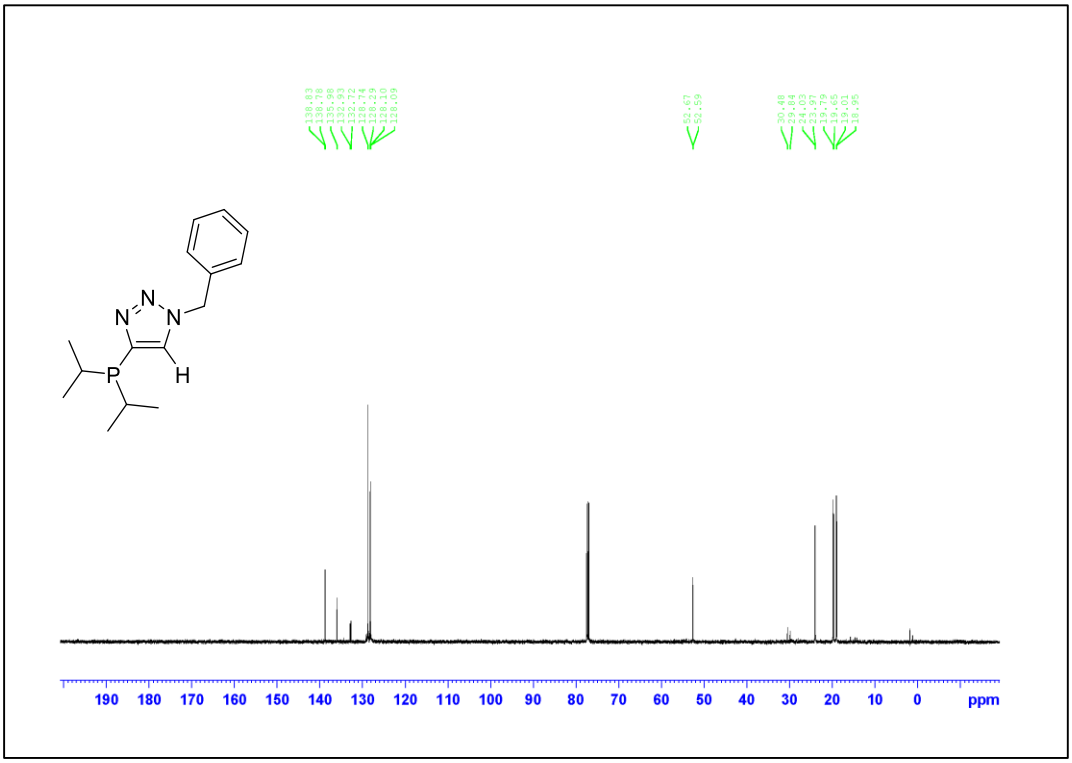

Figure A.330. ^{13}C NMR Spectrum of Compound **3.8e** (125 MHz, $CDCl_3$)

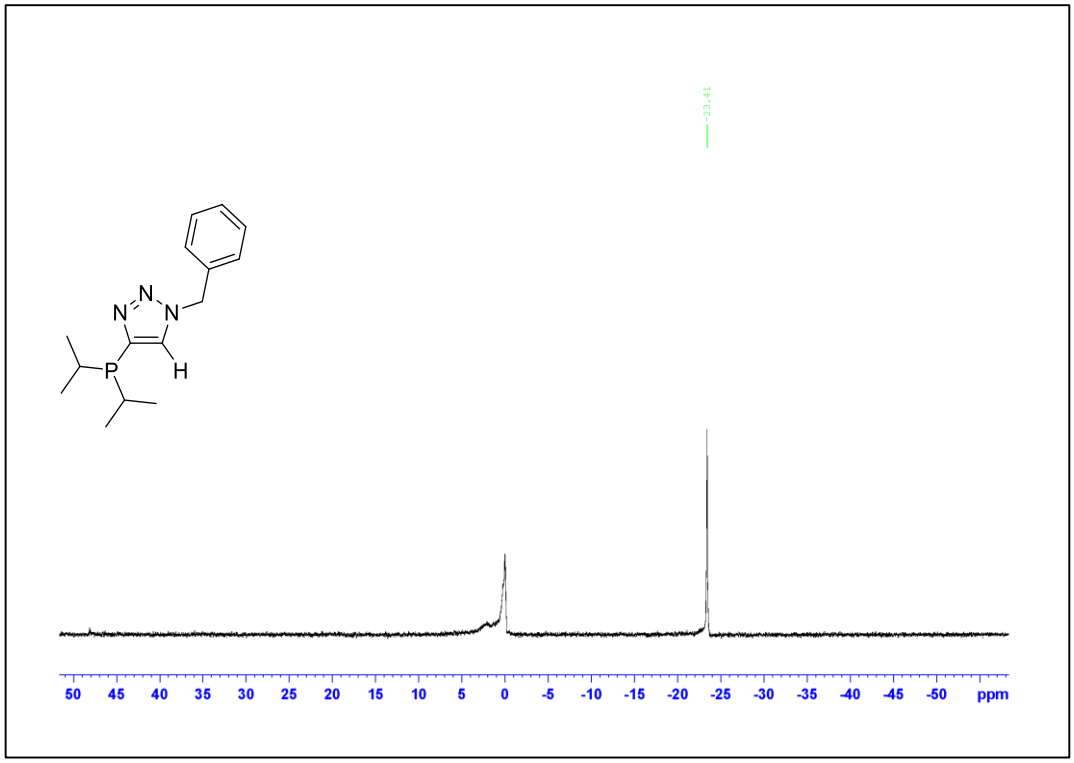

Figure A.331. ^{31}P NMR Spectrum of Compound **3.8e**

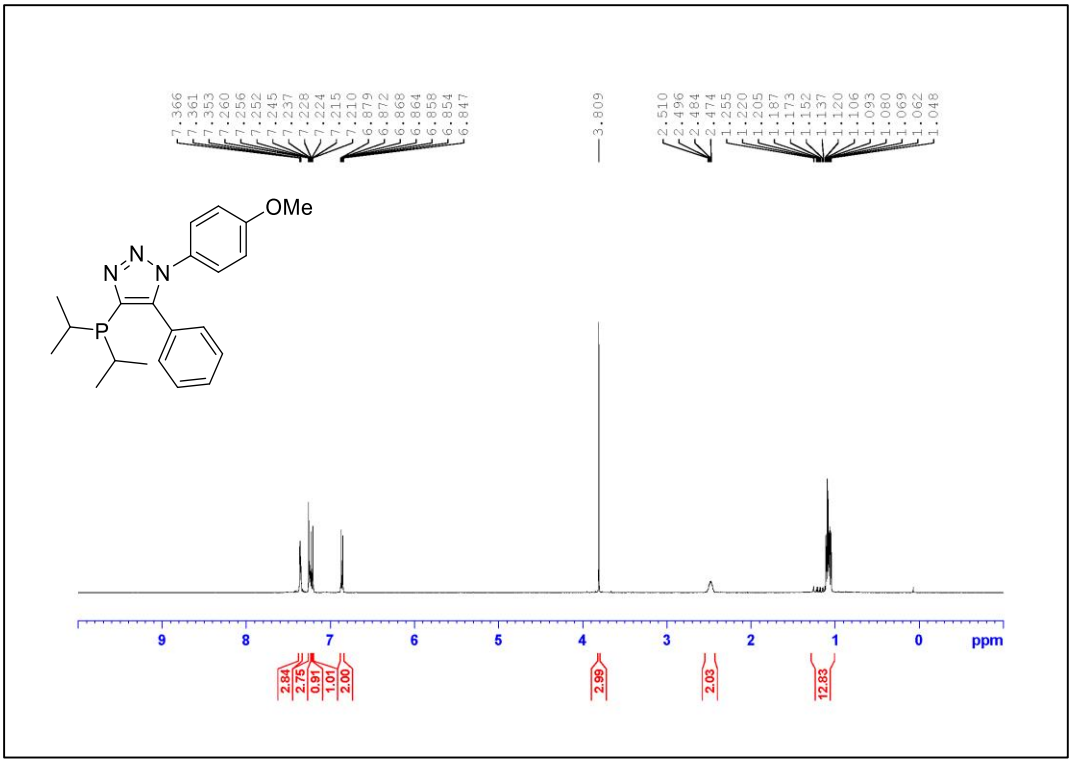

Figure A.332. ^{1}H NMR Spectrum of Compound **3.8k** (500 MHz, $CDCl_3$)

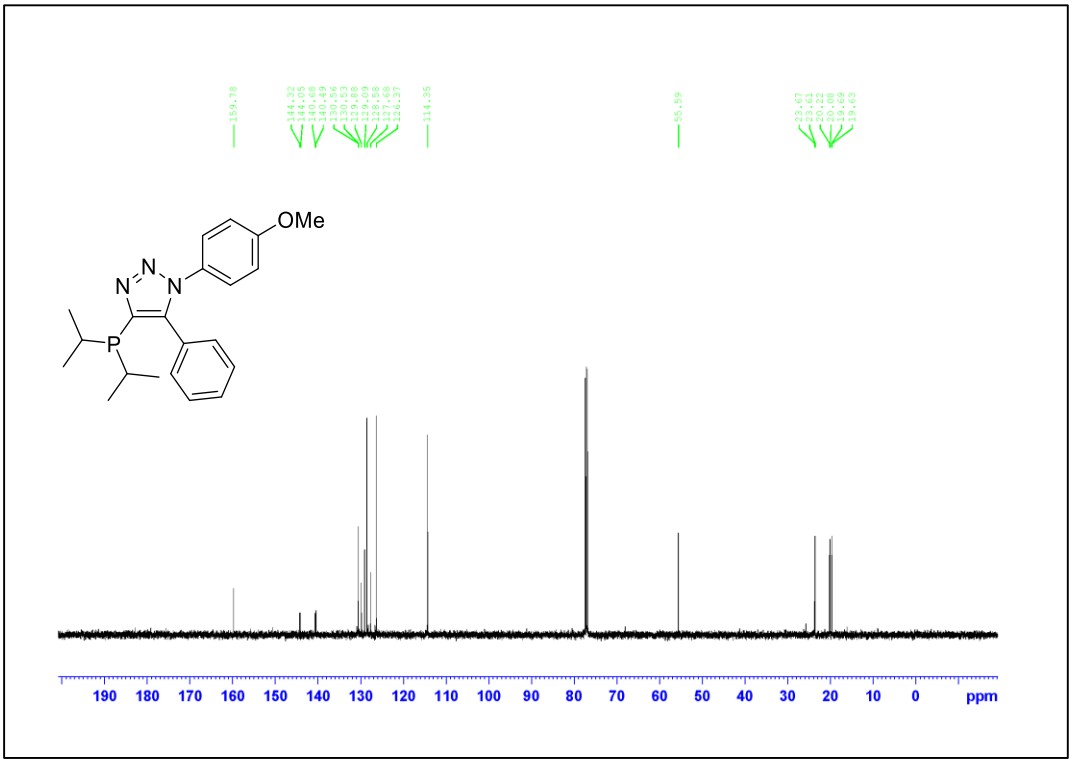

Figure A.333. ^{13}C NMR Spectrum of Compound **3.8k** (125 MHz, $CDCl_3$)

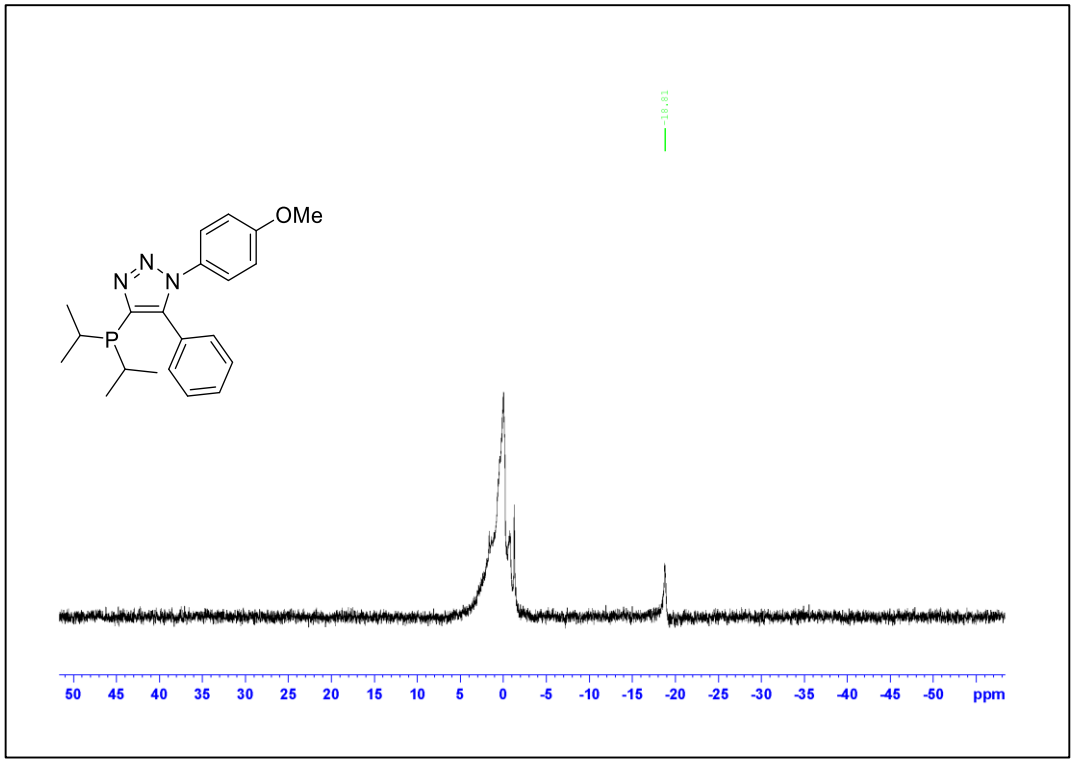

Figure A.334. ^{31}P NMR Spectrum of Compound **3.8k**

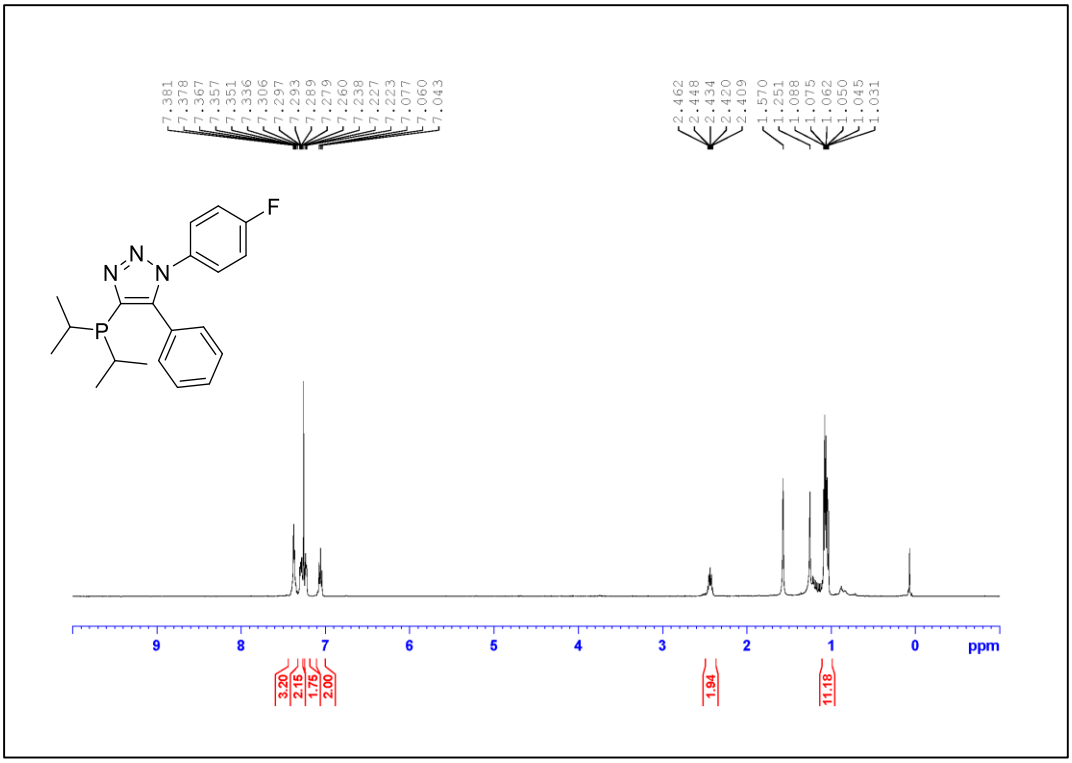

Figure A.335. ^{1}H NMR Spectrum of Compound **3.8p** (500 MHz, $CDCl_3$)

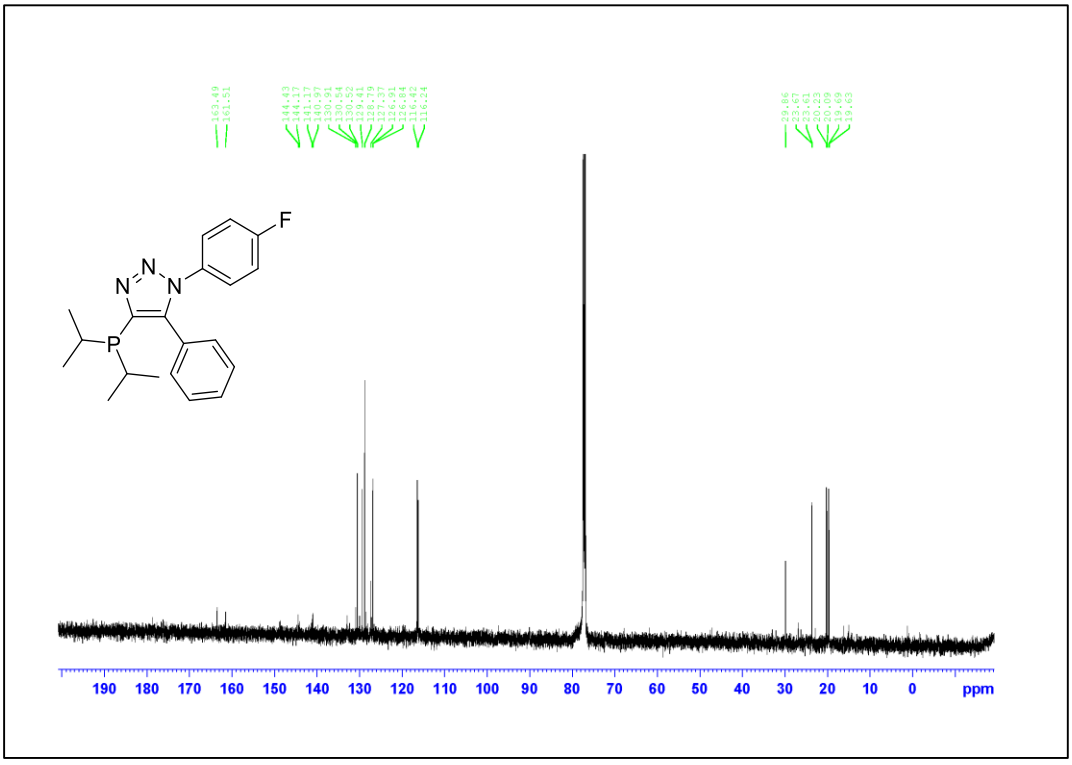

Figure A.336. ^{13}C NMR Spectrum of Compound **3.8p** (125 MHz, $CDCl_3$)

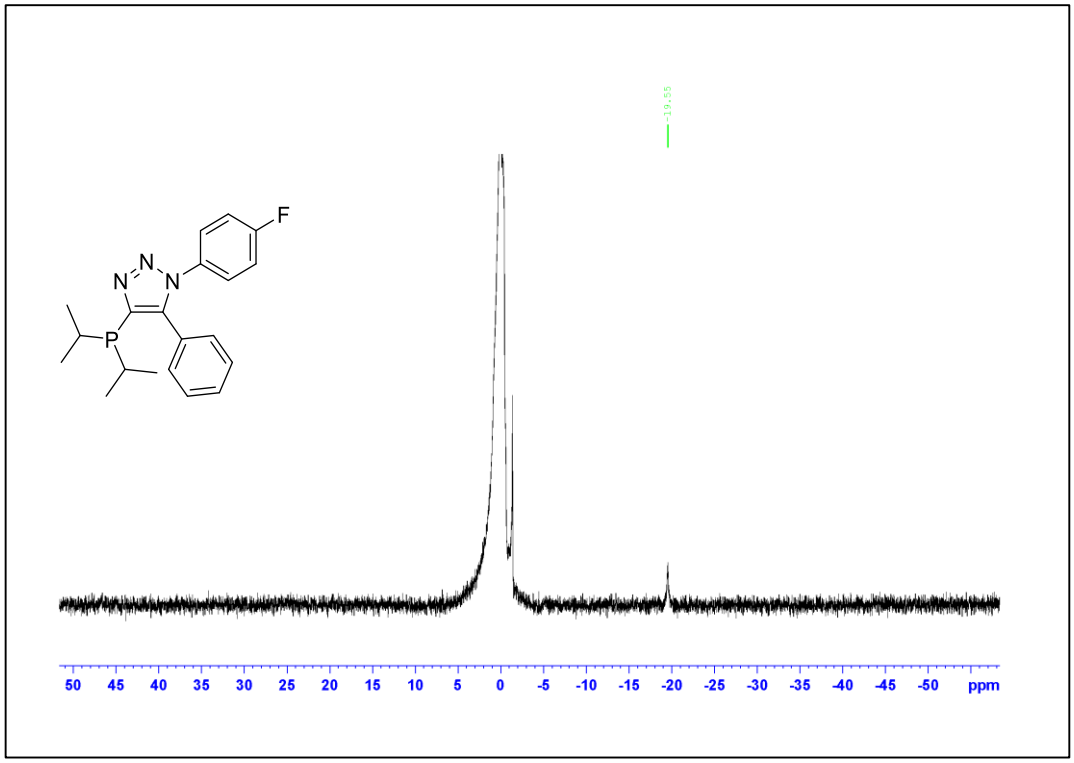

Figure A.337. ^{31}P NMR Spectrum of Compound **3.8p**

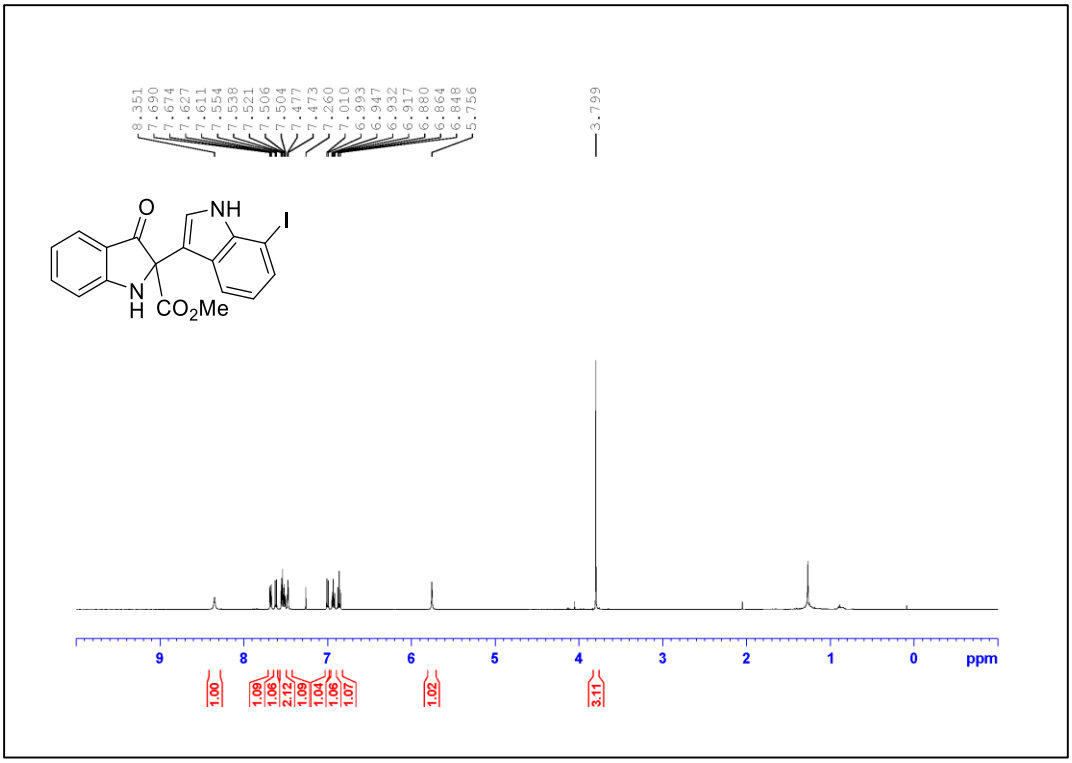

Figure A.338. ^{1}H NMR Spectrum of Compound **4.2c** (500 MHz, $CDCl_3$)

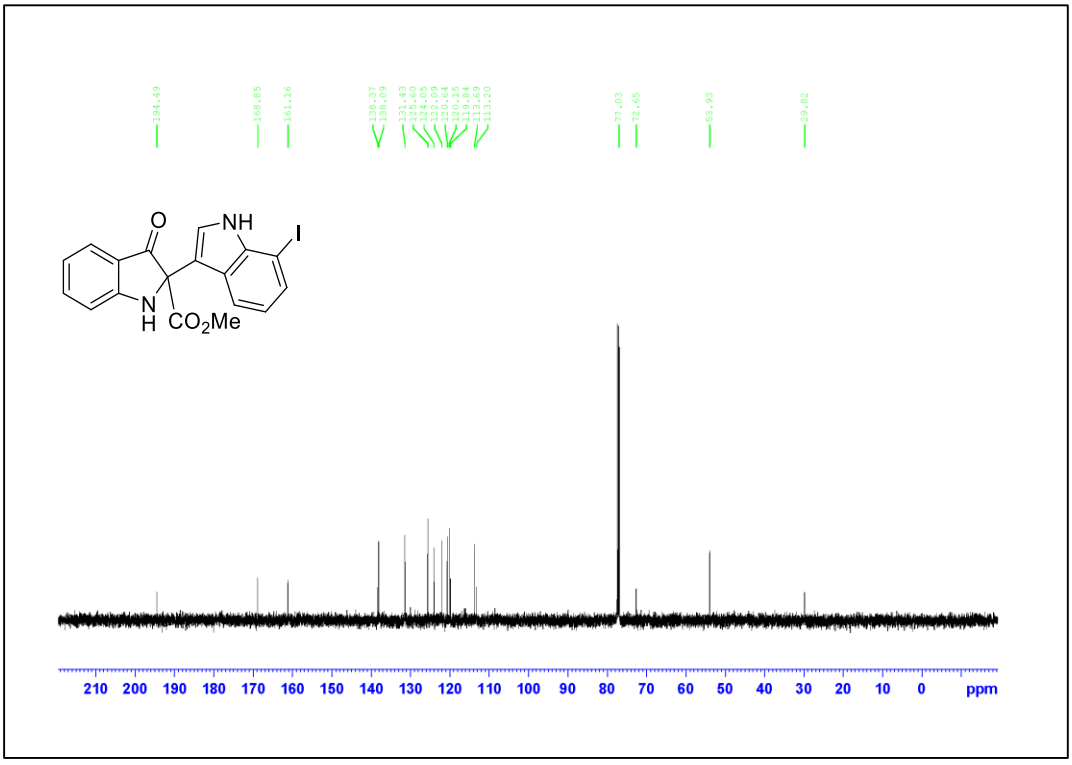

Figure A.339. ^{13}C NMR Spectrum of Compound **4.2c** (125 MHz, $CDCl_3$)

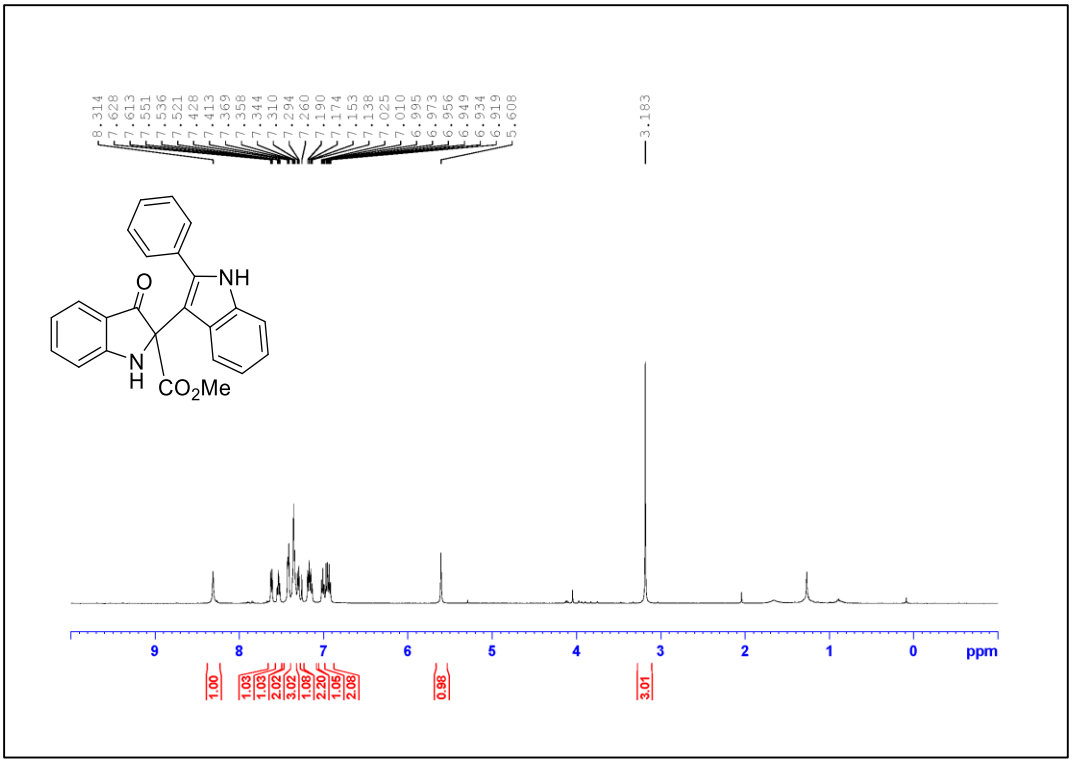

Figure A.340. ^{1}H NMR Spectrum of Compound **4.2f** (500 MHz, $CDCl_3$)

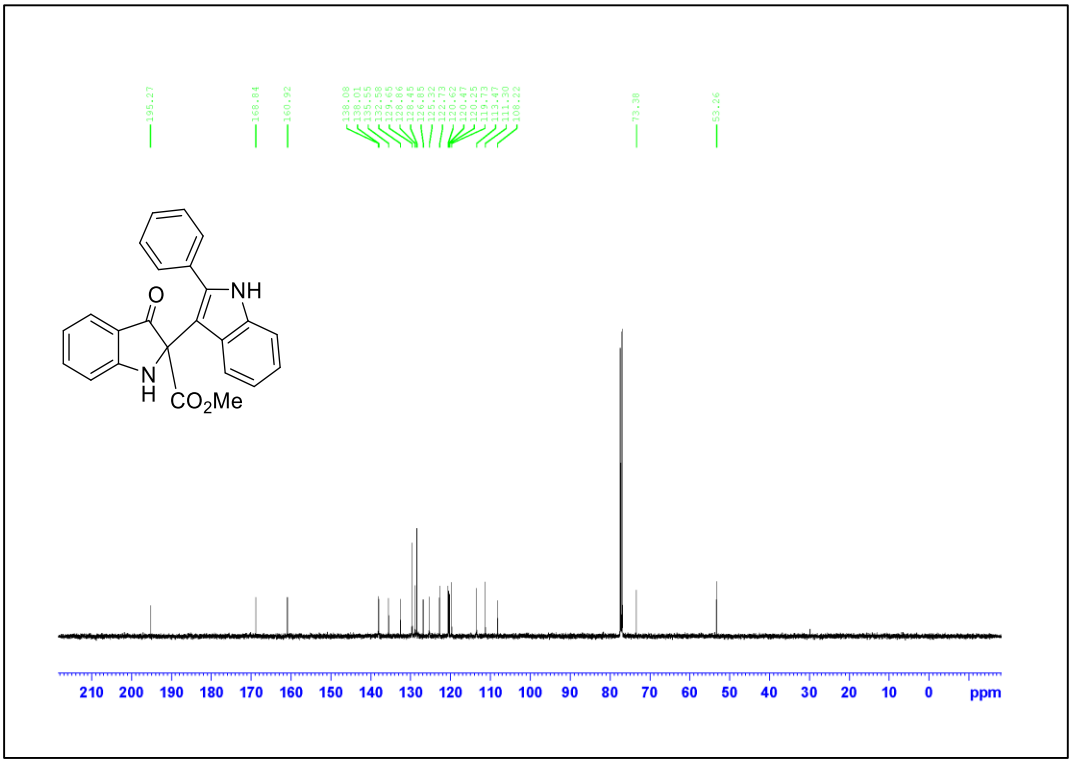

Figure A.341. ^{13}C NMR Spectrum of Compound **4.2f** (125 MHz, $CDCl_3$)

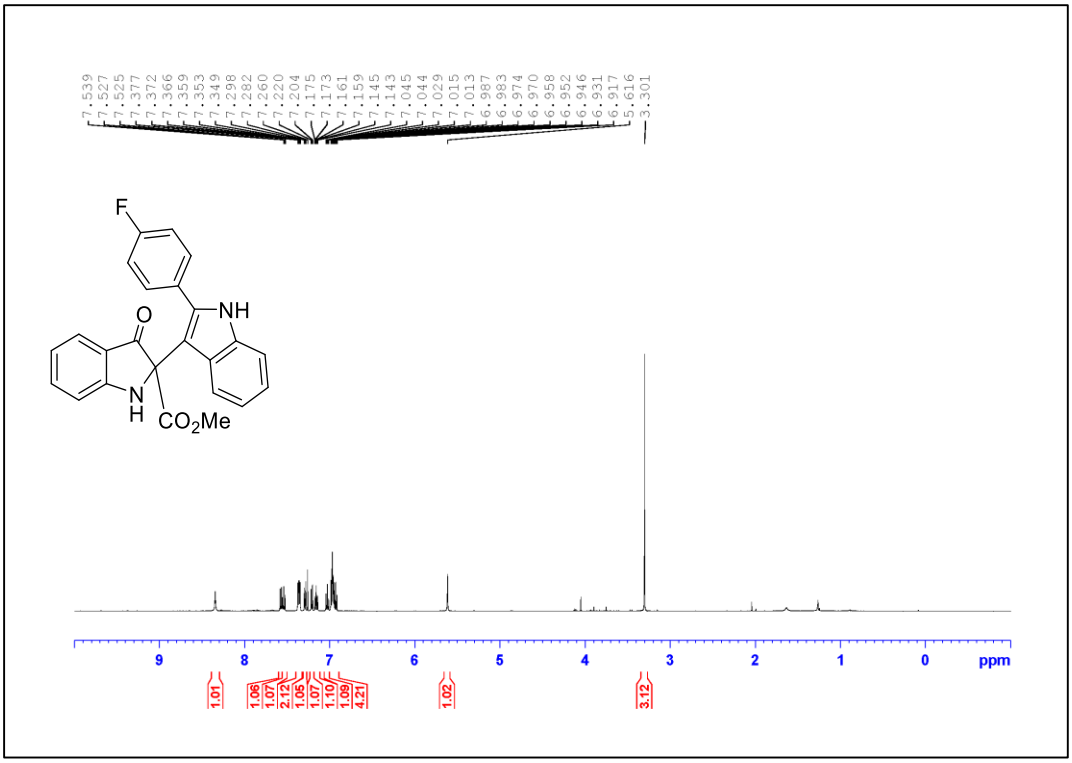

Figure A.342. ^{1}H NMR Spectrum of Compound **4.2g** (500 MHz, $CDCl_3$)

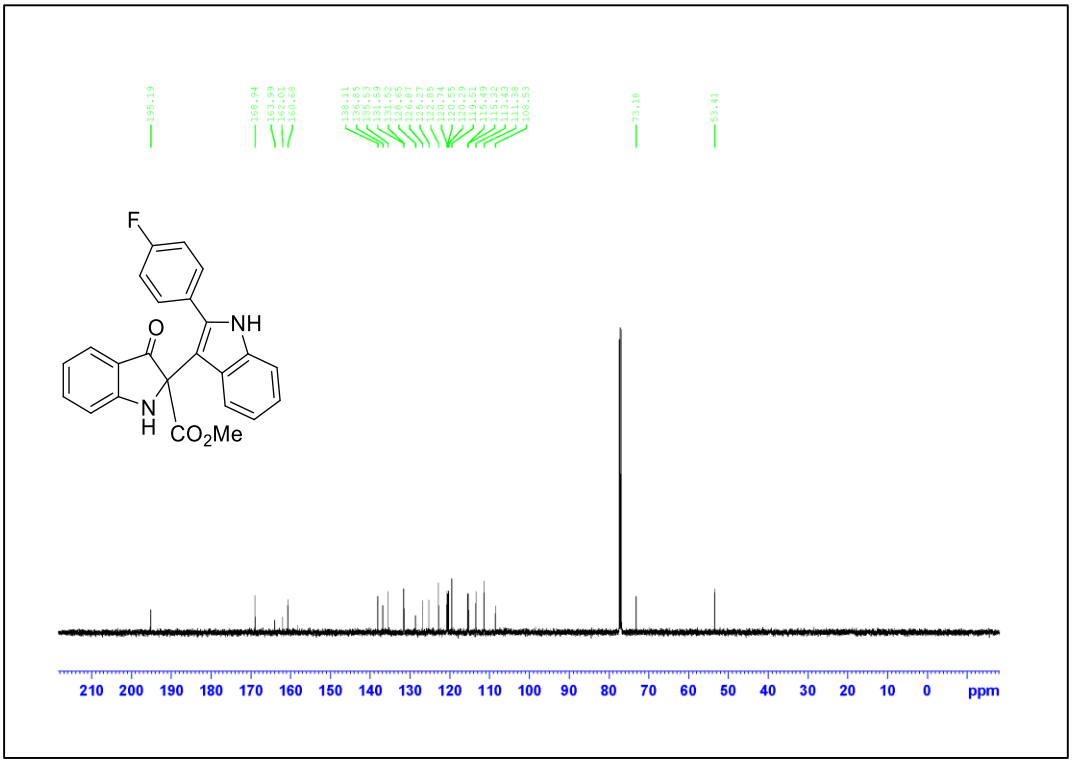

Figure A.343. ^{13}C NMR Spectrum of Compound **4.2g** (125 MHz, $CDCl_3$)

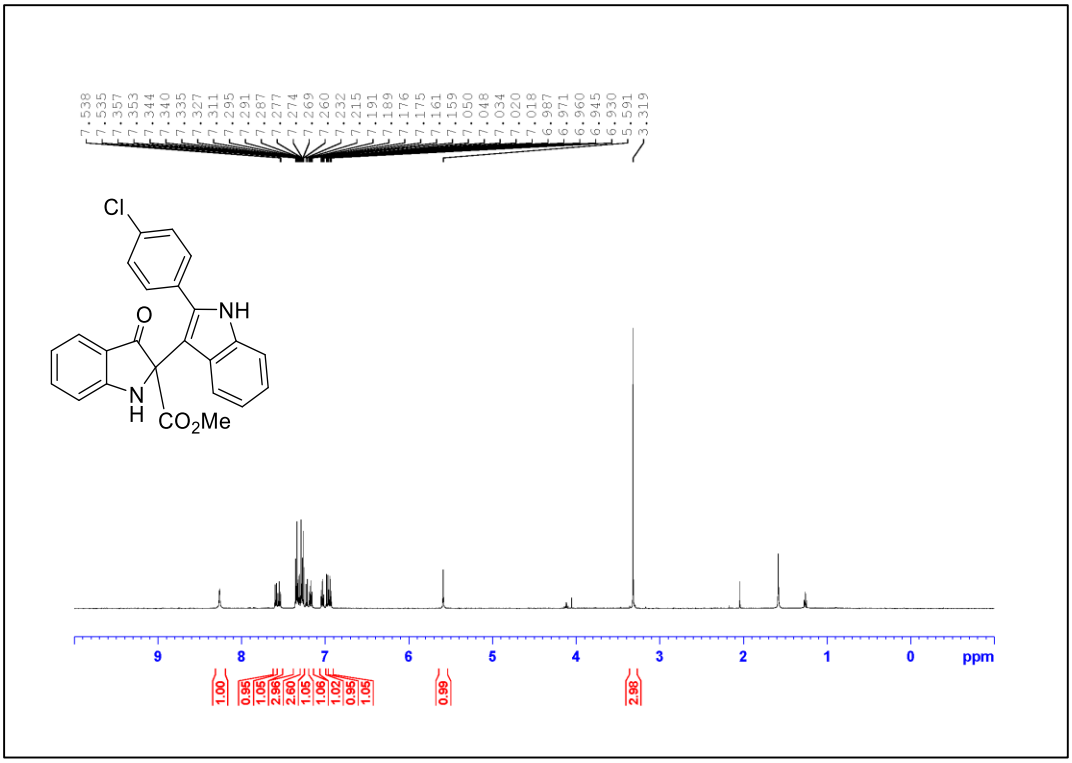

Figure A.344. ^{1}H NMR Spectrum of Compound **4.2h** (500 MHz, $CDCl_3$)

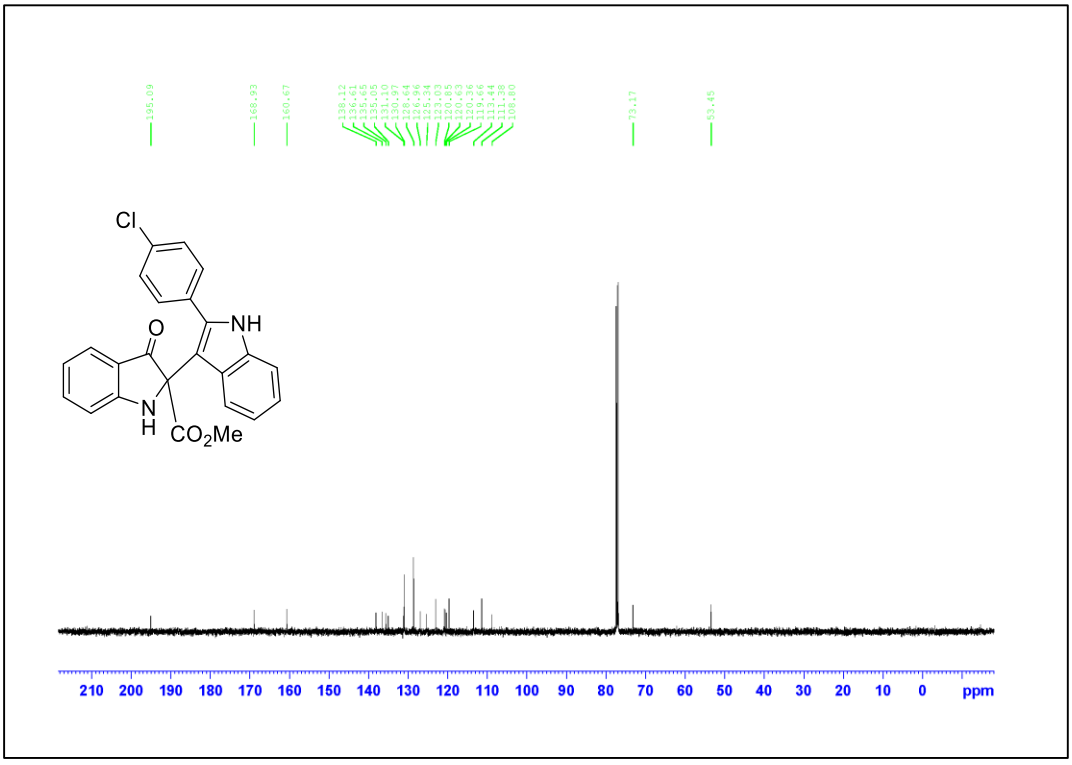

Figure A.345. ^{13}C NMR Spectrum of Compound **4.2h** (125 MHz, $CDCl_3$)

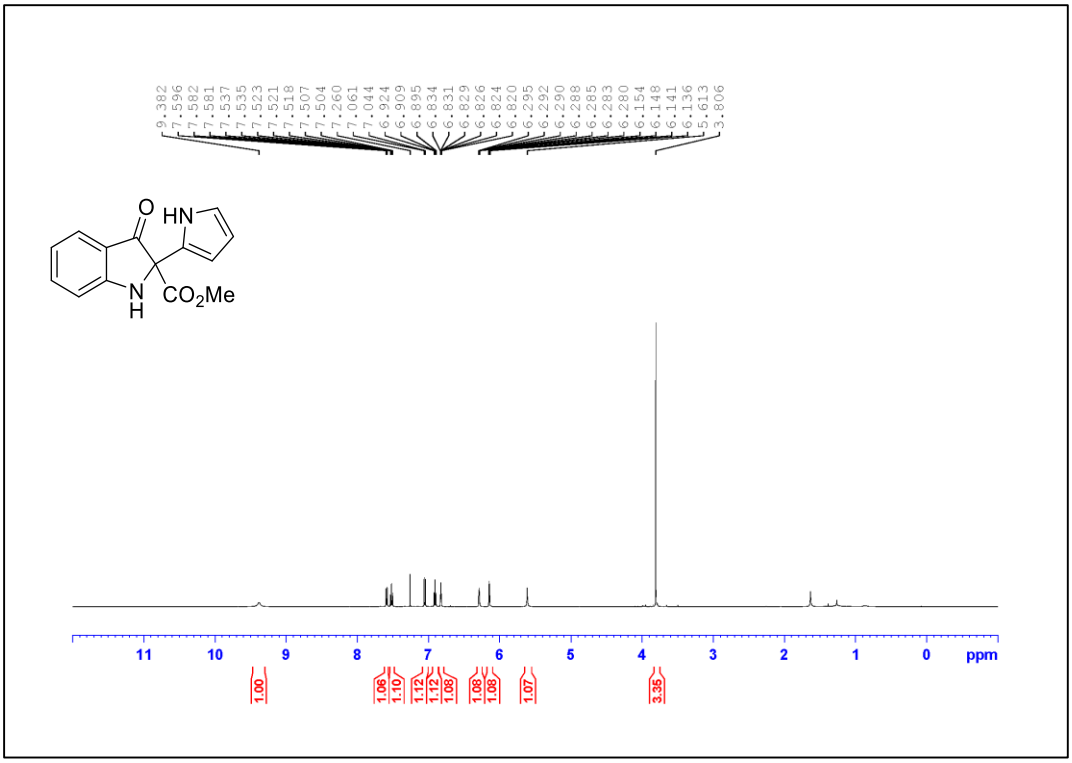

Figure A.346. ^{1}H NMR Spectrum of Compound **4.2m** (500 MHz, $CDCl_3$)

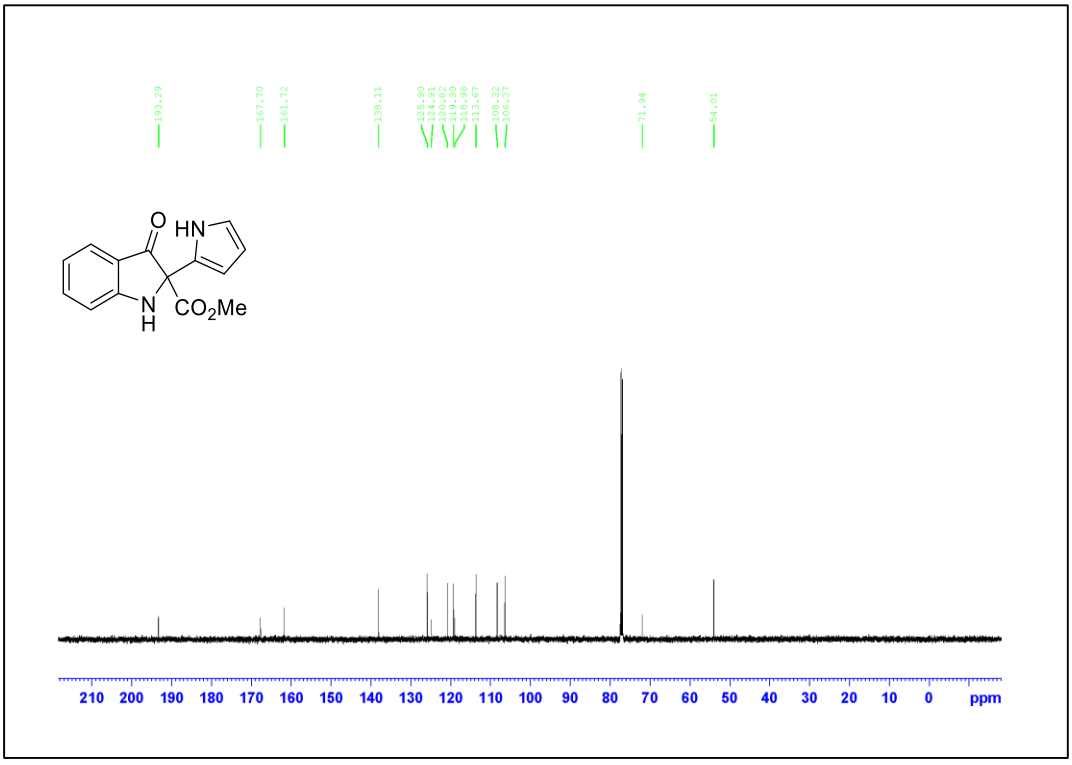

Figure A.347. ^{13}C NMR Spectrum of Compound **4.2m** (125 MHz, $CDCl_3$)

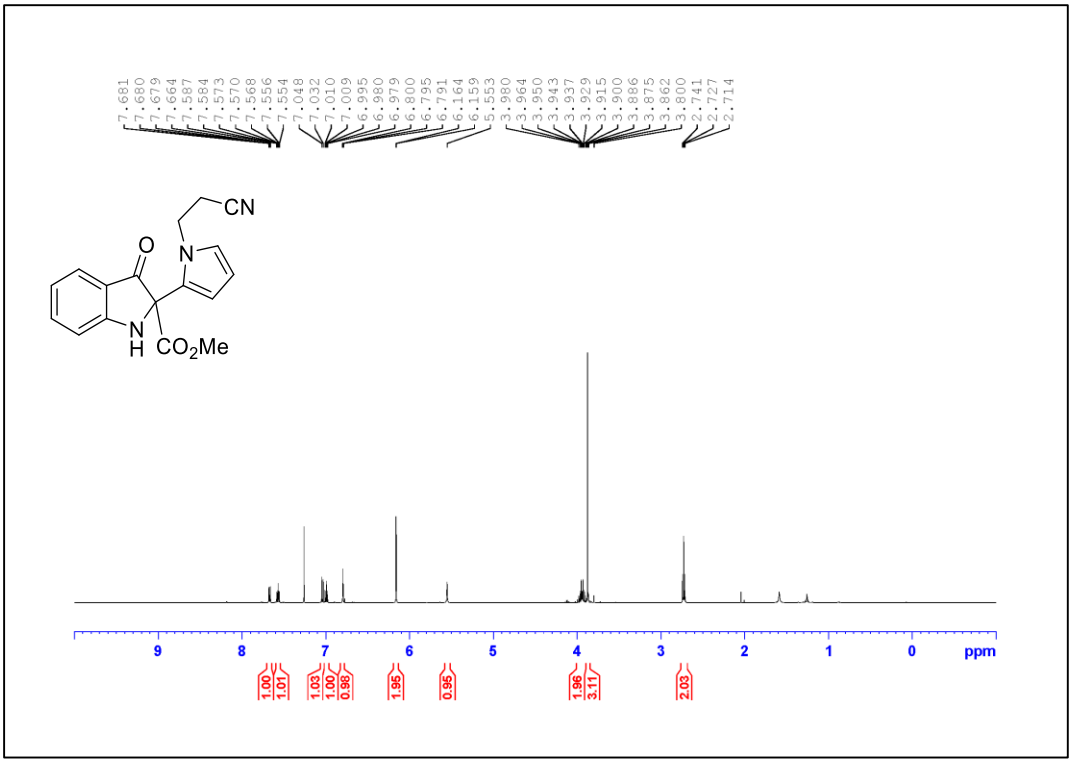

Figure A.348. ^{1}H NMR Spectrum of Compound **4.2p** (500 MHz, $CDCl_3$)

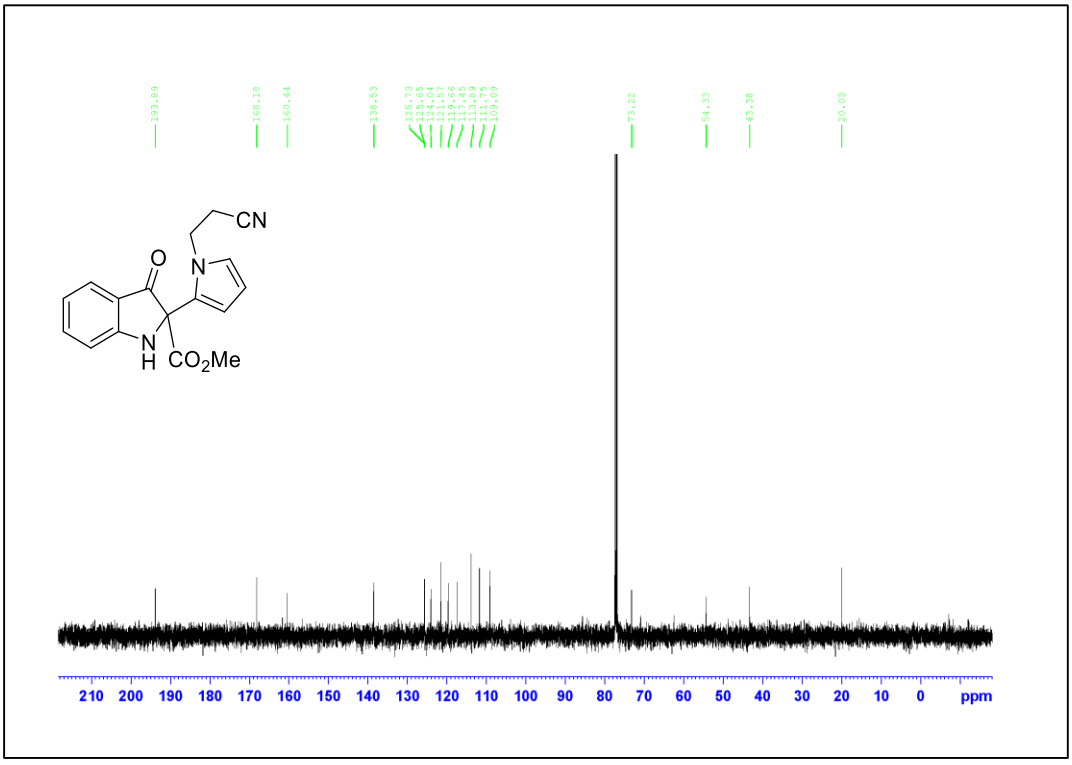

Figure A.349. ^{13}C NMR Spectrum of Compound **4.2p** (125 MHz, $CDCl_3$)

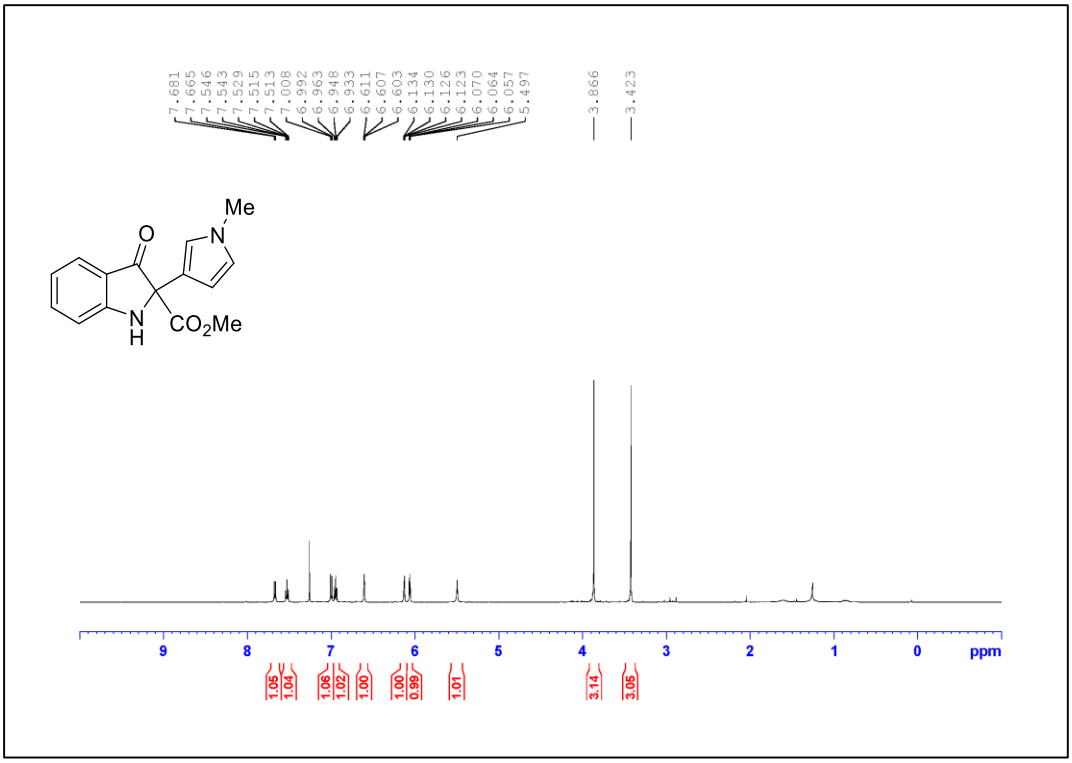

Figure A.350. ^{1}H NMR Spectrum of Compound **4.2q** (500 MHz, $CDCl_3$)

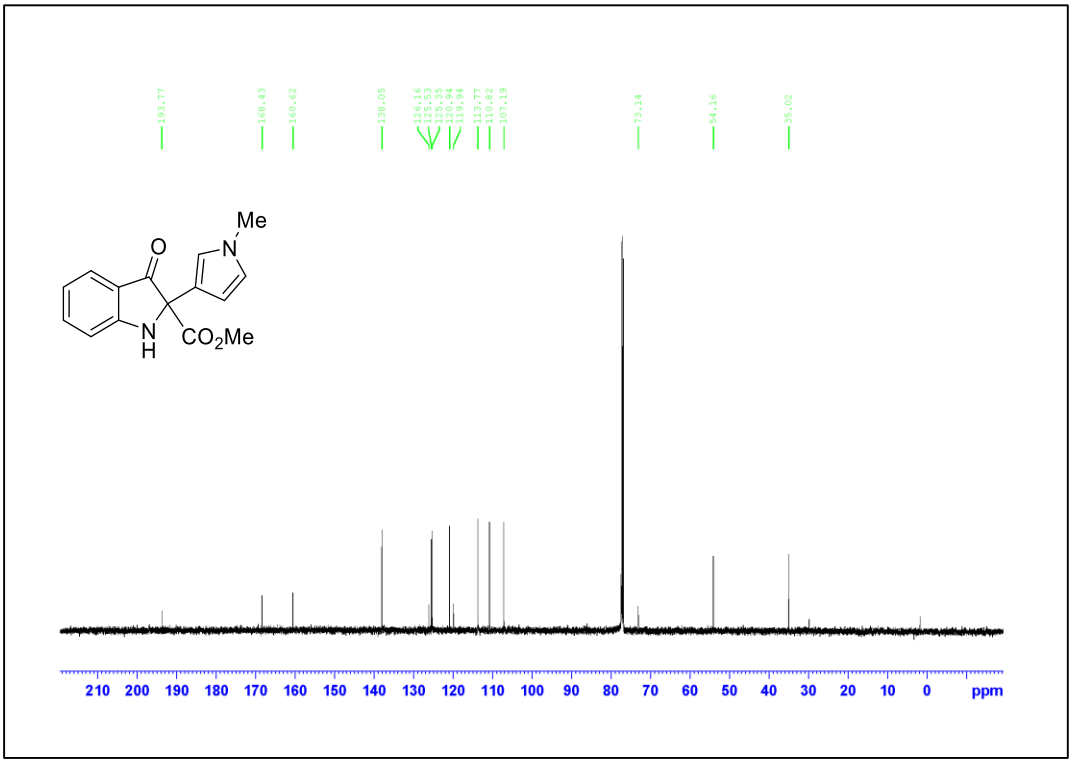

Figure A.351. ^{13}C NMR Spectrum of Compound **4.2q** (125 MHz, $CDCl_3$)

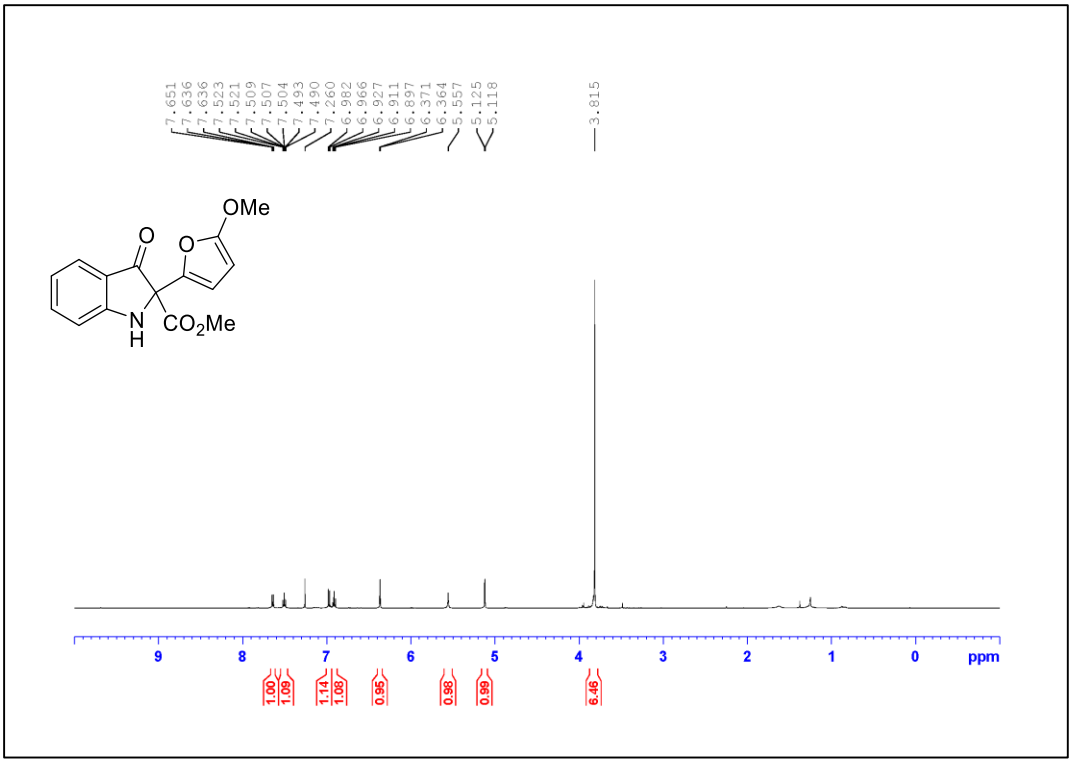

Figure A.352. ^{1}H NMR Spectrum of Compound **4.2r** (500 MHz, $CDCl_3$)

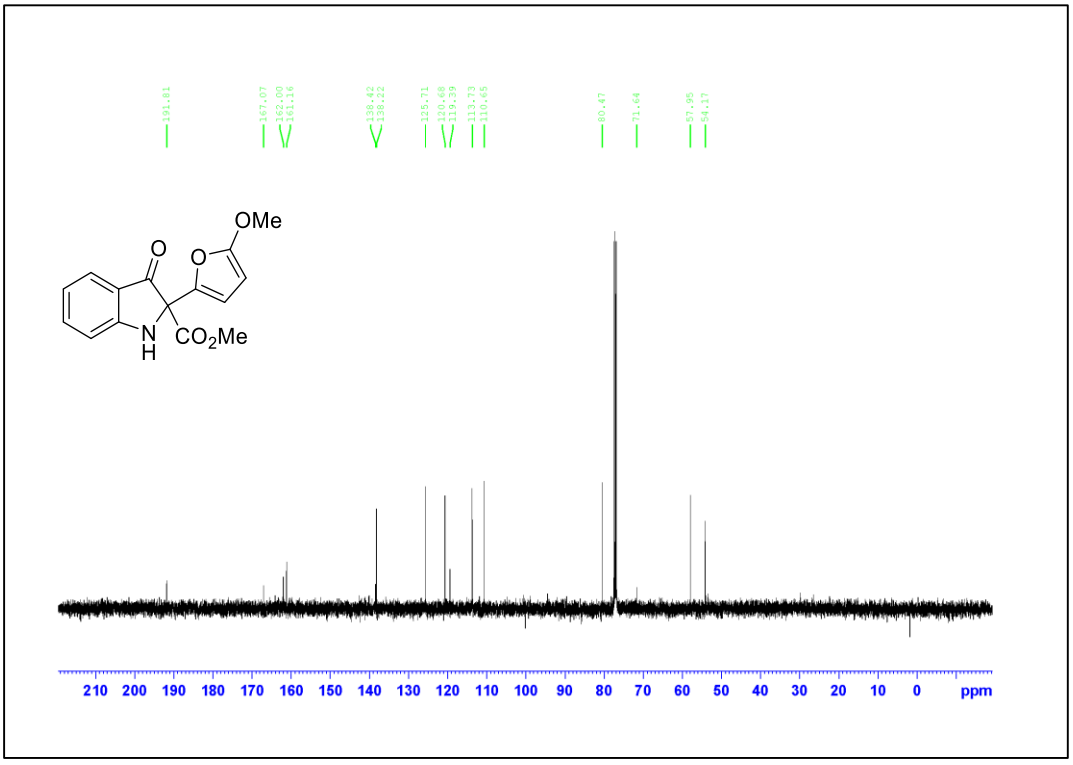

Figure A.353. ^{13}C NMR Spectrum of Compound **4.2r** (125 MHz, $CDCl_3$)

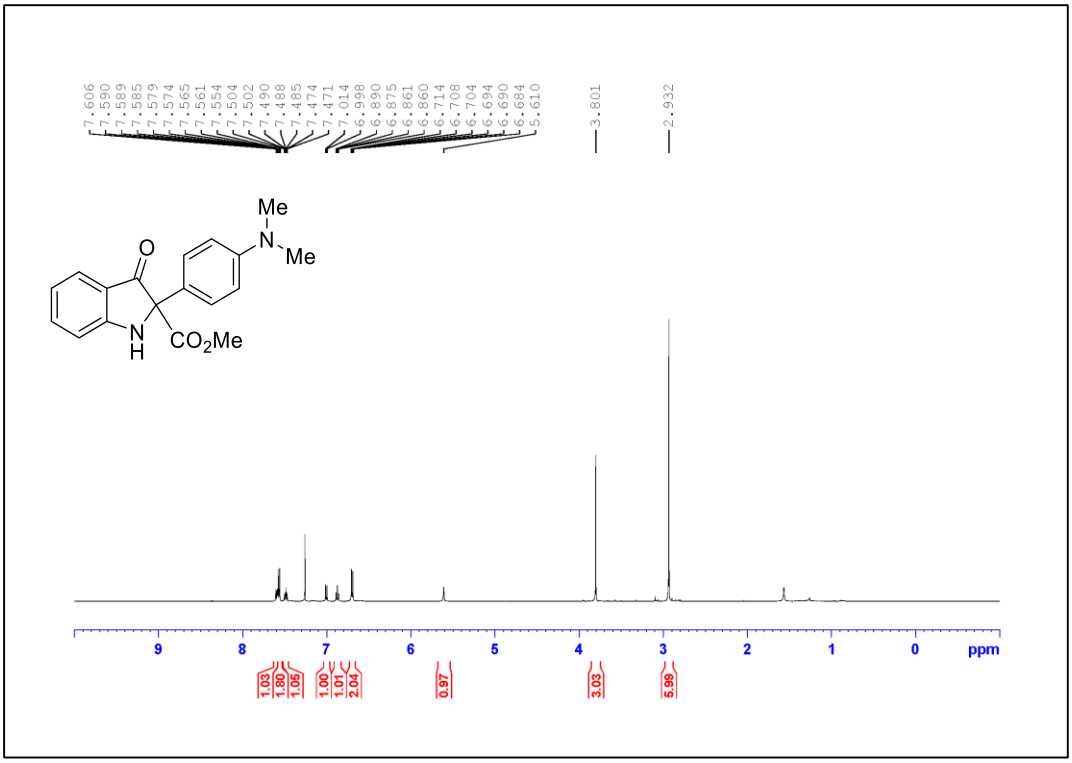

Figure A.354. ^{1}H NMR Spectrum of Compound **4.2s** (500 MHz, $CDCl_3$)

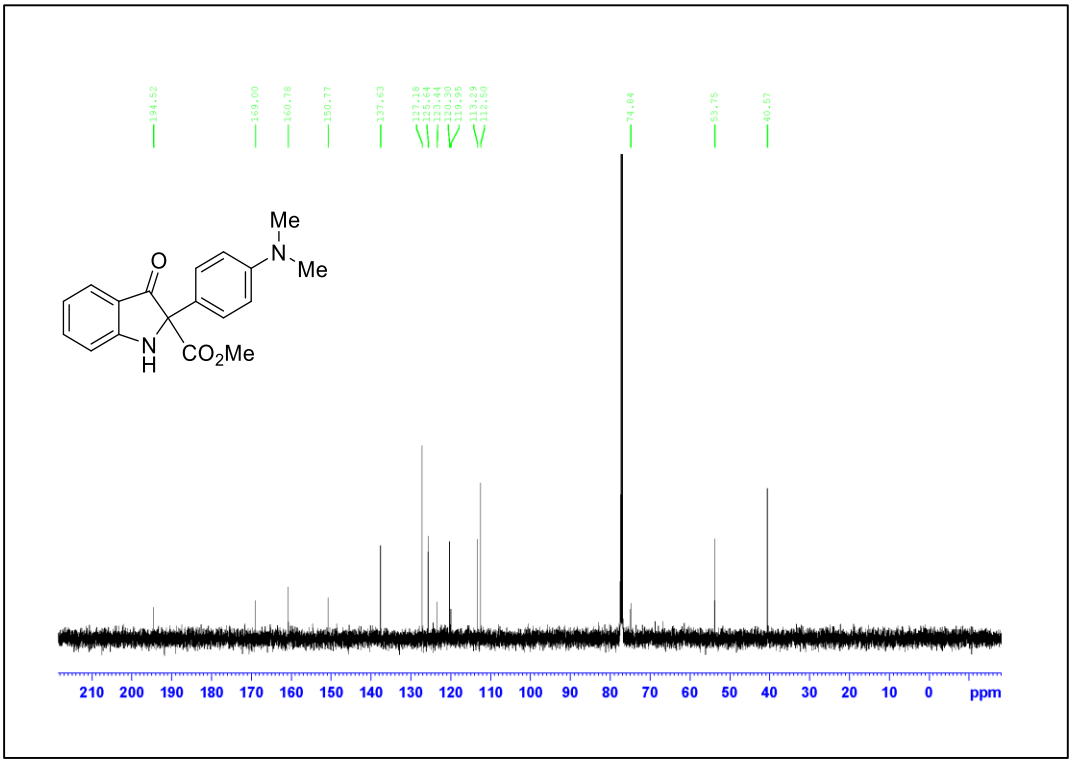

Figure A.355. ^{13}C NMR Spectrum of Compound **4.2s** (125 MHz, $CDCl_3$)

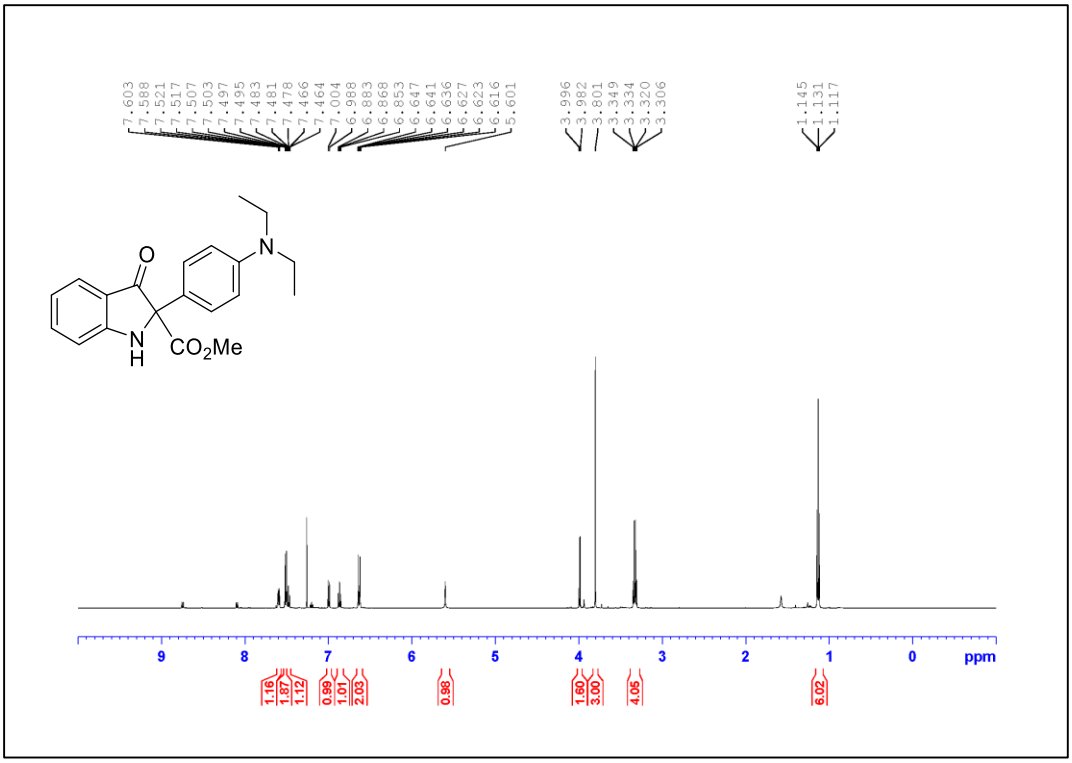

Figure A.356. ^{1}H NMR Spectrum of Compound **4.2t** (500 MHz, $CDCl_3$)

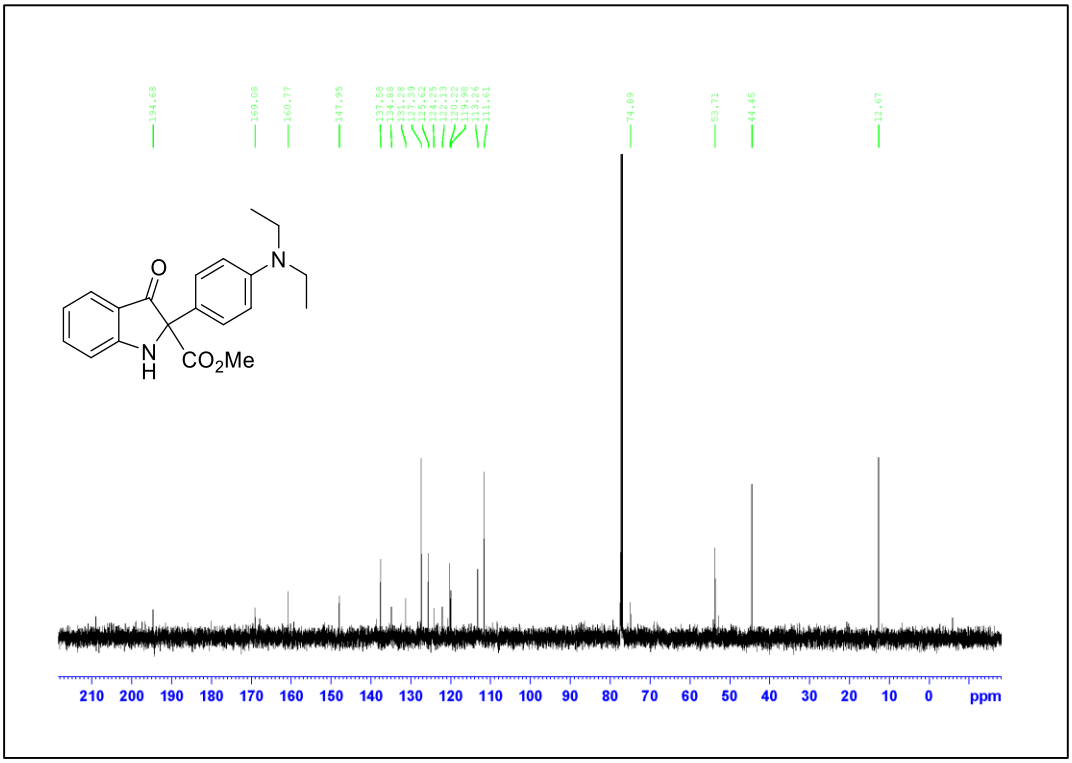

Figure A.357. ^{13}C NMR Spectrum of Compound **4.2t** (125 MHz, $CDCl_3$)

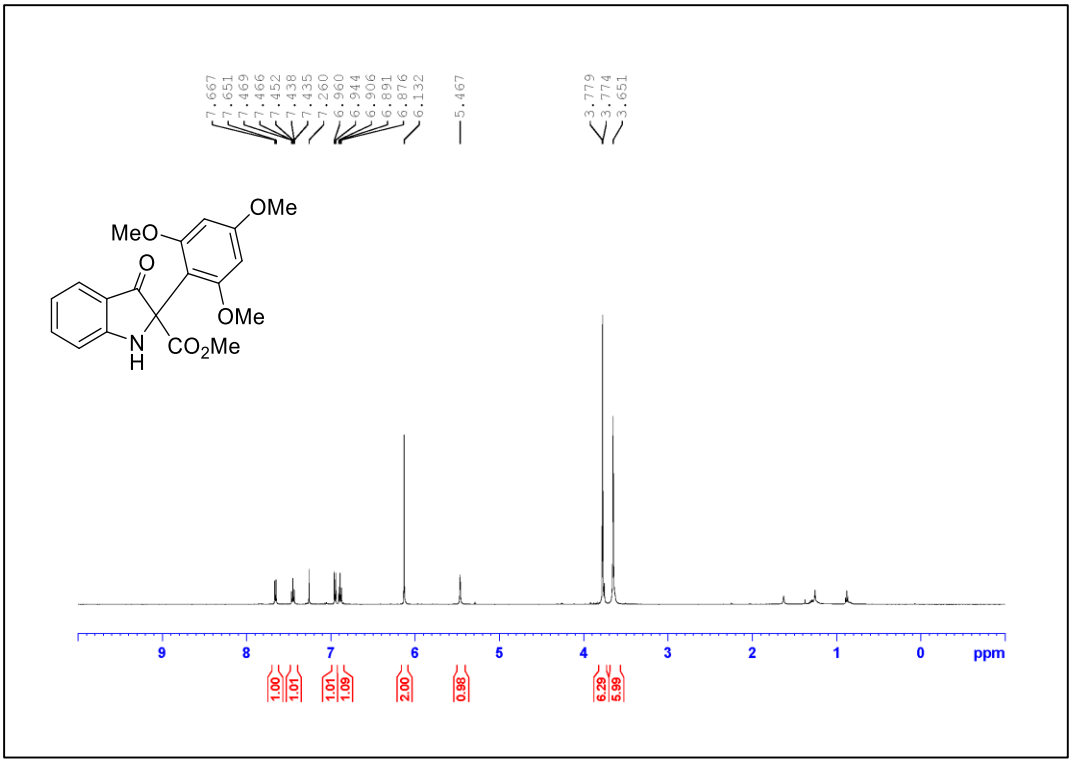

Figure A.358. ^{1}H NMR Spectrum of Compound **4.2u** (500 MHz, $CDCl_3$)

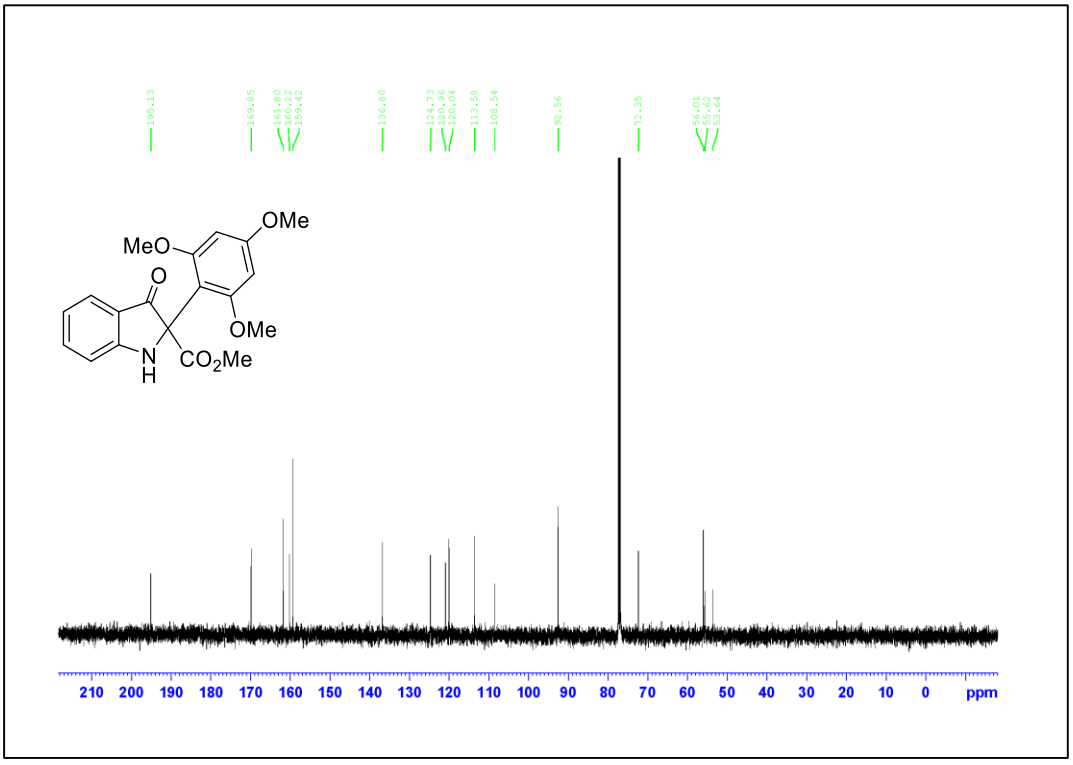

Figure A.359. ^{13}C NMR Spectrum of Compound **4.2u** (125 MHz, $CDCl_3$)

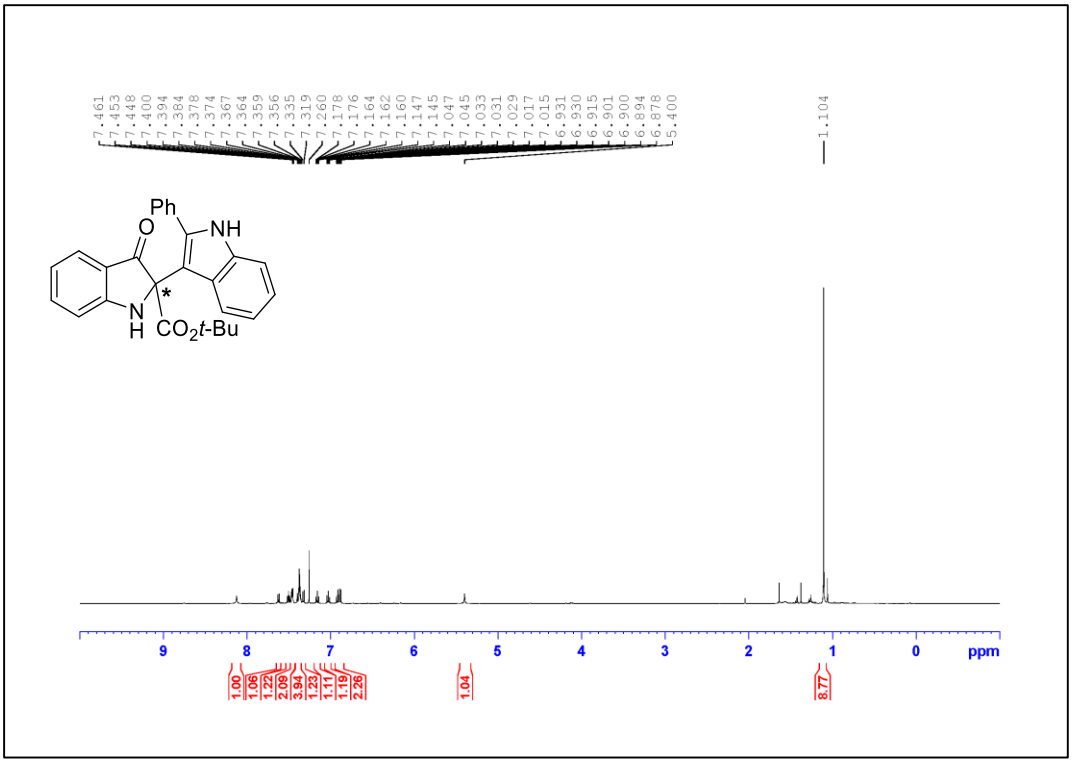

Figure A.360. ^{1}H NMR Spectrum of Compound **4.5f** (500 MHz, $CDCl_3$)

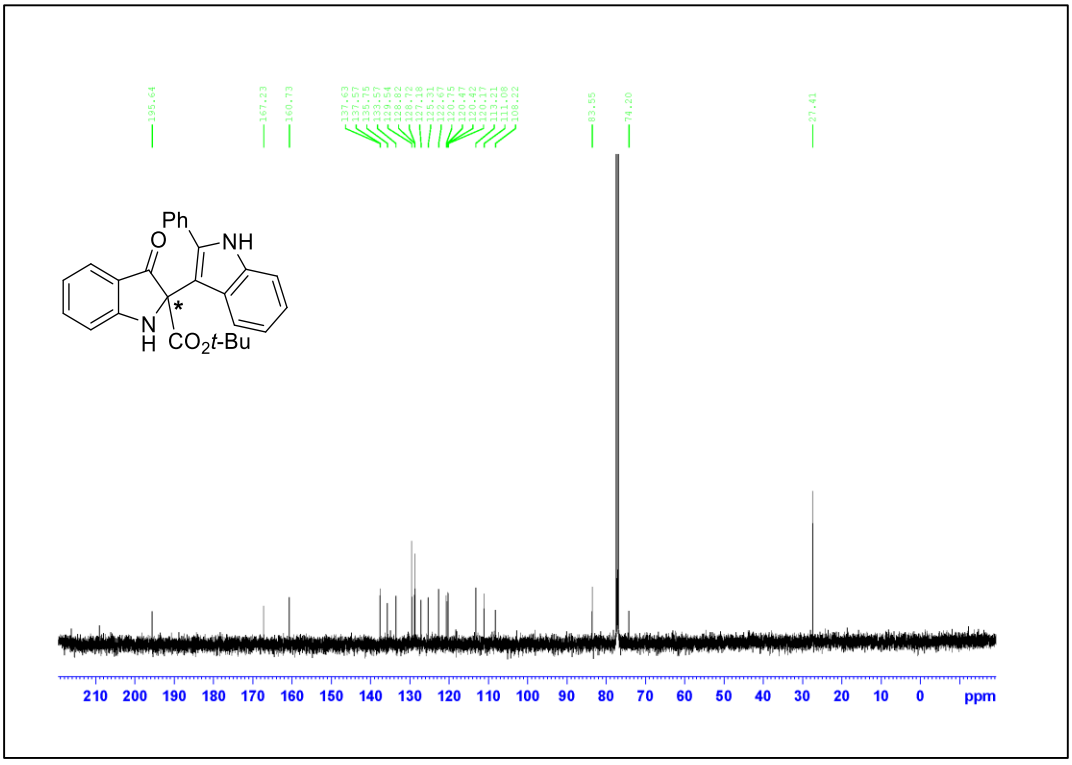

Figure A.361. ^{13}C NMR Spectrum of Compound **4.5f** (125 MHz, $CDCl_3$)

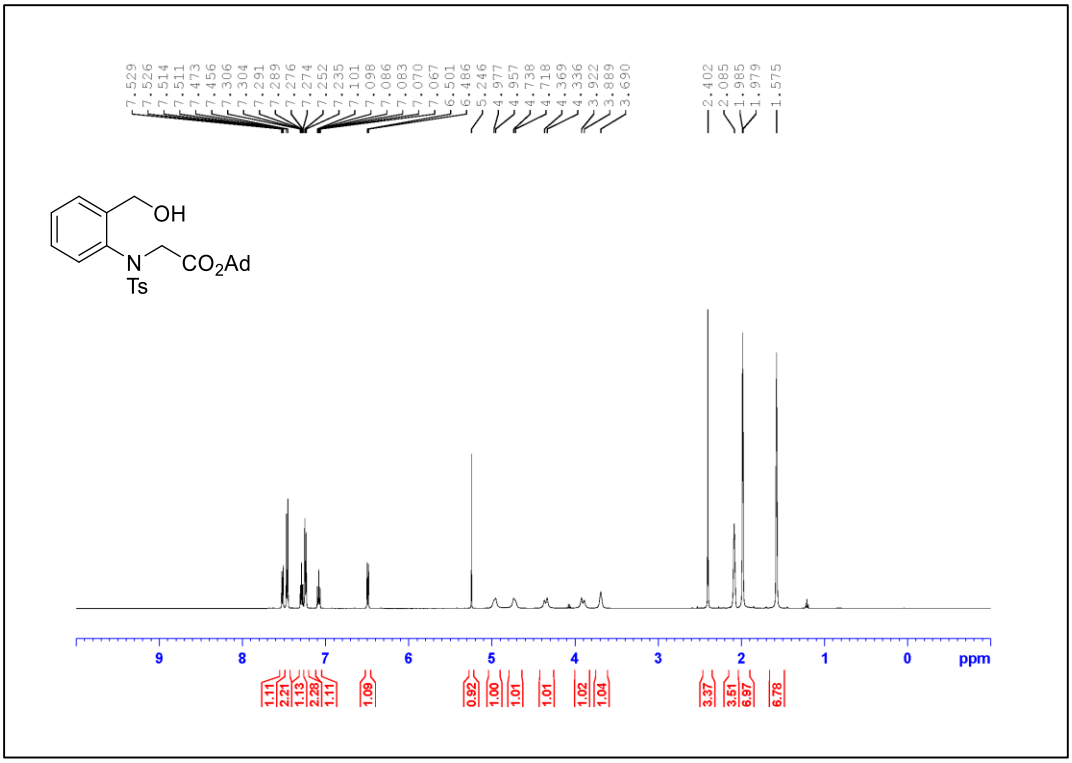

Figure A.362. ^{1}H NMR Spectrum of Compound **4.S1** (500 MHz, $CDCl_3$)

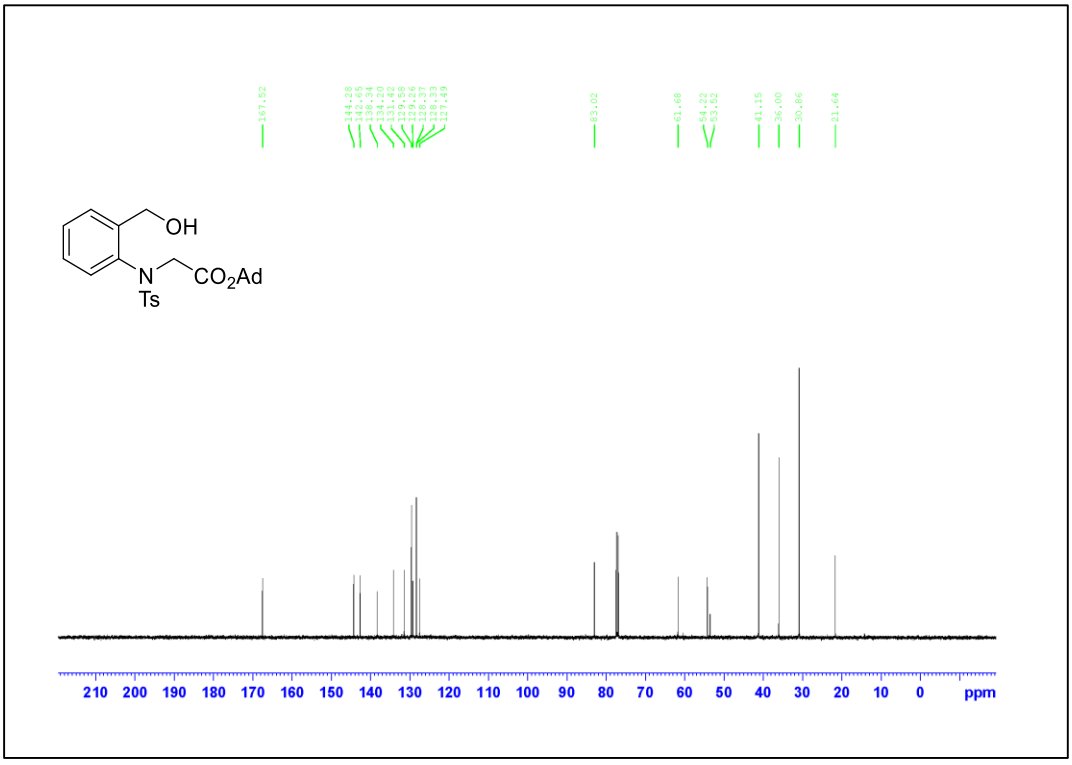

Figure A.363. ^{13}C NMR Spectrum of Compound **4.S1** (125 MHz, $CDCl_3$)

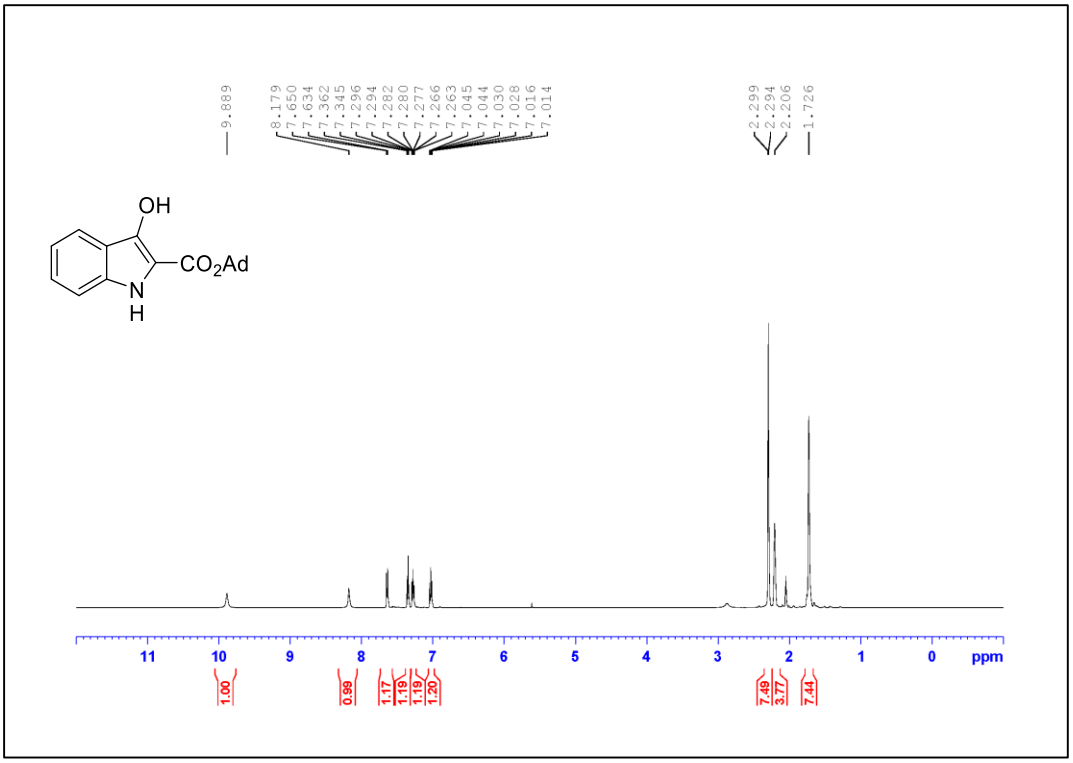

Figure A.364. ^{1}H NMR Spectrum of Compound **4.6** (500 MHz, acetone-d_6)

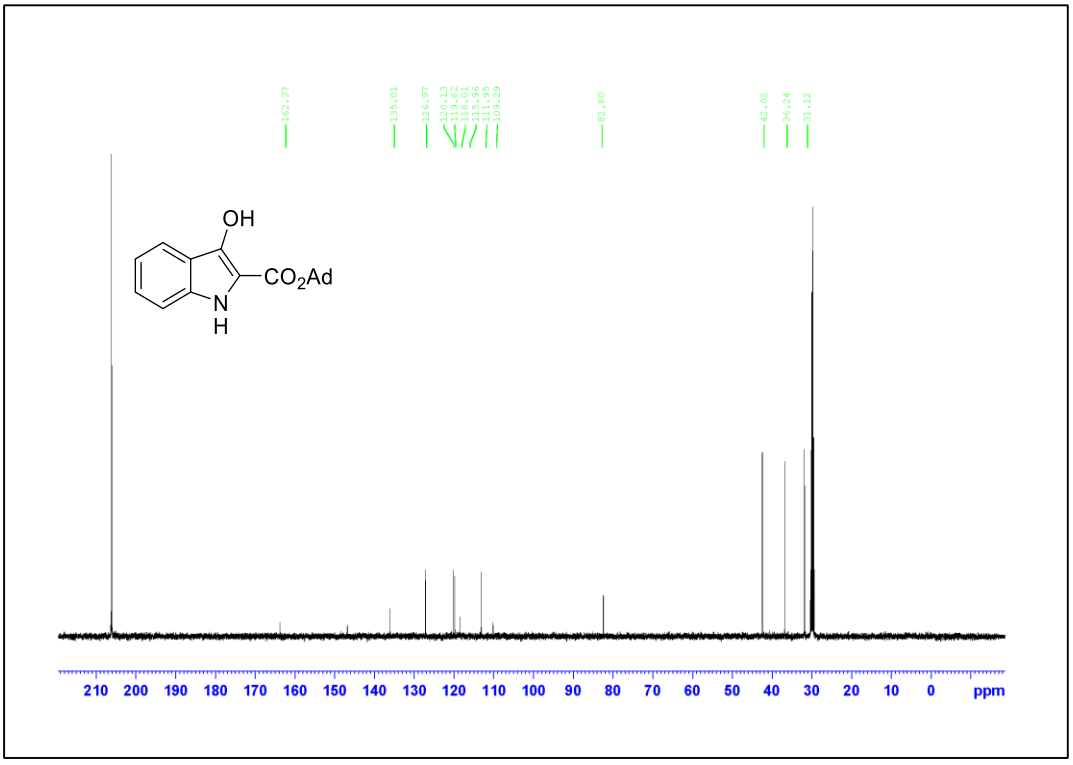

Figure A.365. ^{13}C NMR Spectrum of Compound **4.6** (125 MHz, acetone-d_6)

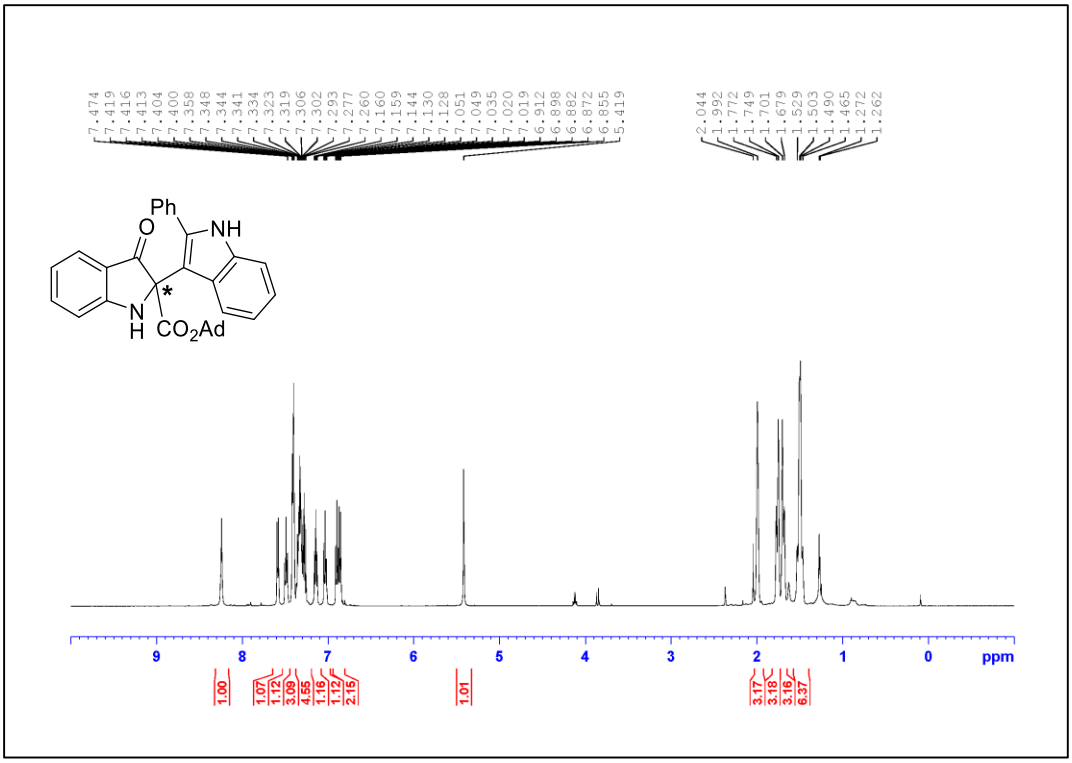

Figure A.366. ^{1}H NMR Spectrum of Compound **4.7f** (500 MHz, $CDCl_3$)

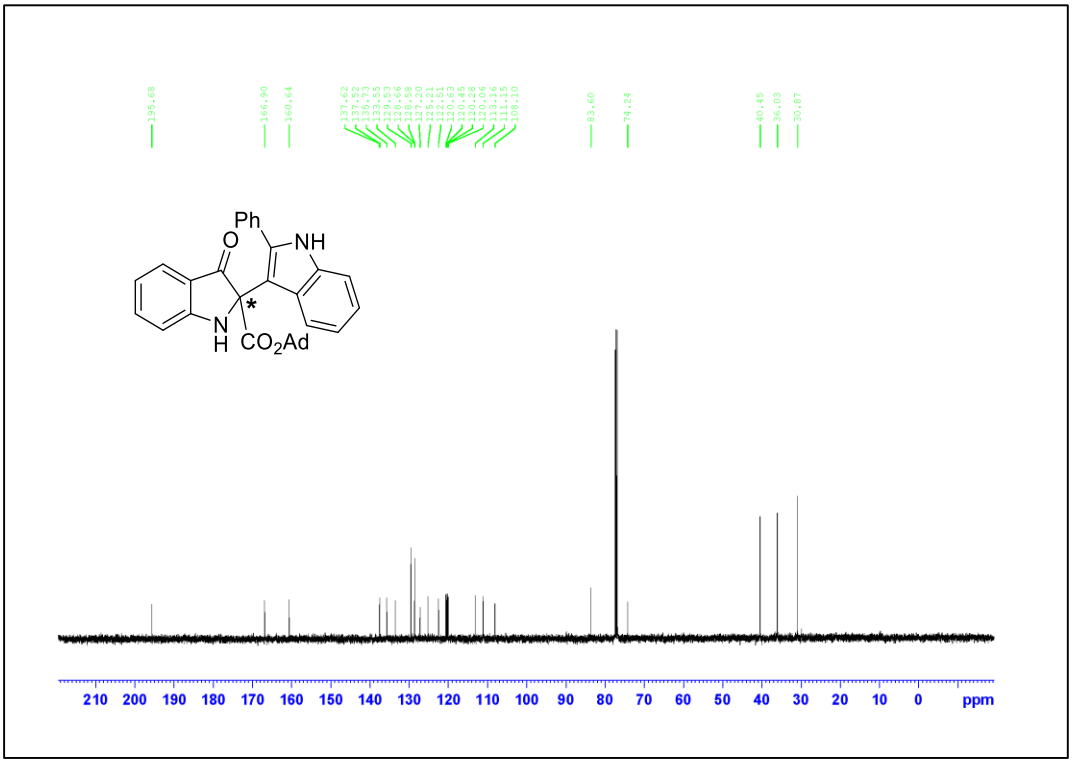

Figure A.367. ^{13}C NMR Spectrum of Compound **4.7f** (125 MHz, $CDCl_3$)

BIBLIOGRAPHY

Akiyama, T.; Hirofuji, H.; Ozaki, S. $AlCl_3$-N,N-Dimethylaniline: A New Benzyl and Allyl Ether Cleavage Reagent. *Tetrahedron Lett.* **1991**, *32* (10), 1321–1324.

Albanese, D.; Landini, D.; Penso, M.; Spanò, G.; Trebicka, A. Chemoselective N-Alkylation of 2-Hydroxycarbazole as a Model for the Synthesis of N-Substituted Pyrrole Derivatives Containing Acidic Functions. *Tetrahedron* **1995**, *51* (19), 5681–5688.

Altinis Kiraz, C. I.; Emge, T. J.; Jimenez, L. S. Oxidation of Indole Substrates by Oxodiperoxomolybdenum·Trialkyl(Aryl)- Phosphine Oxide Complexes. *J. Org. Chem.* **2004**, *69* (6), 2200–2202.

Anxionnat, B.; Gomez Pardo, D.; Ricci, G.; Rossen, K.; Cossy, J. Iridium-Catalyzed Hydrogen Transfer: Synthesis of Substituted Benzofurans, Benzothiophenes, and Indoles from Benzyl Alcohols. *Org. Lett.* **2013**, *15* (15), 3876–3879.

Arai, S.; Nakajima, M.; Nishida, A. A Concise and Versatile Synthesis of Alkaloids from Kopsia Tenuis: Total Synthesis of (±)-Lundurine A and B. *Angew. Chem. Int. Ed.* **2014**, *53* (22), 5569–5572.

Ardakani, M. A.; Smalley, R. K. BASE-INDUCED INTRAMOLECULAR CYCLISATION OF PAZIDOPHENYL SEC-ALKYL KETONES. A NEW SYNTHESIS OF 2,2-DIALKYLINDOXYLS. *Tetrahedron Lett.* **1979**, *20* (49), 4769–4772.

Baba, K.; Tobisu, M.; Chatani, N. Palladium-Catalyzed Synthesis of Six-Membered Benzofuzed Phosphacycles via Carbon–Phosphorus Bond Cleavage. *Org. Lett.* **2015**, *17* (1), 70–73.

Baran, P. S.; Corey, E. J. A Short Synthetic Route to (+)-Austamide, (+)-Deoxyisoaustamide, and (+)-Hydratoaustamide from a Common Precursor by a Novel Palladium-Mediated Indole → Dihydroindoloazocine Cyclization. *J. Am. Chem. Soc.* **2002**, *124* (27), 7904–7905.

Barhate, N. B.; Chen, C.-T. Catalytic Asymmetric Oxidative Couplings of 2-Naphthols by Tridentate N-Ketopinidene-Based Vanadyl Dicarboxylates. *Org. Lett.* **2002**, *4* (15), 2529–2532.

Bedford, R. B.; Betham, M. N-H Carbazole Synthesis from 2-Chloroanilines via Consecutive Amination and C−H Activation. *J. Org. Chem.* **2006**, *71* (25), 9403–9410.

Bedford, R. B.; Betham, M.; Charmant, J. P. H.; Weeks, A. L. Intramolecular Direct Arylation in the Synthesis of Fluorinated Carbazoles. *Tetrahedron* **2008**, *64* (26), 6038–6050.

Boren, B. C.; Narayan, S.; Rasmussen, L. K.; Zhang, L.; Zhao, H.; Lin, Z.; Jia, G.; Fokin, V. V. Ruthenium-Catalyzed Azide−Alkyne Cycloaddition: Scope and Mechanism. *J. Am. Chem. Soc.* **2008**, *130* (28), 8923–8930.

Bringmann, G.; Ledermann, A.; Stahl, M.; Gulden, K. Bismurrayaquinone A: Synthesis, Chromatographic Enantiomer Resolution, and Stereoanalysis by Computational and Experimental CD Investigations. *Tetrahedron* **1995**, *51* (34), 9353–9360.

Brunel, J. M. BINOL: A Versatile Chiral Reagent. *Chem. Rev.* **2005**, *105* (3), 857–898.

Buter, J.; Heijnen, D.; Vila, C.; Hornillos, V.; Otten, E.; Giannerini, M.; Minnaard, A. J.; Feringa, B. L. Palladium-Catalyzed, Tert-Butyllithium-Mediated Dimerization of Aryl Halides and Its Application in the Atropselective Total Synthesis of Mastigophorene A. *Angew. Chem. Int. Ed.* **2016**, *55* (11), 3620–3624.

Chen, Y.-H.; Cheng, D.-J.; Zhang, J.; Wang, Y.; Liu, X.-Y.; Tan, B. Atroposelective Synthesis of Axially Chiral Biaryldiols via Organocatalytic Arylation of 2-Naphthols. *J. Am. Chem. Soc.* **2015**, *137* (48), 15062–15065.

Chu, C.-Y.; Hwang, D.-R.; Wang, S.-K.; Uang, B.-J. Chiral Oxovanadium Complex Catalyzed Enantioselective Oxidative Coupling of 2-Naphthols. *Chem. Commun.* **2001**, *0* (11), 980–981.

Chu, C.-Y.; Uang, B.-J. Catalytic Enantioselective Coupling of 2-Naphthols by New Chiral Oxovanadium Complexes Bearing a Self Accelerating Functional Group. *Tetrahedron Asymmetry* **2003**, *14* (1), 53–55.

Dai, J.; Ma, D.; Fu, C.; Ma, S. Gram Scale Total Synthesis of 2-Hydroxy-3-Methylcarbazole, Pyrano[3,2-a]Carbazole and Prenylcarbazole Alkaloids. *Eur. J. Org. Chem.* **2015**, *2015* (25), 5655–5662.

Dai, Q.; Gao, W.; Liu, D.; Kapes, L. M.; Zhang, X. Triazole-Based Monophosphine Ligands for Palladium-Catalyzed Cross-Coupling Reactions of Aryl Chlorides. *J. Org. Chem.* **2006**, *71* (10), 3928–3934.

Dai, X.; Chen, Y.; Garrell, S.; Liu, H.; Zhang, L.-K.; Palani, A.; Hughes, G.; Nargund, R. Ligand-Dependent Site-Selective Suzuki Cross-Coupling of 3,5-Dichloropyridazines. *J. Org. Chem.* **2013**, *78* (15), 7758–7763.

Dang, H.-S.; Elsegood, M. R. J.; Kim, K.-M.; Roberts, B. P. Radical-Chain Reductive Alkylation of Electron-Rich Alkenes Mediated by Silanes in the Presence of Thiols as Polarity-Reversal Catalysts. *J. Chem. Soc. [Perkin 1]* **1999**, No. 15, 2061–2068.

Daskalaki, E.; Le Droumaguet, B.; Gérard, D.; Velonia, K. Multifunctional Giant Amphiphiles via Simultaneous Copper(i)-Catalyzed Azide–Alkynecycloaddition and Living Radical Polymerization. *Chem Commun* **2012**, *48* (10), 1586–1588.

Degnan, A. P.; Meyers, A. I. Total Syntheses of (−)-Herbertenediol, (−)-Mastigophorene A, and (−)-Mastigophorene B. Combined Utility of Chiral Bicyclic Lactams and Chiral Aryl Oxazolines. *J. Am. Chem. Soc.* **1999**, *121* (12), 2762–2769.

Dhara, K.; Mandal, T.; Das, J.; Dash, J. Synthesis of Carbazole Alkaloids by Ring-Closing Metathesis and Ring Rearrangement–Aromatization. *Angew. Chem. Int. Ed.* **2015**, *54* (52), 15831–15835.

Egami, H.; Katsuki, T. Iron-Catalyzed Asymmetric Aerobic Oxidation: Oxidative Coupling of 2-Naphthols. *J. Am. Chem. Soc.* **2009**, *131* (17), 6082–6083.

Fillion, H.; Bouaziz, Z.; Nebois, P.; Poumaroux, A. Carbazole-1,4-Diones: Syntheses and Properties. *HETEROCYCLES* **2000**, *52* (2), 977.

Fu, W.; Song, Q. Copper-Catalyzed Radical Difluoroalkylation and Redox Annulation of Nitroalkynes for the Construction of C2-Tetrasubstituted Indolin-3-Ones. *Org. Lett.* **2018**, *20* (2), 393–396.

Fukuyama, Y.; Asakawa, Y. Novel Neurotrophic Isocuparane-Type Sesquiterpene Dimers, Mastigophorenes A, B, C and D, Isolated from the Liverwort Mastigophora Diclados. *J. Chem. Soc. [Perkin 1]* **1991**, *0* (11), 2737–2741.

Fukuyama, Y.; Asakawa, Y. Novel Neurotrophic Isocuparane-Type Sesquiterpene Dimers, Mastigophorenes A, B, c and D, Isolated from the Liverwort Mastigophora Didados. *J C H E M SOC P E R K N TRANS* **1991**, 2737.

Goriya, Y.; Ramana, C. V. Synthesis of Pseudo-Indoxyl Derivatives via Sequential Cu-Catalyzed SNAr and Smalley Cyclization. *Chem. Commun.* **2013**, *49* (57), 6376.

Gray, M.; Chapell, B. J.; Felding, J.; Taylor, N. J.; Snieckus, V. The Di- *t* -Butylphosphinyl Directed *Ortho* Metalation Group. Synthesis of Hindered Dialkylarylphosphines. *Synlett* **1998**, *1998* (4), 422–424.

Guchhait, S. K.; Chaudhary, V.; Rana, V. A.; Priyadarshani, G.; Kandekar, S.; Kashyap, M. Oxidative Dearomatization of Indoles via Pd-Catalyzed C–H Oxygenation: An Entry to C2-Quaternary Indolin-3-Ones. *Org. Lett.* **2016**, *18* (7), 1534–1537.

Guo, C.; Schedler, M.; Daniliuc, C. G.; Glorius, F. N-Heterocyclic Carbene Catalyzed Formal [3+2] Annulation Reaction of Enals: An Efficient Enantioselective Access to Spiro-Heterocycles. *Angew. Chem. Int. Ed.* **2014**, *53* (38), 10232–10236.

Guo, Q.-X.; Wu, Z.-J.; Luo, Z.-B.; Liu, Q.-Z.; Ye, J.-L.; Luo, S.-W.; Cun, L.-F.; Gong, L.-Z. Highly Enantioselective Oxidative Couplings of 2-Naphthols Catalyzed by Chiral Bimetallic Oxovanadium Complexes with Either Oxygen or Air as Oxidant. *J. Am. Chem. Soc.* **2007**, *129* (45), 13927–13938.

Han, S.; Movassaghi, M. Concise Total Synthesis and Stereochemical Revision of All (−)-Trigonoliimines. *J. Am. Chem. Soc.* **2011**, *133* (28), 10768–10771.

Hartung, J.; Drees, S.; Greb, M.; Schmidt, P.; Svoboda, I.; Fuess, H.; Murso, A.; Stalke, D. (Schiff-Base)Vanadium(V) Complex-Catalyzed Oxidations of Substituted Bis(Homoallylic) Alcohols − Stereoselective Synthesis of Functionalized Tetrahydrofurans. *Eur. J. Org. Chem.* **2003**, *2003* (13), 2388–2408.

Heiser, B.; Broger, E. A.; Crameri, Y. New Efficient Methods for the Synthesis and In-Situ Preparation of Ruthenium(II) Complexes of Atropisomeric Diphosphines and Their Application in Asymmetric Catalytic Hydrogenations. *Tetrahedron Asymmetry* **1991**, *2* (1), 51–62.

Higuchi, K.; Sato, Y.; Tsuchimochi, M.; Sugiura, K.; Hatori, M.; Kawasaki, T. First Total Synthesis of Hinckdentine A. *Org. Lett.* **2009**, *11* (1), 197–199.

Hon, S.-W.; Li, C.-H.; Kuo, J.-H.; Barhate, N. B.; Liu, Y.-H.; Wang, Y.; Chen, C.-T. Catalytic Asymmetric Coupling of 2-Naphthols by Chiral Tridentate Oxovanadium(IV) Complexes. *Org. Lett.* **2001**, *3* (6), 869–872.

Hu, M.; Li, J.; Q. Yao, S. In Situ “Click” Assembly of Small Molecule Matrix Metalloprotease Inhibitors Containing Zinc-Chelating Groups. *Org. Lett.* **2008**, *10* (24), 5529–5531.

Huisgen, R. 1.3-Dipolare Cycloadditionen Rückschau und Ausblick. *Angew. Chem.* **1963**, *75* (13), 604–637.

Hwang, D.-R.; Chen, C.-P.; Uang, B.-J. Aerobic Catalytic Oxidative Coupling of 2-Naphthols and Phenols by VO(Acac)2. *Chem. Commun.* **1999**, *0* (13), 1207–1208.

Jin, C.-Y.; Wang, Y.; Liu, Y.-Z.; Shen, C.; Xu, P.-F. Organocatalytic Asymmetric Michael Addition of Oxindoles to Nitroolefins for the Synthesis of 2,2-Disubstituted Oxindoles Bearing Adjacent Quaternary and Tertiary Stereocenters. *J. Org. Chem.* **2012**, *77* (24), 11307–11312.

Johansson, J. R.; Beke-Somfai, T.; Said Stålsmeden, A.; Kann, N. Ruthenium-Catalyzed Azide Alkyne Cycloaddition Reaction: Scope, Mechanism, and Applications. *Chem. Rev.* **2016**, *116* (23), 14726–14768.

Karadeolian, A.; Kerr, M. A. Total Synthesis of (+)-Isatisine A. *Angew. Chem. Int. Ed.* **2010**, *49* (6), 1133–1135.

Kang, H.; Lee, Y. E.; Reddy, P. V. G.; Dey, S.; Allen, S. E.; Niederer, K. A.; Sung, P.; Hewitt, K.; Torruellas, C.; Herling, M. R.; et al. Asymmetric Oxidative Coupling of Phenols and Hydroxycarbazoles. *Org. Lett.* **2017**, *19* (20), 5505–5508.

Kawasaki, T.; Higuchi, K.; Masuda, K.; Koseki, T.; Hatori, M.; Sakamoto, M. Asymmetric Alkylation of 2-Monosubstituted Indolin-3-Ones. *HETEROCYCLES* **2007**, *73* (1), 641.

Kenar, J. A. Reaction Chemistry of Gossypol and Its Derivatives. *J. Am. Oil Chem. Soc.* **2006**, *83* (4), 269–302.

Kim, K. H.; Lee, D.-W.; Lee, Y.-S.; Ko, D.-H.; Ha, D.-C. Enantioselective Oxidative Coupling of Methyl 3-Hydroxy-2-Naphthoate Using Mono-N-Alkylated Octahydrobinaphthyl-2,2'-Diamine Ligand. *Tetrahedron* **2004**, *60* (41), 9037–9042.

Knölker, H.-J.; Goesmann, H.; Hofmann, C. Transition Metal Complexes in Organic Synthesis, Part 31.1 A Novel Molybdenum-Mediated Synthesis of Carbazole Derivatives: Application to the Total Synthesis of Mukonal and 1,1'-Bis(2-Hydroxy-3-Methylcarbazole). *Synlett* **1996**, *1996* (8), 737–740.

Kondoh, A.; Yorimitsu, H.; Oshima, K. Synthesis of 2-Indolylphosphines by Palladium-Catalyzed Annulation of 1-Alkynylphosphine Sulfides with 2-Iodoanilines. *Org. Lett.* **2010**, *12* (7), 1476–1479.

Krasiński, A.; Fokin, V. V.; Sharpless, K. B. Direct Synthesis of 1,5-Disubstituted-4-Magnesio-1,2,3-Triazoles, Revisited. *Org. Lett.* **2004**, *6* (8), 1237–1240.

Lee, Y. E.; Cao, T.; Torruellas, C.; Kozlowski, M. C. Selective Oxidative Homo- and Cross-Coupling of Phenols with Aerobic Catalysts. *J. Am. Chem. Soc.* **2014**, *136* (19), 6782–6785.

Li, X.; Yang, J.; Kozlowski, M. C. Enantioselective Oxidative Biaryl Coupling Reactions Catalyzed by 1,5-Diazadecalin Metal Complexes. *Org. Lett.* **2001**, *3* (8), 1137–1140.

Li, Y.; Das, S.; Zhou, S.; Junge, K.; Beller, M. General and Selective Copper-Catalyzed Reduction of Tertiary and Secondary Phosphine Oxides: Convenient Synthesis of Phosphines. *J. Am. Chem. Soc.* **2012**, *134* (23), 9727–9732.

Li, Y.; Lu, L.-Q.; Das, S.; Pisiewicz, S.; Junge, K.; Beller, M. Highly Chemoselective Metal-Free Reduction of Phosphine Oxides to Phosphines. *J. Am. Chem. Soc.* **2012**, *134* (44), 18325–18329.

Li, Y.-J.; Yan, N.; Liu, C.-H.; Yu, Y.; Zhao, Y.-L. Gold/Copper-Co-Catalyzed Tandem Reactions of 2-Alkynylanilines: A Synthetic Strategy for the C2-Quaternary Indolin-3-Ones. *Org. Lett.* **2017**, *19* (5), 1160–1163.

Libman, A.; Shalit, H.; Vainer, Y.; Narute, S.; Kozuch, S.; Pappo, D. Synthetic and Predictive Approach to Unsymmetrical Biphenols by Iron-Catalyzed Chelated Radical–Anion Oxidative Coupling. *J. Am. Chem. Soc.* **2015**, *137* (35), 11453–11460.

Lin, G.; Zhang, A. Synthesis of Optically Pure Clausenamine-A and Its Demethoxylated Analogs. *Tetrahedron* **2000**, *56* (37), 7163–7171.

Littke, A. F.; Dai, C.; Fu, G. C. Versatile Catalysts for the Suzuki Cross-Coupling of Arylboronic Acids with Aryl and Vinyl Halides and Triflates under Mild Conditions. *J. Am. Chem. Soc.* **2000**, *122* (17), 4020–4028.

Littke, A. F.; Fu, G. C. Palladium-Catalyzed Coupling Reactions of Aryl Chlorides. *Angew. Chem. Int. Ed.* **2002**, *41* (22), 4176–4211.

Liu, D.; Gao, W.; Dai, Q.; Zhang, X. Triazole-Based Monophosphines for Suzuki–Miyaura Coupling and Amination Reactions of Aryl Chlorides. *Org. Lett.* **2005**, *7* (22), 4907–4910.

Liu, J.-F.; Jiang, Z.-Y.; Wang, R.-R.; Zheng, Y.-T.; Chen, J.-J.; Zhang, X.-M.; Ma, Y.-B. Isatisine A, a Novel Alkaloid with an Unprecedented Skeleton from Leaves of *Isatis Indigotica*. *Org. Lett.* **2007**, *9* (21), 4127–4129.

Liu, L.; Carroll, P. J.; Kozlowski, M. C. Vanadium-Catalyzed Regioselective Oxidative Coupling of 2-Hydroxycarbazoles. *Org. Lett.* **2015**, *17* (3), 508–511.

Liu, R.-R.; Ye, S.-C.; Lu, C.-J.; Zhuang, G.-L.; Gao, J.-R.; Jia, Y.-X. Dual Catalysis for the Redox Annulation of Nitroalkynes with Indoles: Enantioselective Construction of Indolin-3-Ones Bearing Quaternary Stereocenters. *Angew. Chem. Int. Ed.* **2015**, *54* (38), 11205–11208.

Liu, Y.; McWhorter, W. W. Study of the Addition of Grignard Reagents to 2-Aryl-3 *H* -Indol-3-Ones [1]. *J. Org. Chem.* **2003**, *68* (7), 2618–2622.

Liu, Y.; McWhorter, W. W. Synthesis of 8-Desbromohinckdentine A [1]. *J. Am. Chem. Soc.* **2003**, *125* (14), 4240–4252.

Luo, Z.; Liu, Q.; Gong, L.; Cui, X.; Mi, A.; Jiang, Y. The Rational Design of Novel Chiral Oxovanadium(IV) Complexes for Highly Enantioselective Oxidative Coupling of 2-Naphthols. *Chem. Commun.* **2002**, *0* (8), 914–915.

Majireck, M. M.; Weinreb, S. M. A Study of the Scope and Regioselectivity of the Ruthenium-Catalyzed [3 + 2]-Cycloaddition of Azides with Internal Alkynes. *J. Org. Chem.* **2006**, *71* (22), 8680–8683.

Manabe, K.; Yamaguchi, M. ChemInform Abstract: Catalyst-Controlled Site-Selectivity Switching in Pd-Catalyzed Cross-Coupling of Dihaloarenes. *Catalysts* **2014**, *4*, 307–320.

Melhado, A. D.; Luparia, M.; Toste, F. D. Au(I)-Catalyzed Enantioselective 1,3-Dipolar Cycloadditions of Münchnones with Electron-Deficient Alkenes. *J. Am. Chem. Soc.* **2007**, *129* (42), 12638–12639.

Ming Ge, H.; Yun Zhang, W.; Ding, G.; Saparpakorn, P.; Chun Song, Y.; Hannongbua, S.; Xiang Tan, R. Chaetoglobins A and B, Two Unusual Alkaloids from Endophytic Chaetomium Globosum Culture. *Chem. Commun.* **2008**, 5978-.

Miyaura, N.; Suzuki, A. Palladium-Catalyzed Cross-Coupling Reactions of Organoboron Compounds. *Chem. Rev.* **1995**, *95* (7), 2457–2483.

Moody, C. J.; Shah, P. Diels-Alder Reactivity of Pyrano[3,4-b]Indol-3-Ones. Part 4. Synthesis of the Carbazole Alkaloids Carbazomycin A and B and Hyellazole. *J. Chem. Soc. [Perkin 1]* **1989**, *0* (12), 2463–2471.

Nakajima, M.; Miyoshi, I.; Kanayama, K.; Hashimoto, S.; Noji, M.; Koga, K. Enantioselective Synthesis of Binaphthol Derivatives by Oxidative Coupling of Naphthol Derivatives Catalyzed by Chiral Diamine·Copper Complexes. *J. Org. Chem.* **1999**, *64* (7), 2264–2271.

Narayan, S.; Roush, W. R. Studies Toward the Total Synthesis of Angelmicin B (Hibarimicin B): Synthesis of a Model CD−D′ Arylnaphthoquinone. *Org. Lett.* **2004**, *6* (21), 3789–3792.

Narute, S.; Parnes, R.; Toste, F. D.; Pappo, D. Enantioselective Oxidative Homocoupling and Cross-Coupling of 2-Naphthols Catalyzed by Chiral Iron Phosphate Complexes. *J. Am. Chem. Soc.* **2016**, *138* (50), 16553–16560.

Ngai, M. H.; Yang, P.-Y.; Liu, K.; Shen, Y.; Wenk, M. R.; Yao, S. Q.; Lear, M. J. Click-Based Synthesis and Proteomic Profiling of Lipstatin Analogues. *Chem. Commun.* **2010**, *46* (44), 8335.

Nutan, M. T. .; Hasan, C. .; Rashid, M. . Bismurrayafoline E: A New Dimeric Carbazole Alkaloid from Murraya Koenigii. *Fitoterapia* **1999**, *70* (2), 130–133.

Onodera, G.; Matsumoto, H.; Milton, M. D.; Nishibayashi, Y.; Uemura, S. Ruthenium-Catalyzed Formation of Aryl(Diphenyl)Phosphine Oxides by Reactions of Propargylic Alcohols with Diphenylphosphine Oxide. *Org. Lett.* **2005**, *7* (18), 4029–4032.

Parra, A.; Alfaro, R.; Marzo, L.; Moreno-Carrasco, A.; García Ruano, J. L.; Alemán, J. Enantioselective Aza-Henry Reactions of Cyclic α-Carbonyl Ketimines under Bifunctional Catalysis. *Chem. Commun.* **2012**, *48* (78), 9759.

Pearson, W. H.; Mi, Y.; Lee, I. Y.; Stoy, P. Total Synthesis of the *Kopsia Lapidilecta* Alkaloid (±)-Lapidilectine B. *J. Am. Chem. Soc.* **2001**, *123* (27), 6724–6725.

Qi, X.; Bao, H.; Tambar, U. K. Total Synthesis of (±)-Trigonoliimine C via Oxidative Rearrangement of an Unsymmetrical Bis-Tryptamine. *J. Am. Chem. Soc.* **2011**, *133* (26), 10050–10053.

Qiao, J. X.; Lam, P. Y. S. Copper-Promoted Carbon-Heteroatom Bond Cross-Coupling with Boronic Acids and Derivatives. *Synthesis* **2011**, *2011* (6), 829–856.

Qiu, L.; Kwong, F. Y.; Wu, J.; Lam, W. H.; Chan, S.; Yu, W.-Y.; Li, Y.-M.; Guo, R.; Zhou, Z.; Chan, A. S. C. A New Class of Versatile Chiral-Bridged Atropisomeric Diphosphine Ligands: Remarkably Efficient Ligand Syntheses and Their Applications in Highly Enantioselective Hydrogenation Reactions. *J. Am. Chem. Soc.* **2006**, *128* (17), 5955–5965.

Rossi, R.; Bellina, F.; Lessi, M. Highly Selective Palladium-Catalyzed Suzuki–Miyaura Monocoupling Reactions of Ethene and Arene Derivatives Bearing Two or More Electrophilic Sites. *Tetrahedron* **2011**, *67* (37), 6969–7025.

Rostovtsev, V. V.; Green, L. G.; Fokin, V. V.; Sharpless, K. B. A Stepwise Huisgen Cycloaddition Process: Copper(I)-Catalyzed Regioselective "Ligation" of Azides and Terminal Alkynes. *Angew. Chem. Int. Ed.* **2002**, *41* (14), 2596–2599.

Rueping, M.; Raja, S.; Núñez, A. Asymmetric Brønsted Acid-Catalyzed Friedel-Crafts Reactions of Indoles with Cyclic Imines - Efficient Generation of Nitrogen-Substituted Quaternary Carbon Centers. *Adv. Synth. Catal.* **2011**, *353* (4), 563–568.

S. Baran, P.; Jessing, M. Oxidative Coupling of Indoles with 3-Oxindoles. *HETEROCYCLES* **2010**, *82* (2), 1739.

Sako, M.; Takeuchi, Y.; Tsujihara, T.; Kodera, J.; Kawano, T.; Takizawa, S.; Sasai, H. Efficient Enantioselective Synthesis of Oxahelicenes Using Redox/Acid Cooperative Catalysts. *J. Am. Chem. Soc.* **2016**, *138* (36), 11481–11484.

Schulze, B.; Schubert, U. S. Beyond Click Chemistry – Supramolecular Interactions of 1,2,3-Triazoles. *Chem. Soc. Rev.* **2014**, *43* (8), 2522.

Somei, H.; Asano, Y.; Yoshida, T.; Takizawa, S.; Yamataka, H.; Sasai, H. Dual Activation in a Homolytic Coupling Reaction Promoted by an Enantioselective Dinuclear Vanadium(IV) Catalyst. *Tetrahedron Lett.* **2004**, *45* (9), 1841–1844.

Spinella, S.; Guan, Z.-H.; Chen, J.; Zhang, X. Suzuki Coupling of Heteroaromatic Chlorides Using Highly Electron-Donating ClickPhos Ligands. *Synthesis* **2009**, *2009* (18), 3094–3098.

Spiteri, C.; Moses, J. E. Copper-Catalyzed Azide–Alkyne Cycloaddition: Regioselective Synthesis of 1,4,5-Trisubstituted 1,2,3-Triazoles. *Angew. Chem. Int. Ed.* **2010**, *49* (1), 31–33.

Strotman, N. A.; Chobanian, H. R.; He, J.; Guo, Y.; Dormer, P. G.; Jones, C. M.; Steves, J. E. Catalyst-Controlled Regioselective Suzuki Couplings at Both Positions of Dihaloimidazoles, Dihalooxazoles, and Dihalothiazoles. *J. Org. Chem.* **2010**, *75* (5), 1733–1739.

Tachibana, Y.; Kikuzaki, H.; Lajis, N. H.; Nakatani, N. Comparison of Antioxidative Properties of Carbazole Alkaloids from Murraya Koenigii Leaves. *J. Agric. Food Chem.* **2003**, *51* (22), 6461–6467.

Takizawa, S.; Katayama, T.; Kameyama, C.; Onitsuka, K.; Suzuki, T.; Yanagida, T.; Kawai, T.; Sasai, H. Chiral Dinuclear Vanadium(V) Catalysts for Oxidative Coupling of 2-Naphthols. *Chem. Commun.* **2008**, *0* (15), 1810–1812.

Takizawa, S.; Katayama, T.; Sasai, H. Dinuclear Chiral Vanadium Catalysts for Oxidative Coupling of 2-Naphtholsvia a Dual Activation Mechanism. *Chem. Commun.* **2008**, *0* (35), 4113–4122.

Takizawa, S.; Katayama, T.; Somei, H.; Asano, Y.; Yoshida, T.; Kameyama, C.; Rajesh, D.; Onitsuka, K.; Suzuki, T.; Mikami, M.; et al. Dual Activation in Oxidative Coupling of 2-Naphthols Catalyzed by Chiral Dinuclear Vanadium Complexes. *Tetrahedron* **2008**, *64* (15), 3361–3371.

Takizawa, S.; Kodera, J.; Yoshida, Y.; Sako, M.; Breukers, S.; Enders, D.; Sasai, H. Enantioselective Oxidative-Coupling of Polycyclic Phenols. *Tetrahedron* **2014**, *70* (9), 1786–1793.

Tanaka, Y.; Velen, S. R.; Miller, S. I. Syntheses and Properties of H-1,2,3-Triazoles. *Tetrahedron* **1973**, *29* (21), 3271–3283.

Tsukamoto, S.; Umaoka, H.; Yoshikawa, K.; Ikeda, T.; Hirota, H. Notoamide O, a Structurally Unprecedented Prenylated Indole Alkaloid, and Notoamides P−R from a Marine-Derived Fungus, *Aspergillus* Sp. *J. Nat. Prod.* **2010**, *73* (8), 1438–1440.

Wang, C.; Wang, Z.; Xie, X.; Yao, X.; Li, G.; Zu, L. Total Synthesis of (±)-Grandilodine B. *Org. Lett.* **2017**, *19* (7), 1828–1830.

Wang, J.-Z.; Zhou, J.; Xu, C.; Sun, H.; Kürti, L.; Xu, Q.-L. Symmetry in Cascade Chirality-Transfer Processes: A Catalytic Atroposelective Direct Arylation Approach to BINOL Derivatives. *J. Am. Chem. Soc.* **2016**, *138* (16), 5202–5205.

Wetzel, A.; Gagosz, F. Gold-Catalyzed Transformation of 2-Alkynyl Arylazides: Efficient Access to the Valuable Pseudoindoxyl and Indolyl Frameworks. *Angew. Chem. Int. Ed.* **2011**, *50* (32), 7354–7358.

Wiberg, K. B. The Deuterium Isotope Effect. *Chem. Rev.* **1955**, *55* (4), 713–743.

Witkop, B. The Structure of the So-Called 11-Hydroxytetrahydrocarbazolenine [1]. *J. Am. Chem. Soc.* **1950**, *72* (1), 614–620.

Witkop, B.; Patrick, J. B. The Course and Kinetics of the Acid-Base-Catalyzed Rearrangements of 11-Hydroxytetrahydrocarbazolenine [1]. *J. Am. Chem. Soc.* **1951**, *73* (5), 2188–2195.

Wu, P.-L.; Hsu, Y.-L.; Jao, C.-W. Indole Alkaloids from *Cephalanceropsis Gracilis*. *J. Nat. Prod.* **2006**, *69* (10), 1467–1470.

Xia, Z.; Hu, J.; Gao, Y.-Q.; Yao, Q.; Xie, W. Facile Access to 2,2-Disubstituted Indolin-3-Ones via a Cascade Fischer Indolization/Claisen Rearrangement Reaction. *Chem. Commun.* **2017**, *53* (54), 7485–7488.

Yang, J.; Chen, T.; Zhou, Y.; Yin, S.; Han, L.-B. Palladium-Catalyzed Dehydrogenative Coupling of Terminal Alkynes with Secondary Phosphine Oxides. *Chem. Commun.* **2015**, *51* (17), 3549–3551.

Yin, J.; Rainka, M. P.; Zhang, X.-X.; Buchwald, S. L. A Highly Active Suzuki Catalyst for the Synthesis of Sterically Hindered Biaryls: Novel Ligand Coordination. *J. Am. Chem. Soc.* **2002**, *124* (7), 1162–1163.

Zhang, C.; Li, S.; Bureš, F.; Lee, R.; Ye, X.; Jiang, Z. Visible Light Photocatalytic Aerobic Oxygenation of Indoles and PH as a Chemoselective Switch. *ACS Catal.* **2016**, *6* (10), 6853–6860.

Zhang, L.; Chen, X.; Xue, P.; Sun, H. H. Y.; Williams, I. D.; Sharpless, K. B.; Fokin, V. V.; Jia, G. Ruthenium-Catalyzed Cycloaddition of Alkynes and Organic Azides. *J. Am. Chem. Soc.* **2005**, *127* (46), 15998–15999.

Zhang, X.; Foote, C. S. Dimethyldioxirane Oxidation of Indole Derivatives. Formation of Novel Indole-2,3-Epoxides and a Versatile Synthetic Route to Indolinones and Indolines. *J. Am. Chem. Soc.* **1993**, *115* (19), 8867–8868.

Zhao, Y.-L.; Wang, Y.; Cao, J.; Liang, Y.-M.; Xu, P.-F. Organocatalytic Asymmetric Michael–Michael Cascade for the Construction of Highly Functionalized N-Fused Piperidinoindoline Derivatives. *Org. Lett.* **2014**, *16* (9), 2438–2441.

Zhou, X.-Y.; Chen, X.; Wang, L.-G.; Yang, D.; Li, J.-H. Ruthenium-Catalyzed Oxidative Dearomatization of Indoles for the Construction of C2-Quaternary Indolin-3-Ones. *Synlett* **2018**, *29* (06), 835–839.